AGEDI
مبادرة أبوظبي العالمية للبيانات البيئية
Abu Dhabi Global Environmental Data Initiative

an initiative of

UNEP

هيئة البيئة - أبوظبي
Environment Agency - ABU DHABI

AGEDI | THE ABU DHABI GLOBAL ENVIRONMENTAL DATA INITIATIVE

CLIMATE CHANGE PROGRAMME

Terrestrial Biodiversity Vulnerability to Climate Change

- Atmospheric Modelling
- Arabian Gulf Modelling
- Terrestrial Ecosystems
- Marine Ecosystems
- Transboundary Groundwater
- Water Resource Management
- Al Ain Water Resources
- Coastal Vulnerability Index
- Desalinated Water Supply
- Food Security
- Public Health Benefits of GHG Mitigation
- Sea Level Rise

Full Technical Report

AGEDI .org

AGEDI
مبادرة أبوظبي العالمية للبيانات البيئية
Abu Dhabi Global Environmental Data Initiative

The Principal Investigator for this research is Dr. Matthew Fitzpatrick from the Appalachian Laboratory at the University of Maryland Center for Environmental Science. His co-authors are Kavya Pradhan, and Matthew Lisk.

Suggested Citation: AGEDI. 2015. Technical Report: Regional Terrestrial Biodiversity and Climate Change. LNRCCP. CCRG/University of Maryland – Centre for Environmental Science

Climate Change Research Group

University of Maryland
CENTER FOR ENVIRONMENTAL SCIENCE

AGEDI
مبادرة أبوظبي العالمية للبيانات البيئية
Abu Dhabi Global Environmental Data Initiative

About this Final Technical Report

In October 2013, the Abu Dhabi Global Environmental Data Initiative (AGEDI) launched the "Local, National, and Regional Climate Change (LNRCC) Programme to build upon, expand, and deepen understanding of vulnerability to the impacts of climate change as well as to identify practical adaptive responses at local (Abu Dhabi), national (UAE), and regional (Arabian Peninsula) levels. The design of the Programme was stakeholder---driven, incorporating the perspectives of over 100 local, national, and regional stakeholders in shaping 12 research studies across 5 strategic themes.[1] The "Terrestrial Biodiversity and Climate Change" study within this Programme aims to assess the potential impacts and the vulnerability of terrestrial biodiversity in the Arabian Peninsula region to climate change.

The purpose of this "Final Technical Report" is to offer a summary of what has been learned in carrying out the research activities involved in the "Terrestrial Biodiversity and Climate Change" study. This report seeks to provide the reader with an overall sense of the materials and methods, modeling results, key findings, and other issues that can support future policymaking regarding terrestrial conservation planning under climate change. Ultimately, this report seeks to provide a useful synthesis of all research activities, while offering partners and stakeholders a basis upon which to account for climate change in future biodiversity planning.

[1] For more information on the LNRCC programme and the terrestrial biodiversity sub-project, please contact Jane Glavan (lnrclimatechange@ead.ae).

Climate Change Research Group

University of Maryland
CENTER FOR ENVIRONMENTAL SCIENCE

AGEDI
مبادرة أبوظبي العالمية للبيانات البيئية
Abu Dhabi Global Environmental Data Initiative

Acknowledgments

Many individuals provided invaluable support, guidance, and input to the Terrestrial Biodiversity and Climate Change project.

The authors would like to express their sincere and heartfelt expressions of gratitude for their review by providing comments, feedback and /or data towards the multiple deliverables within the project process including:

- Dr. Abdul Wali Al-Khulaidi, Centre for Middle Eastern Plants
- Dr. Ali El Keblawy, University of Sharjah
- Dr. Benno Boer, UNESCO Arab Region
- Dr. David Mallon, Co-Chair IUCN SSC Antelope Specialist Group
- Mr. Ehab Eid, The Royal Marine Conservation Society of Jordan (JREDS)
- Mr. Hazem Abu Ahmed, Abu Dhabi National Oil Company (ADNOC)
- Dr. Fred Launay, Environment Agency-Abu Dhabi (EAD)
- Dr. Gary Brown, Sultan Qaboos University
- Dr. Jacky Judas, Emirates Wildlife Society (EWS)- WWF
- Mr. Josh Smithson, WardKarlson Consulting
- Ms. Nessrine Al Zahlawi, Environment Agency-Abu Dhabi (EAD)
- Mr. Obaid Al Shamsi, UAE Ministry of Climate Change and Environment (MOCCAE)
- Ms. Paola Ferreira, Emirates Wildlife Society (EWS)- WWF
- Dr. Salim Javed, Environment Agency-Abu Dhabi (EAD)
- Dr. Shahina Ghazanfar, Kew Gardens
- Mr. Tim Hirsch and the informatics team at the Global Biodiversity Information Facility (GBIF)

We are additionally thankful the participation, time and effort that multiple stakeholders across the region who participated in the multitude of meetings and dialogue. The authors would like to especially thank the following stakeholders for their particularly involved participation: Annette Patzelt Oman Botanic Society, Nayla El Beyrouthi of the Ministry of Environment Qatar, Freidhelm Krupp of the Qatar Museum of Science and Nature, Oscar Campbell and Tommy Pedersen of the Emirates Bird Records Committee, Marina Antonopoulou and Nadia Rouchdy of the Emirates Wildlife Society-WWF, Maral Al Shuriqi of Fujairah Municipality, as well as Ahmed Al Hashmi and Naoko Kubo of the UAE Ministry of Environment and Climate Change.

Climate Change Research Group

University of Maryland
CENTER FOR ENVIRONMENTAL SCIENCE

AGEDI
مبادرة أبوظبي العالمية للبيانات البيئية
Abu Dhabi Global Environmental Data Initiative

Table of Contents

Climate Change Research Group

University of Maryland
CENTER FOR ENVIRONMENTAL SCIENCE

List of Tables

page

AGEDI
مبادرة أبوظبي العالمية للبيانات البيئية
Abu Dhabi Global Environmental Data Initiative

List of Figures

page

Climate Change Research Group

University of Maryland
CENTER FOR ENVIRONMENTAL SCIENCE

AGEDI
مبادرة أبوظبي العالمية للبيانات البيئية
Abu Dhabi Global Environmental Data Initiative

List of Acronyms

AR5	Fifth Assessment Report
CLM	Community-Level Model
GBIF	Global Biodiversity Information Facility
GCM	General Circulation Model
GDM	Generalized Dissimilarity Modeling
IPCC	Intergovernmental Panel on Climatic change
NCAR	National Center for Atmospheric Research
RCP	Representative Concentration Pathway
SDM	Species Distribution Model
UAE	United Arab Emirates
WWF	World Wildlife Fund

Climate Change Research Group

University of Maryland
CENTER FOR ENVIRONMENTAL SCIENCE

Introduction

Observations and model-based forecasts provide compelling evidence that the impacts of climatic change on biodiversity are likely to be widespread and significant, including dramatic increases extinction rates and changes to ecosystem structure and function (Walther *et al.* 2002; Root *et al.* 2003; Thuiller *et al.* 2005; Fitzpatrick *et al.* 2008, 2011; Urban 2015). At regional scales, the primary impacts of climatic change are expected to be rapid geographic shifts in climatically suitable habitats (Fischlin *et al.* 2007). As temperatures increase and precipitation patterns change, species will be forced to either adapt to new conditions, migrate to areas that become suitable, or potentially face extinction (Rosenzweig *et al.* 2007; Aitken *et al.* 2008). The increasing isolation and fragmentation of natural habits and the rapid rates of projected climatic change are expected to make migration unfeasible for all but the most vagile and widespread species (Hill *et al.* 1999; Malcolm *et al.* 2002; Travis 2003; Loarie *et al.* 2009).

Dryland ecosystems are expected to be particularly vulnerable to climatic change given their exposure and sensitivity to multiple drivers of global change, including habitat destruction, overgrazing, and invasive species (Talhouk 2009; El-Keblawy 2014). Although quantitative vulnerability assessments remain relatively rare in drylands, existing modeling studies suggest that range contractions (i.e., reduction in suitable habitat) rather than range shifts may be a dominant response of dryland biota to climatic change (Midgley *et al.* 2003; Thuiller *et al.* 2006; Midgley & Thuiller 2007; Fitzpatrick *et al.* 2008; Loarie *et al.* 2008). Such impacts are likely to have significant consequences for human societies given that drylands are home to more than a third of the world's population and support many of the world's food crops and livestock. For these reasons, a critical aspect of climatic change vulnerability assessments and adaptation planning in dryland ecosystems is determining the extent to which future climatic change is expected to alter the geographic distributions of species and patterns of biodiversity.

Background and local context

The Arabian Peninsula houses unique ecosystems that may be particularity vulnerable to climatic change (Talhouk 2009; El-Keblawy 2014). The biodiversity of the region is heavily influenced by its setting between Africa and Eurasia and the mixing of the often distinct taxa of these two realms. Climate history is a primary influence on contemporary patterns of biodiversity as well, as increasing aridity since the last ice age has led to the isolation of Arabian species and the evolution of endemic taxa. Although deserts are the most extensive ecosystem in the hyper-arid portions of the region, other unique systems such as shrub habitats, rangelands, and woodlands occur along coastal areas and highlands (Osman-Elasha & Fisher 2008; Talhouk 2009). In contrast to the species-poor desert regions and their hyper-arid climate, coastal and highland areas typically contain the highest levels of plant and animal biodiversity in the region, while coastal areas support the driest mangrove habitats in the world (Moore *et al.* 2014). Using the

biodiversity hotspot concept (Myers *et al.* 2000), Mallon (2011) identified the mountains and coastal areas of southwestern and southern rim of the Arabian Peninsula, including the lower mountains and coasts of Saudi Arabia, Yemen and the island of Socotra, and Oman, as an area of high biodiversity and notable concentrations of endemic vertebrate species.

The distributions of species within these biodiversity hotspots tend to be tightly coupled to specific climatic regimes and therefore many species may be unlikely to find suitable conditions under a more arid climate (Al Abed & Hellyer 2001). Generally speaking, vulnerability is expected to be greatest for species that are narrowly distributed or which exist at the margins of their environmental tolerances, such as those that thrive at high altitude or otherwise under conditions of moderate heat or moisture or in close proximity to water bodies. Desert fauna that depend on rainfall events to initiate breeding, such as resident birds, and migratory birds whose migration pathways traverse deserts, could also be severely affected (Hardy 2003). The Arabian Gulf region hosts a number of areas considered critical for the overwintering and breeding of birds and of water birds in particular. However, there have been relatively few formal, quantitative assessments of climatic change vulnerability for the region's biodiversity.

Vegetation

The current flora of the Arabian Peninsula reflects the interplay between long-term geologic and evolutionary history, climatic change, local physical factors (e.g., hydrology, soils, topography, etc.) and recent human influences such grazing, agriculture, land use, and introduction of exotic species (Ghazanfar & Fisher 2013). Primary vegetation assemblages include coastal sabkha vegetation, evergreen and deciduous woodlands, drought-deciduous open thorn woodlands, sclerophyllous and succulent shrublands, dwarf shrublands, and open xeromorphic grasslands (Ghazanfar & Fisher 2013). These vegetation assemblages vary across hyper-arid to humid subtropical climates, and more locally with topography and substrate, such as mountains with distinct altitudinal zonation, wadis, sand, rock and gravel deserts, dunes, sandy gravel plains, and mangroves (Miller & Cope 1997). Taking these various factors into consideration, Ghazanfar & Fisher (2013) defined six main vegetation types: (1) coastal and sabkha vegetation, (2) gravel deserts and other scarcely vegetated areas, (3) sand deserts, (4) northern plains and other northern coastal lowlands, (5) montane woodlands and xeromorphic shrublands, and (6) Wadi vegetation.

There are estimated to be somewhere over 6,000 native species of plants in the Arabian Peninsula, with up to ~20% being endemic (Miller & Cope 1997). The majority of the endemic plant taxa in Arabia are associated with mountainous areas (Miller & Cope 1997; El-Keblawy 2014), with the greatest concentrations along coastal regions, notably the western escarpments of Saudi Arabia and Yemen, the Al Hajar Mountains in Oman, and the islands of the Socotra archipelago – a global biodiversity hotspot (Cheung *et al.* 2007; Brown & Mies 2012). In Oman,

an estimated 5% of the flora is threatened, 80% of which occurs in the southern region of the country (Ghazanfar 1998). Yemen has by far the highest overall number of threatened plant species (Talhouk 2009; IUCN 2015), though the actual threat levels for plants in the region are generally poorly known. See Al-Abbasi *et al.* (2010) for criteria used to define important plant conservation areas in the region.

Given that many Arabian plants exhibit adaptation to extremes of heat and drought (Hegazy & Lovett-Doust 2016), much of the vegetation may be considered highly resilient to climatic change, and some taxa could conceivably benefit from increased aridity with expansion of suitable climate conditions. Perhaps for these reasons and given the severe impacts of human activities on dryland ecosystems, the threats of climatic change sometimes have been considered comparatively trivial (Brown & Mies 2012) to other threats. However, species in drylands often exist near the limits of their physiological tolerances (Kassas 1999). Moreover, the decline of some forests in the region already have been attributed at least in part to recent climatic change (e.g., *Juniperus* woodlands, Fisher 1997). Modeling studies have suggested flagship endemics such as the Dragon's Blood Tree (*Dracaena cinnabari*) of Socotra may be threatened by climatic change (Attorre *et al.* 2007) as well. Outside the region, modeling studies have predicted severe consequences of climatic change for dryland plant biodiversity (e.g., Fitzpatrick *et al.* 2008), species of which are often as dependent on the timing of precipitation as the quantity (Cowling *et al.* 2005). Most importantly, climatic change will act as an additional stressor to exacerbate ongoing degradation from the severe impacts from overgrazing and land use change in many areas (Talhouk 2009). In addition, climatic and other conditions required for *regeneration* can differ from those in which *established* plants can persist (Grubb 1977), and as such future climatic change may hinder colonization of disturbed areas or newly suitable habitat and the replacement of individuals lost to mortality.

Fauna

Avifauna

As a bridge between Africa, Asia and Europe, the Arabian Peninsula lies on important bird migration routes and contains numerous stopover habitats for both migrating and overwintering birds (Shobrak 2011). Richness patterns of birds generally follow those for other vertebrates (see below), with the largest concentrations of species generally occurring along coasts and nearby mountainous areas, especially the southwestern portion of the peninsula near the Red Sea (Somveille *et al.* 2013). These areas in Saudi Arabia and Yemen, as well as marshes and wetland areas of southeastern Iraq, are considered globally important bird areas (BirdLife International & NatureServe 2014). Approximately 6% of birds in the region are considered endemic (Mallon 2011).

At present, more than 150 bird species in the region are considered threatened (Talhouk 2009; IUCN 2015), and many more species are considered at high risk from climatic change (Talhouk 2009). Modeling studies have predicted large changes in wintering species richness of Afro-Palearctic migrant passerines due to climatic change, with increases or decreases of +/- 30% in the southwestern corner of the Arabian Peninsula being predicted depending on assumptions regarding dispersal potential (Barbet-Massin *et al.* 2009). Climate simulations predict increases in heat waves in the future and incidental severe heat waves also can lead to catastrophic avian mortality in hot desert environments. One study found that by the 2080s, desert birds could experience reduced survival times and increases in the frequency of catastrophic mortality events (McKechnie & Wolf 2009).

In addition to climatic change, factors such as urbanization, agriculture, wetland drainage, and other forms of habitat destruction also impact regional bird populations (AbuZinada *et al.* 2004). Moreover, climate-driven changes in vegetation will also likely impact birds. For example, the juniper forests at Raydah, Saudi Arabia, support upwards of 125 bird species including high densities of endemic species (Newton & Newton 1996) and recent declines in these forests have been associated with climatic change (Fisher 1997). Lastly, climatic change can impact migratory birds through shifts in phenology that lead to mismatches between critical life history events and food / habitat resources (Heezik & Seddon 1999; Visser *et al.* 2006).

Mammals

Approximately 100 species of native mammals have been recorded in the Arabian Peninsula, from small rodents and bats to large herbivores and carnivores (Kingdon 1990). Mammal species richness is concentrated in the same general areas as that for plants and birds – mostly in coastal mountainous regions of Saudi Arabia, Yemen, and Oman (Ceballos & Ehrlich 2006). Around 10% of the region's mammals are thought to be endemic (Mallon 2011).

Numerous mammal species in the region are already extinct (regionally), threatened with extinction, such as the Arabian oryx and tahr, leopard, wolf, hyena, cheetah, wild ass, and lion, or are declining (Mallon & Budd 2011). Many of the largest extant species are camels, sheep, goats, and gazelles, the last of which make up a bout half of the Bovid fauna (Kingdon 1990). Nearly all of these species have declined greatly over the last several decades (Thouless *et al.* 1991). As a group, carnivores are particularly threatened (Al-Johany 2007; Mallon & Budd 2011). As is the case with other dryland taxa, many desert mammals exist near the upper lethal limits of temperature and have limited access to water. For these reasons, climatic change is expected to have severe consequences across a wide range of desert animals, including mammals (Williams *et al.* 2012). Several studies have modeled the distributions of particular mammal species in the region (e.g., El Alqamy *et al.* 2010; Khosravi *et al.* 2016), but not in the context of climatic change.

Reptiles & Amphibians

Within the Arabian Peninsula, both species richness and the proportion of endemic reptile species are relatively high, with 172 species currently recognized and 89 species (52%) considered endemic (Cox *et al.* 2012). Like other groups, reptile species richness tends to be concentrated along the coastal rim of the Arabian Peninsula, and in particular the southwestern mountains and Dhofar (Farag & Banaja 1980; Mallon 2011). Richness is lowest in the Rub' al Khali (or Empty Quarter). Areas of greatest endemism follow the same general pattern, though the islands of the Socotra archipelago contain a disproportionate number of endemic species (26) (Cox *et al.* 2012). Most of the reptile species in the region are either lizards or snakes, with just two species of turtles and tortoises known from the Arabian Peninsula.

As a group, the reptiles of the Arabian Peninsula currently are relatively well protected, with 144 of the 172 species (84%) represented in protected areas. Only six species are listed as globally threatened, and only 10 are of regional concern. Land use change and agriculture are considered the greatest threats (Cox *et al.* 2012). Experimental studies suggest that reptiles may be particularity sensitive to higher temperatures expected in coming decades, especially for populations existing near the extremes of their thermal tolerance limits (Bestion *et al.* 2015). The extent to which protected areas will allow for persistence under climatic change is unknown.

Given the arid nature of the Arabian Peninsula, it should come as little surprise that the region is home to relatively few amphibian species. Only nine species (frogs and toads only) are known to be present, of which six are considered endemic (Balletto *et al.* 1985). As a rule, these species are limited to areas where standing water is present, however infrequently, to allow development of juvenile stages. For these reasons, most amphibian species are restricted to mountainous areas, wadis, oases, and man made areas.

Motivation & approach

Beyond broad generalities, the lack of quantitative assessments of the impacts of climatic change on terrestrial biodiversity in region make it difficult assess the region's vulnerability and how this varies across species and taxonomic groups. Such assessments are needed in order to understand what climatic change could mean for the region's unique biodiversity and to develop strategic plans for climate adaptation to ensure that the ecosystems upon which humans depend may be minimally impacted. Over the last decade, statistical methods for modeling potential changes in the geographic distributions of species and patterns of biodiversity in response to climatic change have advanced considerably (Elith *et al.* 2006; Ferrier *et al.* 2007; Elith & Leathwick 2009; Franklin 2009). These modeling advances have been supported by increases in the availability of species occurrence data (Graham *et al.* 2004) and high-resolution gridded datasets describing current and future environmental conditions for the globe (Hijmans *et al.* 2005). As such, the tools and

datasets necessary to perform a first-pass quantitative assessment of climatic change impacts on biodiversity in the Arabian Peninsula are now in place.

Objective

The overall objective of this study was to provide a comprehensive assessment of the potential vulnerability of terrestrial biodiversity in the Arabian Gulf countries to climatic change. To support this effort, we identified a set of priority species and sought occurrence records describing their distributions. In addition, we obtained data for thousands of species occurring in the region and beyond in order to consider the effects of climatic change above the level of individual priority species. In addition to these occurrence datasets, we assembled gridded data layers for both current and potential future climate conditions, including (1) 62 climate scenarios from numerous general circulation models (GCMs) and two representative concentration pathways (RCPs[2]; 4.5 and 8.5) and (2) regional climate projections for two spatial domains (also for RCPs 4.5 and 8.5) developed as part of the Regional Atmospheric Modeling sub-project. Using numerous climate simulations allowed us to project our biodiversity models to a range of possible future conditions and quantify uncertainty in projected impacts by highlighting areas where disagreement among models is high / low.

To assess vulnerability, we pursued two types of complimentary statistical modeling approaches. For the priority species, we used species distribution models (SDMs), specifically MaxEnt (Phillips *et al.* 2006), to model current climate suitability for each species with adequate occurrence data (95 total). For species with MaxEnt models exhibiting acceptable performance (75 total), we projected models to the future climate scenarios. Outputs from the MaxEnt models highlight potential changes in climate suitability for individual species, including areas where species may no longer persist and areas that may become suitable for colonization in the future. To provide a broader assessment of climatic change impacts on biodiversity beyond the level of individual priority species, we used a type of community-level model (CLM; Ferrier & Guisan 2006; D'Amen *et al.* 2015) called Generalized Dissimilarity Modeling (GDM; Ferrier *et al.* 2007) to estimate the potential magnitude of change in species composition for thousands of species of plants, birds, mammals, reptiles, and amphibians. Rather than providing species-level projections as SDMs do, GDM translates sets of variables from future climate scenarios into a single measure of the significance of future climatic change for biodiversity based on how it is distributed at

[2] RCPs are greenhouse gas concentration trajectories adopted by the Intergovernmental Panel on Climatic change (IPCC) for the fifth Assessment Report (AR5). They describe possible climate futures, all of which are considered possible depending on how much greenhouse gases are emitted in the future. The four RCPs (2.6, 4.5, 6.0, and 8.5) are named after a possible range of radiative forcing values in the year 2100 relative to pre-industrial values (+2.6, +4.5, +6.0, and +8.5 W/m^2, respectively). RCP's 4.5 and 8.5 were used in this study.

present. The resulting maps from both methods can be used to identify species and regions most vulnerable to climatic change.

After providing a general methodological overview and specifics regarding the two modeling approaches, we discuss the technical results and their interpretation in light of uncertainties inherent in the modeling process. We conclude with a discussion of the findings and data challenges.

Conceptual framework

The fundamental concept underlying the vulnerability assessment is that climate-driven changes in habitat suitability will place species at risk by reducing the area that can support populations and/or by forcing individuals to shift their geographic ranges to track suitable climate regimes. These changes in the distributions of individuals will lead to the disassembly of existing communities and the formation of new ones, which in turn will alter ecosystem structure and function. These biogeographical changes represent just a handful of expected ecological consequences of climatic change. However, for the vast majority of species there is little information available to develop quantitative predictions regarding all possible types and magnitude of changes expected. As a result, many vulnerability assessments rely on regional-scale estimates of changes in habitat suitability derived from SDMs. SDMs require information only on species occurrence and climate. For this reason, they represent an ideal framework to provide a pragmatic first-cut assessment of climatic change risks to species. including spatially explicit outputs that can inform regional adaptation strategies and guide further research.

Despite their strengths, projections from SDMs are subject to a wide range of uncertainties and assumptions (Hampe 2004; Heikkinen *et al.* 2006; Dormann 2007) and understanding these uncertainties is critical for correctly interpreting and potentially implementing SDM-based vulnerability assessments. Perhaps less well appreciated is that SDMs also are constrained for statistical reasons to modeling only those species that have been adequately sampled. Adequately sampled typically means a *minimum* of 20 spatially unique points per species spread at random (i.e., no spatial sampling bias) across the full range of environments in which the species can occur. These data constraints are rarely met, which makes developing robust SDMs for all but the best-studied species in the most densely sampled regions difficult. During this study, data challenges were found are especially pronounced in the Arabian Gulf countries. For these reasons, SDMs alone may provide a limited or even biased perspective on potential climatic change impacts in the region.

To overcome some of the shortcomings and challenges of SDMs and to provide a more comprehensive and robust perspective on potential climatic change impacts to terrestrial biodiversity, our modeling framework supplements SDM-based analyses with community-level modeling. We have discussed CLMs in other documents and we provide further details below

regarding this second modeling strategy. In brief, CLMs of the type used in this study can make use of very sparse biological data and provide a means to assess vulnerability of biodiversity to climatic change when species-level assessments are not possible. Figure 1 summarizes the basic modeling framework.

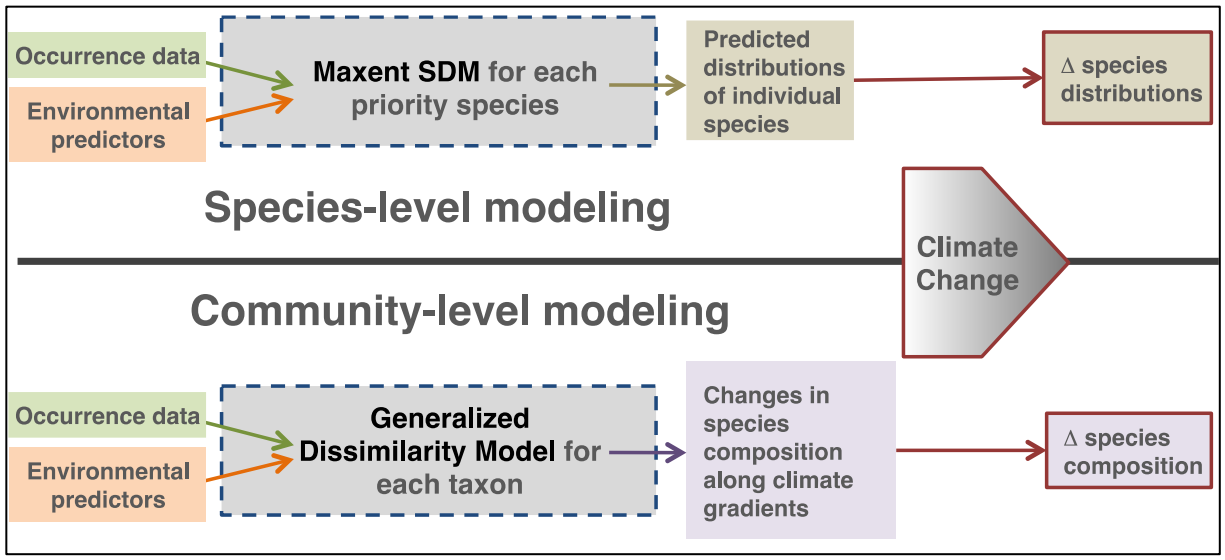

Figure 1 - The two complimentary modeling strategies used for assessing the vulnerability of terrestrial biodiversity to climatic change in this study.

Methodological background

Species distribution modeling

SDMs also known as bioclimatic, ecological niche, or habitat suitability models, are static, correlative models that combine georeferenced observations of species occurrence with environmental data to explain and predict species distributions across a region of interest (Guisan & Zimmermann 2000; Guisan & Thuiller 2005; Elith & Leathwick 2009; Franklin 2009). Once developed from current observations, SDMs can be "projected" in time to scenarios of future climate to estimate how the spatial arrangement of suitable habitat may change for species individually (Fig. 2), including areas where populations may no longer be able to persist given their current environmental tolerances and new areas where populations may establish should individuals be able to reach them via dispersal. The primary output from SDMs are mapped predictions in the form of digital maps indicating a continuous measure (0-1) of the spatial distribution of habitat suitability, or a binary (1/0) prediction of species presence or absence, depending on the data and algorithm used and the goals of the study. Such mapped projections

from individual SDMs provide a broad scale estimate of the vulnerability of different species to changes in climate suitability (Dawson *et al.* 2011).

Numerous statistical approaches exist for fitting SDMs, from regression-based methods such as Generalized Additive Models (Thuiller *et al.* 2003) to more advanced machine learning techniques such as artificial neural networks (Pearson *et al.* 2002). For this study, SDMs were developed using MaxEnt (Phillips *et al.* 2006), widely considered one of the more robust SDM methods (Elith *et al.* 2006, 2011), especially for small sample sizes (Pearson *et al.* 2006a). MaxEnt is an implementation of a statistical approach called maximum entropy that characterizes probability distributions from incomplete information (Phillips *et al.* 2006). In the context of modeling distributions of species using maximum entropy, the assumptions are that (1) occurrence data represent an incomplete sample of an empirical probability distribution, that (2) this unknown distribution can be most appropriately estimated as the distribution with maximum entropy (i.e. the probability distribution that is most uniform) subject to constraints imposed by environmental variables, and that (3) this distribution of maximum entropy approximates the potential geographic distribution of the species.

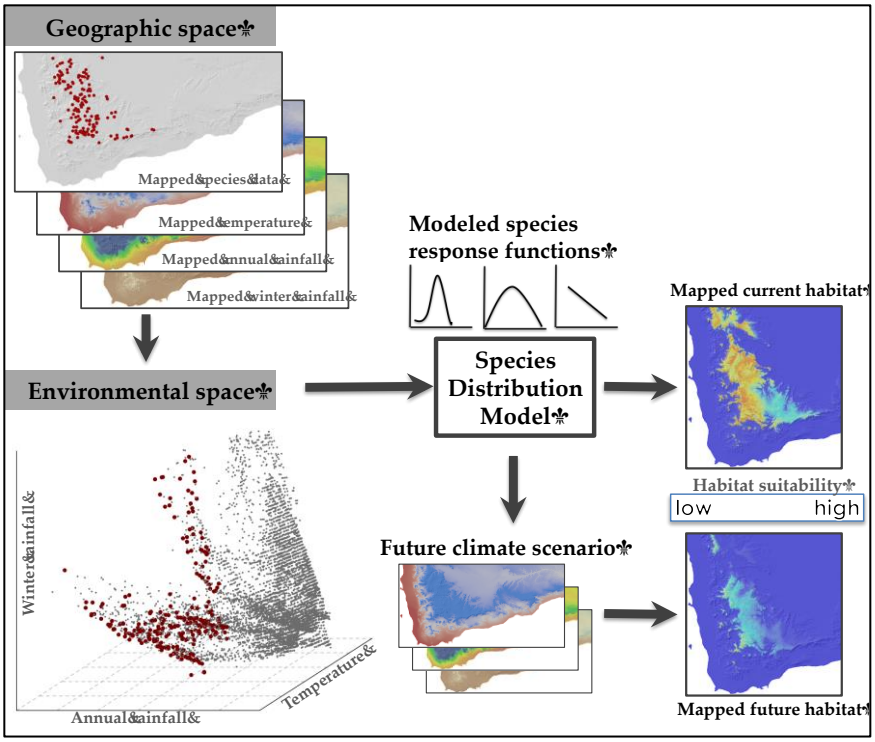

Figure 2 - Graphical representation of the species distribution modeling process, including inputs in both geographic and environmental space, modeled response curves describing species-climate relationships, and resulting output maps of habitat suitability under current and future conditions.

Community-level modeling

Rather than modeling individual species distributions, CLMs 'assemble and predict together' all species within a single integrated process to analyze and map geographic patterns of biodiversity at a collective community level instead of, or in addition to, the level of individual species (Ferrier & Guisan 2006; D'Amen *et al.* 2015). As is the case for SDMs, there are several varieties of CLM algorithms. To model changes in overall patterns of biodiversity in this study, we used Generalized Dissimilarity Modeling (GDM; Ferrier *et al.* 2007). GDM is a nonlinear matrix regression technique for analyzing spatial patterns in species composition between pairs of locations using distance matrices – specifically by relating dissimilarity in species composition (biological distance, the response variable) between all site pairs to a set of predictor variables describing how much sites differ in their environmental conditions (environmental distance) and how isolated they are from one another (geographical distance). GDM has been used in several studies to estimate climatic change vulnerability (Ferrier *et al.* 2010; Fitzpatrick *et al.* 2011, 2013; Dunlop *et al.* 2012) and a major benefit is its ability to make use of sparse biological data. As such, GDM provides a means to assess vulnerability of biodiversity to climatic change when species-level assessments are limited by data availability. We provide technical details regarding GDM in Annex I.

Our aim with GDM was to convert (or, more appropriately, *scale*) future climate scenarios into a single measure reflecting the potential vulnerability of biodiversity based on how it is currently distributed across the study region. Appropriately scaling between climate and biodiversity is complex because both are multidimensional and species will respond in complex ways to climatic change. To accomplish this scaling, GDM is first fit to current biodiversity patterns to determine how species composition changes along existing spatial climate gradients (e.g., temperature, precipitation, etc.). The fitted model can then be used to estimate the potential change in species composition expected at any location by comparing the current environment at a location with future climate for that location. Thus, GDM estimates vulnerability for a given location in terms of the predicted dissimilarity in present-day species composition expected between two locations whose current climates differ by the same magnitude as the projected change in climate at the location of interest (Ferrier *et al.* 2010). It is important to note that GDM models compositional turnover as a single number ranging from 0 (no change in species composition) to 1 (complete change in species composition), and therefore it predicts only the expected magnitude of change in composition, *not the identity of species contributing to change in composition*.

Ensemble forecasting

To deal with methodological and theoretical uncertainties, it is now widely advocated that climatic change vulnerability assessments consider multiple model algorithms and many scenarios of future climatic change (Pearson *et al.* 2006b; Araujo & New 2007; Thuiller *et al.* 2009). Given species data constraints, we were limited in the number of different SDM and CLM algorithms we could use. However, we projected each of our models to a large number of future climate scenarios and these projections were combined by taking the mean of all MaxEnt or GDM projections to produce a single ensemble forecast of expected vulnerability. The general approach used for MaxEnt models is shown in Figure 3. We performed the same procedure for GDM, with the important difference that the projections from GDM represent the magnitude of expected change in species composition rather than changes in climate suitability. Otherwise the process for GDM was the same as for MaxEnt. We produced ensemble forecasts using all global climate scenarios together as well as for the two RCPs individually and for all regional climate model scenarios. This ensemble approach (1) identifies where models agree in terms of projected changes in climate suitability (or change in species composition in the case of GDM) and (2) the spatial distribution and magnitude of uncertainty in these projections.

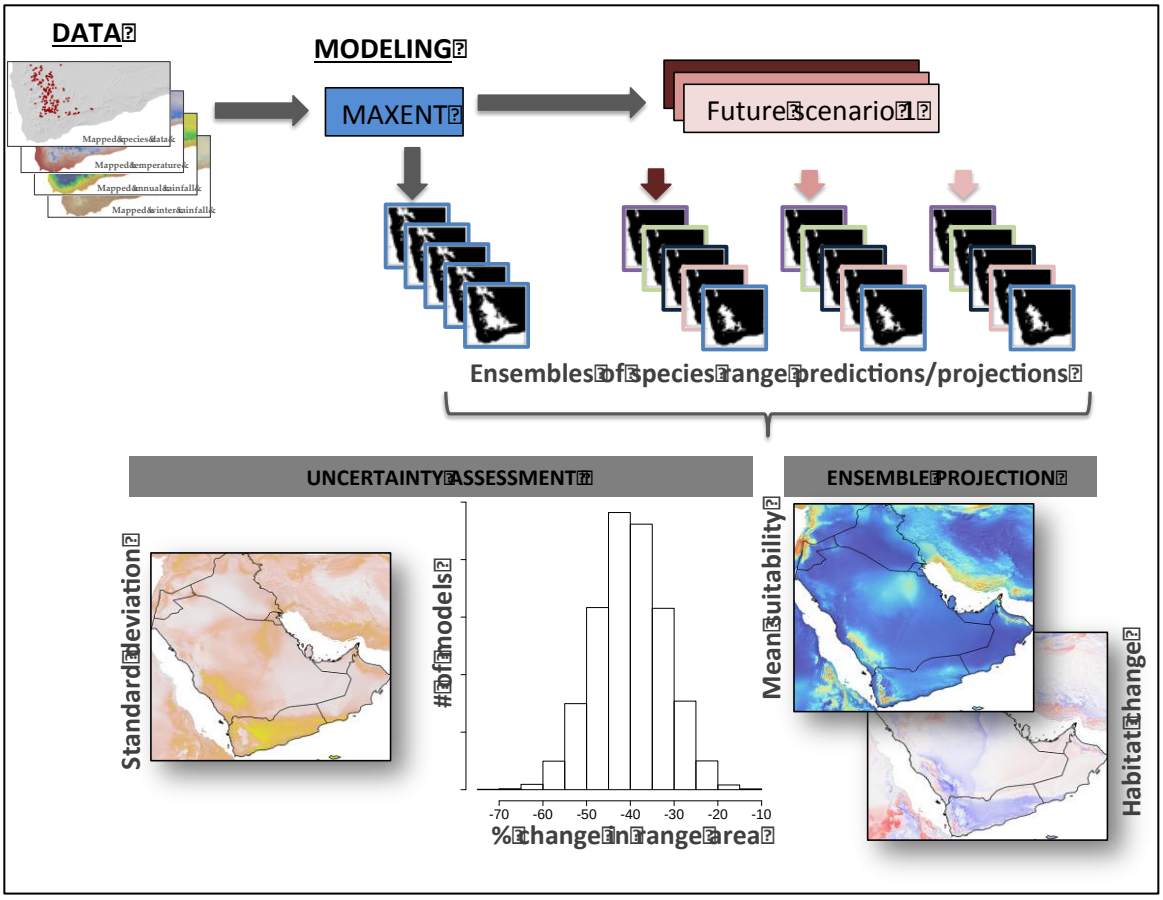

Figure 3 - Modeling framework using ensemble forecasting. The framework in the figure demonstrates the approach using MaxEnt. The same method also was used for GDM, though the ensemble projections are for the magnitude of change in species composition rather than species-level suitability.

Technical methods

In this section, we provide an overview of the technical methods used in this project. Greater details and specifics regarding the occurrence datasets and statistical modeling can be found in Annex I.

Study area

Figure 4 shows the study area as defined for this project. To identify the spatial extent of the model fitting regions, we considered geopolitical boundaries, ecological principles, and data availability. From a modeling perspective, there are two main considerations. First, to ensure that the SDMs capture the full range of environmental conditions the study species can tolerate, all available occurrence data should be used (i.e., occurrence data should not be "clipped" to only those records falling within the study countries). Because species distributions rarely coincide with political boundaries, the study region extends beyond the Arab Gulf countries to include adjacent regions with occurrence data for the priority species. We further enlarged the modeling region to capture complete gradients of environmental space that the study species could reasonably encounter, including consideration of dispersal ability and major biogeographical barriers or transitions (Fitzpatrick & Hargrove 2009). Delineating such areas is often subjective due to data constraints, but we estimated them by considering: (1) species range polygons when available and (2) boundaries of ecoregions or biomes to which the study species are endemic and which represent biologically-relevant ecological and environmental transitions. To delineate the area for fitting GDMs, we used the World Wildlife Fund's (WWF) terrestrial ecoregions (Olson *et al.* 2001). We used these ecoregions to identify dryland ecosystems within and outside of the Arabian Peninsula that contain broadly similar environmental conditions as those found within the study area (green shading, Fig. 4).

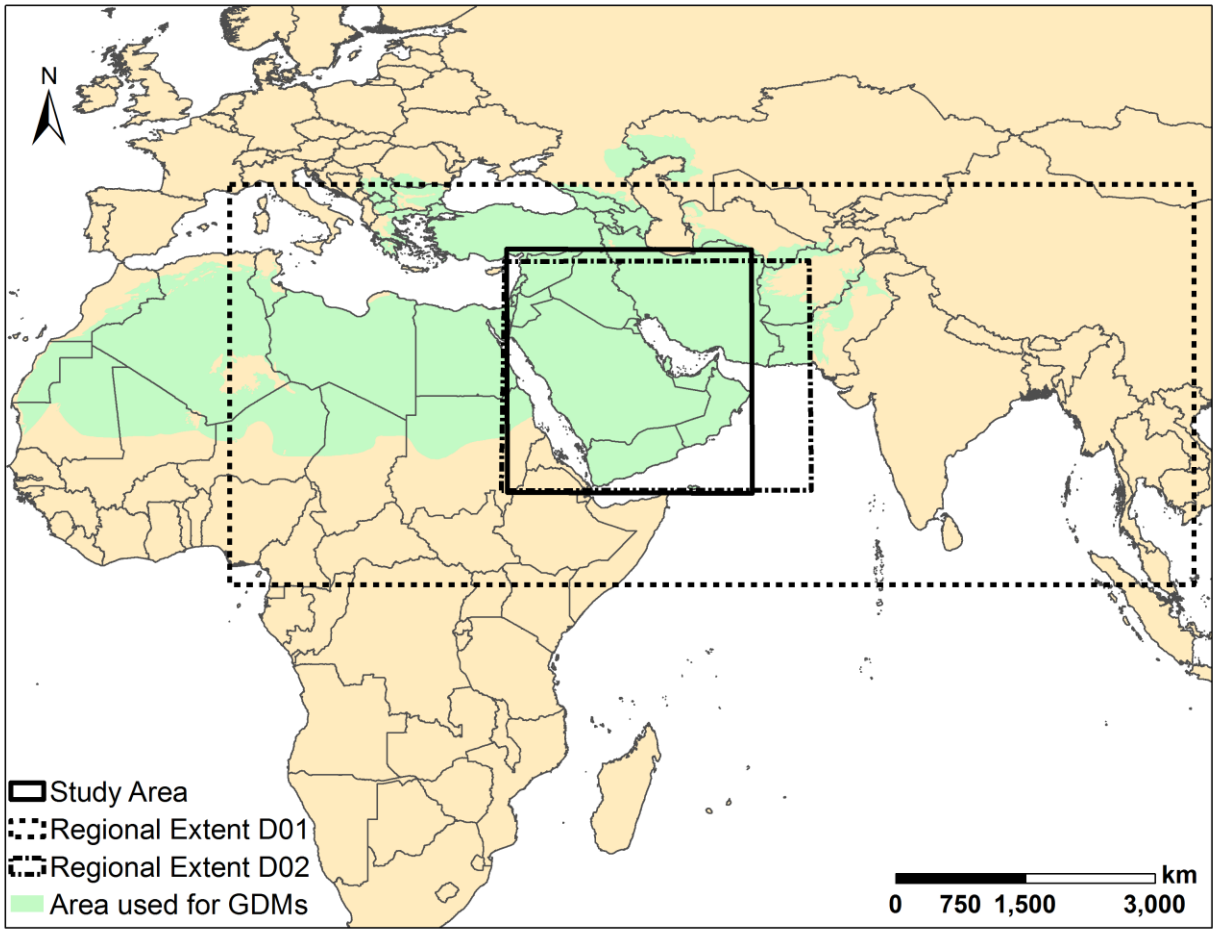

Figure 4 - Map of study region (black rectangle) and general extent of areas used to fit most SDMs (tan) and GDMs (green). Note that occurrence records for some species extend beyond the region shown in this map. The dashed rectangles delineate the extents of the domains for the regional atmospheric modeling.

Model inputs

Species occurrence data

The first step in obtaining the species occurrence data was developing a list of species for which to seek records. We used different approaches to assemble lists of priority species as candidates for SDMs and a more comprehensive list of species for GDM. To identify candidate priority species for modeling, we used a "bottom-up" approach whereby we first reviewed existing literature and published assessments of species of concern in the region and then sought occurrence records for these species (Table 1).

To assemble a more comprehensive list of terrestrial vertebrates (mammals, birds, reptiles, and amphibians) known to occur within the study region, we used species listed as present within any of the WWF terrestrial ecoregions that overlapped countries within the study region. Besides delineating areas with unique climate, geology, and evolutionary history, the WWF ecoregions include a list of all vertebrate species known to occur in each ecoregion. Because the WWF ecoregions do not identify plant species, we used a "top-down" approach to assemble a candidate list of terrestrial plant species in the study region. Instead of first developing a species list, and seeking occurrence records for those species, we simply downloaded all known occurrence records for plants within the Arabian Gulf countries from the Global Biodiversity Information Facility (GBIF). Any plant species with occurrences in the study region were placed on a master list based on these records. This master list was then checked against known taxonomy and records were update and/or removed to match current nomenclature. To the extent possible, we scrutinized these data to generate a final regional species list for plants.

With assistance from colleagues at GBIF[3], we obtained all available occurrence records globally for our species lists, resulting in nearly 100 million records total (including duplicates, records without spatial reference information, etc). We performed numerous quality control measures on these records (see Annex I) to prepare them for modeling.

[3] The dataset obtained through consultations with the GBIF Secretariat was a customized Global data export accessed on 21 May 2015 (GBIF, 2015)

AGEDI
مبادرة أبوظبي العالمية للبيانات البيئية
Abu Dhabi Global Environmental Data Initiative

Table 1 - Summary of priority species considered for vulnerability assessment using MaxEnt. The number of global records is the total number of spatially unique records obtained from GBIF and regional partners. The number of records usable for SDMs is the total number of spatially unique records at 10 arc-minute resolution remaining after quality control (Annex I). Species for which MaxEnt models could not be fit (>= 10 usable records) have "NA" in the Boyce Index column. Only models with a (i) Boyce Index >>0 and (ii) which were found to be adequate performance based on expert opinion were projected to future climate scenarios (Future Projections = YES).

Species	Common Name(s)	Taxon	Global Records	Records Usable for SDMs	Boyce Index	Future Projections
Bufo arabicus	Arabian Toad	Amphibian	26	18	0.7852	YES
Bufo dhufarensis	Dhofar Toad	Amphibian	19	15	0.5602	YES
Hyla savignyi	Lemon-yellow Tree Frog	Amphibian	110	57	0.9351	YES
Bufo tihamicus	NA	Amphibian	10	7	NA	NO
Euphlyctis ehrenbergii	NA	Amphibian	9	9	NA	NO
Chlamydotis macqueenii	Houbara Bustard	Bird (breeding)	56	31	0.9111	YES
Egretta gularis	Western Reef Heron	Bird (breeding)	448	150	0.9612	YES
Coracias garrulus	European Roller	Bird (breeding)	2386	497	0.9841	NO
Gyps fulvus	Griffon Vulture, Eurasian Griffon	Bird (breeding)	1538	318	0.9765	NO
Marmaronetta angustirostris	Marbled Teal	Bird (breeding)	144	50	0.8583	NO
Neophron percnopterus	Egyptian Vulture	Bird (breeding)	1450	429	0.9939	NO
Aquila clanga	Greater Spotted Eagle	Bird (nonbreeding)	591	53	0.9078	YES
Calidris tenuirostris	Great Knot	Bird (nonbreeding)	745	248	0.9746	YES
Chlamydotis macqueenii	Houbara Bustard	Bird (nonbreeding)	56	23	0.6424	YES
Egretta gularis	Western Reef Heron	Bird (nonbreeding)	448	176	0.9592	YES
Marmaronetta angustirostris	Marbled Teal	Bird (nonbreeding)	144	47	0.9102	YES
Neophron percnopterus	Egyptian Vulture	Bird (nonbreeding)	1450	200	0.9829	YES
Vanellus gregarius	Sociable Lapwing	Bird (nonbreeding)	118	27	0.9206	YES
Aquila chrysaetos	Golden Eagle	Bird (nonbreeding)	14931	767	0.991	NO
Coracias garrulus	European Roller	Bird (nonbreeding)	2386	308	0.9886	NO
Falco cherrug	Saker Falcon	Bird (nonbreeding)	312	104	0.8973	NO
Gyps fulvus	Griffon Vulture, Eurasian Griffon	Bird (nonbreeding)	1538	363	0.9713	NO
Alectoris melanocephala	Arabian Partridge	Bird (resident)	21	12	0.8691	YES

Climate Change Research Group

University of Maryland
CENTER FOR ENVIRONMENTAL SCIENCE

Ammoperdix heyi	Sand Patridge	Bird (resident)	121	39	0.9443	YES
Corvus ruficollis	Brown-necked Raven	Bird (resident)	460	229	0.9806	YES
Emberiza cineracea	Cinereous Bunting	Bird (resident)	65	37	0.8975	YES
Phalacrocorax nigrogularis	Socotra Cormorant	Bird (resident)	134	36	0.7955	YES
Puffinus persicus	Persian Shearwater	Bird (resident)	32	11	0.7674	YES
Serinus rothschildi	Olive-rumped Serin, Arabian Canary	Bird (resident)	16	10	0.7217	YES
Sylvia leucomelaena	Arabian Warbler, Red Sea Warbler	Bird (resident)	54	32	0.8813	YES
Turdoides squamiceps	Arabian Babbler	Bird (resident)	159	59	0.9415	YES
Estrilda rufibarba	Arabian Waxbill	Bird (resident)	9	9	NA	NO
Passer euchlorus	Arabian Golden Sparrow	Bird (resident)	14	8	NA	NO
Serinus menachensis	Yemen Serin	Bird (resident)	11	7	NA	NO
Sylvia buryi	Yemen Warbler	Bird (resident)	8	8	NA	NO
Turdus menachensis	Yemen Thrush	Bird (resident)	9	9	NA	NO
Asellia tridens	Trident Leaf-nosed Bat	Mammal	52	34	0.7973	YES
Canis aureus	Common Jackal	Mammal	173	83	0.924	YES
Capra ibex nubiana	Nubian Ibex	Mammal	32	89	0.9133	YES
Caracal caracal	Caracal	Mammal	101	35	0.8521	YES
Eidolon helvum	Straw-colored Fruit Bat	Mammal	220	146	0.9876	YES
Felis margarita	Sand Cat	Mammal	22	15	0.4557	YES
Gazella gazella	Mountain Gazelle	Mammal	126	129	0.9793	YES
Gazella subgutturosa	Goitered Gazelle	Mammal	55	30	0.8102	YES
Gerbillus cheesmani	Cheesman's Gerbil	Mammal	51	24	0.6564	YES
Gerbillus nanus	Dwarf Gerbil, Baluchistan Gerbil	Mammal	99	67	0.9473	YES
Hipposideros caffer	Lesser Leaf-nosed Bat	Mammal	213	153	0.953	YES
Hyaena hyaena	Hyaena	Mammal	191	57	0.6733	YES
Hystrix indica	Indian Crested Porcupine	Mammal	126	36	0.8817	YES
Jaculus jaculus	Lesser Egyptian Jerboa	Mammal	257	150	0.9544	YES
Lepus capensis	Cape Hare, Arabian Hare	Mammal	2542	240	0.966	YES

Meriones crassus	Sundevall's Jird	Mammal	164	99	0.8943	YES
Meriones libycus	Libyan Jird	Mammal	172	116	0.9674	YES
Panthera pardus	Leopard	Mammal	453	171	0.9646	YES
Procavia capensis	Rock Hyrax, Rock Dassie	Mammal	215	122	0.9547	YES
Psammomys obesus	Fat Sand Rat	Mammal	115	51	0.9311	YES
Rhinolophus blasii	Horseshoe Bat	Mammal	55	34	0.8378	YES
Sekeetamys calurus	Bushy-tailed Jird	Mammal	31	15	0.8564	YES
Allactaga euphratica	Euphrates Jerboa	Mammal	34	18	0.9147	NO
Felis silvestris	WildCat	Mammal	2448	353	0.9813	NO
Gerbillus famulus	Black-tufted Gerbil	Mammal	6	6	NA	NO
Mellivora capensis	Honey Badger	Mammal	90	65	0.9509	NO
Oryx leucoryx	Arabian Oryx	Mammal	21	9	NA	NO
Vulpes cana	Blanford's Fox	Mammal	19	9	NA	NO
Vulpes rueppellii	Ruppell's Fox	Mammal	3	3	NA	NO
Acacia tortilis	Umbrella Thorn	Plant	120	72	0.9491	YES
Arthrocnemum macrostachyum	Glaucous Glasswort, Soap Soda	Plant	279	73	0.9086	YES
Atriplex leucoclada	Orache, Raghal	Plant	102	34	0.8656	YES
Avicennia marina	Grey Mangrove	Plant	520	242	0.9767	YES
Calligonum comosum	Arta`, A`bal , Waragat Alshams	Plant	51	25	0.8519	YES
Cleome amblyocarpa	Spider Flower, Adheer	Plant	60	23	0.7262	YES
Cyperus conglomeratus	Thenda, Dune Grass, Sedge	Plant	148	61	0.9045	YES
Delonix elata	Gul Mohur, Creamy Peacock Flower	Plant	33	26	0.8883	YES
Dodonaea viscosa	Hopbush, Candlewood	Plant	86	55	0.8694	YES
Eremobium aegyptiacum	Eremobium aegyptium, sleisla	Plant	42	19	0.9348	YES
Halopyrum mucronatum	NA	Plant	19	14	0.8781	YES
Haloxylon salicornicum	Saxaul	Plant	107	26	0.873	YES
Heliotropium digynum	Kary, Jery	Plant	31	14	0.7344	YES
Juniperus procera	African Juniper	Plant	100	59	0.9307	YES

Limeum arabicum	Berjan	Plant	19	12	0.6282	YES
Moringa peregrina	Wispy-needled yasar tree	Plant	21	12	0.8628	YES
Panicum turgidum	desert grass	Plant	168	84	0.9437	YES
Prosopis cineraria	Ghaf	Plant	37	16	0.9001	YES
Rhazya stricta	Senhwar, Sahaer, Dogbane, Harmal	Plant	44	28	0.8646	YES
Ziziphus spina-christi	Christ's Thorn Jujube	Plant	148	60	0.8638	YES
Convolvulus deserti	Field bindweed	Plant	3	3	NA	NO
Cornulaca monacantha	Had, Djouri, Tahara	Plant	30	16	0.6214	NO
Crotalaria persica	Rattlepod, Rattlebox	Plant	18	13	0.608	NO
Heliotropium kotschyi	Ramram	Plant	23	15	0.7931	NO
Indigofera argentea	NA	Plant	8	8	NA	NO
Salsola imbricata	NA	Plant	59	25	0.8754	NO
Salvadora persica	Toothbrush Tree	Plant	232	147	0.9476	NO
Silene villosa	Desert Campion, terba, turbah	Plant	36	13	0.6671	NO
Sphaerocoma aucheri	NA	Plant	7	7	NA	NO
Stipagrostis plumosa	Desert Grass	Plant	126	57	0.9315	NO
Suaeda vermiculata	Seablite, suwaid	Plant	71	24	0.6108	NO
Tribulus omanense	Puncture Vie	Plant	21	10	0.446	NO
Zygophyllum qatarense	Bean Caper, Qatari	Plant	62	9	NA	NO
Bunopus tuberculatus	Baluch Ground Gecko	Reptile	227	99	0.9501	YES
Cerastes cerastes	Horned Viper	Reptile	45	34	0.8983	YES
Chamaeleo chamaeleon	Mediterranean Chameleon	Reptile	189	58	0.9253	YES
Cyrtopodion scabrum	Rough-tailed Gecko	Reptile	103	62	0.8994	YES
Echis carinatus	Saw Scaled Viper, Carpet Viper	Reptile	71	30	0.8199	YES
Echis coloratus	Palestine Saw-scaled Viper	Reptile	72	35	0.9137	YES
Eryx jayakari	Arabian Sand Boa	Reptile	51	23	0.4368	YES
Hemidactylus persicus	Persian Leaf-toed Gecko	Reptile	63	36	0.8137	YES
Pristurus carteri	Carter's Rock Gecko	Reptile	19	12	0.5931	YES

Pristurus flavipunctatus	Middle Eastern Rock Gecko	Reptile	17	16	0.8089	YES
Pristurus rupestris	Dwarf Rock Gecko	Reptile	62	32	0.9168	YES
Stenodactylus doriae	Middle Eastern Short-fingered Gecko	Reptile	71	35	0.7434	YES
Pristurus minimus	Arnold's Rock Gecko	Reptile	12	8	NA	NO

Climate data

In addition to species occurrence data, our models require information on current climatic conditions (for model fitting) and scenarios of future climate (for forecasting changes in habitat suitability and species composition). In order to account for a range of potential future conditions, we assembled a large number of future climate simulations, including output from (1) a set of climate models run at global extent and debiased and downscaled and (2) output from regional climate model simulations developed as part of the Regional Atmospheric Modeling sub-project. For both current and future climate we used the same set of 19 standard bioclimatic variables (Table 2, Annex II) commonly used to model biodiversity and which quantify annual, seasonal, and monthly means, minima, maxima, and variation of temperature (**°**C) and precipitation (mm). To describe current climatology, we used the WorldClim (http://www.worldclim.org/) dataset at 10 arc-minute resolution. Worldclim is a database of globally-contiguous gridded representations of climate developed from interpolations of observed data for the period 1950-2000 (Hijmans *et al.* 2005). For future climate, we used a set of 62 future climate simulations (Table 3, Annex III) at 2.5 arc-minute spatial resolution and global extent for decades 2030, 2050, 2070, and 2080. These simulations were developed as part of the IPCC AR5 and represent different combinations of GCMs and RCPs and were obtained from the Research Program on Climatic change, Agriculture and Food Security (http://www.ccafs-climate.org). Details regarding the regional climate model simulations developed as part of the Regional Atmospheric Modeling sub-project can be found in another report. For this project, we used simulations run at two spatial domains (D01 at 36 km resolution and D02 at 12 km resolution; Fig. 4.) for RCP4.5 and 8.5 and for decade 2070.

Statistical modeling

MaxEnt modeling of priority species

To avoid potential problems relating to small sample sizes, we developed MaxEnt models only for priority species that had at least 10 spatially unique distribution records. We removed correlated predictor variables for each species separately, so not all species were modeled with the same set of climate variables. Lastly, we used published methods to (1) control model complexity and reduce overfitting (Warren & Seifert 2011) and (2) to account for sampling bias (Phillips *et al.* 2009). We evaluated the ability of models to discriminate known presences from background data using the continuous Boyce Index (Hirzel *et al.* 2006). The Boyce Index ranges from -1 to 1 such that values below 0 indicate an incorrect model, values close to zero indicate a model no different from random, and positive values indicate a model that is predicting better than random.

We projected MaxEnt models for priority species to future climate scenarios if they met two conditions: (1) a Boyce Index >>0 and (2) predicted habitat suitability under current climate was broadly congruent with the known distribution (based on literature searches and / or expert opinion). When these conditions were met, we projected the models to all future climate scenarios (global, regional, both RCPs, all decades). From these projections for each species, we calculated the mean and standard deviation of predicted climate suitability and the change in climate suitability (future - current) between current and each future climate scenario. In addition, we also plotted histograms and the projected change in range area for each model to provide a sense of model variability and agreement in the context of potential losses / gains in range size. Lastly, we calculated similar metrics for (1) all species collectively and (2) each taxon collectively to estimate mean projected change in priority species richness and associated uncertainty. See Annex I for further details.

Generalized Dissimilarity Modeling of regional biodiversity

To assess climatic change vulnerability to terrestrial biodiversity beyond the priority species, we used GDM to relate compositional dissimilarity between locations to their current environmental and geographic separation. Next, we used these models to predict how species composition would be expected to change in time given the amount of environmental separation between current and future climate at each location using each of the future climate scenarios (Fitzpatrick *et al.* 2011; Dunlop *et al.* 2012; Blois *et al.* 2013). The implicit assumption when GDM is used in this context is that the amount of compositional change modeled between two locations as a function of current environmental separation in *space* can be used to approximate how much a single location will differ in composition given an amount of environmental change in *time*. Recent studies have found support for the validity of this assumption (Blois *et al.* 2013).

GDMs were fit by analyzing the dissimilarity in species composition (quantified with the Sørensen index) between pairs of locations across the study region as a function of differences in climate and geographic separation between each location, where locations are the 10 arc-minute current climate grid cells. The Sørensen index ranges between 0 (when two locations have exactly the same species) and 1 (when two locations have no species in common). We adjusted for issues related to the use of presence-only data and associated sampling bias using multiple model weighting methods as described in Annex I. For climate predictor variables, we selected a subset of five uncorrelated bioclimatic variables from the full set of 19 (Annex II), including annual mean temperature (bio1), temperature seasonality (bio4), mean temperature of the warmest month (bio5), annual precipitation (bio12), and precipitation of the warmest quarter (bio18). In addition to climate predictors, we included geographical coordinates of cell centroids to calculate Euclidean distance between sites as an additional predictor variable. We applied this approach to taxonomic groups separately (i.e., plants, mammals, birds, amphibians, reptiles). We mapped current biodiversity patterns for each taxon and, as for the MaxEnt models, we calculated the

mean and standard deviation of projected changes in species composition from GDM. See Annex I for details.

Results

Species occurrence data

All told, we obtained approximately 100 million occurrence records *globally* from GBIF. We supplemented these records with data from regional partners. After removing duplicate records and performing other quality control procedures (Annex I), approximately 30 million records for more than 6,000 species remained. After further processing, we retained nearly 8,000 occurrence records for over 100 priority species for MaxEnt modeling and more than 150,000 occurrence records for approximately 4,600 additional species for GDM. Summaries of the occurrence data used for MaxEnt and GDM can be found in Tables 1 and 2 respectively. Figure 5 shows the spatial distribution and density of occurrence records for priority species across the study region. A summary of each priority species, including physical description, distribution, habitat, conservation status, and a map of occurrence data used in model fitting can be found in Annex IV.

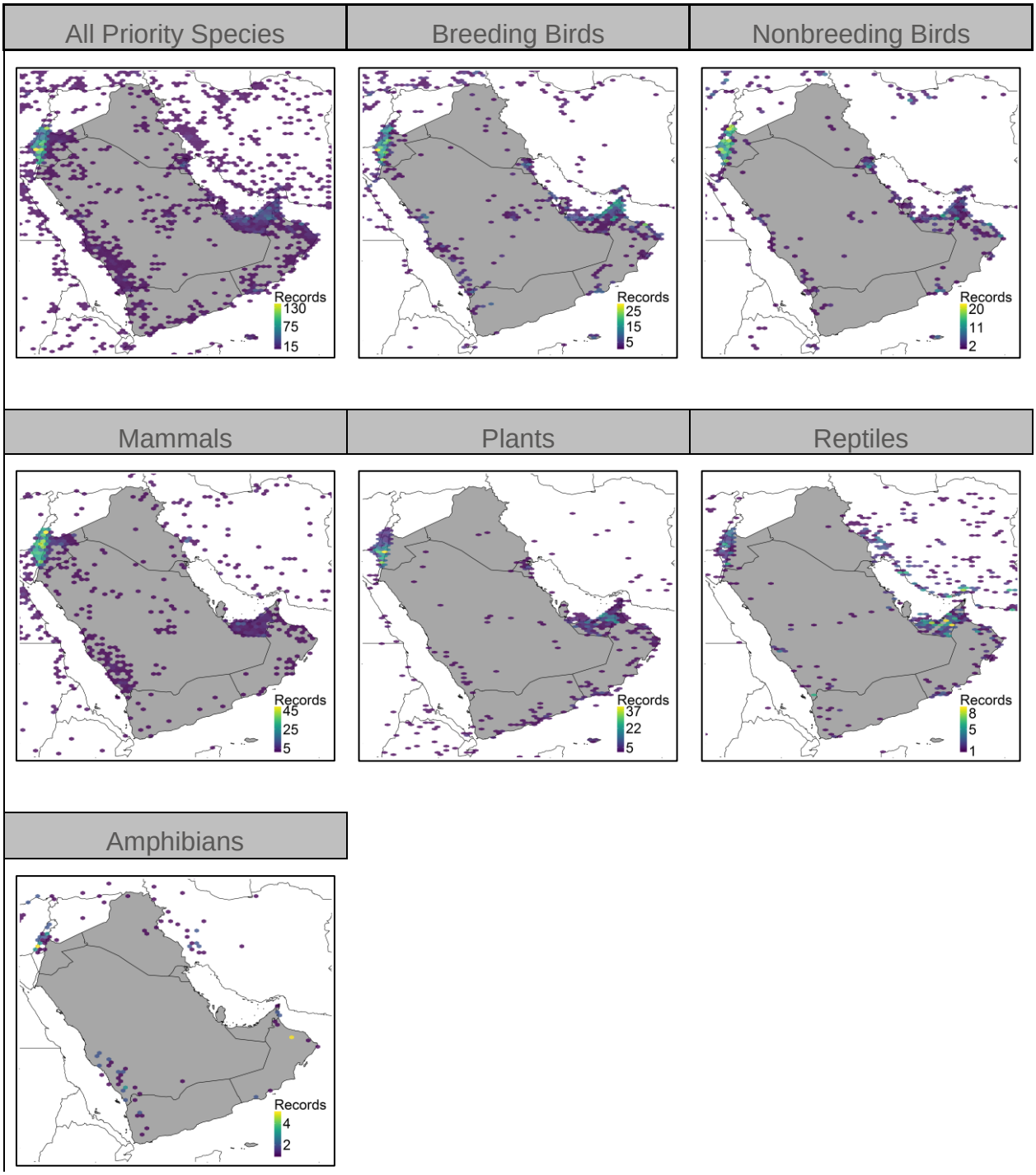

Figure 5- Spatial distribution and density of available occurrence records for priority species.

Predictions of current habitat suitability for priority species

When combined across all priority species, areas of greatest habitat suitability were concentrated in the southern half the study region and along coasts (Fig. 7, top left panel). Predicted patterns of current habitat suitability showed notable differences between taxa (Fig. 8, first row of panels). For example, for nonbreeding birds, high habitat suitability was concentrated mainly along coastlines. For amphibians, habitat suitability was highest mainly in mountainous regions near the southwestern and southeastern coasts, and in particular in the Al Hajar, Hadhramaut, and Asir Mountain ranges. Mammals and breeding birds followed similar patterns to amphibians, but high habitat suitability for these groups being somewhat less restricted to mountainous regions. The highest habitat suitability for plants was restricted mainly to areas along coasts and the southeastern third of the study region.

Projections of changes in habitat suitability for priority species

Based on Boyce Indices and thorough qualitative evaluation of the MaxEnt models, we projected models for 75 of the 95 modeled priority species, including 3 amphibians, 18 birds, 22 mammals, 20 plants, and 12 reptiles (Table 1), to all future global and regional climate scenarios. Annexes V-IX present, for each priority species, (1) occurrence data used to fit models, (2) current habitat suitability, (3) future habitat suitability for decades 2030 and 2070 (global and regional climate scenarios), (4) changes in habitat suitability between current and future climate for decades 2030 and 2070 (global and regional climate scenarios), (5) climate-scenario based uncertainty (global scenarios only as there were not enough regional scenarios to derive uncertainty estimates), and (6) a histogram showing the distribution of projected changes in range area across the 62 global climate scenarios. Projections of future habitat provided in Annexes V-IX represent a ensemble across all global or regional scenarios. Model results for addition times (2050, 2080), individual RCPs (4.5 and 8.5), etc. are provided as an electronic resource at http://www.ccr-group.org/terrestrial/ . Here we report ensemble results across all priority species collectively and each taxon individually.

Projections to Global Scenarios – all priority species combined

When considered collectively by summing changes in habitat suitability across all priority species and global climate scenarios, large areas of the Arab Gulf countries were projected to either lose or gain suitable climate habitat for priority species (Fig. 7; first column of panels). The spatial pattern of losses and gains of suitable habitat remained largely constant through time, though the *magnitude* of projected habitat changes in each location tended to increase from 2030 and 2070 (see electronic resource for other time periods). That said, reductions in habitat suitability (Fig. 7; red shading) tended to become more widespread through time than gains and were concentrated along western and southeastern Saudi Arabia and throughout Yemen, Oman, Qatar, the UAE, and Jordan. Potential increases in habitat suitability for priority species (Fig. 7;

blue shading) were projected for most of Iraq, north central Saudi Arabia, extreme western portions of Oman, and the Al Hajar Mountains. The greatest magnitude of climate-scenario based uncertainty in model projections occurred in the southwestern corner of the study region (Fig. 7; second column of panels), suggesting projections of habitat change differed most across species and climate scenarios in this region.

Projections to Global Scenarios – taxon-level

As for the all-species results, the most pronounced difference in projected change in habitat suitability between 2030 and 2070 was an increase in the magnitude of projected change (either increases or decreases in habitat suitability) rather than changes in the spatial pattern of change per se (Fig.8; compare second and third row of panels). Breeding birds, mammals, and amphibians were projected to have the most extensive reductions in suitable habitat, which covered nearly all of the study region for these taxa. In contrast, nonbreeding birds, plants, and reptiles were projected to gain suitable habitat across much of the study region, with the exception of coastal regions of extreme southwestern Saudi Arabia and western Yemen. Plants and reptiles were projected to lose suitable habitat across the UAE and easternmost Oman, with the exception of the Al Hajar mountains, where these taxa were projected to gain suitable habitat.

Projections to Regional Scenarios– all priority species combined

When combined across all priority species, model projections based on the regional future climate scenarios (Fig. 7; bottom two left panels) were similar to those from the global scenarios exhibited, but exhibited more spatial heterogeneity. This greater spatial heterogeneity likely reflects the fact that the global scenarios are statistically downscaled from a much higher spatial resolution (2.5° grid size) and therefore do not capture fine scale topographic features. Like the global scenarios, model projections to the regional scenarios also highlighted much of Yemen, Oman, the UAE and the southern third of Saudi Arabia as areas expected to decline in habitat suitability, including pronounced reductions across the Rub al' Khali. Projected increases in habitat suitability mainly were limited to the northern portion of the study region and the Al Hajar Mountains. Comparatively smaller changes in habitat suitability were projected elsewhere. Projections generally agreed across the two regional spatial domains, with the notable exception of Qatar, which was predicted to lose suitable habitat in the D02 domain and gain suitable habitat in the D01 domain.

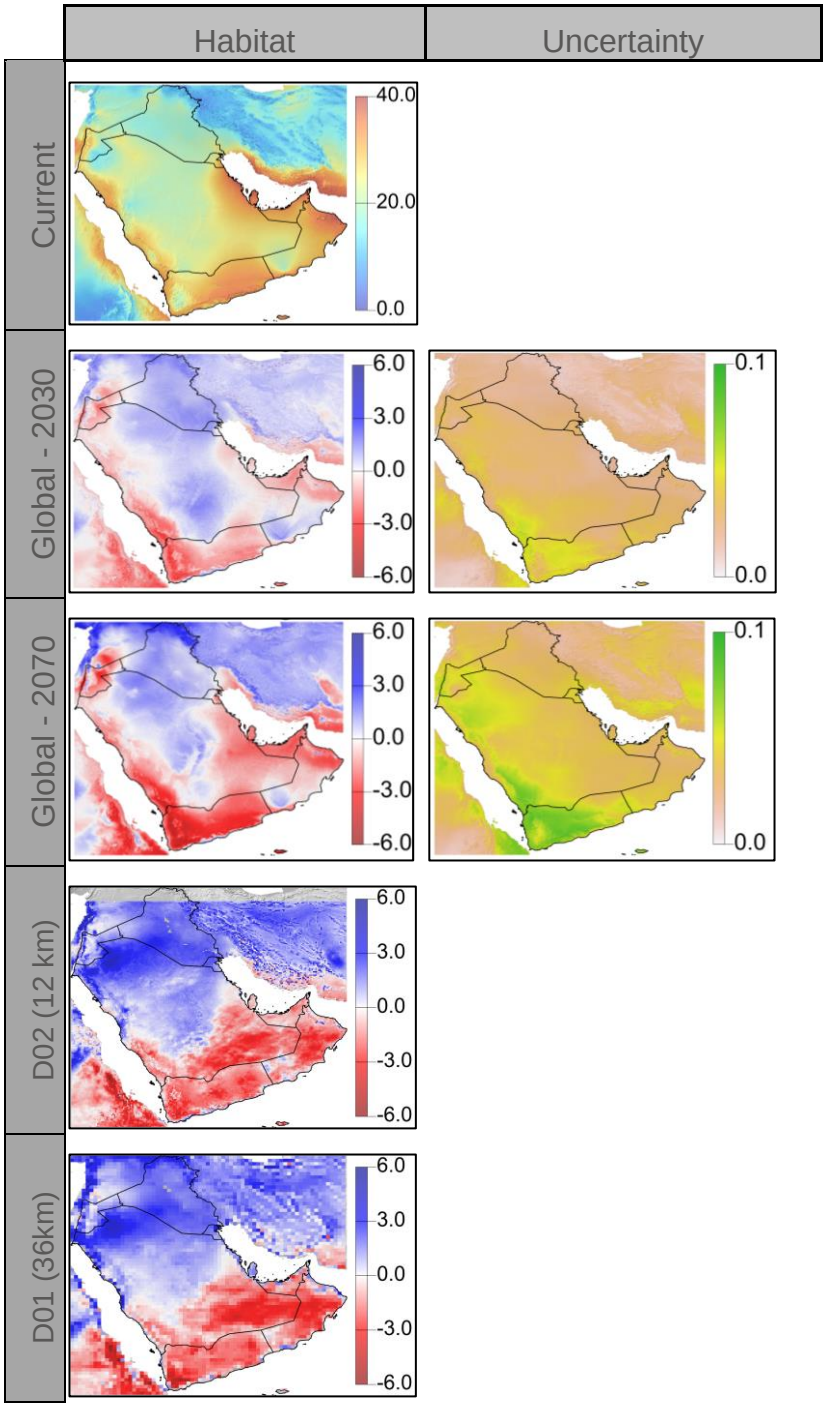

Figure 6 – Mean current habitat suitability and all-scenario ensemble projections of change in habitat suitability across all priority species for global (2030 and 2070) and regional (2070 only) future climate scenarios. Panels to the right of the global scenarios

show the standard deviation of projected changes in habitat suitability for that decade and represent scenario-based uncertainty in future projections.

Projections to Regional Scenarios – taxon-level

At the taxon level, the projected changes in habitat suitability based on the regional climate scenarios (Fig. 8; bottom two rows of panels) were largely consistent with those based on the global climate scenarios (Fig. 8; second and third row of panels). Notable exceptions to this pattern include projected increases in habitat suitability for amphibians in northern Saudi Arabia and Iraq and more extensive declines in habitat suitability in the Rub Al Kali for most taxa. As with the all-priority-species results, the projections to the regional scenarios tended to show greater spatial heterogeneity than those based on the global scenarios.

AGEDI
مبادرة أبوظبي العالمية للبيانات البيئية
Abu Dhabi Global Environmental Data Initiative

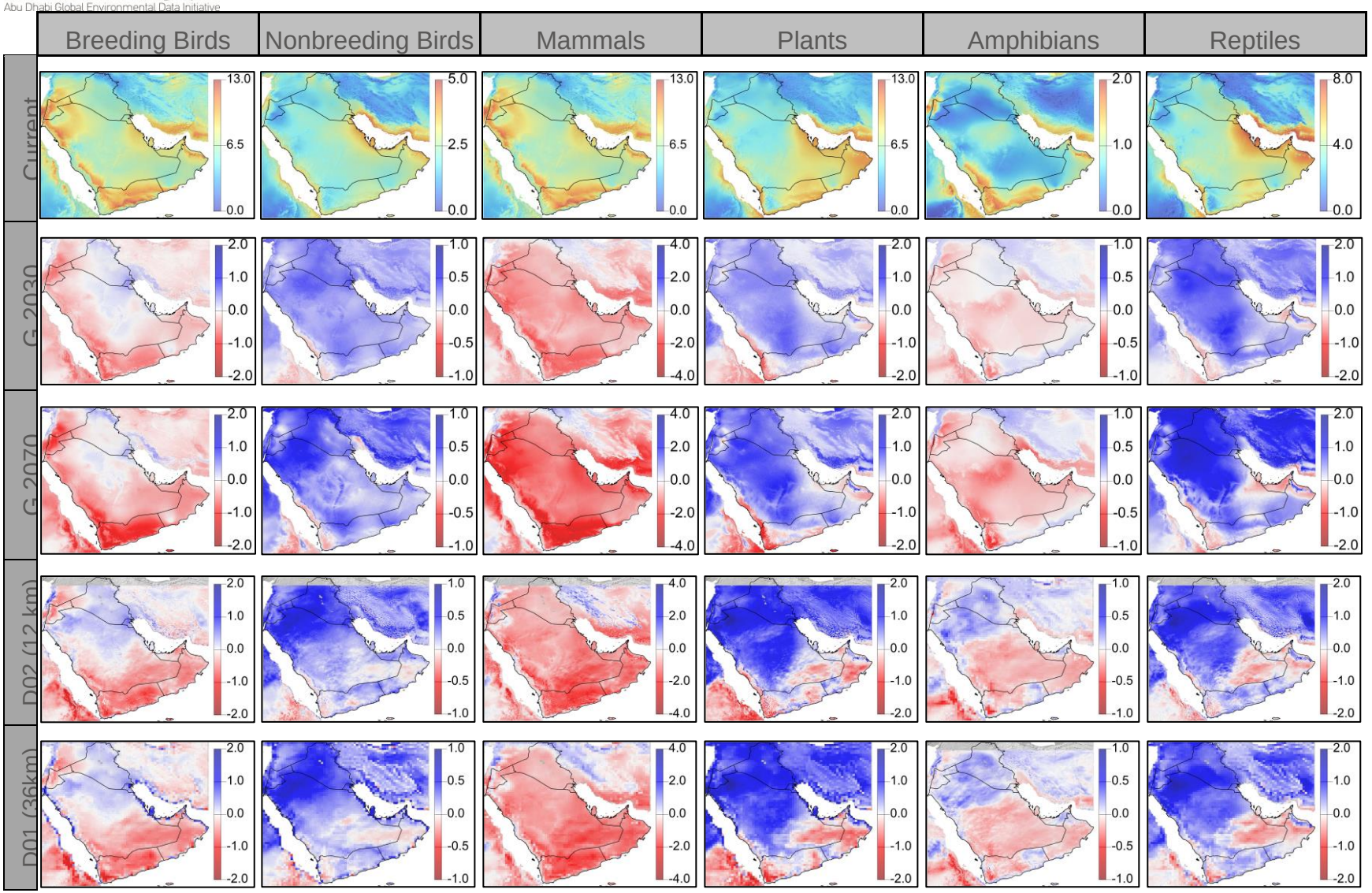

Climate Change Research Group

University of Maryland
CENTER FOR ENVIRONMENTAL SCIENCE

Figure 7. Mean current habitat suitability and all-scenario ensemble projections of projected change in habitat suitability across all priority species by taxonomic group for global (2030 and 2070) and regional (2070 only) future climate scenarios.

Vulnerability assessment of regional biodiversity using GDM

The GDM models incorporated over 200,000 occurrence records for thousands of species. When fit to these current biodiversity patterns, GDM was able to explain a substantial portion of the deviance in compositional differences between locations, especially for plants, mammals, and reptiles (Table 2). The lowest percent deviance explained was for amphibians (41.0%), which had the fewest occurrence data of any modeled taxonomic group.

Table 2 – Summary of data used in fitting GDMs. Percent deviance explained is a metric of model fit whereas the "Weighting Threshold" column refer to settings used to accommodate presence-only data and sampling bias in model fitting (see Annex I for details).

Taxon	Number of Species	Number of Occurrence Records	Number of Sites	Weighting Threshold	Percent Deviance Explained
Birds	657	75,754	348	60	42.9%
Mammals	123	5,440	115	10	51.2%
Plants	3,700	121,564	288	75	56.7%
Amphibians	87	2,120	85	5	41.0%
Reptiles	122	2,727	142	5	48.4%

Predictions of current biodiversity patterns

Of the five taxonomic groups modeled using GDM, plants exhibited the least predicted spatial variation in species composition in the study region (Fig. 9, top row of panels, areas of similar color are expected to harbor similar composition of species). For mammals, much of the study region was predicted to have similar species composition, with the exception of extreme western Yemen (Fig. 9; yellow vs. red shading in the current prediction panel for mammals) and to a lessor extent northern Iraq (Fig. X; blue vs. red shading), which were predicted to harbor assemblages of mammal species that differed from those across most of the study region. In contrast, the composition of bird, amphibian, and reptile species assemblages, was predicted to vary across the study region, with reptiles in particular showing fine scale compositional variation as a function of environmental and topographic gradients.

Projections to Global Scenarios

When projected to future climate scenarios, GDM estimates the expected percent change in species composition at each location as a function of how much climate is expected to change in that location, weighted by the importance of different climate gradients in determining current

biodiversity patterns. A value of zero indicates no expected change in composition and a value of one indicates an expected 100% turnover in species composition (i.e., current and future assemblages share no species in common). Given lags in species responses to changes in climate, these estimates are best interpreted as an index of climatic stress on each taxonomic group at each location (Dunlop *et al.* 2012), with higher values indicating greater climatic stress.

As for the MaxEnt results for priority species, projected impacts between 2030 and 2070 (Fig. 9, compare second and third row of panels) were mainly in degree rather than kind, though areas of climatic stress tended to increase and expand through time for all taxa with the exception of mammals. GDM projections reptiles had some of the most widespread and highest forecasted impacts of any of the taxonomic group. These results suggest that, from the perspective of reptiles, local assemblages could be very different in species composition in the future and may be under pronounced climatic stress as climate changes. Projected impacts were also widespread for birds and amphibians by 2070, but were of a lower magnitude than for all other taxonomic groups. Mammals were projected to experience the least widespread climatic stress, for which the severest of projected impacts largely were limited to the northernmost portion of the study region. For all taxonomic groups except mammals, mountainous regions in the southwestern corner of the study region were identified as potential climate change refugia as this area was projected to have comparatively low climatic stress. Note that model results for addition times (2050, 2080), individual RCPs (4.5 and 8.5), etc. are provided as an electronic resource at http://www.ccr-group.org/terrestrial.

Projections to Regional Scenarios

GDM projections to the two regional climate scenarios (Fig. 9; bottom two rows of panels) showed highly similar results so these are not discussed separately. The regional projections for all taxonomic groups largely mirrored those to the global scenarios, including the south western corner of the study region being projected to serve as a climate refugia in the future. In contrast, the Al Hajar Mountains were predicted to experience high climatic stress for all taxonomic groups but birds. However, the projections to the regional scenarios tended to more severe in terms of both spatial extent and magnitude of projected climatic stress than those to the global scenarios. This pattern was especially evident for plants. For this group, the regional scenarios suggest nearly 100% change in plant species composition across nearly all of the study region.

AGEDI

مبادرة أبوظبي العالمية للبيانات البيئية

Abu Dhabi Global Environmental Data Initiative

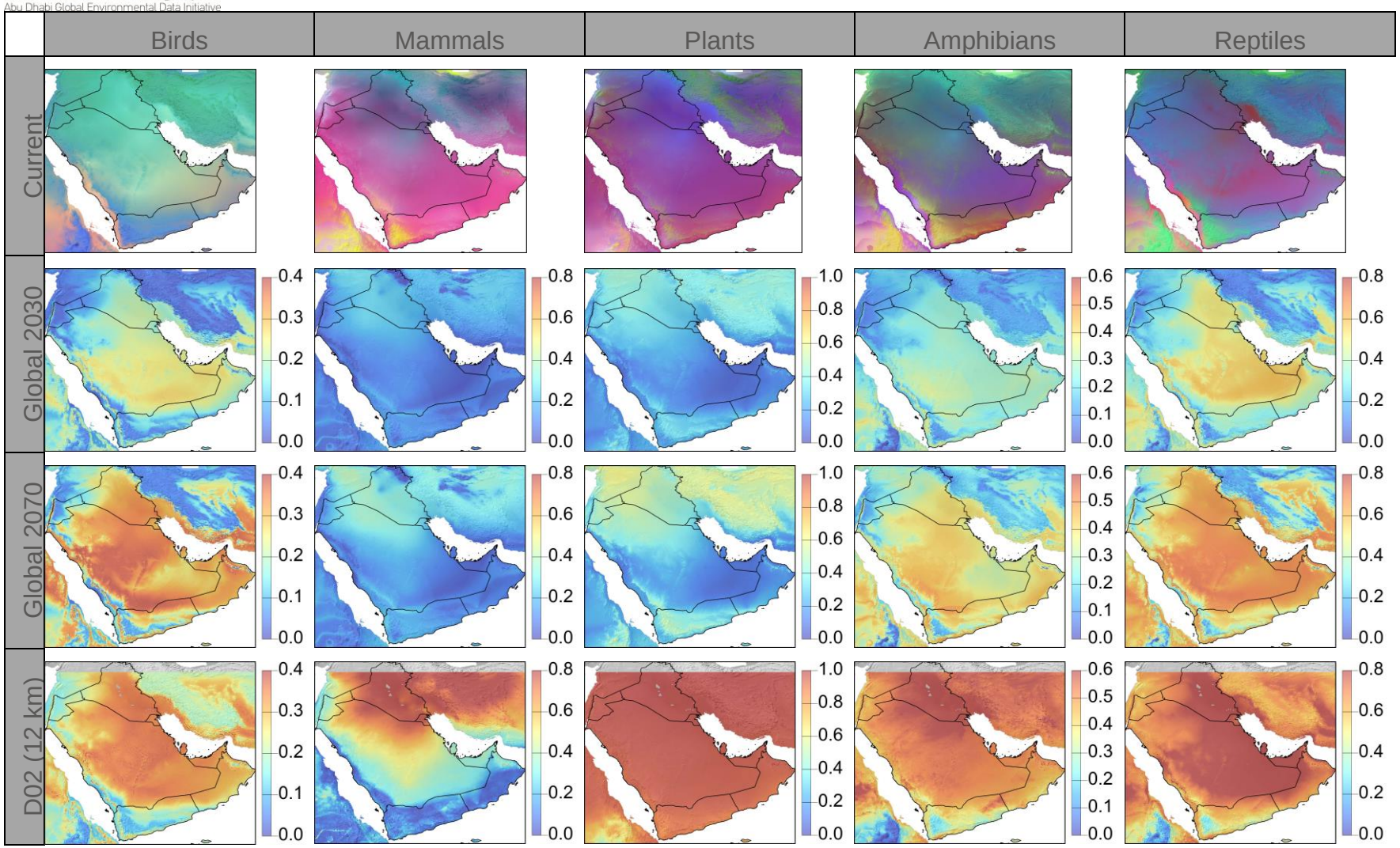

Climate Change Research Group

University of Maryland
CENTER FOR ENVIRONMENTAL SCIENCE

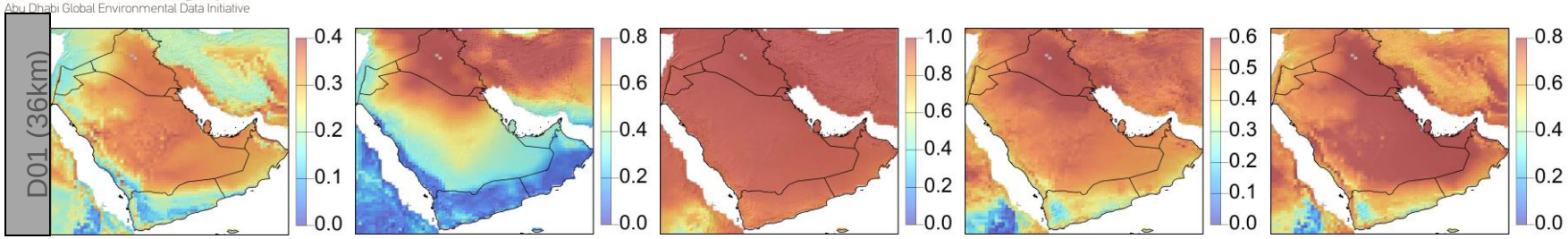

Figure 8 – Current predicted patterns of species composition by taxonomic group (top row of panels, locations with similar colors are expected to harbor assemblages with similar species composition) and all-scenario ensemble projections of expected change in species composition between current and future climate for global (2030 and 2070) and regional future climate scenarios.

Discussion

Vulnerability of terrestrial biodiversity to climate change

Ensemble projections from MaxEnt and GDM to numerous climate scenarios provide a comprehensive overview of the potential future of terrestrial biodiversity in the Arabian Gulf countries from the perspective of both individual species and from biodiversity as a whole. When considered collectively in terms of species, taxonomic groups, climate scenarios, and modeling methods, similarities in projected outcomes reveal impacts that are largely insensitive to particular characteristics of species or assumptions regarding models. With this in mind, findings from this study suggest climate change has to potential to cause widespread changes in species distributions and patterns of biodiversity across the Arabian Peninsula and that the magnitude and spatial extent of impacts will increase through time.

For the 75 priority species for which MaxEnt models were projected, loss of suitable habitat is expected to be most pronounced in the southern half of the study region, including Qatar, the UAE, Yemen (including the island of Socotra), and Oman, and along the western coast of Saudi Arabia (Fig. 7). However, these losses may be offset to some extent by gains in suitable habitat in north central Saudi Arabia and Iraq. The extent to which such gains in habitat may be exploited by species in the future depends on the ability of species to successfully disperse to new habitats and how well these areas provide other aspects of habitat not included in the models, such as shelter, food resources, etc., among other factors. It is also important to note that projections to later decades (i.e., 2080) suggest increases in suitable habitat may be temporary (see electronic resource).

For biodiversity as a whole, findings from GDM suggest that both northern and southern areas may undergo substantial changes in species composition (high climatic stress). Only a fraction of the southern portion of the study region – and the southwestern corner in particular – was projected to experience low climatic stresses and therefore comparatively little changes in species composition. However, these generalities do not necessarily apply across all taxonomic groups or climate scenarios. For example, plants were projected to experience low climatic stress across nearly all of the study region based on the global climate scenarios and very high climatic stress across the entire study region under the regional projections.

The climates of the Arabian Gulf region are some of the most extreme globally in terms of high temperatures and low precipitation. While species in the region are adapted to such extreme environments, many species also exist near the limits of their climatic tolerances and survive by opportunistically exploiting microrefugia in space and/or time. Such factors are difficult to represent using the empirical models and broad scale climatic gradients. However, GDM was able to explain a substantial proportion of deviance in changes in species composition as a function of differences in climate alone, suggesting that gradients of temperature and precipitation are tightly coupled with patterns of biodiversity and/or are correlated with factors that structure assemblages in the region. For

this reason, it is expected that climate change will result in widespread alteration of existing assemblages, including local extinction of species.

Comparing results from MaxEnt and GDM

When viewed together, MaxEnt and GDM collectively provide complimentary and contrasting inferences regarding areas where changes in biodiversity may be greatest / least in the study region. On the surface, it may appear that MaxEnt and GDM largely disagreed given that GDM projected extensive impacts across the entire study region except the southernmost portion, while the projected impacts from MaxEnt tended to be less extensive and mainly limited to the southern portion of the study region. However, that these models produced contrasting results is not necessary a correct interpretation.

MaxEnt emphasizes individual priority species and produces estimates of changes in habitat suitability (*both gains and losses*) for each species. When combined across species, MaxEnt highlights were multiple species may gain or lose habitat. However, both increases and decreases in habitat suitability would be expected to result in changes in species composition, with some areas gaining new species and others experiencing local extinction. In contrast, GDM considers biodiversity collectively and provides inference regarding the expected *magnitude* of change in species composition, but not the nature of this change (i.e., whether the projected changes in species composition arise due to losses / gains of species in a location). When considered together and in this light, both modeling methods agree that climate change may cause widespread changes in species composition across terrestrial environments of the Arabian Gulf countries. MaxEnt provides the additional insight that these changes may be driven largely by local extinction in the south and increases in species richness to the north, while GDM suggests that the lowest changes overall mainly may be limited to the southwestern portion of the Arabian Peninsula.

Caveats

Several important caveats must be considered when interpreting model projections. Foremost, it must be kept in mind that the models used in the report are modeling the effects of *climate only* on biodiversity patterns and ignore all other factors determining habitat suitability. Other abiotic and biotic factors, such as soils, access to groundwater, species interactions, dispersal, etc., can all influence species distributions, but were not included in this study. For higher taxa such as mammals and birds, vegetation is an important component of habitat that provides food resources and shelter. Therefore models fit with climate variables alone may not fully reflect habitat requirements. In addition, climate-driven changes to vegetation will also affect higher taxa. For example, GDM predicts the greatest magnitude and most widespread changes for plant assemblages (Fig. 9). Therefore, in addition to climate change itself, dramatic changes to vegetation structure will also impact species that depend on certain vegetation types.

The models also ignore dispersal constraints, both in constraining current patterns and in the colonization of habitat that becomes suitable in the future. In essence, the model projections assume “unlimited” dispersal in that species are assumed to immediately colonize any and all habitats that

become suitable, no matter how distant those location are from current populations. For these reasons, reductions in habitat suitability are likely more reliable indicators of vulnerability, whereas increases in habitat suitability should be considered as future opportunities for range expansion.

Data challenges

This study suffered from a lack of comprehensive, unbiased species occurrence records, and especially so for priority species. Much of the available occurrence data used for fitting biodiversity models in this study were highly biased to a few geographic areas (Fig. 5). As a result, not only were species distributions poorly represented and MaxEnt models data limited, some environments were overrepresented while others were not represented at all. We took multiple steps in an attempt to rectify and account for these biases in model fitting (Annex I). However, we suspect that for many of the priority species the fitted relationships between species distributions and climate may not fully represent the climatic tolerances of the study organisms. For these reasons, results for individual priority species should be interpreted with caution. Because GDMs were fitted with thousands of records for thousands of species, these results should exhibit less influence of bias and therefore may be considered more robust than the individual species results. Nonetheless, data uncertainties likely represent the single largest source of uncertainty in this study and exceeds that arising from different assumptions regarding future climate, etc. For this reason, we strongly recommend the future efforts focus on improving the availability of species occurrence data in the region, both through the digitization of existing records as well as through targeted field studies designed to sample poorly represented environments throughout the study region. None of the countries in the target region are currently participating members of GBIF (which operates as an intergovernmental initiative), and the development of GBIF 'nodes' in the Arabian peninsula would significantly improve the availability of data for analysis such as this, and thus improve the information available to governments regarding climate change impacts

Climate adaptation context

Targeted management efforts designed to increase the resilience of natural systems and provide a means for species to migrate between suitable habitats may help reduce the impacts of climate change in coming decades. Because climate change is just one among many threats to terrestrial ecosystems in the region, reducing other human perturbations such as overgrazing, invasive species, and land use change, will be critical to ensure resilience in the face of climate change. In addition, is important to note that the impact of climatic change will be felt by biodiversity collectively, not just by priority species, and will be ongoing for many decades if not centuries. A systematic management response rather than a short-term focus on individual species is likely to be most successful, yet most challenging. The magnitude of uncertainty regarding the impacts of future climatic change on terrestrial biodiversity are exceedingly high and there is little time left to reduce uncertainty by observing early impacts given that climate-driven changes will be difficult to detect against the backdrop of other threats and

environmental variation and because impacts will be felt everywhere. This uncertainty makes prediction very difficult, even when high quality data are available.

For these reasons, conservation and management actions should emphasize the preservation of ecological processes (Lawler *et al.* 2015), while allowing or facilitating changes in biodiversity states. These goals might most effectively be met through the design and implementation of a network of protected areas that facilitate movement to and from regions of projected high / low changes in species composition. Efforts should focus on areas where different models and future climate scenarios agree that projected changes in biodiversity could be most pronounced and regions that models suggest could serve as climate refugia in the future. Results from the present study suggest that the mountainous regions in the southwestern corner of the Arabian Peninsula may serve as refugia and therefore may be candidates for protection and/or restoration in the context the protected area network that facilitates migration to the northern portion of the Arabian Peninsula.

Such regions may serve as refugia under future climate and may therefore be candidates for protection and/or restoration.

AGEDI
مبادرة أبوظبي العالمية للبيانات البيئية
Abu Dhabi Global Environmental Data Initiative

Literature Cited

AbuZinada, A.H., Robinson, E.R., Nader, I.A. & Al Wetaid, Y.I. (2004). First Saudi Arabian National Report on the Convention on Biological Diversity. *Natl. Comm. Wildl. Conserv. Dev. Riyadh*

Aiello-Lammens, M.E., Boria, R.A., Radosavljevic, A., Vilela, B. & Anderson, R.P. (2015). spThin: an R package for spatial thinning of species occurrence records for use in ecological niche models. *Ecography*, 38, 541–545

Aitken, S.N., Yeaman, S., Holliday, J.A., Wang, T. & Curtis-McLane, S. (2008). Adaptation, migration or extirpation: climate change outcomes for tree populations. *Evol. Appl.*, 1, 95–111

Al Abed, I. & Hellyer, P. (2001). *United Arab Emirates: a new perspective*. Trident Press Ltd

Al-Abbasi, T.M., Al-Farhan, A., Al-Khulaidi, A.W., Hall, M., Llewellyn, O.A., Miller, A.G., *et al.* (2010). Important plant areas in the Arabian Peninsula. *Edinb. J. Bot.*, 67, 25–35

Al-Johany, A.M.H. (2007). Distribution and conservation of the Arabian Leopard Panthera pardus nimr in Saudi Arabia. *J. Arid Environ.*, 68, 20–30

Araujo, M.B. & New, M. (2007). Ensemble forecasting of species distributions. *Trends Ecol. Evol.*, 22, 42–47

Attorre, F., Francesconi, F., Taleb, N., Scholte, P., Saed, A., Alfo, M., *et al.* (2007). Will dragonblood survive the next period of climate change? Current and future potential distribution of Dracaena cinnabari (Socotra, Yemen). *Biol. Conserv.*, 138, 430–439

Balletto, E., Cherchi, M.A. & Gasperetti, J. (1985). Amphibians of the Arabian Peninsula.

Barbet-Massin, M., Walther, B.A., Thuiller, W., Rahbek, C. & Jiguet, F. (2009). Potential impacts of climate change on the winter distribution of Afro-Palaearctic migrant passerines. *Biol. Lett.*, rsbl. 2008.0715

Bestion, E., Teyssier, A., Richard, M., Clobert, J. & Cote, J. (2015). Live fast, die young: experimental evidence of population extinction risk due to climate change. *PLoS Biol*, 13, e1002281

Climate Change Research Group

University of Maryland
CENTER FOR ENVIRONMENTAL SCIENCE

BirdLife International & NatureServe. (2014). Bird species distribution maps of the world. BirdLife International, Cambridge, UK

Blois, J.L., Williams, J.W., Fitzpatrick, M.C., Jackson, S.T. & Ferrier, S. (2013). Space can substitute for time in predicting climate-change effects on biodiversity. *Proc. Natl. Acad. Sci.*, 110, 9374–9379

Boyce, M.S., Vernier, P.R., Nielsen, S.E. & Schmiegelow, F.K.A. (2002). Evaluating resource selection functions. *Ecol. Model.*, 157, 281–300

Broennimann, O., Di Cola, V. & Guisan, A. (2016). *ecospat: Spatial Ecology Miscellaneous Methods.*

Brown, G. & Mies, B. (2012). *Vegetation ecology of Socotra*. Springer Science & Business Media

Ceballos, G. & Ehrlich, P.R. (2006). Global mammal distributions, biodiversity hotspots, and conservation. *Proc. Natl. Acad. Sci.*, 103, 19374–19379

Chavent, M., Kuentz, V., Liquet, B. & Saracco, J. (2013). *ClustOfVar: Clustering of variables*

Cheung, C.C., DeVantier, L.L. & Van Damme, K.K. (2007). Socotra A Natural History of the Islands and their People

Cowling, R.M., Ojeda, F., Lamont, B.B., Rundel, P.W. & Lechmere-Oertel, R. (2005). Rainfall reliability, a neglected factor in explaining convergence and divergence of plant traits in fire-prone mediterranean-climate ecosystems. *Glob. Ecol. Biogeogr.*, 14, 509–519

Cox, N.A., Mallon, D., Bowles, P., Els, J. & Tognelli, M.F. (2012). The Conservation Status and Distribution of Reptiles of the Arabian Peninsula. *Camb. UK Gland Switz. IUCN Sharjah UAE Environ. Prot. Areas Auth.*

D'Amen, M., Rahbek, C., Zimmermann, N.E. & Guisan, A. (2015). Spatial predictions at the community level: from current approaches to future frameworks. *Biol. Rev.*

Dawson, T.P., Jackson, S.T., House, J.I., Prentice, I.C. & Mace, G.M. (2011). Beyond predictions: Biodiversity conservation in a changing climate. *Science*, 332, 53–58

Dormann, C.F. (2007). Promising the future? Global change projections of species distributions. *Basic Appl. Ecol.*, 8, 387–397

Dunlop, M., Hilbert, D.W., Ferrier, S., House, A., Liedloff, A., Prober, S.M., *et al.* (2012). The implications of climate change for biodiversity conservation and the National Reserve System: final synthesis. *Canberra CSIRO*

El Alqamy, H., Ismael, A., Abdelhameed, A., Nagy, A., Hamada, A., Rashad, S., *et al.* (2010). Predicting the status and distribution of the Nubian Ibex (Capra nubiana) in the high-altitude Mountains of South Sinai (Egypt). *Galemys Bol. Inf. Soc. Esp. Para Conserv. Estud. Los Mamíferos*, 22, 517–530

Elith, J., Graham, C.H., Anderson, R.P., Dudik, M., Ferrier, S., Guisan, A., *et al.* (2006). Novel methods improve prediction of species' distributions from occurrence data. *Ecography*, 29, 129–151

Elith, J. & Leathwick, J.R. (2009). Species distribution models: ecological explanation and prediction across space and time. *Annu. Rev. Ecol. Evol. Syst.*, 40, 677–697

Elith, J., Phillips, S.J., Hastie, T., Dudík, M., Chee, Y.E. & Yates, C.J. (2011). A statistical explanation of MaxEnt for ecologists. *Divers. Distrib.*

El-Keblawy, A. (2014). Impact of Climate Change on Biodiversity Loss and Extinction of Endemic plants of Arid Land Mountains. *J. Biodivers. Endanger. Species*

Farag, A.A. & Banaja, A.A. (1980). Amphibians and reptiles from the western region of Saudi Arabia. *Bull Fac Sci King Aziz Univ*, 4, 5–29

Ferrier, S. & Guisan, A. (2006). Spatial modelling of biodiversity at the community level. *J. Appl. Ecol.*, 43, 393–404

Ferrier, S., Harwood, T. & Williams, K.J. (2010). Using generalised dissimilarity modelling to assess potential impacts of climate change on biodiversity composition in Australia, and on the representativeness of the National Reserve System. *Rep. Dep. Environ. Water Herit. Arts Canberra Aust.*

Ferrier, S., Manion, G., Elith, J. & Richardson, K. (2007). Using generalized dissimilarity modelling to analyse and predict patterns of beta diversity in regional biodiversity assessment. *Divers. Distrib.*, 13, 252–264

Ferrier, S., Watson, G., Pearce, J. & Drielsma, M. (2002). Extended statistical approaches to modelling spatial pattern in biodiversity in northeast New South Wales. I. Species-level modelling. *Biodivers. Conserv.*, 11, 2275–2307

Fischlin, A., Midgley, G.F., Price, J.T., Leemans, R., Gopal, B., Turley, C., *et al.* (2007). Ecosystems, their properties, goods, and services. In: *Climate Change 2007: Impacts, Adaptation and Vulnerability. Contribution of Working Group II to the Fourth Assessment Report of the Intergovernmental Panel on Climate Change*. Cambridge University Press, Cambridge, pp. 211–272

Fisher, M. (1997). Decline in the juniper woodlands of Raydah Reserve in southwestern Saudi Arabia: a response to climate changes? *Glob. Ecol. Biogeogr. Lett.*, 379–386

Fitzpatrick, M. & Hargrove, W. (2009). The projection of species distribution models and the problem of non-analog climate. *Biodivers. Conserv.*, 18, 2255–2261

Fitzpatrick, M.C., Gove, A.D., Sanders, N.J. & Dunn, R.R. (2008). Climate change, plant migration, and range collapse in a global biodiversity hotspot: the Banksia (Proteaceae) of Western Australia. *Glob. Change Biol.*, 14, 1337–1352

Fitzpatrick, M.C., Sanders, N.J., Ferrier, S., Longino, J.T., Weiser, M.D. & Dunn, R. (2011). Forecasting the future of biodiversity: a test of single- and multi-species models for ants in North America. *Ecography*, 34, 836–847

Fitzpatrick, M.C., Sanders, N.J., Normand, S., Svenning, J.-C., Ferrier, S., Gove, A.D., *et al.* (2013). Environmental and historical imprints on beta diversity: insights from variation in rates of species turnover along gradients. *Proc. R. Soc. B Biol. Sci.*, 280

Franklin, J. (2009). *Mapping species distributions: spatial inference and prediction*. Cambridge University Press Cambridge, UK

Ghazanfar, S.A. (1998). Status of the flora and plant conservation in the Sultanate of Oman. *Biol. Conserv.*, 85, 287–295

Ghazanfar, S.A. & Fisher, M. (2013). *Vegetation of the Arabian peninsula*. Springer Science & Business Media

Graham, C.H., Ferrier, S., Huettman, F., Moritz, C. & Peterson, A.T. (2004). New developments in museum-based informatics and applications in biodiversity analysis. *Trends Ecol. Evol.*, 19, 497–503

Global Biodiversity Information Facility (GBIF) custom data export (accessed 21st May 2015; (http://www.gbif.org)

Grubb, P.J. (1977). The maintenance of species-richness in plant communities: the importance of the regeneration niche. *Biol. Rev.*, 52, 107–145

Guisan, A. & Thuiller, W. (2005). Predicting species distribution: offering more than simple habitat models. *Ecol. Lett.*, 8, 993–1009

Guisan, A. & Zimmermann, N.E. (2000). Predictive habitat distribution models in ecology. *Ecol. Model.*, 135, 147–186

Hampe, A. (2004). Bioclimate envelope models: what they detect and what they hide. *Glob. Ecol. Biogeogr.*, 13, 469–471

Hardy, J.T. (2003). *Climate change: causes, effects, and solutions*. Wiley

Heezik, Y.V. & Seddon, P.J. (1999). Seasonal changes in habitat use by Houbara Bustards Chlamydotis [undulata] macqueenii in northern Saudi Arabia. *Ibis*, 141, 208–215

Hegazy, A. & Lovett-Doust, J. (2016). *Plant Ecology in the Middle East*. Oxford University Press

Heikkinen, R.K., Luoto, M., Araujo, M.B., Virkkala, R., Thuiller, W. & Sykes, M.T. (2006). Methods and uncertainties in bioclimatic envelope modelling under climate change. *Prog. Phys. Geogr.*, 30, 751–777

Hijmans, R.J., Cameron, S.E., Parra, J.L., Jones, P.G. & Jarvis, A. (2005). Very high resolution interpolated climate surfaces for global land areas. *Int. J. Climatol.*, 25, 1965–1978

Hijmans, R.J., Phillips, S.J., Leathwick, J.R. & Elith, J. (2012). *dismo: Species distribution modeling. R package version 0.7-23.*

Hill, J.K., Thomas, C.D. & Huntley, B. (1999). Climate and habitat availability determine 20th century changes in a butterfly's range margin. *Proc. R. Soc. Lond. Ser. B-Biol. Sci.*, 266, 1197–1206

Hirzel, A.H., Le Lay, G., Helfer, V., Randin, C. & Guisan, A. (2006). Evaluating the ability of habitat suitability models to predict species presences. *Ecol. Model.*, 199, 142–152

IUCN. (2015). *The IUCN Red List of Threatened Species*

Kassas, M. (1999). Rescuing drylands: a project for the world. *Futures*, 31, 949–958

Khosravi, R., Hemami, M.-R., Malekian, M., Flint, A.L. & Flint, L.E. (2016). Maxent modeling for predicting potential distribution of goitered gazelle in central Iran: the effect of extent and grain size on performance of the model. *Turk. J. Zool.*, 40

Kingdon, J. (1990). *Arabian mammals: a natural history*. Academic Press New York

Lawler, J.J., Ackerly, D.D., Albano, C.M., Anderson, M.G., Dobrowski, S.Z., Gill, J.L., *et al.* (2015). The theory behind, and the challenges of, conserving nature's stage in a time of rapid change. *Conserv. Biol.*, 29, 618–629

Liu, C.R., Berry, P.M., Dawson, T.P. & Pearson, R.G. (2005). Selecting thresholds of occurrence in the prediction of species distributions. *Ecography*, 28, 385–393

Loarie, S.R., Carter, B.E., Hayhoe, K., McMahon, S., Moe, R., Knight, C.A., *et al.* (2008). Climate change and the future of California's endemic flora. *PLoS One*, 3, e2502

Loarie, S.R., Duffy, P.B., Hamilton, H., Asner, G.P., Field, C.B. & Ackerly, D.D. (2009). The velocity of climate change. *Nature*, 462, 1052–1055

Lobo, J.M., Jiménez-Valverde, A. & Real, R. (2008). AUC: a misleading measure of the performance of predictive distribution models. *Glob. Ecol. Biogeogr.*, 17, 145–151

Malcolm, J.R., Markham, A., Neilson, R.P. & Garaci, M. (2002). Estimated migration rates under scenarios of global climate change. *J. Biogeogr.*, 29, 835–849

Mallon, D. & Budd, K. (2011). Regional Red List status of carnivores in the Arabian Peninsula. *IUCN and*

Mallon, D.P. (2011). Global hotspots in the Arabian Peninsula. *Zool. Middle East*, 54, 13–20

Manion, G., Ferrier, S., Lisk, M. & Fitzpatrick, M.C. (2016). *gdm: Functions for Generalised Dissimilarity Modelling.*

McKechnie, A.E. & Wolf, B.O. (2009). Climate change increases the likelihood of catastrophic avian mortality events during extreme heat waves. *Biol. Lett.*, rsbl20090702

Midgley, G.F., Hannah, L., Millar, D., Thuiller, W. & Booth, A. (2003). Developing regional and species-level assessments of climate change impacts on biodiversity in the Cape Floristic Region. *Biol. Conserv.*, 112, 87–97

Midgley, G.F. & Thuiller, W. (2007). Potential vulnerability of Namaqualand plant diversity to anthropogenic climate change. *J. Arid Environ.*, 70, 615–628

Miller, A.G. & Cope, T.A. (1997). Flora of the Arabian Peninsula and Socotra. Vol. 1. *Bot. Jahrbucher Syst. Pflanzengesch. Pflanzengeogr.*, 119, 141–141

Moore, G.E., Grizzle, R.E., Ward, K.M. & Alshihi, R.M. (2014). Distribution, Pore-Water Chemistry, and Stand Characteristics of the Mangroves of the United Arab Emirates. *J. Coast. Res.*, 31, 957–963

Muscarella, R., Galante, P.J., Soley-Guardia, M., Boria, R.A., Kass, J.M., Uriarte, M., *et al.* (2014). ENMeval: An R package for conducting spatially independent evaluations and estimating optimal model complexity for Maxent ecological niche models. *Methods Ecol. Evol.*, 5, 1198–1205

Myers, N., Mittermeier, R.A., Mittermeier, C.G., da Fonseca, G.A.B. & Kent, J. (2000). Biodiversity hotspots for conservation priorities. *Nature*, 403, 853–858

Newton, S.F. & Newton, A.V. (1996). Seasonal changes in the abundance and diversity of birds in threatened juniper forest in the southern Asir mountains, Saudi Arabia. *Bird Conserv. Int.*, 6, 371–392

Olson, D.M., Dinerstein, E., Wikramanayake, E.D., Burgess, N.D., Powell, G.V.N., Underwood, E.C., *et al.* (2001). Terrestrial ecoregions of the world: a new map of life on earth. *BioScience*, 51, 933–938

Osman-Elasha, B. & Fisher, J. (2008). *Part IV: Climate Change Impacts, Vulnerability, & Adaptation: Dryland Ecosystems in Abu Dhabi*

Pearson, R.G., Dawson, T.P., Berry, P.M. & Harrison, P.A. (2002). SPECIES: A Spatial Evaluation of Climate Impact on the Envelope of Species. *Ecol. Model.*, 154, 289–300

Pearson, R.G., Raxworthy, C.J., Nakamura, M. & Townsend Peterson, A. (2006a). Predicting species distributions from small numbers of occurrence records: a test case using cryptic geckos in Madagascar. *J. Biogeogr.*, 34, 102–117

Pearson, R.G., Thuiller, W., Araujo, M.B., Martinez-Meyer, E., Brotons, L., McClean, C., *et al.* (2006b). Model-based uncertainty in species range prediction. *J. Biogeogr.*, 33, 1704–1711

Phillips, S.J., Anderson, R.P. & Schapire, R.E. (2006). Maximum entropy modeling of species geographic distributions. *Ecol. Model.*, 190, 231–259

Phillips, S.J., Dudík, M., Elith, J., Graham, C.H., Lehmann, A., Leathwick, J., *et al.* (2009). Sample selection bias and presence-only distribution models: implications for background and pseudo-absence data. *Ecol. Appl.*, 19, 181–197

Root, T.L., Price, J.T., Hall, K.R., Schneider, S.H., Rosenzweig, C. & Pounds, J.A. (2003). Fingerprints of global warming on wild animals and plants. *Nature*, 421, 57–60

Rosenzweig, C., Casassa, G., Karoly, D.J., Imeson, A., Liu, C., Menzel, A., *et al.* (2007). Assessment of observed changes and responses in natural and managed systems. In: *Climate Change 2007: Impacts, Adaptation and Vulnerability. Contribution of Working Group II to the Fourth Assessment Report of the Intergovernmental Panel on Climate Change*. Cambridge University Press, Cambridge, UK, pp. 79–131

Sala, O.E., Chapin, F.S., Armesto, J.J., Berlow, E., Bloomfield, J., Dirzo, R., *et al.* (2000). Biodiversity - Global biodiversity scenarios for the year 2100. *Science*, 287, 1770–1774

Shobrak, M. (2011). Bird flyways and stopover conservation sites in the Arabian Peninsula. *Zool. Middle East*, 54, 27–30

Somveille, M., Manica, A., Butchart, S.H. & Rodrigues, A.S. (2013). Mapping global diversity patterns for migratory birds. *PLoS One*, 8, e70907

Talhouk, S. (2009). Ecosystems and Biodiversity. In: *Arab Environment and Climate Change: Impact of climate change on Arab countries*, 2009 Report of the Arab Forum for Environment and Development (eds. Tolba, M.K. & Saab, N.W.)

Team, R.C. (2016). *R: A Language and Environment for Statistical Computing*. Vienna, Austria

Thouless, C.R., Grainger, J.G., Shobrak, M. & Habibi, K. (1991). Conservation status of gazelles in Saudi Arabia. *Biol. Conserv.*, 58, 85–98

Thuiller, W., Araujo, M.B. & Lavorel, S. (2003). Generalized models vs. classification tree analysis: Predicting spatial distributions of plant species at different scales. *J. Veg. Sci.*, 14, 669–680

Thuiller, W., Lafourcade, B., Engler, R. & Araújo, M.B. (2009). BIOMOD - a platform for ensemble forecasting of species distributions. *Ecography*, 32, 369–373

Thuiller, W., Lavorel, S., Araujo, M.B., Sykes, M.T. & Prentice, I.C. (2005). Climate change threats to plant diversity in Europe. *Proc. Natl. Acad. Sci. U. S. A.*, 102, 8245–8250

Thuiller, W., Midgley, G.F., Hughes, G.O., Bomhard, B., Drew, G., Rutherford, M.C., *et al.* (2006). Endemic species and ecosystem sensitivity to climate change in Namibia. *Glob. Change Biol.*, 12, 759–776

Travis, J.M.J. (2003). Climate change and habitat destruction: a deadly anthropogenic cocktail. *Proc. R. Soc. Lond. Ser. B-Biol. Sci.*, 270, 467–473

Urban, M.C. (2015). Accelerating extinction risk from climate change. *Science*, 348, 571–573

Visser, M.E., Holleman, L.J. & Gienapp, P. (2006). Shifts in caterpillar biomass phenology due to climate change and its impact on the breeding biology of an insectivorous bird. *Oecologia*, 147, 164–172

Walther, G.R., Post, E., Convey, P., Menzel, A., Parmesan, C., Beebee, T.J.C., *et al.* (2002). Ecological responses to recent climate change. *Nature*, 416, 389–395

Warren, D.L. & Seifert, S.N. (2011). Ecological niche modeling in Maxent: the importance of model complexity and the performance of model selection criteria. *Ecol. Appl.*, 21, 335–342

Warren, D.L., Wright, A.N., Seifert, S.N. & Shaffer, H.B. (2014). Incorporating model complexity and spatial sampling bias into ecological niche models of climate change risks faced by 90 California vertebrate species of concern. *Divers. Distrib.*, 20, 334–343

Williams, J.B., Shobrak, M., Wilms, T.M., Arif, I.A. & Khan, H.A. (2012). Climate change and animals in Saudi Arabia. *Saudi J. Biol. Sci.*, 19, 121–130

AGEDI
مبادرة أبوظبي العالمية للبيانات البيئية
Abu Dhabi Global Environmental Data Initiative

Annex I – Detailed technical methods

Species occurrence data quality control

We took several steps to prepare the species occurrence data from GBIF to ensure only data of the highest quality were used in modeling. As a first pass, points that met any of the following criteria we removed: (1) no geographic (latitude-longitude) coordinates or low spatial precision, (2) uncertain taxonomy, (3) coordinates far outside the known native range, (4) coordinates matching the centroids of political entities. Next, we removed all spatial replicates (i.e., records for the same species with identical coordinates).

When available, we augmented the GBIF records with occurrence data provided by regional partners. These data were subjected to the same processing as described for GBIF data, then were combined with the GBIF data for model fitting. Table 1 summarizes occurrence records for each priority species.

MaxEnt

For each priority species for which we could obtain a polygon range map, we overlaid the point occurrence data with the range polygon for that species. Range polygons for birds came from BirdLife International & NatureServe (2014) and from IUCN (2015) for mammals, amphibians and reptiles. We then identified and removed extreme outliers as any points falling far beyond the range polygon, based on our best professional judgment. We did not have range polygons for plants and some reptiles, so performed literature and web searches to determine likely geographic ranges and remove potential outliers based on these estimates. Lastly, we overlaid the remaining point occurrence data with the gridded climate surfaces for current climate (10 arc-minute resolution) and retained only one spatially unique occurrence record per grid cell. In other words, if two points for the same species fell within the same 10 arc-minute grid cell, it was counted as a single record. For two species - *Capra nubiana* and *Gazella gazella* – we supplemented point occurrences using range polygons for these species. We extracted all cells that fell within the species range polygons and filtered them such that all remaining points were separated by a minimum of 50 km using the spThin package (Aiello-Lammens *et al.* 2015) in R (R Core Team 2016).

GDM

Preparation of occurrence data for GDM generally followed that for the MaxEnt models with two notable exceptions. First, we retained GBIF and regional partner occurrence data for all species of plants, mammals, birds, and reptiles and amphibians, not just priority species. Second, rather than using range polygons to retain occurrence records, we retained all records falling within dryland ecoregions as defined by the World Wildlife Fund (WWF) that fall within our study region (green shading, Figure 4). We intersected the remaining records falling within regional dryland ecoregions with the current climate surfaces (10 arc-minute resolution) and removed spatial duplicates (i.e., occurrence records for the same species falling within the same grid cell). Using these records, we then constructed

site-by-species and site-by-climate matrices for each taxon (where sites are 10 arc-minute climate grid cells). Subsequent processing of these matrices to prepare them for modeling was performed using the 'formatsitepair' function in the 'gdm' package (Manion *et al.* 2016) for R (R Core Team 2016).

Statistical Modeling

MaxEnt

We fit MaxEnt models using the 'dismo' package (Hijmans *et al.* 2012) and MaxEnt 3.3.3E in R (R Core Team 2016). Except for changes as described below, we fit models using the default values for all settings. We pursued fitting of MaxEnt models for any species with at least 10 spatially unique occurrence records as other published studies successfully have fit MaxEnt models with fewer than 20 records (Pearson *et al.* 2006a). For priority species with at least 20 unique records, we partitioned the occurrence data for each species randomly 10 times into calibration (70%) and evaluation (30%) datasets, and models were run on each of the 10 resulting datasets. The multiple models for each species resulting from different random splits of the occurrence data into training and test partitions were combined into a single ensemble by averaging. Thus, maps of current habitat suitability reported in this document show the mean of these ten models for each species. Note that due to statistical limitations, the test/training partitioning was not performed for species with fewer than 20 records.

To avoid over-fitting models with the small number of occurrence records, we used only a subset of the 19 bioclimatic variables from the WorldClim database (http://www.worldclim.org; (Hijmans *et al.* 2005). Variables were first clustered using the 'ClustOfVar' package (Chavent *et al.* 2013) in R (R Core Team 2016). We reduced the full set of 19 potential predictor variables by selecting variables to minimize multicollinearity ($r < 0.7$), but retained uncorrelated pairs of variables that were, in our opinion, most biologically informative. This selection process reduced the 19 covariates to fewer than seven variables per species, which were then used in model fitting and predictive mapping under current and future climates. To restrict predictions to near-shore environments for coastal species, we used distance from the coast as additional predictor for coastal species. Lastly, we included elevation as a predictor for *Capra nubiana*.

Controlling model complexity

Model complexity was altered to prevent overfitting using the regularization parameter. The regularization parameter determines how closely the model fits the calibration data and can be altered using a beta-multiplier to either amplify or dampen the effect of the regularization coefficient. Species specific values for the beta-multiplier were selected by fitting models using a range of beta-multiplier values (0 to 15 in steps of 0.2) and then comparing these models on the basis of the sample-size corrected Akaike Information Criterion (AICc; Warren & Seifert 2011; Warren *et al.* 2014) using the 'ENMeval' package (Muscarella *et al.* 2014) in R (R Core Team 2016).

Model evaluation

The evaluation of the predictive accuracy of presence-only species distribution models is an ongoing challenge; we focused on evaluation criteria that require only information on presence (Franklin 2009). We calcualted the continuous Boyce Index (Hirzel *et al.* 2006), which is a modified version of the Boyce Index (Boyce *et al.* 2002), using the 'ecospat' package (Broennimann *et al.* 2016) in R (R Core Team 2016). This index is calculated by first partitioning the habitat suitability as predicted by the model into classes based on a moving window. Then, for each habitat class the ratio of the predicted frequency to the expected frequency (from a random distribution) at a set of evaluation points is calculated and the Boyce index is determined by obtaining the Spearman rank correlation coefficient between this ratio and class. The Boyce Index thus varies from -1 to 1 such that values below 0 indicate an incorrect model, values close to zero indicate a model no different from random, and positive values indicate a model better than random.

MaxEnt projections

MaxEnt models with a Boyce Index less than 0 (no better than random) were not considered for projection to future climate scenarios. For models with a Boyce Index of at least 0, we reviewed the current range predictions from MaxEnt against the known geographic range and only projected models with predictions that reasonably matched known distribution patterns, based on our best professional judgment. The lowest Boyce Index of any projected model was 0.437 and the maximum value was 0.988 (see previous Table 1). Note that due to spatial sampling bias, models can have a high Boyce Index, yet fail to replicate the known geographic range. For this reason, some models with a high Boyce Index (e.g., greater than 0.9) were not projected.

Suitable MaxEnt models were projected to all 62 global scenarios (see Table 4, Annex III) of future climate for decades 2030, 2050, 2070 and 2080 and to the regional atmospheric models for 2070 (see previous Figure 4). To summarize the output projections, we report for the following:

1. Range map with occurrence data used to fit MaxEnt models
2. Current predicted habitat suitability
3. Mean projected future habitat suitability across all 62 future climate scenarios (ensemble projection)
4. Difference between mean projected future habitat suitability across all 62 future scenarios and predicted current habitat suitability (ensemble habitat change)
5. Standard deviation of projected future habitat suitability across all 62 scenarios (estimate of climate scenario related uncertainty in MaxEnt model projections)
6. Range change histogram across all 62 future scenarios (estimate of likelihood of increase/decrease in range area)

We also report versions of outputs 3-6 above for (1) only RCP4.5, (2) only RCP8.5, and (3) the regional atmospheric modeling (ensemble, RCP4.5, and RCP8.5 across two spatial domains; 2070 only). We also report versions of these figures summarized at the taxon level (e.g., all plants, etc.).

Mapping range area

To map range area and calculate percent change in range area between present and future, we converted the mapped continuous habitat suitability predictions (0-1) from MaxEnt into binary presence-absence (0/1) using the threshold that maximized the sum of sensitivity plus specificity (Liu *et al.* 2005; Lobo *et al.* 2008).

GDM

Background

Ferrier *et al.* (2002, 2007) developed Generalized Dissimilarity Modeling (GDM) as a means to characterize species turnover between locations as a function of their environmental and geographic separation. Rather than modeling individual species distributions, GDM models compositional dissimilarity (i.e. spatial turnover of species composition) between all possible pairs of locations as a function of environmental differences between these locations and their spatial isolation from one another. Potential strengths of the GDM approach relative to SDMs in assessing spatial patterns of biodiversity and for quantifying or forecasting biodiversity change, include an ability to 1) rapidly analyze datasets containing very large numbers of species; 2) make use of data for all species in these datasets, regardless of the number of records per species; and 3) extrapolate patterns in compositional turnover beyond sampled communities. Importantly, and unlike some community-based modeling approaches, using GDM to forecast impacts of climatic change on biodiversity does not assume that species will move together as fixed community types. Rather, GDM assumes that emergent rates of spatial turnover along environmental gradients under current climatic conditions can act as a reliable surrogate for temporal turnover given environmental change in time (Ferrier *et al.* 2007; Blois *et al.* 2013).

GDM is a nonlinear matrix regression technique for analyzing spatial patterns in the compositional dissimilarity (i.e., beta diversity quantified with the Sørensen measure) between pairs of locations as a function of environmental dissimilarity and geographical distance (Ferrier *et al.* 2007). Unlike classical linear matrix regression, GDM accommodates (i) variation in the rate of compositional turnover (non-stationarity) at different positions along a given gradient, and (ii) the curvilinear relationship between compositional dissimilarity and increasing environmental/geographical distance between sites. To address non-stationarity, GDM first uses maximum-likelihood estimation and flexible I-splines to transform each of the predictor variables and provide the best supported relationship between intersite environmental/geographical separation and compositional dissimilarity (Ferrier *et al.* 2007). Second, this scaled combination of intersite distances is transformed via a link function to accommodate the curvilinear relationship between compositional dissimilarity (constrained between 0 and 1) and environmental and/or geographical separation.

When plotted, the maximum height of each I-spline represents the total amount of compositional turnover associated with that variable, holding all other variables constant. As such, the I-splines are partial regression fits that serve as an indication of the importance of each variable in determining

patterns of beta diversity. Second, the slope of the I-spline indicates the rate of species turnover and, importantly, how this rate varies at any point along the gradient concerned (holding all other variables constant). Lastly, the difference in height between any two sites along the I-spline corresponds to the modeled contribution of that predictor variable to the total ecological distance between those sites. By extension, changes climate in the future along portions of those gradients (i) most strongly associated with changes in composition and (ii) where compositional turnover is most rapid would be expected to result in the largest changes in species composition in time (i.e., as a result of climatic change; Fitzpatrick *et al.* 2013).

Weighting schemes to handle presence-only data

GDM requires information on both presence and absence of species, but has been used with presence-only data (Fitzpatrick *et al.* 2011) given that certain corrections are made. Our site-by-species matrices assume that if a species had not been collected in a grid cell it could be considered absent at that location. This is not true in many instances. Therefore we took two measures to account for potential biases introduced by the use of presence-only data and by differences in collection effort between locations. First, we removed poorly sampled locations by eliminating sites with species richness much lower than average species richness across all locations (these taxon-specific thresholds are listed in Table 2. Second, for the remaining sites, we used the 'richness' weighting function within the 'gdm' function in the 'gdm' package (Manion *et al.* 2016) in R (R Core Team 2016). Richness weighting weights sites proportionally to the number of species observed at that site, such that sites with few species carried less weight, and therefore less influence, in model fitting than sites with larger numbers of species (where sampling bias should be less prominent). This approach is likely the safest option to use if sampling effort is known to have varied substantially between sites, but it has the disadvantage of downweighting marginal sites that actually have low richness.

Mapping current biodiversity patterns using GDM

To map current spatial biodiversity patterns for each taxa, we used the non-linear compositional turnover functions from GDM to transform the environmental variables into biological importance values using the 'gdm.transform' function in the 'gdm' package (Manion *et al.* 2016). To map the resulting multidimensional biodiversity patterns, we used Principal Components Analysis (PCA) to reduce the transformed environmental variables into three factors. The PCA was centered but not scale transformed to preserve differences in the magnitude of biological importance among the environmental variables. For each taxon, the expected difference in species composition between grid cells was mapped by assigning the first three PCs to a RGB color palette, with resulting color similarity corresponding to the similarity of expected patterns of species composition. Thus, the resulting map highlights how species composition changes from one location to another, with grid cells of similar color predicted to have more similar species composition.

AGEDI
مبادرة أبوظبي العالمية للبيانات البيئية
Abu Dhabi Global Environmental Data Initiative

GDM projections

Our use of GDM to assess potential climatic change impacts proceeded in two steps. First, we used GDM to relate compositional dissimilarity between pairs of sites (i.e., all grid cells where species of each taxon were recorded) to their current environmental separation. This model-fitting step provided functions that describe how community composition changes as a function of environmental separation as it is distributed at present. Next, we used this model to predict how community composition would change in time given the amount of environmental separation between current and future climate at each location. In this case, environmental separation occurs not in space but in time because the climate at each location changes from t1 to t2 (e.g., 2030, 2050, etc.). As described above for MaxEnt, we combined projections and mapped their mean and standard deviation.). Specifically, we report the following results for each taxon:

1. Map with occurrence data used to fit GDM
2. Current predicted spatial variation in species composition
3. Mean projected dissimilarity between current and future species composition across all 62 future climate scenarios (ensemble projection)
4. Standard deviation of projected dissimilarity between current and future species composition across all 62 future climate scenarios (estimate of climate scenario related uncertainty in GDM projections)

We also report versions of outputs 3 and 4 above for (1) only RCP4.5, (2) only RCP8.5, and (3) the regional atmospheric modeling (ensemble, RCP4.5, and RCP8.5 across two spatial domains; 2070 only).

AGEDI
مبادرة أبوظبي العالمية للبيانات البيئية
Abu Dhabi Global Environmental Data Initiative

Annex II – Bioclimatic variables considered for biodiversity modeling

Table 3: 19 bioclimatic variables commonly used for biodiversity modeling. The units for temperature and precipitation are °C and mm respectively unless otherwise indicated.

Code	Description
BIO1	Annual Mean Temperature
BIO2	Mean Diurnal Range (Mean of monthly (max temp - min temp))
BIO3	Isothermality (BIO2/BIO7) (* 100)
BIO4	Temperature Seasonality (standard deviation *100)
BIO5	Maximum Temperature of Warmest Month
BIO6	Minimum Temperature of Coldest Month
BIO7	Temperature Annual Range (BIO5-BIO6)
BIO8	Mean Temperature of Wettest Quarter
BIO9	Mean Temperature of Driest Quarter
BIO10	Mean Temperature of Warmest Quarter
BIO11	Mean Temperature of Coldest Quarter
BIO12	Annual Precipitation
BIO13	Precipitation of Wettest Month
BIO14	Precipitation of Driest Month
BIO15	Precipitation Seasonality (Coefficient of Variation)
BIO16	Precipitation of Wettest Quarter
BIO17	Precipitation of Driest Quarter
BIO18	Precipitation of Warmest Quarter
BIO19	Precipitation of Coldest Quarter

AGEDI
مبادرة أبوظبي العالمية للبيانات البيئية
Abu Dhabi Global Environmental Data Initiative

Annex III – Future climate simulations used in biodiversity modeling (global extent)

Table 4: Sixty-two future climate scenarios assembled in support of the terrestrial biodiversity vulnerability assessment. Note that each GCM by RCP combination is available for future decades 2030, 2050, 2070, and 2080. All simulations are available at 2.5 arc-minute spatial resolution and cover the entire planet.

		RCP	
	GCM	**4.5**	**8.5**
1.	bcc_csm1_1_m	X	X
2.	bcc_csm1_1	X	X
3.	bnu_esm	X	X
4.	cccma_canesm2	X	X
5.	cesm1_bgc	X	X
6.	cesm1_cam5	X	X
7.	csiro_access1_0	X	X
8.	csiro_access1_3	X	X
9.	csiro_mk3_6_0	X	X
10.	ec_earth		X
11.	fio_esm	X	X
12.	gfdl_cm3	X	X
13.	gfdl_esm2g	X	X
14.	gfdl_esm2m	X	X
15.	giss_e2_h		X
16.	giss_e2_h_cc	X	
17.	giss_e2_r	X	X
18.	giss_e2_r_cc	X	
19.	inm_cm4	X	X
20.	ipsl_cm5a_lr	X	X
21.	ipsl_cm5a_mr	X	X

22.	ipsl_cm5b_lr		X
23.	lasg_fgoals_g2	X	X
24.	miroc_esm	X	X
25.	miroc_esm_chem	X	X
26.	miroc_miroc5	X	X
27.	mohc_hadgem2_cc	X	X
28.	mohc_hadgem2_es	X	X
29.	mpi_esm_lr	X	X
30.	mpi_esm_mr		X
31.	mri_cgcm3	X	X
32.	ncar_ccsm4	X	X
33.	ncc_noresm1_m	X	X
34.	nimr_hadgem2_ao	X	X

AGEDI
مبادرة أبوظبي العالمية للبيانات البيئية
Abu Dhabi Global Environmental Data Initiative

Annex IV – Summaries of species for which MaxEnt models were developed for this study

Climate Change Research Group

University of Maryland
CENTER FOR ENVIRONMENTAL SCIENCE

Plants

Acacia tortilis

Common Name: Umbrella Thorn

Description: Medium to large tree with a distinct flat topped, umbrella shape. It is generally a larger tree than subsp. *heteracantha*, except where young specimens are heavily browsed upon on a regular basis. The pods of subsp. *spirocarpa* are more laxly curled and covered in velvety hairs and small red glands. The young branches are also pubescent. This species is easily distinguished from other Acacias by the coiled pods and the presence of both long straight thorns and short hooked thorns. Subsp. *heteracantha* is normally a shrub or small to medium sized tree. It is a smaller, more shrubby tree than subsp. *spirocarpa*, which has less tightly coiled pods and has more pubescent pods and young branches (Encyclopedia of Life 2016). Image source: http://www.asergeev.com/.

Global Distribution: North Africa, east Africa, south Africa, Arabia (Encyclopedia of Life 2016). Range map can be found at: http://www.fao.org/docrep/006/q2934e/q2934e05.htm

Distribution within Arabian Gulf Countries: Widespread.

Habitat: *Acacia tortilis* occurs from sand dunes and rocky scarps to alluvial valley bottoms, avoiding seasonally waterlogged sites. A very drought resistant species, the umbrella thorn grows in areas with annual rainfall as low as 40 mm and as much as 1200 mm, with dry seasons of 1-12 months. The tree favors alkaline soils but will colonize saline and gypseous soils.

Current Status: This species has yet to be assessed by the IUCN. Subspecies: A.t. heteracantha classified as Least Concern (LC) (ARKive 2016).

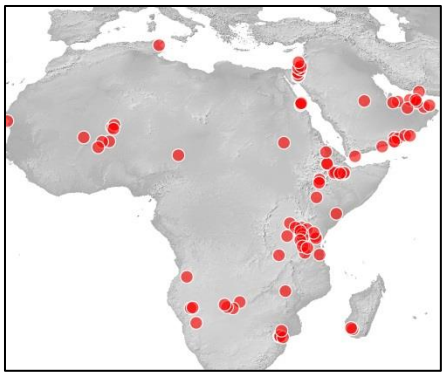

Figure 1 Points used to fit Maxent model.

Arthrocnemum macrostachyum

Common Name: Glaucous Glasswort, Scorpiurus, soap soda

Description: Suffruticose, robust monoecious perennial, up to 150 cm tall, diffuse, glaucous - green; stem up to 1 cm in diam. woody; branches prostrate to erect, fleshy and jointed, 3-4 mm in diam. Flowers in horizontal groups of 3, embedded in axils. Male flowers in c. 2-3 cm long spikes; stamen usually 1, anther c. 0.8 mm long, ovoid, protruding from the joints. Female flowers on similar 'spikes', with only stigmas protruding out of the joints; perianth irregularly toothed or short-lobed; fruiting calyx spongy, c. 3 x 2 mm, adherent to the horny pericarp; seed c. 1 mm long (Encyclopedia of Life 2016). Image source: http://www.asergeev.com/.

Global Distribution: Mediterranean coast of S.Europe, N. Africa, Egypt, Saudi Arabia, Middle East, Iran and Pakistan (Encyclopedia of Life 2016).

Distribution within Arabian Gulf Countries: Saudi Arabia, Yemen, Socotra, Oman, UAE, Qatar, Bahrain, Map 328 (Miller & Cope 1996).

Habitat: Seashores, mud-flats, coastal dunes and salt-marshes; sea-level (Miller & Cope 1996).

Current Status: *Arthrocnemum macrostachyum* is not yet classified on the IUCN Red List (ARKive 2016).

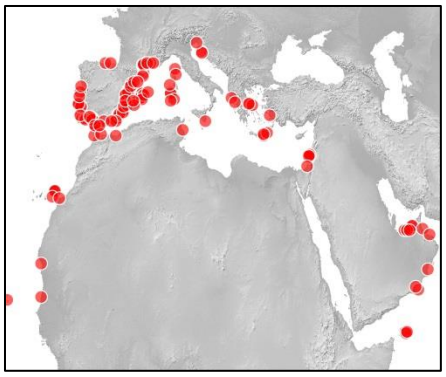

Figure 2 Points used to fit Maxent model.

Atriplex leucoclada

Common Name: Orache, Raghal

Description: Perennial herb up to 80cm, basal part and lower branches woody; stems decumbent to erect, slender, branched mainly from the base. Leaves petiolate to sessile, triangular-deltoid to broadly ovate-cordate, 0.5-2.5x0.2-2cm, acute at the tip, entire, undulate or sinuate-dentate, hastate to almost rounded at the base. Flowers in axillary and terminal spikes or panicles, the axillary pistillate, the terminal staminate and pistillate. Fuiting bracteoles deltoid, quadrangular or campanulate, 3-5x2-5mm, lobed or toothed, connate at the base, free above (Miller & Cope 1996). Image source: http://www.asergeev.com/.

Global Distribution: Egypt to SW Asia[14]

Distribution within Arabian Gulf Countries: Saudi Arabia, Yemen, Oman, UAE, Bahrain, Kuwait, Map 315 and Map 316 (Miller & Cope 1996).

Habitat: Coastal plains and desert wadis on limestone, sandstone, or volcanic soils; 0-2500m. (Miller & Cope 1996).

Current Status: *Atriplex leucoclada* has not yet been assessed by the IUCN Red List (ARKive 2016).

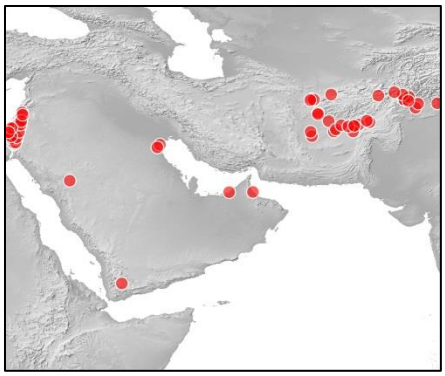

Figure 3 Points used to fit Maxent model.

Avicennia marina

Common Name: Gray Mangrove

Description: Evergreen shrub or small tree 1–10 m high, trunk to 40 cm in diameter. Numerous upright pneumatophores 10–15 cm high and 6 mm in diameter. Trunk often with masses of small air roots but no prop or stilt roots. Bark whitish to grayish or yellow-green, smooth, often powdery with raised dots, scaly, exposing greenish inner bark. Leaves opposite, ovate, lanceolate to elliptical, 3.5–12 cm long, 1.5–5 cm wide, mostly acute at both ends, entire, thick leathery, shiny green and hairless upper surface, pale whitish-gray and finely hairy underneath. Petiole 5–10 mm long, hairy. Heads or cymes ball-like, upright on long stalks at ends and sides of twigs. Flowers few to many, sessile, 4 mm long, 5 mm across. Calyx 5-lobed, green, hairy, persistent; corolla tubular, white.turning yellow or orange with 4 nearly equal, short lobes. Image source: http://www.asergeev.com/.

Global Distribution: It can be found in East Africa and the Middle East including Bahrain, Djbouti, Egypt, Eritrea, Iran, Kenya, Madagascar, Maldives, Mozambique, Oman, Qatar, Saudi Arabia, Seychelles, Somalia, South Africa, Sudan, Tanzania, United Arab Emirates, and Yemen (IUCN 2016).

Distribution within Arabian Gulf Countries:

Habitat: Avicennia marina is a shrub to medium sized tree, 2-5 m tall. This species is found from downstream to intermediate estuarine zones in all intertidal regions. It is found at the mouth of rivers or in lower tidal areas. It is shade intolerant with a maximum porewater salinity of 85 ppt. Optimal growth occurs at a salinity of 0-30 ppt.
This is a pioneer species on newly formed habitats of mud with a high proportion of sand, but does not seem to grow on pure mud. It is a hardy species in natural conditions and regenerates quickly from coppices, both as individuals and as a species. It is a colonizing species on newly formed mudflats in SE Asia and has a high tolerance to hypersaline conditions (IUCN 2016).

Current Status: Least Concern (IUCN 2016).

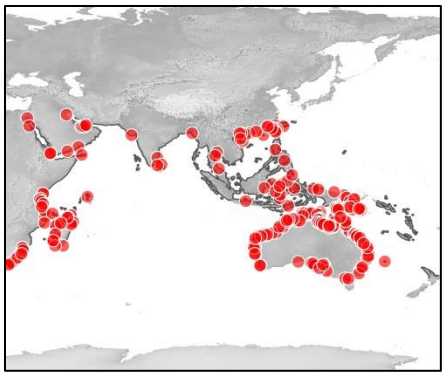

Figure 4 Points used to fit Maxent model. Range polygon from IUCN 2016.

Calligonum comosum

Common Name: Arta`, A`bal , Waragat Alshams

Description: Virtually leafless perennial shrub up to 2.5m tall, stem much branched from thick woody rootstock. Main stems dark and rough often with peeling bark, older branches white with swollen nodes, less rough but angular and fragile and often dropping. Twigs slender, dark green looks from a distance like long trailing hairs. Image source: http://www.free-photos.biz/.

Global Distribution: Distributed around northeast Africa, Egypt, Sinai, Palestine, Arabia to Pakistan.

Distribution within Arabian Gulf Countries: Map 160 (Miller & Cope 1996).

Habitat: Sand plains, dunes and roadsides.

Current Status: Not Evaluated.

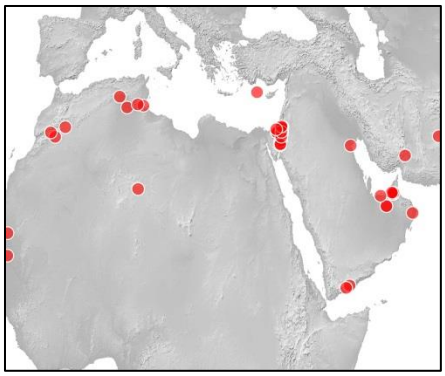

Figure 5 Points used to fit Maxent model.

Cleome amblyocarpa

Common Name: Spider Flower, Adheer

Description: Annual or sometimes perennial, erect, densely glandular herb with unpleasant smell, much branched, up to 50cm high. Image source: http://www.asergeev.com/.

Global Distribution: North and east Africa, Sinai, Palestine Arabia, Iraq, Iran (Encyclopedia of Life 2016).

Distribution within Arabian Gulf Countries: Saudi Arabia (NW-Saudi Arabia: Hejaz), Sinai peninsula (Central Sinai, Northern Sinai, Southern Sinai), Yemen (Aden Desert, Inner Hadhramaut, N-Inner Yemen, SW-Yemen, W-Yemen), Oman, United Arab Emirates, Iran (S-Iran), Iraq (S-Iraq: Desert, W-Iraq: Desert) (GBIF 2016). Map 479 (Miller & Cope 1996).

Habitat: Sandy coastal dunes, waste ground, desert wadis and plains (Encyclopedia of Life 2016). Sand and disturbed land, gravel and rocky limestone places.

Current Status: *Cleome amblyocarpa* is not yet classifed on the IUCN Red List (ARKive 2016).

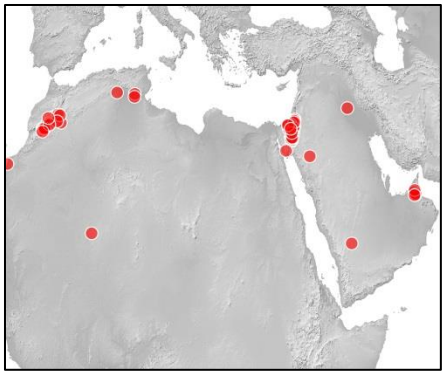

Figure 6 Points used to fit Maxent model.

Cyperus conglomeratus

Common Name: Thenda, Dune Grass, Sedge

Description: Perennial sedge, variable in aspect from dwarf form with single stem a few centimetres high to bushy plants with several stems up to 70cm in height. Roots rigid, fibrous and woolly covered with a thick coating of sand; base of the plant usually surrounded by old brown leaf sheaths. Stems stout; young growth pale green but for much of year plant is dull brown or straw-like . Image source: http://www.asergeev.com/.

Global Distribution: Mauritania, Morocco, Algeria, Tunisia, Libya, Egypt, Palestine, Syria, Iraq, Arabia, Iran, Afghanistan, Pakistan, Senegal, Mali, Niger, Chad, central African Republic, Sudan, Ethiopia, Eritrea, Somalia (Encyclopedia of Life 2016).

Distribution within Arabian Gulf Countries: *Arabian Peninsula* Gulf States Kuwait, Oman, Saudi Arabia, Yemen

Habitat: Sandy places, including sand dunes. Quickly colonizes disturbed ground, drought resistant. One of the few plants that colonize the mobile dunes of the interior desert . Inland and coastal sand dunes, desert sandy plains (Encyclopedia of Life 2016).

Current Status: Status not found, however: Very common and widespread in UAE . The most dominant plant species in the sand of the UAE is *Cyperus conglomeratus*.

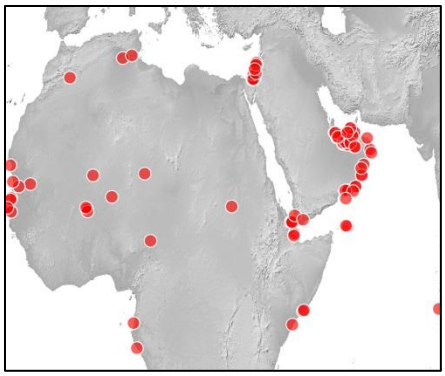

Figure 7 Points used to fit Maxent model.

Delonix elata

Common Name: White Gul Mohur, Yellow Gul Mohur, Creamy Peacock Flower

Description: An erect tree, 6-10 m tall, bark ash-coloured. Leaves 6-20 cm long, bipinnate¬ly compound, pinnae 4-8 pairs, 4-6 cm long, leaflets l0-20 pairs, sessile or subsessile, linear-oblong, obtuse, sometimes slightly mucronate, narrowed towards the base, 7-15 mm long, c. 2-3 mm wide. Inflorescence terminal raceme, the lower flower with the longest pedicel, pedicel hairy, up to 2.5 (-3) cm long. Calyx 2-3 cm long, fused at the base, leathery, silky pubescent, oblong, narrow and sharp pointed. Corolla white in the beginning, turning yellow, the upper petal is smaller and darker in colour; sub-orbicular, curled at the margins, c. 2.5 cm long. Stamens hairy, dark coloured, 5-10 cm long, thickened at the base. Pods 12.5-20 cm long, c. 6-25 mm broad, smooth, narrow at both the ends. Seeds 4-8 (Encyclopedia of Life 2016). Image source: https://www.flickr.com/.

Global Distribution: The species is found naturally between 25 degrees north to 8 degrees south. From India (possibly planted) in the west, across Oman, Saudi Arabia, Yemen and Egypt, down through Ethiopia, Somalia, Kenya, Tanzania and across to the Democratic Republic of the Congo. Also widely cultivated as an avenue tree and for shade and green manure. Recorded from sea level up to 2,000 m and occasionally as high as 4,000 m (Encyclopedia of Life 2016).

Distribution within Arabian Gulf Countries: Native: Saudi Arabia, Yemen; Introduced: Oman (IUCN 2016).

Habitat: A perennial medium-sized tree found growing in woodland or thicket vegetation. Capable of growing on poor soil (IUCN 2016).

Current Status: Least Concern (IUCN 2016).

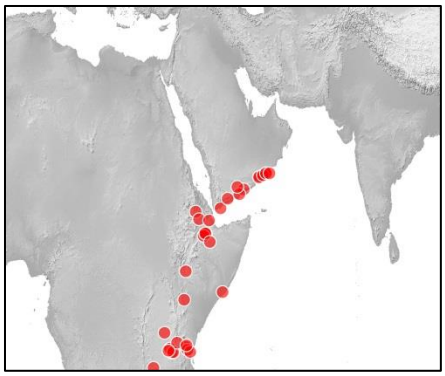

Figure 8 Points used to fit Maxent model.

Dodonaea viscosa

Common Name: Hopbush, Candlewood

Description: Shrub or small tree. Leaves *simple* yellowish-green, glabrous, *resinous*; lamina narrowly elliptic; apex acute or acuminate; base decurrent into the petiole. Inflorescences terminal on the branches. Flowers greenish-yellow at first, often turning reddish later. Stamens 6. Style 4-6 mm long. Fruits with 2-3 papery wings (Encyclopedia of Life 2016). Image source: http://www.asergeev.com/.
Global Distribution: Widely distributed through the southern hemisphere including Australia, New Zealand, South and Southeast Asia, Africa and Latin America; also occurring in the southern United States. It is tolerant of drought and can grow in coastal environments. It is intolerant of frost and does not grow well in shade (Royal Botanic Gardens 2016).

Distribution within Arabian Gulf Countries: Arabia (Encyclopedia of Life 2016).

Habitat: Forest margins, savannahs, coastal vegetation on or behind sandy beaches (Encyclopedia of Life 2016).

Current Status: *Dodonaea viscosa* has yet to be classified by the IUCN Red List (Royal Botanic Gardens 2016).

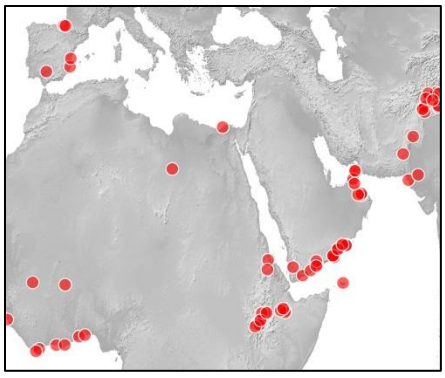

Figure 9 Points used to fit Maxent model.

Eremobium aegyptiacum

Common Name: Eremobium, Ghurayra, Sleisla

Description: Small, greyish–green, annual to 35cm high, usually shorter with several thin slender stems branching prostrate or ascending from the base. Hairy, young stems are sticky and are therefore often covered with sand; white color but can be reddish .
Global Distribution: Sinai, Palestine, Arabia, Iraq, Iran, Pakistan (Encyclopedia of Life 2016).

Distribution within Arabian Gulf Countries: Qatar (Flora of Qatar 2016), Iraq, UAE, possibly other countries (Encyclopedia of Life 2016).

Habitat: Desert plant, common in the UAE in a variety of habitats, including gravel plains, hillsides, wadis and plantations, often in association with Acacia tortilis and Prosopis cineraria .

Current Status: Not Evaluated (ARKive 2016).

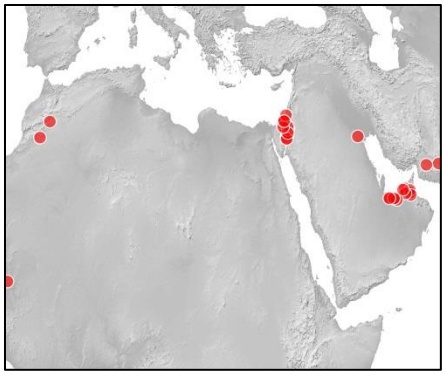

Figure 10 Points used to fit Maxent model.

Halopyrum mucronatum

Common Name:

Description: Tough stoloniferous perennial, the stolons rooting to form dense tussocks; roots thick and tomentose; culms up to 1 m or more high, rigid, woody, branching, producing fascicles of shoots at the nodes. Leaf-blades up to 45 cm long, involute or opening out and up to 4 mm wide, stiff, mostly glaucous. Inflorescence linear to narrowly lanceolate, 1040 cm long, the branches loosely 3-7-spiculate. Spikelets 8-25-flowered, lanceolate to ovate or oblong, 12-26 mm long, 5-7 mm wide, straw-coloured or tinged with purple; glumes narrowly ovate, 6-9 mm long, coriaceous, acute; lemmas lanceolate to oblong-lanceolate, 7-9 mm long, asperulous or very minutely hairy; callus and rhachilla-tip bearded with white hairs 4-5 mm long (Encyclopedia of Life 2016). Image source: http://www.asergeev.com/.

Global Distribution: Africa: north, northeast tropical, east tropical, southern tropical, and western Indian ocean. Asia-temperate: western Asia and Arabia. Asia-tropical: India (Royal Botanic Gardens 2016).

Distribution within Arabian Gulf Countries:

Habitat: Coastal dunes, growing up through successive accretions of sand (Encyclopedia of Life 2016).

Current Status: This species has yet to be classified by the IUCN (ARKive 2016).

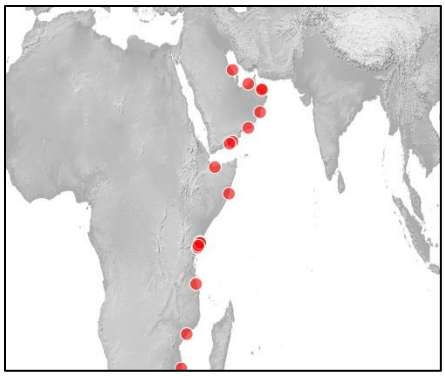

Figure 11 Points used to fit Maxent model.

Haloxylon salicornicum

Common Name: Rimth

Description: Large perennial woody plants, much branched, erect, almost leafless shrub up to 150cm high, usually with accumulated sands around the base. Branches thick and jointed, erect or ascending, bluish-green and fleshy when young, gradually hardening to dirty grey in colour and drying yellow .
Global Distribution: The plant is native to: Egypt; Libya; Tunisia; Algeria; Palestine; Jordan; Syria; Lebanon; Iraq; Kuwait; Central and Eastern of the Arabian Peninsula; Iran; Afghanistan; Pakistan; and India .

Distribution within Arabian Gulf Countries: Iraq; Kuwait; Central and Eastern of the Arabian Peninsula .

Habitat: Stable sand, especially in the central areas and on alluvial gravel plains of stony desert (Encyclopedia of Life 2016).

Current Status: Not Evaluated (Encyclopedia of Life 2016).

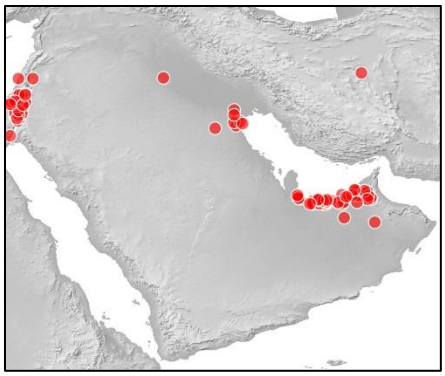

Figure 12 Points used to fit Maxent model.

Heliotropium digynum

Common Name: Kary, Jery

Description: Perennial densely branched shrub with woody base, stems round, whitish, small plant erect; older ones spreading outwards, up to 60 cm .
Global Distribution: The species is native to North Africa (Egypt, Tunisia, and Algeria), Arabian Peninsula, Iraq, Israel and Jordan .

Distribution within Arabian Gulf Countries: Arabian Peninsula, Iraq .

Habitat: Sand between dunes and sandy plains. Widespread in sandy deserts, between dunes and sandy plains, also in shade of Eucalyptus plantations .

Current Status: Not Evaluated .

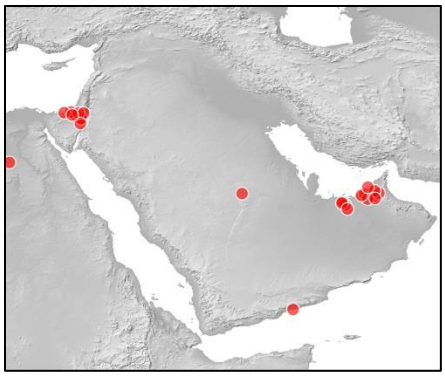

Figure 13 Points used to fit Maxent model.

Juniperus procera

Common Name: African Pencil Cedar, East African Cedarwood, African Juniper

Description: The African pencil cedar (Juniperus procera), the tallest of all juniper species in the world, acquired its name from its extensive use in the manufacturing of pencils. The trunk is straight and sharply tapered, covered with bark varying in colour from pale brown to reddish brown. Young African pencil cedars have needle-like leaves, one to two centimetres long, and as the plant ages the foliage gradually changes to the scale-like adult leaves, which are light-green or yellowish-green and only up to six millimetres long. Male African pencil cedars bear numerous, tiny male cones at the ends of branches. These greenish to orangey-brown structures are composed of scales, each containing two to three pollen sacs. Female plants bear the female cones; reddish-brown to blue-black, berry-like structures made of fleshy scales, each one containing a single ovule (ARKive 2016). Image source: https://www.flickr.com/.

Global Distribution: Recorded from NE, E and S Tropical Africa: Democratic Republic of the Congo, Djibouti, Eritrea, Ethiopia, Kenya, Malawi, Somalia, Sudan (near Red Sea), Tanzania, Uganda, NE Zimbabwe; Arabian Peninsula: Saudi Arabia (Asir Range), Yemen. Widespread from Arabia to Zimbabwe. Existing populations in the Arabian Peninsula represent a small fragment of the woodlands that once existed. Outlying populations in Zimbabwe, the Democratic Republic of the Congo and Malawi are extremely small and threatened (IUCN 2016).

Distribution within Arabian Gulf Countries: Saudi Arabia, Yemen (IUCN 2016).

Habitat: The African pencil cedar is found in mountainous areas and highlands, on rocky ground. In Africa, it occurs at altitudes between 1,050 and 3,600 metres, but is most common between 1,800 and 2,700 metres. Juniperus procera occurs on mountain slopes, summits, on escarpments and outcrops and in forested ravines in sand, loam or clay over various rock types, e.g. basalt, volcanic ash and cinders, granite, limestone, or metamorphic rock. The altitudinal range is 1,370-3,000 m a.s.l. The climate is tropical montane, with a prolonged dry season (IUCN 2016).

Current Status: Least Concern (IUCN 2016).

Figure 14 Points used to fit Maxent model.

Limeum arabicum

Common Name: Berjan

Description: Straggly perennial erect shrub up to 80cm, stems intricately tangled; very thin waxy-white angular stems, branches gently zigzagging at 3-5cm intervals. Whole plant appears fragile and covered with minute glands to which fine sands tend to cling . Image source: http://www.asergeev.com/.

Global Distribution: Saudi Arabia (NE-Saudi Arabia, C-Saudi Arabia, S-Saudi Arabia: Rub al Khali), Oman, United Arab Emirates, S-Yemen (GBIF 2016).

Distribution within Arabian Gulf Countries: Saudi Arabia (NE-Saudi Arabia, C-Saudi Arabia, S-Saudi Arabia: Rub al Khali), Oman, United Arab Emirates, S-Yemen (GBIF 2016). Map 184 (Miller & Cope 1996).

Habitat: Lower sand dunes. Common locally in central desert always in deeper sand away from the coast .

Current Status: Not Evaluated[1] *Limeum arabicum* has not yet been assessed by the IUCN (ARKive 2016).

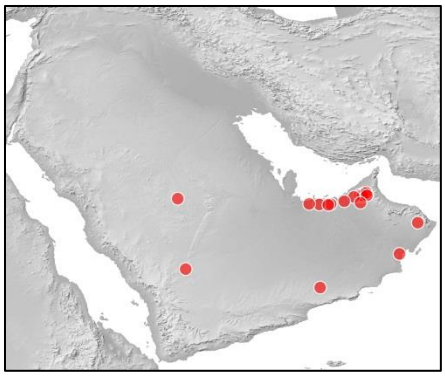

Figure 15 Points used to fit Maxent model.

Moringa peregrina

Common Name: Wispy-needled yasar tree

Description: Shrub or small tree up to 10 m tall, with tuberous rootstock; bole up to 40 cm in diameter; bark grey, purple-grey or bright brown; crown ovoid; branches terete, slender, young stems grey-white or waxy blue-green; twigs brittle. Leaves alternate, in bunches at the ends of branches, 15–40 cm long, 2–pinnate, with 2–5 pairs of pinnae; leaflets opposite or alternate, obovate, oblanceolate or spatulate, 3–20(–35) mm × 2–10(–13) mm, base cuneate to rounded, apex rounded or notched, grey or waxy green. Inflorescence an axillary, lax, much-branched panicle 18–30 cm long. Flowers bisexual, slightly zygomorphic, 5-merous, white with purple heart or pink-flushed, sometimes scented; pedicel 2–9 mm long, jointed; sepals free, oblong to lanceolate, 7–9 mm × 1.5–3 mm, acuminate, hairy on both surfaces; petals free, narrowly oblong, obovate or spatulate, 8–15 mm × 2–5 mm, hairy inside; stamens 5, free, 4.5–7 mm long, alternating with 5 staminodes, 4–5 mm long; ovary superior, shortly stalked, cylindrical, hairy, 1-celled, style slender. Fruit an elongate capsule (10–)32–39 cm × (1–)1.5–1.7 cm, somewhat trigonous, slightly narrowed between the seeds, with a beak, glabrous, dehiscent with 3 valves. Seeds globose to ovoid or trigonous, 10–12 mm × 10–12 mm, brown ("PROTA4U" 2016).
Global Distribution: Tropical Northeast Africa, Southwest Asia (Encyclopedia of Life 2016).

Distribution within Arabian Gulf Countries: Saudi Arabia, Oman, Yemen, United Arab Emirates (Encyclopedia of Life 2016).

Habitat: Rocky Slopes and Wadis (Encyclopedia of Life 2016).

Current Status: This species has not yet been classified by the IUCN (ARKive 2016).

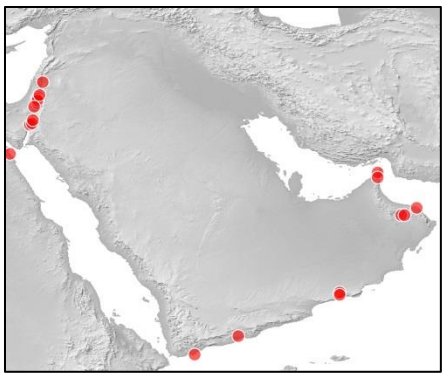

Figure 16 Points used to fit Maxent model.

Panicum turgidum

Common Name: Thamam, Merkba

Description: Glaucous suffruticose perennial forming bushes 40-100(-200) cm high and often as much through; culms erect or ascending, woody, usually dichotomously branched at the nodes, sometimes also forming fastigiate tufts of branches. Leaf-blades linear-lanceolate, (0.5)2-15 cm long, 16 mm wide, flat, folded or convolute, glabrous and glaucous, stiff and pungent, often much shorter than their sheath. rarely filiform and up to 30 cm long. Panicle subpyramidal, 2.5-15(-30) cm long, lax, the branches distant and eventually spreading, spiculate to the base. Spikelets ovoid, (3.1-)3.4-4.4(-5) mm long, glabrous, acute or acuminate, turgid and often widely gaping at anthesis; lower glume broadly ovate, three-quarters to almost as long as the spikelet, 5-9-nerved; upper glume 7-9-nerved; lower lemma 9-11-nerved, its palea almost as long; upper lemma pallid or yellowish, smooth and shining (Encyclopedia of Life 2016). Image source: http://www.asergeev.com/.
Global Distribution: Mauritania, Morocco, Tunisia, Libya, Egypt, Cyprus, Palestine, Arabia, Iraq, Iran, Pakistan, Sudan, Ethiopia, Eritrea, Somalia (Encyclopedia of Life 2016).

Distribution within Arabian Gulf Countries: Through the Arabian peninsula (FAO 2016).

Habitat: Sand and gravel.[1] Sand dunes on the edge of the Sahara, the arid Red Sea coast, and dunes in India. It is usually found on deep dune sand, but will grow in a well-drained latosol (FAO 2016).

Current Status:

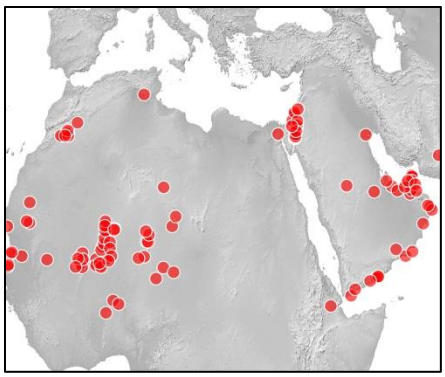

Figure 17 Points used to fit Maxent model.

Prosopis cineraria

Common Name: Khejri, Jandi, Jand, Ghaf

Description: Small tree 3-5 m high with a rounded canopy, often lopped to feed stock. Life expectancy is about 200 years or more, branches and twigs bear short (3-6 mm) thorns all along the internodes, by contrast with the new-world species where thorns are axillary. Leaves are bipinnate 1.2-5 cm long bearing 1-3 pairs of pinnae having 7-14 pairs of sub-sessil leaflets 4-15 mm long x 2-4 mm wide, each. Flowers are small, cream-yellow clustered in acute spikes 5-23 cm long with a 1-2.5 mm long peduncle. Pods are pale yellow, 8-25 cm long x 4-8 mm wide, cylindrical and hanging, containing 10-25 seeds ovoid in shape and dark brown in color, packed in a brown pulp. Flowering in India occurs in February-March in the mid-dry season, pods are mature in May-June before the onset of the rains (FAO 2016). Image source: https://www.flickr.com/.

Global Distribution: Occurs naturally in the dry regions of India, Pakistan, Afghanistan, Iran, and Arabia. Extremely drought tolerant, growing in areas with less than 75mm annual rain fall and temperatures of up to 50°C .

Distribution within Arabian Gulf Countries: Oman, Pakistan, Saudi Arabia, the United Arab Emirates, and Yemen (Encyclopedia of Life 2016).

Habitat: Sand plains, dunes and wadi banks. Grows at altitude from sea level up to 600m above sea level; favoured habitat sand plains and dunes or wadi banks .

Current Status: Not Evaluated .

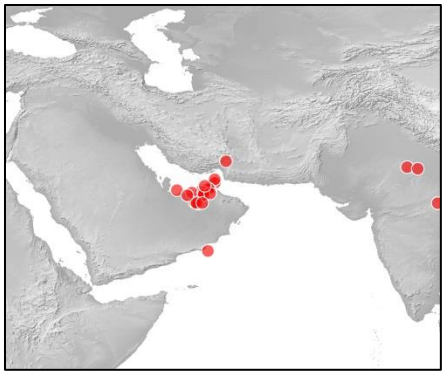

Figure 18 Points used to fit Maxent model.

Rhazya stricta

Common Name: Harmal, Senhwar, Sahaer, Dogbane

Description: Rhazya stricta is an evergreen dwarf shrub of the Apocianaceae family, which contains around 1,300 herbs, shrubs and trees, many of which have important medicinal and economical value. Growing in deserts and arid valleys, the appearance of Rhazya stricta depends upon its habitat. The shrub is stunted and yellowish-green where the soil is formed of coarse materials and rainfall is low, but is bigger and dark green where the soil is fine and water is in abundance. The leaves are highly variable in shape, but are often narrowly oval. The flowers are arranged into a flattened cluster and are borne on short stalks, with the round petals being bluish-green on the outside of the flower and white on the inside. The cylindrical, long fruit pods encase narrowly-winged, flattened, brown seeds (ARKive 2016).

Global Distribution: Rhazya stricta is widely distributed around the coastlines of the Arabian peninsula, ranging into Iran, southern Afghanistan and Pakistan (ARKive 2016).

Distribution within Arabian Gulf Countries:

Habitat: Rhazya stricta occurs in deserts and dry valleys (known as wadis) (ARKive 2016).

Current Status: Not Evaluated (ARKive 2016).

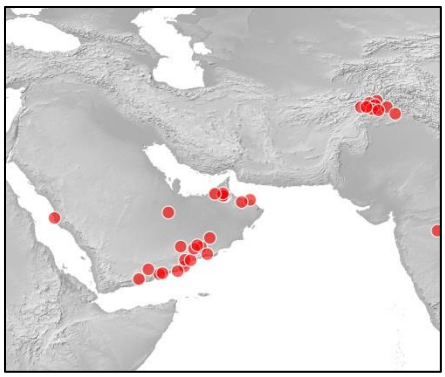

Figure 19 Points used to fit Maxent model.

Ziziphus spina-christi

Common Name: Christ's Thorn Jujube, Gaba, Kurkura, Areen, Sidra

Description: A medium-size tree, with spreading, greyish white branches, glabrous or slightly pubescent. Stipular spines in pairs, one erect, c. 2 cm long, the other recurved 5-8 mm long, sometimes spines absent. Leaves 2-6 x 1-4 cm ovate-elliptic or suborbiculer, glabrous or pubscent on nerves beneath, rounded to subcordate at base, obtuse or shortly acuminate, margin entire or obsoletely crenate, 3-nerved; petiole 3-12 mm long, glabrous or puberulous. Inflorescence axillary tomentose, pedicel woolly, c. 3-5 mm long. Flowers 4-6 mm across, greenish yellow. Calyx c. 1 mm long, keeled within, pubescent, ovate, ± acute, petals spathulate; 1.25 mm long. Disc prominently 10-lobed, glabrous, grooved (Encyclopedia of Life 2016).

Global Distribution: Christ's thorn is found in West and North Africa, the Middle East, northwest India and the eastern Mediterranean (ARKive 2016).

Distribution within Arabian Gulf Countries: Arabia (Encyclopedia of Life 2016).

Habitat: Christ's thorn is typically found in areas of relatively low rainfall and is capable of growing in areas of desert or semi-desert where the soils are often silty (containing fine deposits of mud and clay particles). It grows up to elevations of around 600 metres, although it has been reported at 1,500 metres in the United Arab Emirates (ARKive 2016).

Current Status: *Ziziphus spina-christi* has yet to be classified by the IUCN (ARKive 2016).

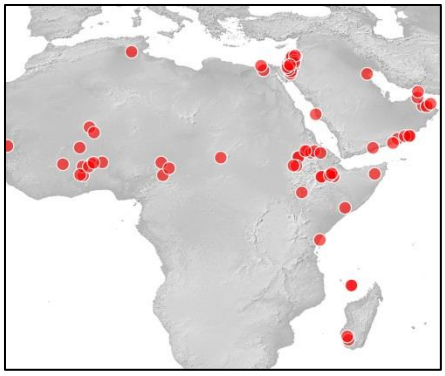

Figure 20 Points used to fit Maxent model.

Amphibians

Bufo arabicus

Common Name: Arabian Toad

Description: The Arabian toad (Bufo arabicus) is one of only nine species of amphibian found in the Arabian Peninsula, and by far the most common of the two toad species that occur in the United Arab Emirates. The Arabian toad's body varies in colour, appearing green, tan, brown and even grey, usually with vivid, golden speckling on the upperparts. Other distinctive features of this species include a rounded head and snout, along with small eardrums located behind the large, prominent eyes. The female is also significantly larger than the male. The vocalisation of the Arabian toad is a prolonged "krrraaaa", reminiscent of a creaking door hinge (ARKive 2016).

Global Distribution: Endemic to the Arabian Peninsula, the Arabian toad occurs in widely separated areas within north-west, central and south-west Saudi Arabia, as well as the offshore Farasan Islands. It can also be found in west and south-central Yemen, north Oman and the United Arab Emirates. The Arabian toad has been recorded from sea-level to elevations of 2,300 metres (ARKive 2016).

Distribution within Arabian Gulf Countries: Oman, Saudi Arabia, United Arab Emirates, Yemen (IUCN 2016).

Habitat: The Arabian toad is restricted to areas with surface water, occurring opportunistically wherever these sites occur. This species' natural distribution encompasses mountain regions, where it inhabits springs, as well as permanent and seasonal small rivers, and lowland gravel plains, where it occupies oases. The Arabian toad may also be found in artificial water sources, such as garden ponds and irrigation canals (ARKive 2016).

Current Status: Least Concern (IUCN 2016).

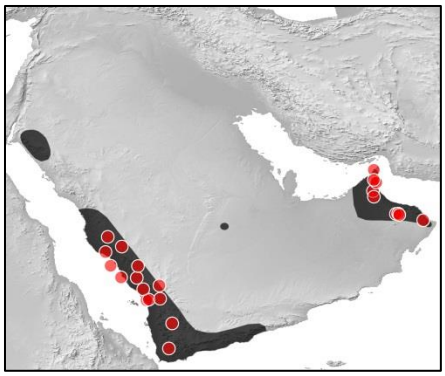

Figure 21 Points used to fit Maxent model. Range polygon from IUCN 2016.

Bufo dhufarensis or *Duttaphrynus dhufarensis*

Common Name: Dhofar Toad

Description: The Dhofar toad is one of only two amphibians in the United Arab Emirates, and, incredibly, one of just nine in the whole of the Arabian Peninsula. Exhibiting considerable variation in colour and pattern, the body of this relatively small Bufo can range from green to tan to brown, and be either mottled or uniform. Distinctive features of this species include large, prominent eardrums positioned immediately behind the protruding eyes, and a distinctive staccato "kra-kra-kra" breeding call (ARKive 2016).

Global Distribution: The Dhofar toad occurs throughout much of the southern Arabian Peninsula, including Oman, Saudi Arabia, the United Arab Emirates and Yemen, as well as on the Farasan Islands and several other offshore islands (ARKive 2016). The altitudinal range of the species is sea level to 2,200m asl (IUCN 2016).

Distribution within Arabian Gulf Countries:

Habitat: Found wherever there are water sources, including gardens, oases, springs, canals and small rivers, but this arid environment specialist is also frequently found some distance from permanent water bodies (ARKive 2016).

Current Status: Least Concern (IUCN 2016).

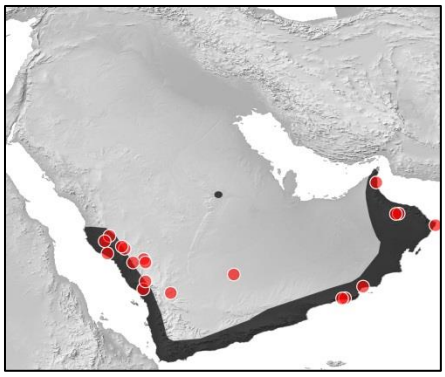

Figure 22 Points used to fit Maxent model. Range polygon from IUCN 2016.

Hyla savignyi

Common Name: Lemon-yellow Tree Frog

Description: The lemon-yellow tree frog (Hyla savignyi) is a medium-sized frog with long hind limbs and slight webbing between the digits on the feet. The tips of the digits are expanded into discs, which are smaller on the hind limbs than on the forelimbs. The back of the lemon-yellow tree frog is smooth, while the throat and underside have a rough texture.
As its common name suggests, the lemon-yellow tree frog is typically yellowish to light green, but variations of brown and straw colouration can also exist. Its overall colouration varies depending on factors such as the external temperature and the colour of the substrate that the frog lives on. The underside of the lemon-yellow tree frog is white, and a dark line extends along the side of the body from the nostrils to the hind legs.
The male and female lemon-yellow tree frog are very similar in appearance, but can be distinguished from one another by the large vocal sac that is visible externally on the male frog, appearing as darker folds and wrinkles of skin on the throat.
The lemon-yellow tree frog was previously considered to be a subspecies of the common tree frog (Hyla arborea), but differs slightly in its colouration and in its calls (ARKive 2016).
Image source: https://www.flickr.com/.

Global Distribution: The lemon-yellow tree frog has a widespread distribution across western Asia and the Middle East, from Cyprus and Turkey, through Syria, Georgia, Armenia, Iraq and Azerbaijan to Iran. It also occurs south into Israel and Jordan, and in a small area in north-eastern Sinai, Egypt, near the border with Israel. An isolated population also occurs in the south-western Arabian Peninsula, in Saudi Arabia and Yemen (ARKive 2016).**Distribution within Arabian Gulf Countries:** Iran, Iraq, Saudi Arabia, Yemen (IUCN 2016).

Habitat: This species lives in much drier landscapes than H. arborea schelkownikowi, including steppes, deserts and semi-deserts. It occurs mainly near water bodies, in wet sites, oases, gardens, bushlands, and mountain forest edges. Individuals may be found sitting on trees, bushes, leafs and on land under logs, stones and in burrows. Animals may even be found at long distances from water bodies in xeric environments, such as rocky slopes and on the xerophytic bushes. Reproduction occurs in small stagnant water bodies (ponds and puddles, some of which are very small) and slowly flowing brooks with dense herbaceous and shrub vegetation (Encyclopedia of Life 2016).

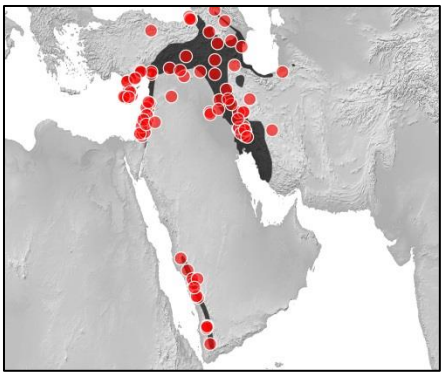

Figure 23 Points used to fit Maxent model. Range polygon from IUCN 2016.

Current Status: Least Concern (IUCN 2016).

Reptiles

Bunopus tuberculatus

Common Name: Baluch Rock Gecko, Baluch Ground Gecko, Button-scaled Gecko

Description: The Baluch ground gecko (Bunopus tuberculatus) is a small, ground-dwelling gecko with rather short, straight toes, a long tail, and conspicuous tubercles on the back and flanks. The body is generally tan coloured, giving good camouflage against its sandy habitat, and the tail is barred. Young Baluch ground geckos have a prominent dark stripe through the eye, which may fade with age, and the eye itself has a vertical pupil. As in other geckos, the eyelids are fused together, forming a transparent covering to the eye. However, unlike many other geckos, the Baluch ground gecko lacks expanded toe pads, and is therefore unable to climb vertical surfaces (ARKive 2016). Image source: http://www.asergeev.com/.

Global Distribution: The Baluch ground gecko is found in the Middle East, Arabian Peninsula and southwest Asia, from Israel, Jordan and Syria, south into Saudi Arabia, United Arab Emirates and Oman, north to Turkmenistan, and east to Pakistan (ARKive 2016). This species ranges from the Arava Valley in southern Israel, through Jordan, northeastern Syria, to Iraq, Iran and Central Asia (southern Turkmenistan, Afghanistan and eastern Pakistan). It is also widespread on the Arabian Peninsula in much of Saudi Arabia, Kuwait, the United Arab Emirates, Oman and northeastern Yemen. It occurs from the lowlands up to 2,100 m above sea level (Afghanistan) (IUCN 2016).

Distribution within Arabian Gulf Countries: Iran, Iraq, Kuwait, Oman, Saudi Arabia, United Arab Emirates, Yemen (IUCN 2016).

Habitat: The Baluch ground gecko is reported to be abundant and widespread in vegetated sandy plains and in coastal habitats.[6] This nocturnal, ground dwelling species is found on a variety of different desert soil substrates, both soft and hard. Animals can be found resting in dead palm trees and under ground cover. The female lays clutches of two eggs. It can be found in lightly modified habitats, such as sandy fields, in rural areas (IUCN 2016).

Current Status: Least Concern (IUCN 2016).

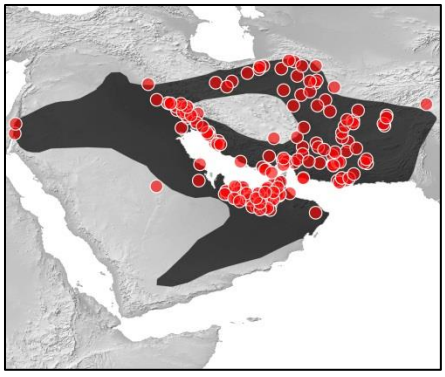

Figure 24 Points used to fit Maxent model. Range polygon from IUCN 2016.

Cerastes cerastes

Common Name: Desert Horned Viper, Saharan Horned Viper

Description: A medium to fairly large snake, with a short, stocky body. Largest Egyptian specimen has a total length of 735 mm. Tail short, tail / total length = 0.08-0.13. Nostril round; 11-15 supralabials; eye moderate, separated from supralabials by 4-5 scales, pupil vertical; scales on dorsal side of head moderate, more than 14 interorbitals; a supraocular horn made of a single spine-like scale, present or absent; dorsals strongly keeled, 28-39 scale rows around mid-body; 137-156 ventrals, 23-45 paired subcaudals; anal entire. Dorsum sandy, with a usual pattern of large, brownish, rounded or square spots along mid-dorsum, alternating with smaller lateral dark spots; a dark band between the posterior of the eye to the angle of the mouth. Venter plain white (ARKive 2016). Image source: https://www.flickr.com/.

Global Distribution: Sahara horned vipers are among the most abundant and easily distinguishable of the venomous snakes of the North African and Middle Eastern deserts. Cerastes gasperettii is generally distributed all across North Africa, including southwestern Arabia and southwestern Israel. Common in the Sahara desert, it is most frequently found between Egypt and Morocco. Its range extends to southward to northern Mali, Niger, northern Chad, Sudan, and Mauritania (ARKive 2016).

Distribution within Arabian Gulf Countries: Oman, Saudi Arabia (ARKive 2016).

Habitat: Found throughout the Sahara in Northern Africa, C. cerastes inhabits a variety of habitats within the desert, including rock hills, sandy deserts, and wadis. Members of this species can sometimes be found in dunes, and are rarely found on rock pavement and gravel plains.
It has been determined that there is a strong correlation between microclimate and the general distribution of this species. Saharan horned vipers generally prefer cooler temperatures, with annual averages of 20°C or lower, and are usually found in altitudes of up to 1500m. Even humidity is important when considering the locality of these snakes. Temperatures must be high enough for the snake to bask and obtain heat, and humid enough to retain a maximum amount of water present in the body, as the only source of water is from prey (ARKive 2016).

Current Status: Least Concern (ARKive 2016).

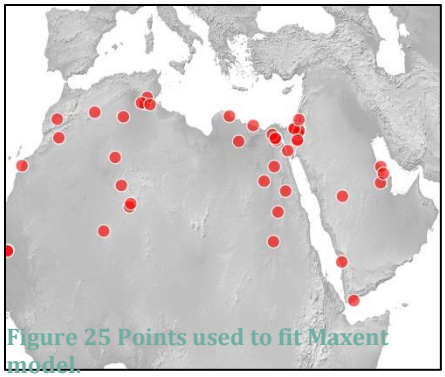

Figure 25 Points used to fit Maxent model.

Chamaeleo chamaeleon

Common Name: Mediterranean Chameleon

Description: Due to its amazing ability to change colour, the Mediterranean chameleon (Chamaeleo chamaeleon) can vary from bright green to dull brown, tan or grey. Females may also display yellow, orange or green spots during the mating season, and are generally slightly heavier than the males. Whatever its background colour, the Mediterranean chameleon generally has two light stripes along each side of its body, with the stripes often being broken into a series of dashes or spots .
Like other chameleons, the Mediterranean chameleon is well known for its long, sticky tongue which, when extended, can be twice the length of the body. Chameleons have very sharp eyesight and each eyeball is able to move independently of the other. The Mediterranean chameleon is well adapted to living in bushes and trees, with strong feet to hold firmly onto branches and a long, prehensile tail.
The Mediterranean chameleon has a light crest of scales along its throat, and a crest of small, serrated scales along its back (ARKive 2016). Image source: https://www.flickr.com/.

Global Distribution: The Mediterranean chameleon's range is the broadest of all chameleon species, extending from northern Africa to southwest Asia and southern Europe. Although not originally native there, this species has also been introduced to parts of Italy, Portugal, Spain and the Canary Islands (ARKive 2016).

Distribution within Arabian Gulf Countries: Iraq, Saudi Arabia, Yemen (IUCN 2016).

Habitat: The Mediterranean chameleon is found in a variety of habitats including open pine woodland, shrubland, plantations, gardens and orchards. It spends the majority of its time in trees or bushes, preferring dense cover for camouflage. However, this habit changes during the mating season when males move to the ground to find a mate and females descend to a lower level of vegetation.
Differences have been found in the habitat use of different age groups of Mediterranean chameleons, with juveniles occupying low grasses instead of bushes and trees (ARKive 2016).

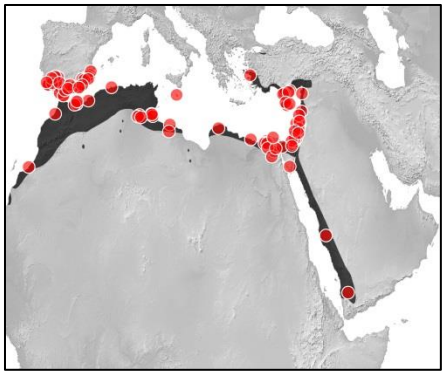

Figure 26 Points used to fit Maxent model. Range polygon from IUCN 2016.

Current Status: Least Concern (IUCN 2016).

Cyrtopodion scabrum

Common Name: Rough Bent-toed Gecko, Rough-tailed Bowfoot Gecko, Keeled Gecko, Rough-tailed Gecko

Description: Belonging to one of the most diverse families of lizards, the rough-tailed bowfoot gecko is a small, nocturnal ground gecko, with exceptionally long, angular toes and two pairs of enlarged scales under the chin. It is sandy in colour and whiter underneath, marked with regular brown spots on the body, and brown bands on the tail. The head is flattened downwards, and the eyes are large, lacking eyelids, with vertical pupils that can be contracted during the day to prevent light from damaging the retina. The tail is longer than the head and body and is relatively flat and tapered, with rows of prominent keeled scales. The rough-tailed bowfoot gecko also has a series of ridged, wart-like bumps, called tubercles, which are arranged regularly along the length of the back, and are separated by small scales, while the underside has around twenty large scales across the middle of the belly (ARKive 2016). Image source: http://www.asergeev.com/.

Global Distribution: The rough-tailed bowfoot gecko is distributed throughout southwest Asia, including south east Turkey, Iraq, the Arabian Peninsula, Iran, Afghanistan and Pakistan. This species has also become naturalised in Israel, and has been introduced and become established in Texas, USA (ARKive 2016).

Distribution within Arabian Gulf Countries: most of Iraq, northwestern, northern and eastern Saudi Arabia (with isolated central populations), southwestern Yemen, Kuwait, Qatar, northern United Arab Emirates, eastern and southern Oman. Introduced: Iran (IUCN 2016).

Habitat: In its native range, the rough-tailed gecko is primarily found in disturbed habitats such as towns, oil camps and desert farms, while in Texas it is known only from the Port of Galveston, where it is found along the commercial fishing docks (ARKive 2016).

Current Status: Least Concern (IUCN 2016).

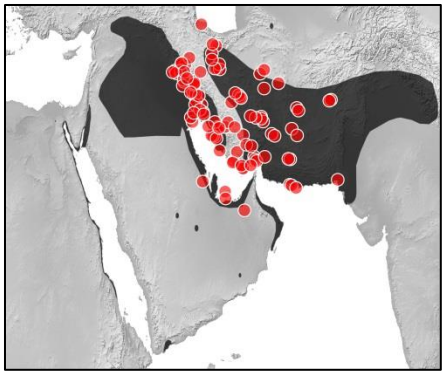

Figure 27 Points used to fit Maxent model. Range polygon from IUCN 2016.

Echis carinatus

Common Name: Saw Scaled Viper, Carpet Viper

Description: Body short, robust and stout. Highly keeled pointed scales of dry appearance found in all over the dorsal body. Body color ranges from light to dark brown, gray, brick red or reddish-brown. Light color spots of light yellow or very light brown margined by dark color found in whole dorsal surface; these spots may be more symmetric on mid body; usually guarded and connected by two undulating lines from both sides (head to posterior body). Belly color white with dark brown or blackish spots in all ventral scales; these spots become larger and more prominent on side ventrals. Subcaudal scales undivided. Head triangular with small shaped keeled scale; clearly broader than neck. One Arrow or cruciform shaped or somewhat plus shaped mark always exist on the top of the head which may have long or short arms. Large eyes with vertical pupil. Two long foldable fangs present on the fore side of the mouth in all life stages. Short tail with a pointed tip, covered with keeled scales; typical dorsal patterns may be absent or faint (Indiansnakes.org 2016). Image source: https://www.flickr.com/.

Global Distribution: Afghanistan, Iran, India (Rajasthan, Punjab, , Andhra Pradesh, Tamil Nadu, Maharashtra (Salher, Marunji, probably all over) [A. Captain, pers. Comm.]), Pakistan, Sri Lanka, Bangladesh, United Arab Emirates, Oman, Turkmenistan, Uzbekistan, Tajikistan (Encyclopedia of Life 2016).

Distribution within Arabian Gulf Countries: United Arab Emirates, Oman (Encyclopedia of Life 2016).

Habitat: Found both in moderate elevation and plains. Distributed in variety of forests including deserts, semi-deserts, rainforest, scrub forest, mixed, dry and moist deciduous forest, grassland etc. Habitat includes dry open lands, agricultural field, scrubs, rocky terrain, open plains etc. Hides in mounds, holes, piles, caves, cracks, dense leaf litters, rocks etc. Saw-scaled Viper is a nocturnal species which remains active from late evening to late nights for foraging and other life activities. Can be seen at day time while basking on habitat. Activity usually terrestrial but climbs on scrub vegetation for basking (Indiansnakes.org 2016).

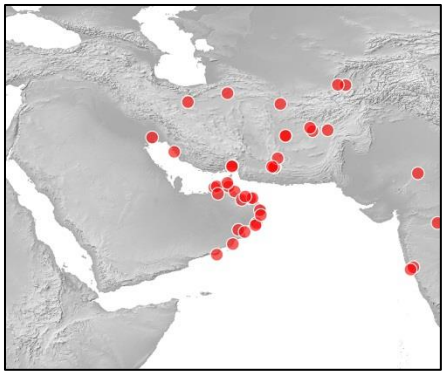

Figure 28 Points used to fit Maxent model.

Current Status: No status found, however subspecies Echis carinatus sochureki has not been evaluated (ARKive 2016)

Echis coloratus

Common Name: Palestine Saw-scaled Viper

Description: A medium-sized snake, with a short, stocky body. Largest Egyptian specimen has a total length of 530 mm, up to 750 mm elsewhere. Tail short, tail / total length = 0.09-0.12. It has 12-15 supralabials; eye moderate, separated from supralabials by 3-4 scales, pupil vertical; scales on dorsal side of head moderate, 13-15 interorbitals; dorsals strongly keeled, 31-35 scale rows around mid-body; 174-205 ventrals, 42-52 single subcaudals; anal entire. Dorsum buffish gray, with a mid-dorsalseries of dark-edged pale-gray saddles, interspersed with large rufous-brown blotches; a lateral series of smaller dark spots; dorsal side of head plain brownish; a diagnostic broad, dark-gray band, from the eye to corner of mouth. Venter white (Encyclopedia of Life 2016). Image source: https://www.flickr.com/.

Global Distribution: The Palestine saw-scaled viper occurs across Egypt, the Middle East and the Arabian Peninsula, including Israel, Jordan, Saudi Arabia, Yemen, northern Oman and the United Arab Emirates. In Egypt, it occurs east of the River Nile (ARKive 2016).

Distribution within Arabian Gulf Countries: Yemen, Saudi Arabi, United Arab Emirate, N Oman (Encyclopedia of Life 2016).

Habitat: Like many viper species, the Palestine saw-scaled viper inhabits rocky, arid areas. It avoids sandy habitats, preferring rocky or hard terrain, and is often found near sources of water. The Palestine saw-scaled viper has been recorded at elevations of up to 2,000 metres in the southern Sinai Peninsula (ARKive 2016).

Current Status: Not Evaluated (ARKive 2016).

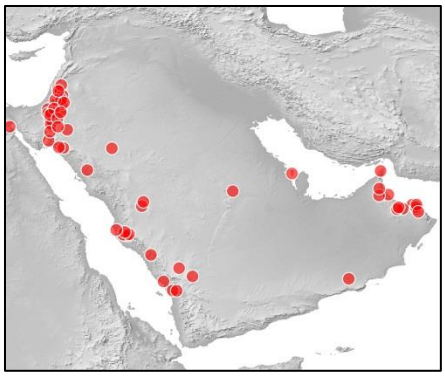

Figure 29 Points used to fit Maxent model.

Eryx jayakari

Common Name: Arabian Sand Boa

Description: One of the smallest boa species, the Arabian sand boa is the only boa found in south-east Arabia, and one of the most common snakes in the United Arab Emirates. The body is covered in smooth, glossy scales, and colored yellow, with an irregular patterning of brown bars and blotches. The features of the head are unusual, with a chisel- shaped snout, and eyes that are positioned on the top of the head, rather than the sides. Boas are one of the most primitive snake groups, and retain vestigial features of the four-legged ancestors from which they evolved. In this species, the remnants of hind limbs are apparent as small claws towards the snake's rear (ARKive 2016). Image source: https://www.flickr.com/.

Global Distribution: The Arabian sand boa is found throughout the Arabian Peninsula and also in Iran (ARKive 2016).

Distribution within Arabian Gulf Countries: This species is found on the Arabian Peninsula in Yemen, Oman, eastern Saudi Arabia and Kuwait, and is also present within Iran where it has been recorded from Khuzistan Province, Bushahr Province, Kerman Province (west of Sirjan) and is probably present in all active dunes within this area (IUCN 2016).

Habitat: As its name suggests, the Arabian sand boa is found in arid, sandy deserts.[6] It has been recorded from deserts, and may be found burrowing in sand and soft soils. Animals are found usually quite deep in sand rising to shallower levels and the surface during the night to wait for prey (IUCN 2016).

Current Status: Least Concern (IUCN 2016)

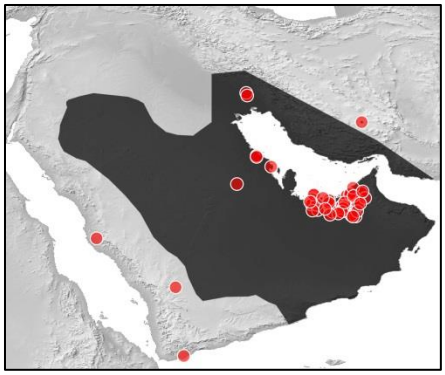

Figure 30 Points used to fit Maxent model. Range polygon from IUCN 2016.

Hemidactylus persicus

Common Name: Persian Leaf-toed Gecko

Description: The Persian leaf-toed gecko is a member of a species-rich group of reptiles possessing unique, leaf-like adhesive pads that do not reach to the toe-tips, a feature alluded to by the name Hemidactylus, which means 'half-finger' in Latin. This relatively large gecko has a pointed snout, curved forehead and a cylindrical, tapering tail. The upper-body surface is covered in small, irregular, flat scales mixed with rather large, triangular, ridged tubercles, which are loosely arranged into 16 lines running along the length of the body. The snout is covered in large, curved scales, with the largest scales sitting between the eyes and the nostrils. The pale yellowish-brown skin of the Persian leaf-toed gecko is very fragile and breaks easily, forming conspicuous scars. Several faint brownish bands traverse the upperside of the body, with the tubercles being almost black, and the lips are whitish (ARKive 2016). Image source: http://www.asergeev.com/.

Global Distribution: The Persian leaf-toed gecko is known from arid regions in the Middle East and South Asia, ranging from northern Oman and the United Arab Emirates through the Arabian Peninsula to southern Iran, Pakistan and northern India (ARKive 2016).

Distribution within Arabian Gulf Countries: S Iran, Iraq, Saudi Arabia, N Oman, United Arab Emirates, Bahrain, Kuwait (Encyclopedia of Life 2016).

Habitat: The Persian leaf-toed gecko inhabits rocky areas in arid regions, including those in limestone outcrops were it clings to cliffs, boulders and bushes (ARKive 2016).

Current Status: Not Evaluated (ARKive 2016).

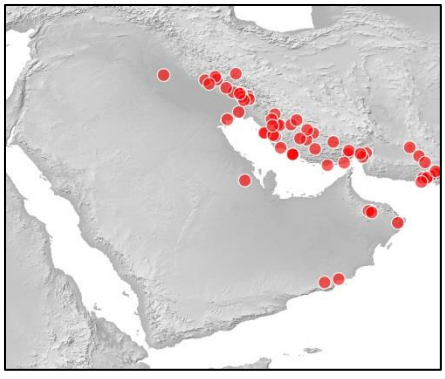

Figure 31 Points used to fit Maxent model.

Pristurus carteri

Common Name: Carter's Semaphore Gecko, Carter's Rock Gecko

Description: The largest member of the Pristurus carteri group (up to 60 mm from snout to vent in many populations but sometimes up to 78 mm); snout elongated, rounded or bluntly pointed; mental not markedly shorter than rostral and lips not turned downwards anteriorly; axillary mite pockets may be large to absent; enlarged tubercles on flanks are sometimes quite well developed; 10-12 lamellae under first hind toe, 18-22 beneath fourth. Tailless than 90% of snout- vent distance, often considerably, its upper crest at least partly heterogeneous and sometimes strongly so, the tip often rounded; autotomy and regeneration almost always taking place only at the base. Usually no large dark spots on sides of throat, which may be generally dark; dark collar absent or at most very weakly indicated; six, sometimes seven dark areas on the back from neck to vent,which may be divided, one at level of forelegs and three or four between the fore and hind limbs (The Reptile Database 2016).

Global Distribution: This species is endemic to the southern Arabian Peninsula, where it ranges from central Oman from Dibab southwards, via Masirah Island, and the adjoining mainland. A disjunct population occurs in north Yemen, where it is known from two records. There is a single record from the United Arab Emirates, on the border with Oman (IUCN 2016).

Distribution within Arabian Gulf Countries:

Habitat: It is ground dwelling and exclusively diurnal. This species is associated with gravelly habitats with little or no vegetation. Arnold (1980) recorded it from open, dry flattish areas although occasionally found on slopes as well if the gradient is not too abrupt. Gardner (2009) recorded it from rocky plateau outcrops and from wadi gravels and outwash (ARKive 2016).

Current Status: Least Concern (IUCN 2016).

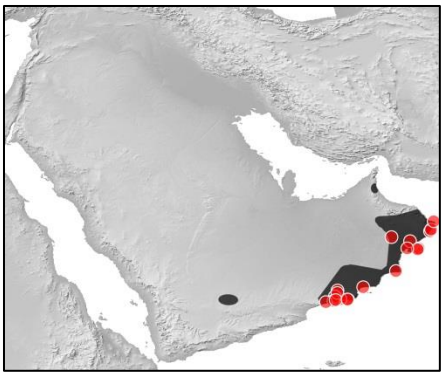

Figure 32 Points used to fit Maxent model. Range polygon from IUCN 2016.

Pristurus flavipunctatus

Common Name: Middle Eastern Rock Gecko, Rüppell's Semaphore Gecko

Description: The Middle Eastern rock gecko is a tiny gecko with a grey body and up to eight dark, 'V' shaped markings along the lower back. Dark brown spots and bands can be seen along the sides of the body, and a dark stripe runs along each side of the head from the mouth to behind the ears. The underside of the Middle Eastern rock gecko is a plain, pale grey with no patterning. The eyes of this species are large and golden brown.
The male and female Middle Eastern rock gecko are similar in appearance, but the male has much clearer patterning and bolder colouration. The male Middle Eastern rock gecko also has an unusual crest on the underside of the tail, which is not found in the female. In addition, the male's abdomen is very long and narrow, whereas in the female it is cylindrical in shape. Juvenile Middle Eastern rock geckos are similar in appearance to the adult female, with a bold stripe along the lower back.
Whereas many other geckos use calls to communicate, members of the genus Pristurus use body postures and movements of their long, narrow tail, giving them the name 'semaphore geckos' (ARKive 2016).

Global Distribution: The Middle Eastern rock gecko has a large range covering parts of Somalia, east Ethiopia, Eritrea, Djibouti, Sudan, Egypt, Saudi Arabia and Jordan (ARKive 2016).

Distribution within Arabian Gulf Countries: Saudi Arabia (The Reptile Database 2016).

Habitat: An arboreal species, the Middle Eastern rock gecko lives among a variety of plants including Acacia trees, using the spiky branches for shelter and protection from birds and other predators.
Vegetation in the regions it inhabits is often sparse, and many individuals have been known to live together on a single isolated tree or shrub (ARKive 2016).

Current Status: Not Evaluated (ARKive 2016).

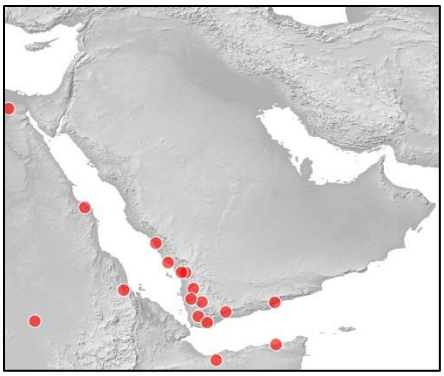

Figure 33 Points used to fit Maxent model.

Pristurus rupestris

Common Name: Blandford's Semaphore Gecko, Dwarf Rock Gecko, Persia Rock Gecko

Description: The rock semaphore gecko (Pristurus rupestris) is a tiny gecko which, like other members of the genus Pristurus, is notable for being active during the day rather that at night. Whereas most other geckos are nocturnal and use calls to communicate, Pristurus species signal to each other with body postures and tail movements, earning them the name 'semaphore geckos'.
The rock semaphore gecko has a relatively flattened, soft-skinned body. Its eyes are quite small compared to most other geckos, and the rounded pupils do not contract to slits in bright light. The limbs of the rock semaphore gecko are quite long and slender, and the slender tail is longer than the head and body combined. Male rock semaphore geckos have a crest of pointed scales along the top of the tail.
The body of the rock semaphore gecko is generally greyish-brown or olive above, with darker and lighter spots, and sometimes with small red spots on the sides. A dark streak passes through the eye, and there may be a light reddish band along the back. Three subspecies are sometimes recognised: Pristurus rupestris rupestris, Pristurus rupestris iranicus and Pristurus rupestris guweirensis. The rock semaphore gecko closely resembles the bar-tailed semaphore gecko (Pristurus celerrimus), but is smaller, with a shorter and less conspicuously banded tail (ARKive 2016). Image source: https://www.flickr.com/.

Global Distribution: The rock semaphore gecko occurs in southwest Jordan, Saudi Arabia, Iran, Oman, the United Arab Emirates and possibly in Pakistan. It is also found in Africa, where it has been recorded from Eritrea, Djibouti, Ethiopia and northern Somalia. The subspecies P. r. iranicus occurs in Iran and possibly western Pakistan, while P. r. guweirensis occurs in Jordan. The rock semaphore gecko may have been accidentally introduced in parts of its range (ARKive 2016).

Distribution within Arabian Gulf Countries: Iran, Oman, Saudi Arabia, United Arab Emirates (IUCN 2016).

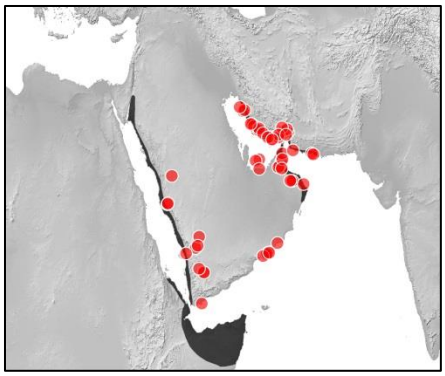

Figure 34 Points used to fit Maxent model. Range polygon from IUCN 2016.

Habitat: This species occurs in rocky formations within flat, hard, sandy desert and gravelly plains (dry wadis). It also occurs in open, dry woodland and shrubland. It can be found under stones, on the walls of abandoned buildings, on beaches and among rocks. It is an egg-laying species (IUCN 2016). This common gecko is found in rocky areas within sandy desert and gravel plains, as

well as open, dry woodland and shrubland. The rock semaphore gecko also occurs in cities and can be found in gardens. It is typically found on rocks, under stones, or on walls, and has been recorded from sea level up to elevations of around 3,000 metres (ARKive 2016).

Current Status: Least Concern (IUCN 2016).

Stenodactylus doriae

Common Name: Middle Eastern Short-fingered Gecko, Sand Gecko, Dune Sand Gecko

Description: The Middle Eastern short-fingered gecko is the largest of the desert-dwelling sand geckos (genus Stenodactylus) found in the United Arab Emirates. This species is well-adapted to its desert habitat, with eyes bordered by large scales to protect from sand while burrowing, and flattened toes, with a projecting fringe of long scales, to increase surface area contact with the loose substrate. The skin is soft, mainly comprising small scales, interspersed with scattered larger, raised scales, termed "tubercles". The overall colouration is pale sandy above, marked with indistinct dark transverse bands and a darker line running from the eyes down each side, and whitish below. The eyes are large, and the tail is long and cylindrical, tapering to a fine point (ARKive 2016).

Global Distribution: Inhabiting the Middle East and the Arabian Peninsula, the Middle Eastern short-fingered gecko can be found in Saudi Arabia, Iran, Iraq, Israel, The United Arab Emirates, Oman and Jordan (ARKive 2016).

Distribution within Arabian Gulf Countries: Iran, Iraq, Oman, Saudi Arabia, United Arab Emirates, Yemen (IUCN 2016).

Habitat: The Middle Eastern short-fingered gecko can be found on the loose, wind-blown sands of dunes and sandy plains (ARKive 2016). This terrestrial species is only found in the areas between mobile sandy dunes, where there is a 'green crust' substrate in which the species can dig burrows. The females lay clutches of one to two eggs. It is not present in agricultural land (IUCN 2016).

Current Status: Least Concern (IUCN 2016).

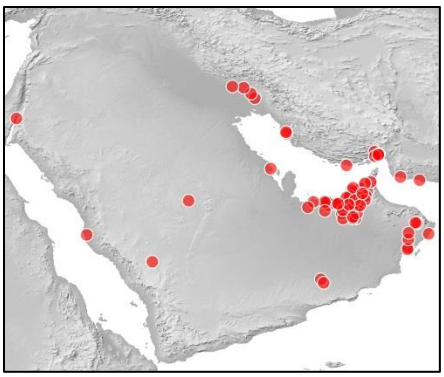

Figure 35 Points used to fit Maxent model.

Mammals

Allactaga euphratica

Common Name: Euphrates Jerboa

Description: Like other dipodids, Euphrates jerboas have very large hind feet and small forelimbs. The length of their feet is usually 50 to 61 mm, body length is 230 to 310 mm and tail length is 144 to 195 mm. Allactaga euphratica use their long tails for balance while they are bounding. They also have rather tall, narrow ears, measuring from 27 to 42 mm. There are tufts of hair around the openings of their ears to keep sand out. A distinguishing feature of the genus Allactaga is that, while they have five toes, two of them on each of their feet are vestigial and are found high up on the hind foot. The hind feet also have tufts of hair on the bottom to provide friction against the sand while walking and jumping. Allactaga euphratica have furry coats with either red and black upper parts and white under parts or sandy colored upper parts and white under parts, depending on the color of the soil where they are found. All Allactaga euphratica have one white stripe on their hips. They also have black and white tufts of fur on the ends of their tails. These tufts are often used by individuals while bounding to signal to other jerboas. Euphrates jerboas living at higher elevations tend to have darker coats than those at lower elevations. All Euphrates jerboas have well-developed whiskers (Encyclopedia of Life 2016).

Global Distribution: Recorded from Turkey, Syria, and eastern Jordan, through northern Saudi Arabia and Iraq to Kuwait and Iran. It has recently been recorded in Lebanon. The southern and eastern limits of the range are poorly defined. The species occurs up to 2,660 m in Lebanon (IUCN 2016).

Distribution within Arabian Gulf Countries: Iraq, Kuwait; Saudi Arabia (IUCN 2016).

Habitat: The species occurs in steppe and semi-desert habitats. There are some records from cultivated plains. Like all Allactaga species, this species is not found in loose sands. Primarily, jerboas are nocturnal rodents spending most of the daylight hours in underground burrows emerging at night to forage. Most species have a vegetarian diet (IUCN 2016).

Current Status: Near Threatened (IUCN 2016).

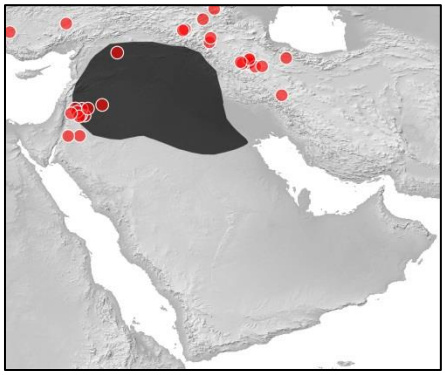

Figure 36 Points used to fit Maxent model. Range polygon from IUCN 2016.

Asellia tridens

Common Name: Geoffroy's Trident Leaf-nosed Bat, Trident Bat, Trident Leaf-nosed Bat

Description: The trident leaf-nosed bat is named after its distinctive nose-leaf, a fleshy structure surrounding the nose, common to many bats, which on this species has three projections; the outer two projections have blunt tips while the central one is pointed. The fur of the trident leaf-nosed bat varies in colour, from pale greyish-brown to a pale yellow, and the underside is whitish. The ears are very large and almost hairless, and the tail projects up to five millimetres beyond the flight membrane. The trident leaf-nosed bat is also distinguished by the lack of a tragus (the bump in front of the opening of the ear), which is very well-developed in most bats (ARKive 2016). Image source: https://www.flickr.com/.

Global Distribution: The trident leaf-nosed bat is found throughout northern Africa and the Middle East. Its range extends from Mauritania in the west to Pakistan in the east, and from Iraq in the north to Ethiopia in the south (ARKive 2016).

Distribution within Arabian Gulf Countries: Saudi Arabia, Yemen (IUCN 2016).

Habitat: This is a gregarious and colonial species which occurs in crevices or in cliffs in arid and semi-desert habitats. It roosts in temples, caves, mines, open-wells, underground irrigation tunnels and old tombs and buildings. Forages over desert and semi-desert vegetation zones, mainly in oases. Forages by slow hawking, has been observed foraging around palm trees and buildings, and over water (IUCN 2016).

Current Status: Least Concern (IUCN 2016).

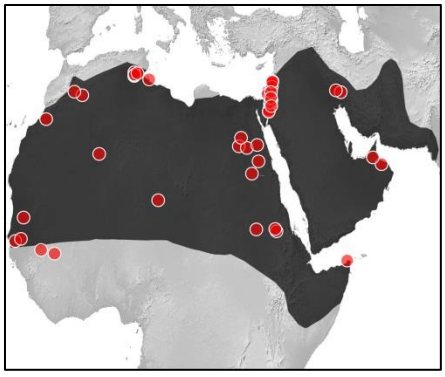

Figure 37 Points used to fit Maxent model. Range polygon from IUCN 2016.

Canis aureus

Common Name: Golden Jackal, Asiatic Jackal, Common Jackal

Description: The golden jackal is a slender, medium-sized canid with long legs, a long, pointed muzzle, and a relatively short, bushy tail. The coat is rather coarse, and, as the name suggests, is generally golden or yellowish in color, although individuals vary from pale cream to tawny, and coat color may also vary between seasons. The back is often mottled black, brown and white, while the head, ears, sides and limbs may have a reddish-brown hue. The underparts are pale. The golden jackal can be distinguished from other jackal species by the black tip to the tail. Occasional dark (melanistic) individuals are reported, and several subspecies of golden jackal are recognized. The golden jackal is a very vocal species, using a variety of barking, growling, cackling and whining calls. The most distinctive is the high-pitched, wailing howl, often given in chorus at dawn and dusk, and thought to reinforce family bonds or advertise territory ownership (ARKive 2016). Image source: https://www.flickr.com/.

Global Distribution: The Golden Jackal is widespread in North and north-east Africa, occurring from Senegal on the west coast of Africa to Egypt in the east, in a range that includes Morocco, Algeria, and Libya in the north to Nigeria, Chad and Tanzania in the south. They also occur in the Arabian Peninsula and have expanded their range into Europe, where they have a patchy distribution, being resident in the Balkans and, since recent times, in Hungary and south-western Ukraine. It is regularly found as a vagrant in Austria, Slovakia, Slovenia and north-eastern Italy. Eastwards they range into Turkey, Syria, Iraq, Iran, Central Asia, the entire Indian subcontinent, then east and south to Sri Lanka, Myanmar, Thailand and parts of Indo-China (IUCN 2016).

Distribution within Arabian Gulf Countries: Iran, Iraq, Kuwait, Oman, Qatar, Saudi Arabia, United Arab Emirates, Yemen (IUCN 2016).

Habitat: Its tolerance of dry habitats and opportunistic diet enable the golden jackal to inhabit a wide variety of habitats, ranging from desert, to grassland, forest, and even agricultural and semi-urban areas, although it most commonly occurs in dry, open country (ARKive 2016).

Current Status: Least Concern (IUCN 2016).

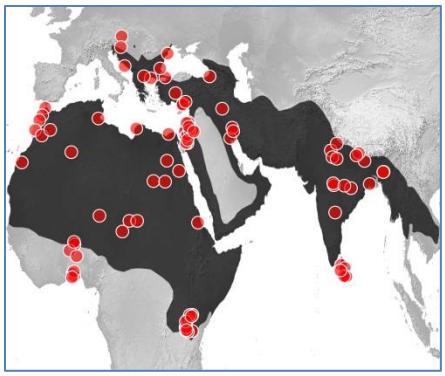

Figure 38 Points used to fit Maxent model. Range polygon from IUCN 2016.

Capra nubiana or *Capra ibex nubiana*

Common Name: Nubian ibex

Description: This relatively small ibex is most easily recognised by the impressive, backward-arching horns of the male, which are long, slender and ridged on their outer curve, casting a magnificent silhouette against the rocky, mountainous terrain of its surroundings. Whilst found in both sexes, these horns are much larger in males than females, growing up to 120 cm on bucks, and only 35 cm on females. The coat is a light sandy brown colour, with a white underbelly, while the legs bear conspicuous black-and-white markings. Bucks have a dark stripe down the back and older males have a long, dark beard. During the October rut, the neck, chest, sides, shoulders and upper legs of the bucks become dark brown to almost black in colour. The differentiation between species and subspecies status in ibexes is very controversial and remains somewhat debated, with all species previously classified under Capra ibex (ARKive 2016). Image source: https://www.flickr.com/.

Global Distribution: Northeastern Africa and parts of Arabia, including Egypt, Ethiopia, Israel, Jordan, Oman, Saudi Arabia, Sudan and Yemen. Formerly also in Lebanon and the Syrian Arab Republic (ARKive 2016).

Distribution within Arabian Gulf Countries: Oman, Saudi Arabia, Yemen (IUCN 2016).

Habitat: Nubian Ibex occur in rocky, desert mountains with steep slopes and hills (which provide vital escape routes), and associated plateaus, canyons and wadis. They consume a wide array of herbaceous and woody plants.[12] A rocky-desert dwelling species found in rough, dry, mountainous terrain. In the summer, the Nubian ibex moves further up the mountain to avoid the heat, returning to lower elevations in the winter (ARKive 2016).

Current Status: Vulnerable (IUCN 2016).

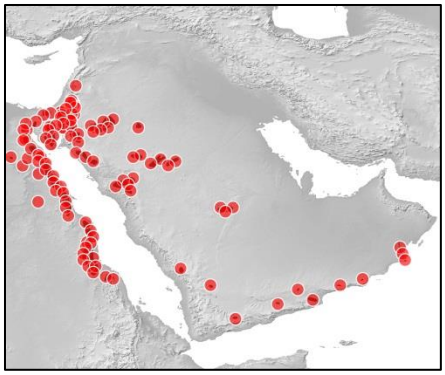

Figure 39 Points used to fit Maxent model.

Caracal caracal

Common Name: Caracal, Desert Lynx, African Caracal, Asian Caracal

Description: The caracal is a slender, graceful cat with a short, dense coat and distinctive, long, black-tufted ears. The body color varies from reddish-brown to tawny-grey, but occasionally entirely black "melanistic" individuals may occur. The chin, throat and underparts are white, with pale red spots or blotches on the belly and the insides of the legs that vary from very faint to distinct in different individuals. Distinctive narrow black stripes run from the eye to the nose and down the center of the forehead, and the eyes are yellow-brown, with the pupil contracting to a circle rather than a slit. The caracal produces a range of vocalizations, including miaows, growls, hisses and coughing calls (ARKive 2016). Image source: https://www.flickr.com/.

Global Distribution: The caracal has a large range, including much of Africa, and also extending through the Arabian and Anatolian Peninsula, and southwestern and central Asia, as far as Kazakhstan and central India. Within Africa, the caracal is only absent from the central Sahara and areas of dense forest around equatorial West Africa (ARKive 2016).

Distribution within Arabian Gulf Countries: Iran, Iraq, Kuwait, Oman, Saudi Arabia, United Arab Emirates, Yemen (IUCN 2016).

Habitat: The caracal occupies a wide variety of habitats from semi-desert to relatively open savanna and scrubland to moist woodland and thicket or evergreen/montane forest (as in the Western Cape of South Africa), but favours drier woodland and savanna regions with lower rainfall and some cover. While drier open country is preferred, they are absent from true desert and are usually associated with some form of vegetative cover. They range up to 2,500 m and exceptionally 3,300 m (exceptionally) in the Ethiopian Highlands (IUCN 2016).

Current Status: Least Concern (IUCN 2016).

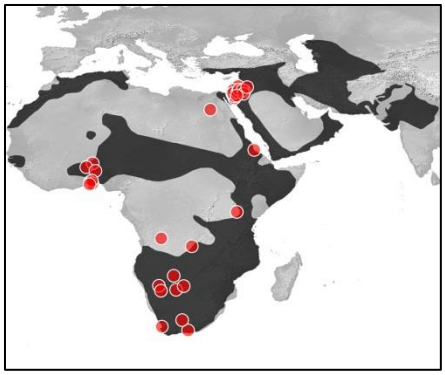

Figure 40 Points used to fit Maxent model. Range polygon from IUCN 2016.

Eidolon helvum

Common Name: Straw-colored Fruit Bat, African Straw-colored Fruit Bat

Description: The straw-coloured fruit bat (Eidolon helvum) is the second largest bat on the African continent. Despite its name, this bat is not a consistent straw-yellow colour, instead ranging from pale yellow to dark brownish-grey. The fur on the rump and legs is often darker than on the more yellowish shoulders, and the underparts are lighter than the upperparts. Adult straw-coloured fruit bats usually have a bright orange, yellow or brownish collar of longer hairs on the throat, which extends upwards onto the back of the neck. This collar overlies glands on the skin that secrete a musky-smelling fluid, and is brighter and more pronounced in males.
The female straw-coloured fruit bat is only slightly smaller than the male and often appears lighter in colour. Juvenile straw-coloured fruit bats are generally darker than the adults, and lack a collar.
The straw-coloured fruit bat has long, dark blackish-brown wings which are quite narrow and pointed. When the bat is at rest, the tips of the wings are folded inwards. The tail membrane is narrow, running along the insides of the thighs, while the tail itself is short and projects beyond the membrane for about half its length. The first finger on the forearm is long and has a strong, curved claw, which is used for climbing among tree branches (ARKive 2016). Image source: https://www.flickr.com/.

Global Distribution: This bat is broadly distributed across the lowland rainforest and savanna zones of Africa from Senegal in the west, through to South Africa in the south and Ethiopia in the east (possibly ranging into Djibouti and southern Eritrea). It is also present on the extreme southwest Arabian Peninsula, where it has been recorded from Yemen and Saudi Arabia. Populations of this bat occur on several offshore islands including the Gulf of Guinea islands and Zanzibar, Pemba and Mafia (off Tanzania). There is a possibly disjunct population in the Air Mountains of Niger. Distribution at northern and southern extremes of the range is patchy and erratic. It is also sparse or absent in large areas of the Horn of Africa, central East Africa, and elsewhere. This bat is a migratory species in parts of its range; populations migrate from the West African forest north into the savanna zone during the major wet season. It ranges from sea level to around 2,000 m asl (IUCN 2016).

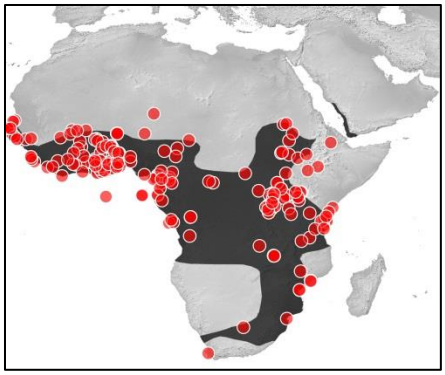

Figure 41 Points used to fit Maxent model. Range polygon from IUCN 2016.

Distribution within Arabian Gulf Countries: Saudi Arabia, Yemen (IUCN 2016).

Habitat: This adaptable species has been recorded from a very wide range of habitats. It is commonly found in moist and dry tropical rain forest, including evergreen forest habitats in the form of coastal (including mangrove) and riverine forest, through moist and dry savanna and mosaics of these and similar habitat types. Populations can persist in modified habitats and the species is often recorded in urban areas, such as wooded city parks (IUCN 2016).

Current Status: Near Threatened (IUCN 2016).

Felis margarita

Common Name: Sand Cat, Sand Dune Cat

Description: The smallest cat species in Arabia, the sand cat is well adapted to its arid desert habitat, obtaining all the water it needs from its food. Prey capture is facilitated by the sand cat's highly sensitive ears, which are large and triangular, and capable of detecting noises from animals both above and below the surface of the sand. Its foot pads are covered with thick hair, enabling it to move easily over quickly moving sands in its desert environment, and insulates them from the surface heat. The fur of the sand cat ranges from yellowish-brown to dull grey, with vague lines on its limbs and several black rings near the black tip of its tail. A dark, reddish streak runs from the corner of the eye down the cheek. The patterns on the sand cat's fur vary between the six subspecies (ARKive 2016). Image source: https://www.flickr.com/.

Global Distribution: The sand cat ranges from northern Africa, through the Arabian Peninsula to central and south-west Asia, but due to its specific habitat requirements, it has a patchy distribution within this range (ARKive 2016). The Sand Cat is the only felid found primarily in true desert, and has a wide but apparently disjunct distribution through the deserts of northern Africa and southwest and central Asia. It is not clear whether the gaps in known range are due to a lack of records or truly reflect species absence. For example, sightings have been reported in Libya and Egypt west of the Nile, but there are no historical records despite intensive collecting effort (IUCN 2016).

Distribution within Arabian Gulf Countries: Iran, Kuwait, Oman, Saudi Arabia, United Arab Emirates, Yemen (IUCN 2016).

Habitat: Sand Cats are specialists of sandy desert, where they are unevenly distributed, localized around sparse vegetation which can support small rodent prey. They are also found in stony desert. With thickly furred feet, the Sand Cat is well adapted to the extremes of a desert environment, living in areas far from water, and tolerant of extremes of hot and cold temperatures, largely because of their fossorial (burrowing) behavior. They are absent from areas where the soil is compacted (IUCN 2016).

Current Status: Near Threatened (IUCN 2016).

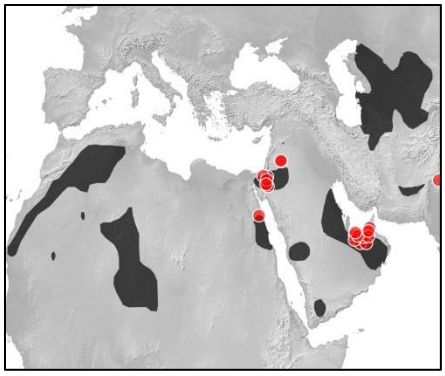

Figure 42 Points used to fit Maxent model. Range polygon from IUCN 2016.

Gazella gazella

Common Name: Mountain Gazelle

Description: Of all Gazella species, the mountain gazelle is the most slender built with relatively the longest neck and legs. The coat is fawn to dark-brown on the back, neck and head, while the belly and buttocks are pure white, with these tones being separated on the flanks by a dark narrow band. G. g. gazella and G. g. muscatensis are darker than the other subspecies. The coat is short, sleek and glossy in summer, reflecting much of the sun's radiation. In winter the pelage is much longer, dense and rainproof and not glossy, enabling the gazelles to withstand the heavy winter rains (800-1000 mm) in northern Israel; although seasonal variations in the pelage are much less in desert subspecies. The face has two conspicuous white stripes extending from the eyes towards the nostrils with dark-brown to black lower margins, coupled usually with a black spot on the muzzle above the nose. The male's horns are quite long (22 – 29.4 cm), straight and thick basally, with a slight lyrate form and prominent rings, while those of females are generally shorter (5.8 - 11.5 cm), un-ringed, irregular in shape, and often bent, crooked or broken. Males of northern subspecies have longer horns than southern desert subspecies, and those of the Persian Gulf region are shortest and more strongly outbowed. Northern Palestine gazelles (G. g. gazella) are generally the largest of the mountain gazelle subspecies, while the southern desert subspecies are much lighter (only 12-16 kg), but longer-legged and with a relatively longer body and ears (Encyclopedia of Life 2016). Image source: https://www.flickr.com/.

Global Distribution: Formerly occurred across most of the Arabian Peninsula, north to southern Syria and extending westwards into Sinai. The last confirmed records for Egypt were in 1932 though there have been some recent unconfirmed reports. There have been no records in Syria since the 1970s, although they may survive on Jabal Hermon and perhaps in upper Galilee. In Lebanon, the species was believed to have become extinct after 1945, but three were seen in 1998 in the Barouk Mountains. The last record from Jordan was in 1986, although Masseti (2004) notes that they were reintroduced into Shaumari Wildlife Reserve (IUCN 2016).

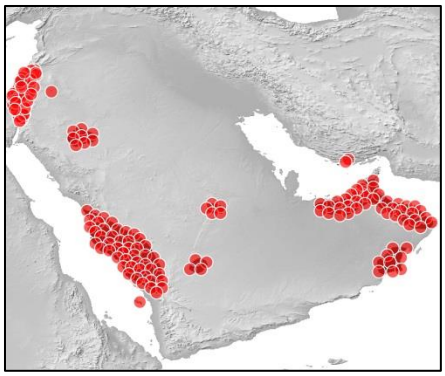

Figure 43 Points used to fit Maxent model.

Distribution within Arabian Gulf Countries: Their current range includes: Israel (widely distributed); Saudi Arabia (occurs on the Farasan islands, in three protected areas, and as scattered populations in the west); Oman (widely distributed, with the largest population in the Arabian Oryx Sanctuary); United Arab Emirates and

Yemen, mainly from the west and south. There is also a small introduced population on Farur Island (Iran) in the Persian Gulf (IUCN 2016).

Habitat: Mountain gazelles live in low altitude mountains, sometimes in very steep terrain, but avoid rocky areas and walking on rocks. They prefer plateaus, hilly relief, foothills and valleys between mountains and open habitats or areas with light forest in gravel or sandy plains, but also occur in regions of real desert and coastal dunes. In Arabia, they usually live on rough terrain of mountain beds, gorges, and rolling hills. Mountain gazelles can withstand severe climatic conditions. They live in very hot and dry Jordan Valley, the Negev Desert, and the Nafud and Dhofar Deserts, where mid-day temperature can reach 45 degrees Celsius, and in northern Israel where sub-zero temperatures are not rare on winter nights and snow can cover the ground for several days (ARKive 2016).

Current Status: Vulnerable (IUCN 2016).

Gazella subgutturosa

Common Name: Goitered Gazelle

Description: This gazelle receives its common name due to the goitre-like swelling on the throat, which is an enlarged cartilaginous cylinder that is larger and more distinctive in males, especially during the breeding season, and allows them to emit loud bellows in courtship. Unlike most gazelles, females of this species are mostly, although not always, hornless, while males boast long, elegantly curved, lyre-like, black horns that diverge outwards and turn back in at the tip. Interestingly, horn development in females increases from Mongolia and China, where they are almost completely hornless, to the Arabian Peninsula, where they have well-developed horns. Goitered gazelles vary in colouration between populations, from nearly white to brown with different tones of grey, red or yellow. Generally, the very light brown colouration of the back darkens towards the flanks, where it meets the white underparts in a crisp line, and the black colouration of the first two thirds of the tail contrasts starkly against the white of the buttocks. In Central and Middle Asia young have distinct facial stripes and spots on a coloured background, which tend to white and fade with age, but in Saudi Arabia even young have a white face without markings. Eyes are large and black, and the ears are long. Legs and neck are relatively long and the tail is quite short. Males are larger and heavier than females (ARKive 2016). Image source: https://www.flickr.com/.

Global Distribution: Occurs from the south of the Arabian Peninsula across the Middle East and Asia to Mongolia, China and Pakistan. Their historical range has contracted greatly, and they are now extinct in Kuwait, Georgia, and perhaps Kyrgyzstan (IUCN 2016).

Distribution within Arabian Gulf Countries: The historical range of Arabian Sand Gazelle (the only subspecies assessed here) covered the Arabian Peninsula north to southern Iraq and Kuwait. The taxon is currently found in Bahrain (Hawar Island and southern part of Bahrain Island); Oman (Dhofar, edge of Rub al Khali to Arabian Oryx Sanctuary); United Arab Emirates (Umm al Zummur area); Saudi Arabia (four populations, all in protected areas); Jordan (north-east); Syria, Iraq and Yemen. It is now extinct in Kuwait (IUCN 2016).

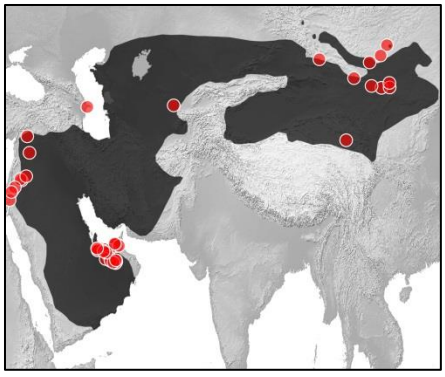

Figure 44 Points used to fit Maxent model. Range polygon from IUCN 2016.

Habitat: Inhabits a wide range of semi-desert and desert habitats. Ascends into foothills and penetrates mountain valleys in Central Asia, to altitudes of 2,700 m in Mongolia. They migrate seasonally in search of pasture

and water. Arabian Sand Gazelle prefers areas of dunes and sandy desert in the Arabian Peninsula (IUCN 2016).

Current Status: Vulnerable (IUCN 2016).

Gerbillus cheesmani

Common Name: Cheesman's Gerbil

Description: A medium-sized gerbil, Cheesman's gerbil is named after the military officer, explorer and ornithologist Colonel Robert Ernest Cheesman. The upperparts of Cheesman's gerbil are sandy-beige, while the belly is white. This species has a relatively long tail, and the soles of its feet are hairy. Like many gerbil species, Cheesman's gerbil is rather mouse-like in appearance, with large, black eyes that are positioned high on its head, giving this small mammal a wide field of vision (ARKive 2016).

Global Distribution: Arabian Peninsula, Iraq and Iran. The species also occurs marginally in Syria (one record) and Jordan. Found from sea level to c.450 m asl (IUCN 2016).

Distribution within Arabian Gulf Countries: Iran, Iraq, Kuwait, Oman, Saudi Arabia, United Arab Emirates, Yemen (IUCN 2016).

Habitat: Cheesman's gerbil is found on sandy soils and mud flats in desert areas. In some areas of its range, this species occurs in sand dunes. In Saudi Arabia, Cheesman's gerbil is found in areas associated with a variety of plants, including *Haloxylon salicornicum*, *Ephera alata* and *Artemesia* bushes, which provide it with shelter (ARKive 2016).

Current Status: Least Concern (IUCN 2016).

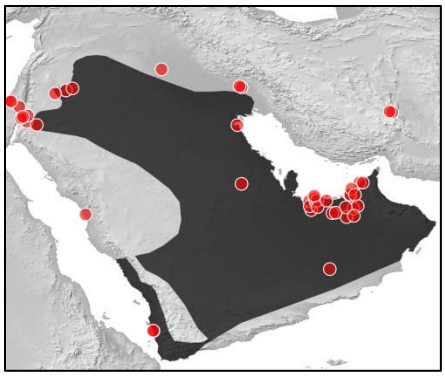

Figure 45 Points used to fit Maxent model. Range polygon from IUCN 2016.

Gerbillus nanus

Common Name: Dwarf Gerbil, Baluchistan Gerbil

Description: Baluchistan gerbil is a medium-sized gerbil. Hairs of the upperparts reddish yellow. Underparts, forelimbs and feet white. Upper surface color of the tail as back with gray spots at distal end and underside silver. Tail brush pale gray and obvious. Palm and sole of the feet with hairs, extending between pads (Encyclopedia of Life 2016).

Global Distribution: Occurs in the western part of the Sahara and Sahel (from Morocco to Tunisia in the north and from Mauritania through northern Mali and Niger to Chad in the south). Also present in the Arabian Peninsula and the Middle East through Afghanistan and Pakistan to northwest India (IUCN 2016).

Distribution within Arabian Gulf Countries: Iran, Iraq, Oman, Saudi Arabia, United Arab Emirates, Yemen (IUCN 2016).

Habitat: Found in desert, semi-desert, arable land and gardens. Mostly found in parts of the desert with relatively deep soil and abundant vegetation, such as wadis, oases, sebkhas edges and sand-clay plains or basins (IUCN 2016).

Current Status: Least Concern (IUCN 2016).

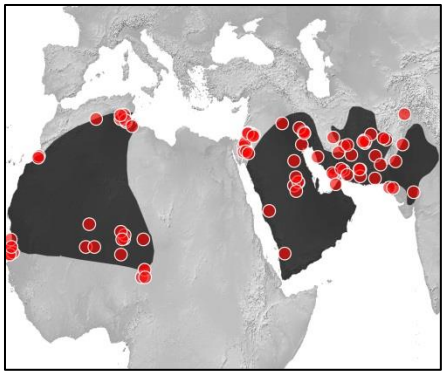

Figure 46 Points used to fit Maxent model. Range polygon from IUCN 2016.

Hipposideros caffer

Common Name: Sundevall's Leaf-nosed Bat, Sundevall's Roundleaf Bat, Lesser Leaf-nosed Bat

Description: Sundevall's roundleaf bat is a medium-sized bat, with a head-body length of 8 to 9 cm (3.1 to 3.5 in), and a wingspan of 20 to 29 cm (7.9 to 11.4 in). Adults have a body weight of 8 to 10 g (0.28 to 0.35 oz). They have long fur, which may be either grey or a bright golden-orange in colour, and brown wings. The fur is generally paler on the underside of the body.http://www.inaturalist.org/taxa/244897-Hipposideros-caffer - cite_note-Wright2009-4
The bats have large, rounded, ears with a well-developed antitragus, and a horseshoe-shaped nose-leaf, with a distinctive small projection on either side. There is also an additional serrated ridge of skin behind the main nose-leaf. Both females and males have an extra pair of teats in the pubic region. Although these are vestigial in the males, they can be as long as 4 cm (1.6 in) in some females (almost half the body length), yet are never functional. These false teats may be only present to allow the young something to hold on to while clinging to their mothers (iNaturalist 2016). Image source: https://www.flickr.com/.

Global Distribution: A very wide ranging species, occurring from the south-western Arabian Peninsula (including Yemen) and across most of sub-Saharan Africa (except for central forested regions). This species has also been recorded in southern Algeria, central Niger, eastern Chad, the Senegal/Mauritania border. H. caffer tephrus is confined to the coastal areas of northern Morocco. A supposed record from southern Algeria requires confirmation. Elevation ranges from sea level to 2,500 m in this area (IUCN 2016).

Distribution within Arabian Gulf Countries: Saudi Arabia, Yemen (IUCN 2016).

Habitat: This species occurs in savanna, bushveld and coastal forest, and is usually associated with rivers and other water resources, provided there are caves or buildings where it can roost during the day. Colony size varies from small to medium-sized groups of tens or hundreds of individuals, exceptionally up to 500,000 (IUCN 2016).

Current Status: Least Concern (IUCN 2016).

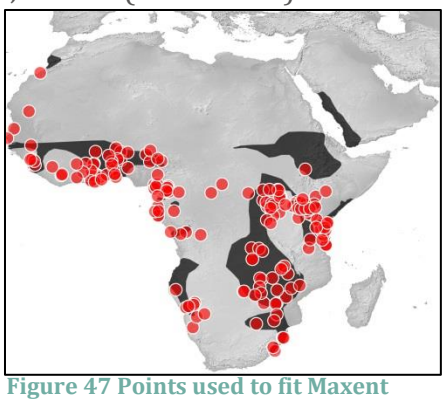

Figure 47 Points used to fit Maxent model. Range polygon from IUCN 2016.

Hyaena hyaena

Common Name: Striped Hyaena

Description: Like other hyaenas, the striped hyaena is dog-like in appearance, with powerful forequarters and a back that slopes down towards the tail. It gets its name from the black stripes on the sides of the pale grey or beige coat, which is long and shaggy except for on the face and limbs. A crest of particularly long hair, running from the head to the tail, is erected in situations of conflict to make the hyaena look larger and more intimidating. The striped hyaena has a long, thick neck, which along with the strong skull and jaw bones enables the hyaena to break up dry bones. The black and white tail is long and bushy and the feet bear short, blunt claws (ARKive 2016). Image source: https://www.flickr.com/.

Global Distribution: The Striped Hyaena has a very large, albeit now patchy distribution, extending from Africa, north of and including the Sahel, and including much of east and northeast Africa south to about central Tanzania, through the Middle East and Arabian Peninsula, Turkey, the Caucasus, Central Asia, and the Indian subcontinent, though not reaching Assam, Bhutan or Myanmar. They may have recently expanded into Nepal. Although historically present, there are few reliable recent records of occurrence in Sudan, Eritrea, Somalia, Qatar, Kuwait, and the United Arab Emirates (IUCN 2016).

Distribution within Arabian Gulf Countries: Iran, Iraq, Oman, Saudi Arabia, Yemen (IUCN 2016)

Habitat: In most of its range the Striped Hyaena occurs in open habitat or light thorn bush country in arid to semi-arid environments. These animals avoid open desert (such as the center of the Arabian Desert and the Sahara, though they may occur at low density in the central Saharan massifs), dense thickets and forests. Nevertheless, it was reported from Lebanon and Jordan that they inhabit thick Mediterranean oak forests, and also avoid high altitudes; however, it has been recorded to 3,300 m in Pakistan, 2,700 m in the Moroccan High Atlas, at least to 2,300 m in the Ethiopian Highlands, and 2,200 m in the Lebanese mountains. Striped Hyaenas are sometimes found close to dense human settlements (e.g., Israel, Lebanon and Algeria) (IUCN 2016).

Figure 48 Points used to fit Maxent model. Range polygon from IUCN 2016.

Current Status: Near Threatened (IUCN 2016).

Hystrix indica

Common Name: Indian Crested Porcupine

Description: On average, the Indian porcupine's head and body measure 70-90 centimeters (cm) in length, with the tail adding an additional 8-10 cm. Its hair is highly modified to form multiple layers of spines. Beneath the longer, thinner spines lies a layer of shorter and thicker ones. Each quill is brown or black in color, with alternating bands of white. Spines vary in length, with the neck and shoulder quills being the longest, measuring 15 to 30 cm. The tail is covered with shorter spines that appear white in color. Among these, are longer, hollow, rattling quills that are used to alarm potential predators. The feet and hands are broad, with long claws that are used for burrowing (Encyclopedia of Life 2016). Image source: https://www.flickr.com/.

Global Distribution: The Indian porcupine is found throughout southeast and central Asia and in parts of the Middle East, including such countries as India, Nepal, Bhutan, Bangladesh, Sri Lanka, Pakistan, Israel, Iran and Saudi Arabia (Encyclopedia of Life 2016).

Distribution within Arabian Gulf Countries: Iran, Iraq, Saudi Arabia (Encyclopedia of Life 2016).

Habitat: The Indian porcupine is highly adaptable to multiple environments. Although they usually favor rocky hill sides, the species can also be found in tropical and temperate scrublands, grasslands, and forests. They are also found throughout the Himalayan mountains, reaching up to elevations of 2400 meters (Encyclopedia of Life 2016).

Current Status: Least Concern (IUCN 2016).

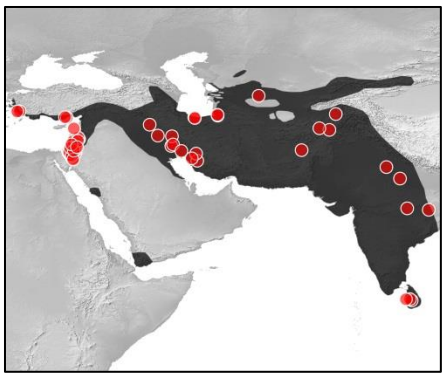

Figure 49 Points used to fit Maxent model. Range polygon from IUCN 2016.

Jaculus jaculus

Common Name: Lesser Egyptian Jerboa

Description: Jaculus jaculus is the smallest species in the genus Jaculus. It is very small with a darkish back and lighter colored underbelly. There is also a light-colored stripe across its hip. Jerboas are a lot like a tiny kangaroo in locomotion and posture. The hind feet are incredibly large, 50 to 75 mm, and used for jumping. Each hind foot has three toes. The tail is very long, 128 to 250 mm, with a clump of hairs at the tip which is used for balance. It has moderately large eyes and ears. Females are larger than males (Encyclopedia of Life 2016). Image source: https://www.flickr.com/.

Global Distribution: This species is particularly abundant in Egypt, hence its common name, but its distribution also extends across North Africa and the Arabian Peninsula, from Morocco as far east as Iran (ARKive 2016).

Distribution within Arabian Gulf Countries: Iran, Iraq, Kuwait, Oman, Qatar, Saudi Arabia, United Arab Emirates, Yemen (IUCN 2016).

Habitat: The habitat of this species varies across the range, from sand dunes to rocky substrates, however, it is always found near to vegetation (IUCN 2016).

Current Status: Least Concern (IUCN 2016).

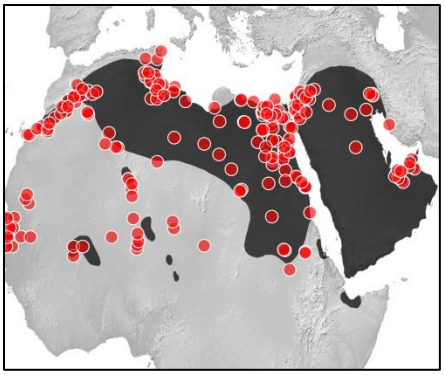

Figure 50 Points used to fit Maxent model. Range polygon from IUCN 2016.

Lepus capensis

Common Name: Cape Hare, Desert Hare, Arabian Hare, Brown Hare

Description: A widespread and abundant species, the Cape hare is a typical hare in appearance, with long, slender limbs, large hind feet, a short tail, large eyes and large ears. The fur is soft and straight, and the feet are well furred. In general, the body colour ranges from pale buff, to grey-brown, to rich, almost reddish-brown, with white underparts and a black and white tail. The backs of the ears have white outer edges and black tips, and may be 'flashed' when the hare is being pursued, possibly to confuse predators. Hares utter a loud, high-pitched scream when caught or injured, and may also produce a warning noise by grinding the teeth together, as well as communicating through drumming or stamping of the feet, and through calls, such as those given to the young.
The female Cape hare is usually slightly larger than the male. The species shows considerable variation in size and appearance across its large range, and many subspecies are recognised. However, the taxonomy of the Cape hare is somewhat unclear, and is under review (ARKive 2016). Image source: https://www.flickr.com/.

Global Distribution: The Cape hare has a very wide distribution, being found across most non-forested regions of Africa, through the Arabian Peninsula and Middle East, and across central Asia. It is also found on the islands of Sardinia and Cyprus. Populations in China, Mongolia and Russia are now thought to be separate species (ARKive 2016).

Distribution within Arabian Gulf Countries: Bahrain, Kuwait, Iraq, Iran, Oman, Qatar, Saudi Arabia, United Arab Emirates, Yemen (IUCN 2016)

Habitat: The Cape hare can be found in almost any open country, from savanna grassland to cold, stony desert. It thrives on overgrazed pasture, and so may be expanding its range in light of an increase in this habitat. Most hares do not dig burrows, instead relying on camouflage and speed to escape danger, but the Cape hare, in addition to using shallow scrapes in the ground ('forms'), may use burrows to escape high desert temperatures (ARKive 2016).

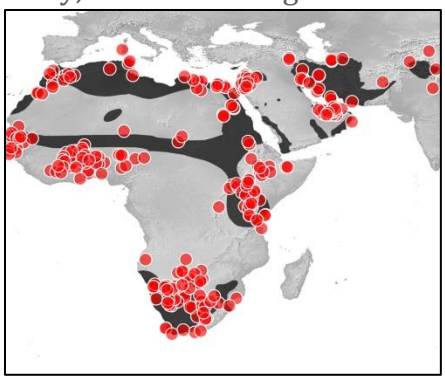

Figure 51 Points used to fit Maxent model. Range polygon from IUCN 2016.

Current Status: Least Concern (IUCN 2016).

Meriones crassus

Common Name: Sundevall's Jird

Description: Similar in appearance to the gerbils to which it is related, Sundevall's jird is a relatively small but robust rodent with soft, fine fur, a broad head, large eyes, elongated hind legs, and a long tail ending in a black tuft. The fur is yellowish to brownish in colour, although individuals vary in colouration depending on the habitat, providing good camouflage against predators. The contrasting colour of the tail tuft may serve to attract potential predators towards the tail and away from the more vulnerable head and body. The underparts of Sundevall's jird are white, and the claws are pale, helping to distinguish this species from the slightly larger Libyan jird,Meriones libycus, which has dark or black claws (ARKive 2016). Image source: https://www.flickr.com/.

Global Distribution: Sundevall's jird is widely distributed across North Africa, from Morocco to Egypt and Sudan, as well as in southwest Asia, including the Arabian Peninsula, north to Turkey, and as far east as Pakistan (ARKive 2016).

Distribution within Arabian Gulf Countries: Bahrain, Iran, Iraq, Oman, Saudi Arabia, United Arab Emirates (IUCN 2016).

Habitat: Sundevall's jird occurs in dry, sandy or gravel deserts, where it often burrows beneath sandy hummocks. It may avoid more rocky habitats, and is absent from mountain areas (ARKive 2016).

Current Status: Least Concern (IUCN 2016).

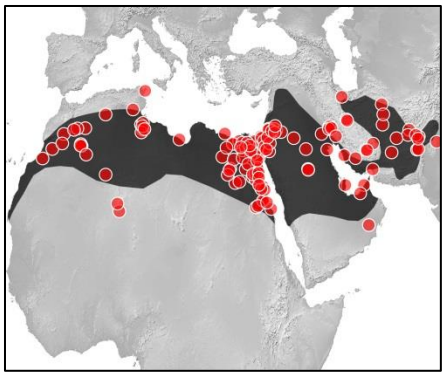

Figure 52 Points used to fit Maxent model. Range polygon from IUCN 2016.

Meriones libycus

Common Name: Libyan Jird

Description: Similar in appearance to the gerbils to which it is related, the Libyan jird is a fairly small but robust rodent, with soft, fine fur, a broad head, large eyes, and elongated hind legs. The body is generally reddish brown in colour, faintly speckled with black, with greyish-white underparts, and a long tail that ends in a black tuft. While the body colouration provides good camouflage, the contrasting colour of the tail tuft may serve to attract a predator's attention towards the tail and away from the more vulnerable head and body. The Libyan jird can be distinguished from the similar Sundevall's jird (Meriones crassus) by its dark rather than white claws, its larger size, and the longer tail, which has a more developed tuft (ARKive 2016).

Global Distribution: The Libyan jird has an extensive range, occurring across North Africa, through the Arabian Peninsula and into Asia, as far east as China. There is some confusion as to whether the species found in parts of the Arabian Peninsula, such as in the United Arab Emirates, is the Libyan jird or the very similar Arabian jird (Meriones arimalius), previously considered a subspecies of the Libyan jird (ARKive 2016).

Distribution within Arabian Gulf Countries: Iran, Iraq, Kuwait, Qatar, Saudi Arabia (IUCN 2016).

Habitat: M. libycus occupies desert habitats, generally in areas with stabilized dunes (desert and semi-desert habitats). It becomes most abundant in unflooded river plains and it is often found close to wadis and dayas. It is sometimes found in arable land. It is a highly mobile species, frequently changing burrows or even migrating should forage conditions deteriorate (IUCN 2016).

Current Status: Least Concern (IUCN 2016).

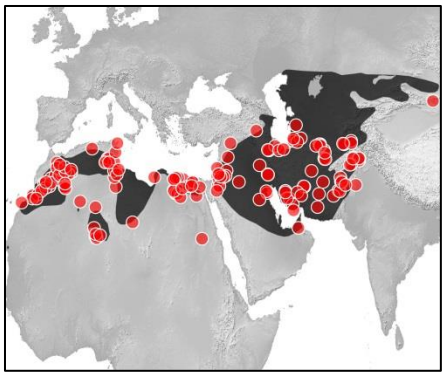

Figure 53 Points used to fit Maxent model. Range polygon from IUCN 2016.

Panthera pardus

Common Name: Leopard

Description: Distinguished by its exceptionally beautiful, black-spotted coat, the leopard is also recognised for its supreme stealth and its remarkable versatility. Despite being the smallest of the 'big cats', the leopard is the most widespread of all wild cat species, and is well known for the variety of prey it takes, as well as its ability to occupy a range of habitats, from deserts and mountains to jungles and swamps.
The leopard can be individually identified by its spot pattern. Its distinctive black spots contrast with the pale background coat colour and the white underparts. Small, solid black spots mark the head, throat, chest and lower limbs, with larger black patches on the belly. The leopard's back, flanks and upper limbs are patterned with pale-centred rosettes, which vary greatly in shape and size.
There is huge variation in coat colour, pattern and body size across the leopard's range, and the appearance of this species is often associated with its habitat (ARKive 2016). Image source: https://www.flickr.com/.

Global Distribution: The leopard has an exceptionally large range, occurring throughout Africa and Asia. It occurs across most of sub-Saharan Africa, with smaller populations in North Africa. Its range extends east to the Arabian Peninsula and throughout southwest Asia to India, China and the Russian Far East, and it is also found on the islands of Java and Sri Lanka.
Nine subspecies of leopard have been recognised, with the nominate subspecies, *P. p. pardus*, occurring in sub-Saharan Africa and North Africa. The Arabian leopard (*P. p. nimr*) occurs throughout Arabia, with the Persian leopard (*P. p. saxicolor*) occurring in Central Asia, the Javan leopard (*P. p. melas*) only on Java and the Sri Lankan leopard (*P. p. kotiya*) in Sri Lanka.
The Indian leopard (*P. p. fusca*) is distributed throughout the Indian sub-continent, while the Indochinese leopard (*P. p. delacourii*) is found throughout southeast Asia into southern China. The North Chinese leopard (*P. p. japonensis*) occurs in northern China, and the Amur leopard (*P. p. orientalis*) in found in the Russian Far East, the Korean peninsula and north-eastern China.
Despite occurring over such a vast area, the leopard has vanished from almost 40 percent of its historic range in Africa, and from over 50 percent of its historic range in Asia. (ARKive 2016).

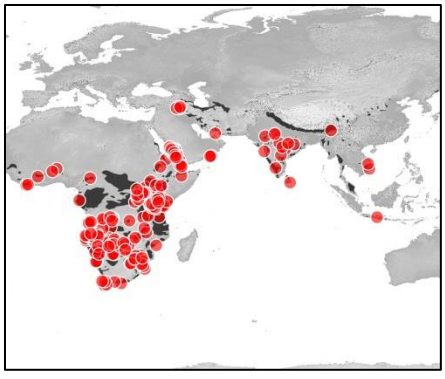

Figure 54 Points used to fit Maxent model. Range polygon from IUCN 2016.

Distribution within Arabian Gulf Countries: Native: Iran, Oman, Saudi Arabia, United Arab Emirates, Yemen, Regionally Extent: Kuwait (IUCN 2016).

Habitat: The leopard has adapted to make use of many different habitat types, ranging from deserts to rocky hills and mountains, lowland forests, woodlands, jungles, grasslands and swamps.
Although the leopard does occur in deserts and arid habitats, it is more common in areas with reasonable amounts of cover, such as rocks or vegetation. This species occurs from sea level to elevations of 5,200 metres (ARKive 2016).

Current Status: Near Threatened (IUCN 2016).

Procavia capensis

Common Name: Rock Hyrax, Rock Dassie

Description: The rock hyrax (Procavia capensis) is a small, tailless mammal which superficially may resemble a guinea pig, but is actually more closely related to elephants and manatees. Also known as the 'dassie', the dense fur of the rock hyrax is variable in colour, but is typically brownish-grey on the upperparts, with lighter underparts. A distinctive patch sits the back of the rock hyrax, which may be black, yellow or orange, and covers a gland that secretes a characteristic odour. The soles of the feet are moist and rubber-like, providing the hyrax with a good grip as it clambers around its steep, rocky habitat.
A rather vocal species, the rock hyrax produces a series of intermittent "harsh yips" which build up to "guttural grunts" to defend its territory, and a sharp bark is used to warn others if danger threatens (ARKive 2016). Image source: https://www.flickr.com/.

Global Distribution: The rock hyrax is found throughout sub-Saharan Africa, with the exception of the Congo basin, and in north-east Africa, eastwards to the western and southern coast of the Arabian Peninsula (ARKive 2016).

Distribution within Arabian Gulf Countries: Saudi Arabia, Oman, Yemen (IUCN 2016).

Habitat: The rock hyrax occupies habitats dominated by rocks and large boulders, including mountain cliffs, scree slopes and outcrops or kopjes (isolated rock hills rising from the African veldt). It requires numerous cavities and crevices that are large enough to shelter in, but small enough to discourage predators. These cavities often face away from strong prevailing winds, have good visibility of the surrounding habitat, and are close to to sunlit areas for basking and suitable foraging areas. The rock hyrax often uses basking and sheltering to control its body temperature, thus the location and layout of its rocky habitat is important – it needs easy access to basking spots when it is cold, as well as deep crevices to escape excessive heat (ARKive 2016).

Current Status: Least Concern (IUCN 2016).

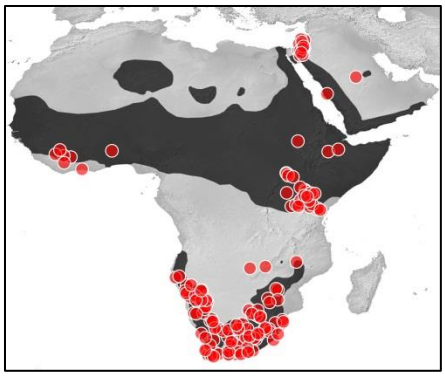

Figure 55 Points used to fit Maxent model. Range polygon from IUCN 2016.

Psammomys obesus

Common Name: Fat Sand Rat

Description: The appropriately named fat sand rat is a heavy-built, gerbil-like rodent, native to desert regions. It typically has dark reddish-brown fur speckled with black on its upperparts and lighter fur on the underside, although the exact colour of the fur may vary depending on the environment. The sturdy limbs bear blackish claws and the short, stout tail has a noticeable black tip. The small, rounded ears are covered with dense whitish to yellowish hair. This species apparently communicates through high-pitched squeaks and by drumming its feet (ARKive 2016). Image source: https://www.flickr.com/.

Global Distribution: This species is found in North Africa from Mauritania and Western Sahara to Egypt, and east through Sinai Peninsula into Saudi Arabia, Israel, Jordan and Syria. It is unevenly distributed probably due to its dependence on succulent plants for moisture. It has been recorded from a harbour in Sudan, where it may have been accidentally introduced (IUCN 2016).

Distribution within Arabian Gulf Countries: Saudi Arabia (IUCN 2016).

Habitat: The species is only found in the vicinity of succulent shrubs, which are its main food source. It is a habitat generalist, found in rocky habitats, grasslands, semi-desert and desert so long as succulent shrubs are present. This mostly diurnal species is colonial and lives in burrow systems in open terrain of soil or sand (IUCN 2016).

Current Status: Least Concern (IUCN 2016).

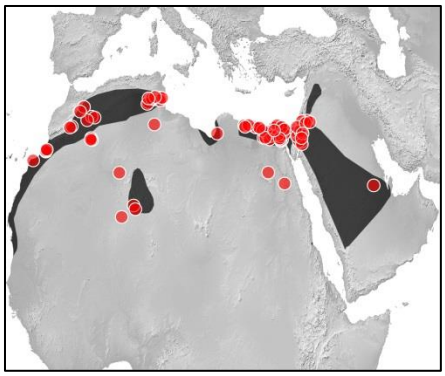

Figure 56 Points used to fit Maxent model. Range polygon from IUCN 2016.

Rhinolophus blasii

Common Name: Blasius's Horseshoe Bat, Peak-saddle Horseshoe Bat, Peters's Horseshoe Bat

Description: Blasius's horseshoe bats are medium sized bats with medium sized ears and broad wings. They are normally light brown with hints of grey, lilac, and cream colors in their long fur. They have distinctive horseshoe shaped noseleaves, from which horseshoe bats take their name. The noseleaf of Blasius's horseshoe bats is broad but covers only part of the muzzle. The wings are short and broad, which allows for greater maneuverability. The skull is gracile, which indicates that its diet consists of soft foods rather than the hard shelled insects eaten by bats with more robust skulls. The negative tilt of the head identifies R. blasii as a nasal emitter; their high frequency echolocation calls radiate from the nostrils as opposed to the mouth. Blasius's horseshoe bats have a 1-1-2-3, 2-1-3-3 dentition, with relatively strong, short upper canines. They are sexually dimorphic, with the female being the larger of the two sexes (Encyclopedia of Life 2016).

Global Distribution: Rhinolophus blasii has a large range in the Palaearctic and the Afrotropics, throughout which it is widely but patchily distributed. Its range extends marginally into the Indomalayan region.
In Africa, it occurs from northeastern South Africa and the Democratic Republic of Congo, through south Malawi, to East African, Ethiopia and Somalia, and in North Africa. Follow Taylor (2000) for southern African distribution. In North African it is only present in Morocco and Algeria (it may occur in Tunisia but there are no confirmed records as yet, and likewise for Egypt). Altitude range is from sea level to 1,200 m.
In Asia, it has a patchy distribution extending from Turkey in the west to Pakistan in the east, and from the Caucasus in the north to Yemen in the south. It was confirmed in Georgia in 2006.
In European, it is extinct in northeastern Italy and has not been recorded in Slovenia during the last 50 years. Also recorded from western Anatolia and from the Levant (Syria, Lebanon, Jordan, Palestine and Israel). It is now restricted to the Balkan peninsula and to some Mediterranean islands including Crete and Cyprus. There are no recent records in Romania and northern Bulgaria despite intensive work by Christian Dietz. Past records from this area are disputed: no specimen has been found in museums in Romania, and the presence of R. euryale in the same area might have caused confusion . It occurs from sea level to 2,215 m in Yemen (IUCN 2016).

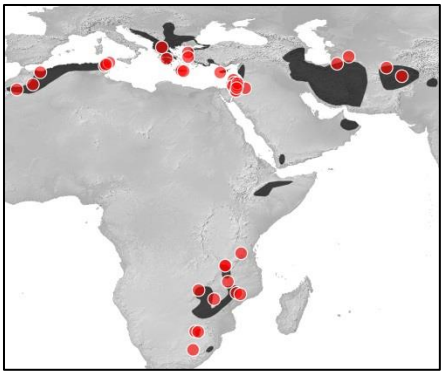

Figure 57 Points used to fit Maxent model. Range polygon from IUCN 2016.

Distribution within Arabian Gulf Countries: Iran, Oman, Yemen (IUCN 2016).

Habitat: Blasius's horseshoe bats live in temperate climates and prefer savanna woodlands, although they are occasionally found in desert regions as well. They

roost in caves, mines, under piles of boulders, and sometimes in human dwellings, roosting in attics and cellars.[2] In the Mediterranean region it typically forages in shrubland and woodland, although it may penetrate to desert habitat. Summer roosts are situated in natural and artificial underground sites, with attics also being used in the northern part of the range. In winter, it hibernates in underground sites. This species is considered to be sedentary (IUCN 2016).

Current Status: Least Concern (IUCN 2016).

Sekeetamys calurus

Common Name: Bushy-tailed Jird

Description: The timid bushy-tailed jird is a small, gerbil-like mammal with a slender body, large eyes and, as the common name suggests, a thick and fluffy covering of fine hairs on the tail. The bushy tail is the most striking feature, having greyish or black fur along most of its length, except for the white tip. The body of the bushy-tailed jird is brownish-yellow and speckled with black on the upperparts, paler on the flanks, and white on the underside. With its slender limbs and long hind feet, the bushy-tailed jird is a proficient, agile climber in its rocky habitat (ARKive 2016). Image source: https://www.flickr.com/.

Global Distribution: The bushy-tailed jird is distributed on the highlands surrounding the Red Sea, in north-eastern Sudan, eastern Egypt, including the southern coast of the Sinai Peninsula, southern Israel, southern Jordan, and western Saudi Arabia (ARKive 2016).

Distribution within Arabian Gulf Countries: Saudi Arabia (IUCN 2016).

Habitat: The bushy-tailed jird inhabits rocky, hot, arid deserts where it rests during the day in a burrow under large rocks or a den amongst boulders. It is able to tolerate extreme temperatures, such as in Sinai, where mountain-dwelling populations can experience snow during the winter and soaring temperatures during the summer (ARKive 2016).

Current Status: Least Concern (IUCN 2016).

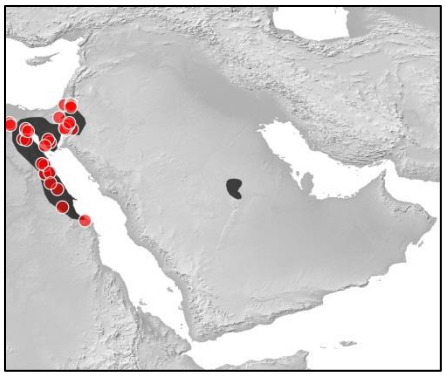

Figure 58 Points used to fit Maxent model. Range polygon from IUCN 2016.

Birds

Alectoris melanocephala

Common Name: Arabian partridge

Description: Much larger than other Alectoris species, the sexes are similar. Often considered the most beautiful of the genus, the crown is black which extends down the nape; a broad white band begins in front of the eye and extends to the back of the head, the chin and upper throat are also white, this is separated from the white above the eye by a narrow black band that starts at the bill, extends to the the cheek and forms a "V" on the neck; the sides of the neck pastel brown; rest of plumage bluish gray as in other members of the genus; pronounced barring on the sides. Females slightly smaller, lack the tarsal knob seen on adult males (gbwf.org 2016).

Global Distribution: Oman, Saudi Arabia, Yemen (IUCN 2016)

Distribution within Arabian Gulf Countries:

Habitat: Arid regions of Arabian Peninsula (Encyclopedia of Life 2016). Rocky hillsides and grassy slopes to 4500 feet. Will often feed on cultivated lands (gbwf.org 2016).

Current Status: Least Concern (IUCN 2016).

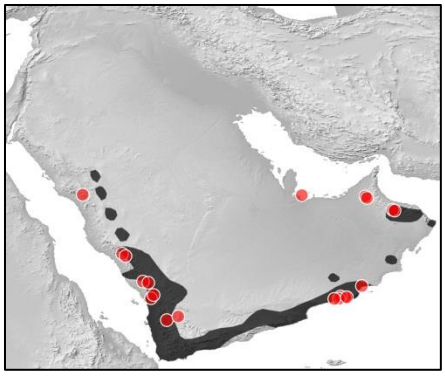

Figure 59 Points used to fit Maxent model, breeding range. Range polygon from Birdlife 2016.

Ammoperdix heyi

Common Name: Sand partridge

Description: Well adapted to living in sweltering desert temperatures, the sand partridge has striking dark red, black and white wavy streaked plumage on its sides, with a sandy-pink underside that darkens towards the back. It has a distinctive blue-grey head, with a white, oval patch on its cheek and a chestnut coloured throat, and the beak is short and yellow. In flight, the sand partridge can be identified by its dark chestnut tail feathers. Both females and juveniles are 'washed-out' versions of the male, being more sandy and grey in colour, with fewer distinct markings. The song of the sand partridge is said to have a yelping quality which often echoes in its rocky surroundings. The male's call includes the sounds qwei-qwei-qwei and when alarmed wuit-wuit-wuit (ARKive 2016). Image source: https://www.flickr.com/.

Global Distribution: The range of the sand partridge extends from Egypt and Sudan, through to Israel and Jordan, and reaches as far as Saudi Arabia and Oman (ARKive 2016).

Distribution within Arabian Gulf Countries: Oman, Saudi Arabia, United Arab Emirates, Yemen (IUCN 2016).

Habitat: This species is found in hot, dry desert habitats, where it usually resides on steep, rocky slopes with scattered vegetation, but can sometimes also be found in sandy, dried-out rivers. This bird often has to tolerate extreme climates; for example, the average summer temperature in the Arava desert of Israel is around 40 degrees Celsius, with an annual rainfall of 50 millimetres (ARKive 2016).

Current Status: Least Concern (IUCN 2016).

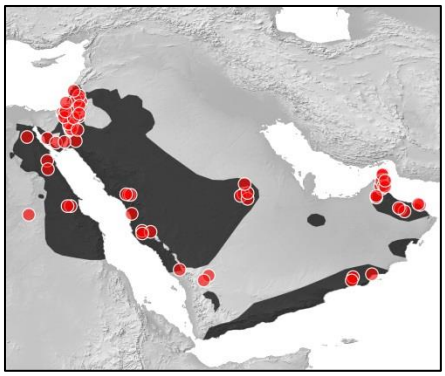

Figure 60 Points used to fit Maxent model, breeding range. Range polygon from Birdlife 2016.

Aquila clanga

Common Name: Greater Spotted Eagle

Description: A medium-sized eagle, the greater spotted eagle only has white spots as a juvenile, when they extend in bands across the upperwing. By adulthood, the spots have faded leaving dark brown feathers across the head, body and wings, with slightly paler flight feathers on the upper side. In gliding flight, the greater spotted eagle holds the feathers at the tips of the wings downward. Although mainly a quiet bird, this eagle has a barking 'kyak' call during the breeding season (ARKive 2016). Image source: https://www.flickr.com/.

Global Distribution: *Aquila clanga* occupies a fragmented range, breeding in Estonia, Poland, Belarus, Moldova, Russia, Ukraine, Kazakhstan, mainland China and Mongolia, and apparently regularly in tiny numbers in Pakistan and north-west India, with some individuals possibly still breeding in Finland, Latvia and Lithuania, although this has not been confirmed recently. Passage or wintering birds occur in small numbers over a vast area, including central and Eastern Europe, North Africa, East Africa, the Middle East, the Arabian Peninsula, the Indian Subcontinent, south Asia and South-East Asia. Wintering birds have also been reported in Hong Kong (China) (BirdLife 2016).

Distribution within Arabian Gulf Countries: Iran, Iraq, Oman, Saudi Arabia, United Arab Emirates, Yemen (IUCN 2016).

Habitat: It occurs in lowland forests near wetlands, nesting in different types of (generally tall) trees, depending on local conditions. It is a migratory species, with birds leaving their breeding grounds in October and November to winter in southern Europe, southern Asia and north-east Africa. They tend to return in February and March. Birds migrate on a broad front, tending to pass in singles, twos and threes with the occasional larger group. They do not concentrate at bottleneck sites to the extent of many other raptors such as *Clanga pomarina* (IUCN 2016).

Current Status: Vulnerable (IUCN 2016).

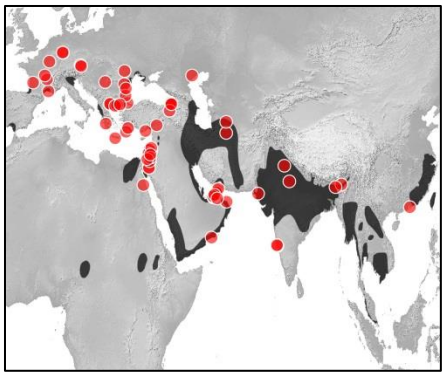

Figure 61 Points used to fit Maxent model, non-breeding range. Range polygon from Birdlife 2016.

Calidris tenuirostris

Common Name: Great Knot

Description: The great knot is a long distance migratory shorebird, with a rather plump body and a stout, straight bill. For most of the year, the great knot has streaky, greyish-brown feathers on its upperparts and head, and white underparts. During flight, a white stripe on the wings and a small, whitish patch on the rump can be seen. During the breeding season, it develops reddish-brown streaks on its back, and black streaks on the head and breast. The bill is black, the irises are brown, and the legs and feet are dark grey to olive green. While usually silent, the great knot may occasionally call with a '*prrt'* sound (ARKive 2016). Image source: https://www.flickr.com/.

Global Distribution: The great knot breeds in north-eastern Siberia (Russia) and winters along the coastlines of Southeast Asia, Australia, India, Bangladesh, Pakistan and the eastern shores of the Arabian Peninsula (ARKive 2016).

Distribution within Arabian Gulf Countries: Iran, Kuwait, Oman, Saudi Arabia, United Arab Emirates (IUCN 2016).

Habitat: *Breeding* The species breeds on gravelly areas covered with lichen and patches of herbs, heather, *Empetrum*spp., *Dryas* spp. and *Vaccinium* spp. or alternatively on areas with a continuous layer of lichen and scattered stunted larch *Larix* spp. or dwarf pine *Pinus pumila*. It occurs on plateaus or gentle slopes with montane tundra in the subarctic at heights of 300-1,600 m. *Non-breeding*In its wintering range the species occurs in sheltered coastal habitats such as inlets, bays, harbours, estuaries and lagoons with large intertidal mud and sandflats, oceanic sandy beaches with nearby mudflats, sandy spits and islets, muddy shorelines with mangroves and occasionally exposed reefs or rock platforms. It roosts in refuges such as shallow water in sheltered sites, on coastal dunes or on saltflats amongst mangroves during high tides. On passage the species stages in estuaries and on intertidal mudflats (Encyclopedia of Life 2016).

Current Status: Vulnerable (ARKive 2016), Endangered (IUCN 2016).

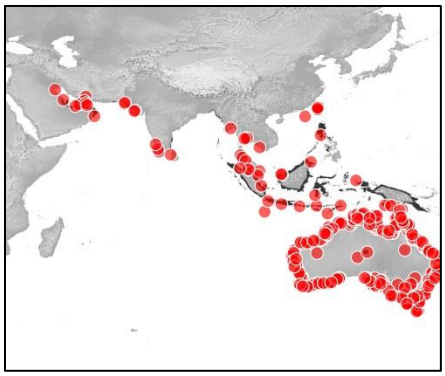

Figure 62 Points used to fit Maxent model, non-breeding range. Range polygon from Birdlife 2016.

Chlamydotis macqueenii or *Chlamydotis undulata*

Common Name: Houbara Bustard

Description: A striking bird resembling a turkey in shape, the houbara bustard is at its most magnificent during the courtship display. It is a slender bird, with a tuft of hairs in the centre of the crown, and long plumes of feathers drooping over the neck, the uppermost feathers being black while the lower ones are white with black tips. The body is pale sandy-buff in colour, with darker brown lines and mottling, while the underside is white. Large areas of black and brown occur on the flight feathers and the long, square tail is sandy-chestnut and patterned with four distinct blue-black bars. Male houbara bustards are slightly larger than females (ARKive 2016). Image source: https://www.flickr.com/.

Global Distribution: There are three subspecies of houbara bustard: Chlamydotis undulata macqueenii is found in the deserts of Russia and the Middle East, including the Arabian Peninsula, while C. u. undulata is found in North Africa andC. u. fuertaventurae is found in the eastern Canary Islands. They differ slightly in their size and colouration, but are not consistent in their migratory tendencies. North African and Middle Eastern birds are resident or partially migratory, moving short distances to find fresh vegetation, whereas other Asian populations are fully migratory (IUCN 2016).

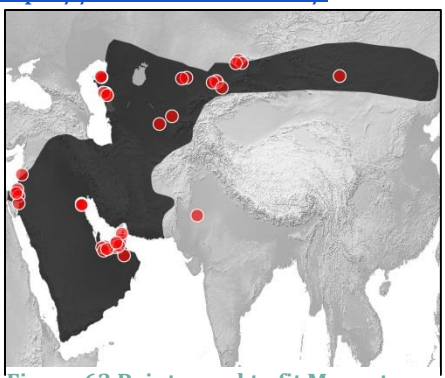

Figure 63 Points used to fit Maxent model, breeding range. Range polygon from Birdlife 2016.

Distribution within Arabian Gulf Countries: Israel,Palestine, Jordan, Syria, Saudi Arabia,Yemen, Oman, U.A.E., Bahrain, Qatar,Iraq, Kuwait, Iran (BirdLife 2016).

Habitat: It inhabits sandy and stony semi-desert and is specialised to arid conditions where trees are absent and both shrub cover and herb layer are sparse (IUCN 2016).

Current Status: Vulnerable (IUCN 2016).

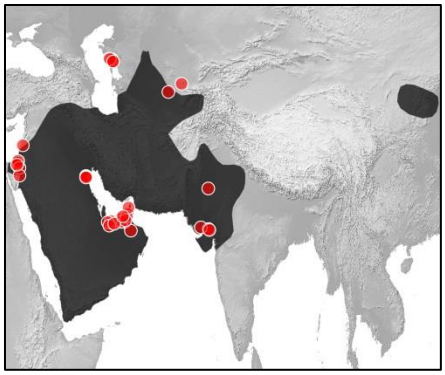

Figure 64 Points used to fit Maxent model, non-breeding range. Range polygon from Birdlife 2016.

Corvus ruficollis

Common Name: Brown-necked Raven

Description: A large, attractive corvid with glossy plumage, the brown-necked raven (*Corvus ruficollis*) has distinctive, elongated, pointed and often forked throat feathers known as hackles, and a large, slightly curved, thick set bill. The lustrous black feathers are tinged with dark green on the crown and upperparts, and violet on the wings, breast, flanks and tail, while the back of the neck, throat and the upper-back is a shiny brown, glossed with bronze-purple. The underparts are sooty-black, the bill and legs are black, and the eyes are brown. The male and female brown-necked raven are similar in appearance, but the juvenile differs in being less glossed, with a duller head and underparts. Although similar in appearance to the common raven (*Corvus corax*), the brown-necked raven is distinguished by its smaller size, slimmer build, shorter wings with a more pointed tip, and brown head and neck (ARKive 2016). Image source: https://www.flickr.com/.

Global Distribution: The brown-necked raven is found from western Africa, eastwards into the Middle East and south-western Asia (ARKive 2016).

Distribution within Arabian Gulf Countries: Native: Iran, Iraq, Saudi Arabia, United Arab Emirates, Yemen, Oman, Vegrant: Bahrain (IUCN 2016).

Habitat: The opportunistic brown-necked raven is found in a variety of natural habitats, including hot desert, rocky areas, savanna, shrubland, freshwater springs and oases, as well as artificial habitats, such as arable land and urban areas, including rubbish dumps. It occurs up to altitudes of 3,700 metres (ARKive 2016).

Current Status: Least Concern (IUCN 2016).

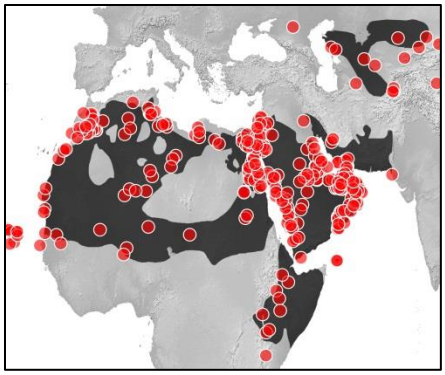

Figure 65 Points used to fit Maxent model, breeding range. Range polygon from Birdlife 2016.

Egretta gularis

Common Name: Western reef-egret

Description: Western reef-egret is the name given to two former subspecies of the little egret (Egretta garzetta), now treated somewhat contentiously as a single separate species. This thin, medium-sized heron occurs in two distinct forms, one of which has mostly dark slaty-grey plumage and a white throat, while the other has predominately white plumage. During the breeding season, both forms develop red lores and distinctive plumes on the head, chest and back. The legs are dark, while the feet are bright yellow, except during the height of courtship when they turn pinkish red (ARKive 2016). Image source: https://www.flickr.com/.

Global Distribution: Native to coastal West Africa from Mauritania to Gabon, and coastal East Africa, through the Red Sea and the Arabian Gulf to India. Vagrant individuals have been recorded as far away as Brazil, the Caribbean, and North America (ARKive 2016).

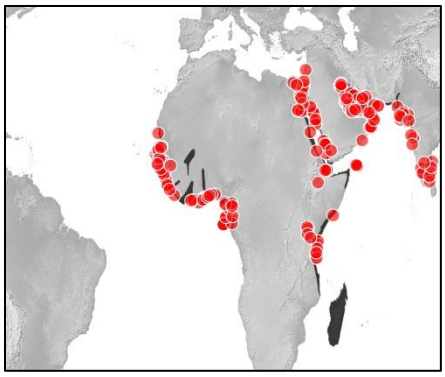

Figure 66 Points used to fit Maxent model, breeding range. Range polygon from Birdlife 2016.

Distribution within Arabian Gulf Countries: Bahrain, Iran, Iraq, Kuwait, Oman, Qatar, Saudi Arabia, United Arab Emirates, Yemen (IUCN 2016).

Habitat: The western reef-egret is a coastal species, occurring mainly on rocky or sandy shores and reefs, but is also found around estuaries, mudflats, saltmarshes, mangroves, tidal creeks and lagoons (ARKive 2016).

Current Status: Least Concern (IUCN 2016).

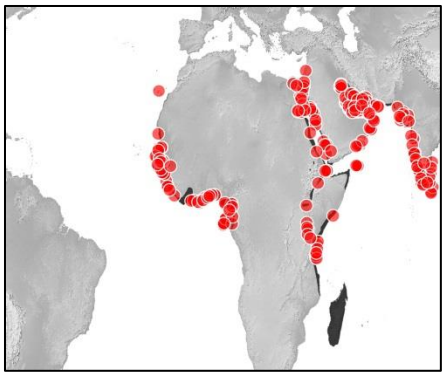

Figure 67 Points used to fit Maxent model, non-breeding range. Range polygon from Birdlife 2016.

Emberiza cineracea

Common Name: Cinereous Bunting

Description: One of the least known bunting species in its range, the cinereous bunting is a rather drab, greyish to brownish bird with a white outer tail. Although described as a relatively featureless species, its main distinguishing character is the olive to yellow head of the male, together with the pale yellow chin and conspicuous white eye ring. The beak is pale grey, and the legs brown. The female cinereous bunting is similar to the male, but darker and duller in color, with more streaked plumage, and a trace of yellow on the throat. The juvenile has slightly browner plumage, and is even more streaked than the female. Two subspecies of cinereous bunting are recognized, which differ mainly in the color of the underparts, with Emberiza cineracea cineracea having a more white or grey belly, and Emberiza cineracea semenowi a brighter yellow one. The song of the cinereous bunting is a simple, ringing, tuneful phrase of five to six notes, while the most common call is a short, metallic kjip (ARKive 2016). Image source: https://www.flickr.com/.

Global Distribution: This species breeds on the islands of Skyros, Lesbos and Chios, Greece, and western Turkey, as well as in south-east Turkey, south-west Iran and Iraq. Statements regarding potential breeding in northern Syria are of uncertain validity. The winter distribution remains poorly known, but includes Eritrea and Yemen, and potentially also Ethiopia, north-east Sudan and south-west Saudi Arabia (where records may solely relate to individuals on migration). In addition, there are passage records along the species' two, well-separated migration routes: Cyprus, Syria, Lebanon, Israel, Jordan, Palestinian Authority Territories and Egypt; and Kuwait, Qatar, Bahrain, United Arab Emirates and Oman. The Turkish breeding population - which at 3,100-5,500 pairs probably constitutes over 90% of the global population - was suspected to have declined by 0-19% during 1990-2000 and in 1990-2013 (IUCN 2016).

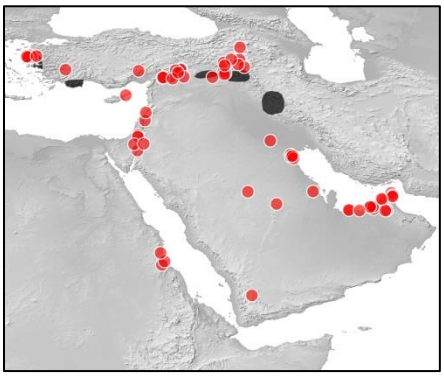

Figure 68 Points used to fit Maxent model, breeding range. Range polygon from Birdlife 2016.

Distribution within Arabian Gulf Countries: Bahrain, Iran, Iraq, Kuwait, Qatar, Saudi Arabia, United Arab Emirates, Yemen (IUCN 2016).

Habitat: The cinereous bunting usually breeds on dry, rocky slopes and uplands with shrubby vegetation and sometimes scattered conifers, although it usually avoids arid areas, and has also been recorded using more lushly vegetated slopes at lower elevations. Migrating individuals may use lowland desert or agricultural land, and in its winter range the species is found in dry, open country, such as semi-desert or coastal plains (ARKive 2016).

Current Status: Near Threatened (IUCN 2016).

Gyps fulvus

Common Name: Griffon Vulture, Eurasian Griffon, Eurasian Griffon Vulture

Description: A large, carnivorous scavenger, the Eurasian griffon may be seen soaring majestically on thermal currents in the warmer, rugged areas of countries surrounding the Mediterranean as it searches for food. The Eurasian griffon has an impressive creamy-white ruff (a ring of conspicuously colored feather which project from around the neck), which matches the color of the head and neck. The body and upper-wing plumage of the Eurasian griffon is pale brown, contrasting beautifully with the dark flight feathers on the rest of the wings and tail. This contrast is most noticeable in juvenile birds which have particularly pale upper-wing feathers. A fairly vocal bird, the Eurasian griffon produces a range of different calls when interacting with other Eurasian griffons. For example, a drawn out hissing sound is produced by dominant birds when feeding, and a wooden-sounding chattering occurs when another Eurasian griffon ventures too close (ARKive 2016). Image source: https://www.flickr.com/.

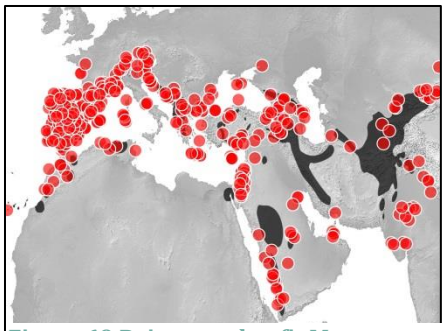

Figure 69 Points used to fit Maxent model, breeding range. Range polygon from Birdlife 2016.

Global Distribution: The Eurasian griffon has an extremely large range, extending over Europe, the Middle East and North Africa. It occurs from India, west to Portugal and Spain. The Eurasian griffon is most common in countries bordering the Mediterranean, although it usually occurs at low densities. The most widespread population occurs in Spain, which supports over three-quarters of the total European population (ARKive 2016).

Distribution within Arabian Gulf Countries: Iran, Iraq, Kuwait, Oman, Saudi Arabia, Yemen (IUCN 2016).

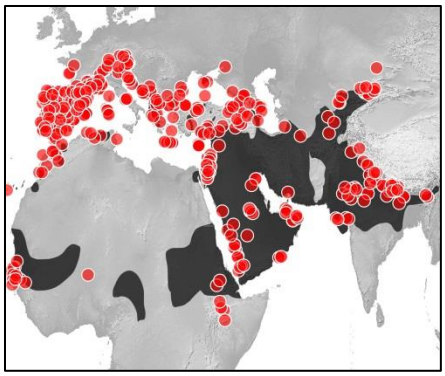

Figure 70 Points used to fit Maxent model, non-breeding range. Range polygon from Birdlife 2016.

Habitat: The Eurasian griffon occurs in a wide range of habitats, including mountains, plateaus, grassland, shrubland and semi-desert. Itis usually found in warm climates, but will tolerate harsher conditions such as cold, rain, mist or even snow to obtain particularly favorable foraging or breeding conditions. The Eurasian griffon tends to avoid forests, wetlands, lakes and marine waters. This species requires high cliffs for roosting and is found at a wide range of elevations, from just above sea level up to 2,500 meters. A large area for foraging is also

required, and rising air currents associated with midday thermals or up-draughts from slopes or cliffs are needed to enable the bird's soaring flight (ARKive 2016).

Current Status: Least Concern (IUCN 2016).

Neophron percnopterus

Common Name: Egyptian Vulture, Egyptian Eagle

Description: A small vulture with a very large range, the Egyptian vulture has an unmistakable appearance. Adults have largely white to pale grey plumage, which contrasts markedly with the black flight-feathers and the bold yellow bare skin on the face. The long, narrow bill has a yellow base and terminates with a black tip. The tail is short and wedge-shaped. The legs may be greyish-white, pink or pale yellow. Two subspecies of the Egyptian vulture are recognized; *Neophron percnopterus ginginianus* is slightly smaller than *Neophron percnopterus percnopterus* and has an entirely yellow bill. Juveniles have much darker plumage than the adults, and may be grey-brown, brown or blackish-brown (ARKive 2016). Image source: https://www.flickr.com/.

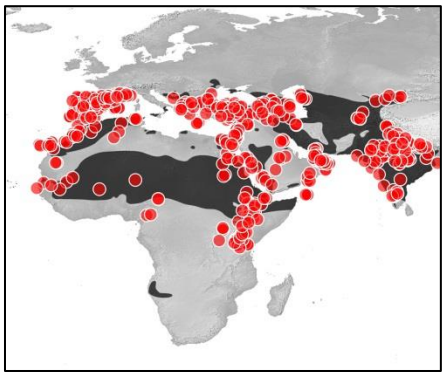

Figure 72 Points used to fit Maxent model, breeding range. Range polygon from Birdlife 2016.

Global Distribution: The Egyptian vulture has a very large range. *N. p. percnopterus* occurs in southern Europe, east to Central Asia and north-west India, and south through North Africa, Arabia and the Sahel zone to northern Tanzania, south-western Angola and north-western Namibia. Isolated populations also occur in the Canary Islands and the Cape Verde Islands. *N. p. ginginianus* can be found in Nepal and India, except for the north-western parts. Most Egyptian vulture populations migrate for winter to the south of the Sahara, but some remain on their breeding grounds.[6] Several resident island populations show genetic isolation (IUCN 2016).

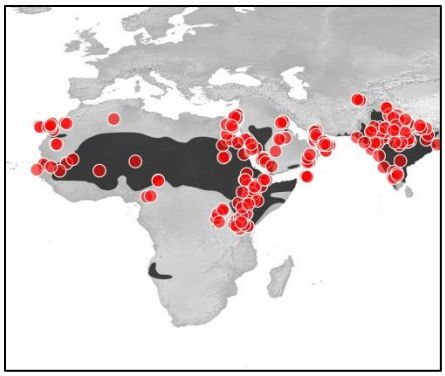

Figure 71 Points used to fit Maxent model, non-breeding range. Range polygon from Birdlife 2016.

Distribution within Arabian Gulf Countries: Iran, Iraq, Kuwait, Oman, Saudi Arabia, United Arab Emirates, Yemen, Socotra.

In Spain, which with at least 1,300 pairs may support as much as 40% of the European breeding population, the number of territories declined by at least 25% between 1987-2000 (i.e. equating to a decline of >50% over three generations), likely due to high mortality rates. Similar declines are reported from the Middle East, e.g. 50-75% in **Israel**, however in **Oman** the population appears stable, although this may be more a reflection of count methods rather than genuine stability in the population.

Around 1,700 birds are resident in a stable population on the island of Socotra (IUCN 2016).

Habitat: Typically nests on ledges or in caves on cliffs, crags and rocky outcrops, but occasionally also in large trees, buildings (mainly in India), electricity pylons and exceptionally on the ground. Forages in lowland and montane regions over open, often arid, country. Also scavenges at human settlements (IUCN 2016).

Current Status: Endangered (IUCN 2016).

Phalacrocorax nigrogularis

Common Name: Socotra Cormorant

Description: 80 cm. Large, blackish cormorant with bronze-green sheen on back and wings. In breeding season, becomes more glossy, with fine, white flecks on neck. **Similar spp.** Great Cormorant *P. carbo* is larger, with stouter bill and white face and chin-patch (BirdLife 2016). Image source: http://www.asergeev.com/.

Global Distribution: This large bird has an extremely restricted range, with two subpopulations now breeding at a total of just nine locations. The northern subpopulation breeds on islands off the Arabian Gulf coasts of Bahrain, United Arab Emirates (UAE), Saudi Arabia, Qatar and possibly the Islamic Republic of Iran (breeding not confirmed since 1972). The much smaller southern population breeds on one or more islands off the Arabian Sea coast of Oman and in the Gulf of Aden off Yemen (BirdLife 2016).

Distribution within Arabian Gulf Countries:

Habitat: The species is exclusively marine and occurs within the range of productive upwellings. *Breeding* It breeds on offshore islands and islets that have shores of level sand or gravel. *Nonbreeding* Outside the breeding season it roosts on coastal cliffs and rocky islets (BirdLife 2016).

Current Status: Vulnerable (BirdLife 2016).

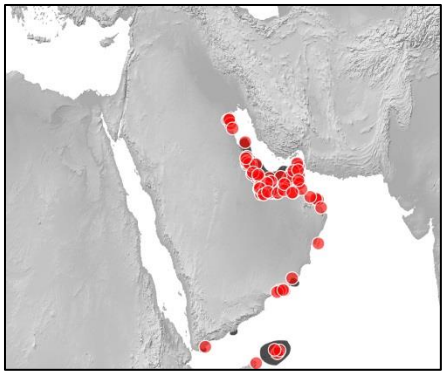

Figure 73 Points used to fit Maxent model, breeding range. Range polygon from Birdlife 2016.

Puffinus persicus

Common Name: Persian Shearwater

Description: The Persian shearwater is a seabird in the Procellariidae family formerly lumped in with Audubon's shearwater (*Puffinus lherminieri*) (iNaturalist 2016).

Global Distribution: After breeding, the northern subspecies ranges from the southern Red Sea, the Gulf of Aden and the Somali coast across the south of the Arabian Peninsula to the Gulf of Oman, Pakistan and western India. The southern subspecies stays in the area around the Comoros and the Tanzanian and northern Mozambican coast (iNaturalist 2016).

Distribution within Arabian Gulf Countries: Iran, Oman, Saudi Arabia, United Arab Emirate, Yemen, Vagrant: Kuwait (IUCN 2016).

Habitat:

Current Status: Least Concern (iNaturalist 2016).

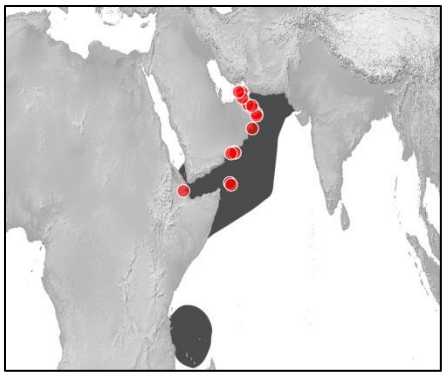

Figure 74 Points used to fit Maxent model, breeding range. Range polygon from Birdlife 2016.

Serinus rothschildi

Common Name: Olive-rumped Serin, Arabian Serin, Arabian Canary

Description: A rather scarce resident of the south-west highlands occurring in scrub land and acacia sites, recorded twice on Raydah escarpment at Raydah Farm and once on the plateau along the Azeezah Road. In 1987 it was recorded more frequently than in 2010, suggesting a possible decline in numbers. Also occurs in the Tihama around Jebal Gaha where a few were seen. Birds have also been seen in the Raghadan Forest area of Baha. (Birds of Saudi Arabia 2016).

Global Distribution:

Distribution within Arabian Gulf Countries: Saudi Arabia, Yemen (IUCN 2016).

Habitat:

Current Status: Least Concern (IUCN 2016).

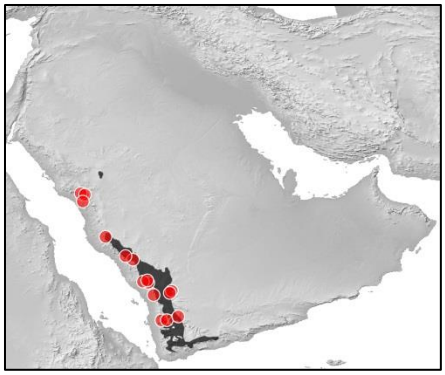

Figure 75 Points used to fit Maxent model, breeding range. Range polygon from Birdlife 2016.

Sylvia leucomelaena

Common Name: Arabian Warbler, Red Sea Warbler

Description: Image source: https://www.flickr.com/.

Global Distribution: Djibouti, Egypt, Eritrea, Israel, Jordan, Oman, Saudi Arabia, Somalia, Sudan, Yemen (IUCN 2016).

Distribution within Arabian Gulf Countries: Oman, Saudi Arabia, Yemen (IUCN 2016).

Habitat: dry savanna (GBIF 2016).

Current Status: Least Concern (IUCN 2016).

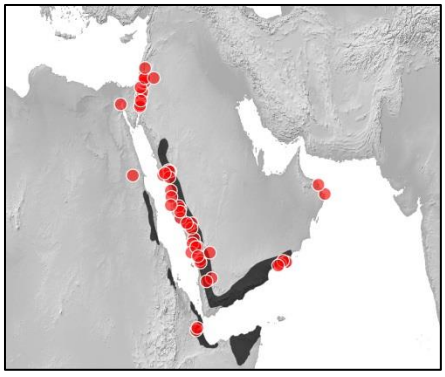

Figure 76 Points used to fit Maxent model, breeding range. Range polygon from Birdlife 2016.

Turdoides squamiceps

Common Name: Arabian Babbler

Description: A superbly camouflaged dark brown bird, from a distance the Arabian babbler appears rather plain, but upon closer inspection the fluffy plumage is in fact quite attractive. The feathers covering the head have dark centers with white edges, giving an appealing mottled effect. The dark centers of the feathers on the underparts become lighter and the white turns a tan color. The Arabian babbler has short, curved wings, an elongated tail that balances the bird as it weaves through dense or thorny vegetation, and a long, thin, slightly downward-pointing bill (ARKive 2016). Image source: https://www.flickr.com/.

Global Distribution: The Arabian Babbler is found from Yemen, Oman and the United Arab Emirates in the southern Arabian Peninsula into Saudi Arabia, Jordan, Israel and Egypt (ARKive 2016).

Distribution within Arabian Gulf Countries: Oman, Saudi Arabia, United Arab Emirates, Yemen (IUCN 2016).

Habitat: The Arabian babbler is found in a variety of different habitats, ranging from arable land and plantations, to grassland, saltmarshes, shrubland and true desert, up to altitudes of 2,800 meters. In the Negev desert of Israel, the Arabian babbler uses *Acacia* bushes for cover and nest sites (ARKive 2016).

Current Status: Least Concern (IUCN 2016).

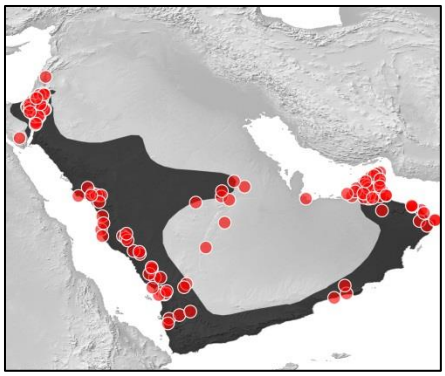

Figure 77 Points used to fit Maxent model, breeding range. Range polygon from Birdlife 2016.

Vanellus gregarius

Common Name: Sociable Lapwing

Description: 27-30 cm. Strikingly patterned plover. Adult greyish with black and chestnut belly. White supercilium and black crown and eye-stripe. Winter adult brownish but retains supercilium and crown pattern. Juvenile brown, slightly scalloped above, and streaked black below with large white supercilium. **Similar spp.**White-tailed Lapwing *V. leucurus* lacks supercilium and crown patch, has longer legs and no black subterminal tail-band. **Voice** Harsh *kretsch kretsch* and a rapid chattering (BirdLife 2016). Image source: https://www.flickr.com/.

Global Distribution: The sociable lapwing breeds in Russia and Kazakhstan, dispersing through Kyrgyzstan, Tajikistan, Uzbekistan, Turkmenistan, Afghanistan, Armenia, Iran, Iraq, Saudi Arabia, Syria and Turkey to winter grounds in Israel, Eritrea, Sudan and north-west India. It may also be found in Pakistan, Sri Lanka and Oman during the winter. However, this species is suffering a very rapid decline in numbers and a severe range reduction (ARKive 2016).

Distribution within Arabian Gulf Countries: In Arabia it often occurs in the desert near the coast (IUCN 2016).

Habitat: Inhabits grassland steppes with salty areas, near water. Winters on dry plains, sandy spots and short grasslands, in close proximity to a water source (ARKive 2016).

Current Status: Critically Endangered (BirdLife 2016).

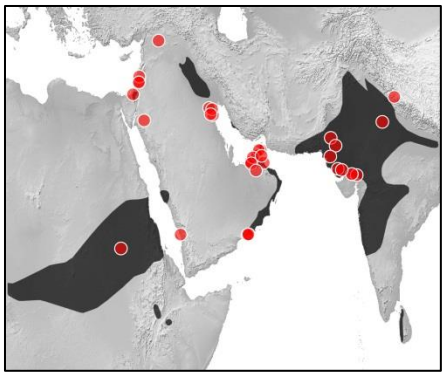

Figure 78 Points used to fit Maxent model, non-breeding range. Range polygon from Birdlife 2016.

1.
ARKive. (2016). *ARKive - Discover the world's most endangered species*. Available at: http://www.arkive.org/. Last accessed 28 March 2016

2.
BirdLife. (2016). *BirdLife | Partnership for nature and people*. Available at: http://www.birdlife.org/. Last accessed 28 March 2016

3.
Birds of Saudi Arabia. (2016). *Birds of Saudi Arabia*. Available at: http://www.birdsofsaudiarabia.com/. Last accessed 20 April 2016

4.
Dubai Desert Conservation Resort. (2016). . Available at: http://www.ddcr.org/florafauna/. Last accessed 25 March 2016

5.
Encyclopedia of Life. (2016). *Encyclopedia of Life*. Available at: http://www.eol.org/. Last accessed 25 March 2016

6.
FAO. (2016). *Food and Agriculture Organization of the United Nations*. Available at: http://www.fao.org/home/en/. Last accessed 25 March 2016

7.
Flora of Qatar. (2016). *Flora of Qatar*. Available at: http://www.floraofqatar.com/. Last accessed 1 September 2016

8.
GBIF. (2016). *Free and Open Access to Biodiversity Data | GBIF.org*. Available at: http://www.gbif.org/. Last accessed 29 March 2016

9.
gbwf.org. (2016). *gbwf.org, Aviculture & Conservation of Galliformes (Game Birds)*. Available at: http://www.gbwf.org/. Last accessed 18 April 2016

10.
iNaturalist. (2016). *iNaturalist.org*. *iNaturalist.org*. Available at: http://www.inaturalist.org/. Last accessed 15 April 2016

11.
Indiansnakes.org. (2016). *Indiansnakes.org | For snakes & snake people*. Available at: http://indiansnakes.org/. Last accessed 19 April 2016

12.
IUCN. (2016). *The IUCN Red List of Threatened Species*. Available at: http://www.iucnredlist.org/. Last accessed 25 March 2016

13.
Miller, A.G. & Cope, T.A. (1996). *Flora of the Arabian Penninsula and Socotia*. Edinburgh University Press

14.
PROTA4U. (2016). . Available at: https://www.prota4u.org/. Last accessed 1 September 2016

15.
Royal Botanic Gardens. (2016). *Royal Botanic Gardens, Kew | Welcome To Our Website*. Available at: http://www.kew.org/. Last accessed 25 March 2016

16.
The Reptile Database. (2016). *The Reptile Database*. Available at: http://reptile-database.reptarium.cz/. Last accessed 19 April 2016

AGEDI
مبادرة أبوظبي العالمية للبيانات البيئية
Abu Dhabi Global Environmental Data Initiative

Annex V – MaxEnt results combined across all priority amphibian species for RCP4.5 and RCP8.5

Climate Change Research Group

University of Maryland
CENTER FOR ENVIRONMENTAL SCIENCE

Figure 1: Current and future climate suitability for *Bufo arabicus*, with associated uncertainty and change in range area based on an ensemble of all future climate scenarios. Range and occurrence data shown for reference.

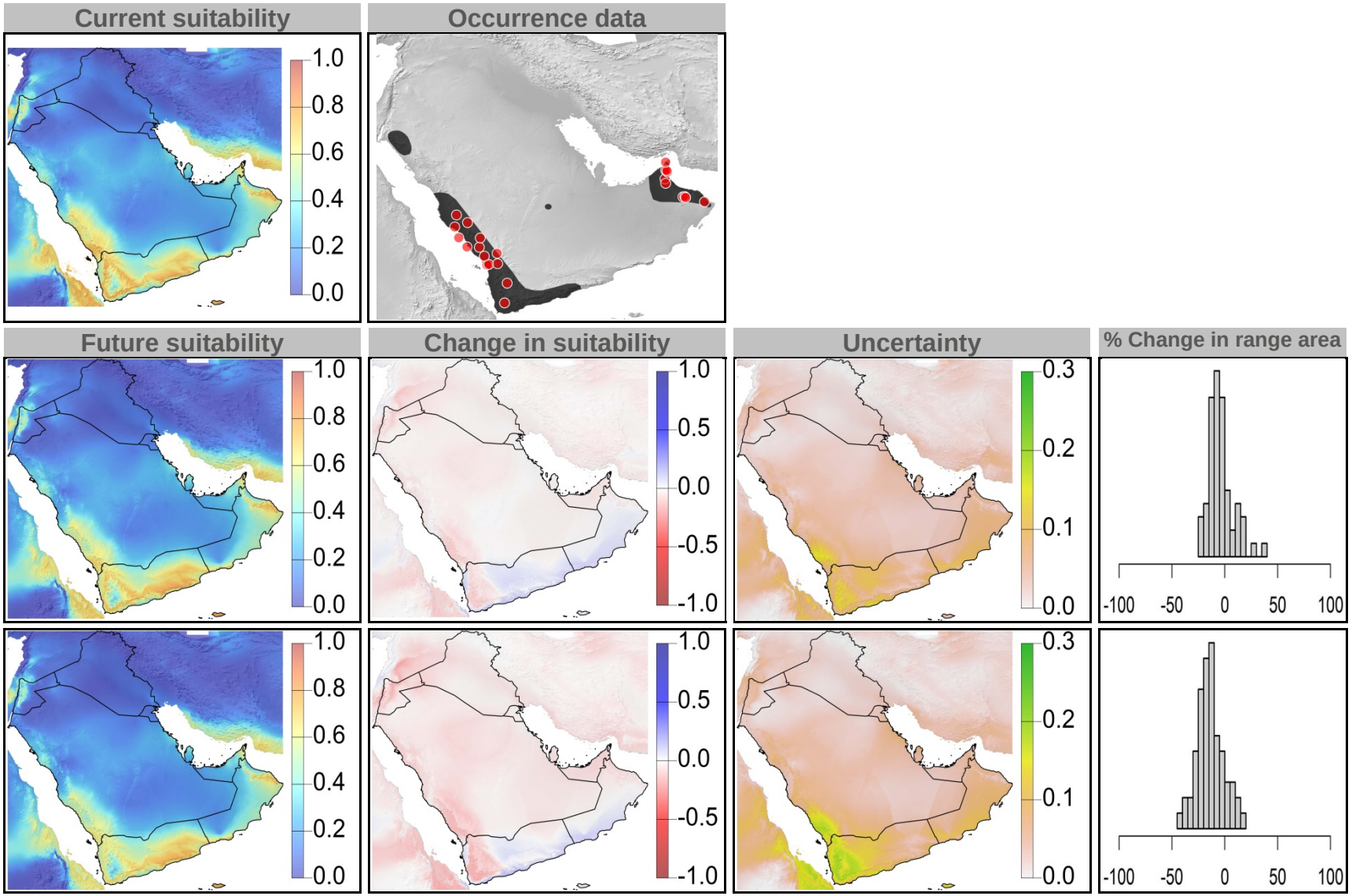

Figure 2: Current and future (2070) climate suitability for *Bufo arabicus*, based on an ensemble of all future climate scenarios from the regional climate modeling effort at two spatial domains. Range and occurrence data shown for reference.

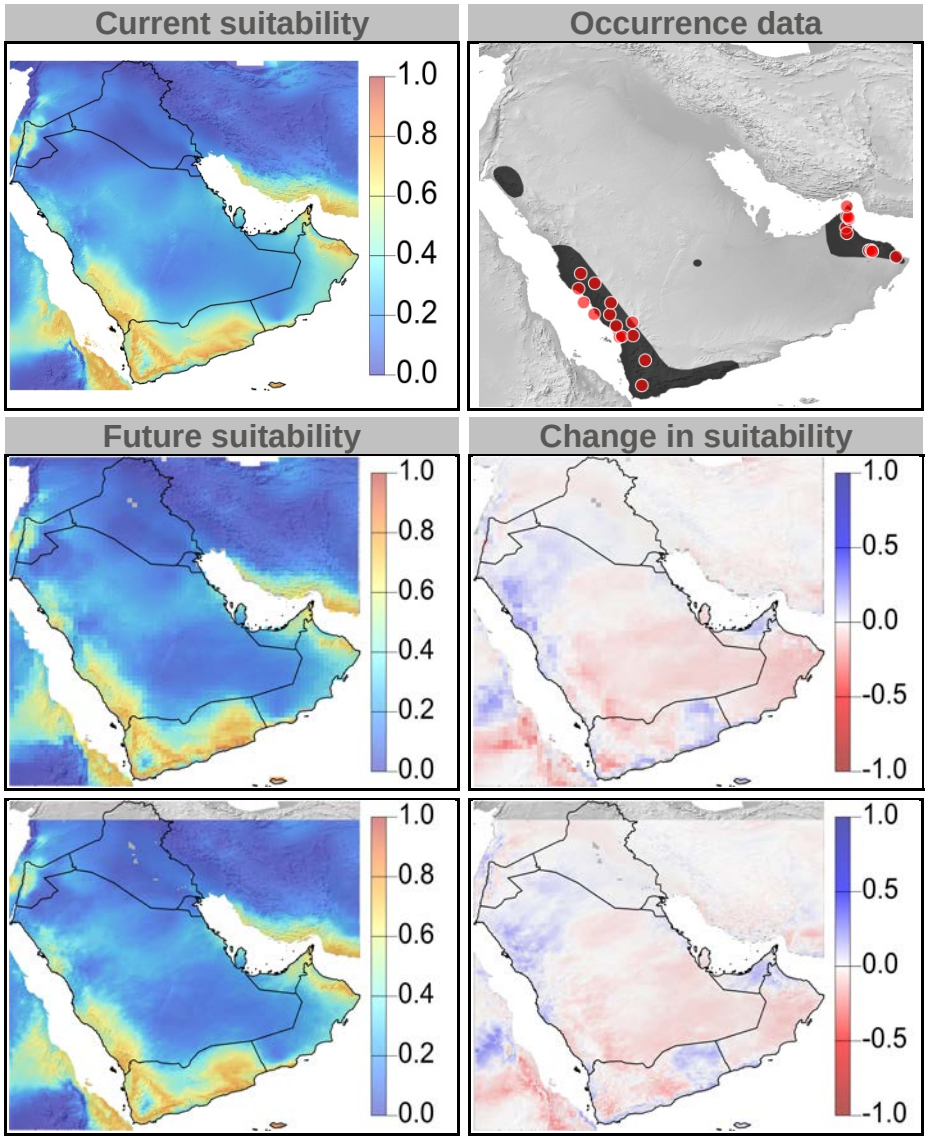

Figure 3: Current and future climate suitability for *Bufo dhufarensis*, with associated uncertainty and change in range area based on an ensemble of all future climate scenarios. Range and occurrence data shown for reference.

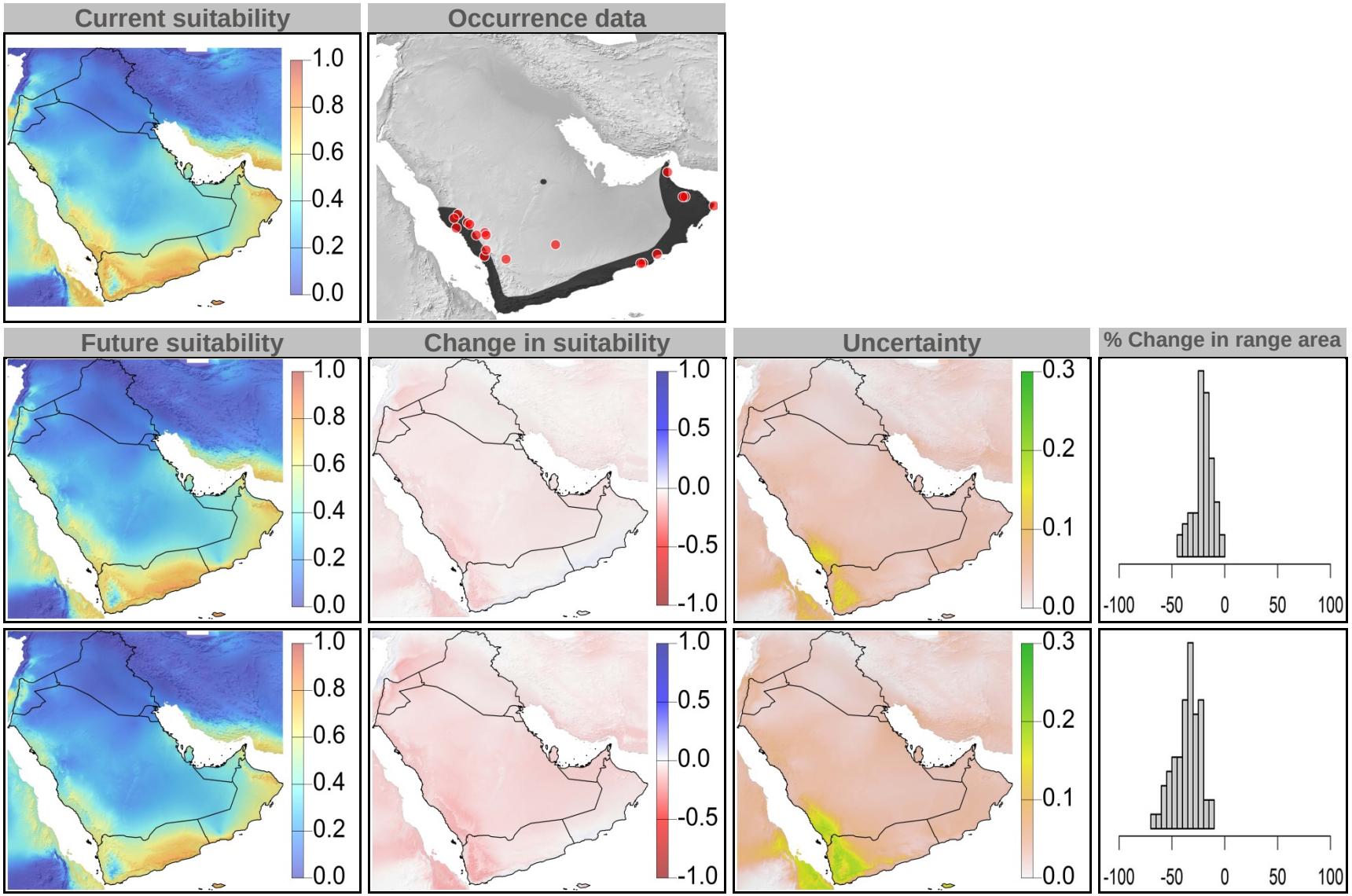

Figure 4: Current and future (2070) climate suitability for *Bufo dhufarensis*, based on an ensemble of all future climate scenarios from the regional climate modeling effort at two spatial domains. Range and occurrence data shown for reference.

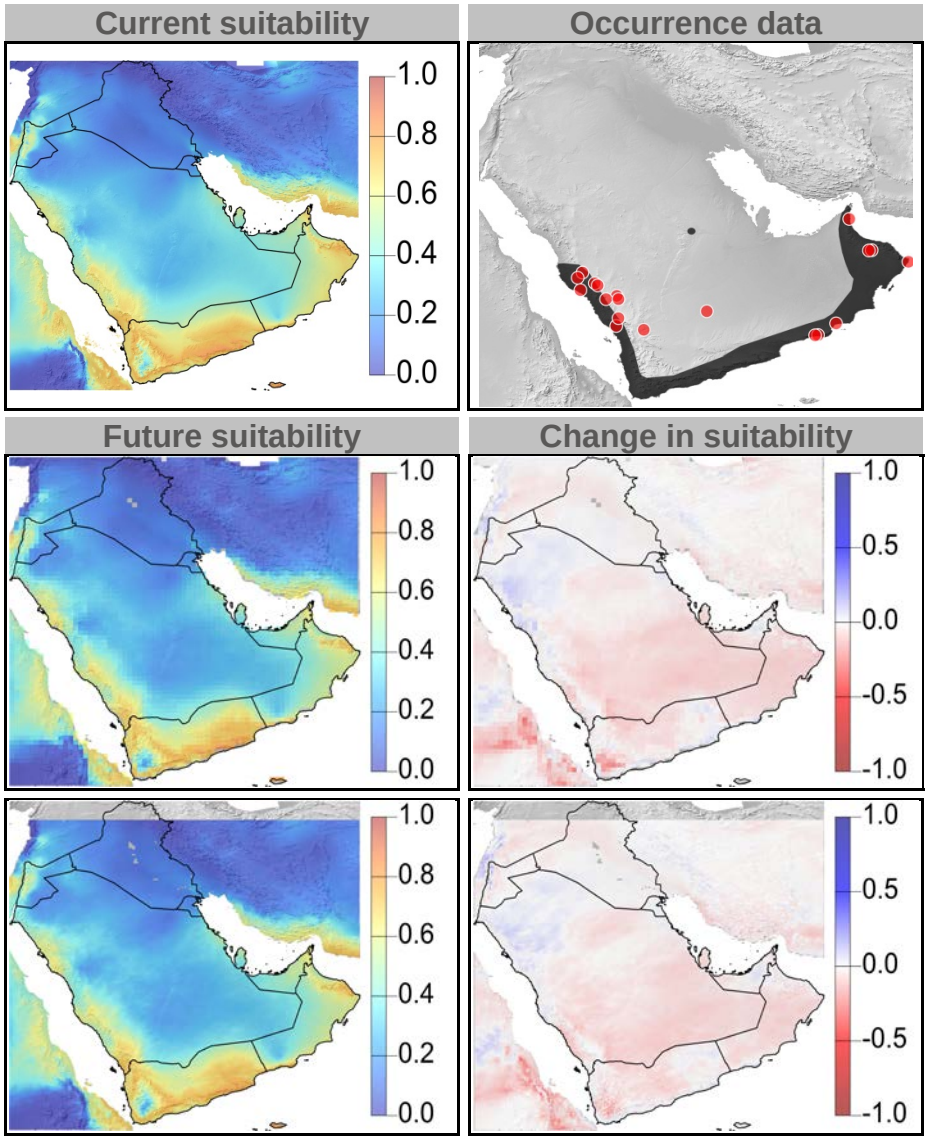

Figure 5: Current and future climate suitability for *Hyla savignyi*, with associated uncertainty and change in range area based on an ensemble of all future climate scenarios. Range and occurrence data shown for reference.

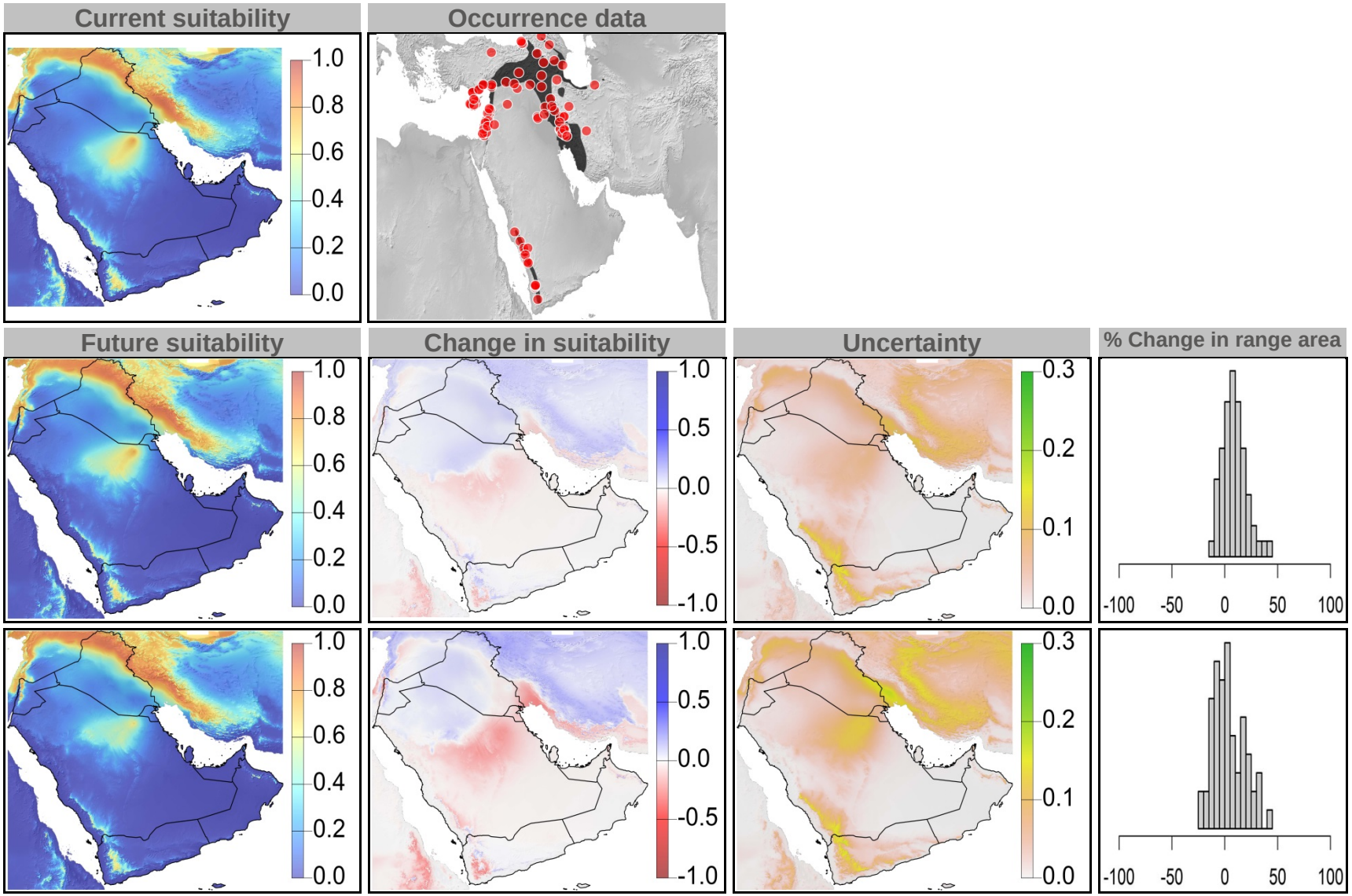

Figure 6: Current and future (2070) climate suitability for *Hyla savignyi*, based on an ensemble of all future climate scenarios from the regional climate modeling effort at two spatial domains. Range and occurrence data shown for reference.

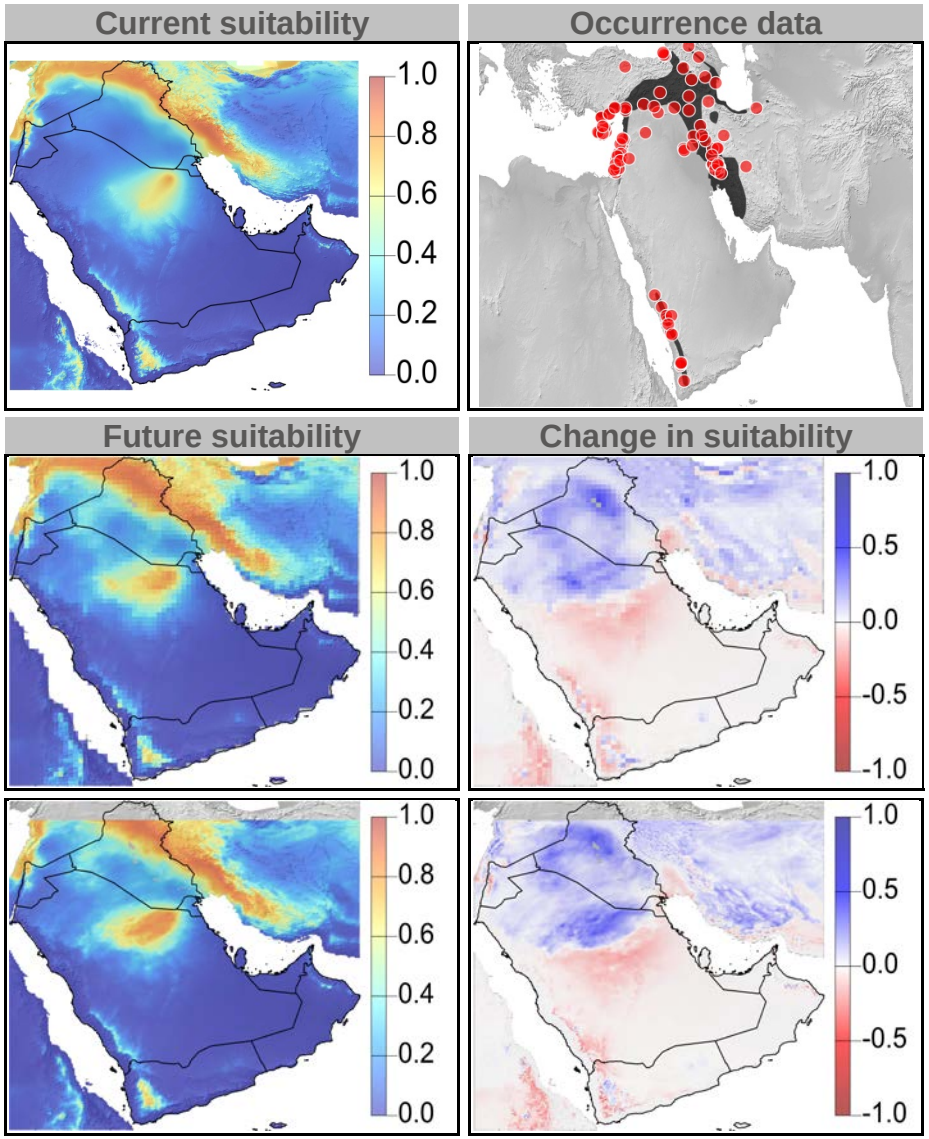

AGEDI
مبادرة أبوظبي العالمية للبيانات البيئية
Abu Dhabi Global Environmental Data Initiative

Annex VI – MaxEnt results combined across all priority bird species for RCP4.5 and RCP8.5

Climate Change Research Group

University of Maryland
CENTER FOR ENVIRONMENTAL SCIENCE

Figure 1: Current and future climate suitability for *Alectoris melanocephala*, with associated uncertainty and change in range area based on an ensemble of all future climate scenarios. Range and occurrence data shown for reference.

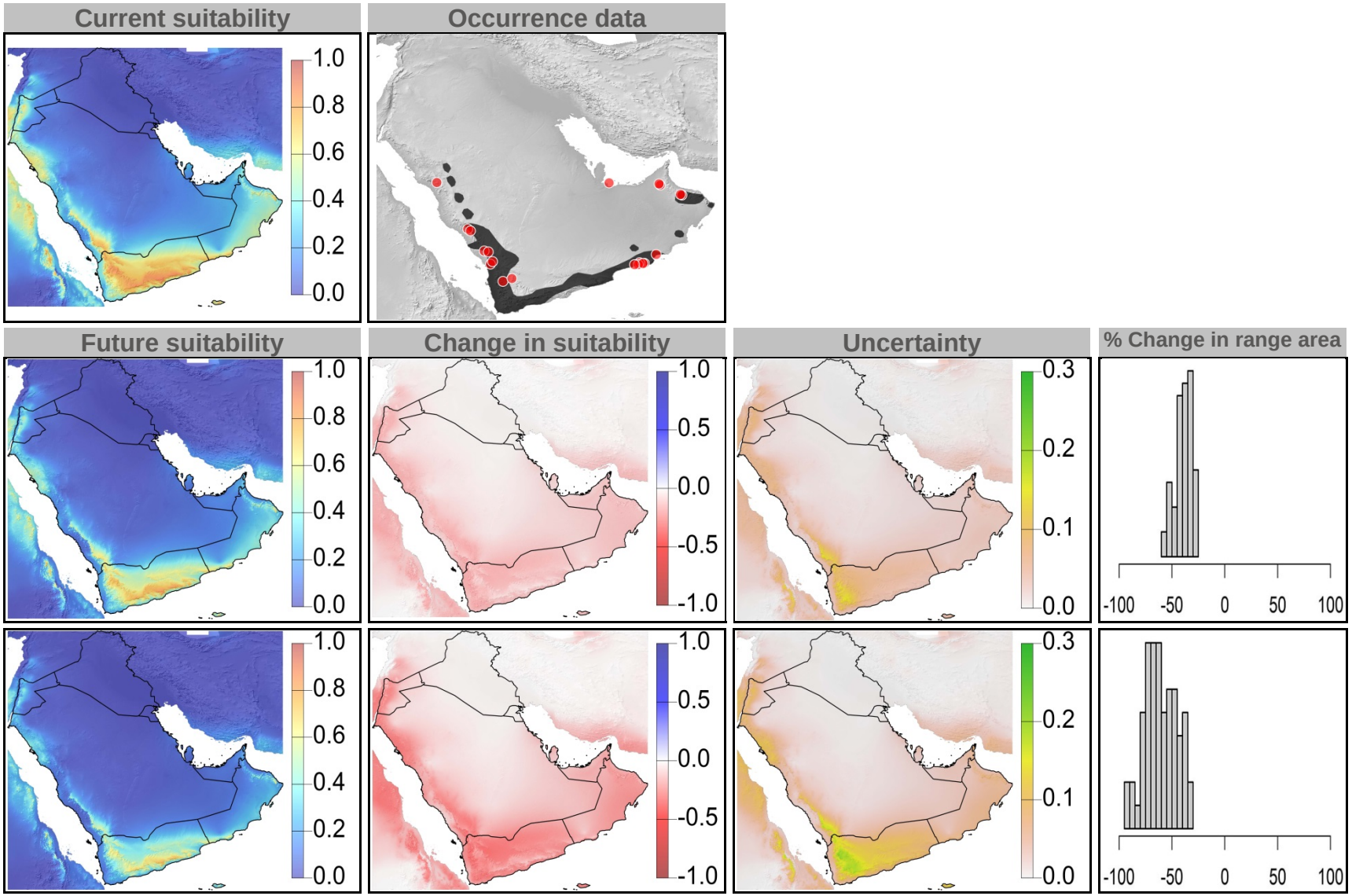

Figure 2: Current and future (2070) climate suitability for *Alectoris melanocephala*, based on an ensemble of all future climate scenarios from the regional climate modeling effort at two spatial domains. Range and occurrence data shown for reference.

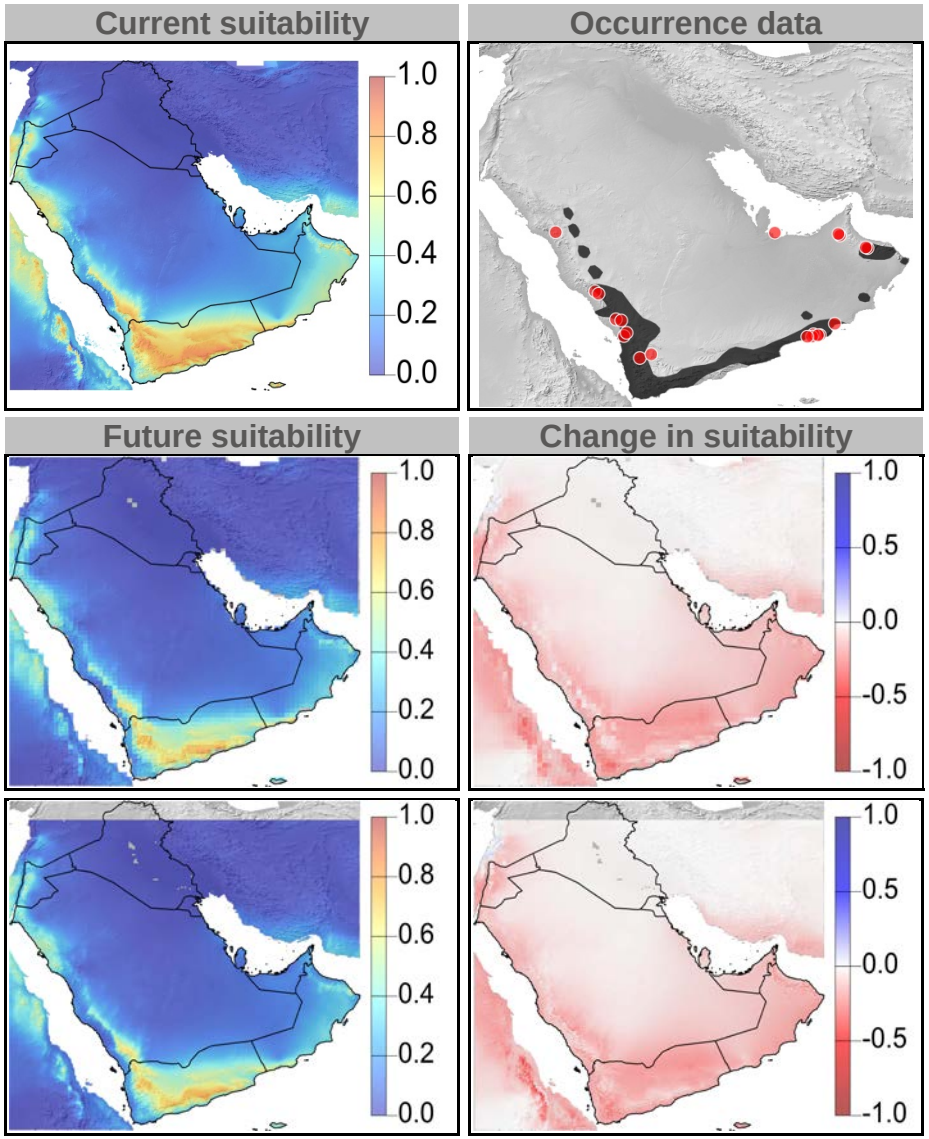

Figure 3: Current and future climate suitability for *Ammoperdix heyi*, with associated uncertainty and change in range area based on an ensemble of all future climate scenarios. Range and occurrence data shown for reference.

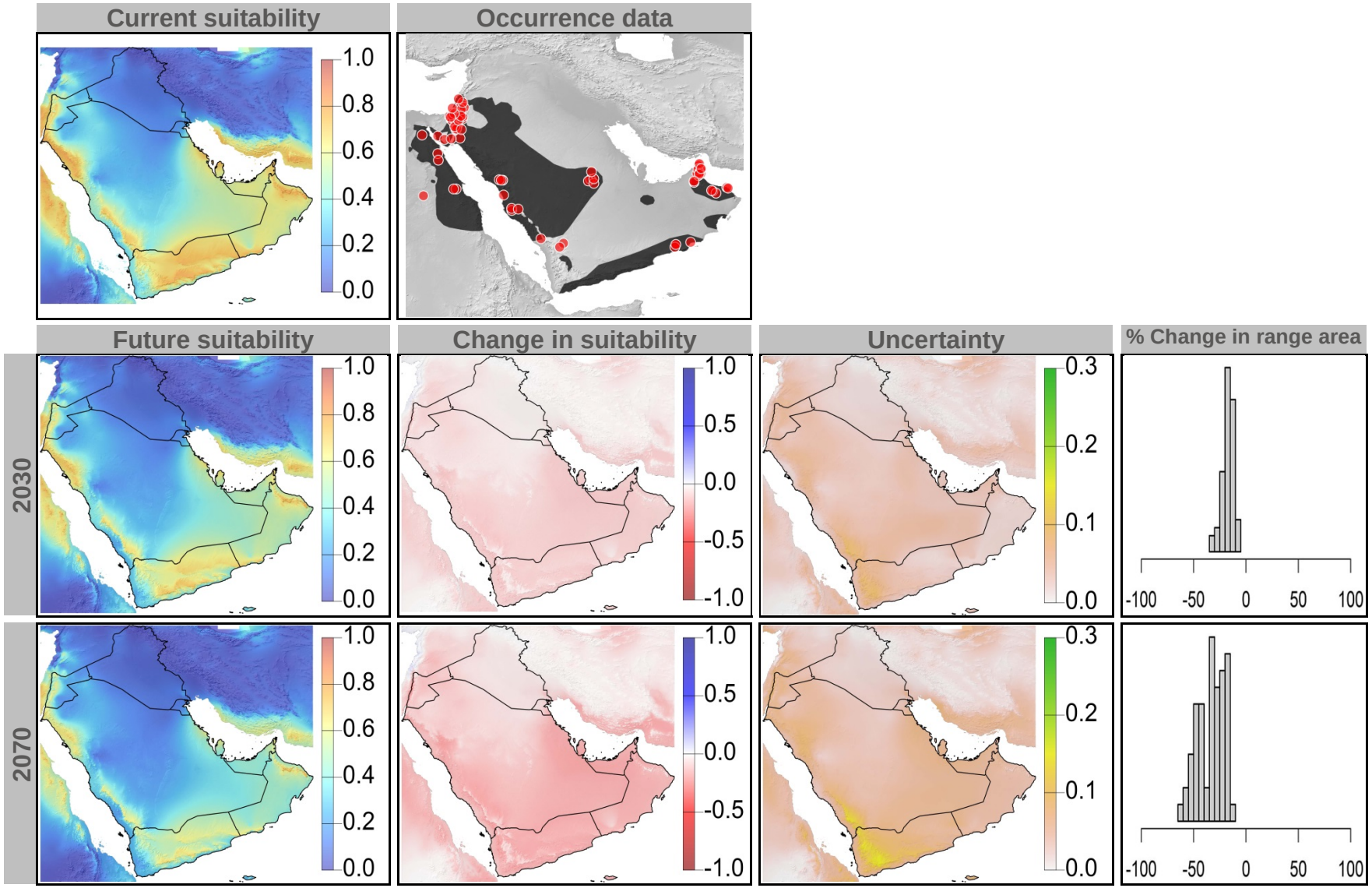

Figure 4: Current and future (2070) climate suitability for *Ammoperdix heyi*, based on an ensemble of all future climate scenarios from the regional climate modeling effort at two spatial domains. Range and occurrence data shown for reference.

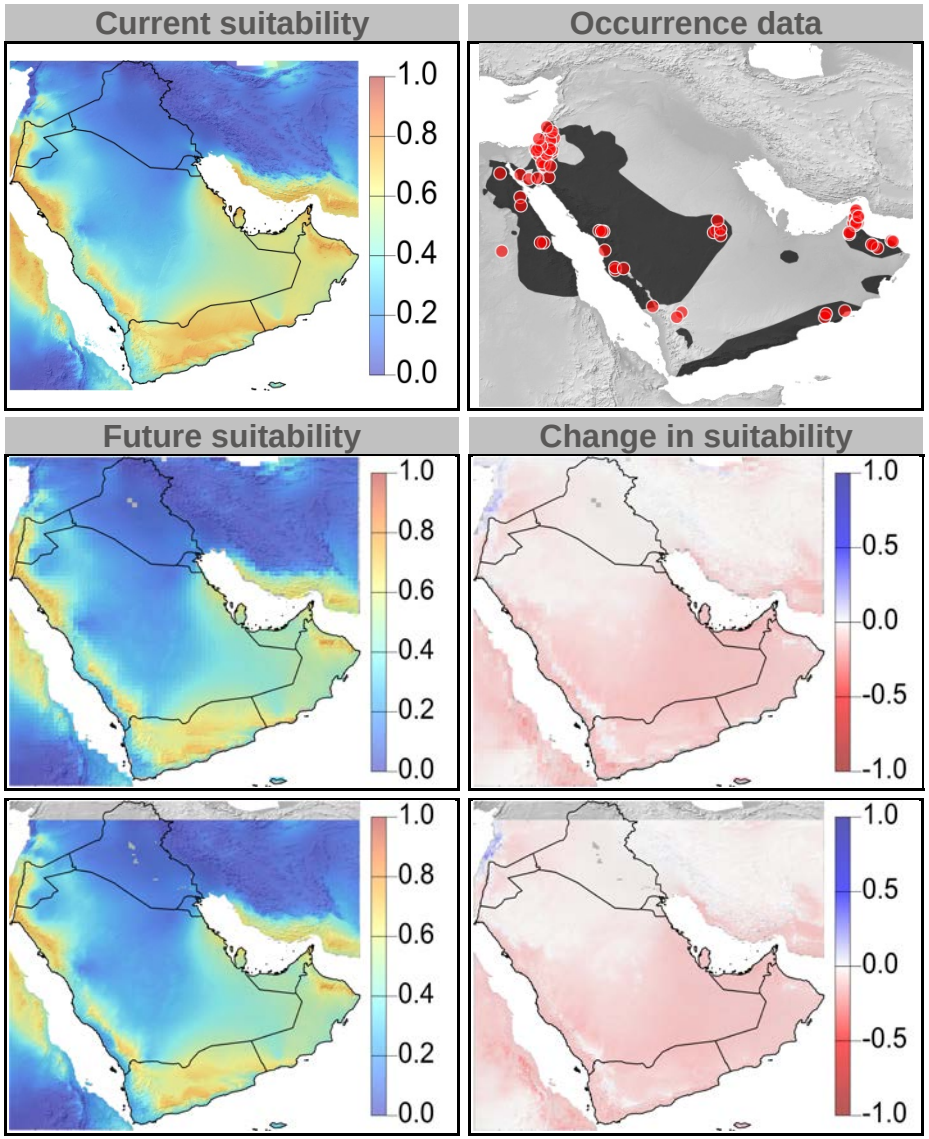

Figure 5: Current and future climate suitability for *Chlamydotis macqueenii* (breeding), with associated uncertainty and change in range area based on an ensemble of all future climate scenarios. Range and occurrence data shown for reference.

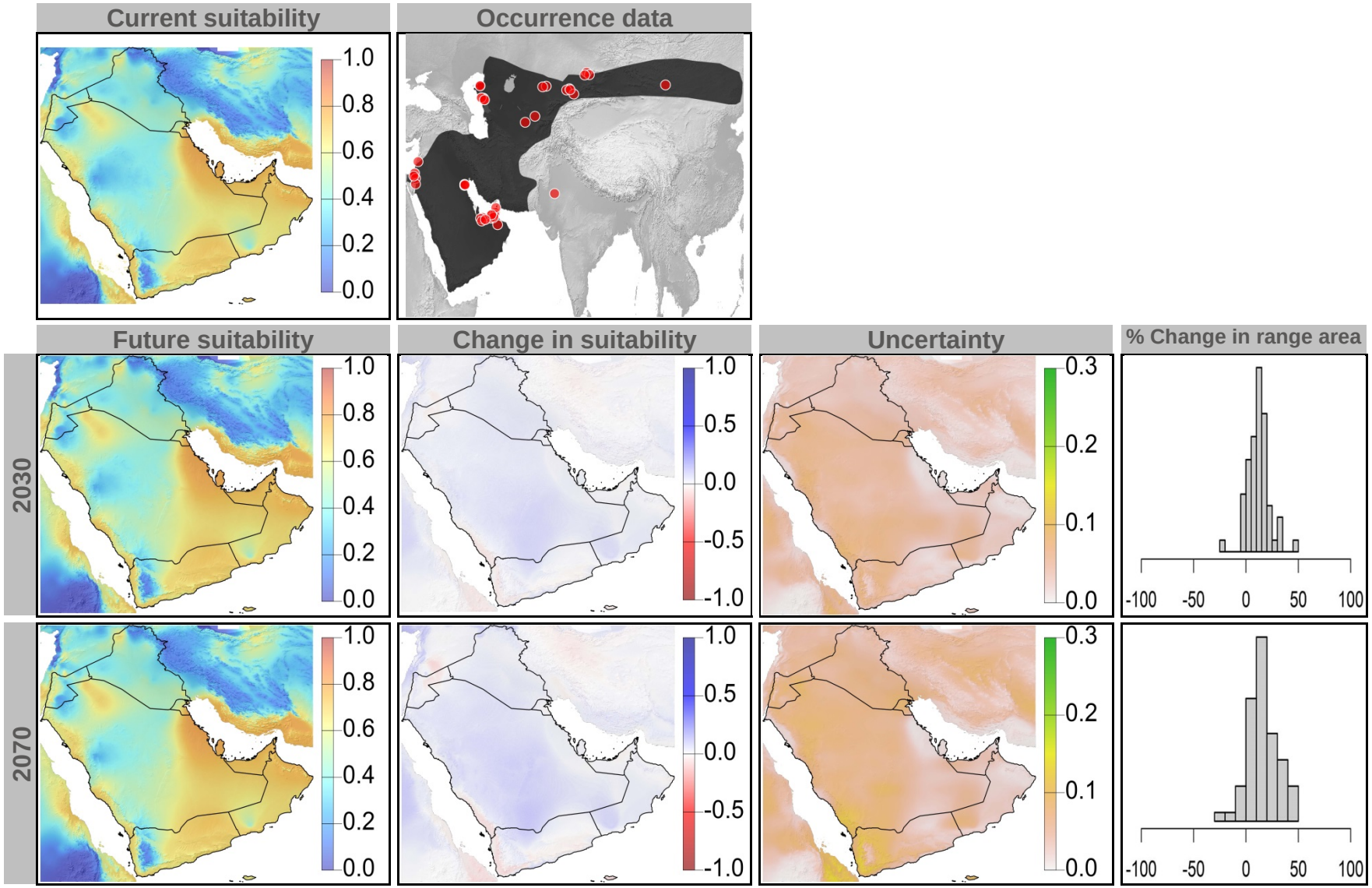

Figure 6: Current and future (2070) climate suitability for *Chlamydotis macqueenii* (breeding), based on an ensemble of all future climate scenarios from the regional climate modeling effort at two spatial domains. Range and occurrence data shown for reference.

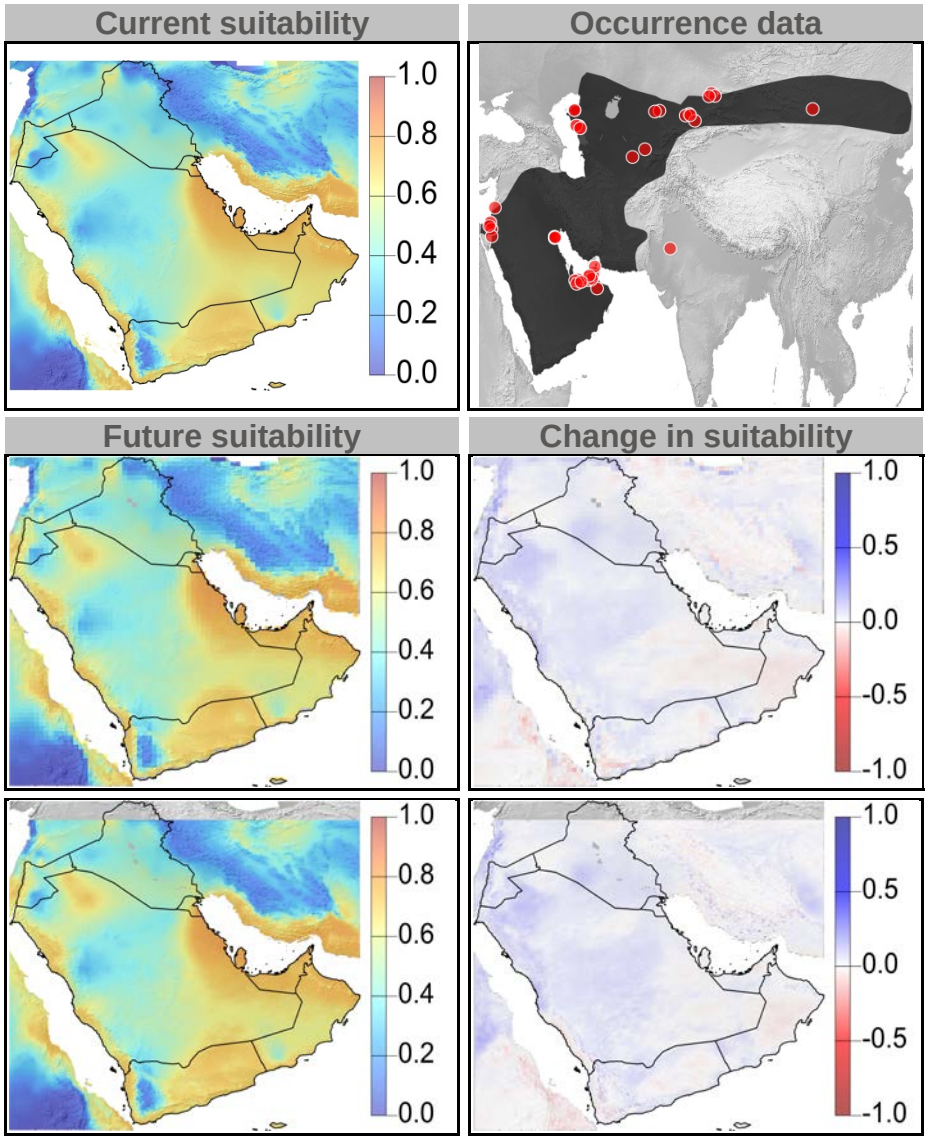

Figure 7: Current and future climate suitability for *Corvus ruficollis*, with associated uncertainty and change in range area based on an ensemble of all future climate scenarios. Range and occurrence data shown for reference.

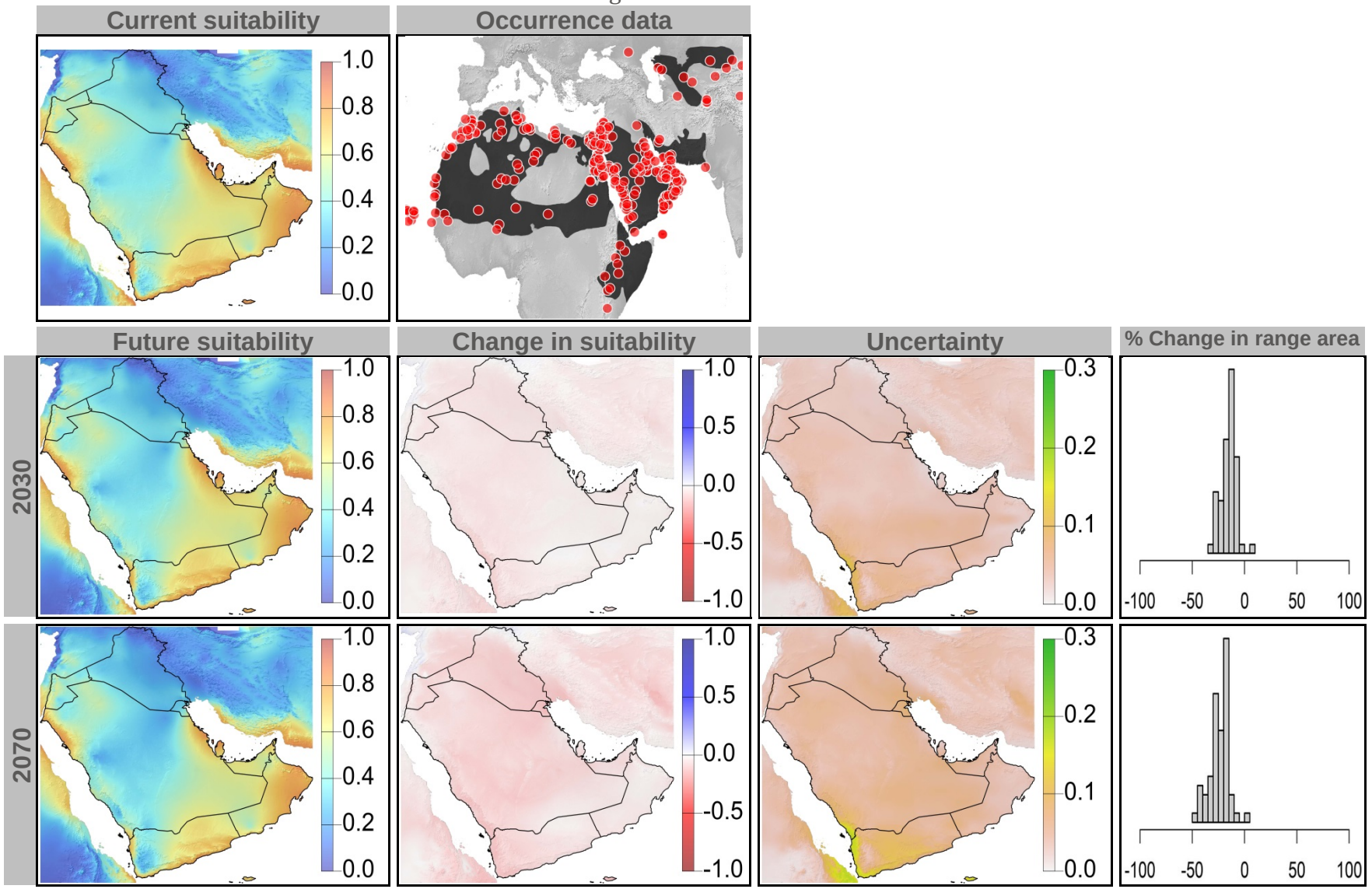

Figure 8: Current and future (2070) climate suitability for *Corvus ruficollis*, based on an ensemble of all future climate scenarios from the regional climate modeling effort at two spatial domains. Range and occurrence data shown for reference.

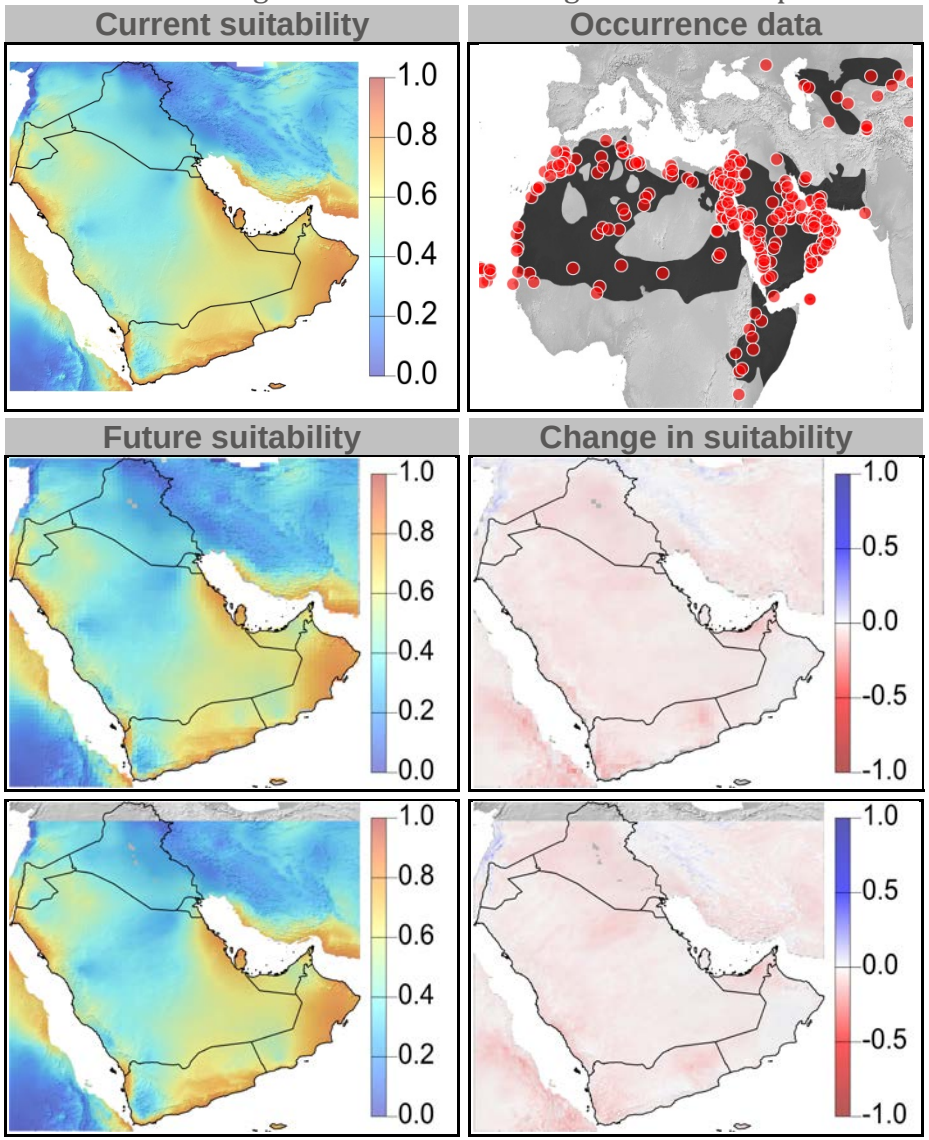

Figure 9: Current and future climate suitability for *Egretta gularis* (breeding), with associated uncertainty and change in range area based on an ensemble of all future climate scenarios. Range and occurrence data shown for reference.

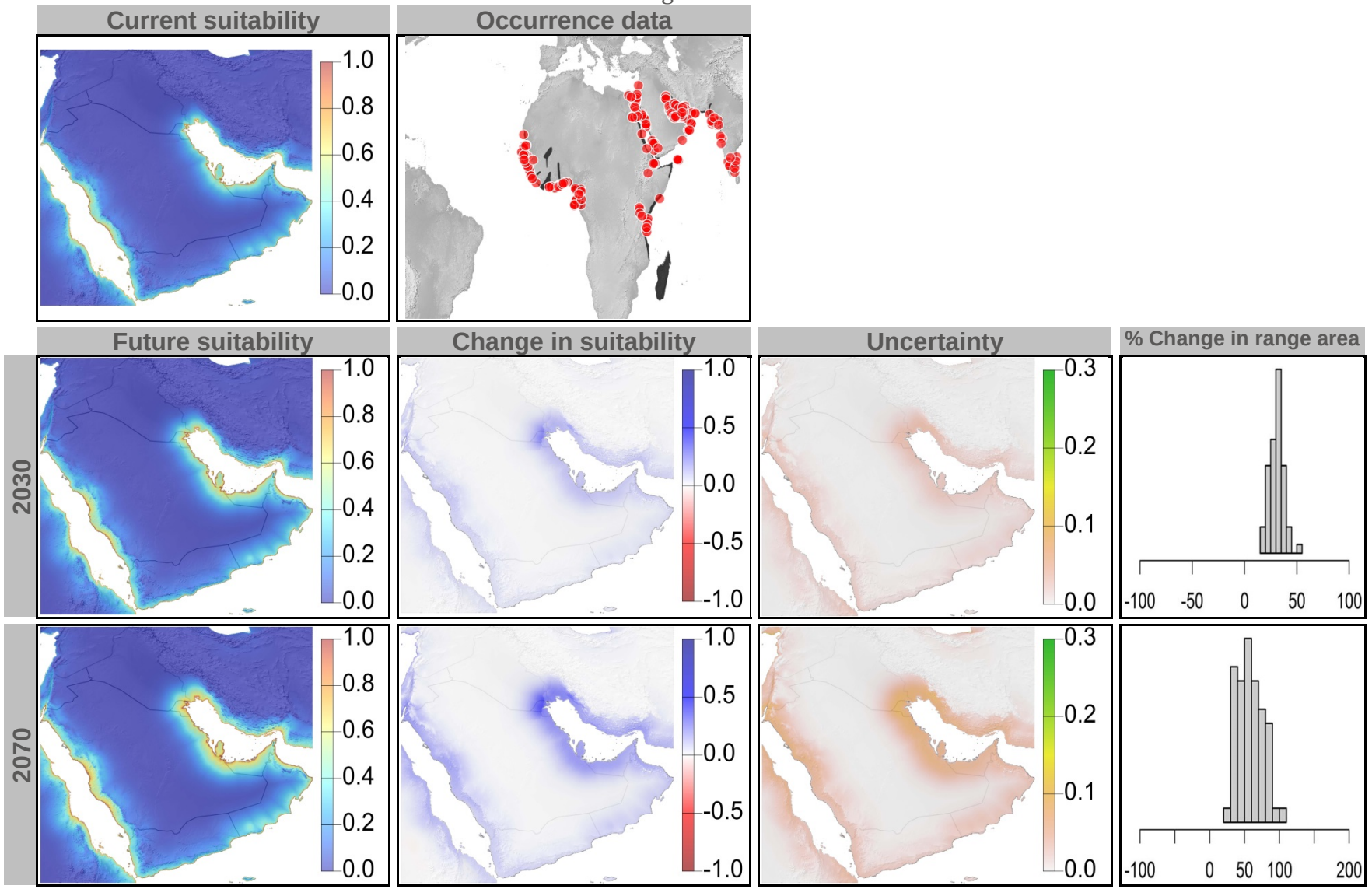

Figure 10: Current and future (2070) climate suitability for *Egretta gularis* (breeding), based on an ensemble of all future climate scenarios from the regional climate modeling effort at two spatial domains. Range and occurrence data shown for reference.

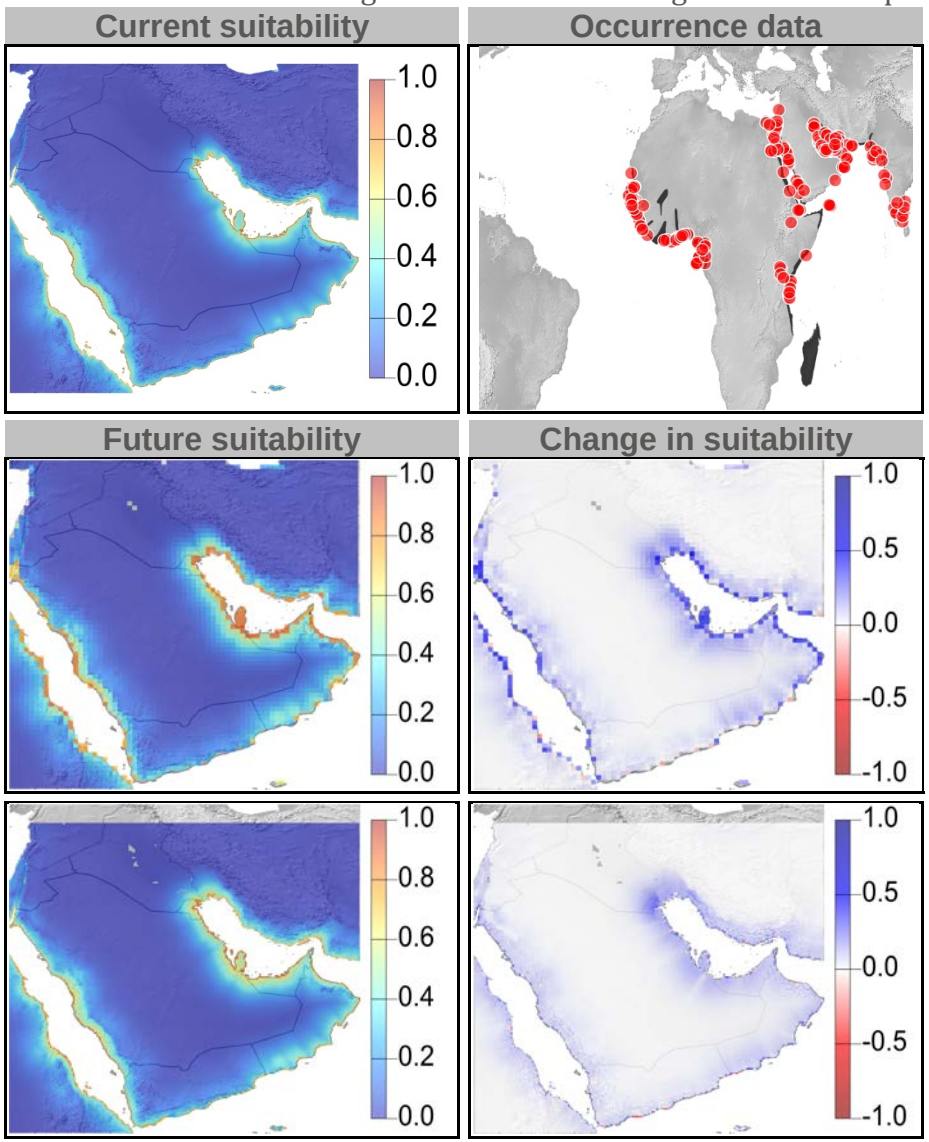

Figure 11: Current and future climate suitability for *Emberiza cineracea*, with associated uncertainty and change in range area based on an ensemble of all future climate scenarios. Range and occurrence data shown for reference.

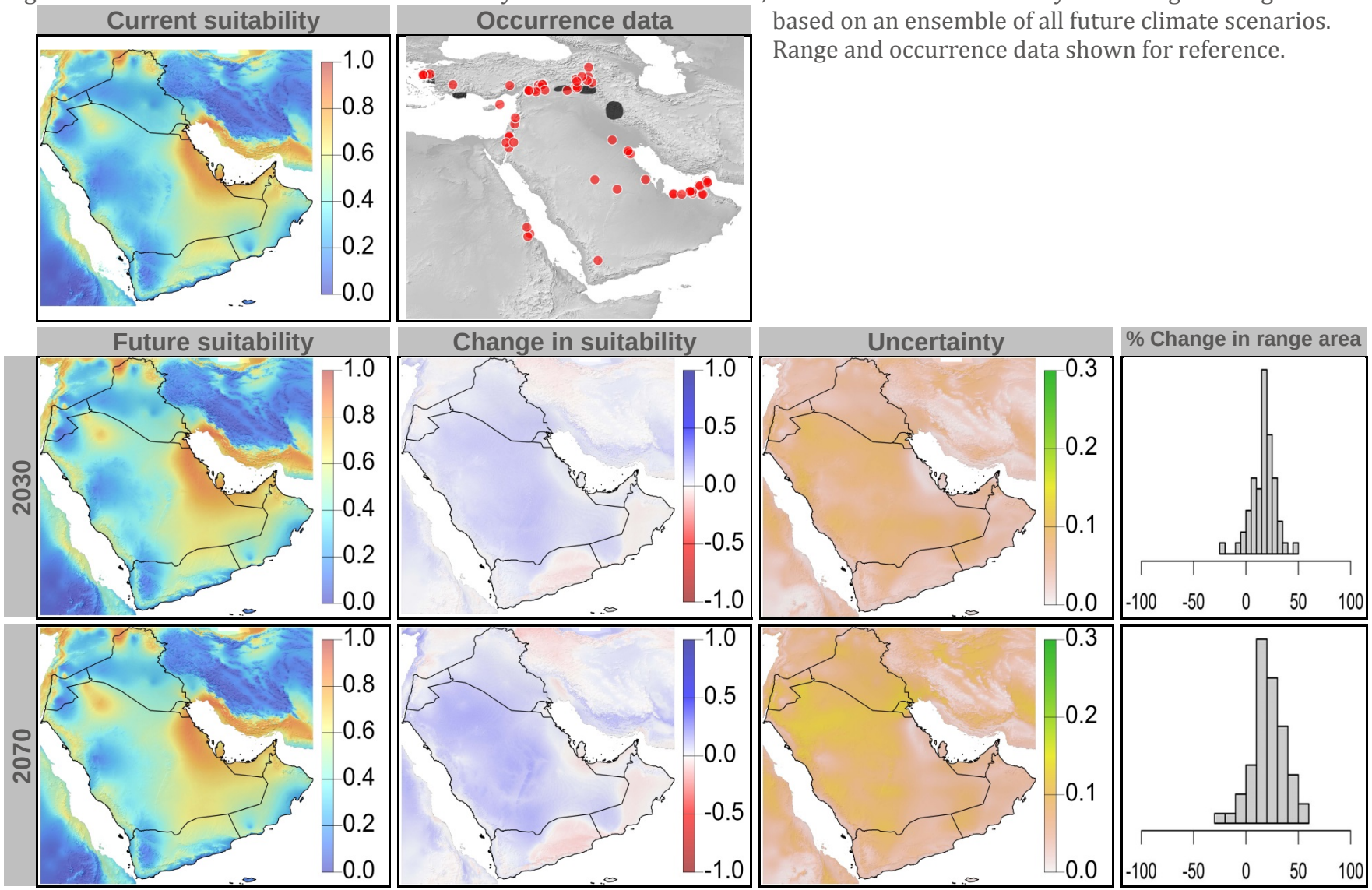

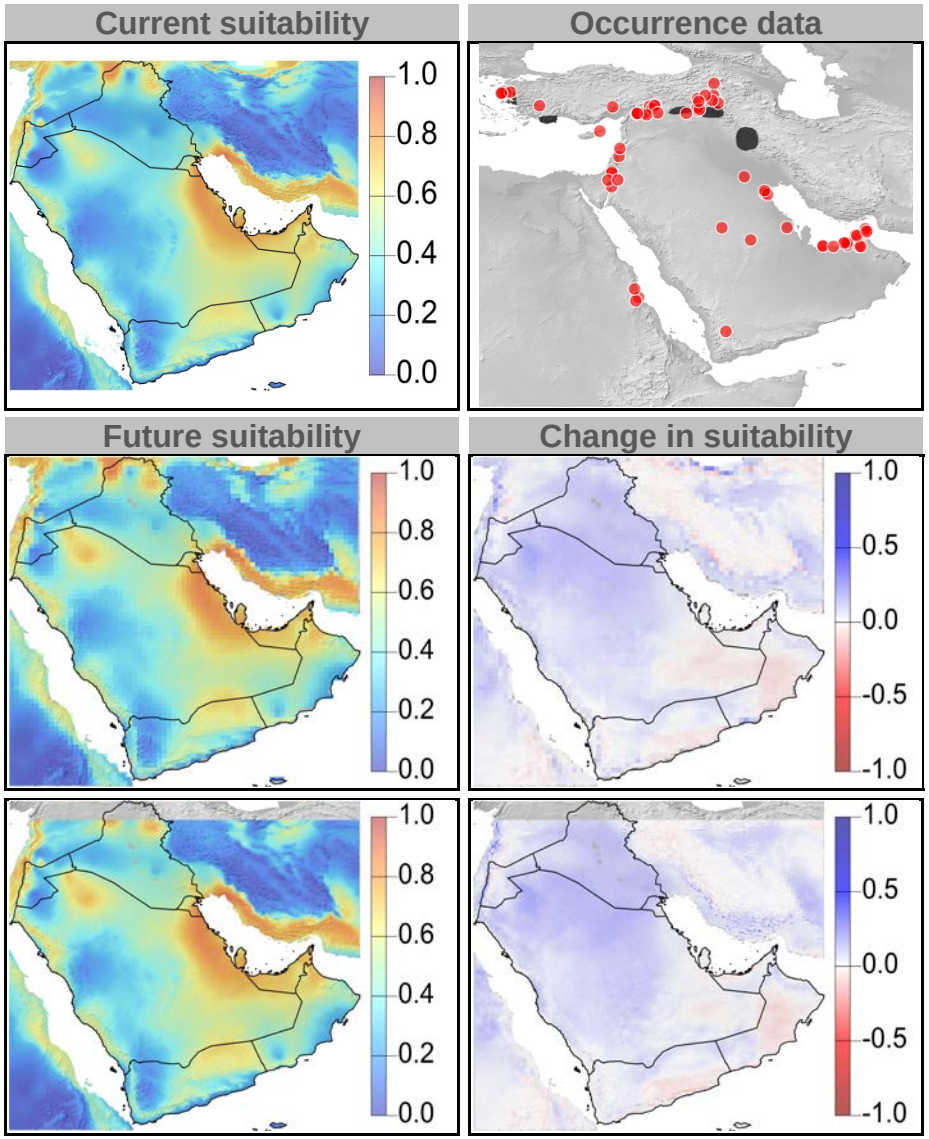

Figure 12: Current and future (2070) climate suitability for *Emberiza cineracea*, based on an ensemble of all future climate scenarios from the regional climate modeling effort at two spatial domains. Range and occurrence data shown for reference.

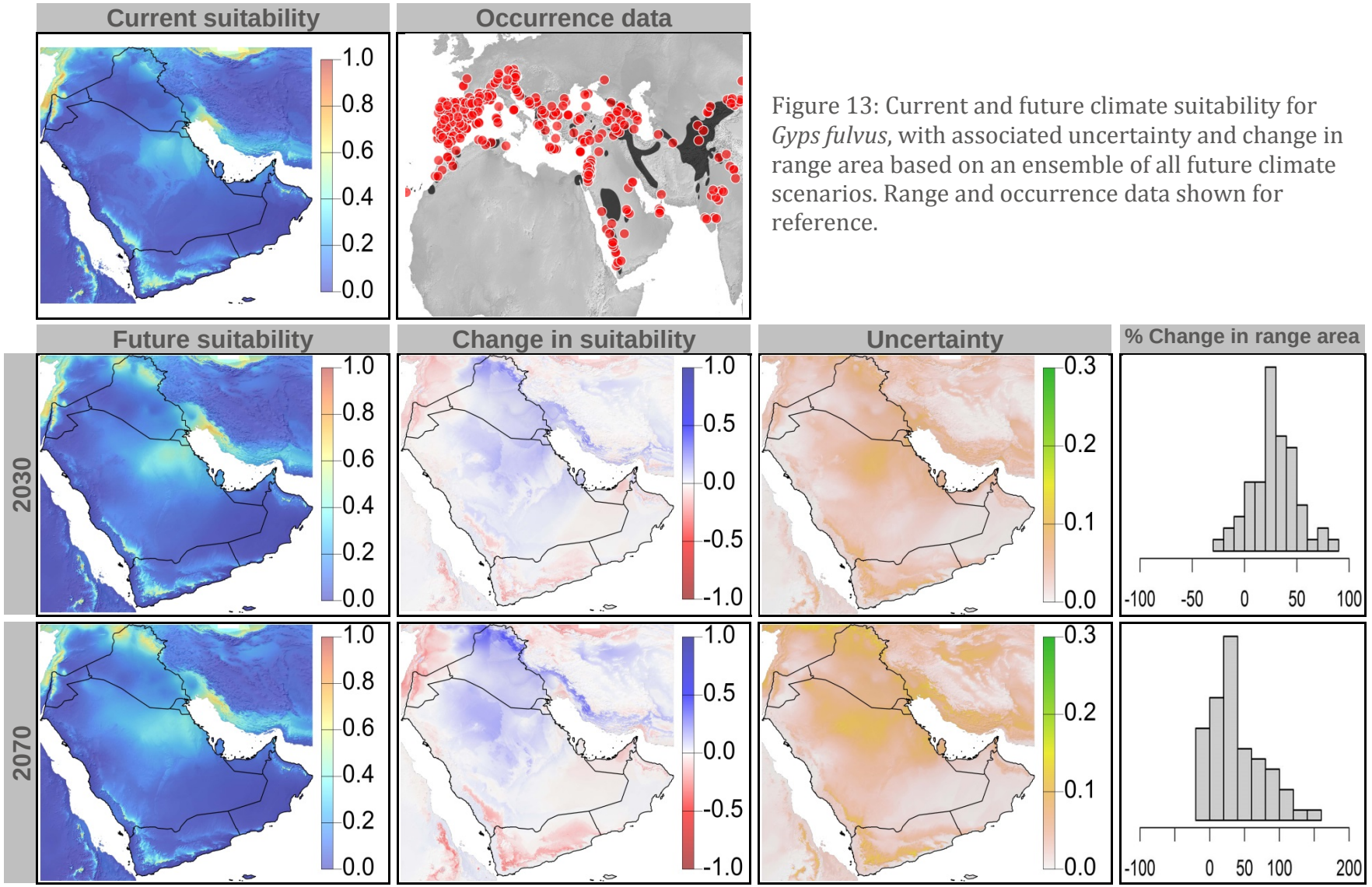

Figure 13: Current and future climate suitability for *Gyps fulvus*, with associated uncertainty and change in range area based on an ensemble of all future climate scenarios. Range and occurrence data shown for reference.

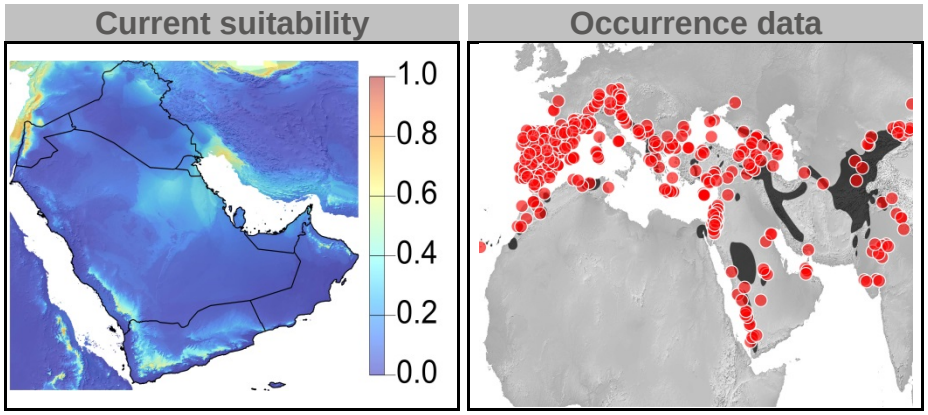

Figure 14: Current and future (2070) climate suitability for *Gyps fulvus*, based on an ensemble of all future climate scenarios from the regional climate modeling effort at two spatial domains. Range and occurrence data shown for reference.

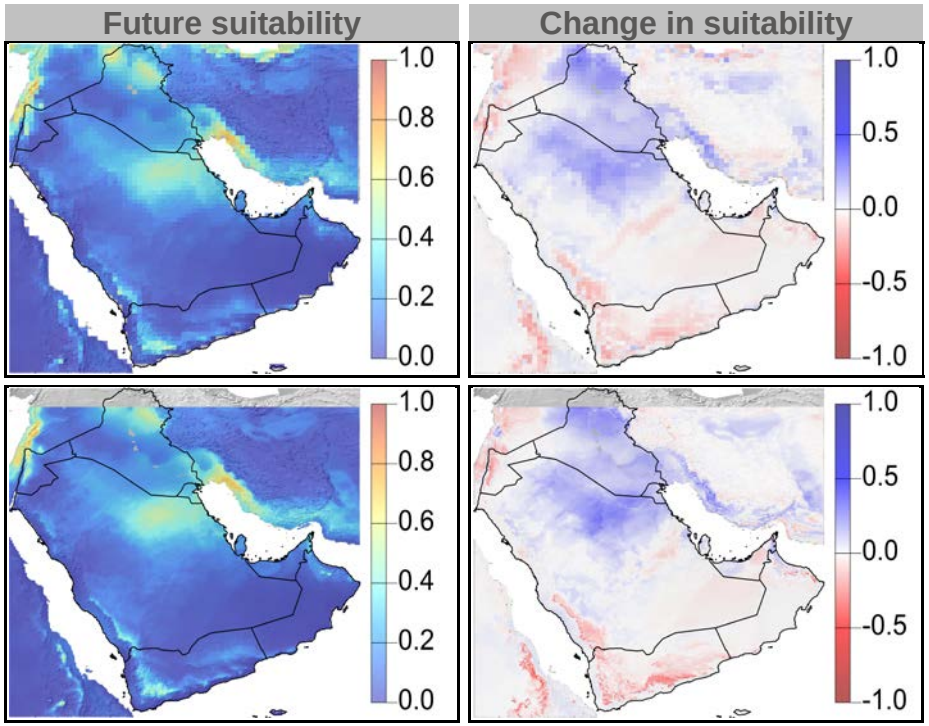

Figure 15: Current and future climate suitability for *Phalacrocorax nigrogularis*, with associated uncertainty and change in range area based on an

ensemble of all future climate scenarios. Range and occurrence data shown for reference.

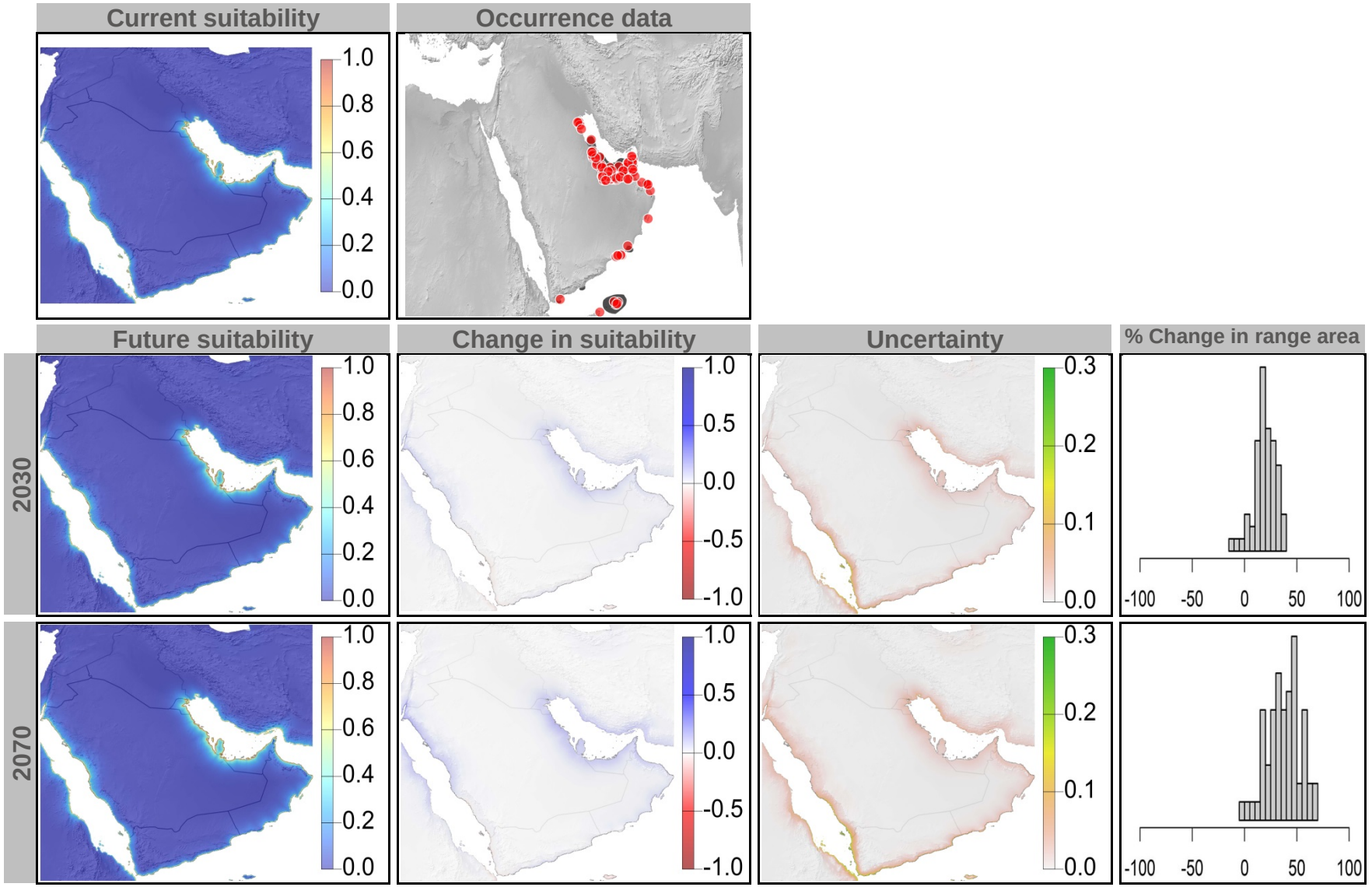

Figure 16: Current and future (2070) climate suitability for *Phalacrocorax nigrogularis*, based on an ensemble of all future climate scenarios from the regional climate modeling effort at two spatial domains. Range and occurrence data shown for reference.

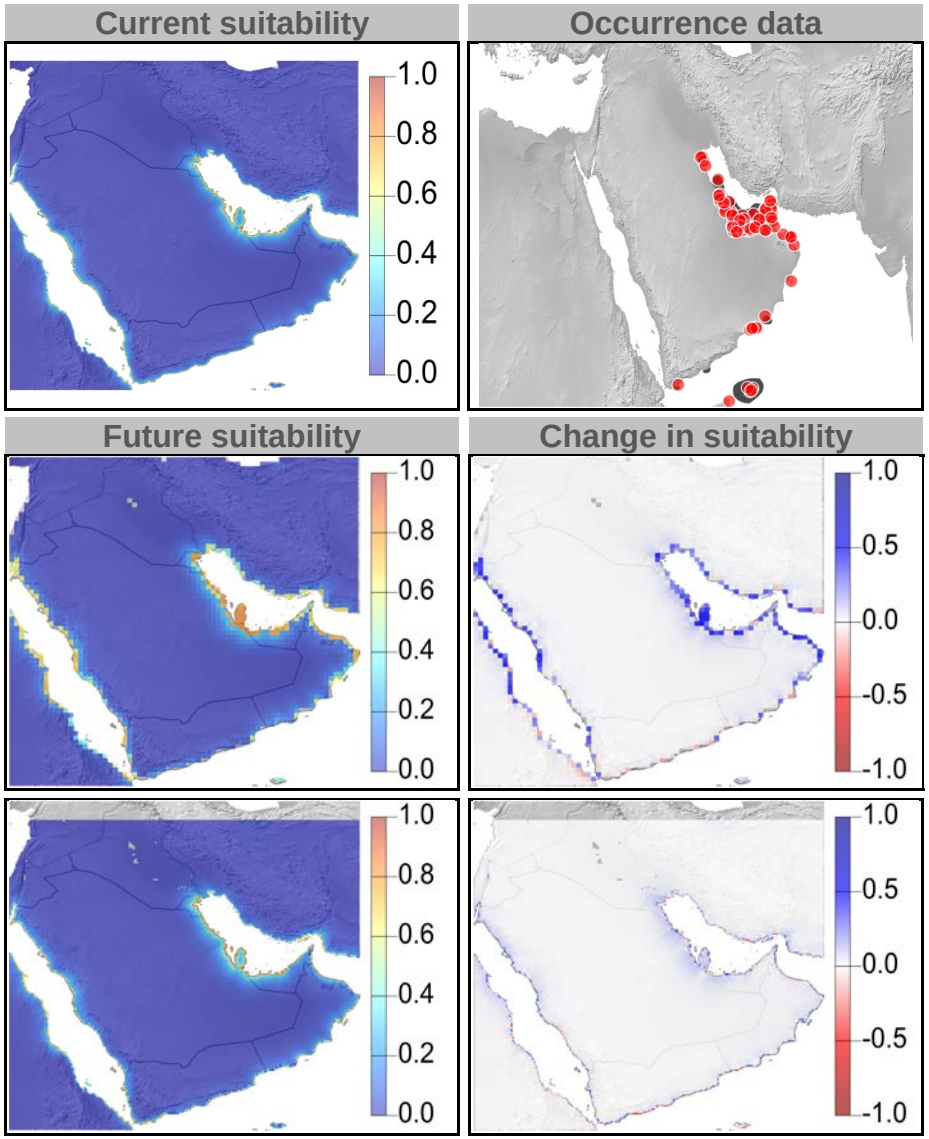

Figure 17: Current and future climate suitability for *Puffinus persicus*, with associated uncertainty and change in range area based on an ensemble of all future climate scenarios. Range and occurrence data shown for reference.

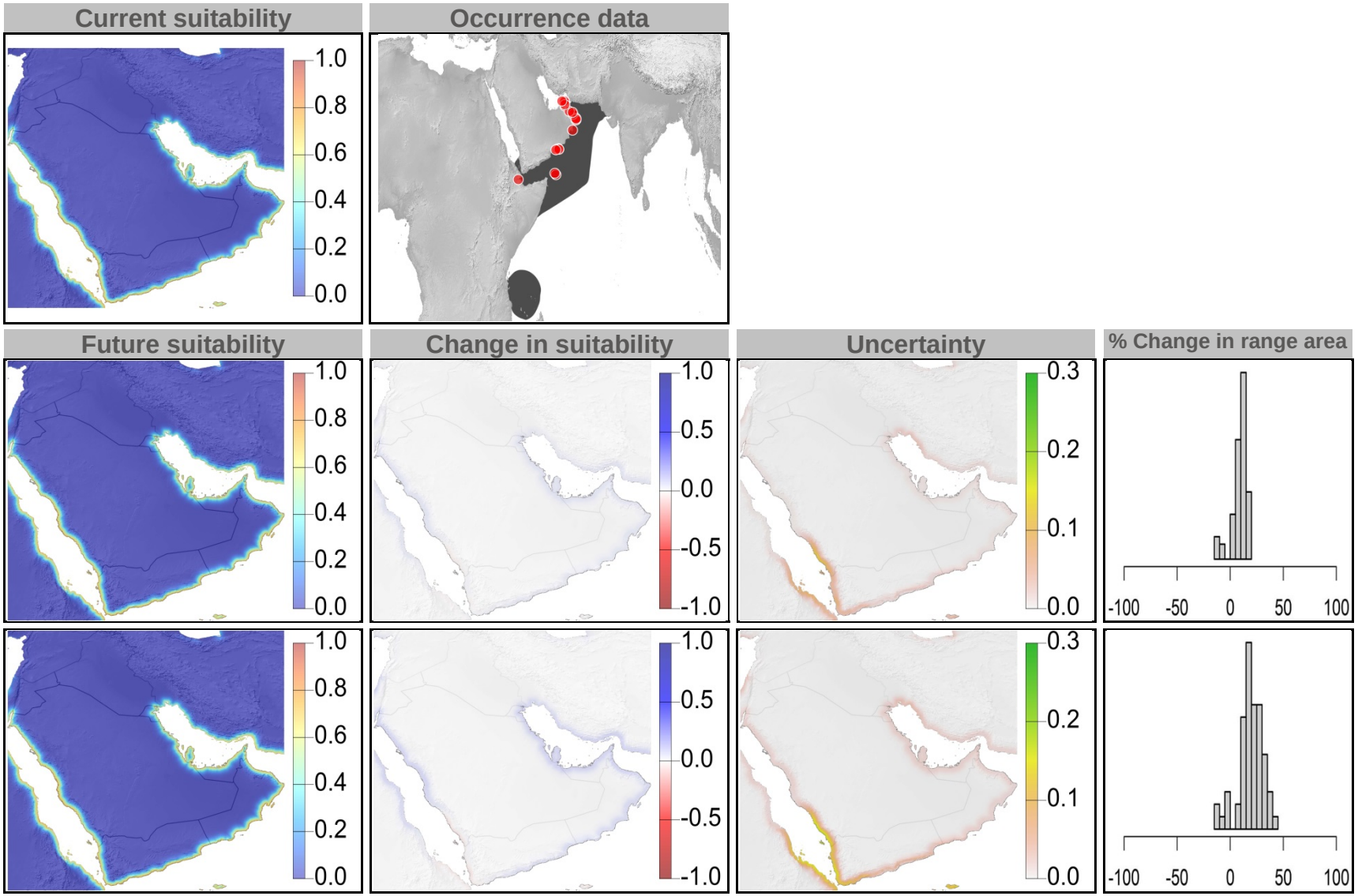

Figure 18: Current and future (2070) climate suitability for *Puffinus persicus*, based on an ensemble of all future climate scenarios from the regional climate modeling effort at two spatial domains. Range and occurrence data shown for reference.

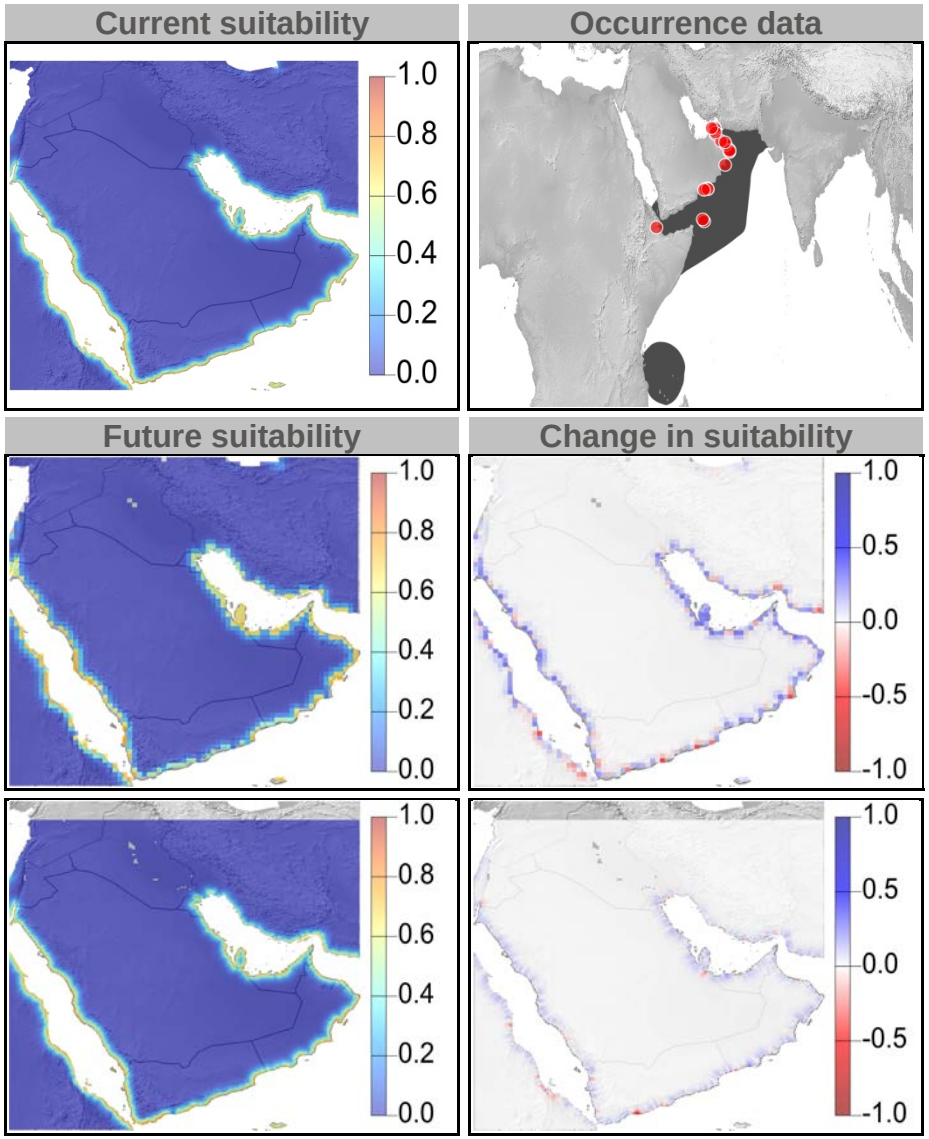

Figure 19: Current and future climate suitability for *Serinus rothschildi*, with associated uncertainty and change in range area based on an ensemble of all future climate scenarios. Range and occurrence data shown for reference.

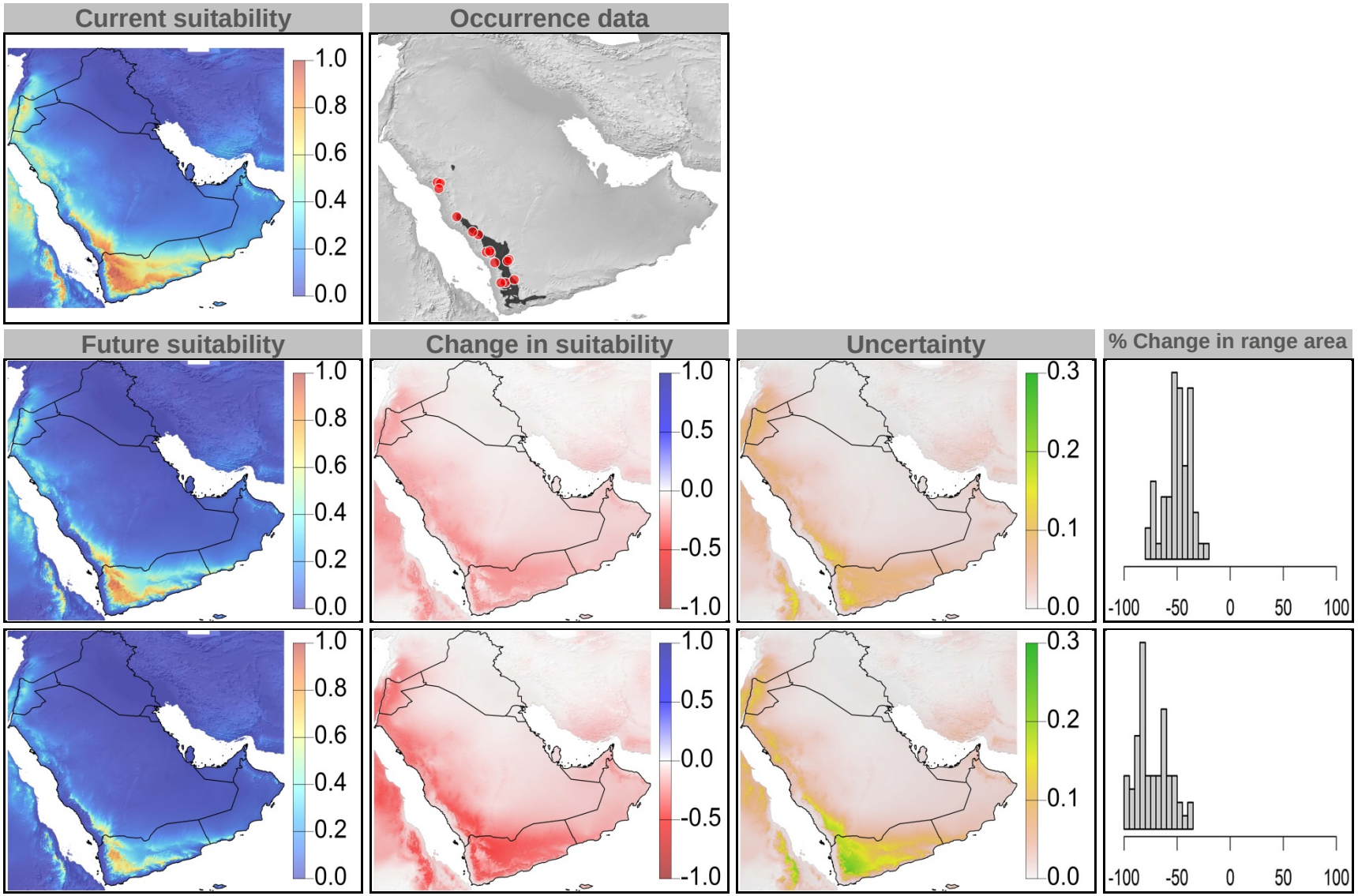

Figure 20: Current and future (2070) climate suitability for *Serinus rothschildi*, based on an ensemble of all future climate scenarios from the regional climate modeling effort at two spatial domains. Range and occurrence data shown for reference.

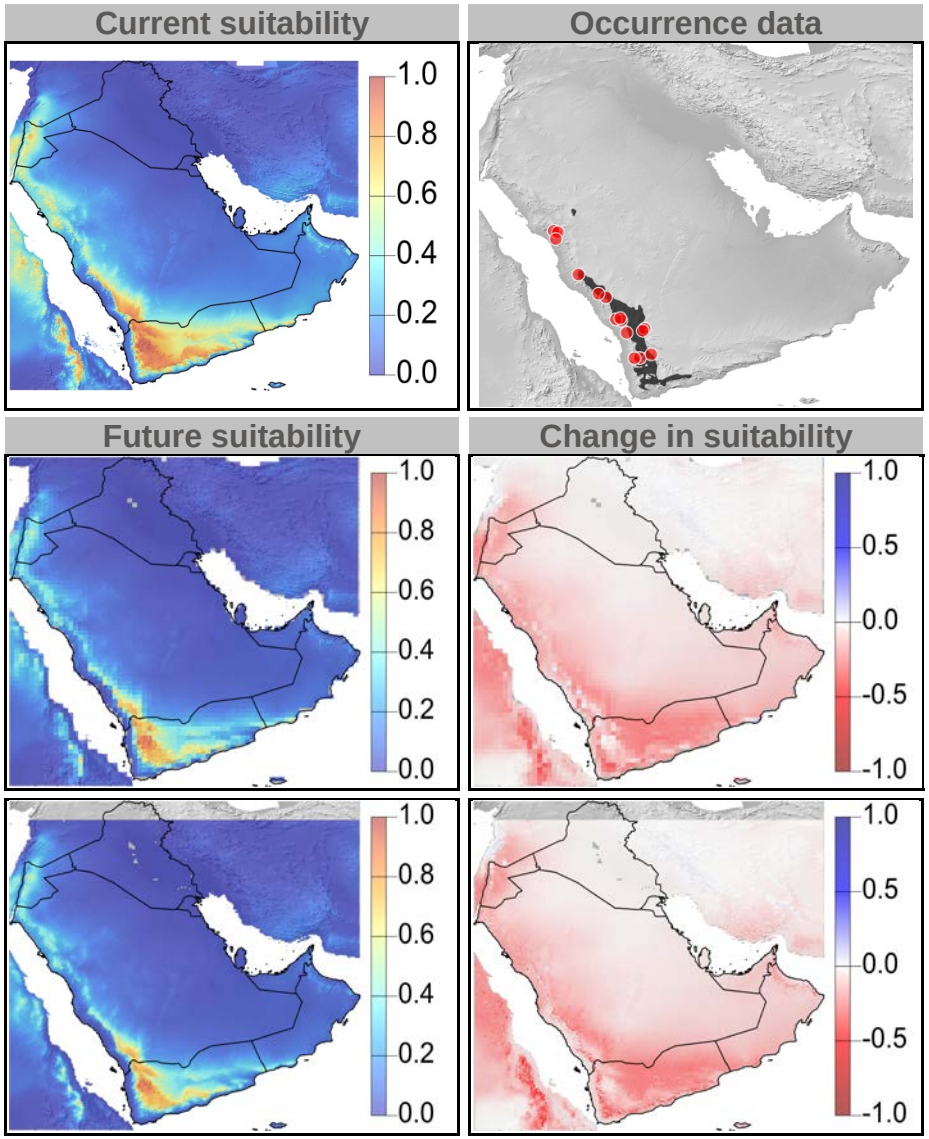

Figure 21: Current and future climate suitability for *Sylvia leucomelaena*, with associated uncertainty and change in range area based on an ensemble of all future climate scenarios. Range and occurrence data shown for reference.

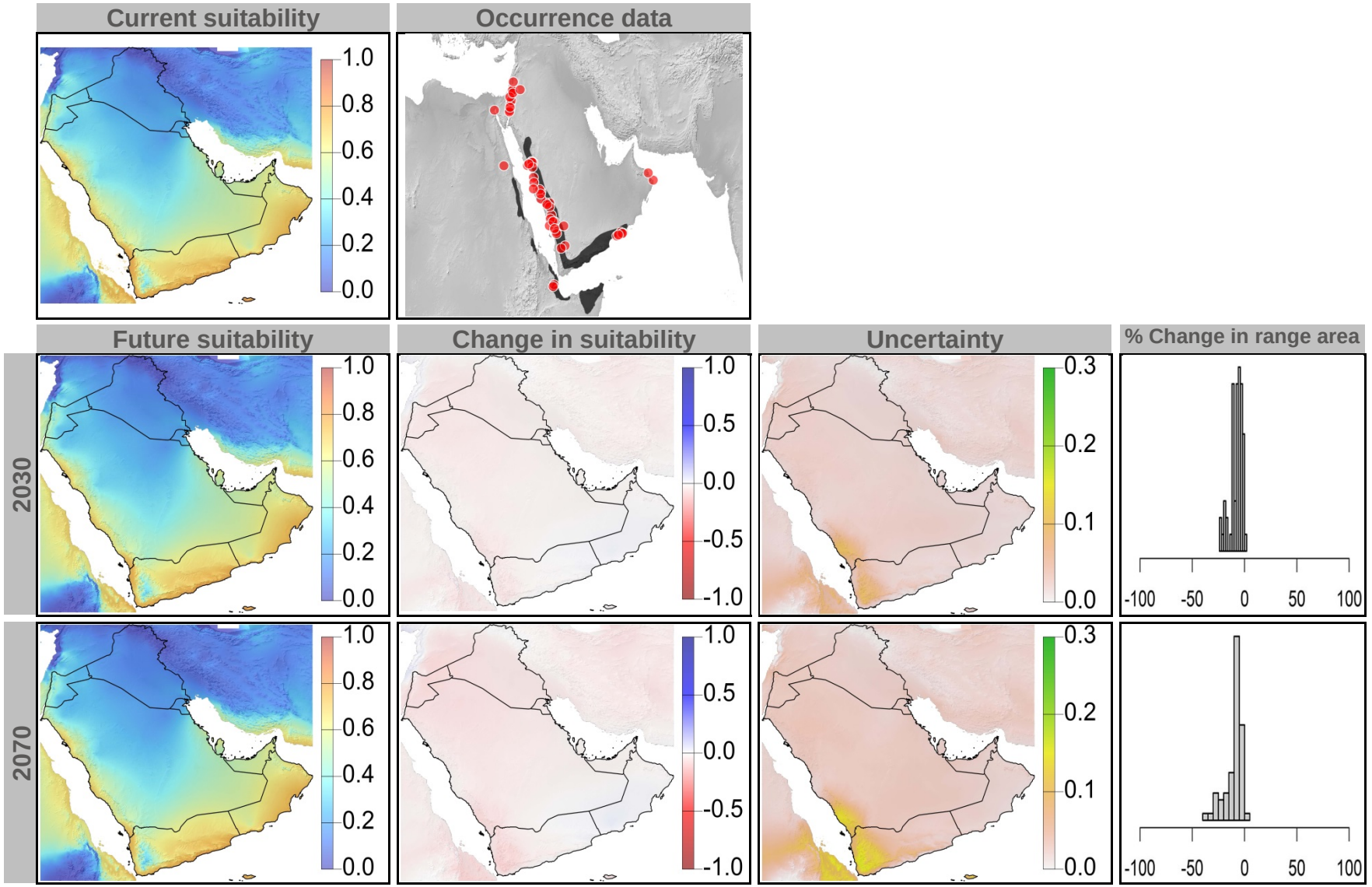

Figure 22: Current and future (2070) climate suitability for *Sylvia leucomelaena*, based on an ensemble of all future climate scenarios from the regional climate modeling effort at two spatial domains. Range and occurrence data shown for reference.

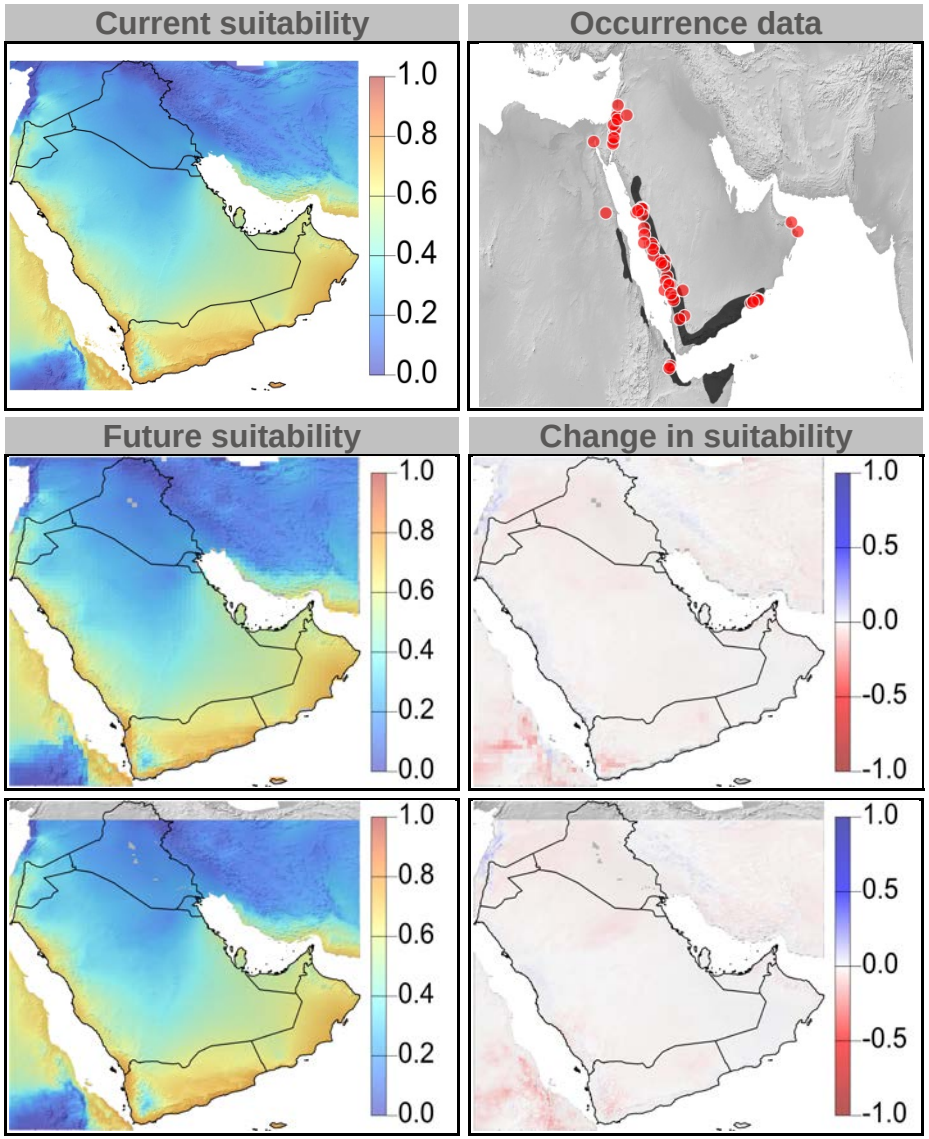

Figure 23: Current and future climate suitability for *Turdoides squamiceps*, with associated uncertainty and change in range area based on an ensemble of all future climate scenarios. Range and occurrence data shown for reference.

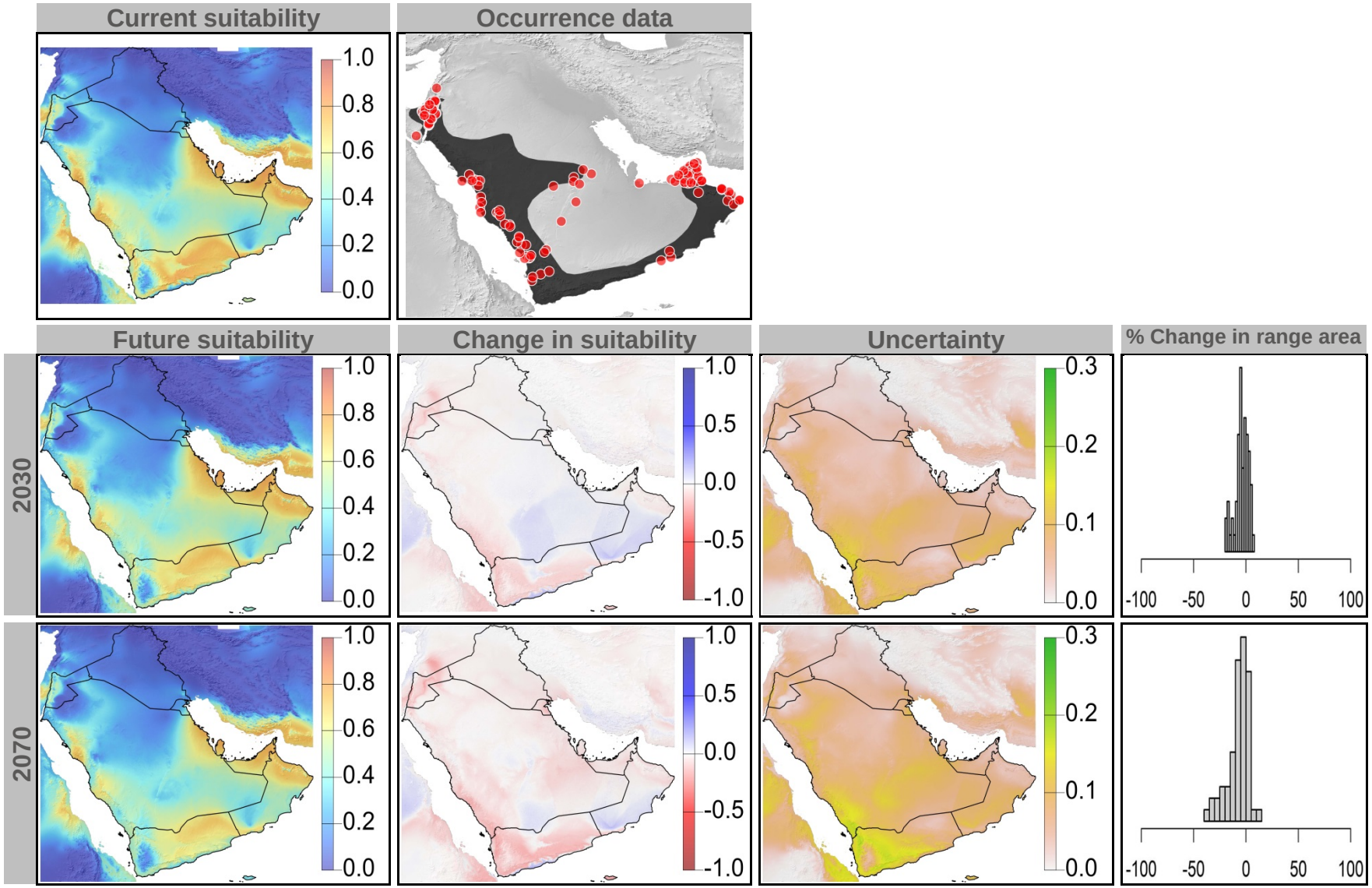

Figure 24: Current and future (2070) climate suitability for *Turdoides squamiceps*, based on an ensemble of all future climate scenarios from the regional climate modeling effort at two spatial domains. Range and occurrence data shown for reference.

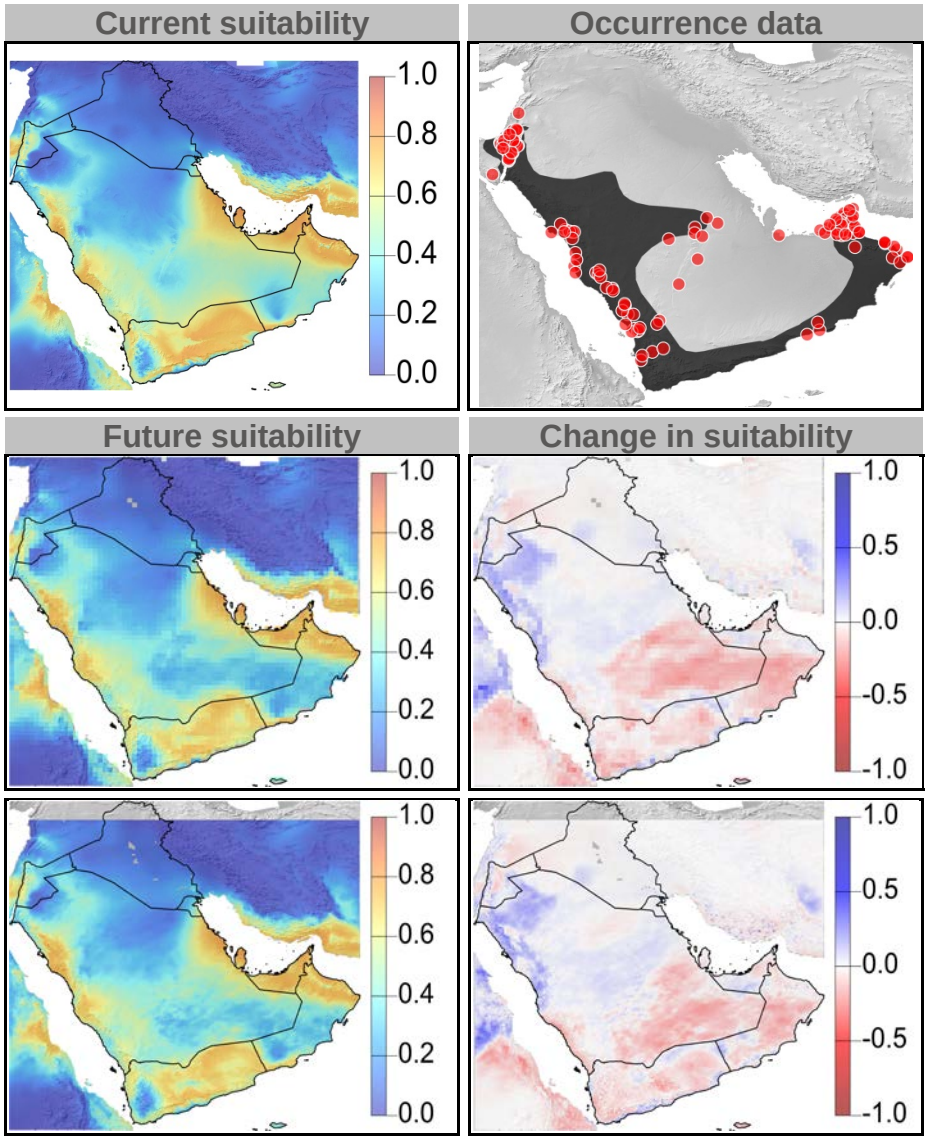

Figure 25: Current and future climate suitability for *Aquila clanga*, with associated uncertainty and change in range area based on an ensemble of all future climate scenarios. Range and occurrence data shown for reference.

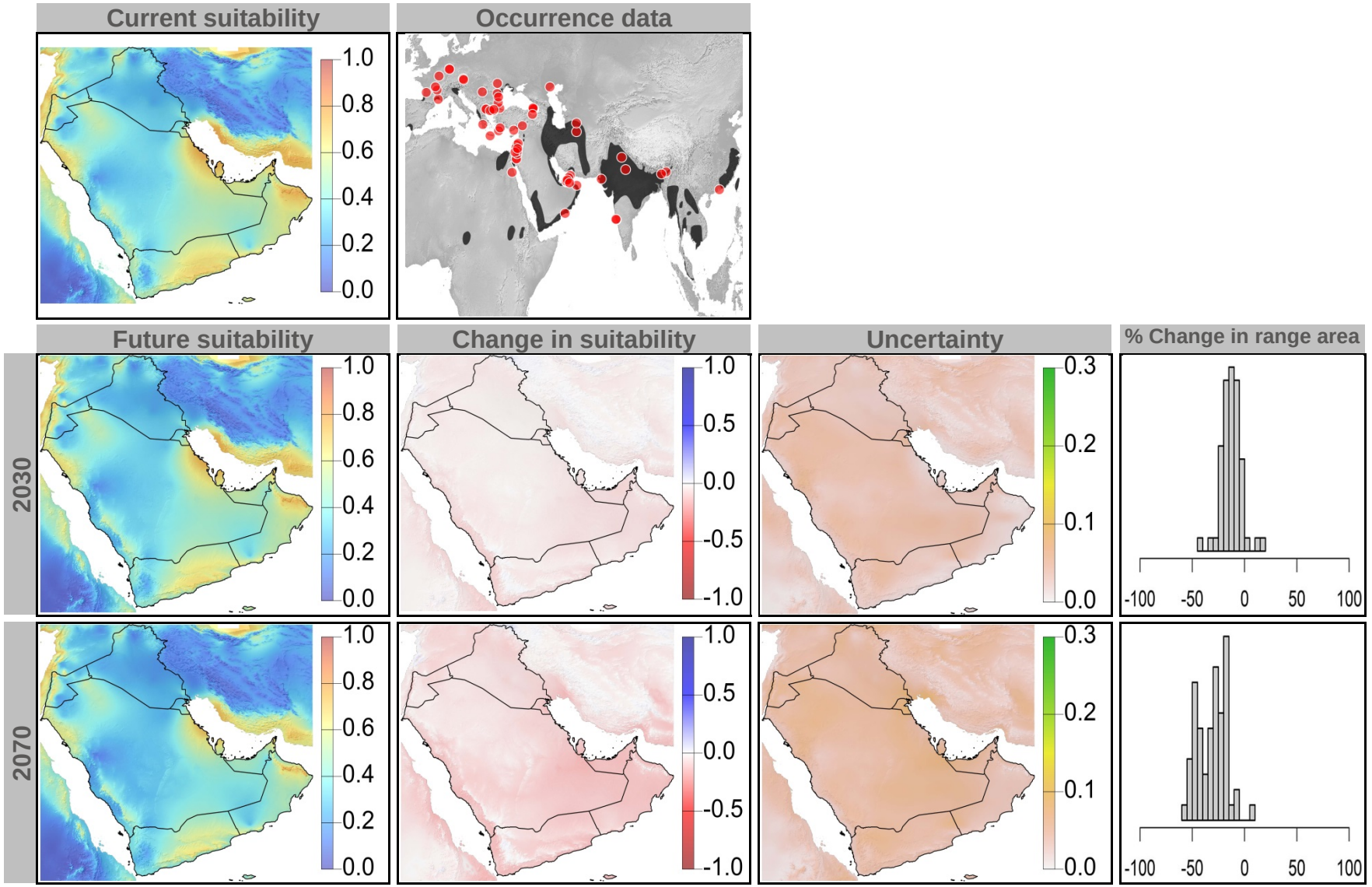

Figure 26: Current and future (2070) climate suitability for *Aquila clanga*, based on an ensemble of all future climate scenarios from the regional climate modeling effort at two spatial domains. Range and occurrence data shown for reference.

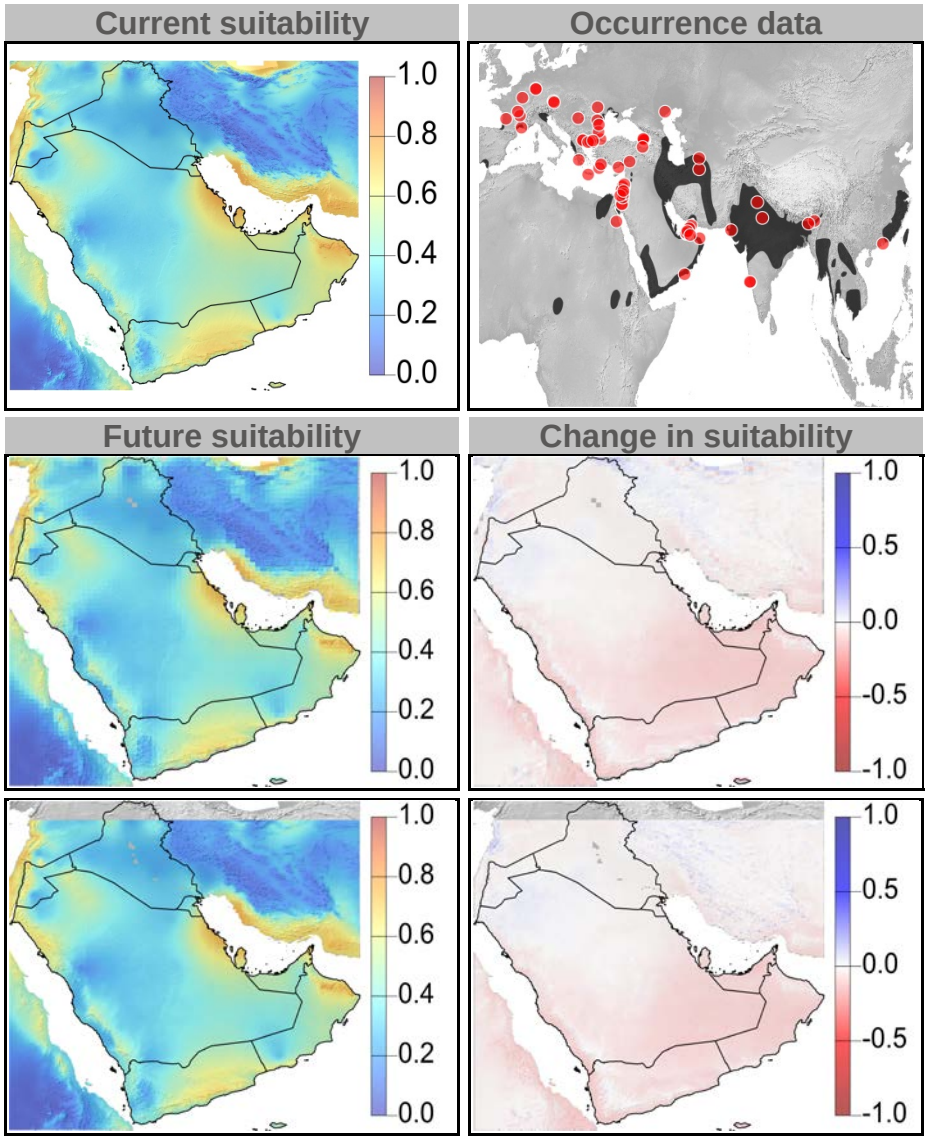

Figure 27: Current and future climate suitability for *Calidris tenuirostris*, with associated uncertainty and change in range area based on an ensemble of all future climate scenarios. Range and occurrence data shown for reference.

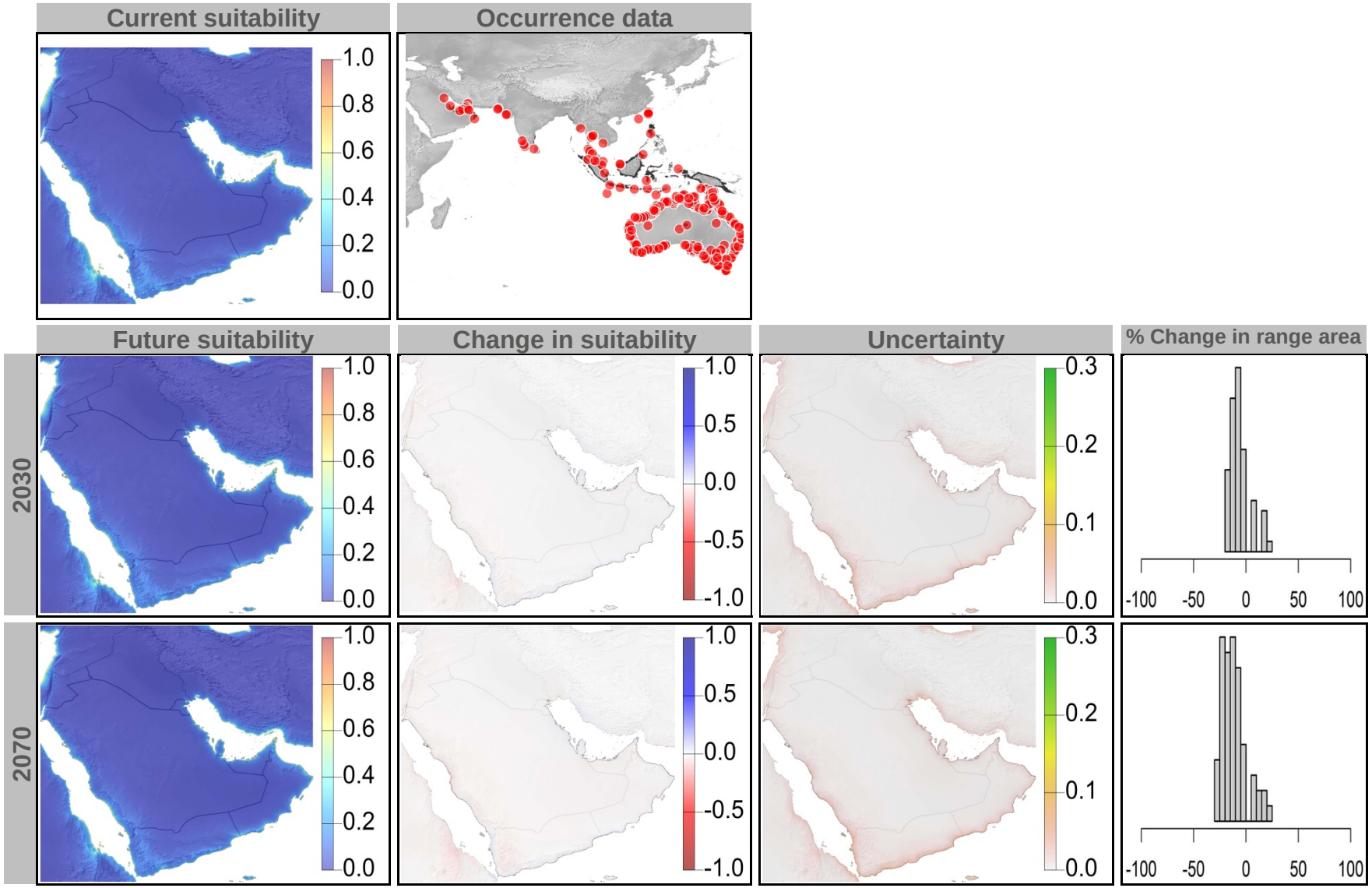

Figure 28: Current and future (2070) climate suitability for *Calidris tenuirostris*, based on an ensemble of all future climate scenarios from the regional climate modeling effort at two spatial domains. Range and occurrence data shown for reference.

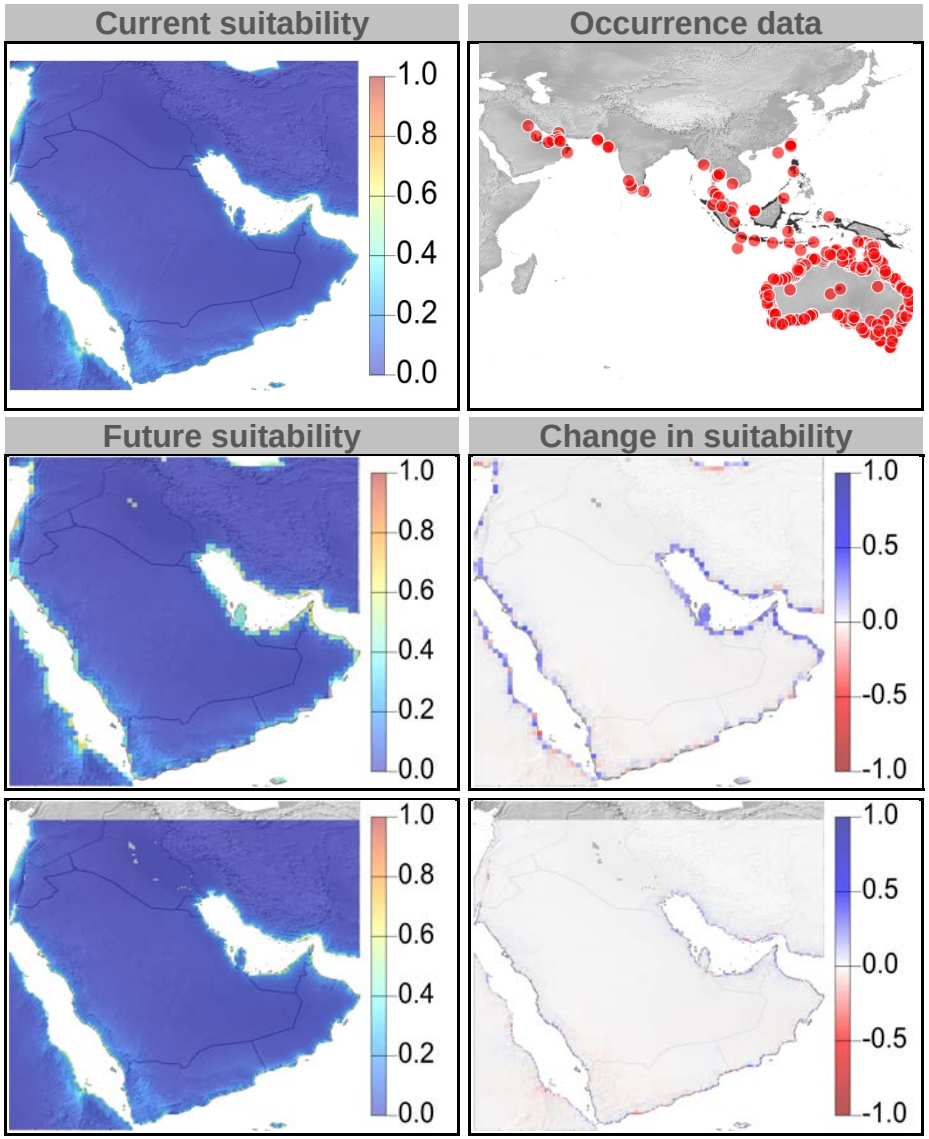

Figure 29: Current and future climate suitability for *Chlamydotis macqueenii* (non-breeding), with associated uncertainty and change in range area based on an ensemble of all future climate scenarios. Range and occurrence data shown for reference.

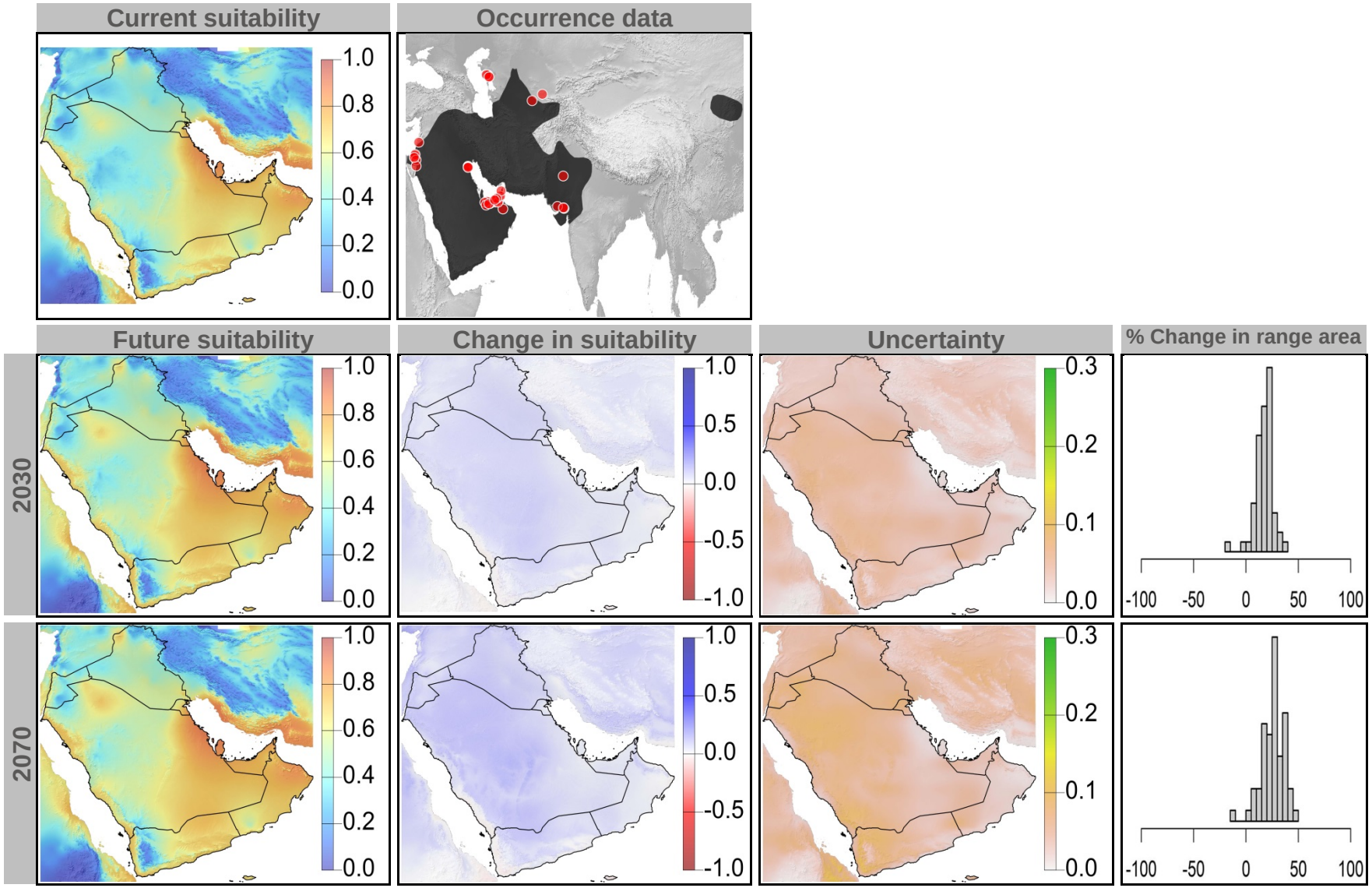

Figure 30: Current and future (2070) climate suitability for *Chlamydotis macqueenii* (non-breeding), based on an ensemble of all future climate scenarios from the regional climate modeling effort at two spatial domains. Range and occurrence data shown for reference.

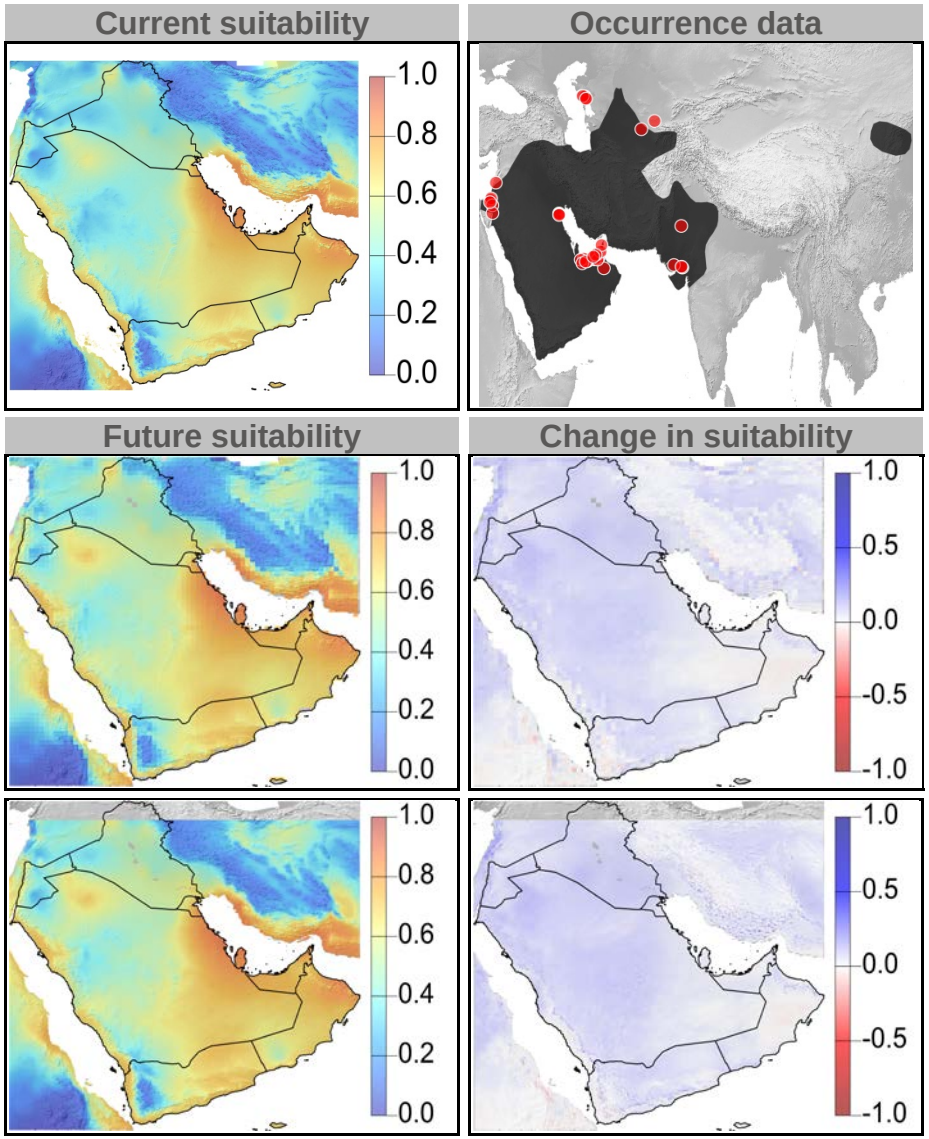

Figure 31: Current and future climate suitability for *Egretta gularis* (non-breeding), with associated uncertainty and change in range area based on an ensemble of all future climate scenarios. Range and occurrence data shown for reference.

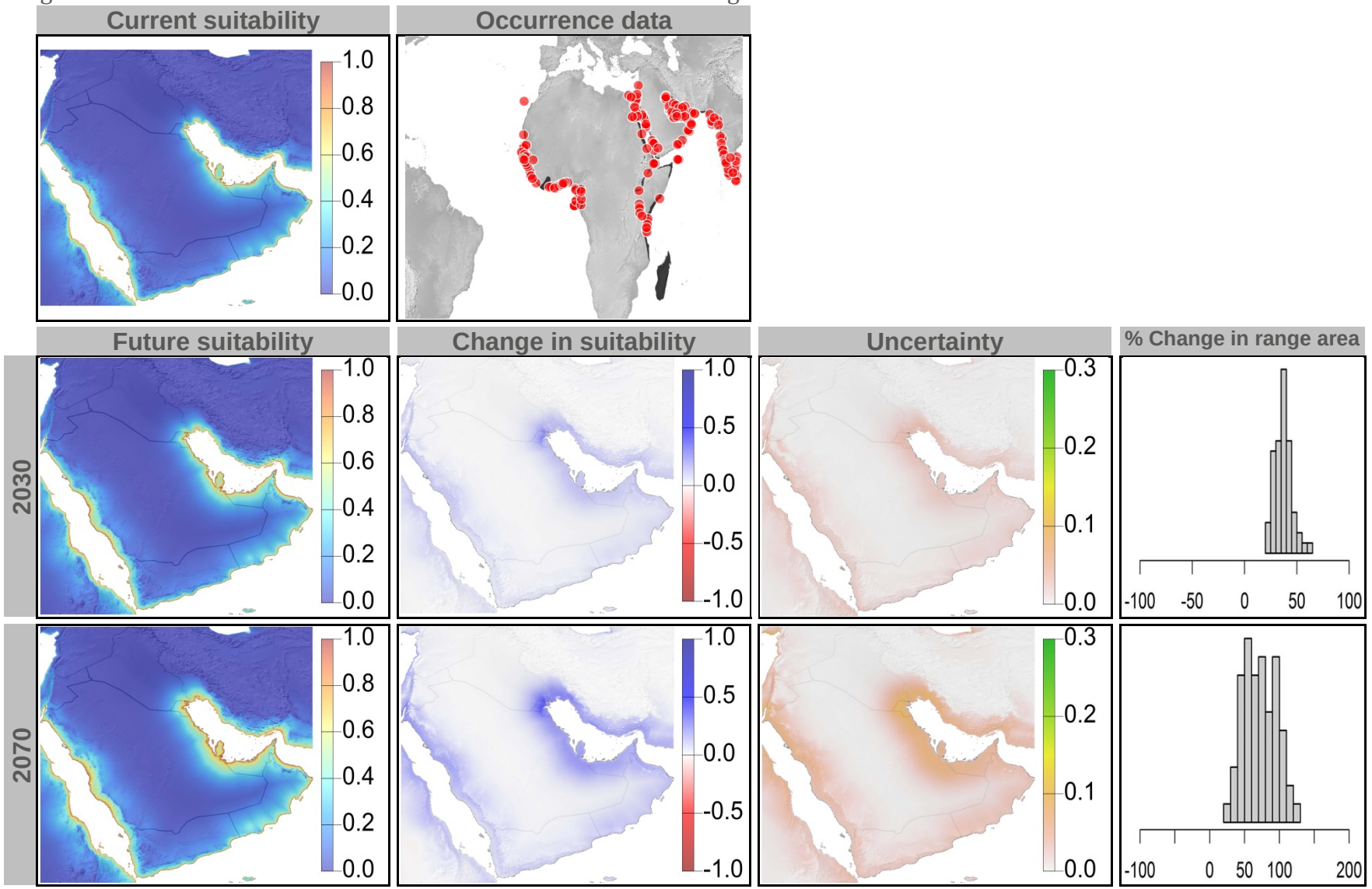

Figure 32: Current and future (2070) climate suitability for *Egretta gularis* (non-breeding), based on an ensemble of all future climate scenarios from the regional climate modeling effort at two spatial domains. Range and occurrence data shown for reference.

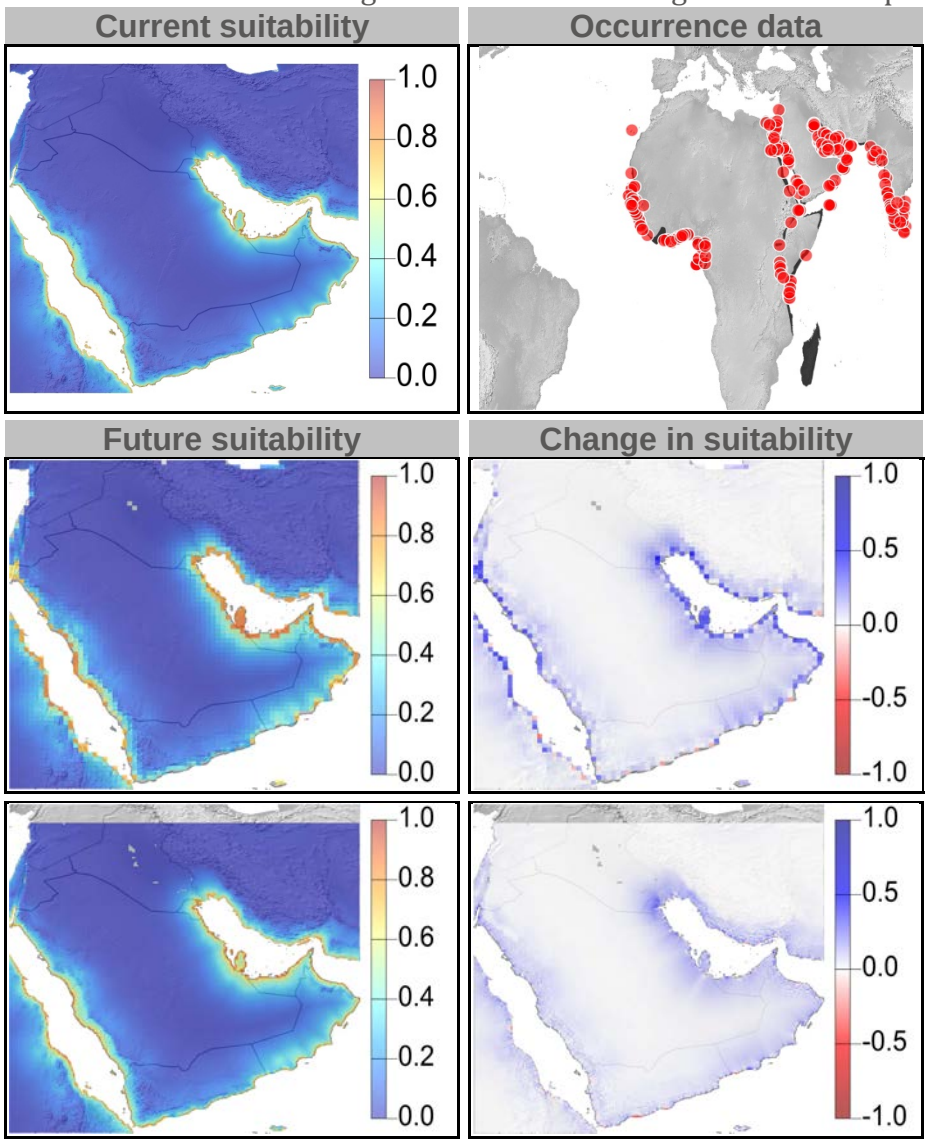

Figure 33: Current and future climate suitability for *Marmaronetta angustirostris*, with associated uncertainty and change in range area based on an ensemble of all future climate scenarios. Range and occurrence data shown for reference.

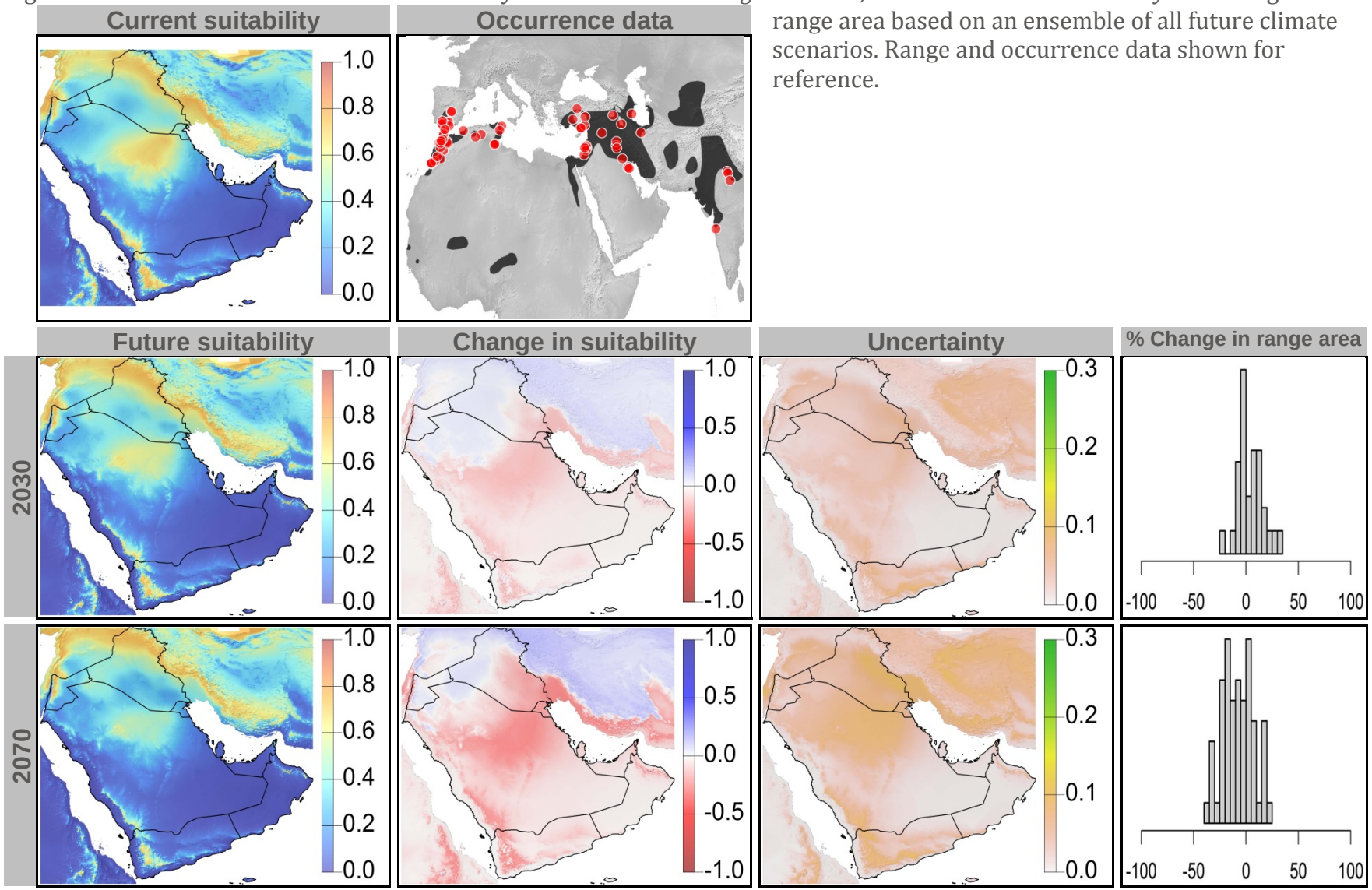

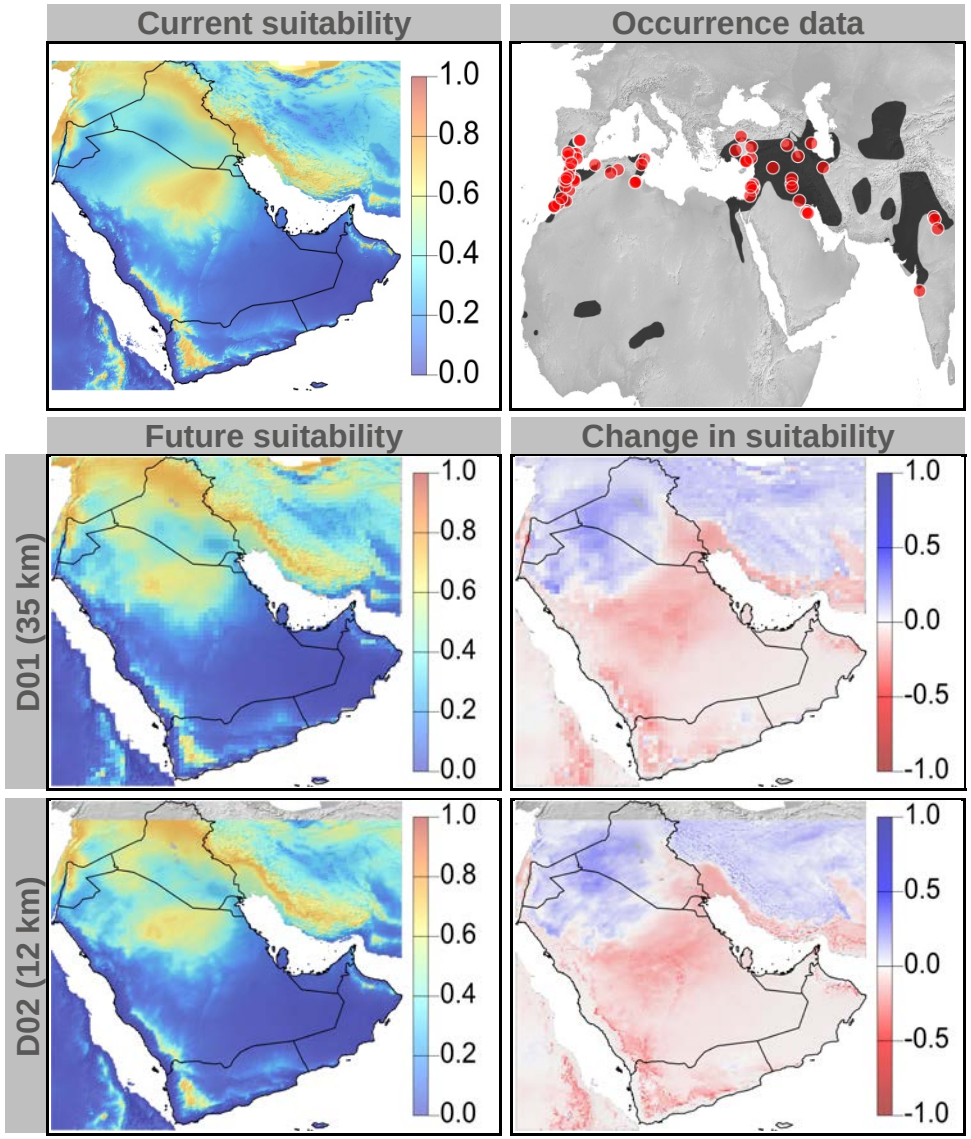

Figure 34: Current and future (2070) climate suitability for *Marmaronetta angustirostris*, based on an ensemble of all future climate scenarios from the regional climate modeling effort at two spatial domains. Range and occurrence data shown for reference.

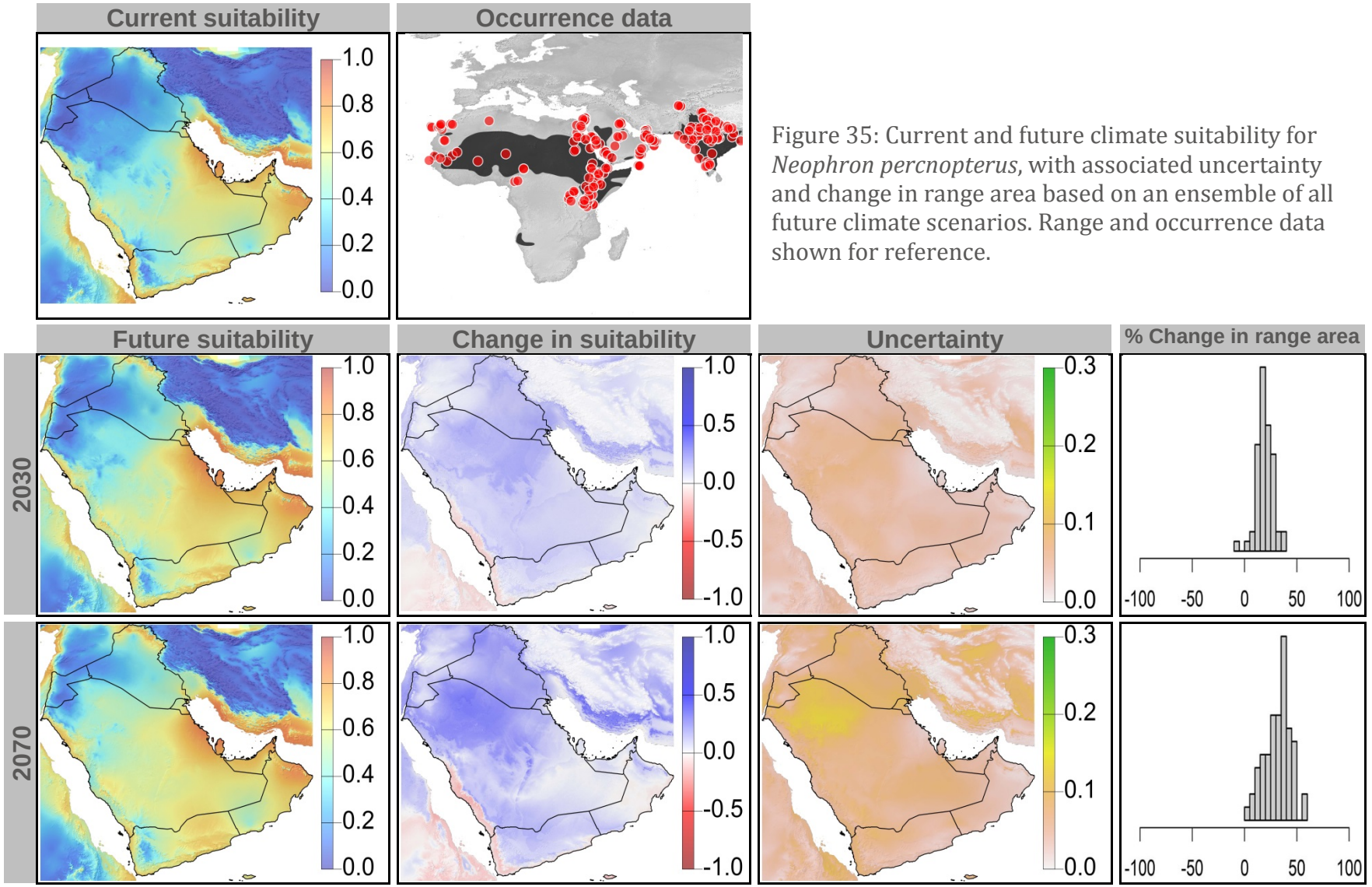

Figure 35: Current and future climate suitability for *Neophron percnopterus*, with associated uncertainty and change in range area based on an ensemble of all future climate scenarios. Range and occurrence data shown for reference.

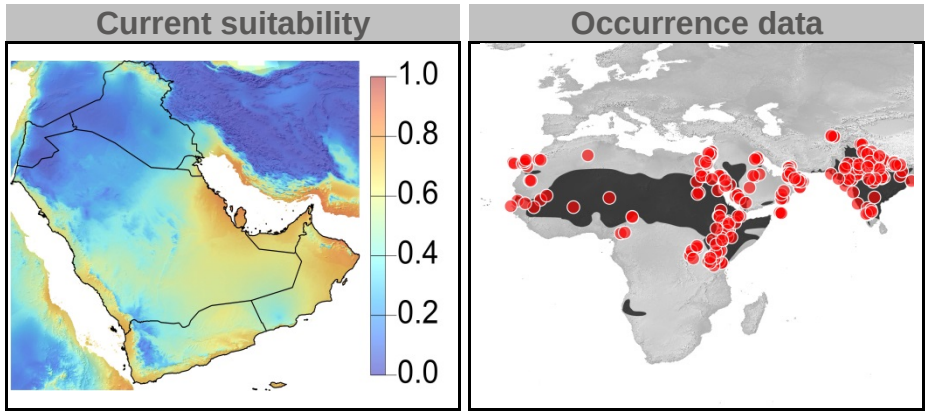

Figure 36: Current and future (2070) climate suitability for *Neophron percnopterus*, based on an ensemble of all future climate scenarios from the regional climate modeling effort at two spatial domains. Range and occurrence data shown for reference.

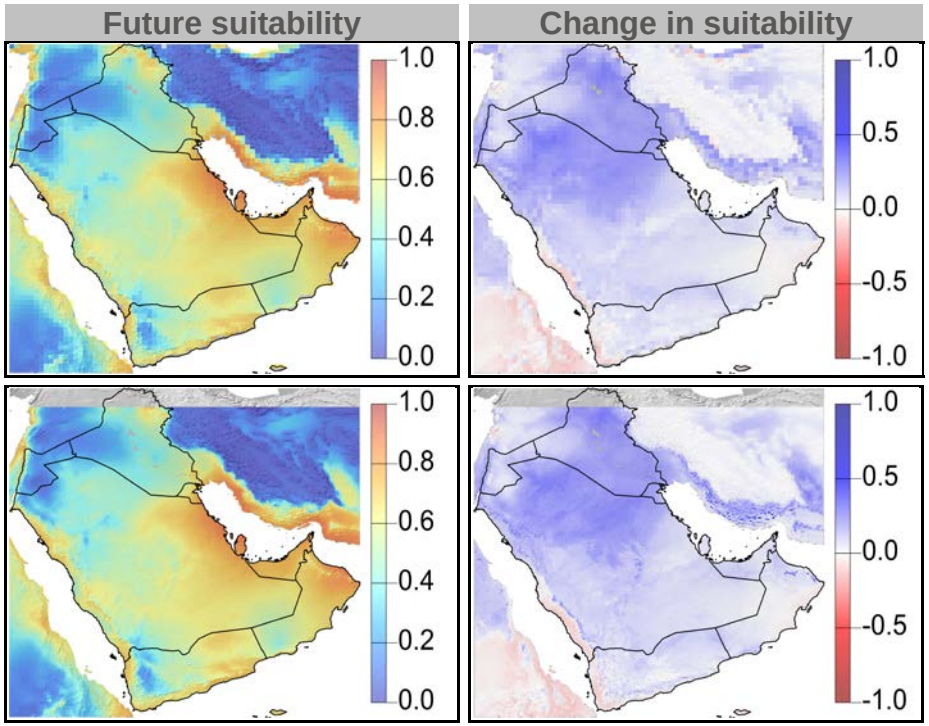

Figure 37: Current and future climate suitability for *Vanellus gregarius*, with associated uncertainty and change in range area based on an ensemble of all

future climate scenarios. Range and occurrence data shown for reference.

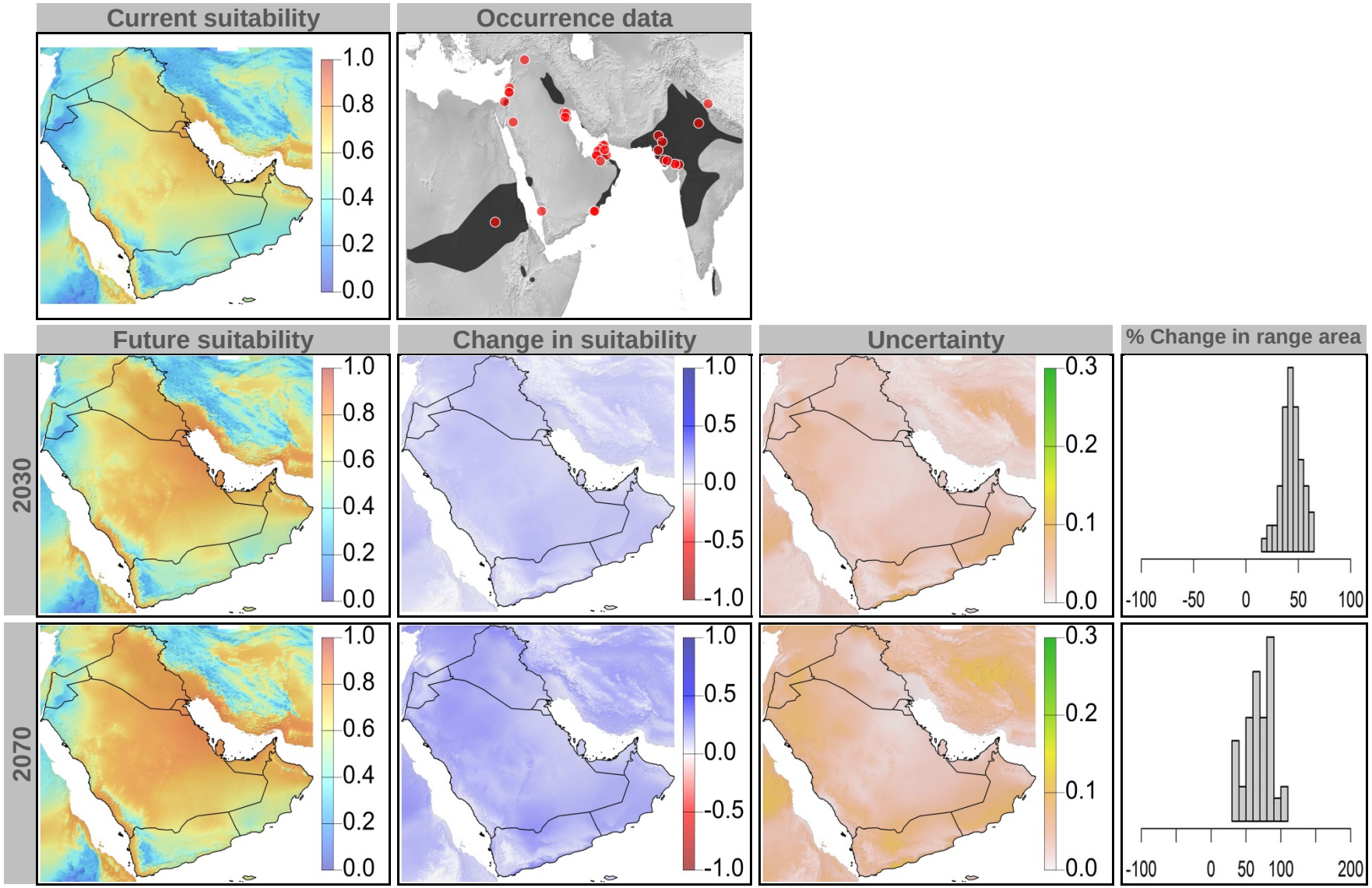

Figure 38: Current and future (2070) climate suitability for *Vanellus gregarius*, based on an ensemble of all future climate scenarios from the regional climate modeling effort at two spatial domains. Range and occurrence data shown for reference.

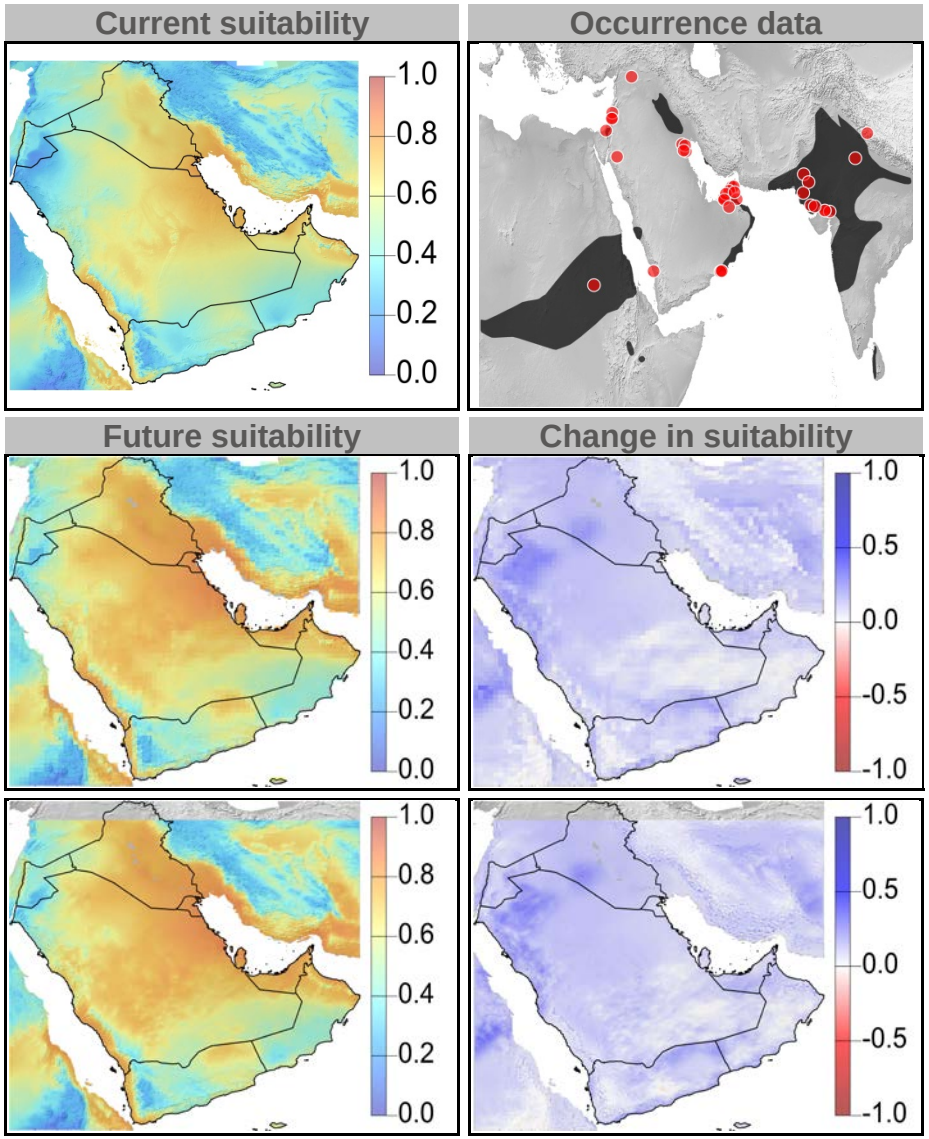

AGEDI
مبادرة أبوظبي العالمية للبيانات البيئية
Abu Dhabi Global Environmental Data Initiative

Annex VII – MaxEnt results combined across all priority mammal species for RCP4.5 and RCP8.5

Climate Change Research Group

University of Maryland
CENTER FOR ENVIRONMENTAL SCIENCE

Figure 1: Current and future climate suitability for *Allactaga euphratica*, with associated uncertainty and change in range area based on an ensemble of all future climate scenarios. Range and occurrence data shown for reference.

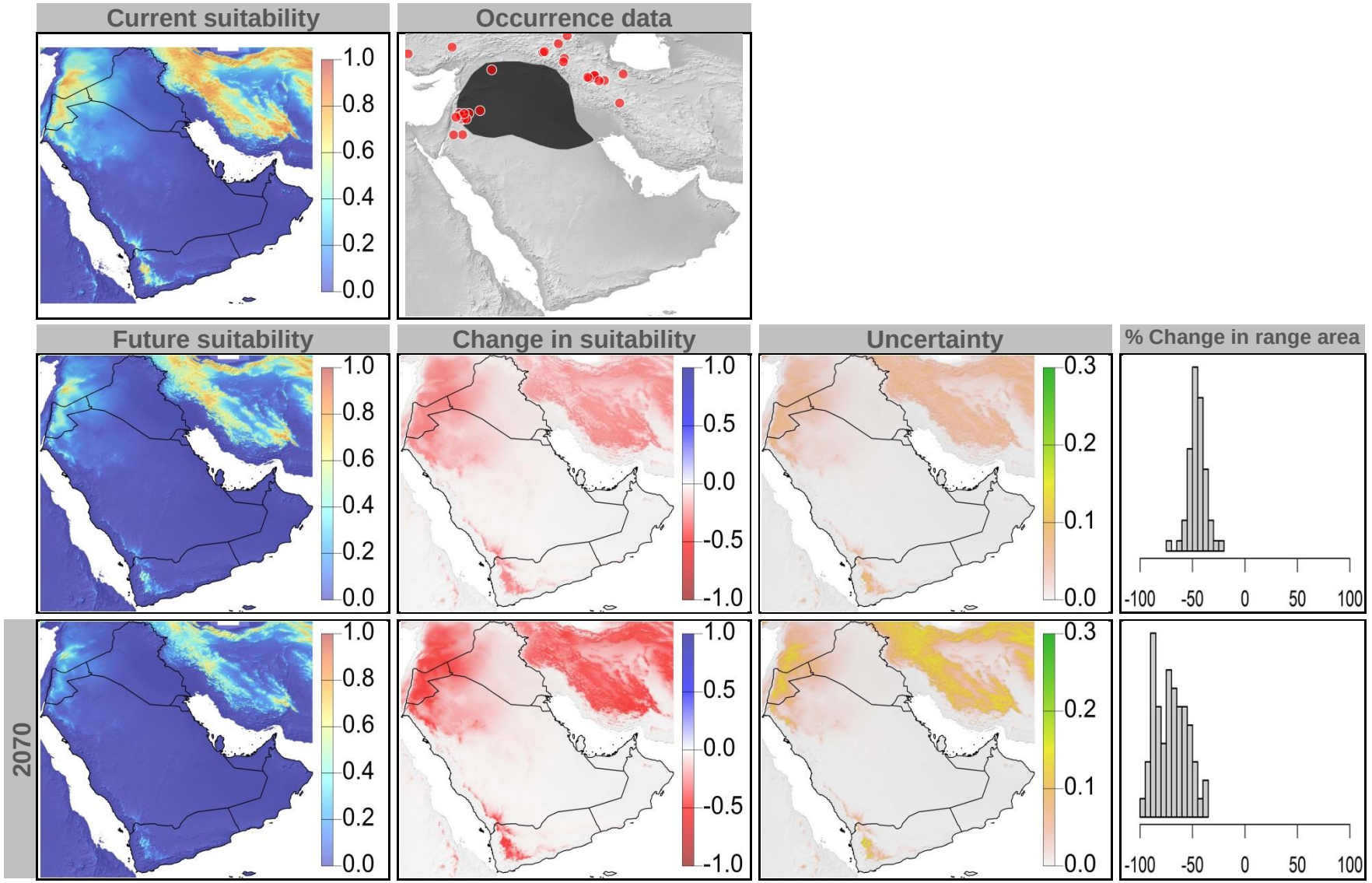

Figure 2: Current and future (2070) climate suitability for *Allactaga euphratica*, based on an ensemble of all future climate scenarios from the regional climate modeling effort at two spatial domains. Range and occurrence data shown for reference.

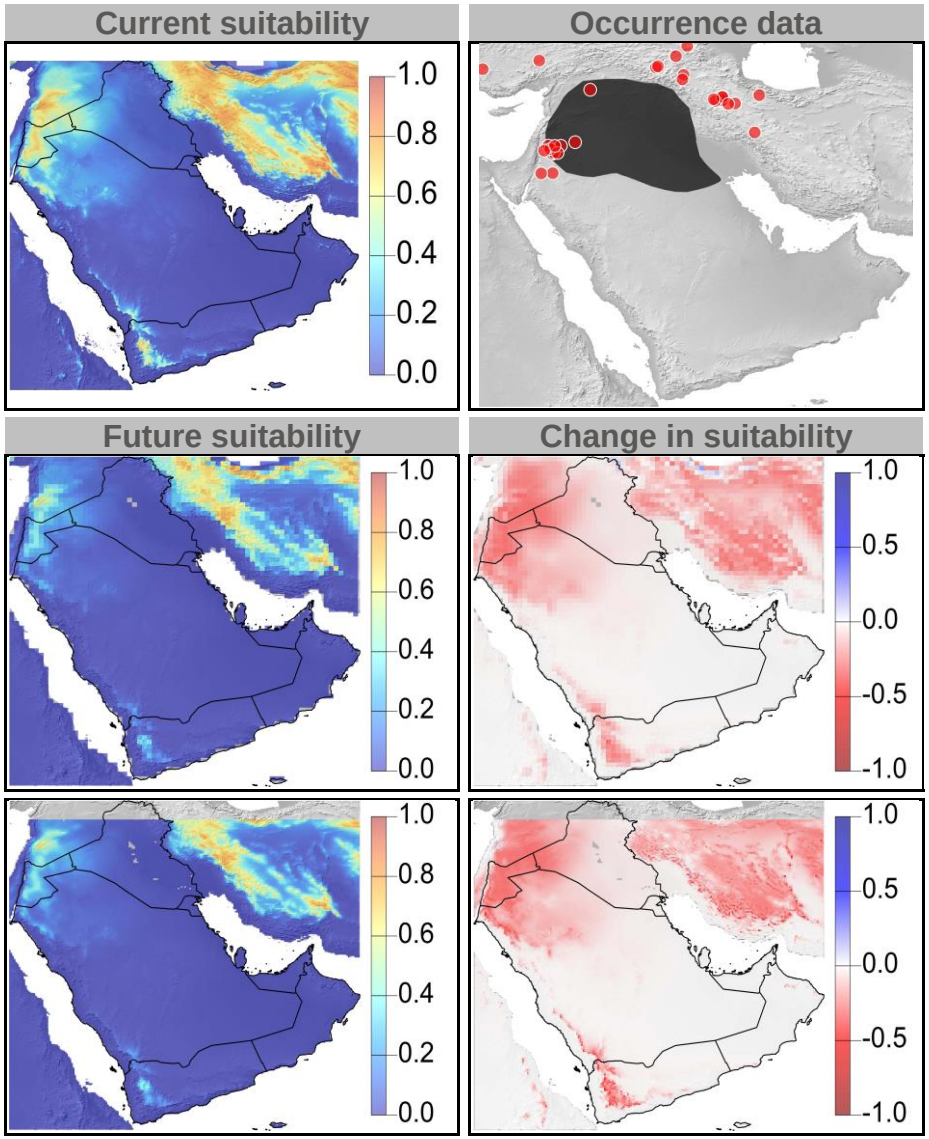

Figure 3: Current and future climate suitability for *Asellia tridens*, with associated uncertainty and change in range area based on an ensemble of all future climate scenarios. Range and occurrence data shown for reference.

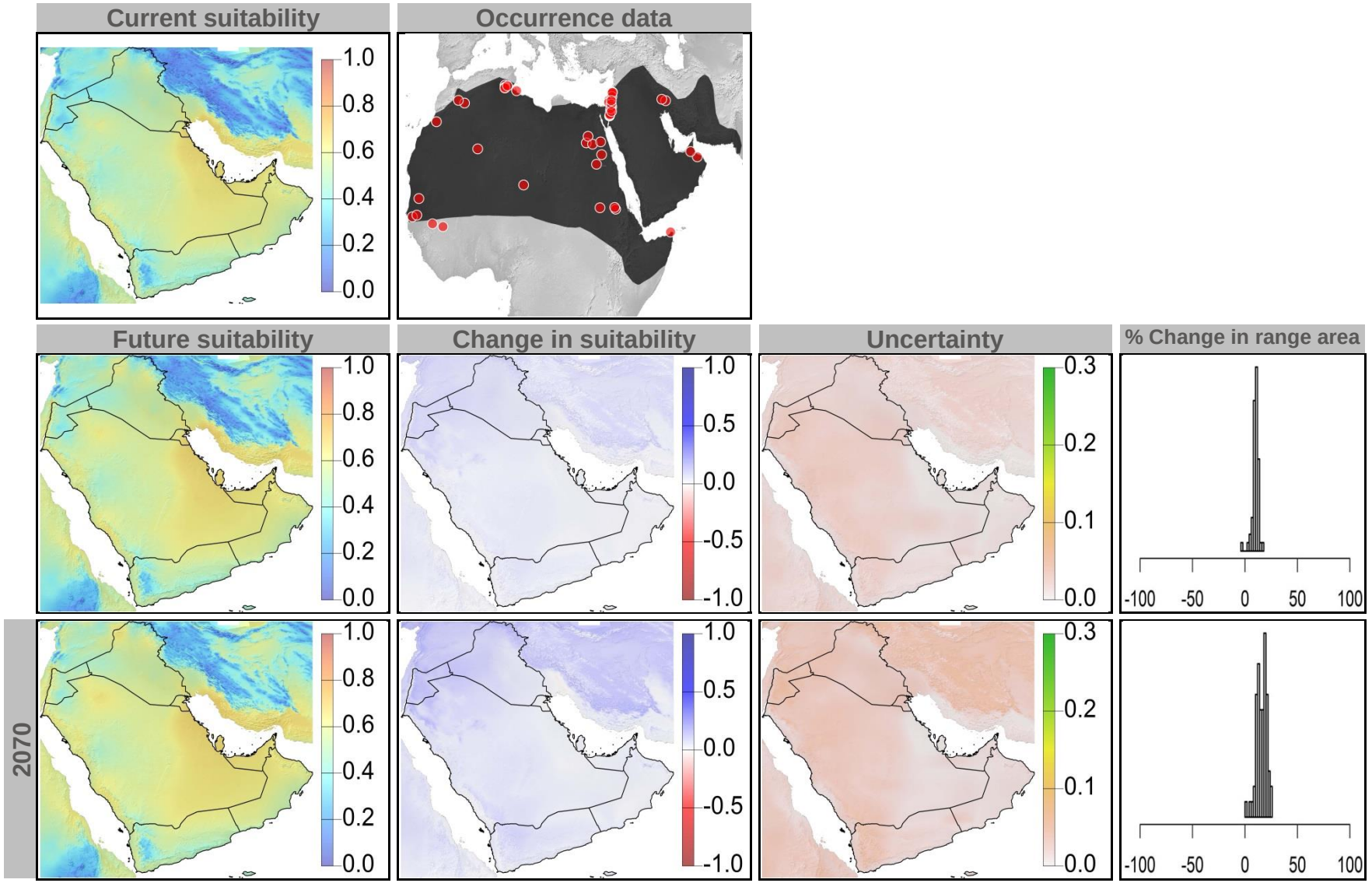

Figure 4: Current and future (2070) climate suitability for *Asellia tridens*, based on an ensemble of all future climate scenarios from the regional climate modeling effort at two spatial domains. Range and occurrence data shown for reference.

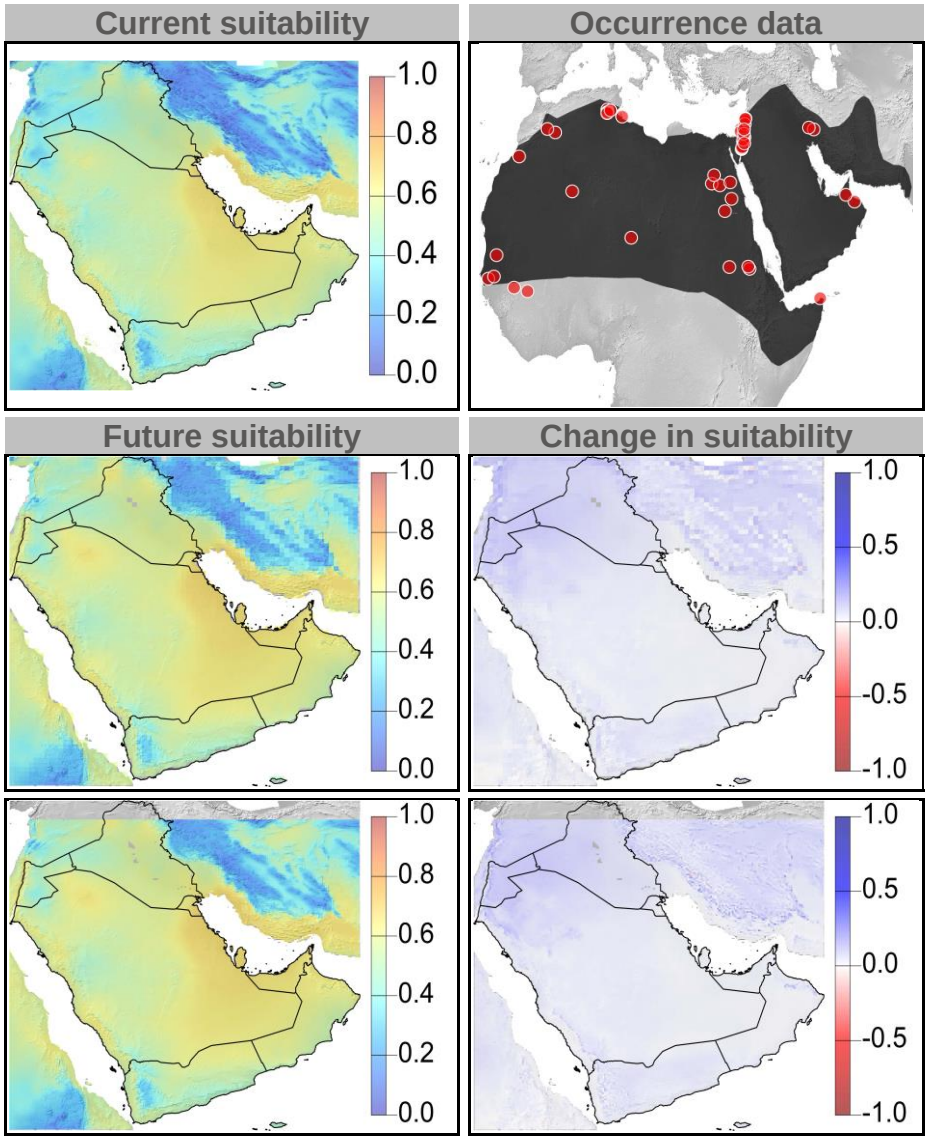

Figure 5: Current and future climate suitability for *Canis aureus*, with associated uncertainty and change in range area based on an ensemble of all future climate scenarios. Range and occurrence data shown for reference.

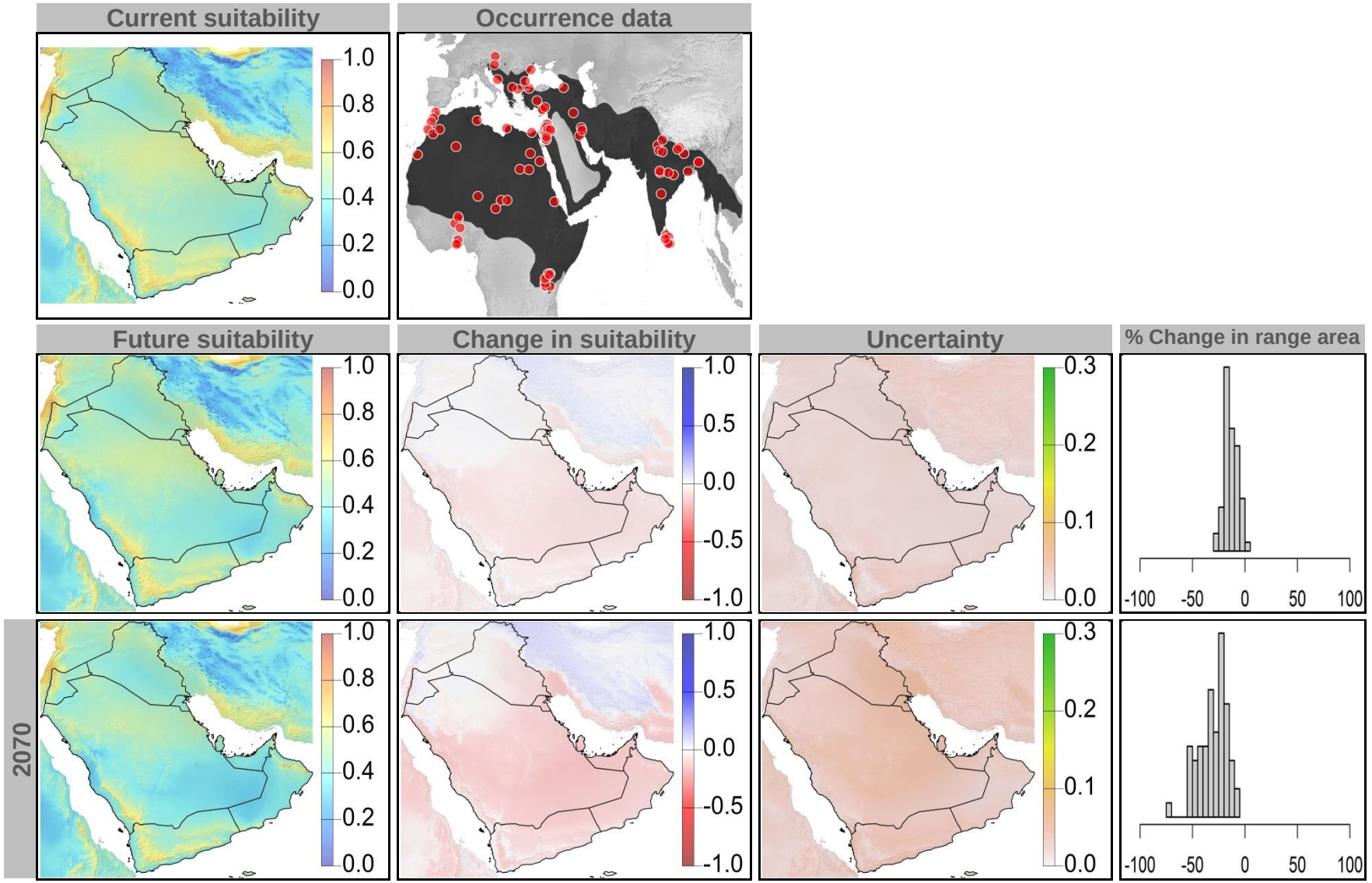

Figure 6: Current and future (2070) climate suitability for *Canis aureus*, based on an ensemble of all future climate scenarios from the regional climate modeling effort at two spatial domains. Range and occurrence data shown for reference.

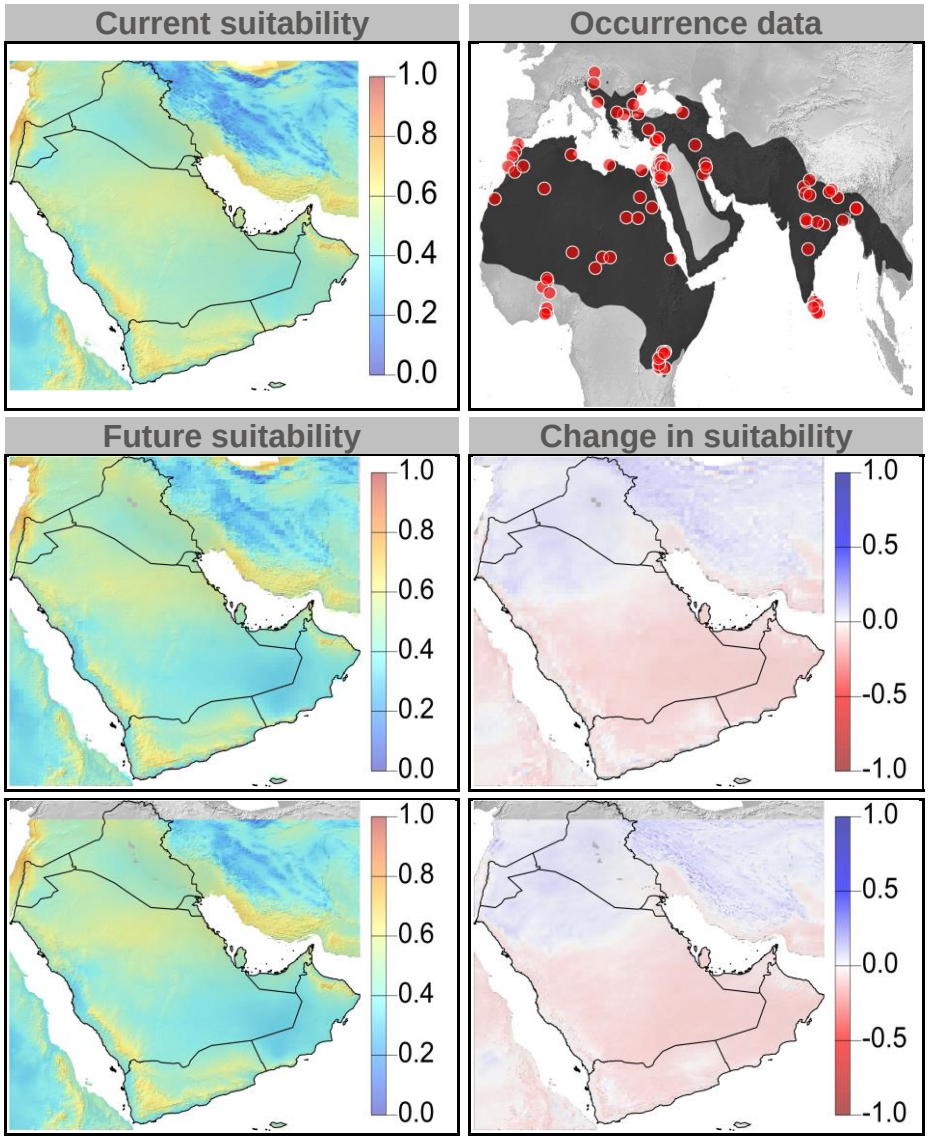

Figure 7: Current and future climate suitability for *Capra nubiana*, with associated uncertainty and change in range area based on an ensemble of all future climate scenarios. Range and occurrence data shown for reference.

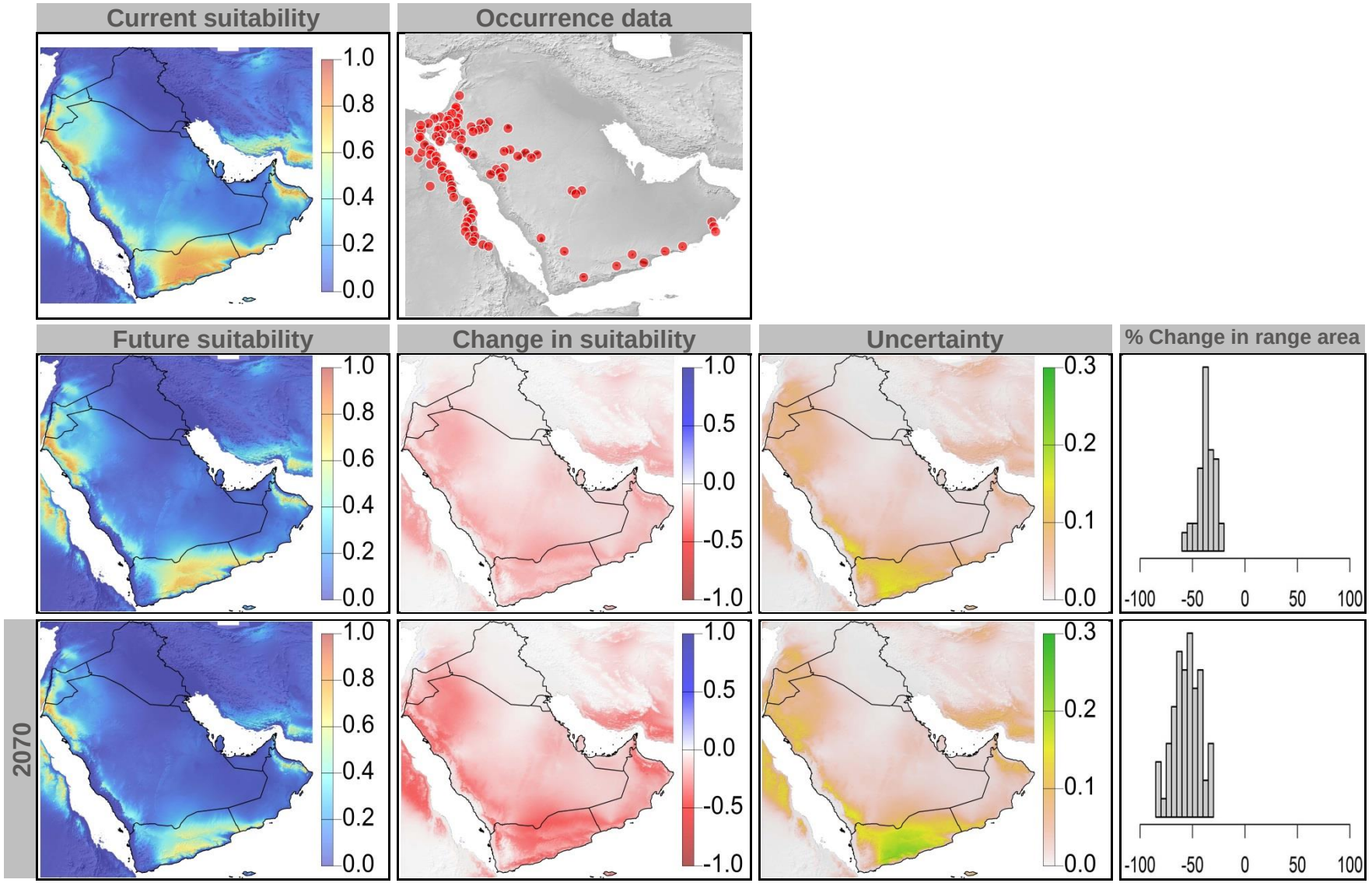

Figure 8: Current and future (2070) climate suitability for *Capra nubiana*, based on an ensemble of all future climate scenarios from the regional climate modeling effort at two spatial domains. Range and occurrence data shown for reference.

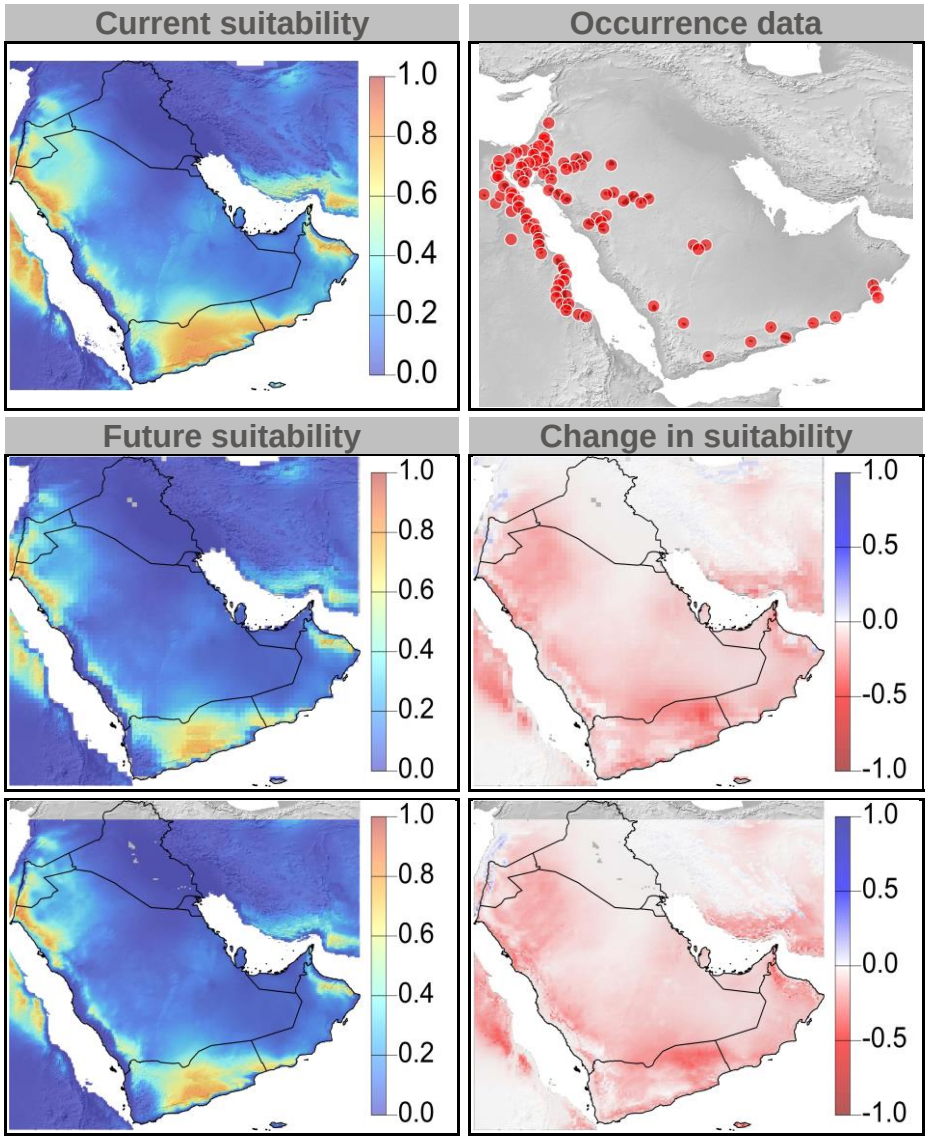

Figure 9: Current and future climate suitability for *Caracal caracal*, with associated uncertainty and change in range area based on an ensemble of all future climate scenarios. Range and occurrence data shown for reference.

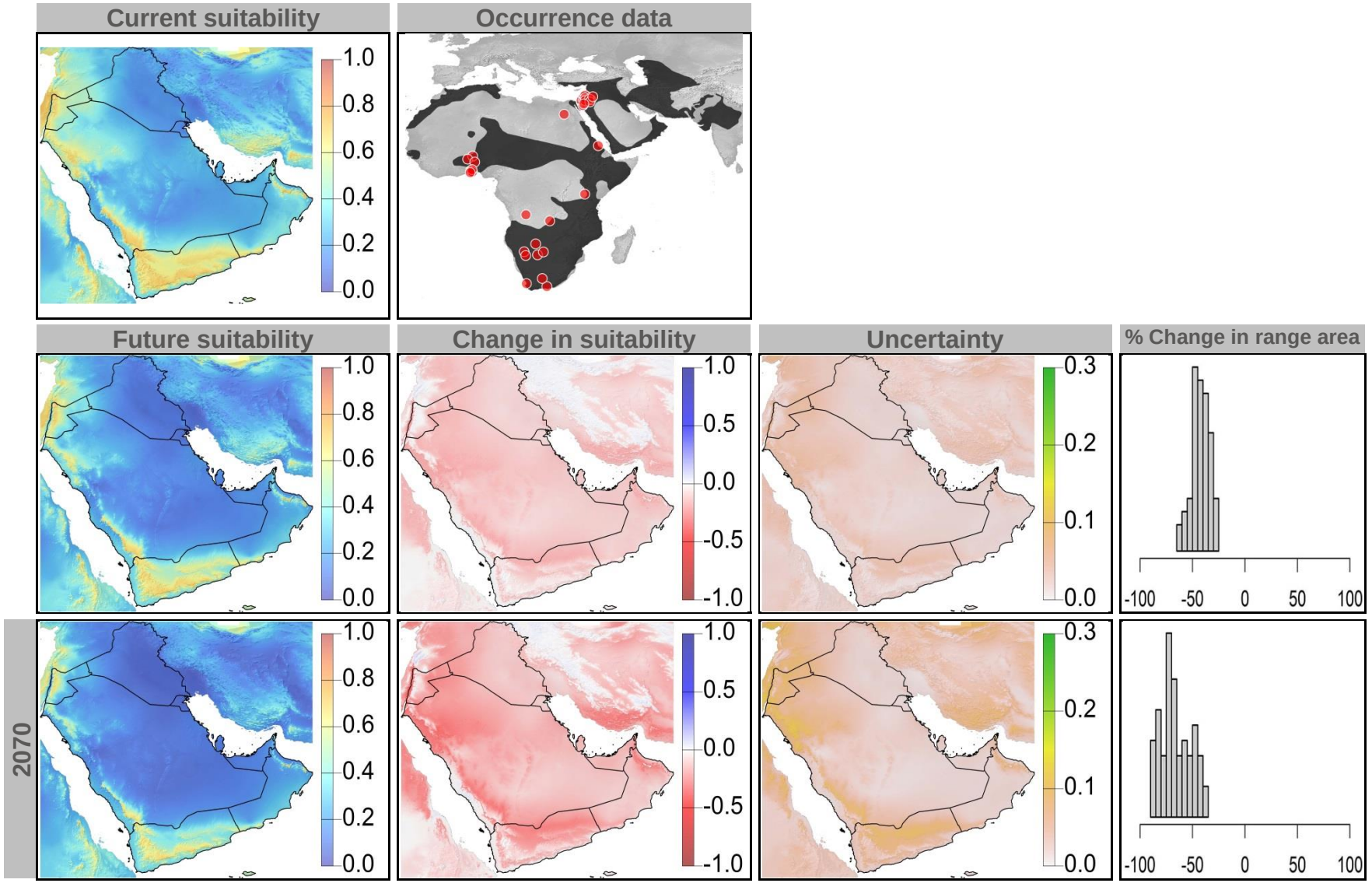

Figure 10: Current and future (2070) climate suitability for *Caracal caracal*, based on an ensemble of all future climate scenarios from the regional climate modeling effort at two spatial domains. Range and occurrence data shown for reference.

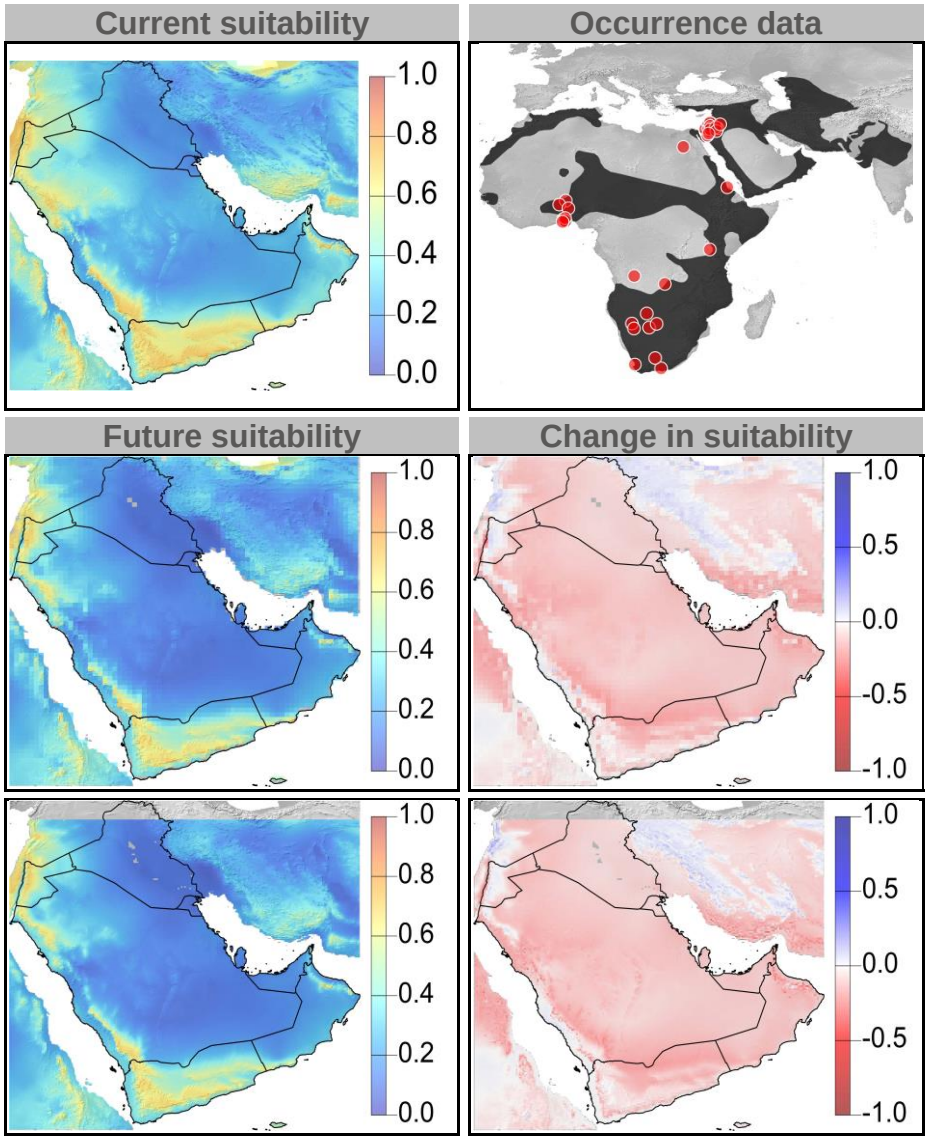

Figure 11: Current and future climate suitability for *Eidolon helvum*, with associated uncertainty and change in range area based on an ensemble of all future climate scenarios. Range and occurrence data shown for reference.

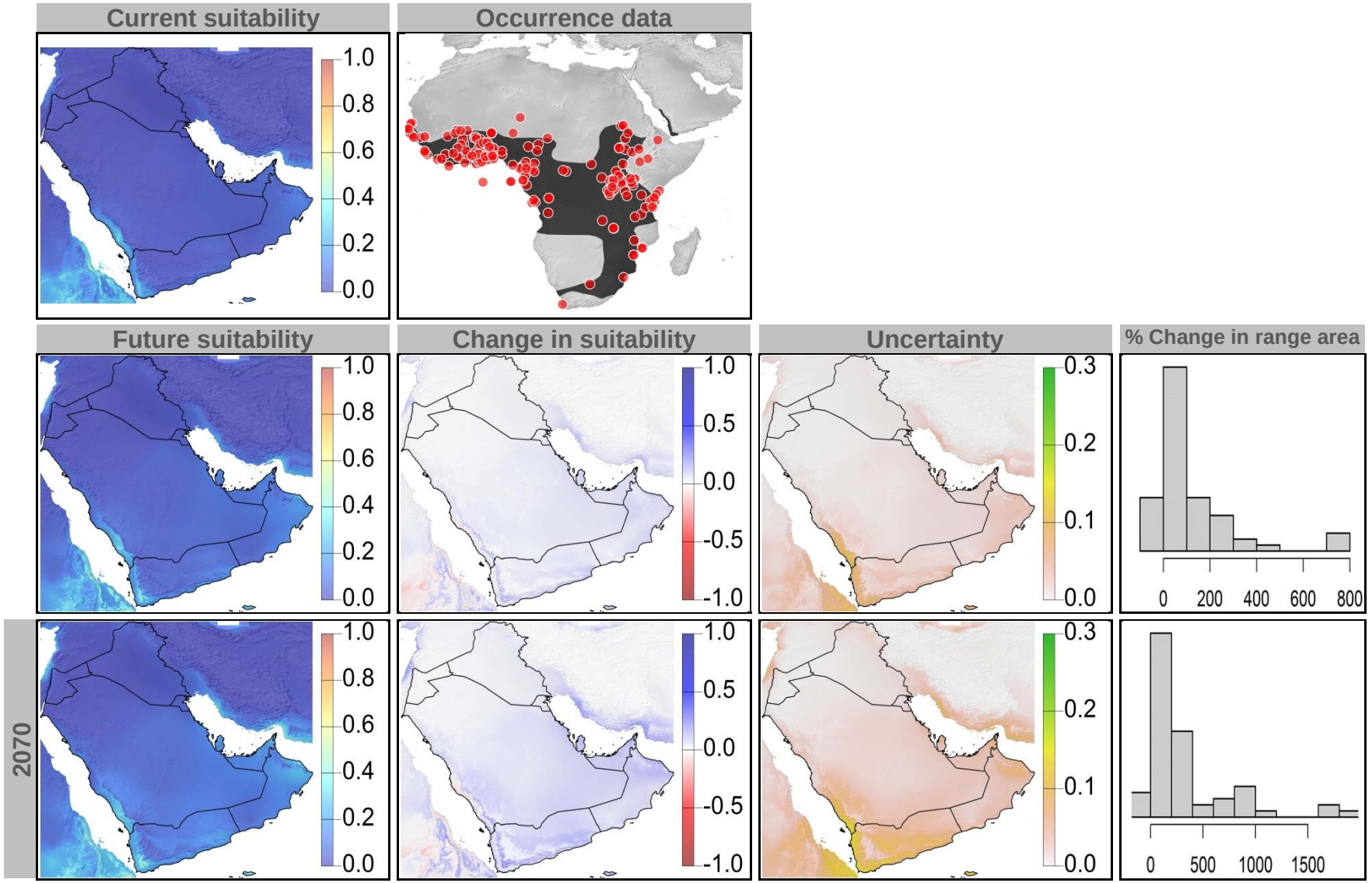

Figure 12: Current and future (2070) climate suitability for *Eidolon helvum*, based on an ensemble of all future climate scenarios from the regional climate modeling effort at two spatial domains. Range and occurrence data shown for reference.

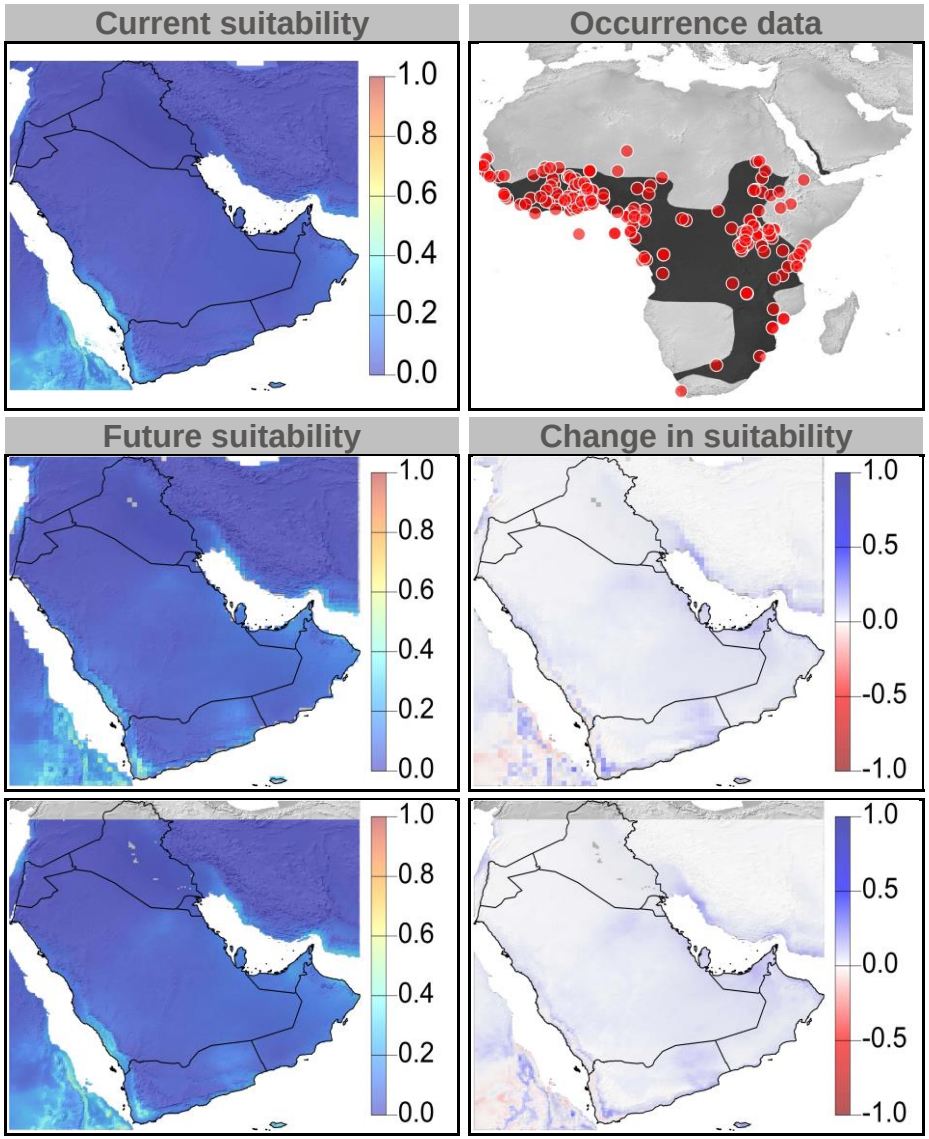

Figure 13: Current and future climate suitability for *Felis margarita*, with associated uncertainty and change in range area based on an ensemble of all future climate scenarios. Range and occurrence data shown for reference.

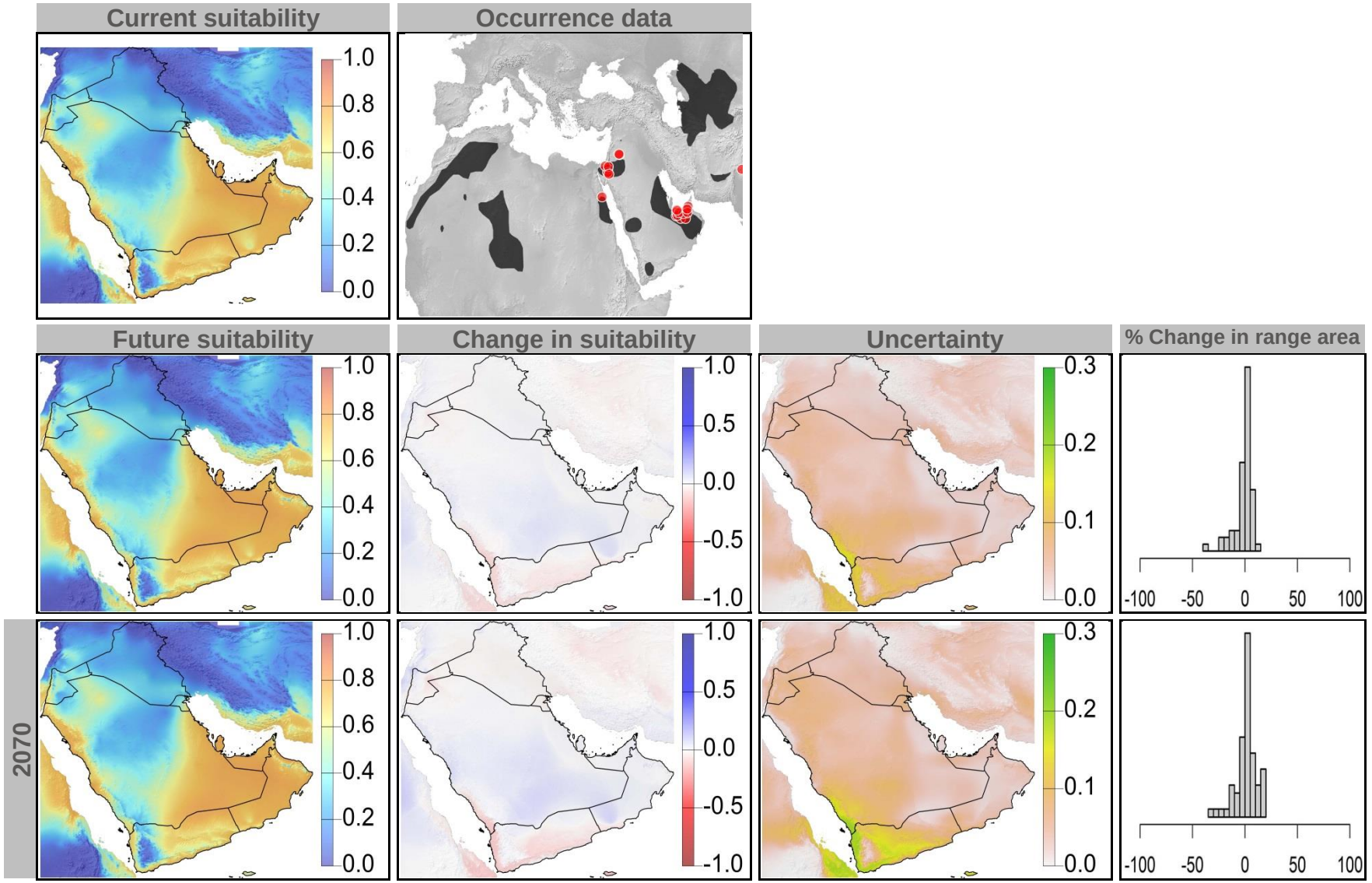

Figure 14: Current and future (2070) climate suitability for *Felis margarita*, based on an ensemble of all future climate scenarios from the regional climate modeling effort at two spatial domains. Range and occurrence data shown for reference.

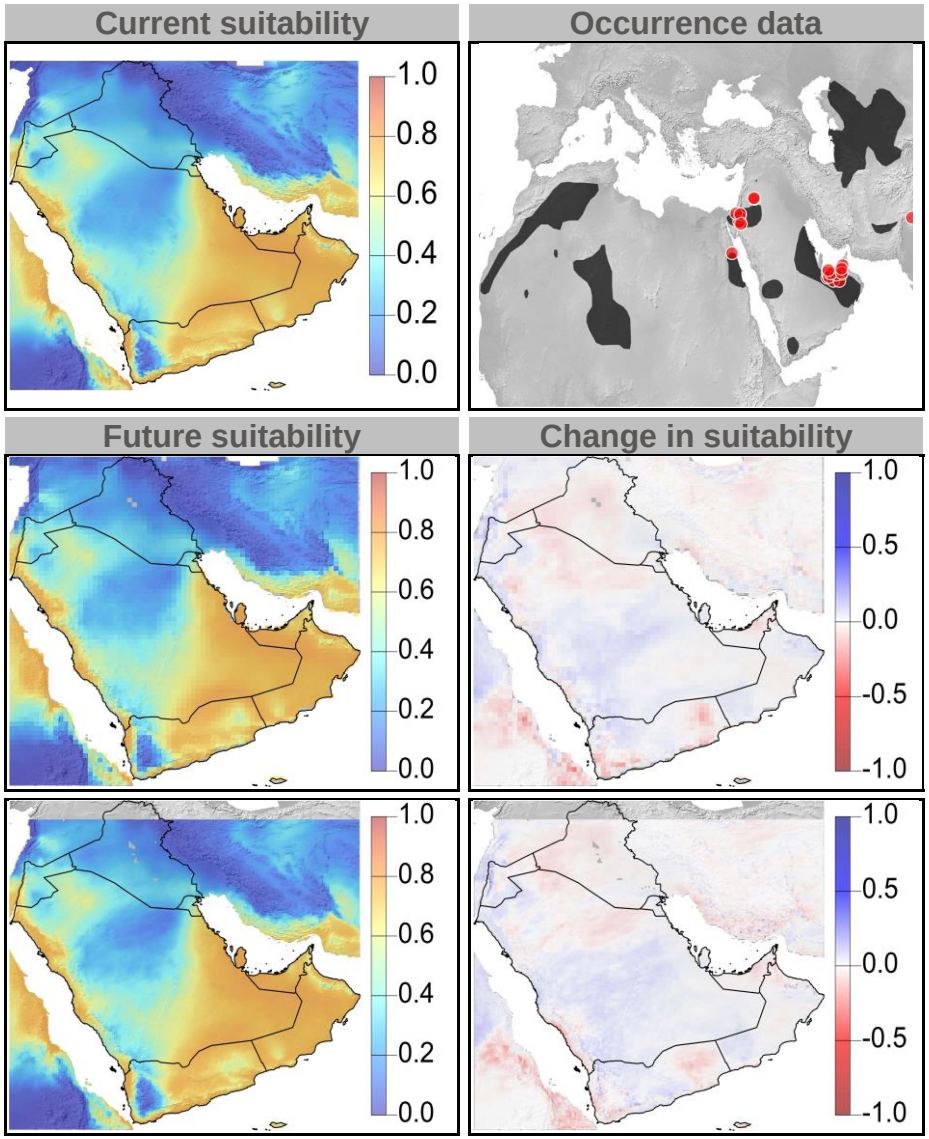

Figure 15: Current and future climate suitability for *Gazella gazella*, with associated uncertainty and change in range area based on an ensemble of all future climate scenarios. Range and occurrence data shown for reference.

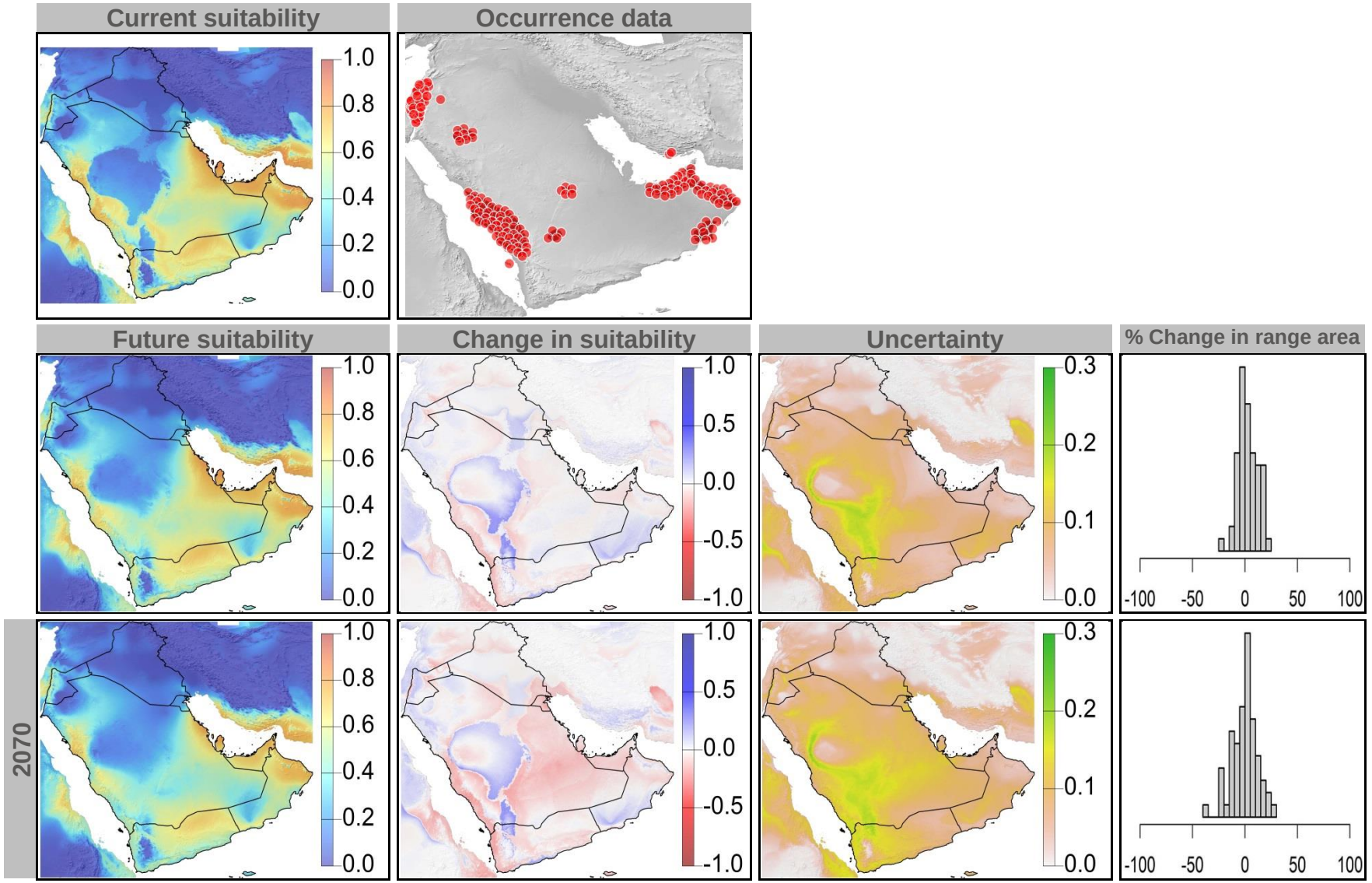

Figure 16: Current and future (2070) climate suitability for *Gazella gazella*, based on an ensemble of all future climate scenarios from the regional climate modeling effort at two spatial domains. Range and occurrence data shown for reference.

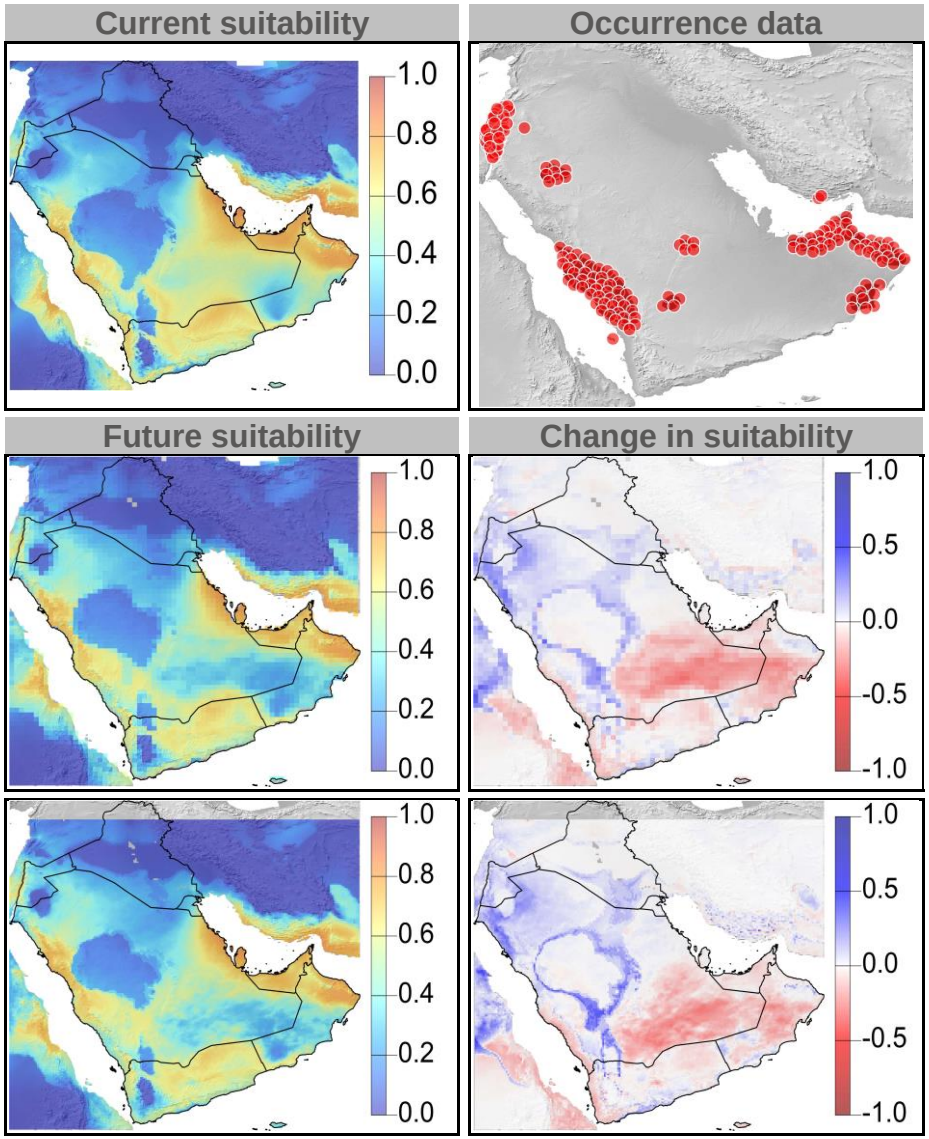

Figure 17: Current and future climate suitability for *Gazella subgutturosa*, with associated uncertainty and change in range area based on an ensemble of all future climate scenarios. Range and occurrence data shown for reference.

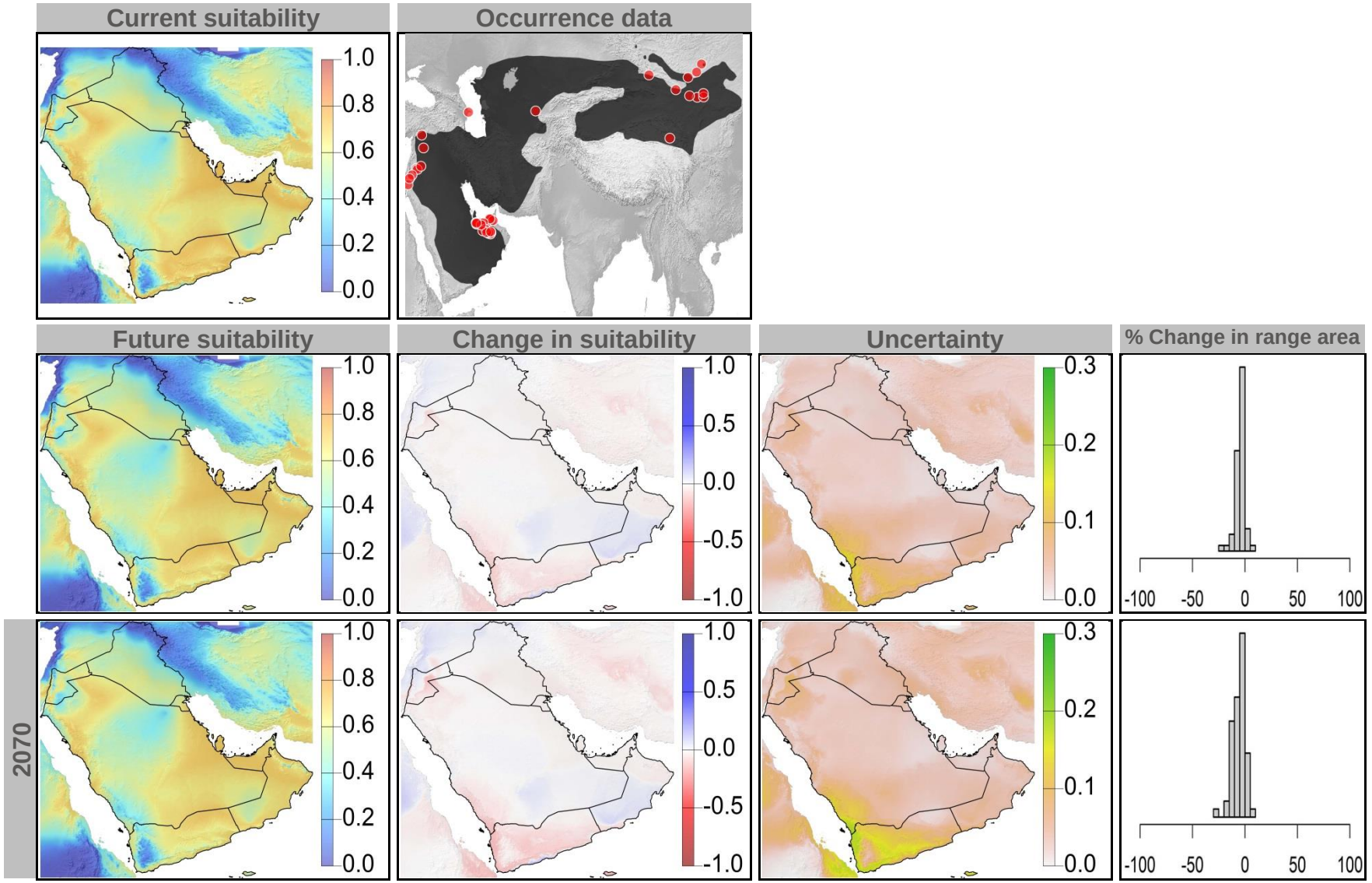

Figure 18: Current and future (2070) climate suitability for *Gazella subgutturosa*, based on an ensemble of all future climate scenarios from the regional climate modeling effort at two spatial domains. Range and occurrence data shown for reference.

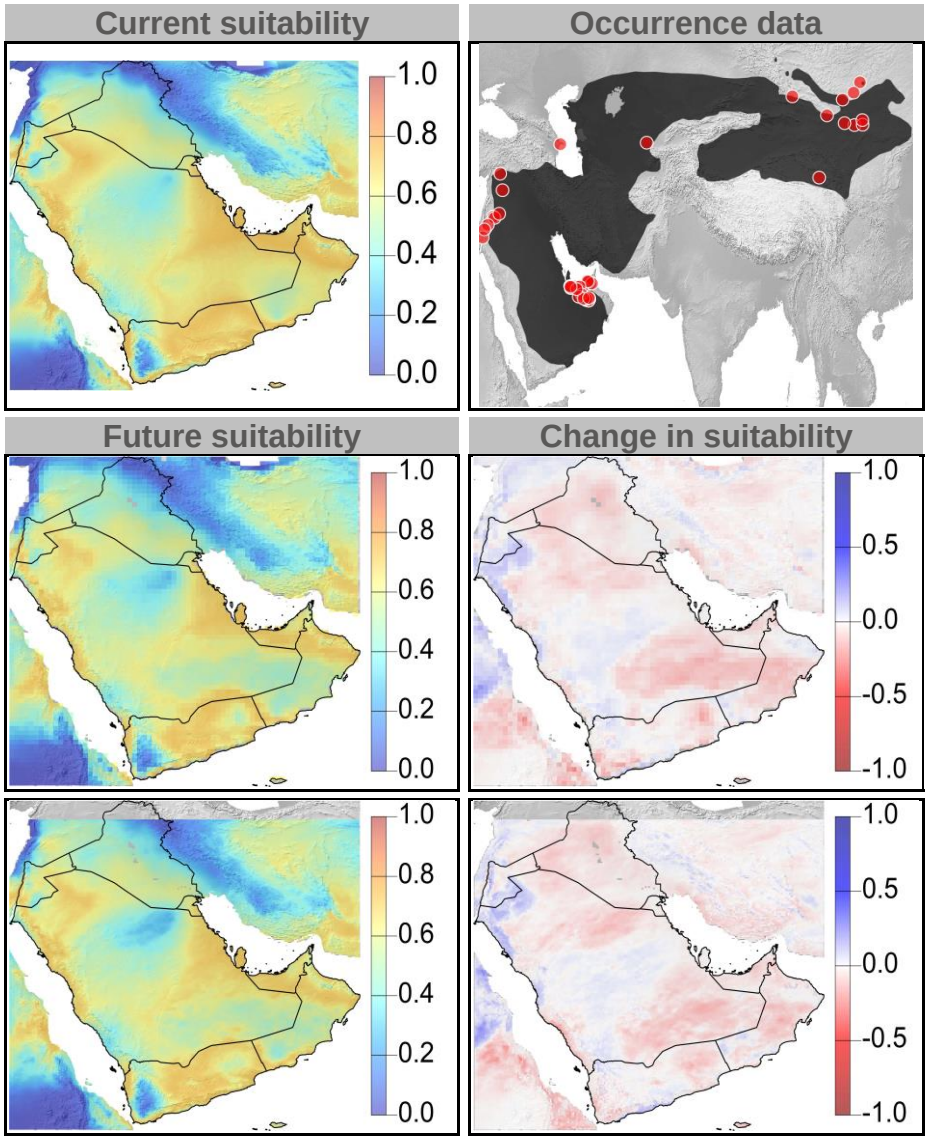

Figure 19: Current and future climate suitability for *Gerbillus cheesmani*, with associated uncertainty and change in range area based on an ensemble of all future climate scenarios. Range and occurrence data shown for reference.

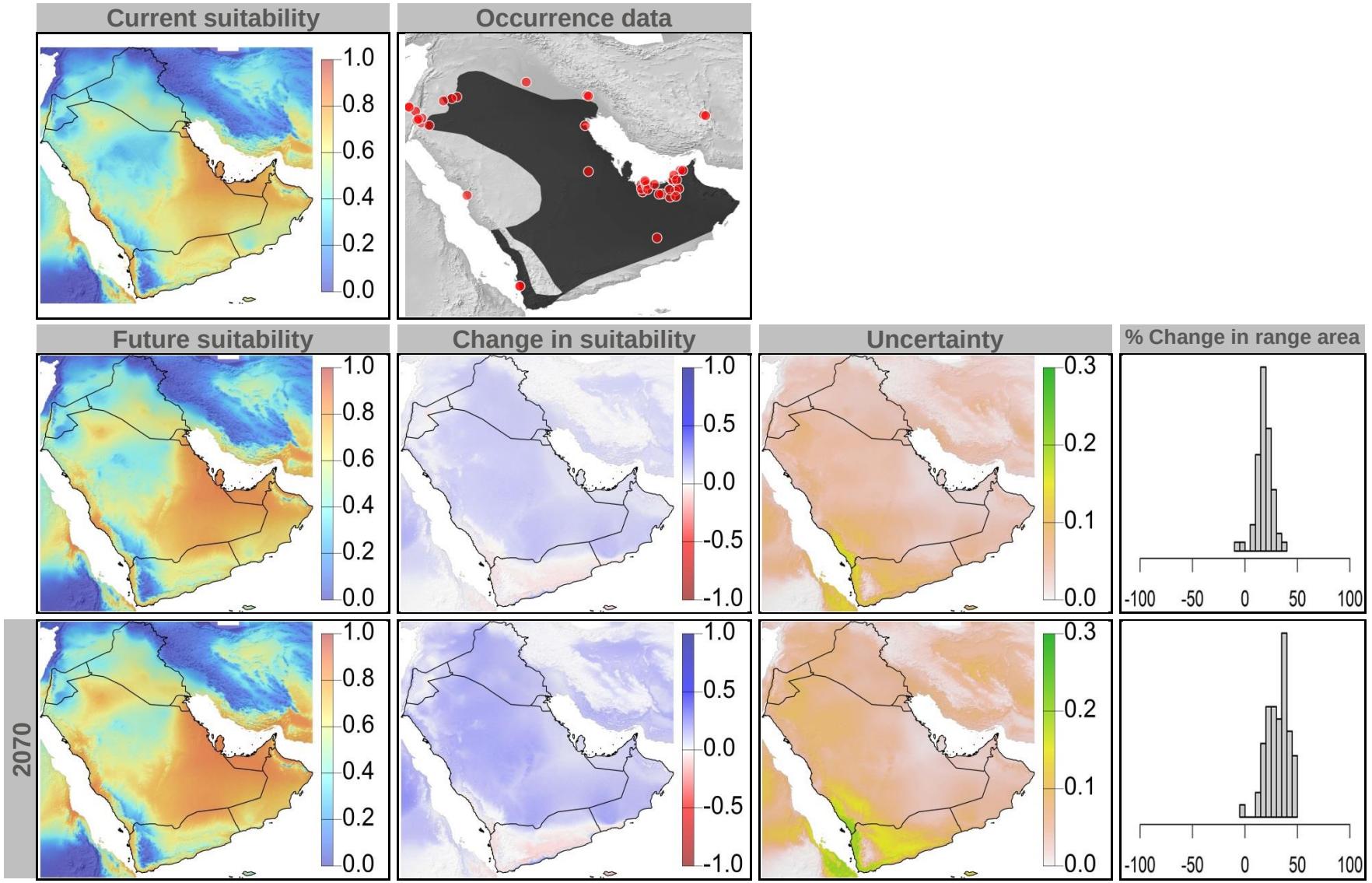

Figure 20: Current and future (2070) climate suitability for *Gerbillus cheesmani*, based on an ensemble of all future climate scenarios from the regional climate modeling effort at two spatial domains. Range and occurrence data shown for reference.

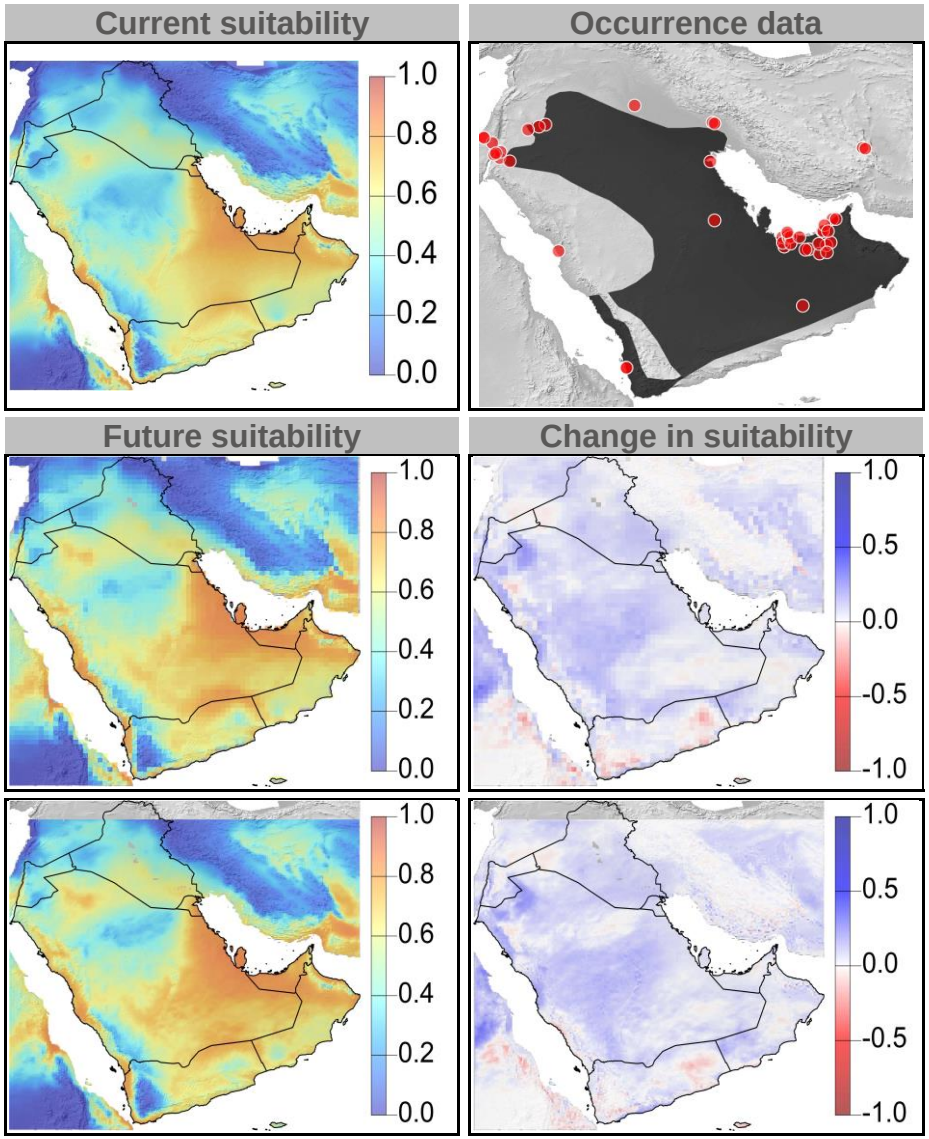

Figure 21: Current and future climate suitability for *Gerbillus nanus*, with associated uncertainty and change in range area based on an ensemble of all future climate scenarios. Range and occurrence data shown for reference.

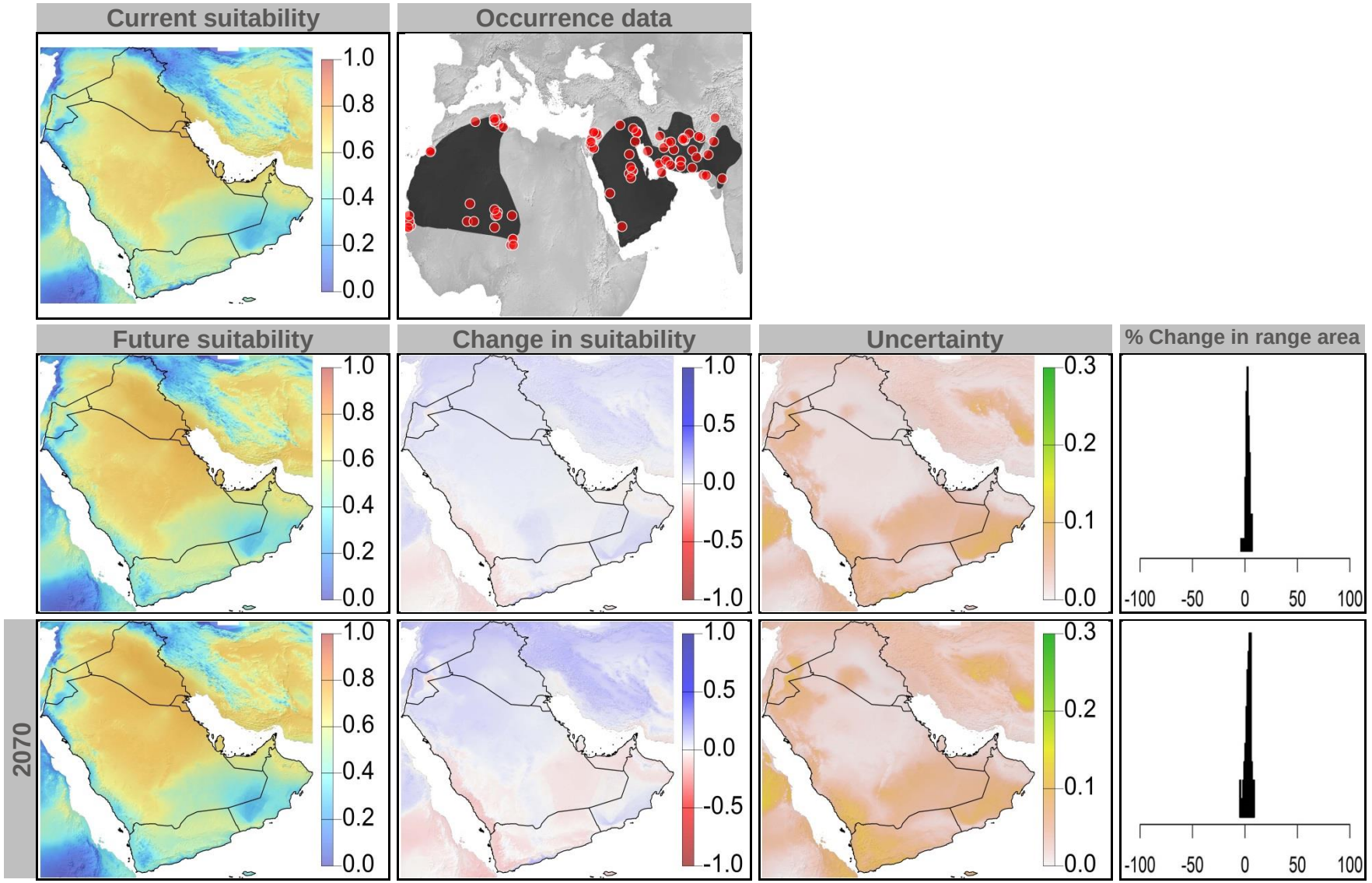

Figure 22: Current and future (2070) climate suitability for *Gerbillus nanus*, based on an ensemble of all future climate scenarios from the regional climate modeling effort at two spatial domains. Range and occurrence data shown for reference.

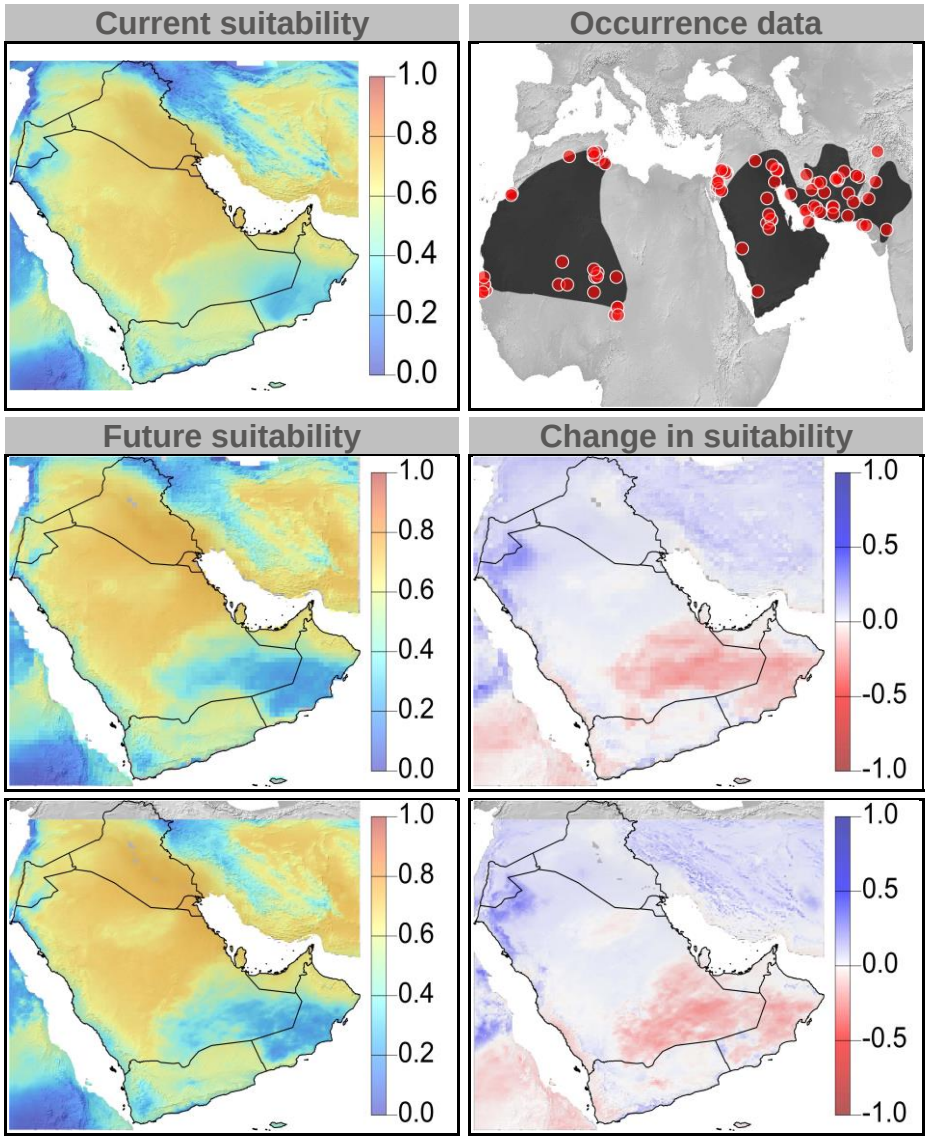

Figure 23: Current and future climate suitability for *Hipposideros caffer*, with associated uncertainty and change in range area based on an ensemble of all future climate scenarios. Range and occurrence data shown for reference.

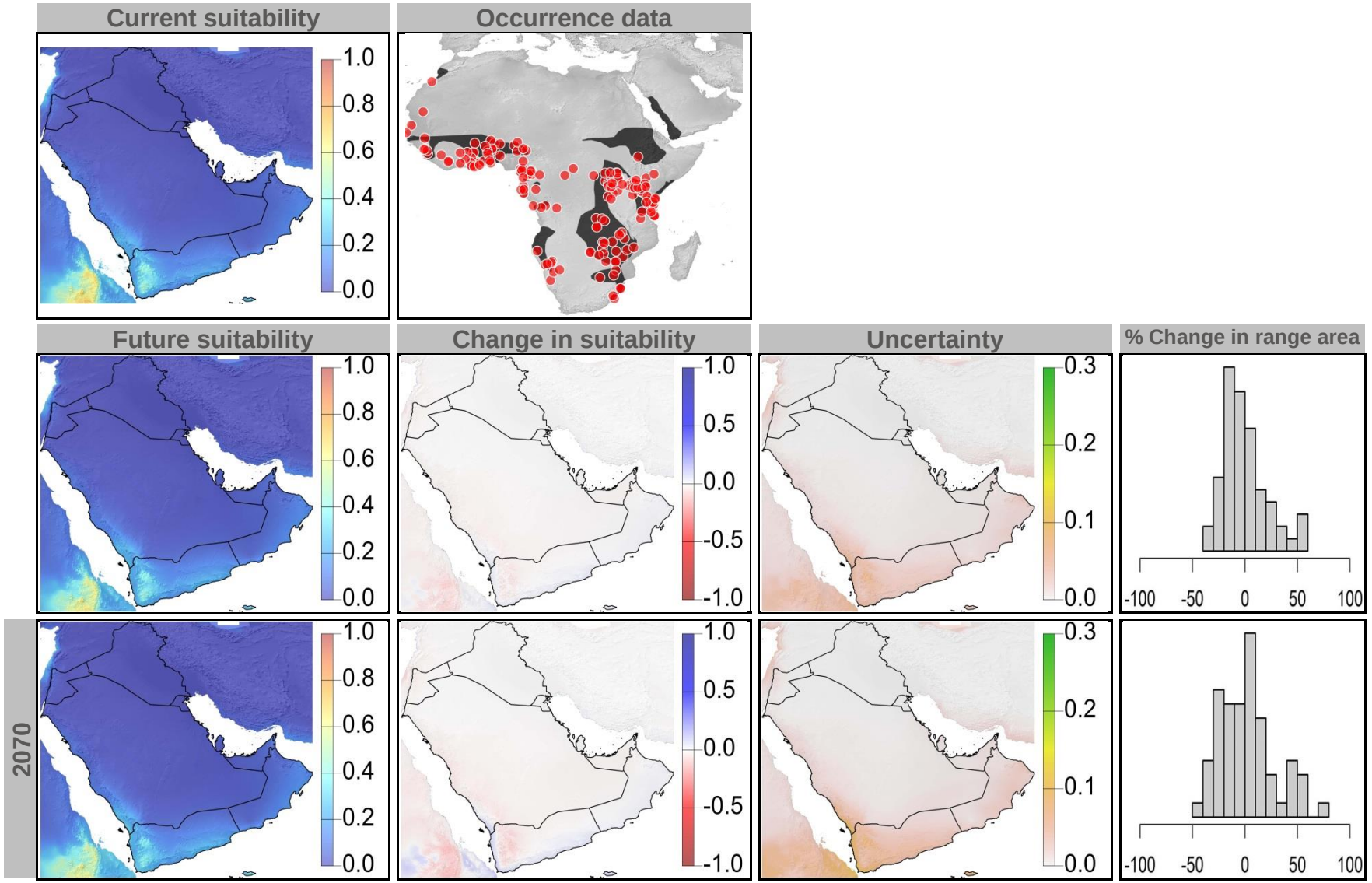

Figure 24: Current and future (2070) climate suitability for *Hipposideros caffer*, based on an ensemble of all future climate scenarios from the regional climate modeling effort at two spatial domains. Range and occurrence data shown for reference.

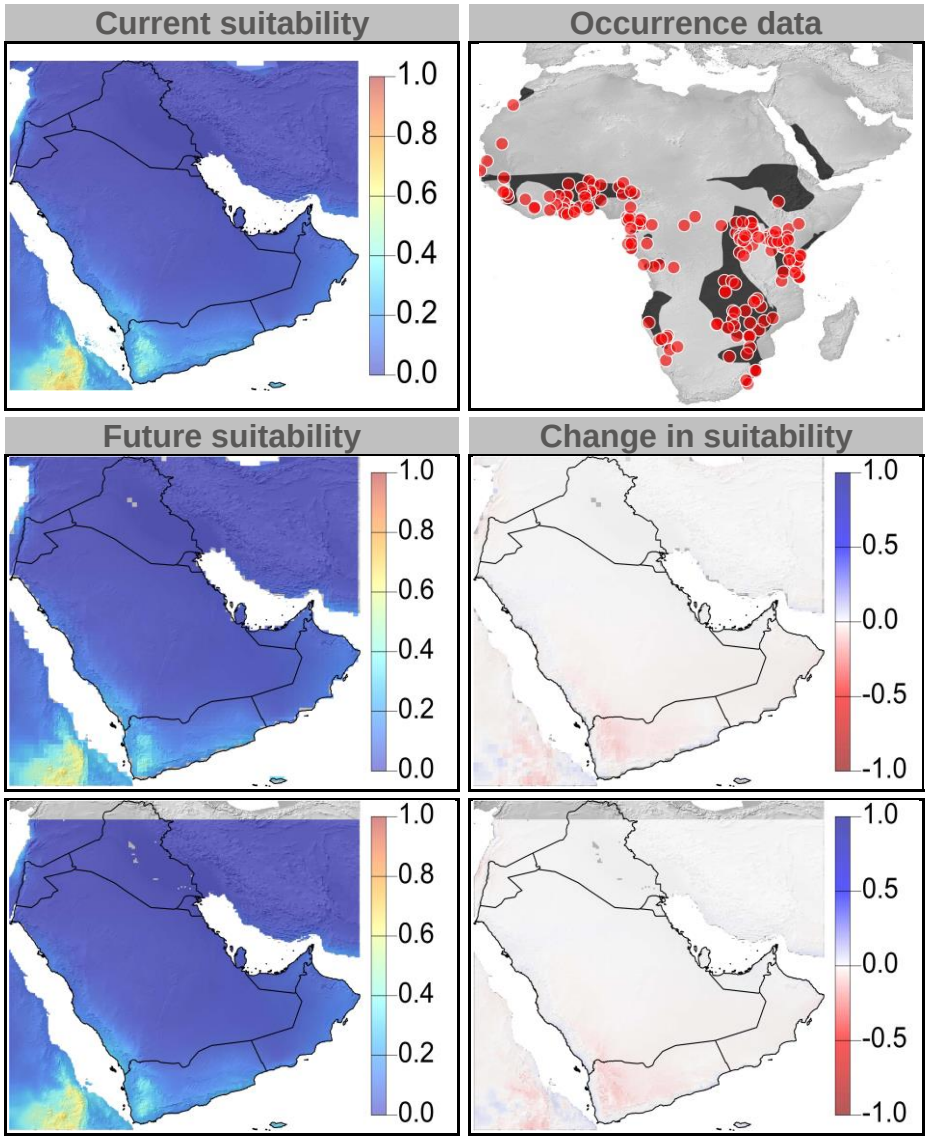

Figure 25: Current and future climate suitability for *Hyaena hyaena*, with associated uncertainty and change in range area based on an ensemble of all future climate scenarios. Range and occurrence data shown for reference.

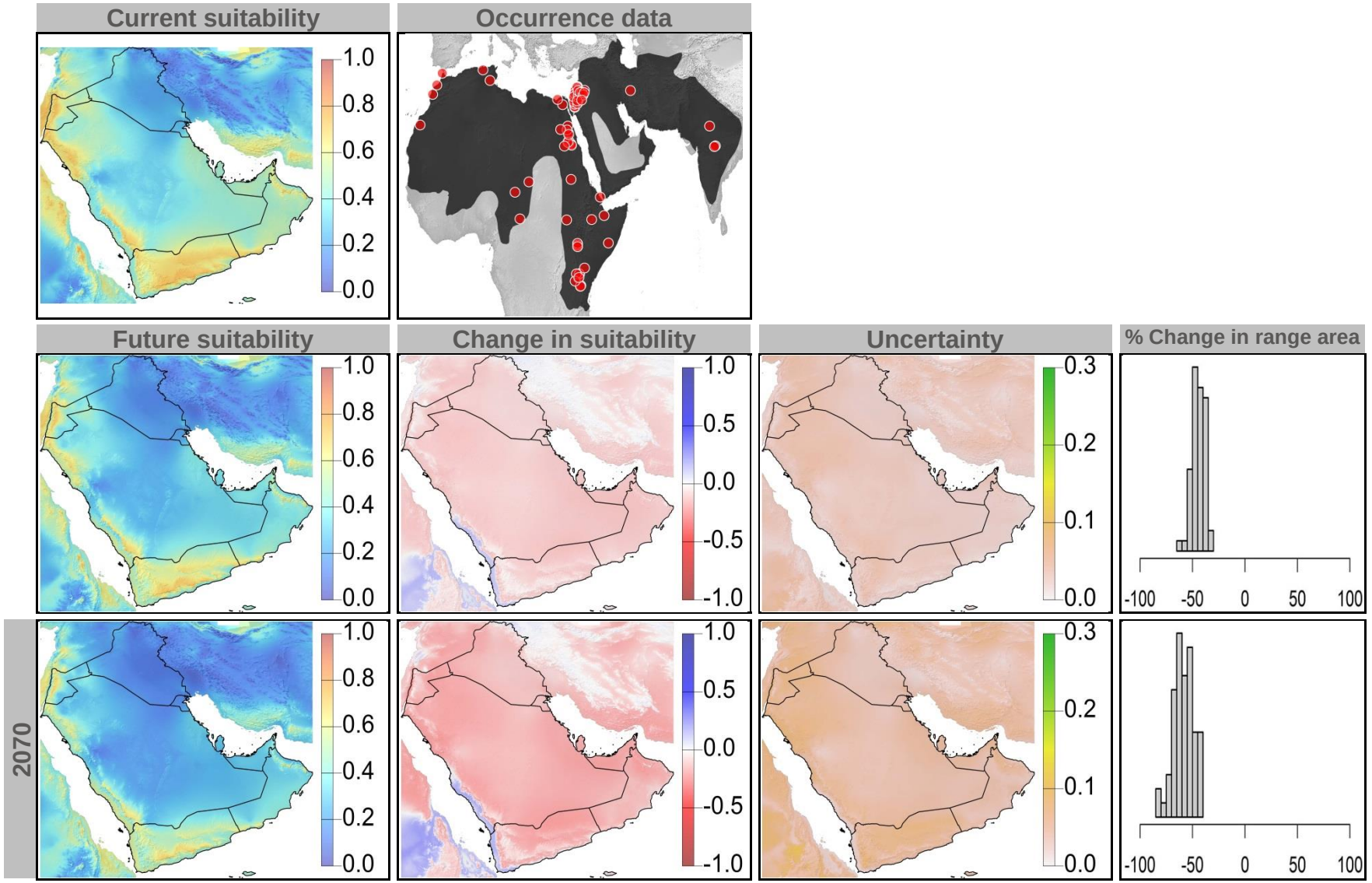

Figure 26: Current and future (2070) climate suitability for *Hyaena hyaena*, based on an ensemble of all future climate scenarios from the regional climate modeling effort at two spatial domains. Range and occurrence data shown for reference.

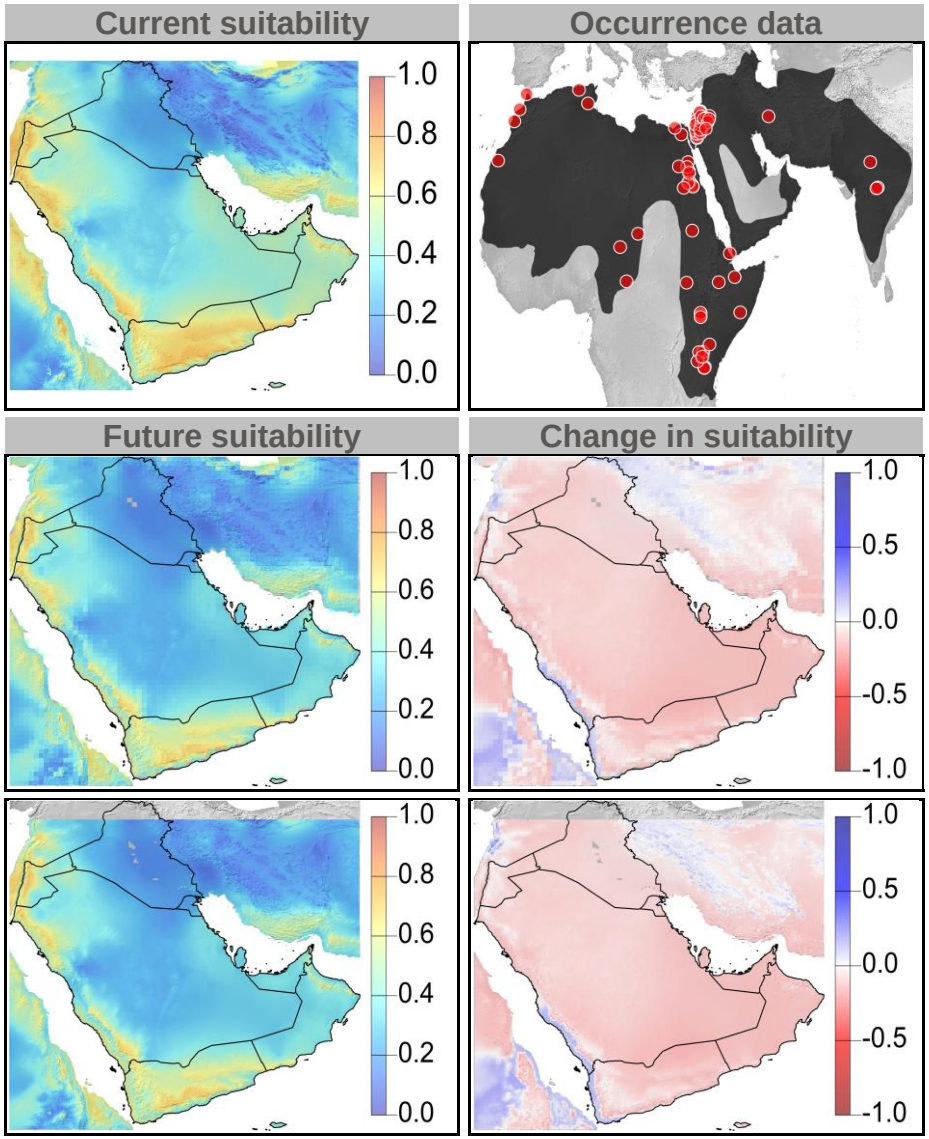

Figure 27: Current and future climate suitability for *Hystrix indica*, with associated uncertainty and change in range area based on an ensemble of all future climate scenarios. Range and occurrence data shown for reference.

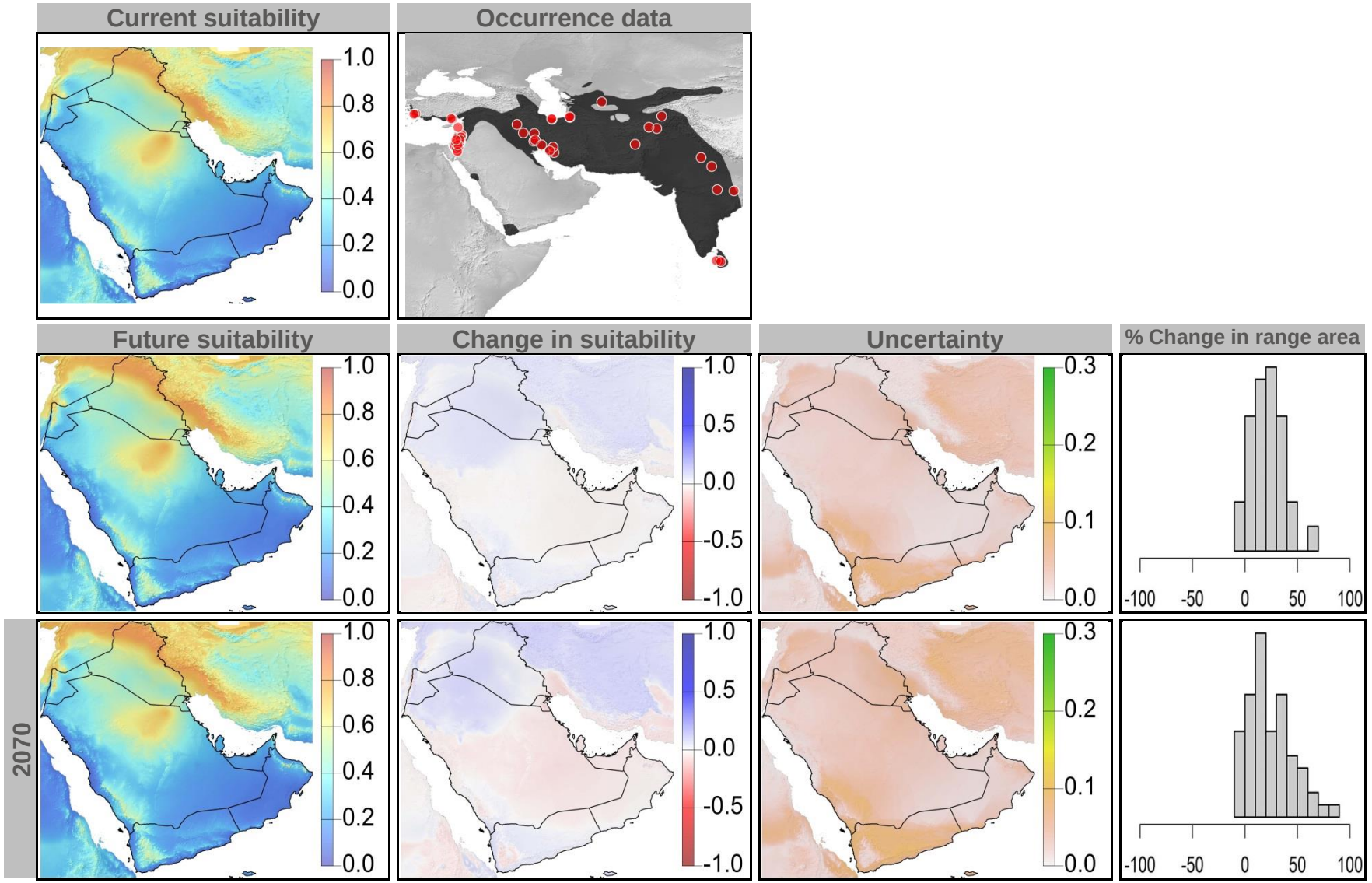

Figure 28: Current and future (2070) climate suitability for *Hystrix indica*, based on an ensemble of all future climate scenarios from the regional climate modeling effort at two spatial domains. Range and occurrence data shown for reference.

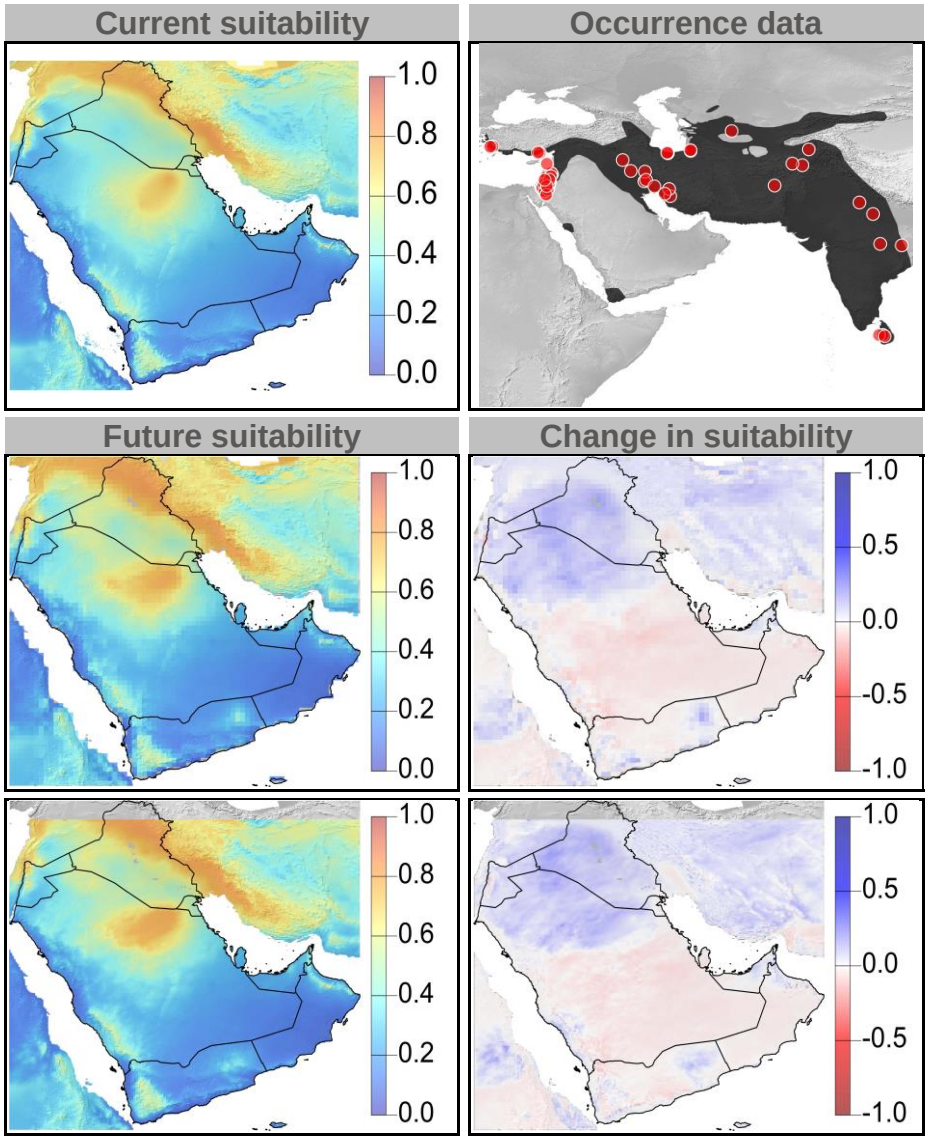

Figure 29: Current and future climate suitability for *Jaculus jaculus*, with associated uncertainty and change in range area based on an ensemble of all future climate scenarios. Range and occurrence data shown for reference.

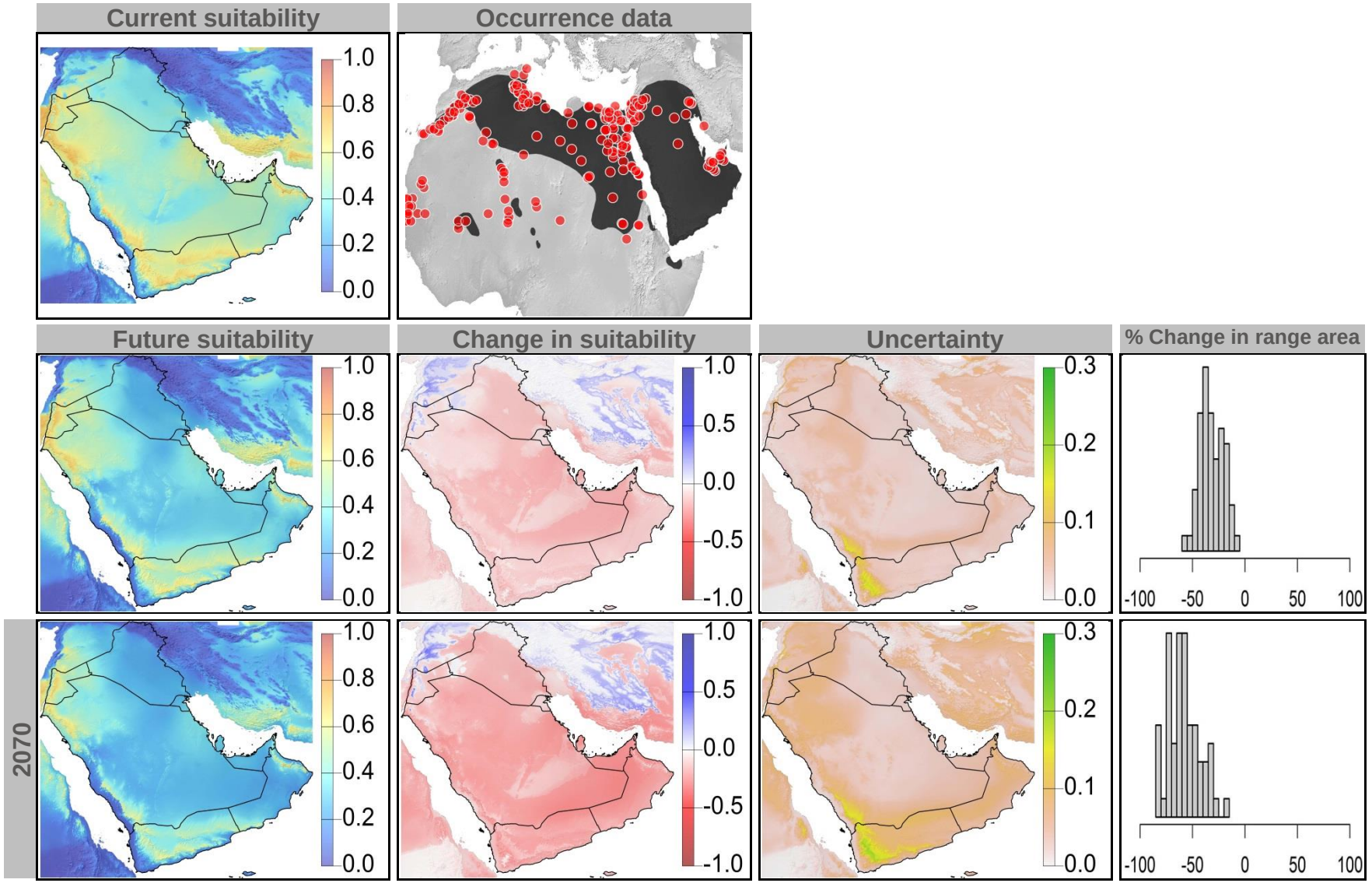

Figure 30: Current and future (2070) climate suitability for *Jaculus jaculus*, based on an ensemble of all future climate scenarios from the regional climate modeling effort at two spatial domains. Range and occurrence data shown for reference.

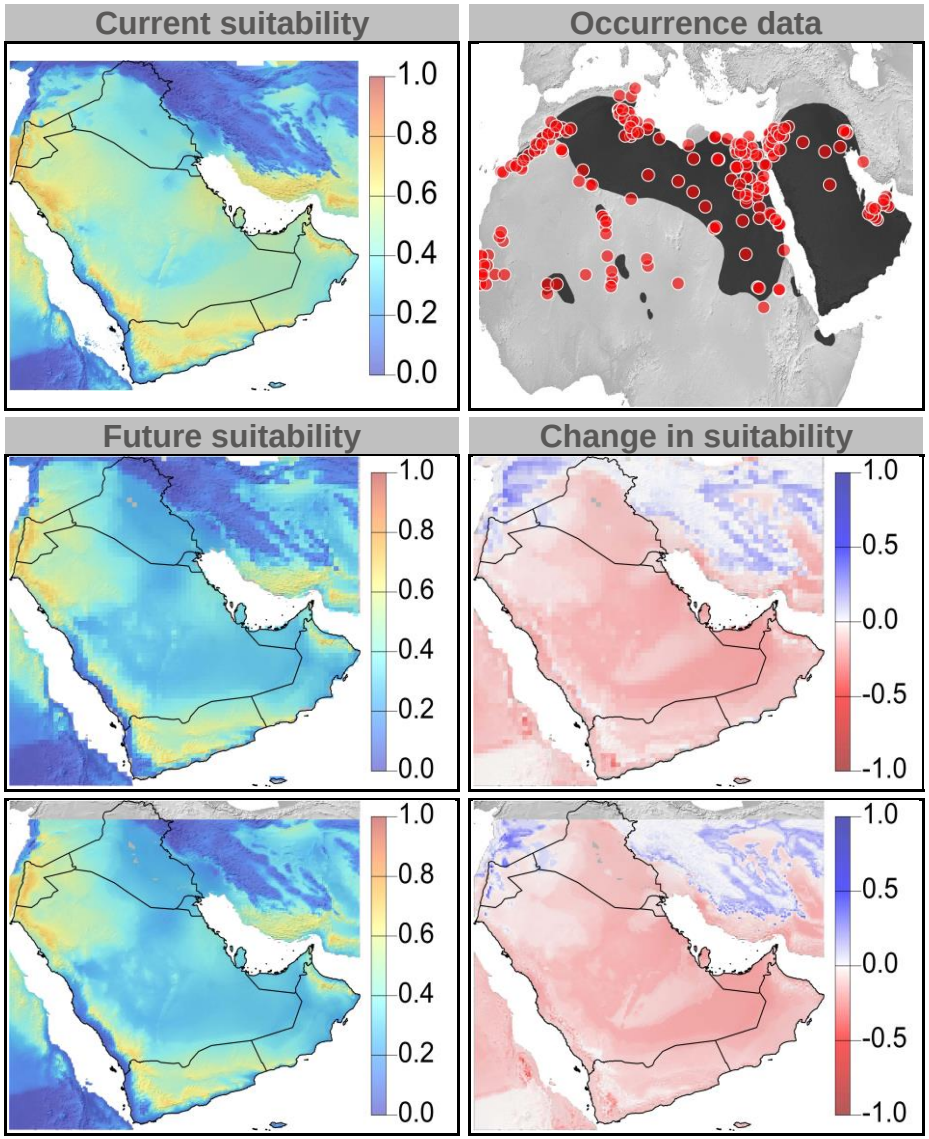

Figure 31: Current and future climate suitability for *Lepus capensis*, with associated uncertainty and change in range area based on an ensemble of all future climate scenarios. Range and occurrence data shown for reference.

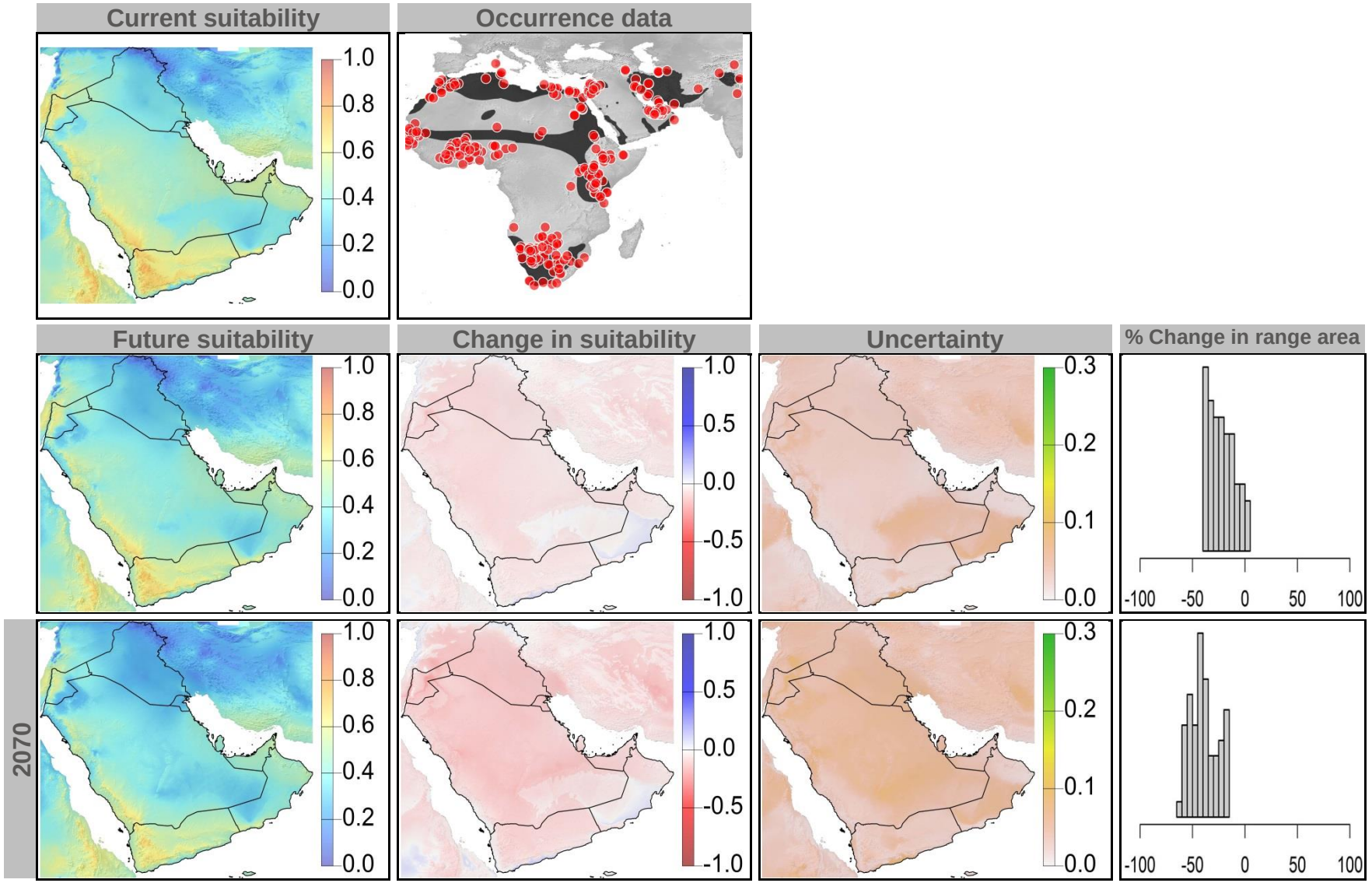

Figure 32: Current and future (2070) climate suitability for *Lepus capensis*, based on an ensemble of all future climate scenarios from the regional climate modeling effort at two spatial domains. Range and occurrence data shown for reference.

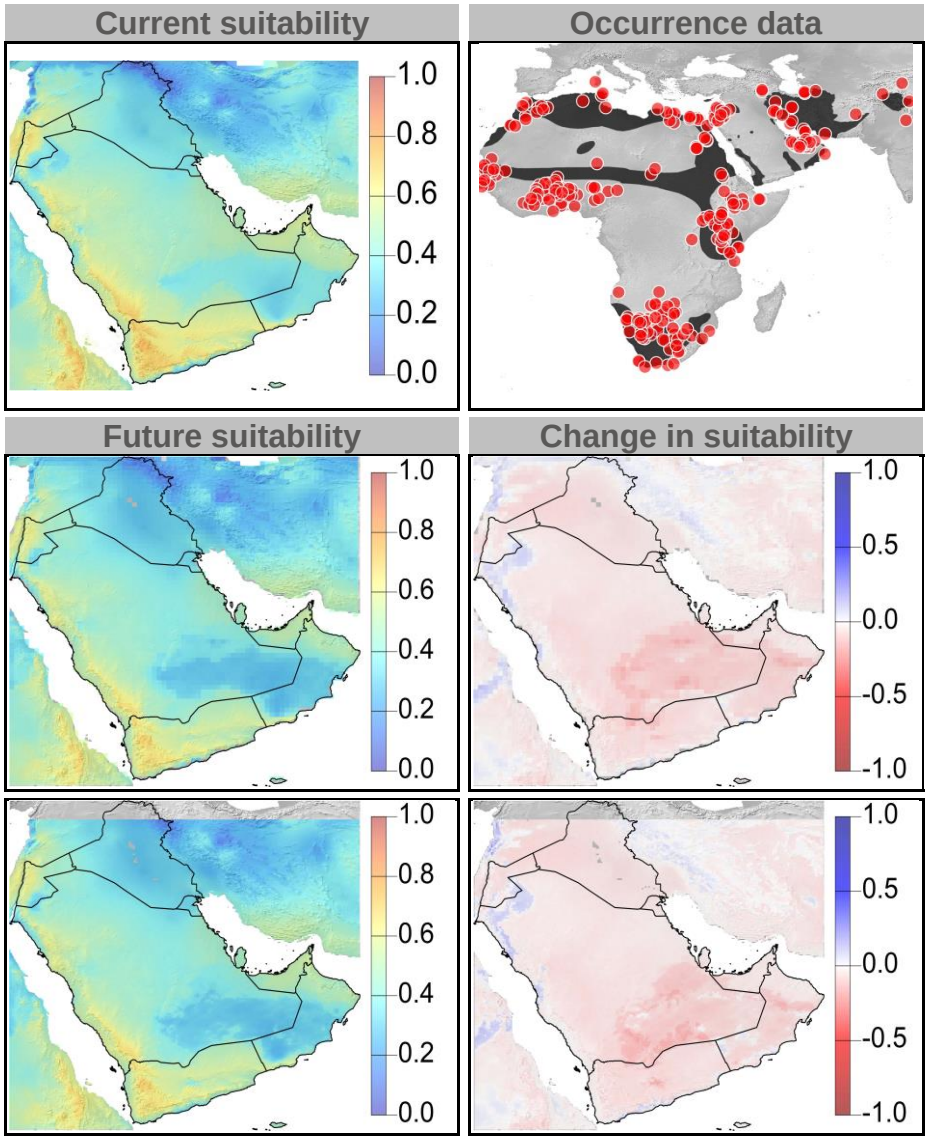

Figure 33: Current and future climate suitability for *Meriones crassus*, with associated uncertainty and change in range area based on an ensemble of all future climate scenarios. Range and occurrence data shown for reference.

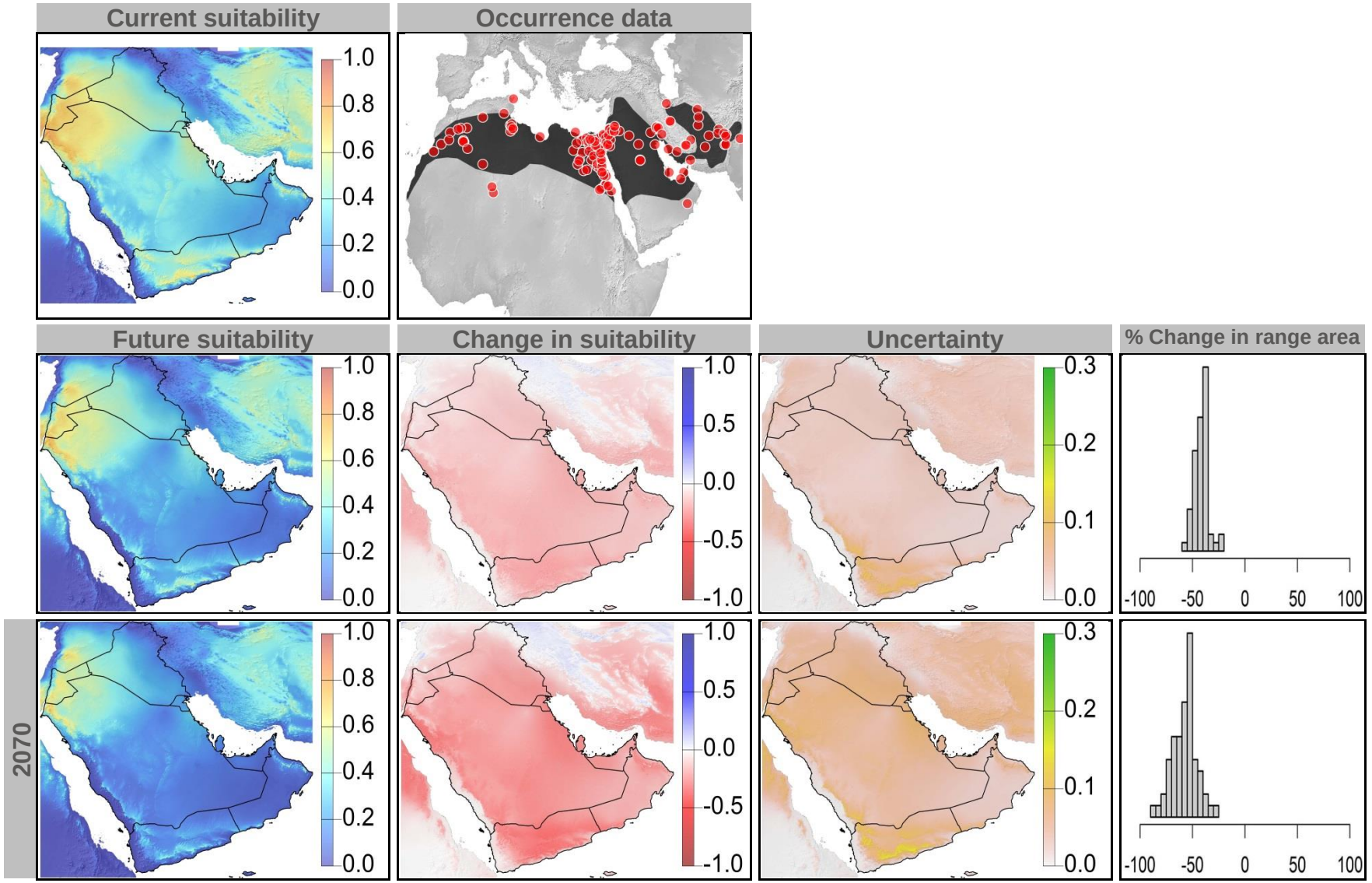

Figure 34: Current and future (2070) climate suitability for *Meriones crassus*, based on an ensemble of all future climate scenarios from the regional climate modeling effort at two spatial domains. Range and occurrence data shown for reference.

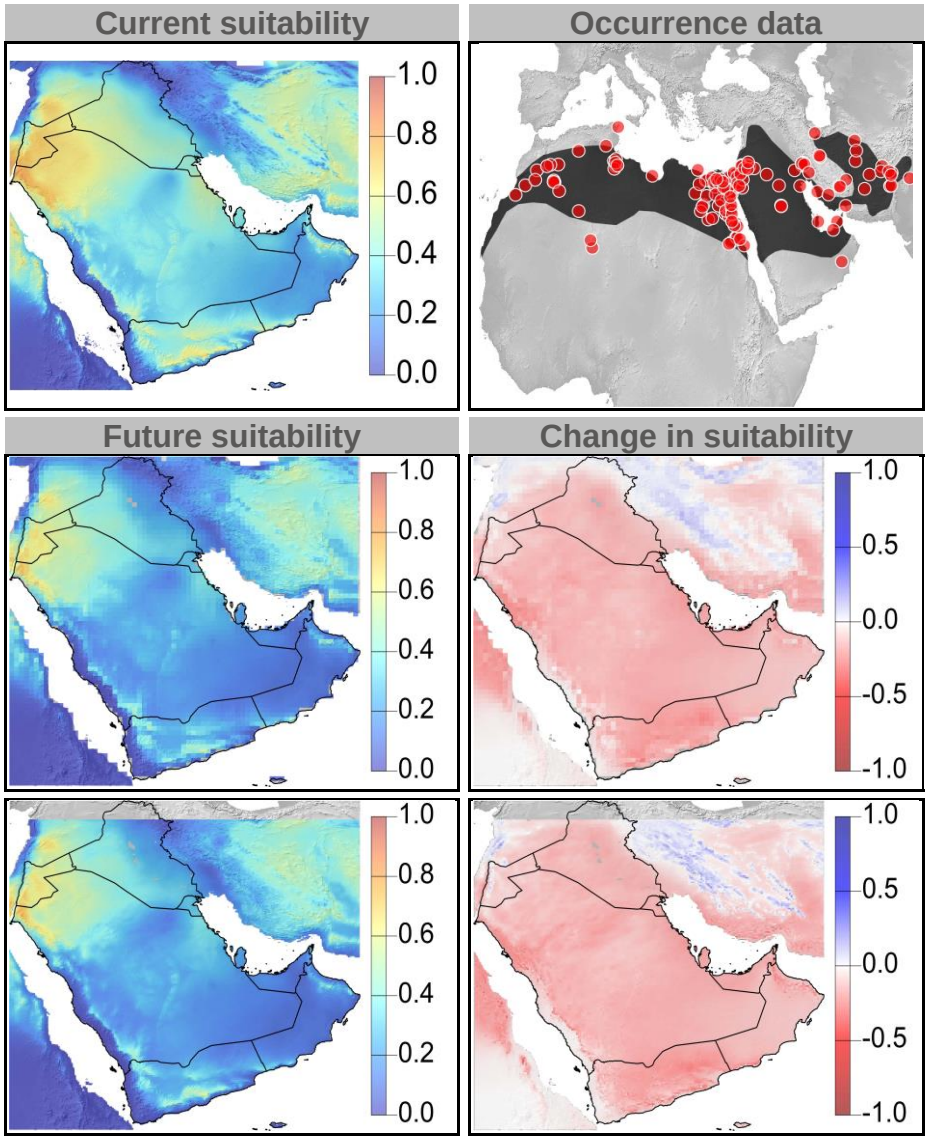

Figure 35: Current and future climate suitability for *Meriones libycus*, with associated uncertainty and change in range area based on an ensemble of all future climate scenarios. Range and occurrence data shown for reference.

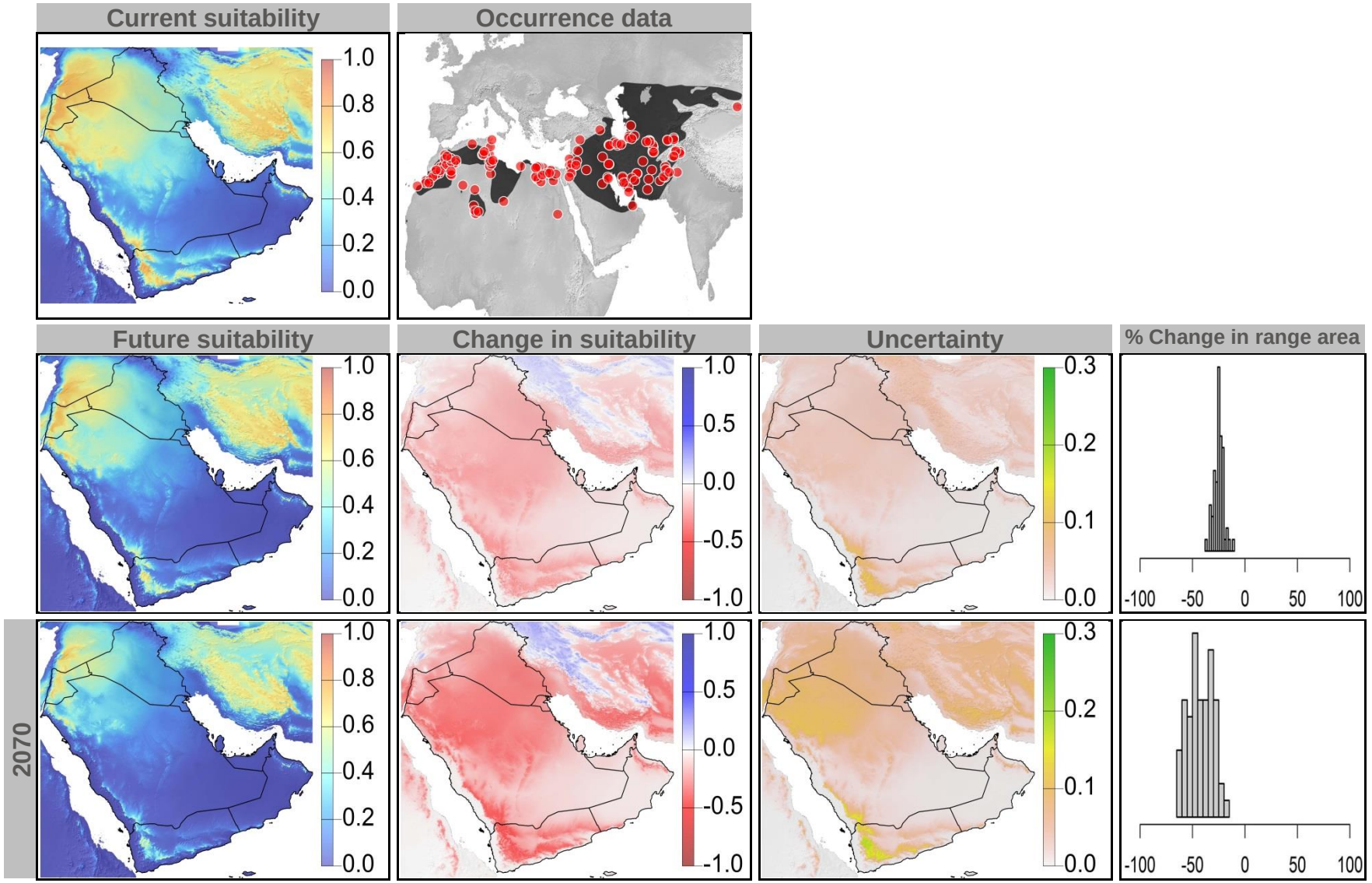

Figure 36: Current and future (2070) climate suitability for *Meriones libycus*, based on an ensemble of all future climate scenarios from the regional climate modeling effort at two spatial domains. Range and occurrence data shown for reference.

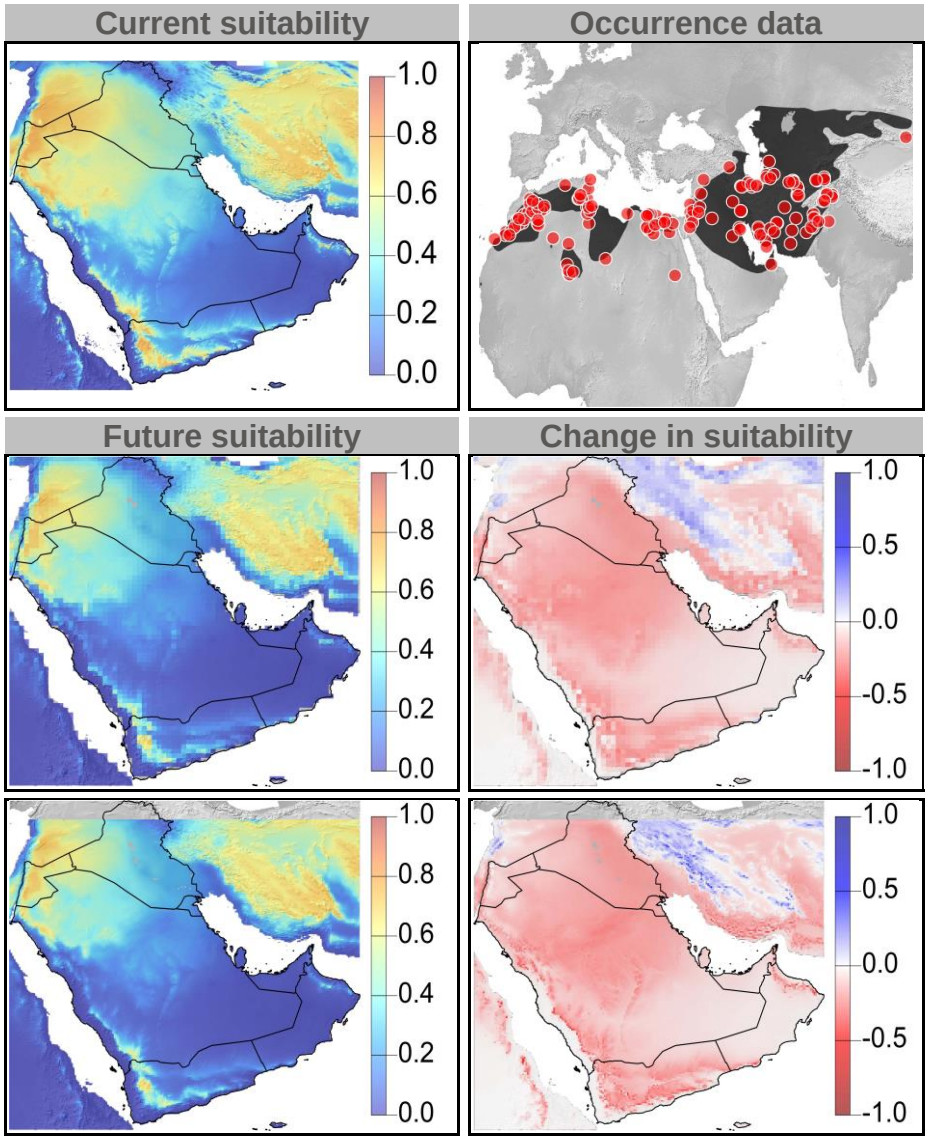

Figure 37: Current and future climate suitability for *Panthera pardus*, with associated uncertainty and change in range area based on an ensemble of all future climate scenarios. Range and occurrence data shown for reference.

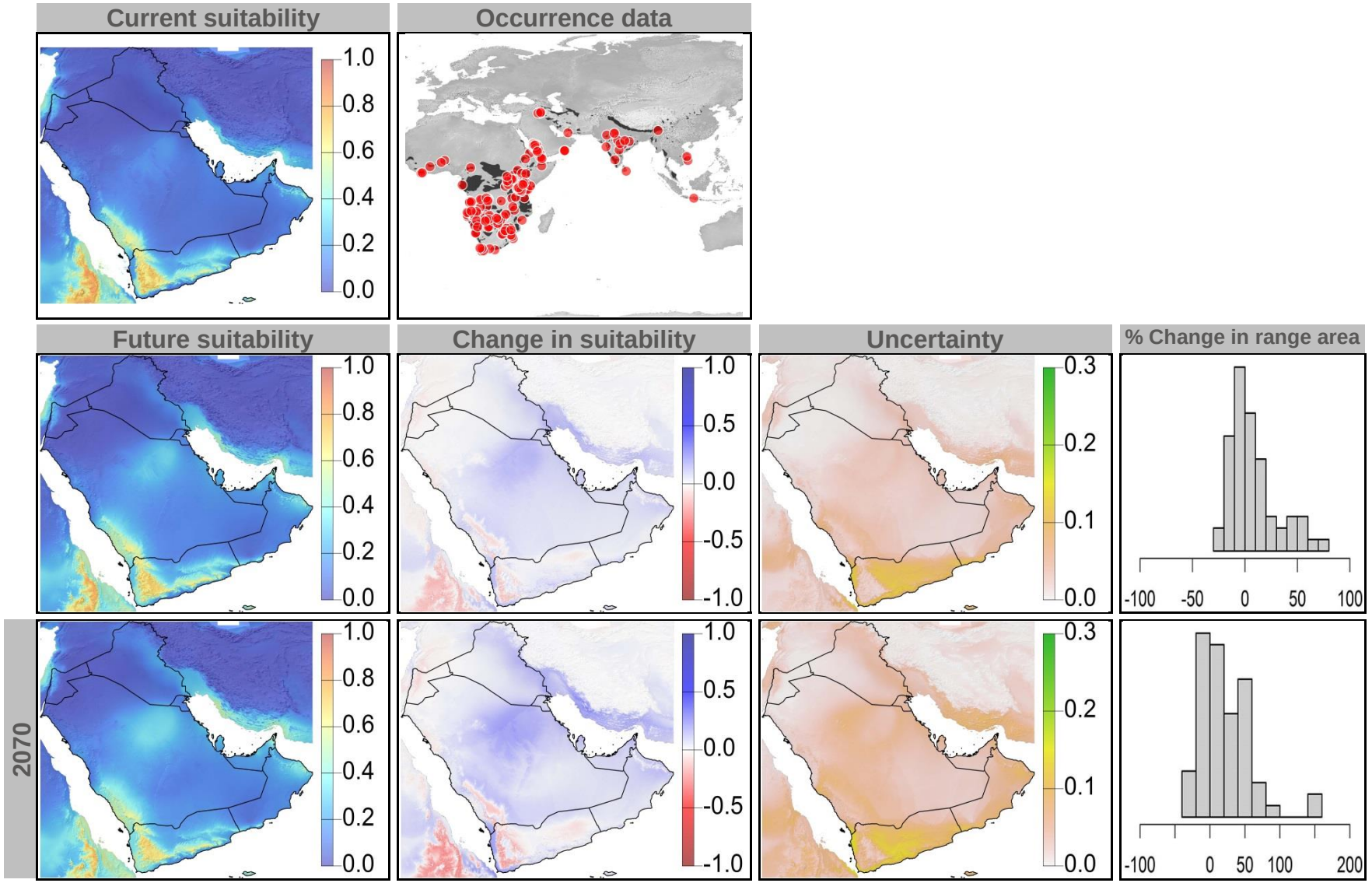

Figure 38: Current and future (2070) climate suitability for *Panthera pardus*, based on an ensemble of all future climate scenarios from the regional climate modeling effort at two spatial domains. Range and occurrence data shown for reference.

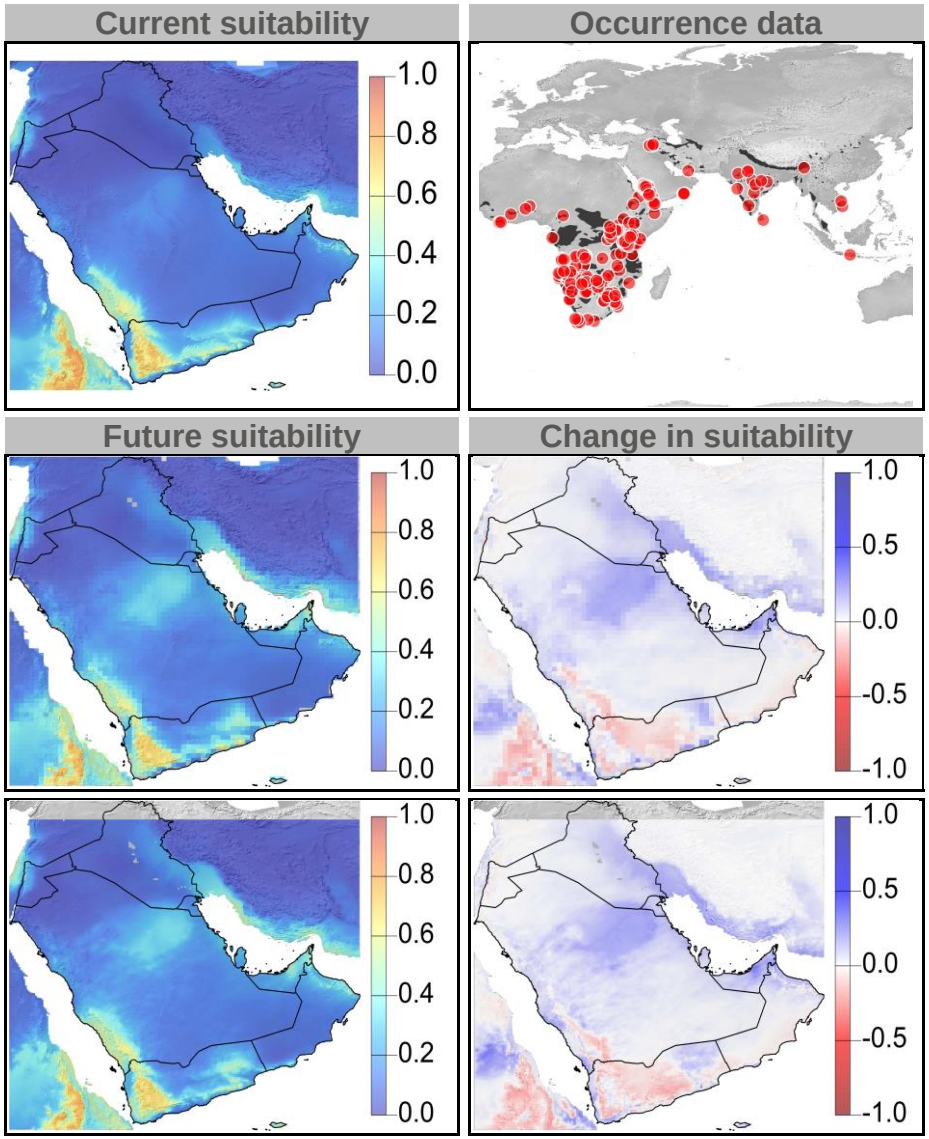

Figure 39: Current and future climate suitability for *Procavia capensis*, with associated uncertainty and change in range area based on an ensemble of all future climate scenarios. Range and occurrence data shown for reference.

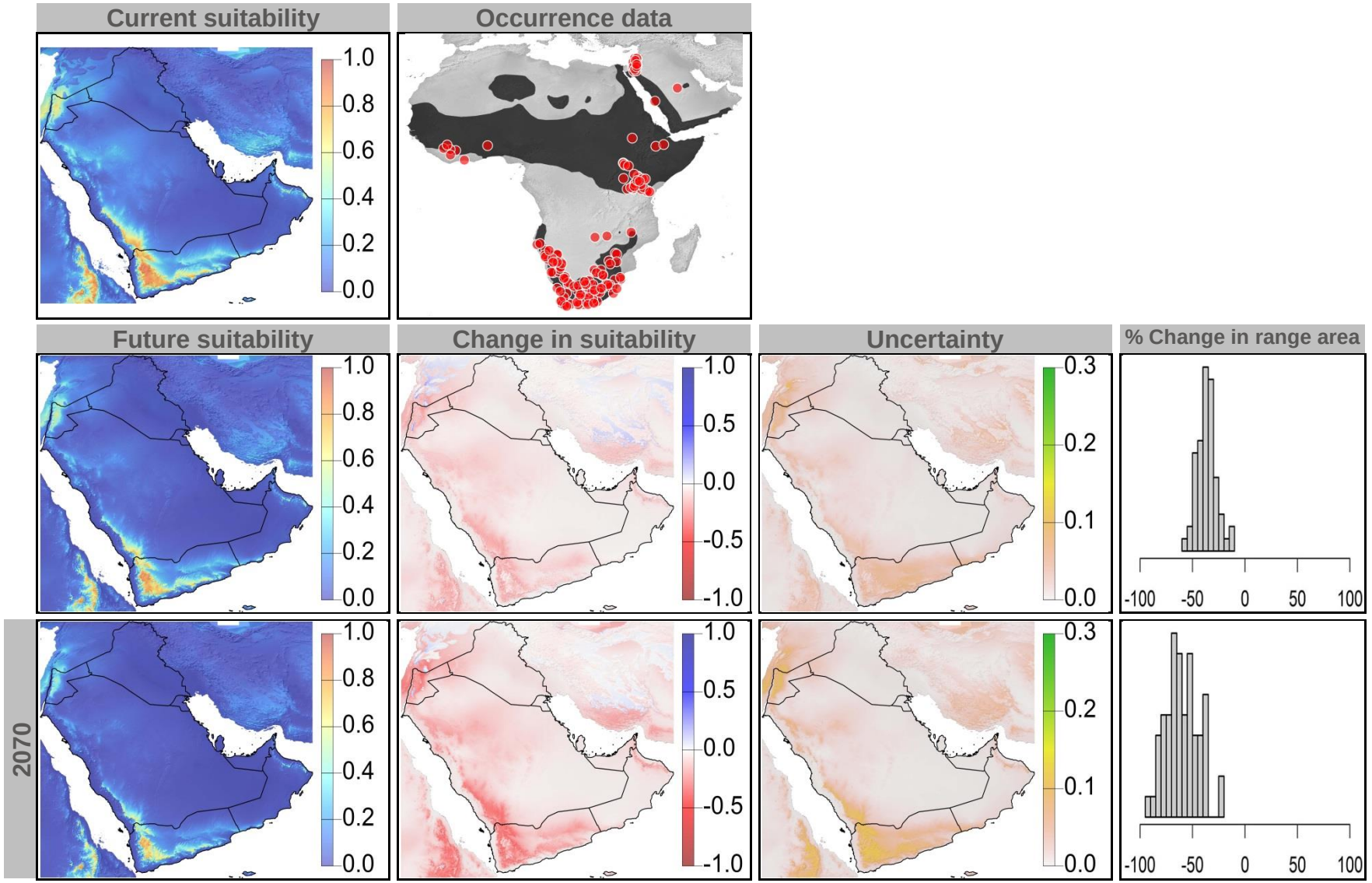

Figure 40: Current and future (2070) climate suitability for *Procavia capensis*, based on an ensemble of all future climate scenarios from the regional climate modeling effort at two spatial domains. Range and occurrence data shown for reference.

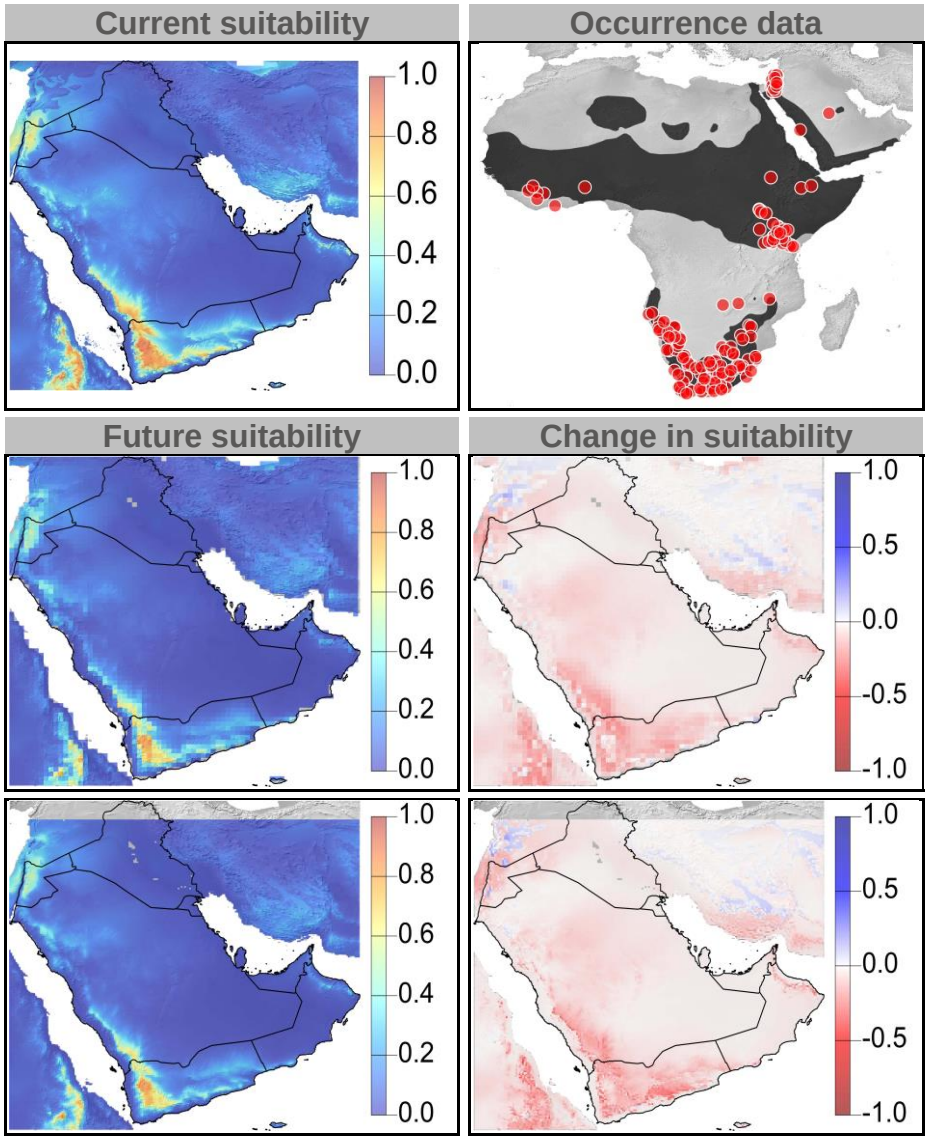

Figure 41: Current and future climate suitability for *Psammomys obesus*, with associated uncertainty and change in range area based on an ensemble of all future climate scenarios. Range and occurrence data shown for reference.

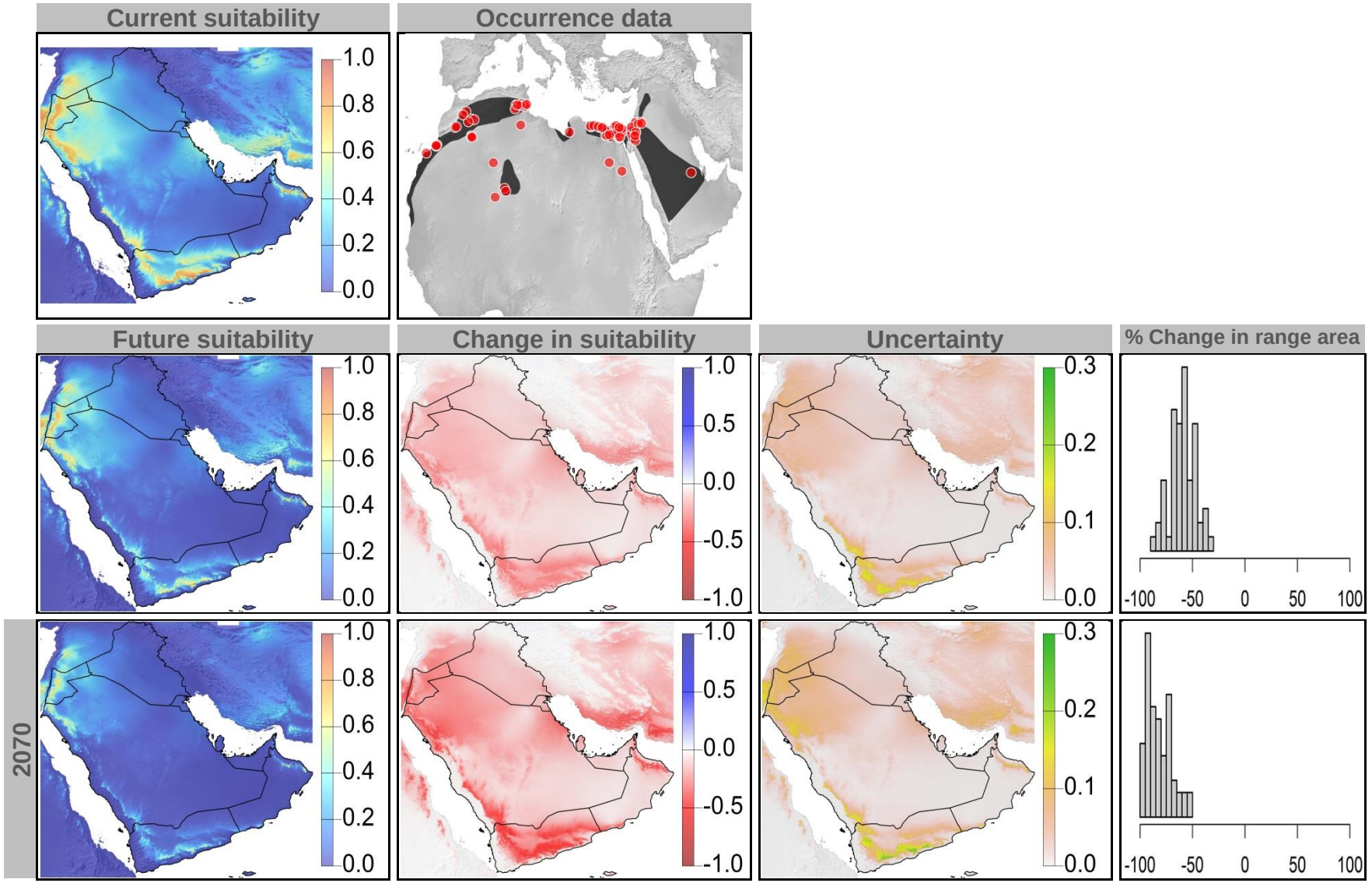

Figure 42: Current and future (2070) climate suitability for *Psammomys obesus*, based on an ensemble of all future climate scenarios from the regional climate modeling effort at two spatial domains. Range and occurrence data shown for reference.

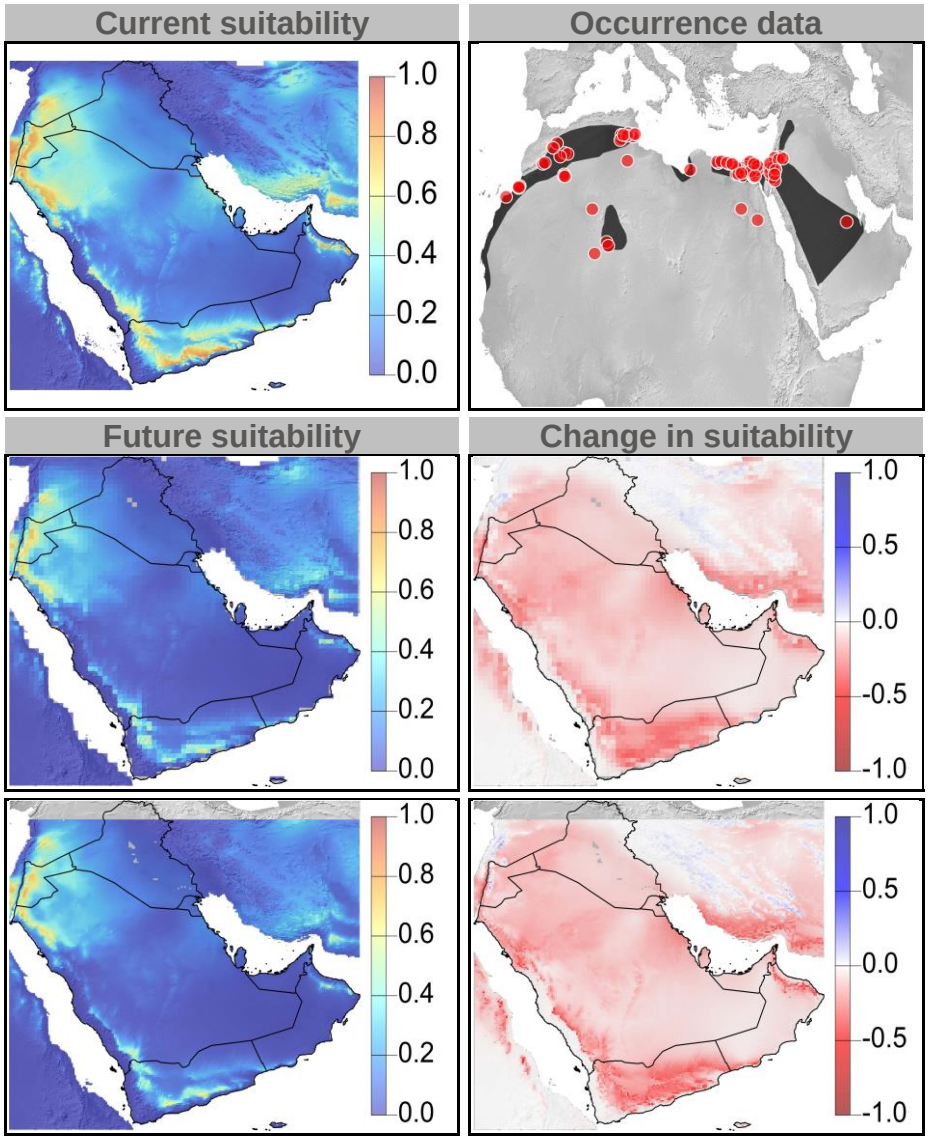

Figure 43: Current and future climate suitability for *Rhinolophus blasii*, with associated uncertainty and change in range area based on an ensemble of all future climate scenarios. Range and occurrence data shown for reference.

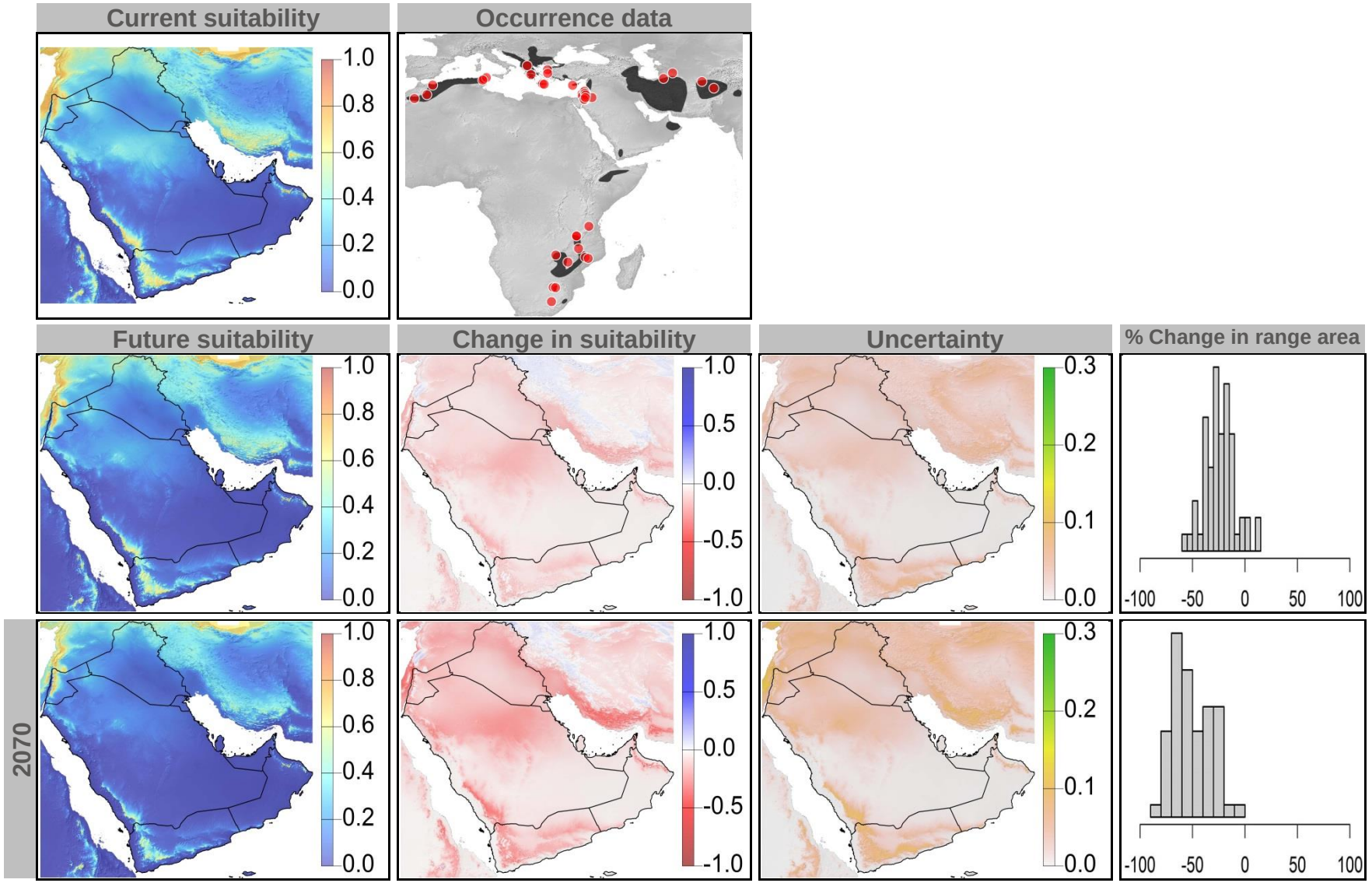

Figure 44: Current and future (2070) climate suitability for *Rhinolophus blasii*, based on an ensemble of all future climate scenarios from the regional climate modeling effort at two spatial domains. Range and occurrence data shown for reference.

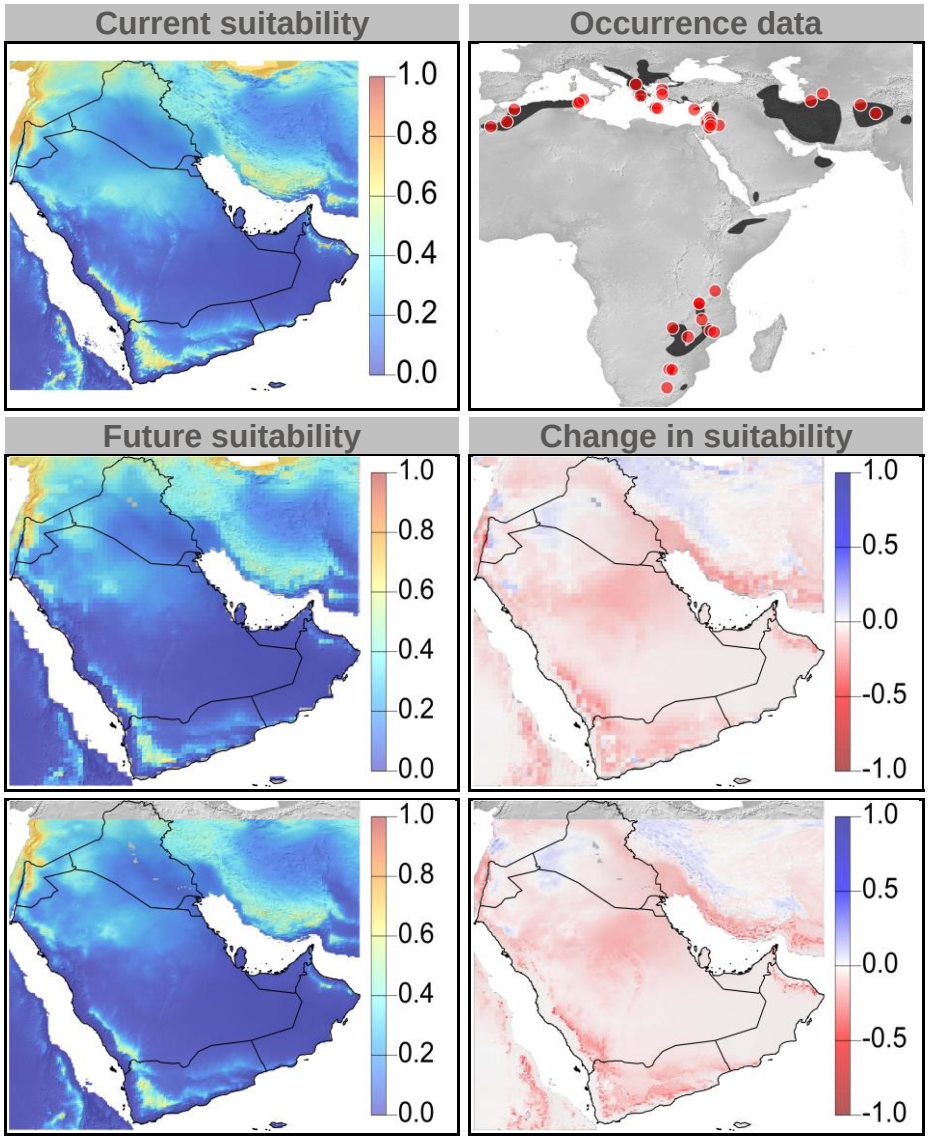

Figure 45: Current and future climate suitability for *Sekeetamys calurus*, with associated uncertainty and change in range area based on an ensemble of all future climate scenarios. Range and occurrence data shown for reference.

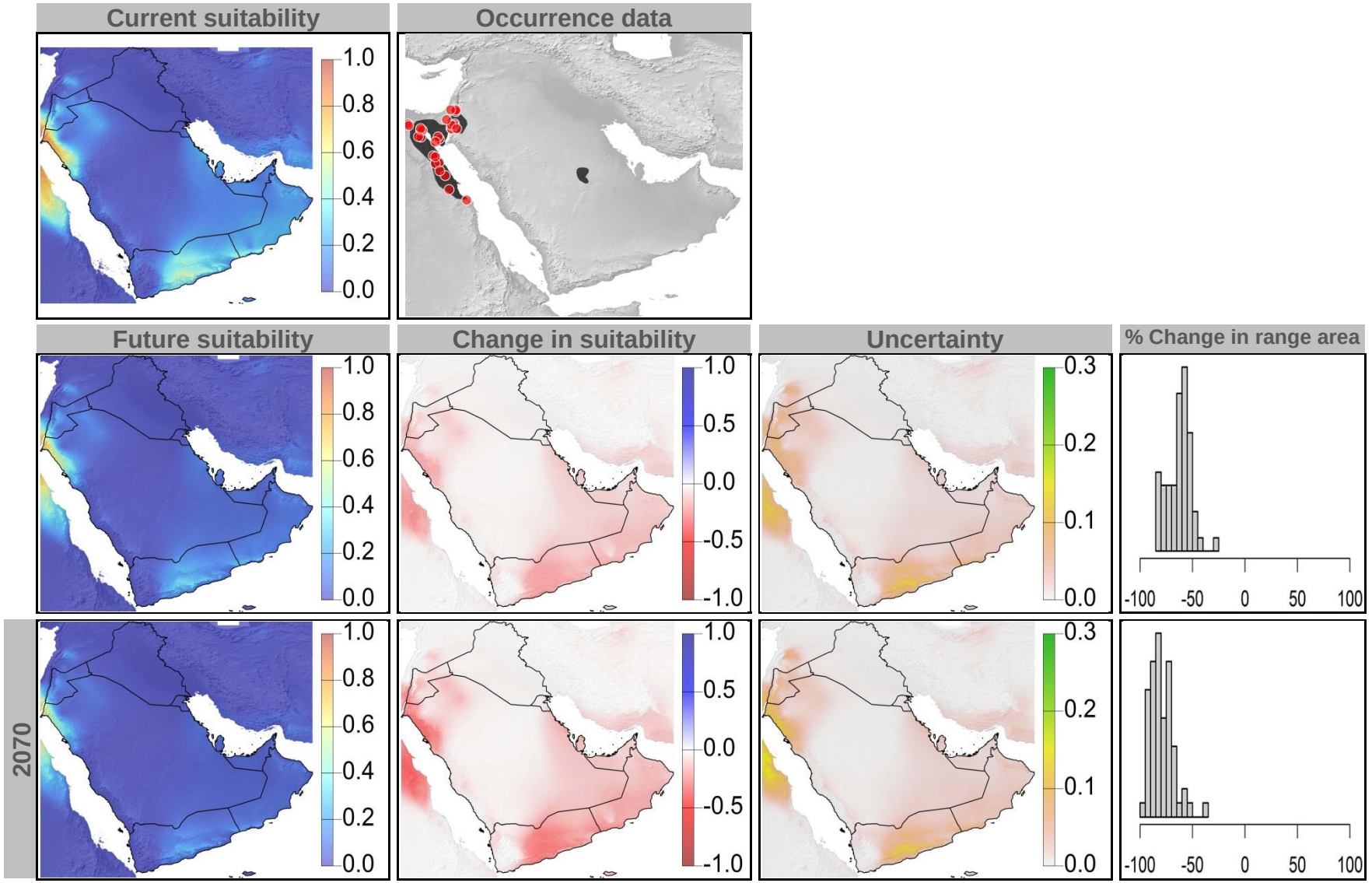

Figure 46: Current and future (2070) climate suitability for *Sekeetamys calurus*, based on an ensemble of all future climate scenarios from the regional climate modeling effort at two spatial domains. Range and occurrence data shown for reference.

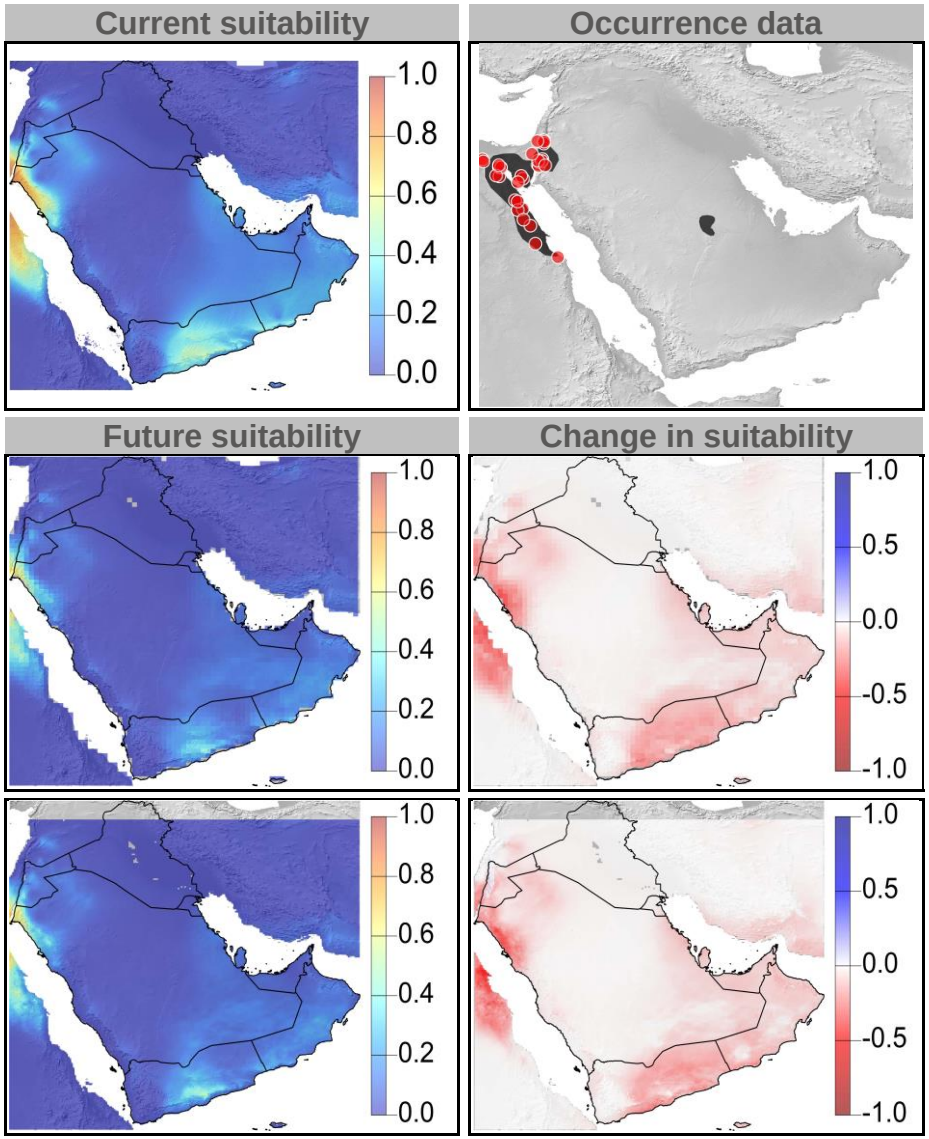

AGEDI
مبادرة أبوظبي العالمية للبيانات البيئية
Abu Dhabi Global Environmental Data Initiative

Annex VIII – MaxEnt results combined across all priority plant species for RCP4.5 and RCP8.5

Climate Change Research Group

University of Maryland
CENTER FOR ENVIRONMENTAL SCIENCE

Figure 1: Current and future climate suitability for *Acacia tortilis*, with associated uncertainty and change in range area based on an ensemble of all future climate scenarios. Range and occurrence data shown for reference.

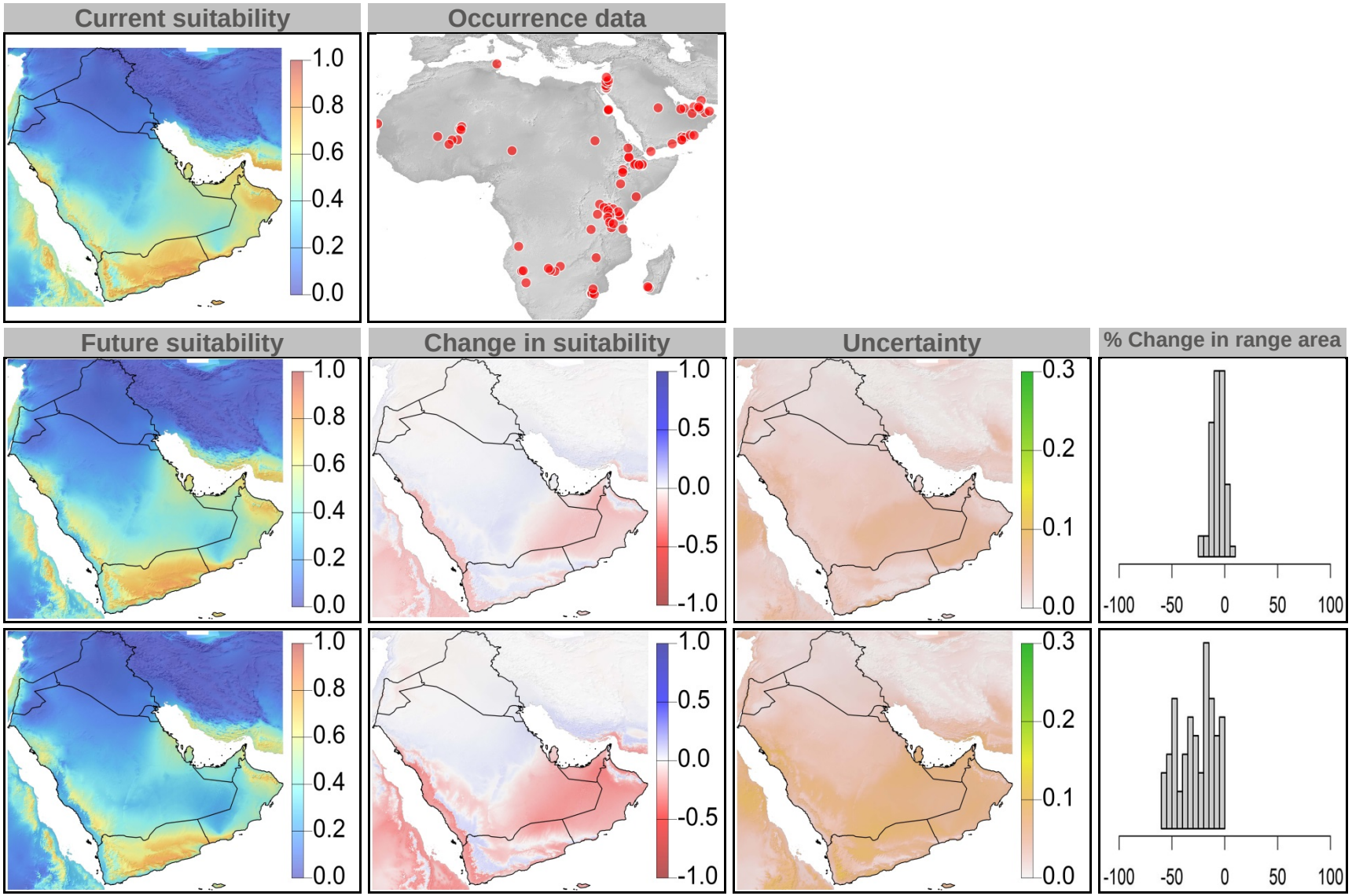

Figure 2: Current and future (2070) climate suitability for *Acacia tortilis*, based on an ensemble of all future climate scenarios from the regional climate modeling effort at two spatial domains. Range and occurrence data shown for reference.

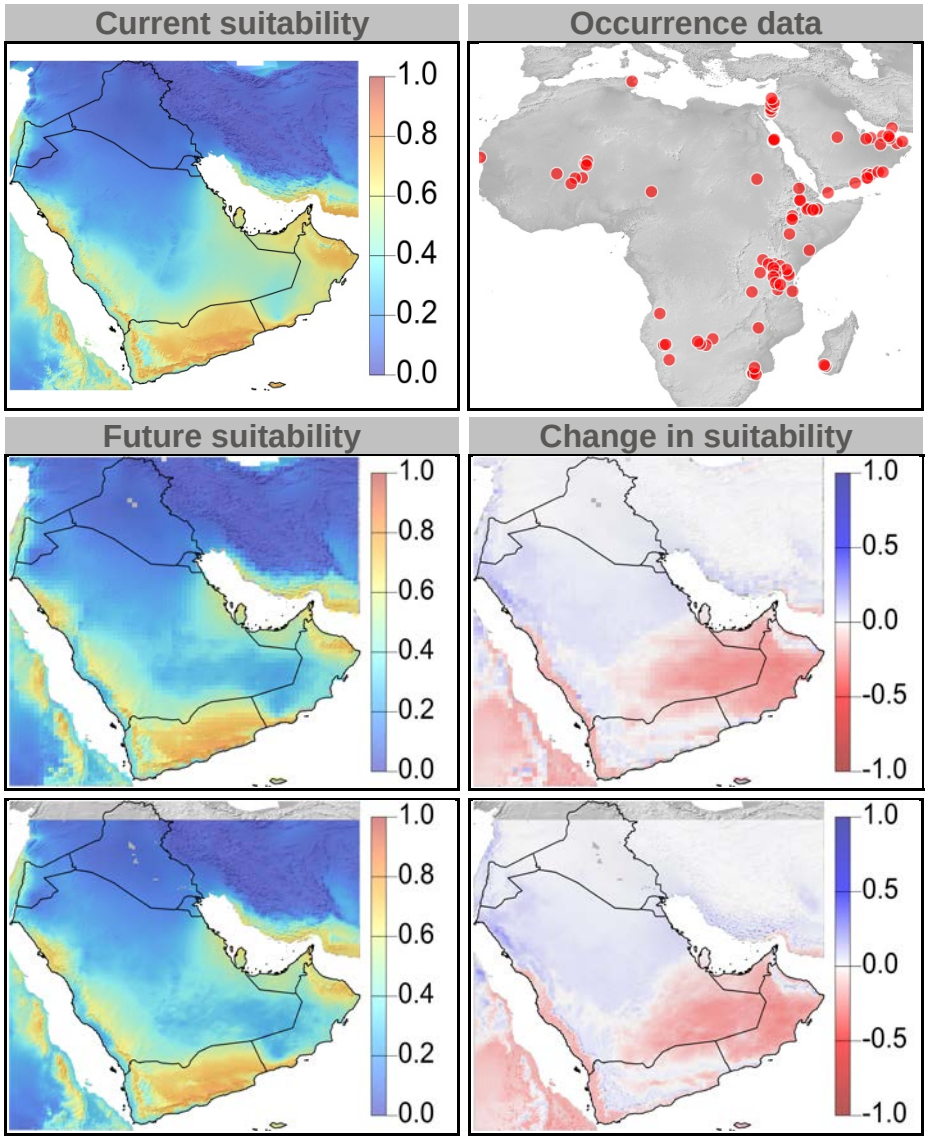

Figure 3: Current and future climate suitability for *Arthrocnemum macrostachyum*, with associated uncertainty and change in range area based on an ensemble of all future climate scenarios. Range and occurrence data shown for reference.

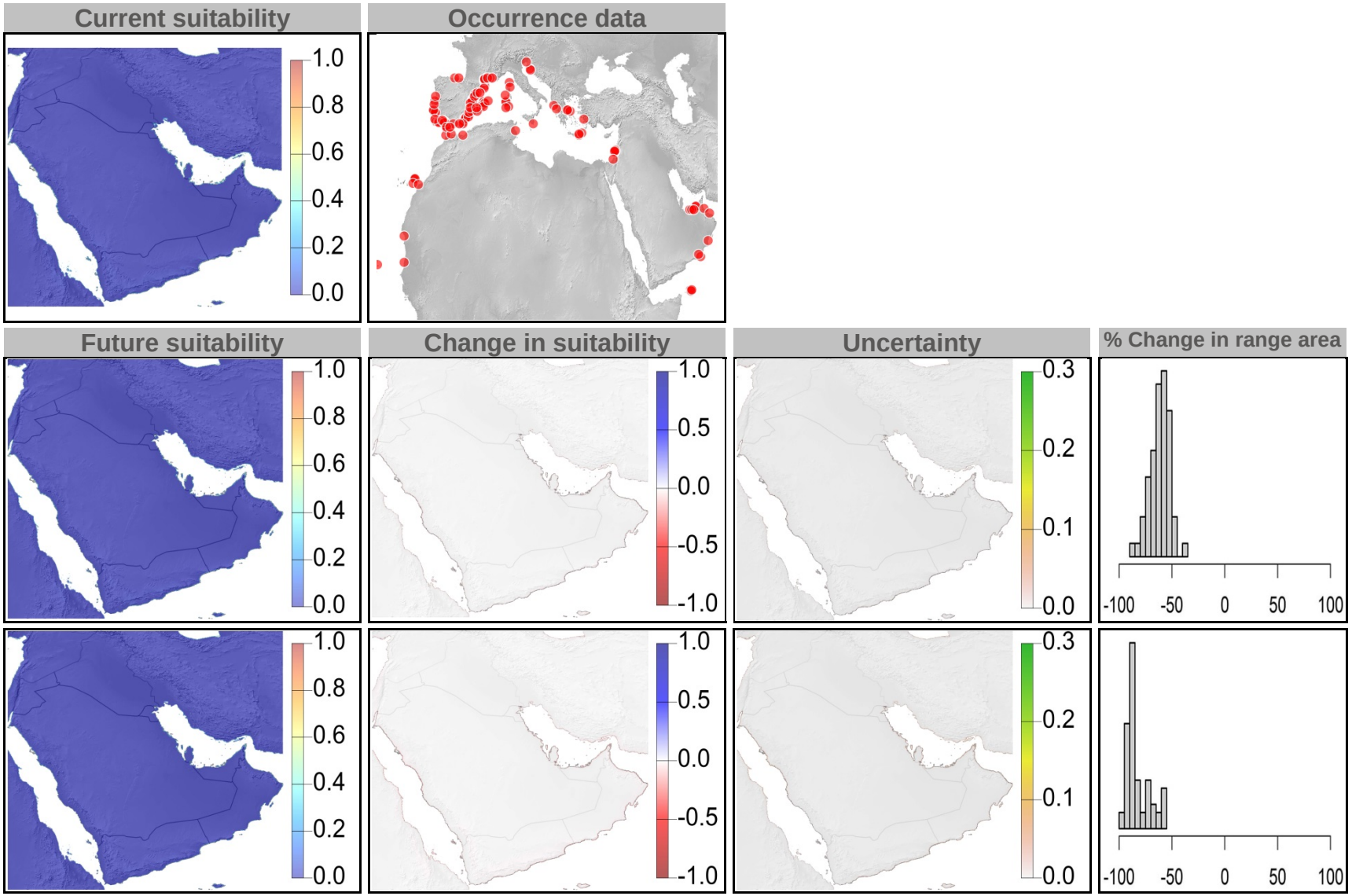

Figure 4: Current and future (2070) climate suitability for *Arthrocnemum macrostachyum*, based on an ensemble of all future climate scenarios from the regional climate modeling effort at two spatial domains. Range and occurrence data shown for reference.

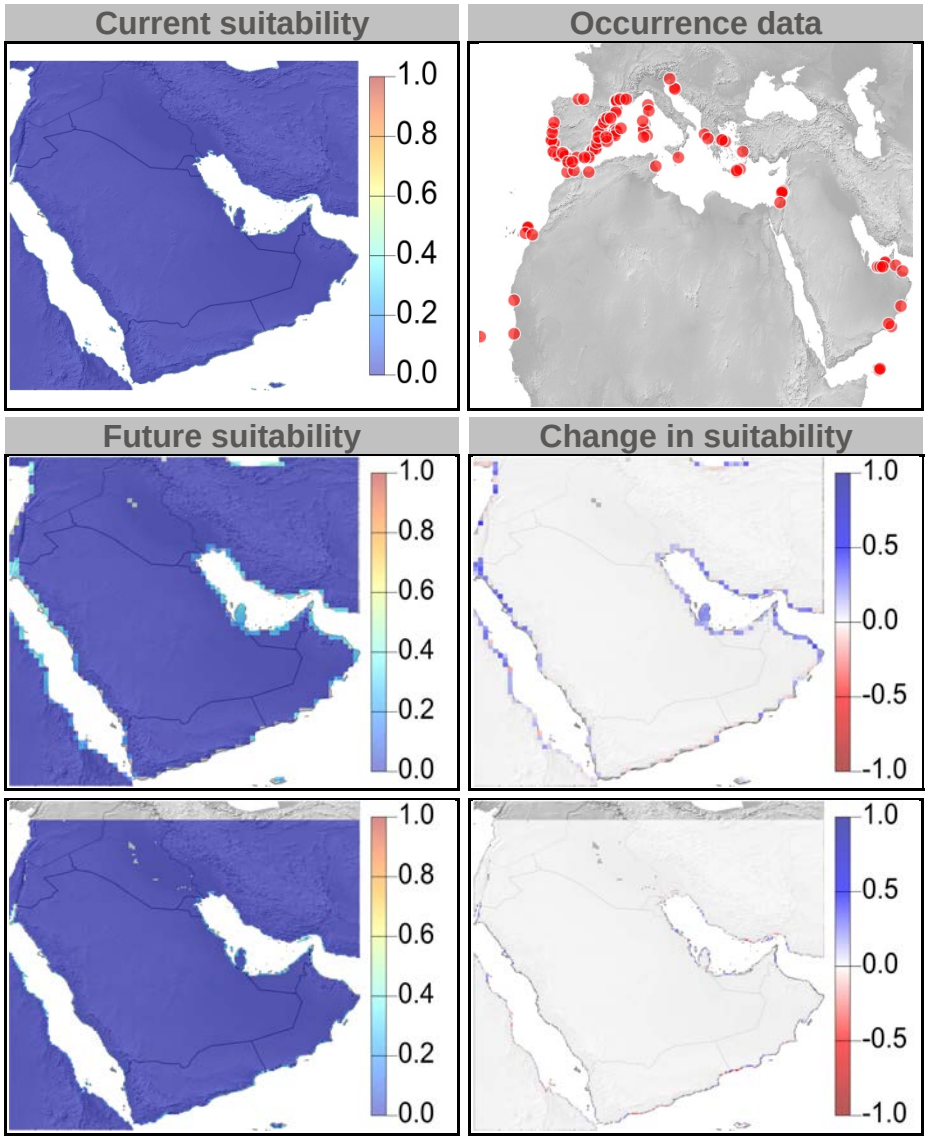

Figure 5: Current and future climate suitability for *Atriplex leucoclada*, with associated uncertainty and change in range area based on an ensemble of all future climate scenarios. Range and occurrence data shown for reference.

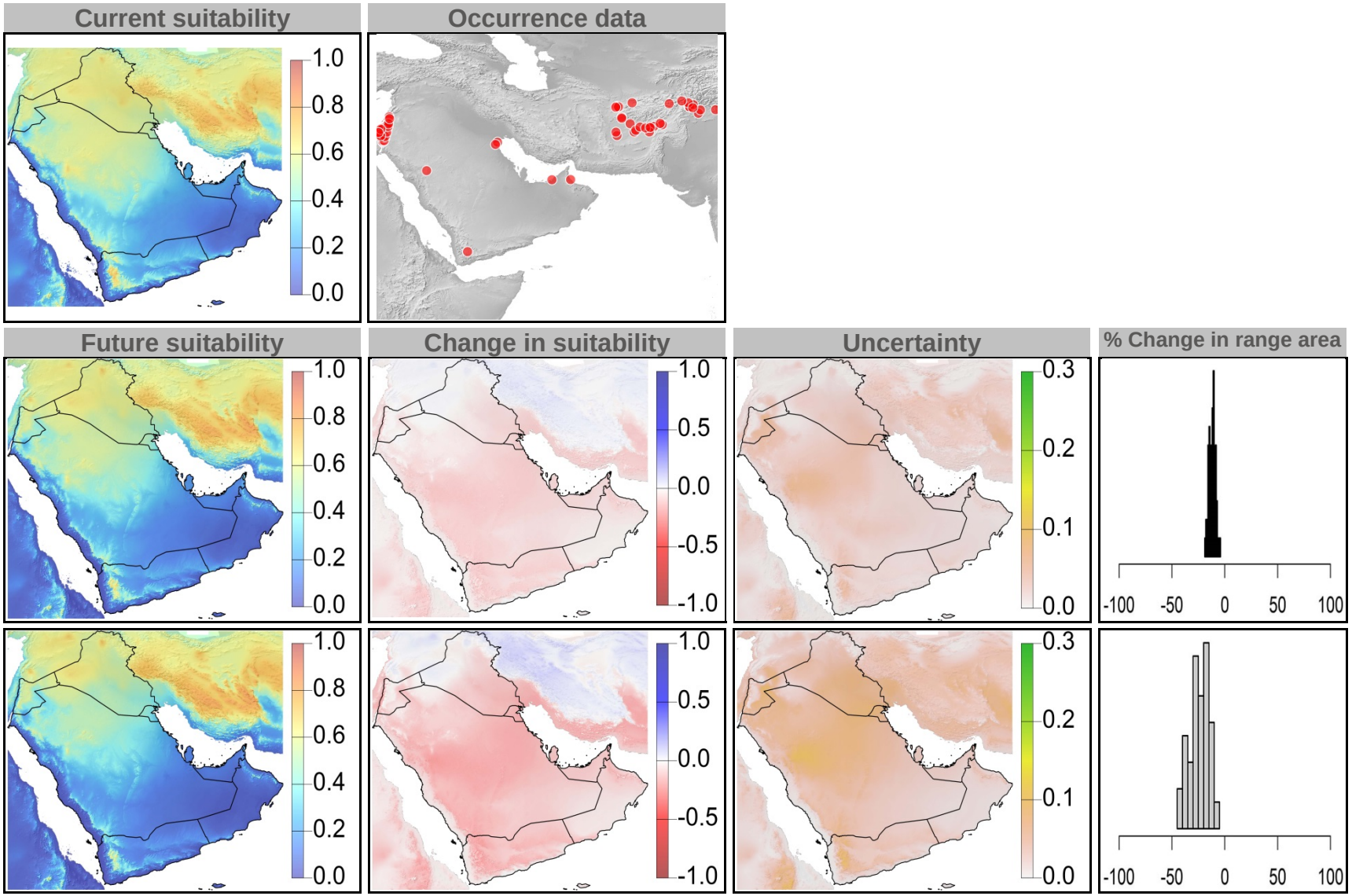

Figure 6: Current and future (2070) climate suitability for *Atriplex leucoclada*, based on an ensemble of all future climate scenarios from the regional climate modeling effort at two spatial domains. Range and occurrence data shown for reference.

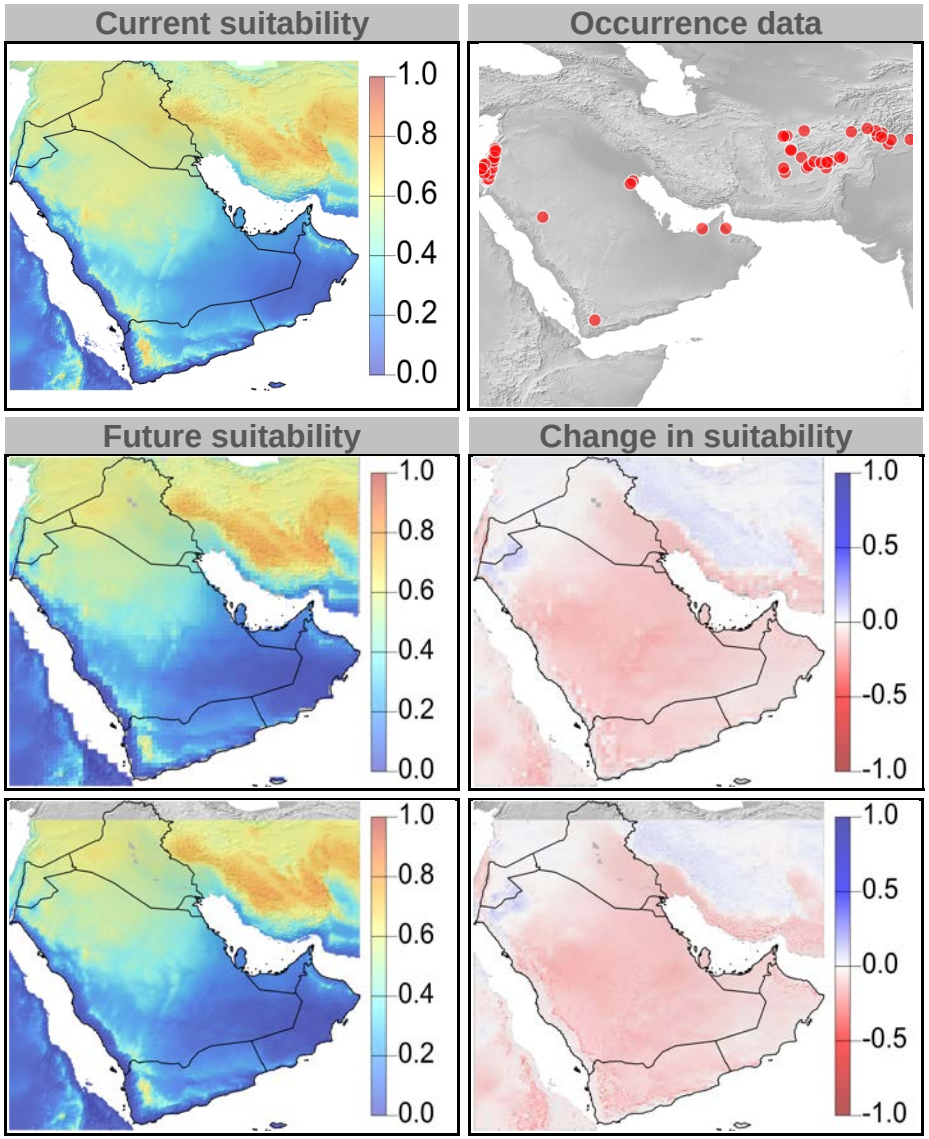

Figure 7: Current and future climate suitability for *Avicennia marina*, with associated uncertainty and change in range area based on an ensemble of all future climate scenarios. Range and occurrence data shown for reference.

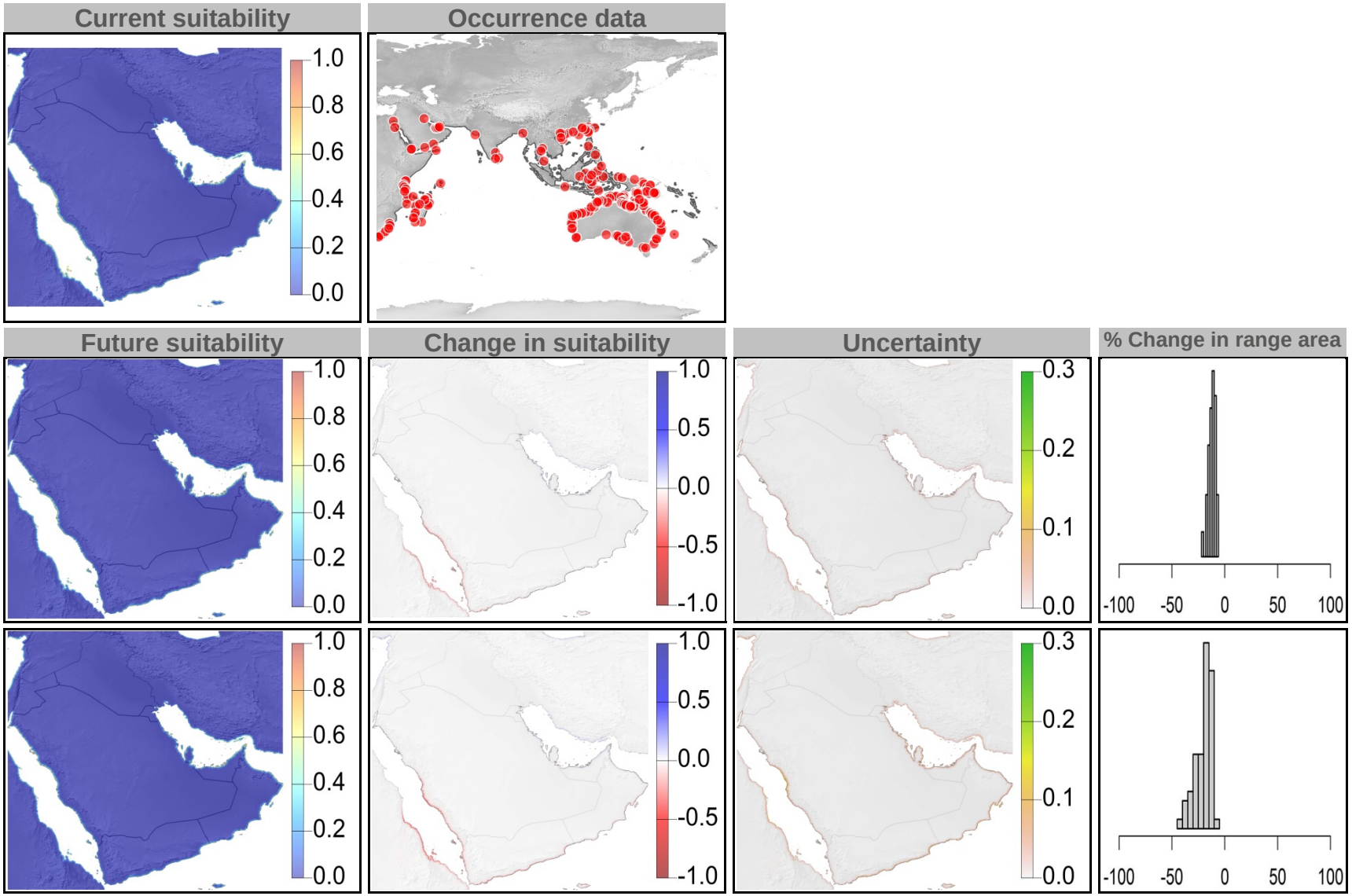

Figure 8: Current and future (2070) climate suitability for *Avicennia marina*, based on an ensemble of all future climate scenarios from the regional climate modeling effort at two spatial domains. Range and occurrence data shown for reference.

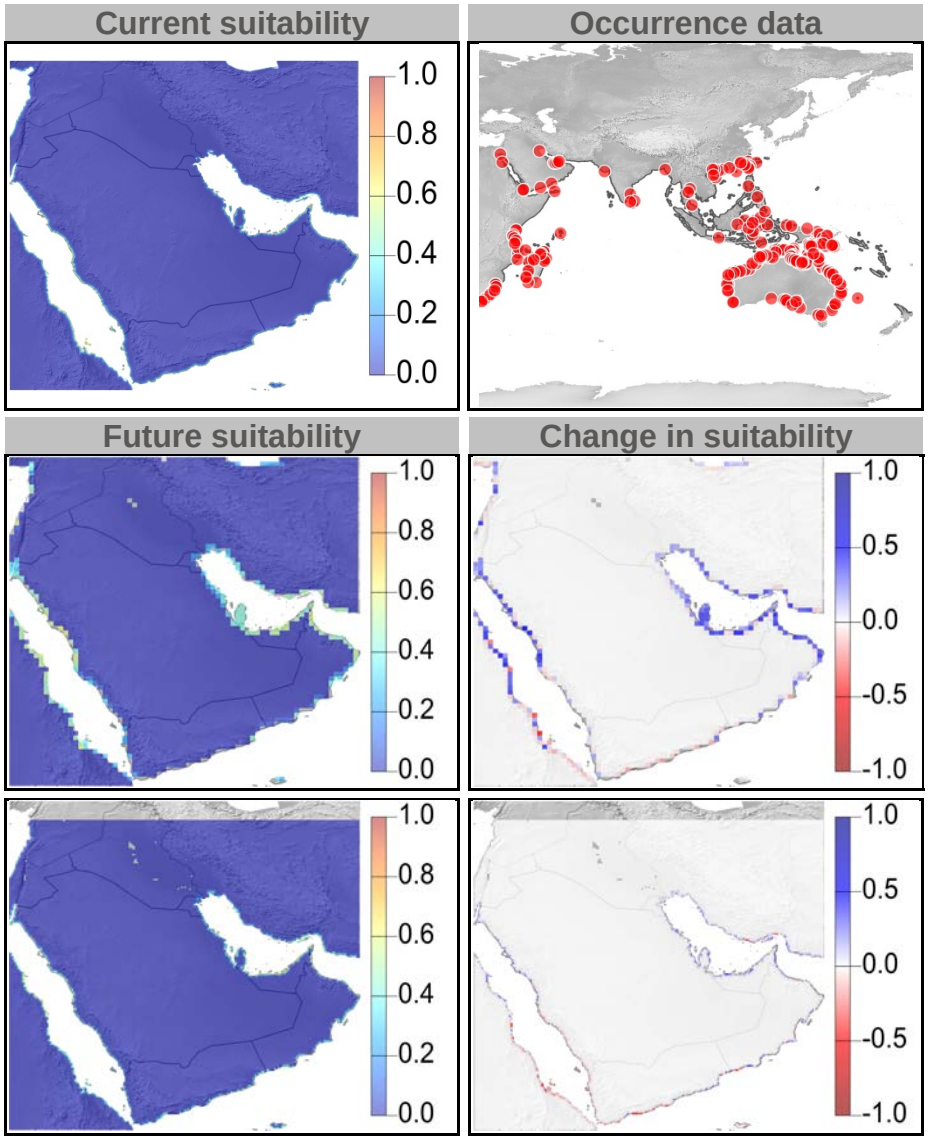

Figure 9: Current and future climate suitability for *Calligonum comosum*, with associated uncertainty and change in range area based on an ensemble of all future climate scenarios. Range and occurrence data shown for reference.

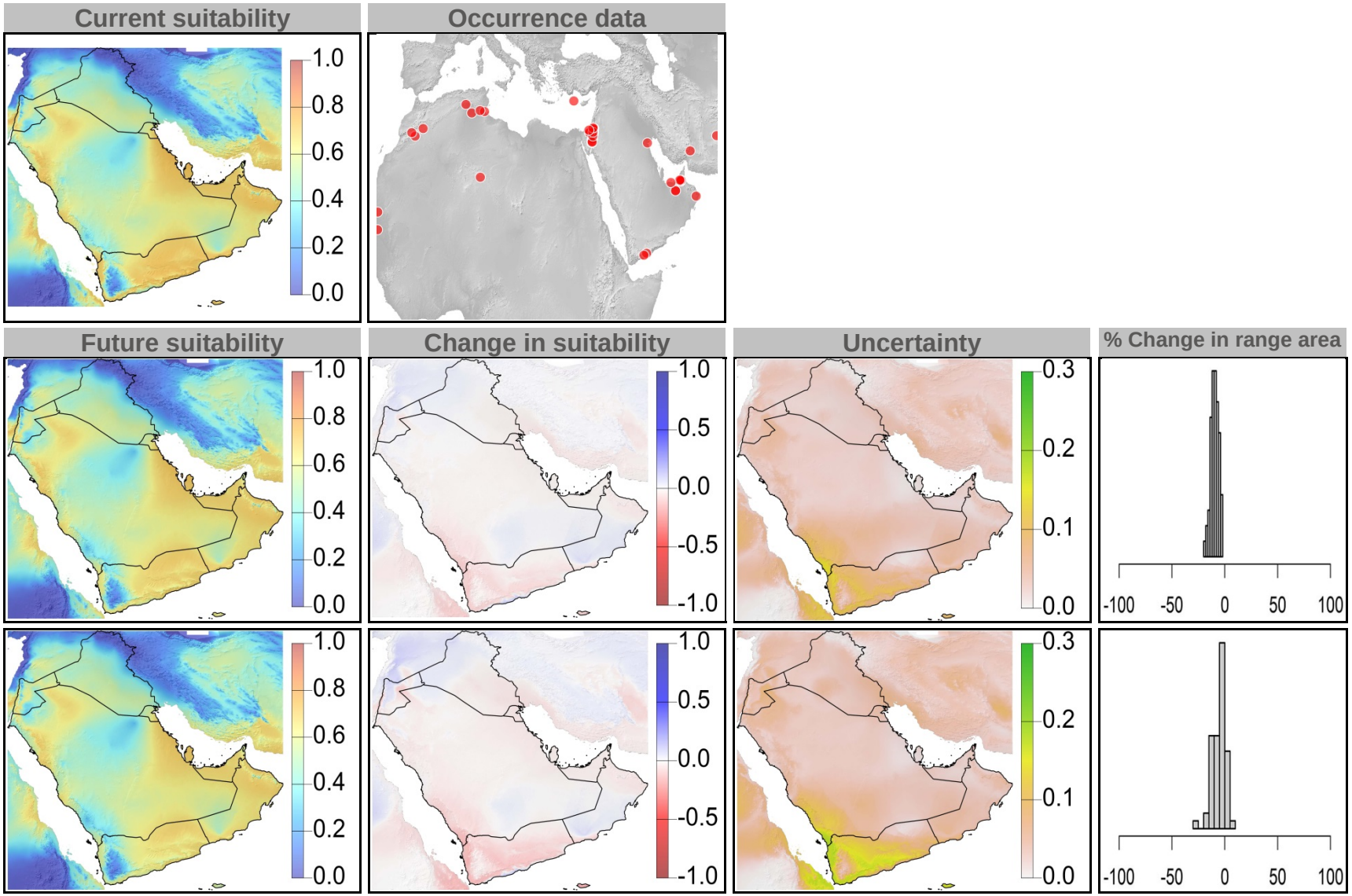

Figure 10: Current and future (2070) climate suitability for *Calligonum comosum*, based on an ensemble of all future climate scenarios from the regional climate modeling effort at two spatial domains. Range and occurrence data shown for reference.

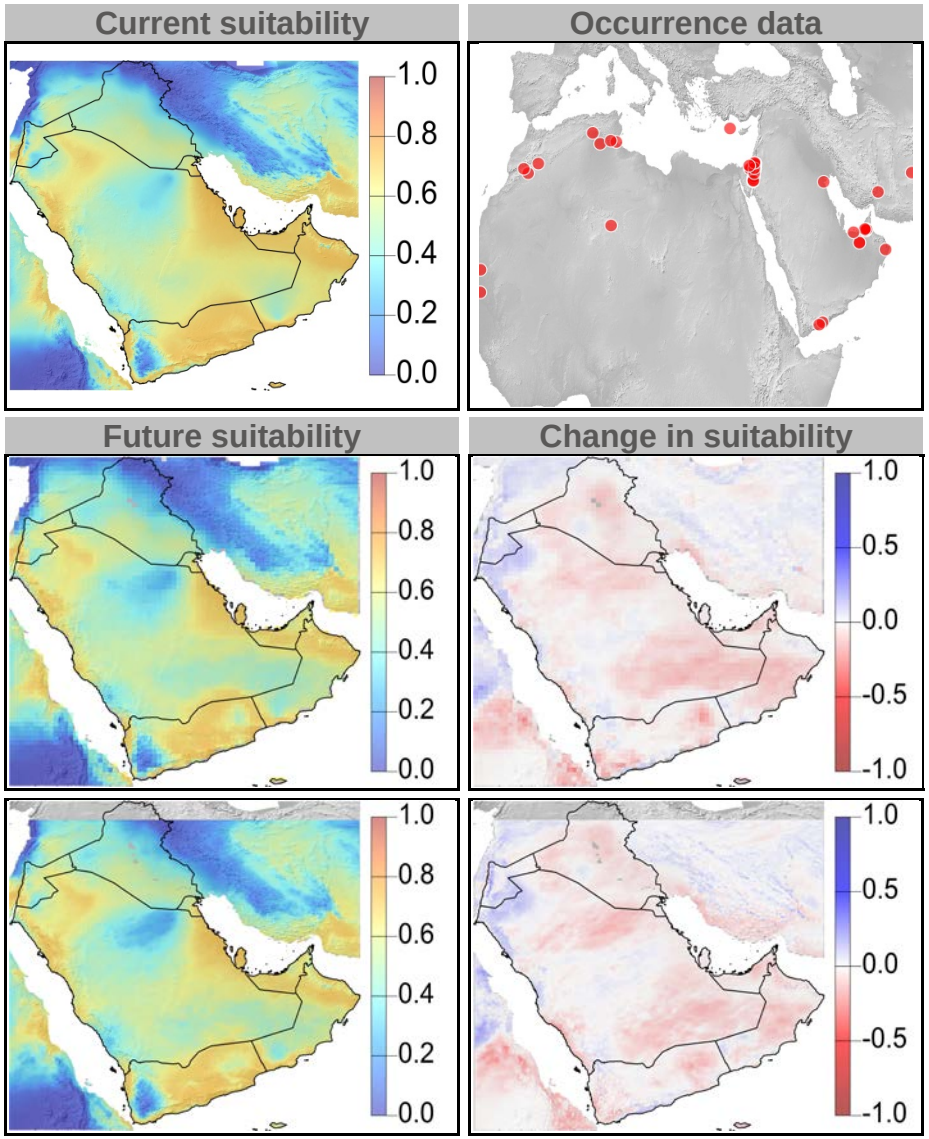

Figure 11: Current and future climate suitability for *Cleome amblyocarpa*, with associated uncertainty and change in range area based on an ensemble of all future climate scenarios. Range and occurrence data shown for reference.

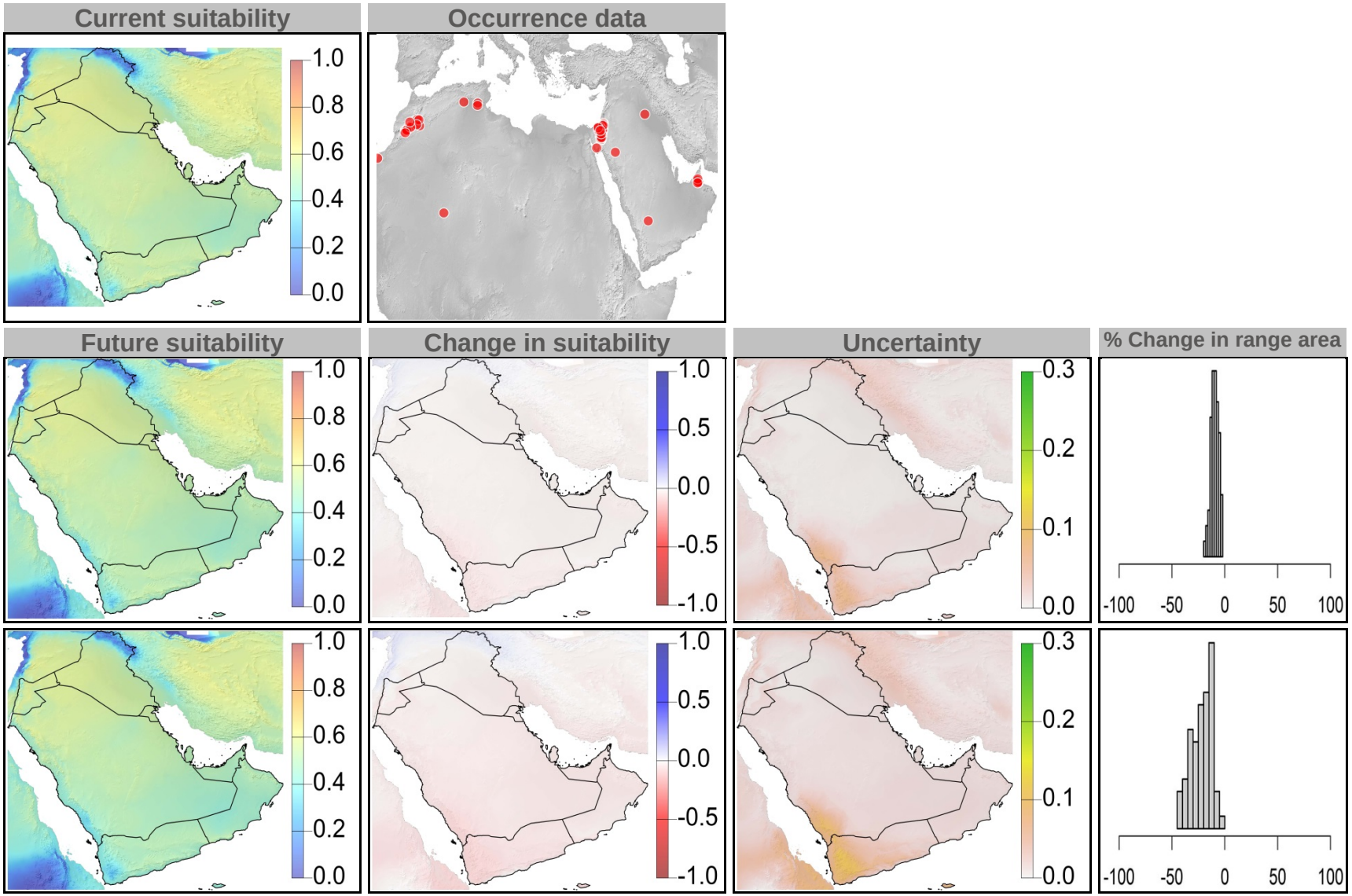

Figure 12: Current and future (2070) climate suitability for *Cleome amblyocarpa*, based on an ensemble of all future climate scenarios from the regional climate modeling effort at two spatial domains. Range and occurrence data shown for reference.

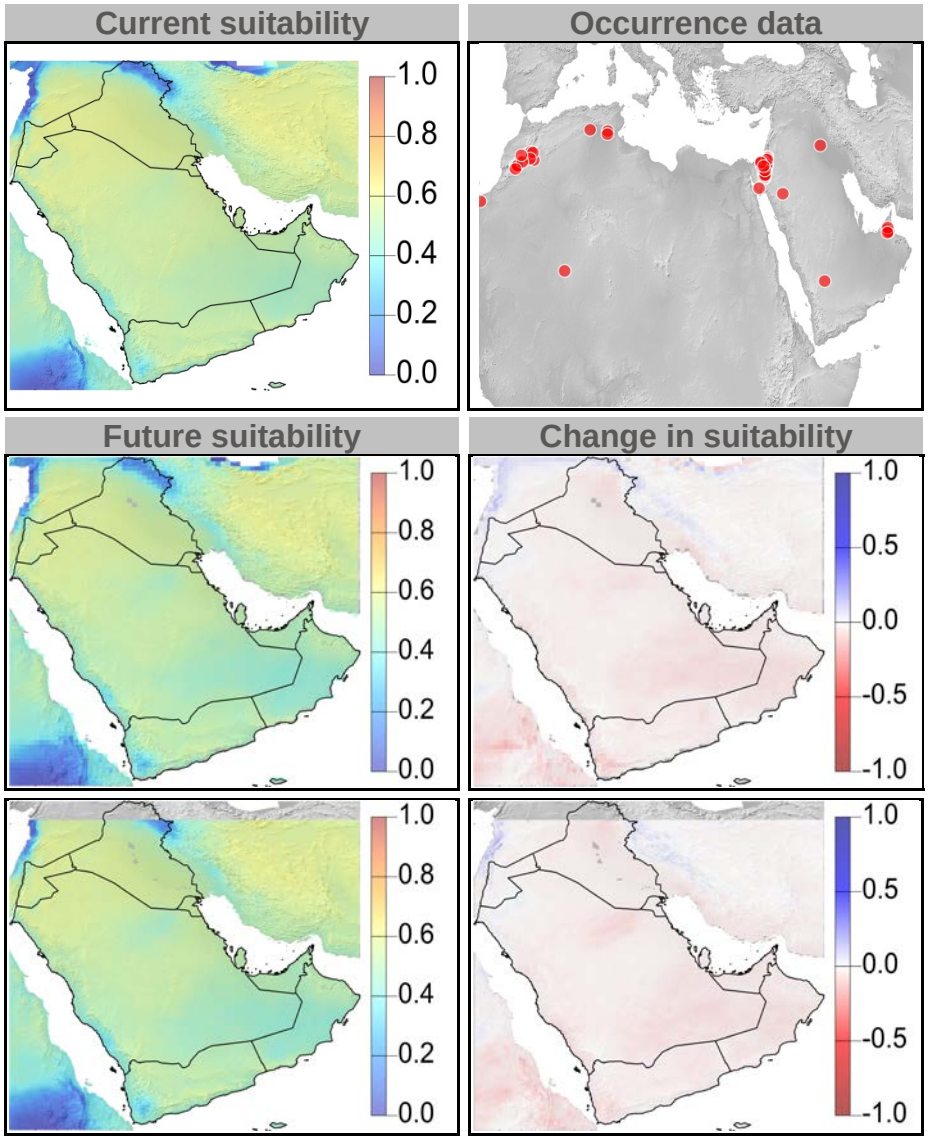

Figure 13: Current and future climate suitability for *Cyperus conglomeratus*, with associated uncertainty and change in range area based on an ensemble of all future climate scenarios. Range and occurrence data shown for reference.

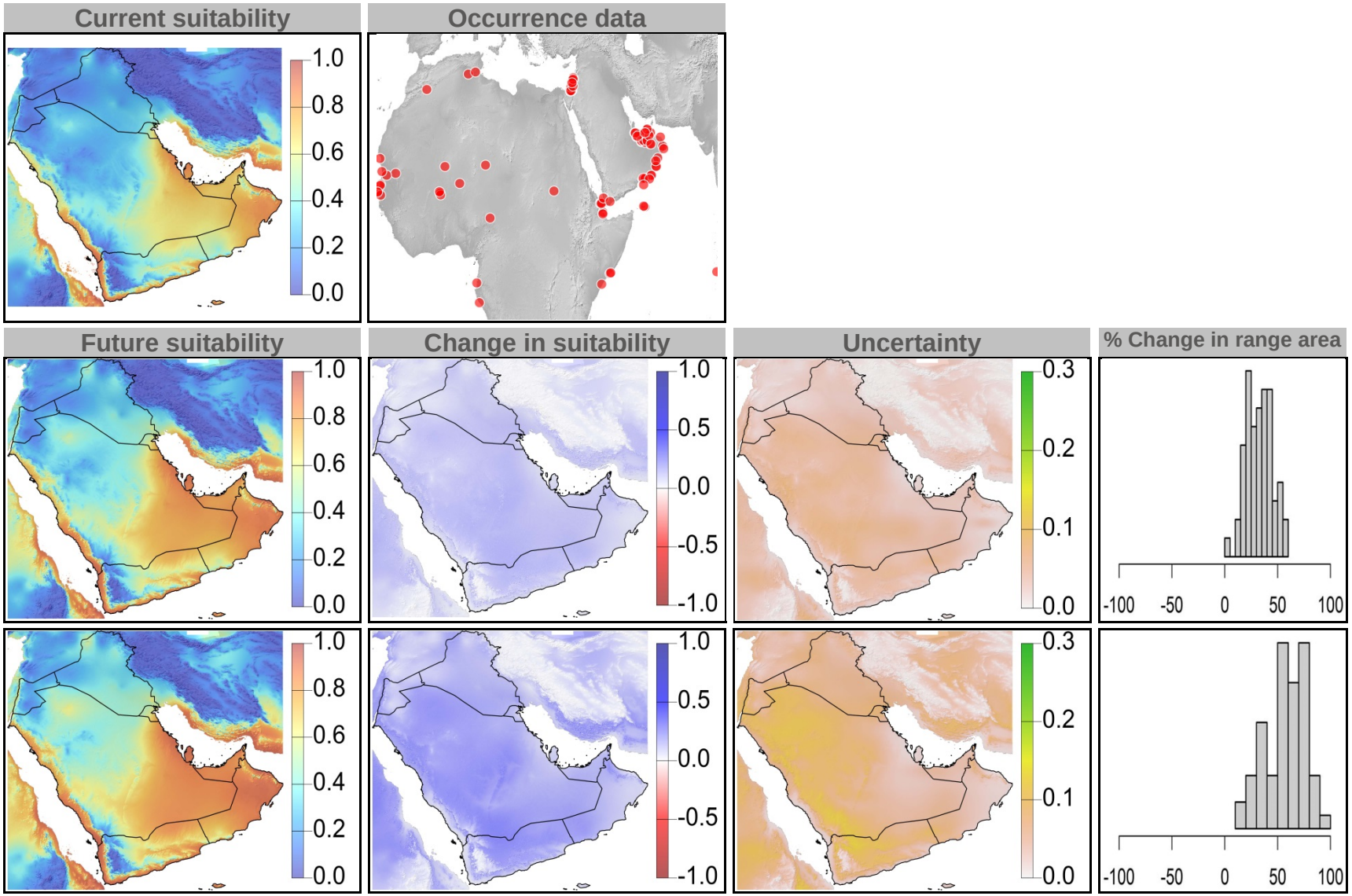

Figure 14: Current and future (2070) climate suitability for *Cyperus conglomeratus*, based on an ensemble of all future climate scenarios from the regional climate modeling effort at two spatial domains. Range and occurrence data shown for reference.

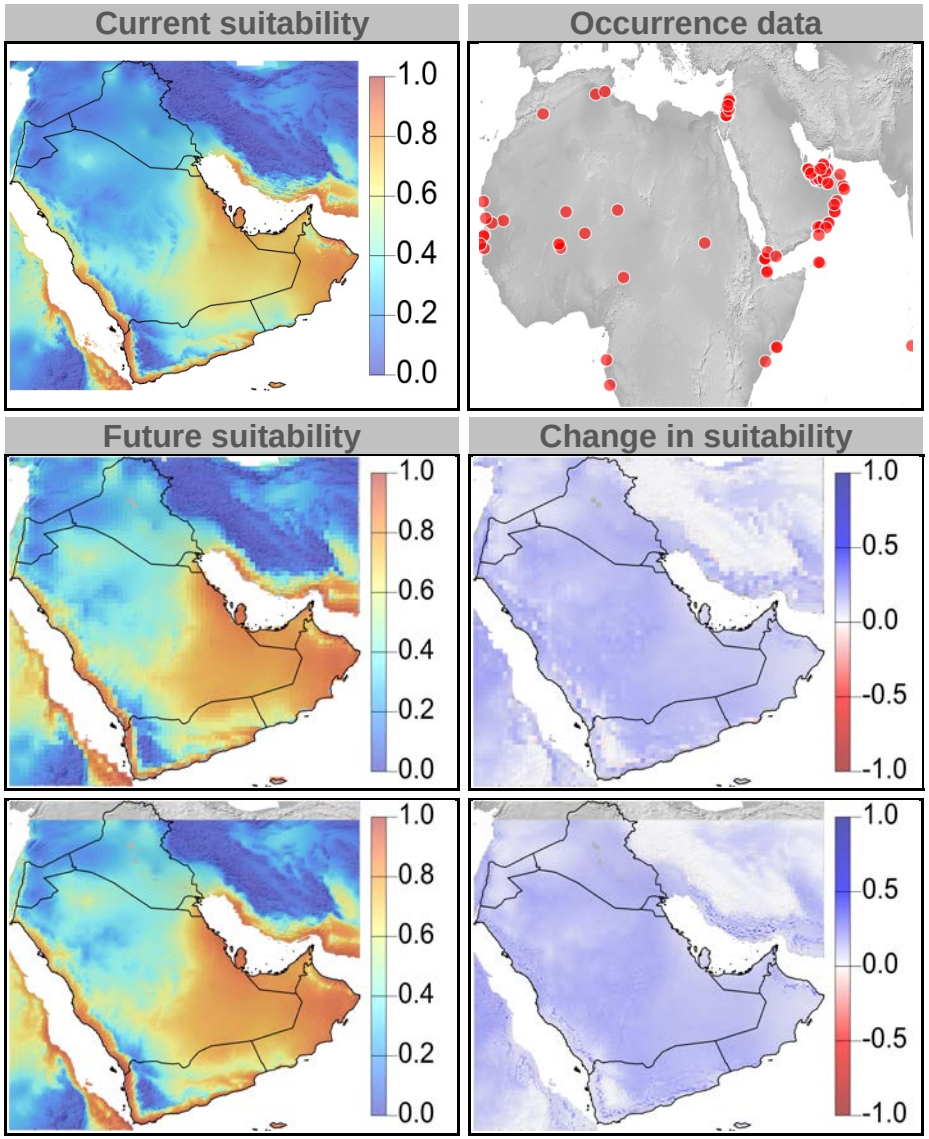

Figure 15: Current and future climate suitability for *Delonix elata*, with associated uncertainty and change in range area based on an ensemble of all future climate scenarios. Range and occurrence data shown for reference.

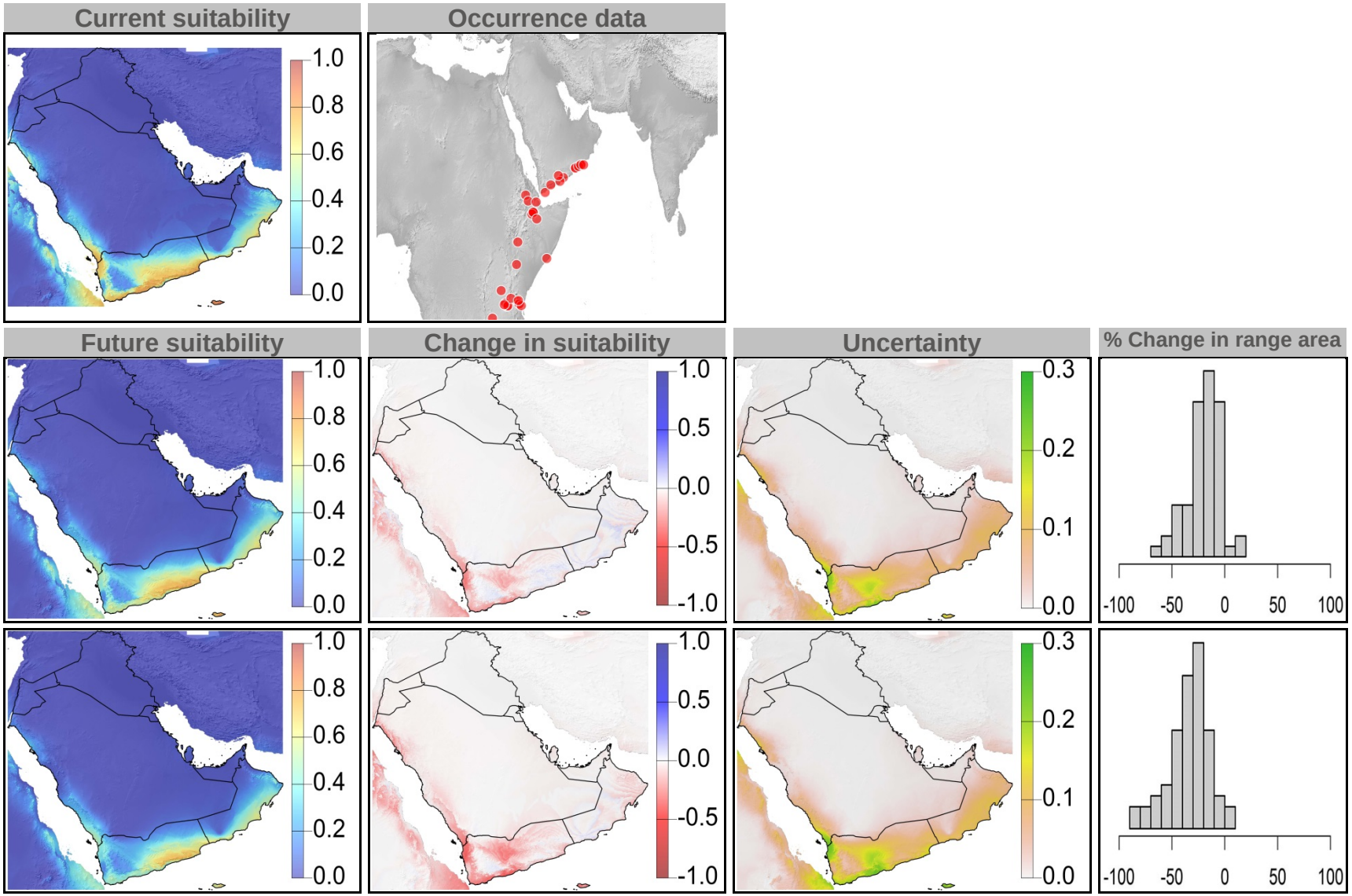

Figure 16: Current and future (2070) climate suitability for *Delonix elata*, based on an ensemble of all future climate scenarios from the regional climate modeling effort at two spatial domains. Range and occurrence data shown for reference.

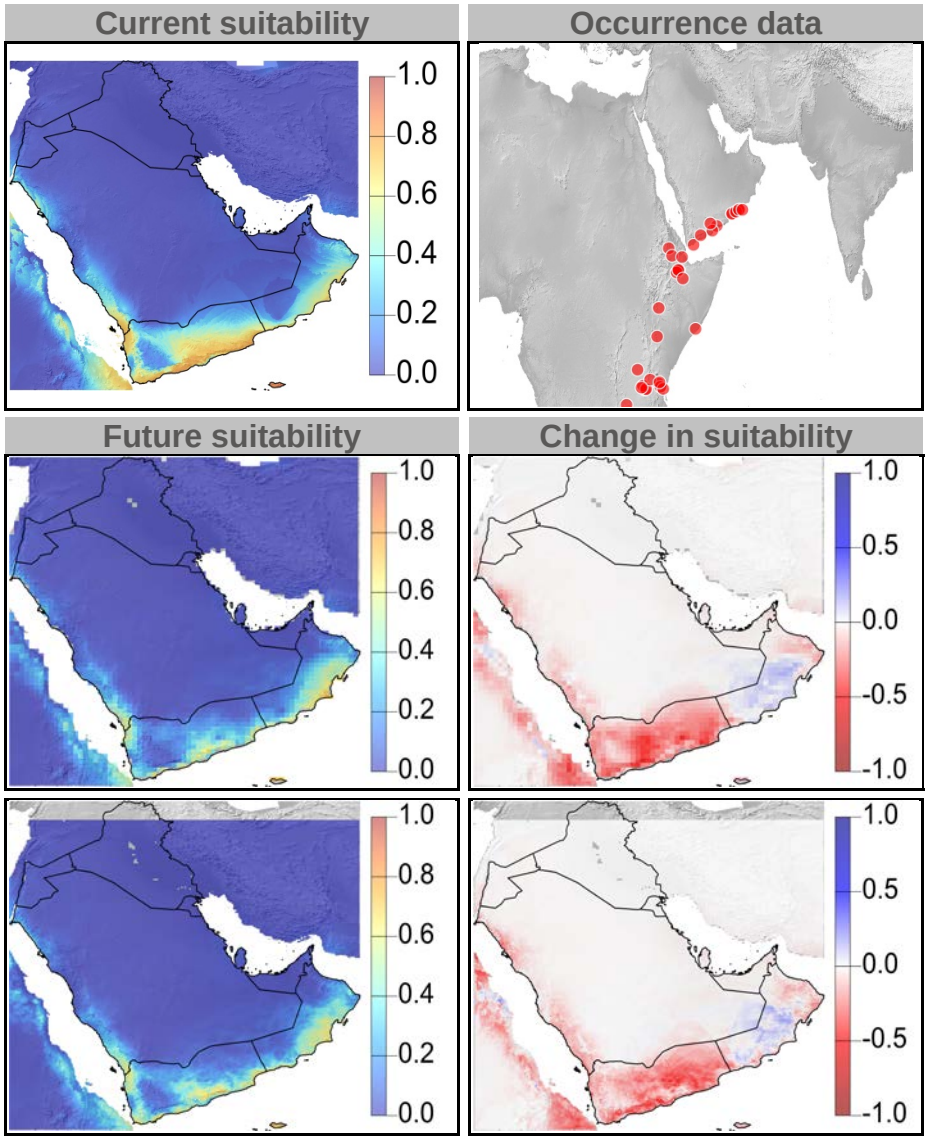

Figure 17: Current and future climate suitability for *Dodonaea viscosa*, with associated uncertainty and change in range area based on an ensemble of all future climate scenarios. Range and occurrence data shown for reference.

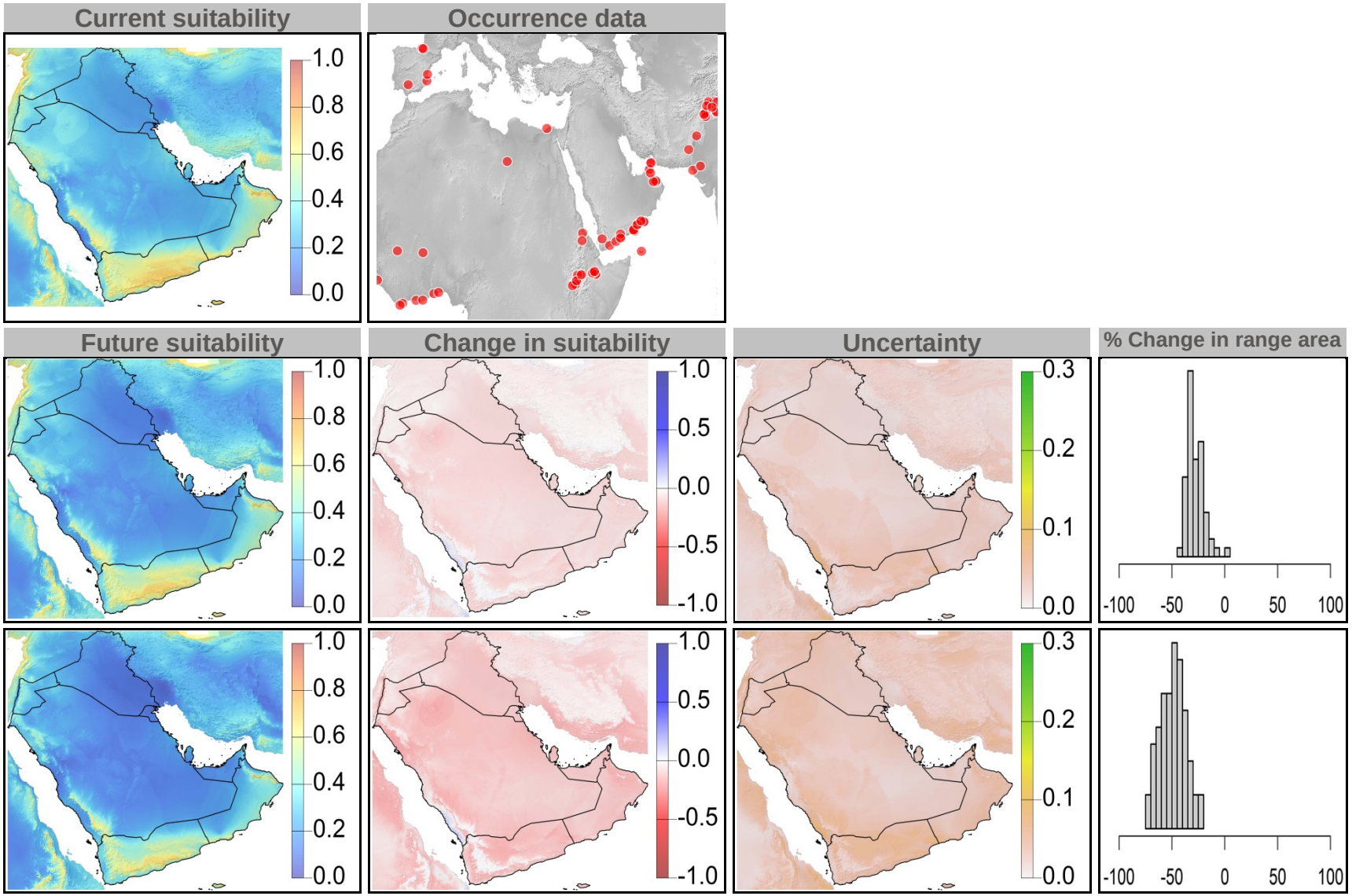

Figure 18: Current and future (2070) climate suitability for *Dodonaea viscosa*, based on an ensemble of all future climate scenarios from the regional climate modeling effort at two spatial domains. Range and occurrence data shown for reference.

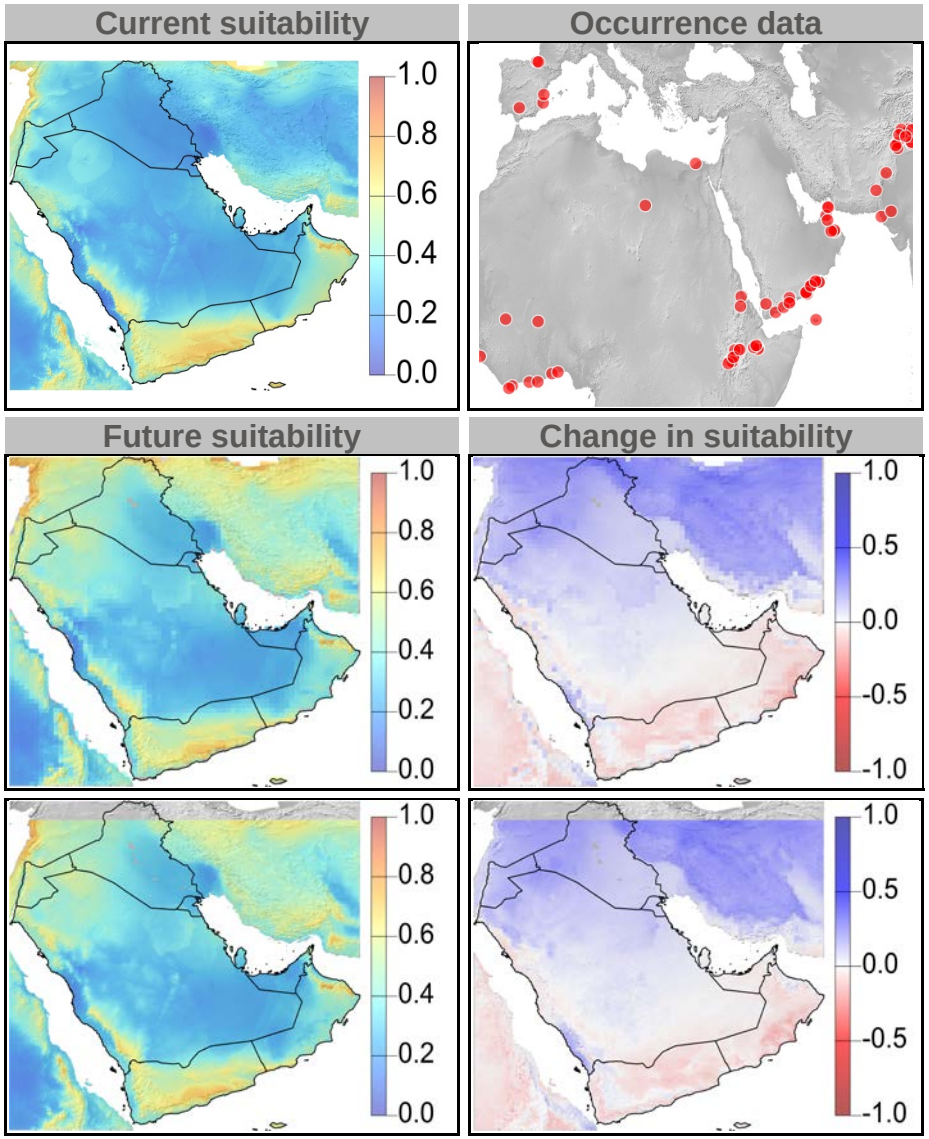

Figure 19: Current and future climate suitability for *Eremobium aegyptiacum*, with associated uncertainty and change in range area based on an ensemble of all future climate scenarios. Range and occurrence data shown for reference.

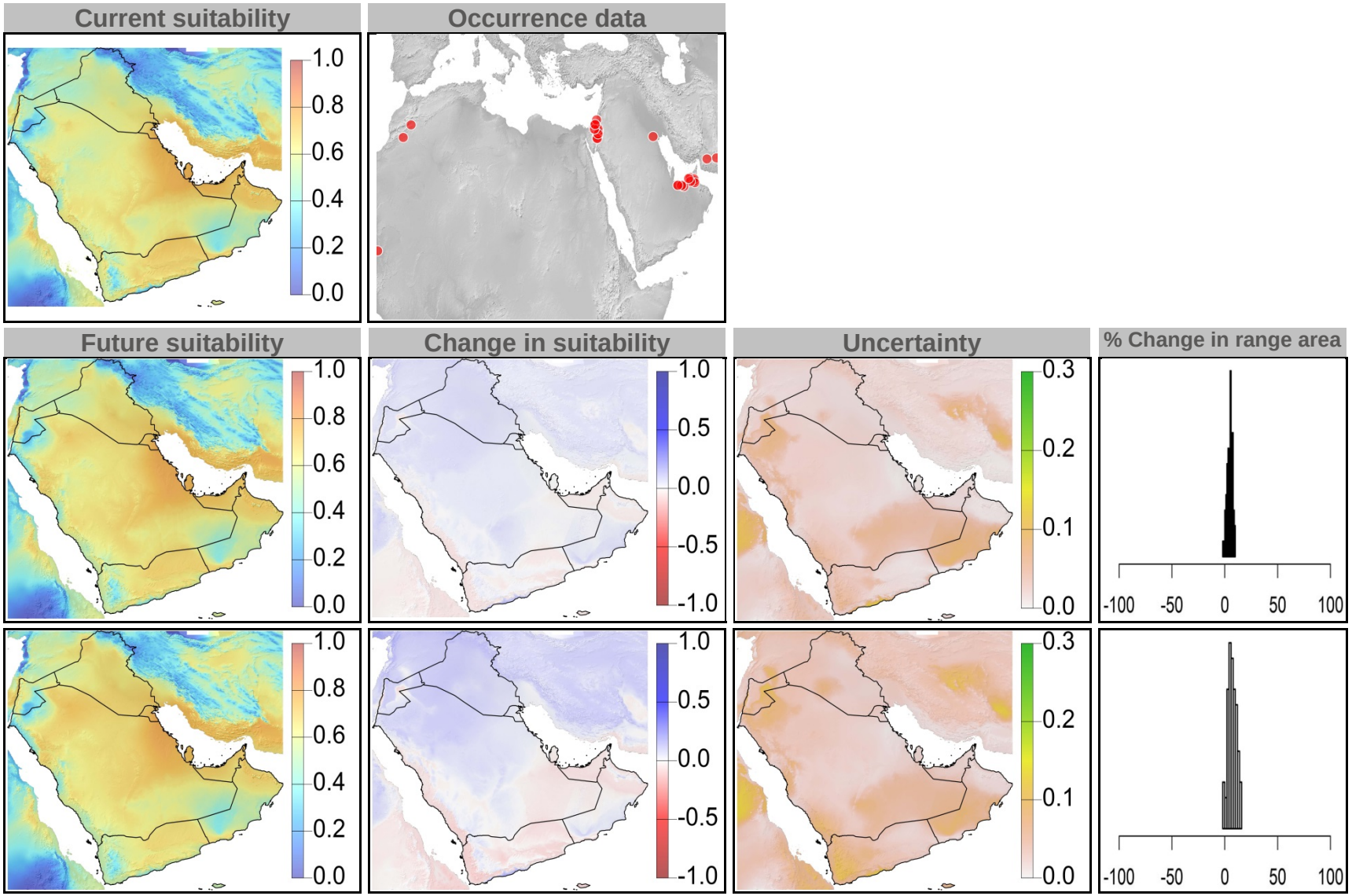

Figure 20: Current and future (2070) climate suitability for *Eremobium aegyptiacum*, based on an ensemble of all future climate scenarios from the regional climate modeling effort at two spatial domains. Range and occurrence data shown for reference.

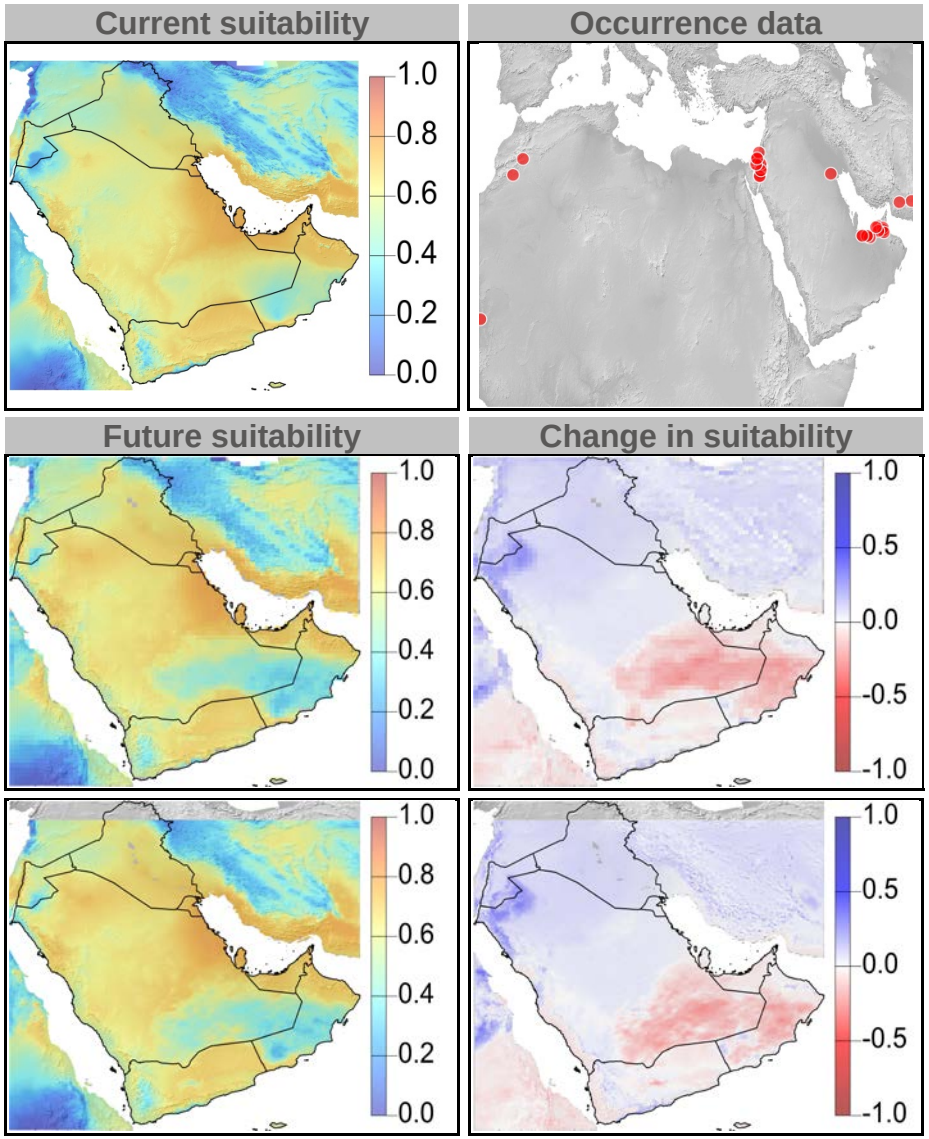

Figure 21: Current and future climate suitability for *Halopyrum mucronatum*, with associated uncertainty and change in range area based on an ensemble of all future climate scenarios. Range and occurrence data shown for reference.

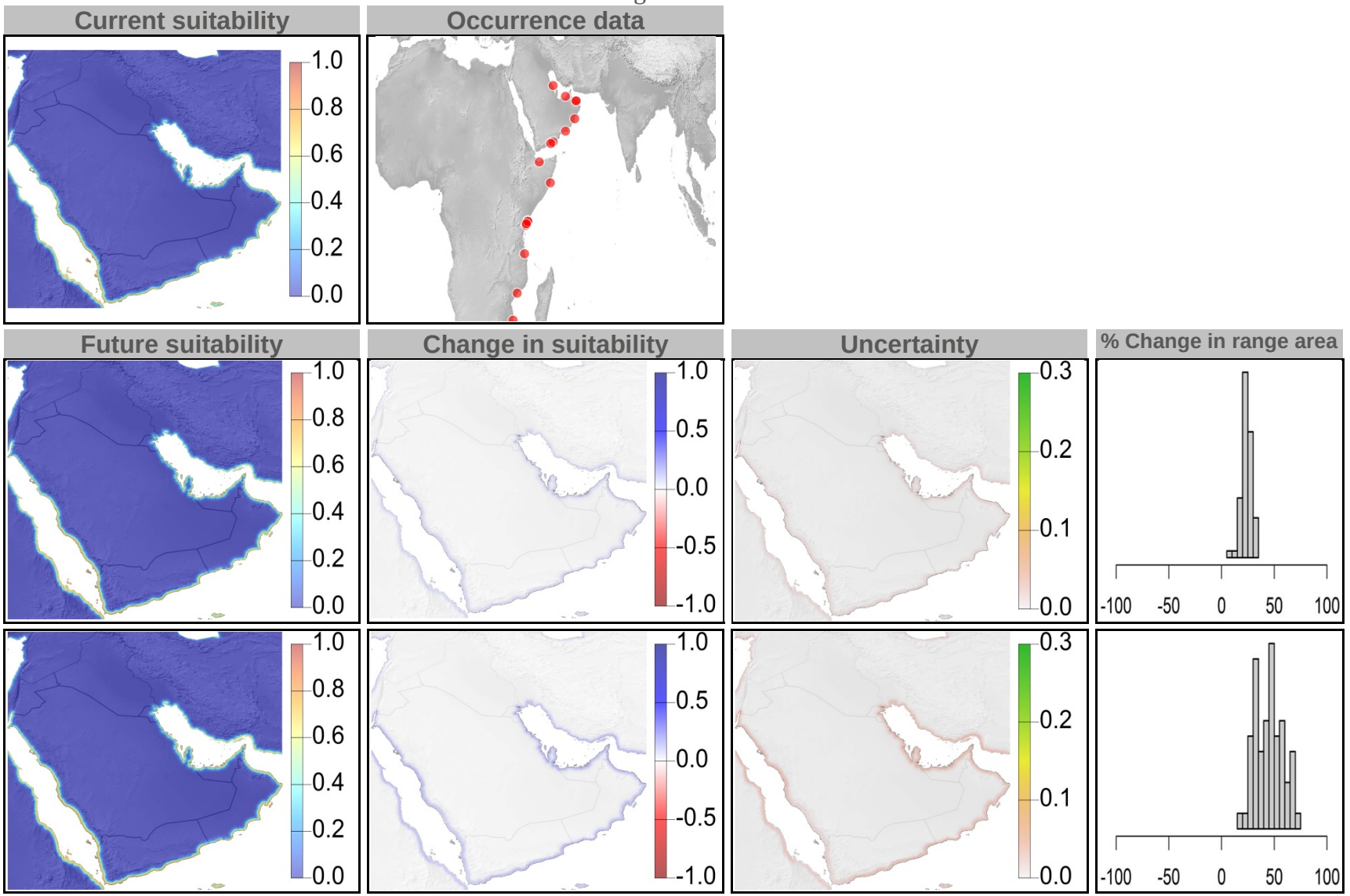

Figure 22: Current and future (2070) climate suitability for *Halopyrum mucronatum*, based on an ensemble of all future climate scenarios from the regional climate modeling effort at two spatial domains. Range and occurrence data shown for reference.

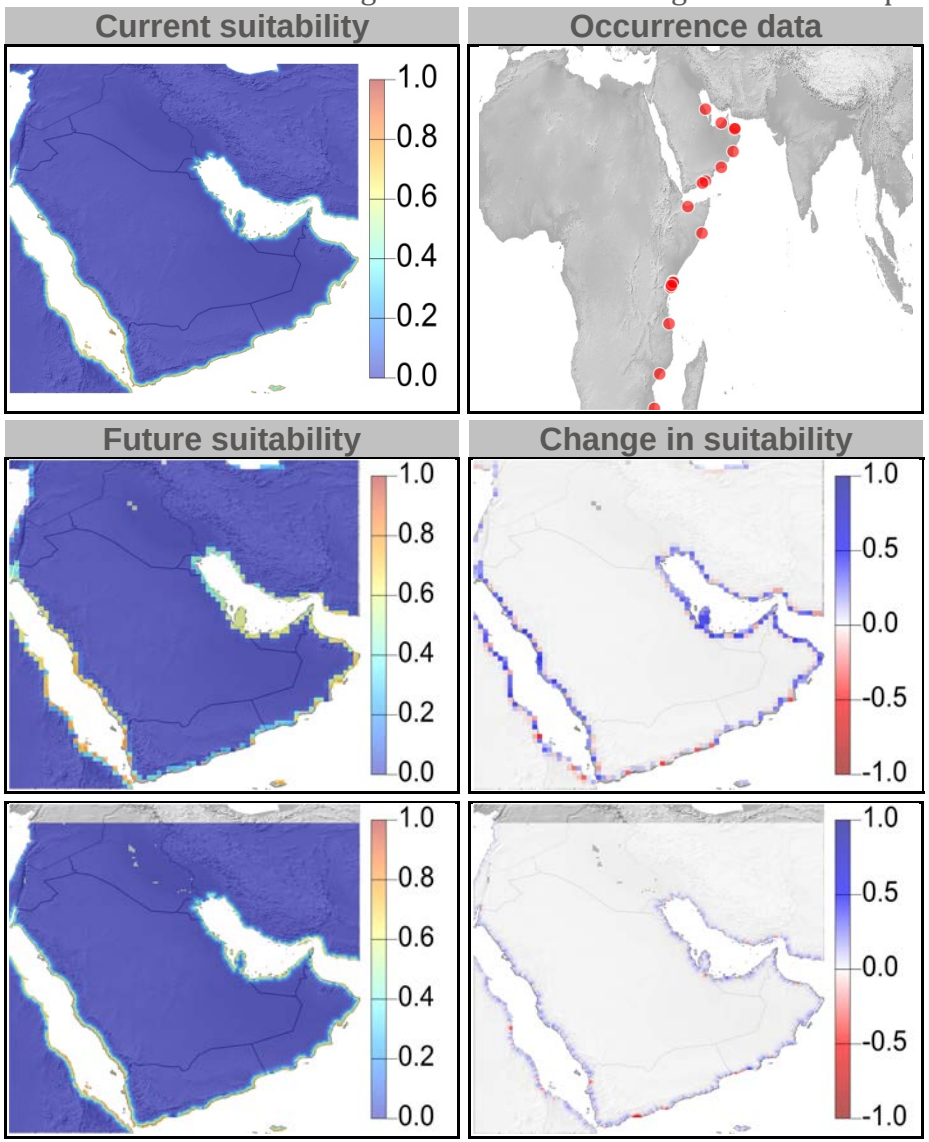

Figure 23: Current and future climate suitability for *Haloxylon salicornicum*, with associated uncertainty and change in range area based on an ensemble of all future climate scenarios. Range and occurrence data shown for reference.

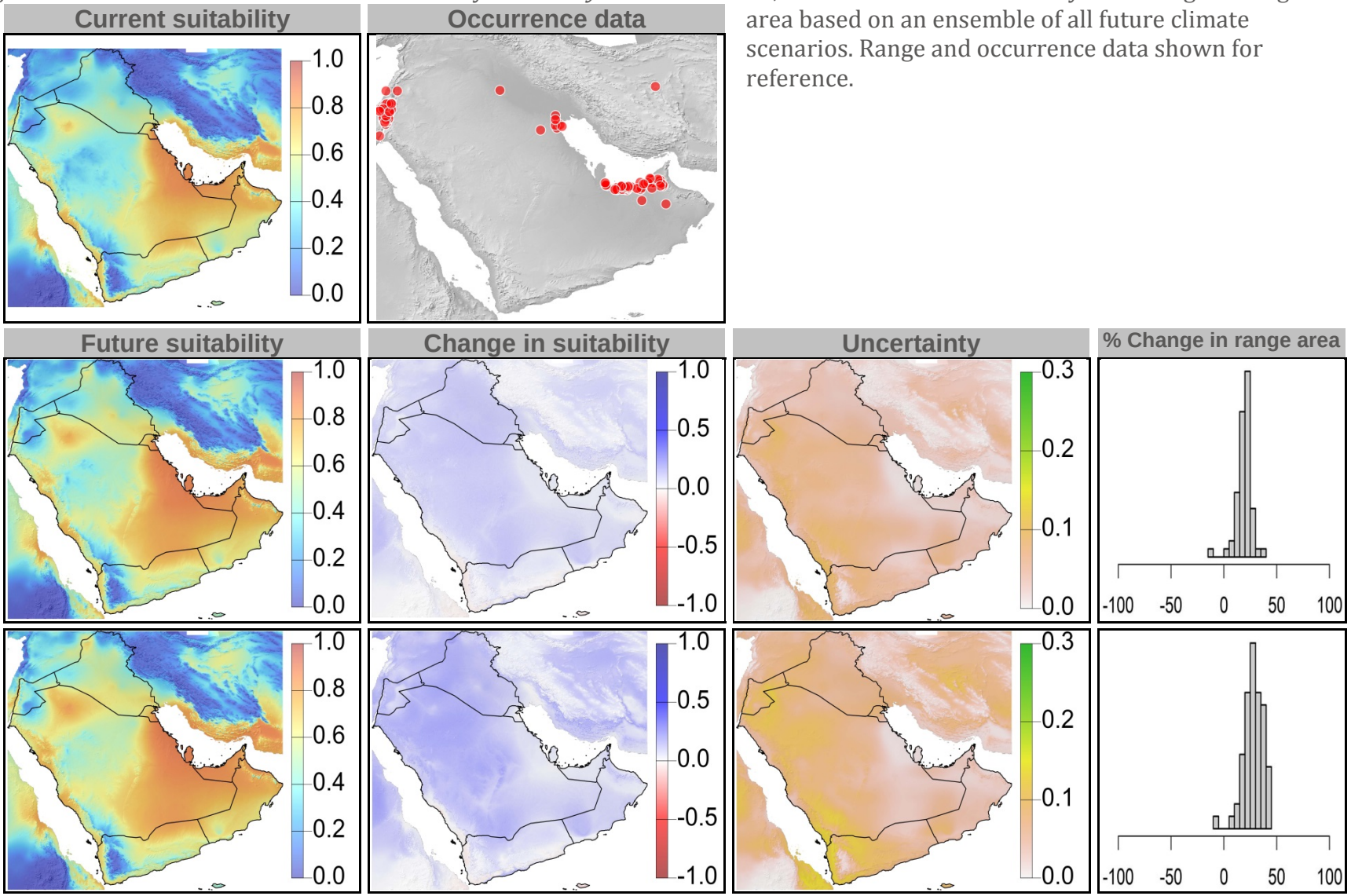

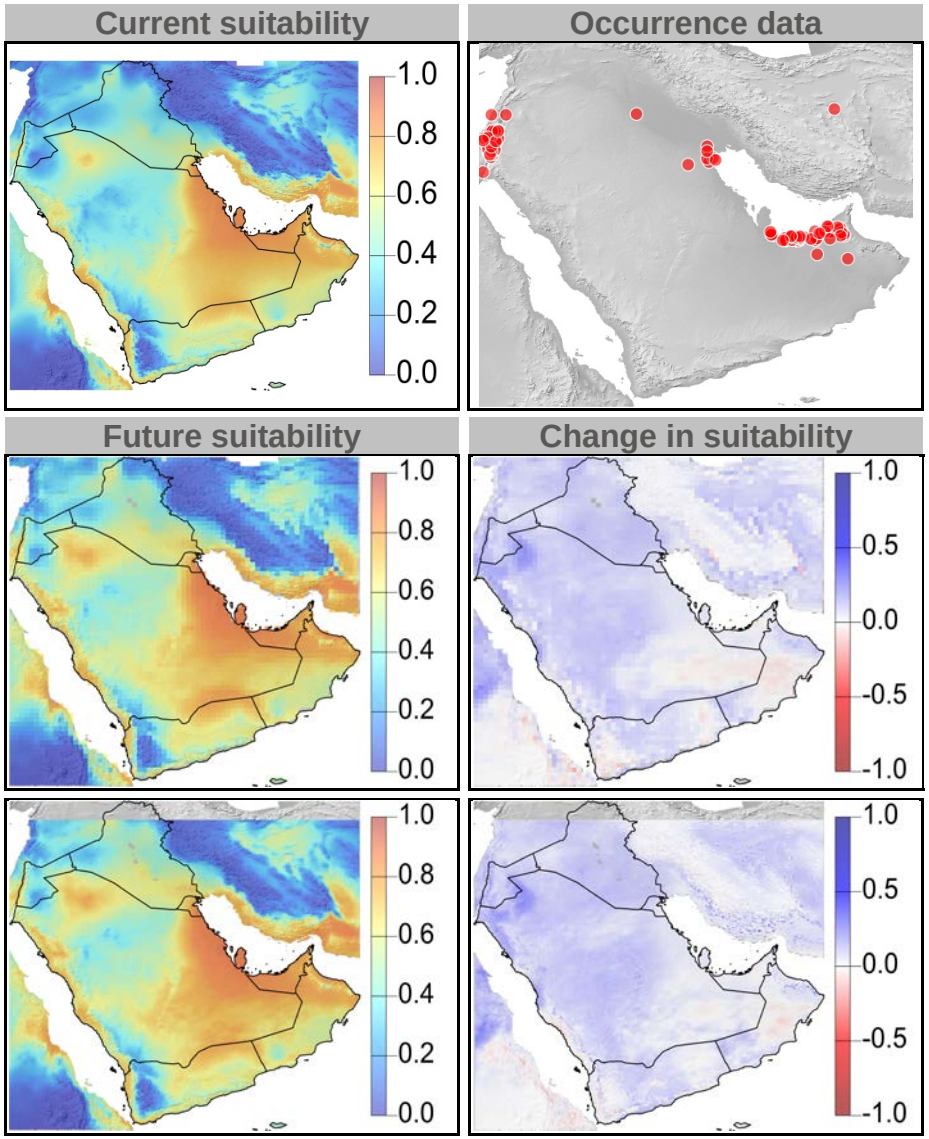

Figure 24: Current and future (2070) climate suitability for *Haloxylon salicornicum*, based on an ensemble of all future climate scenarios from the regional climate modeling effort at two spatial domains. Range and occurrence data shown for reference.

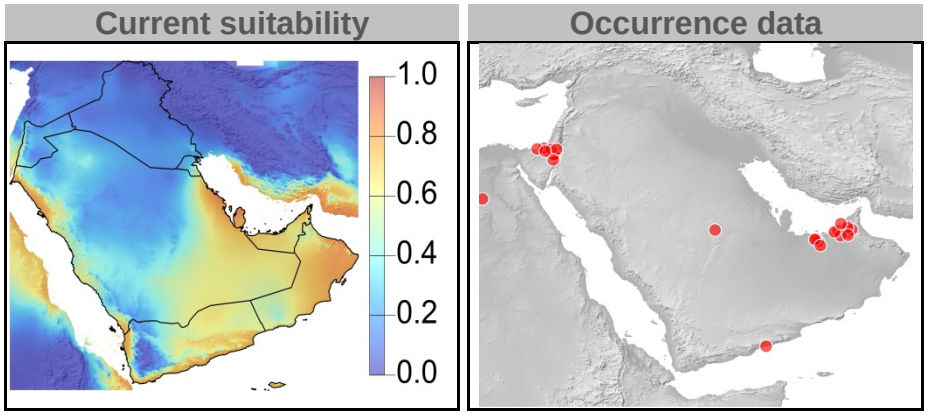

Figure 25: Current and future climate suitability for *Heliotropium digynum*, with associated uncertainty and change in range area based on an ensemble of all future climate scenarios. Range and occurrence data shown for reference.

Figure 26: Current and future (2070) climate suitability for *Heliotropium digynum*, based on an ensemble of all future climate scenarios from the regional climate modeling effort at two spatial domains. Range and occurrence data shown for reference.

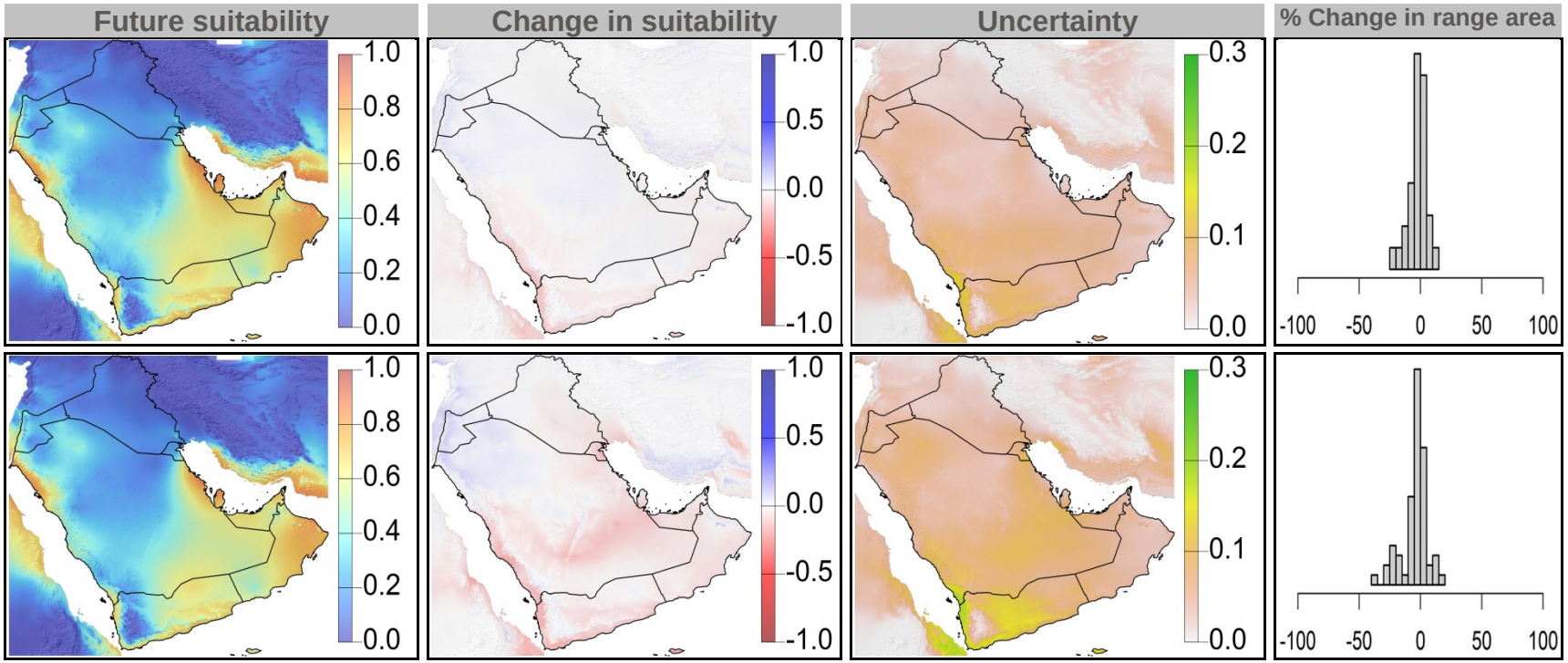

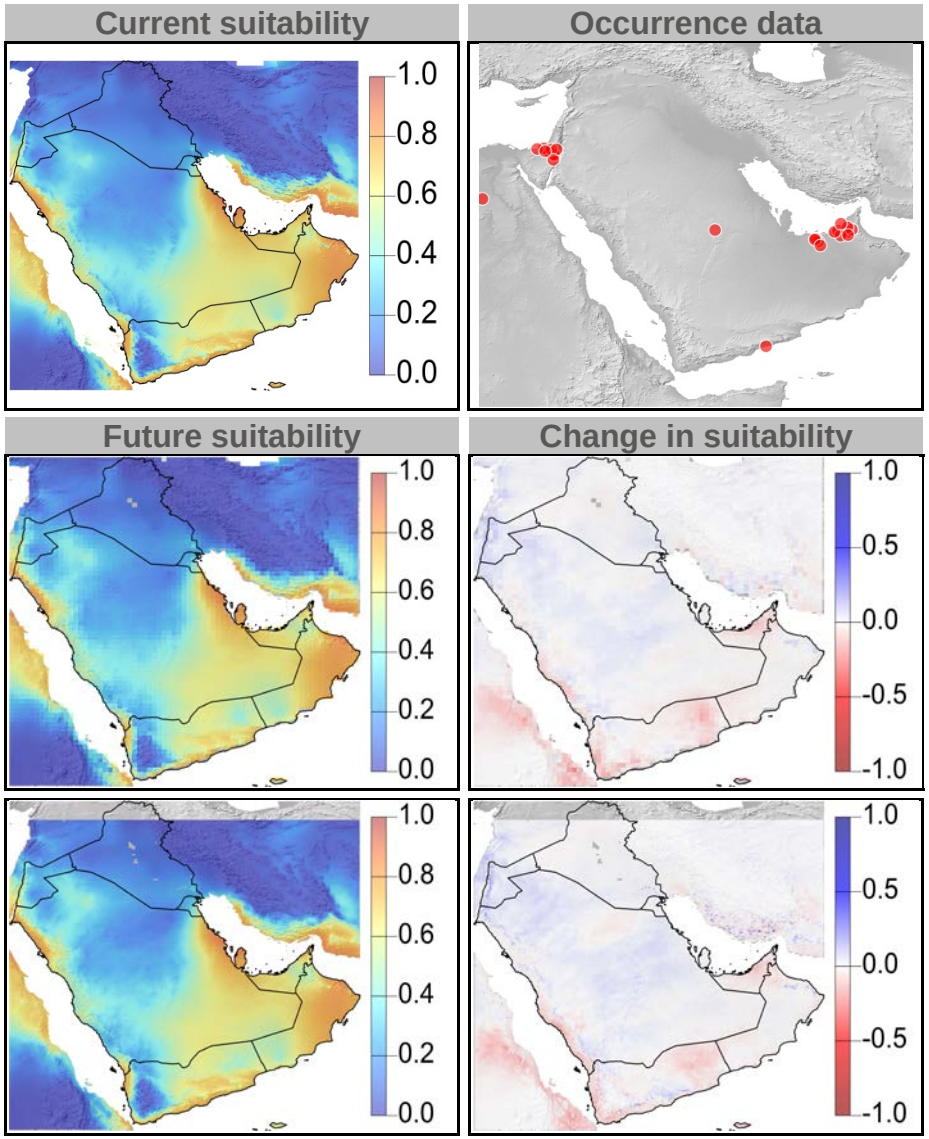

Figure 27: Current and future climate suitability for *Juniperus procera*, with associated uncertainty and

change in range area based on an ensemble of all future climate scenarios. Range and occurrence data shown for reference.

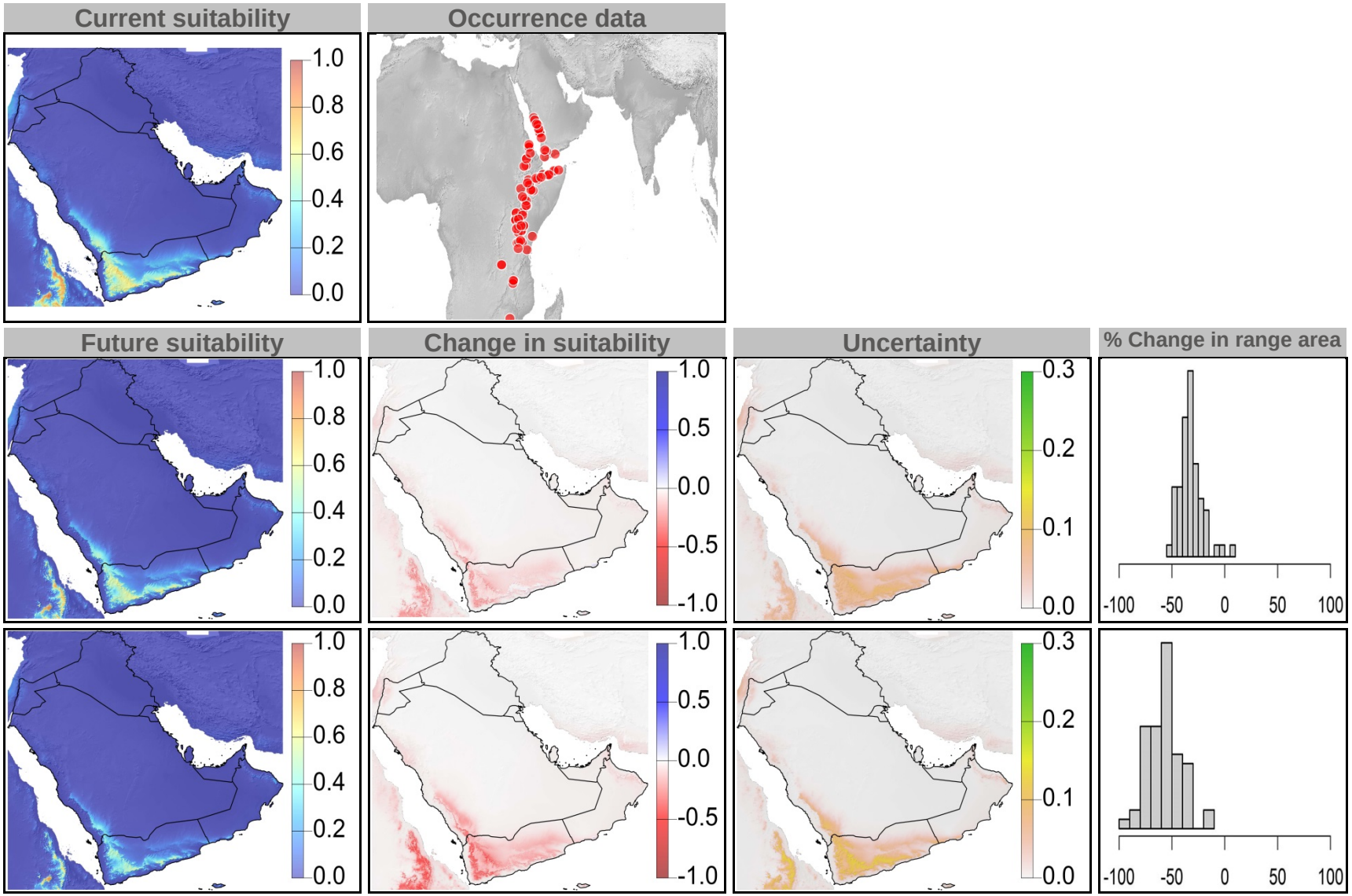

Figure 28: Current and future (2070) climate suitability for *Juniperus procera*, based on an ensemble of all future climate scenarios from the regional climate modeling effort at two spatial domains. Range and occurrence data shown for reference.

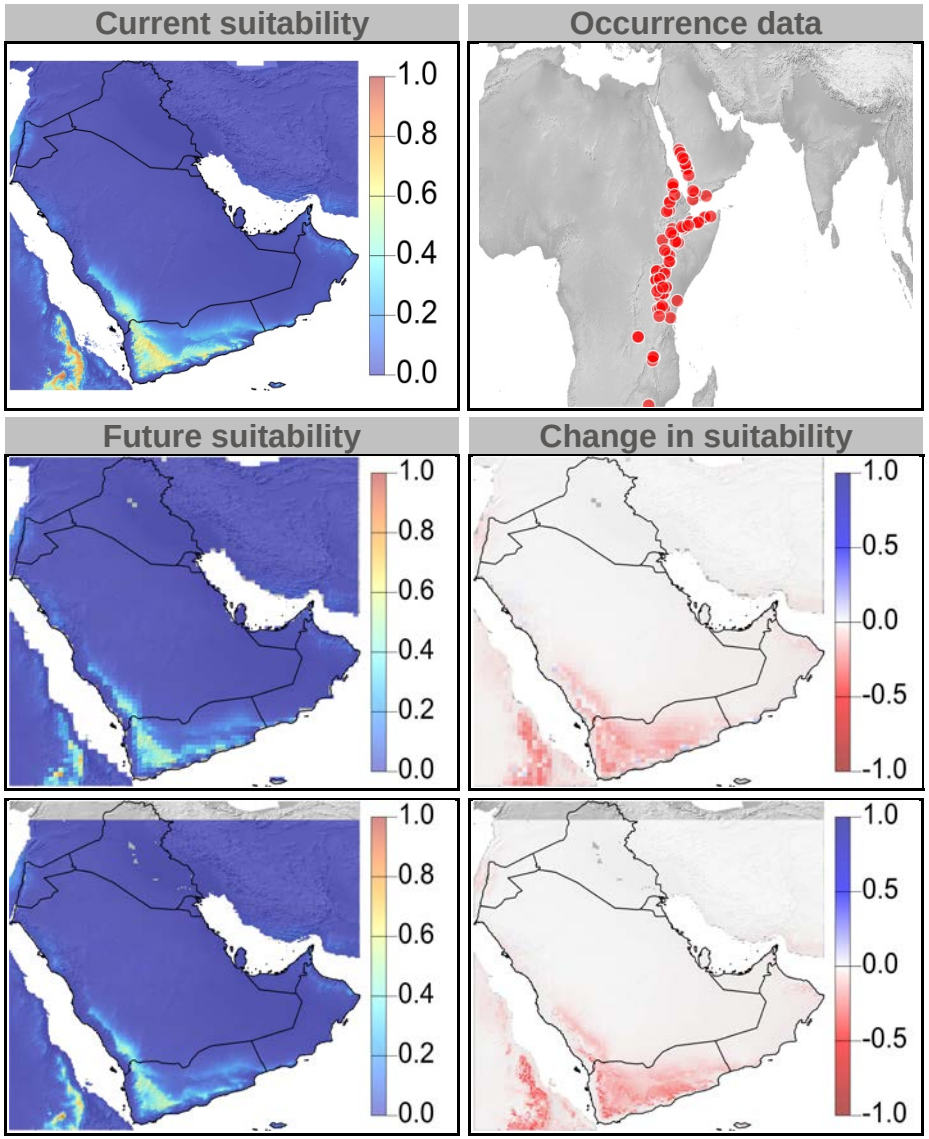

Figure 29: Current and future climate suitability for *Limeum arabicum*, with associated uncertainty and change in range area based on an ensemble of all future climate scenarios. Range and occurrence data shown for reference.

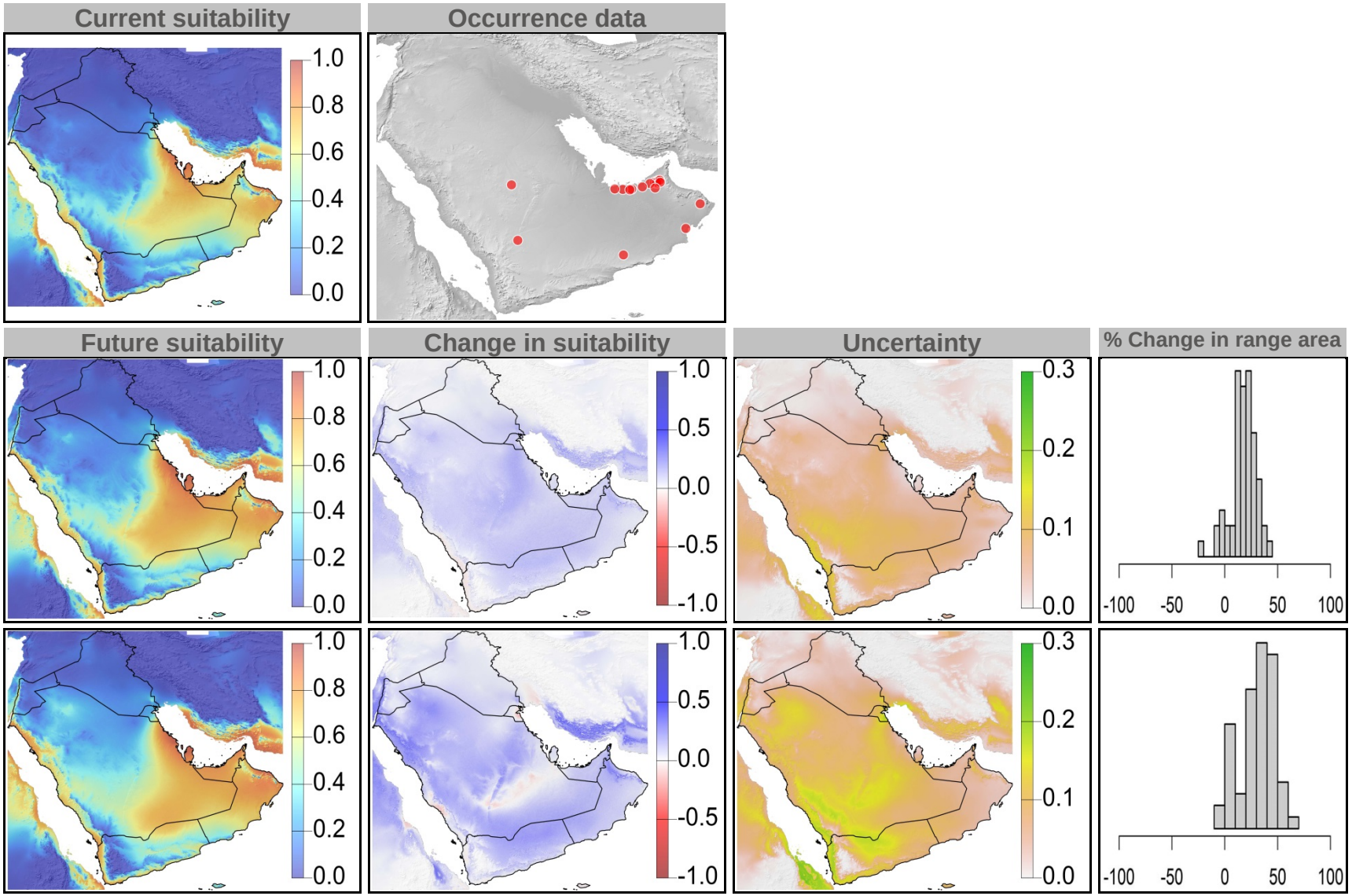

Figure 30: Current and future (2070) climate suitability for *Limeum arabicum*, based on an ensemble of all future climate scenarios from the regional climate modeling effort at two spatial domains. Range and occurrence data shown for reference.

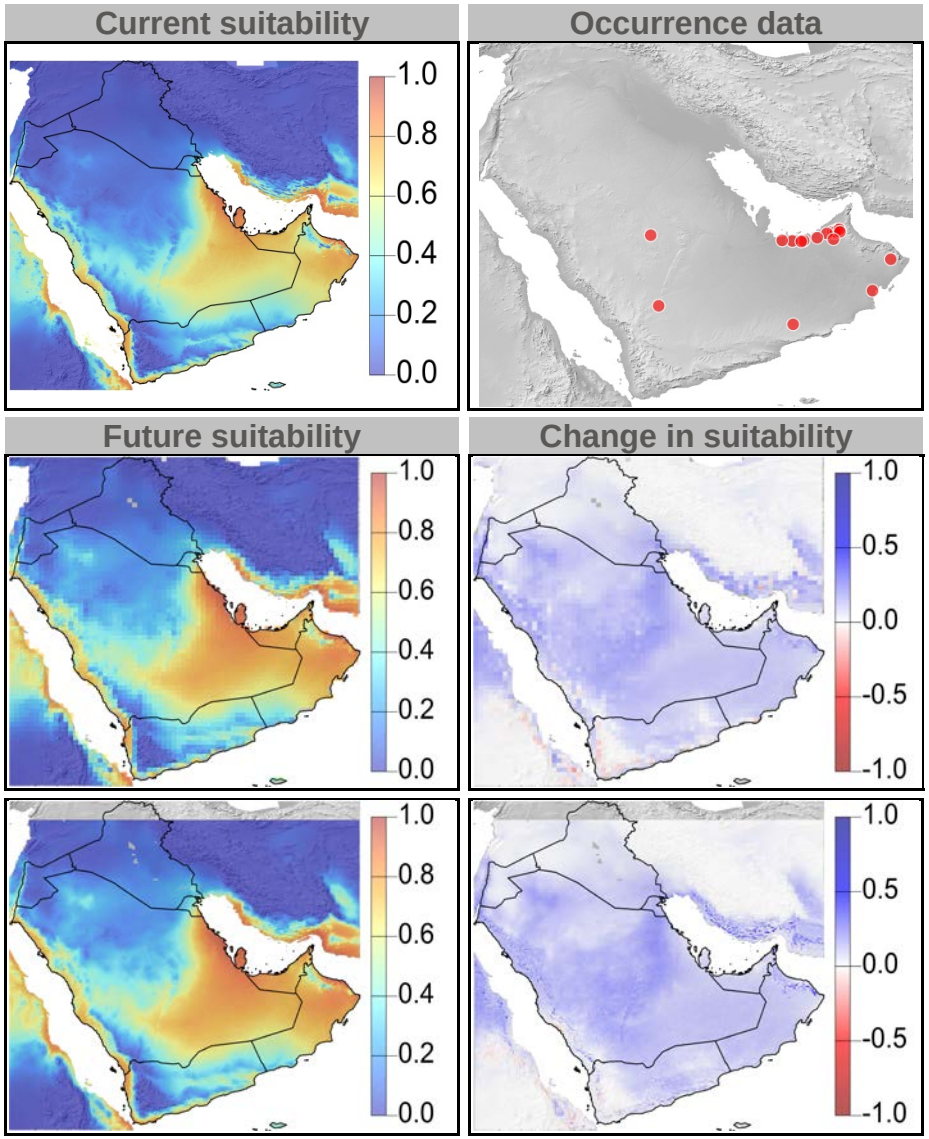

Figure 31: Current and future climate suitability for *Moringa peregrina*, with associated uncertainty and change in range area based on an ensemble of all future climate scenarios. Range and occurrence data shown for reference.

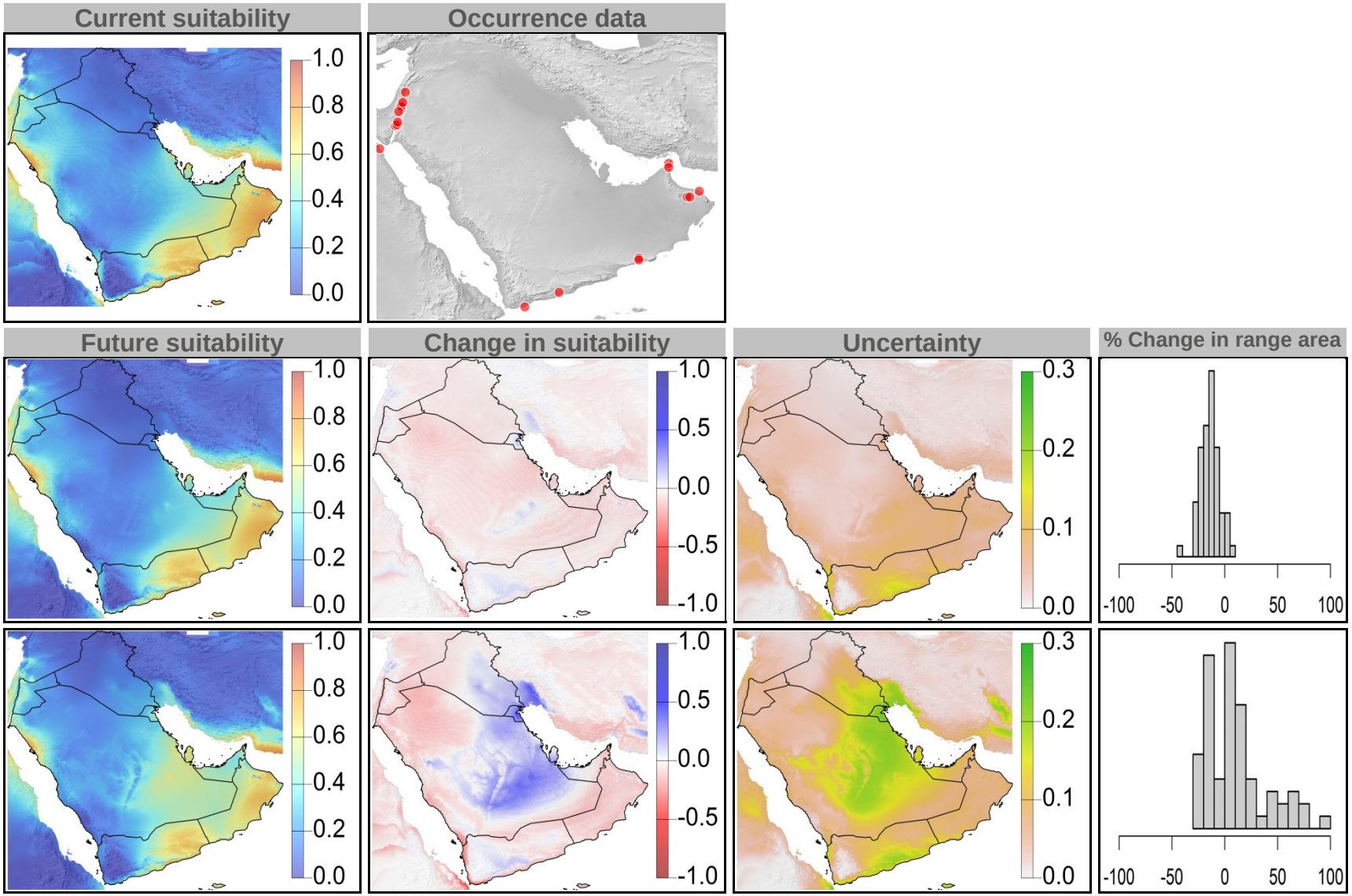

Figure 32: Current and future (2070) climate suitability for *Moringa peregrina*, based on an ensemble of all future climate scenarios from the regional climate modeling effort at two spatial domains. Range and occurrence data shown for reference.

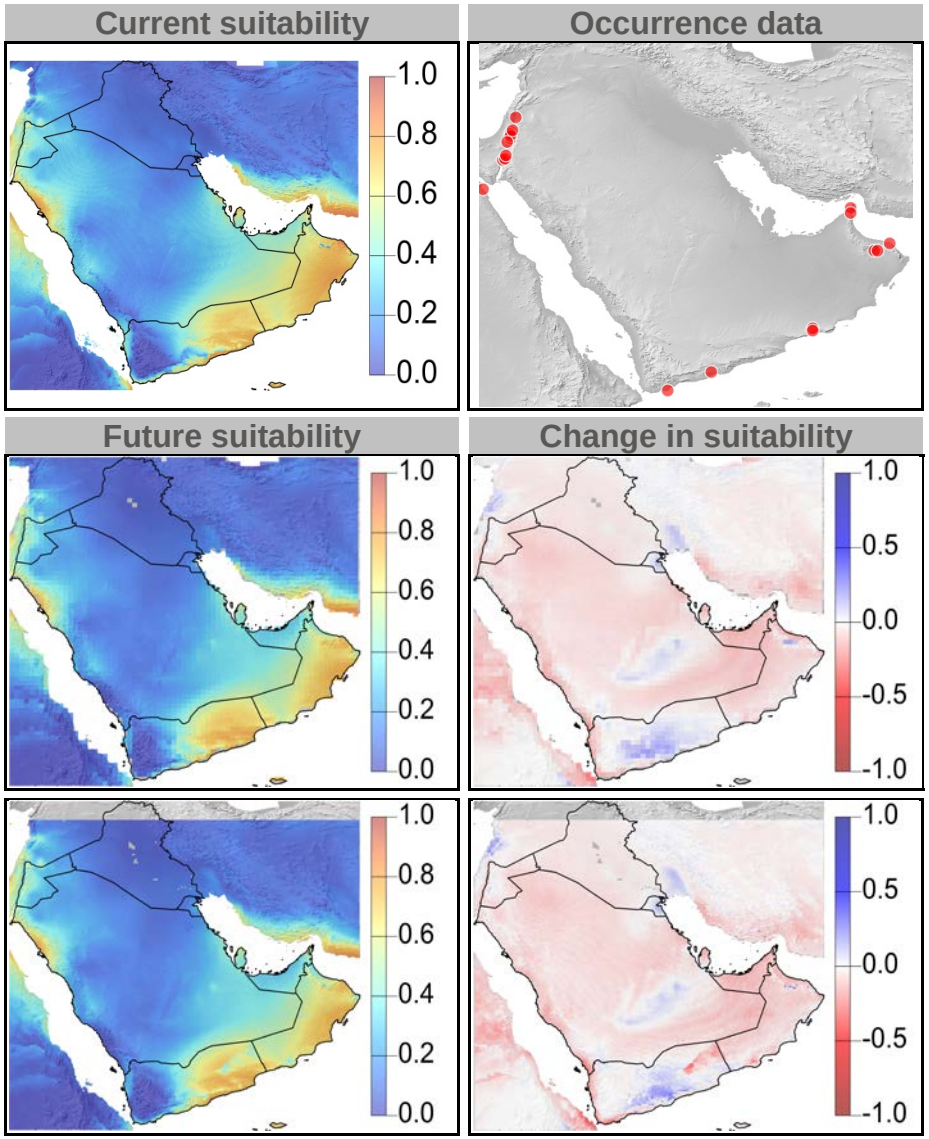

Figure 33: Current and future climate suitability for *Panicum turgidum*, with associated uncertainty and change in range area based on an ensemble of all future climate scenarios. Range and occurrence data shown for reference.

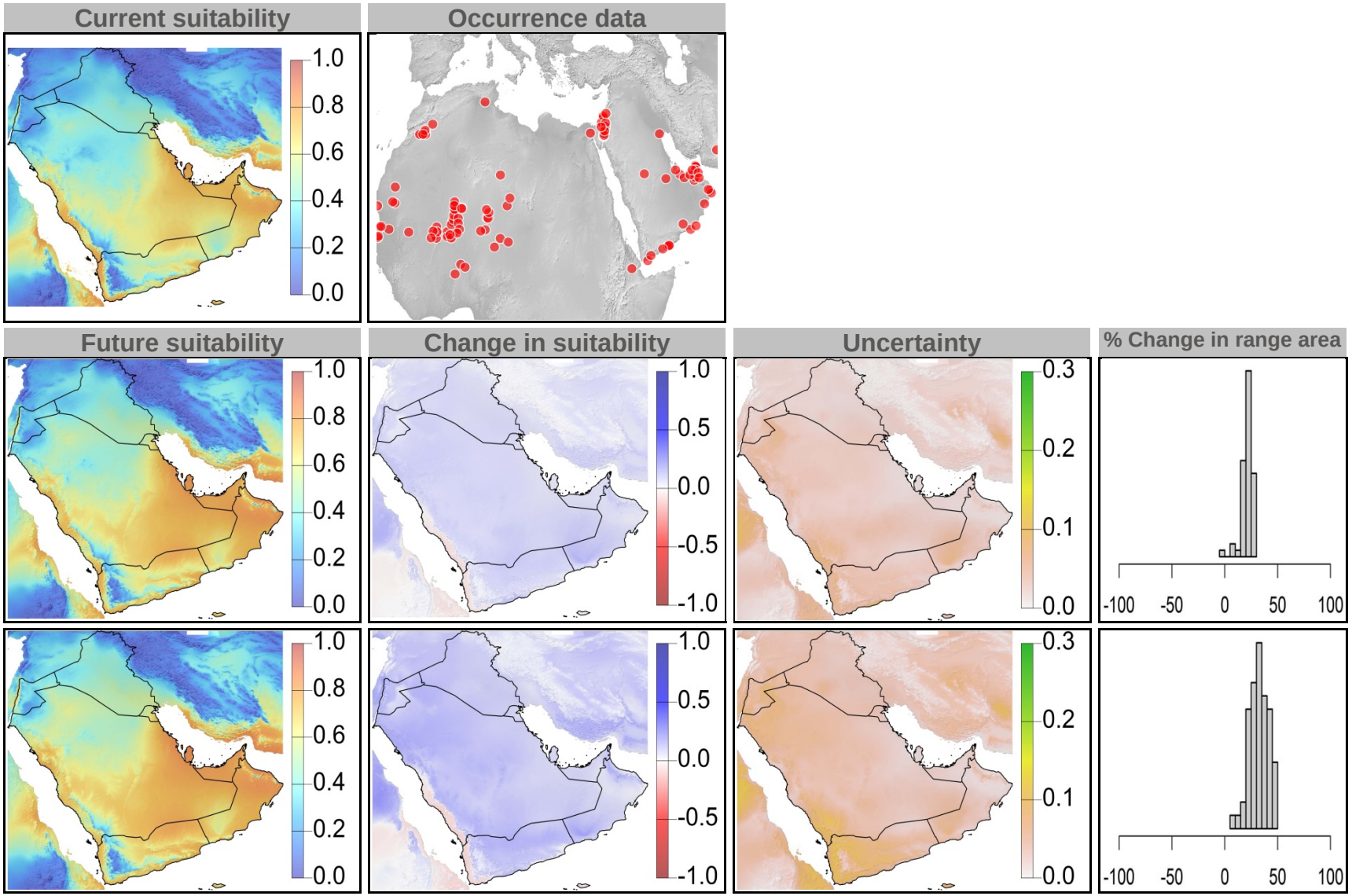

Figure 34: Current and future (2070) climate suitability for *Panicum turgidum*, based on an ensemble of all future climate scenarios from the regional climate modeling effort at two spatial domains. Range and occurrence data shown for reference.

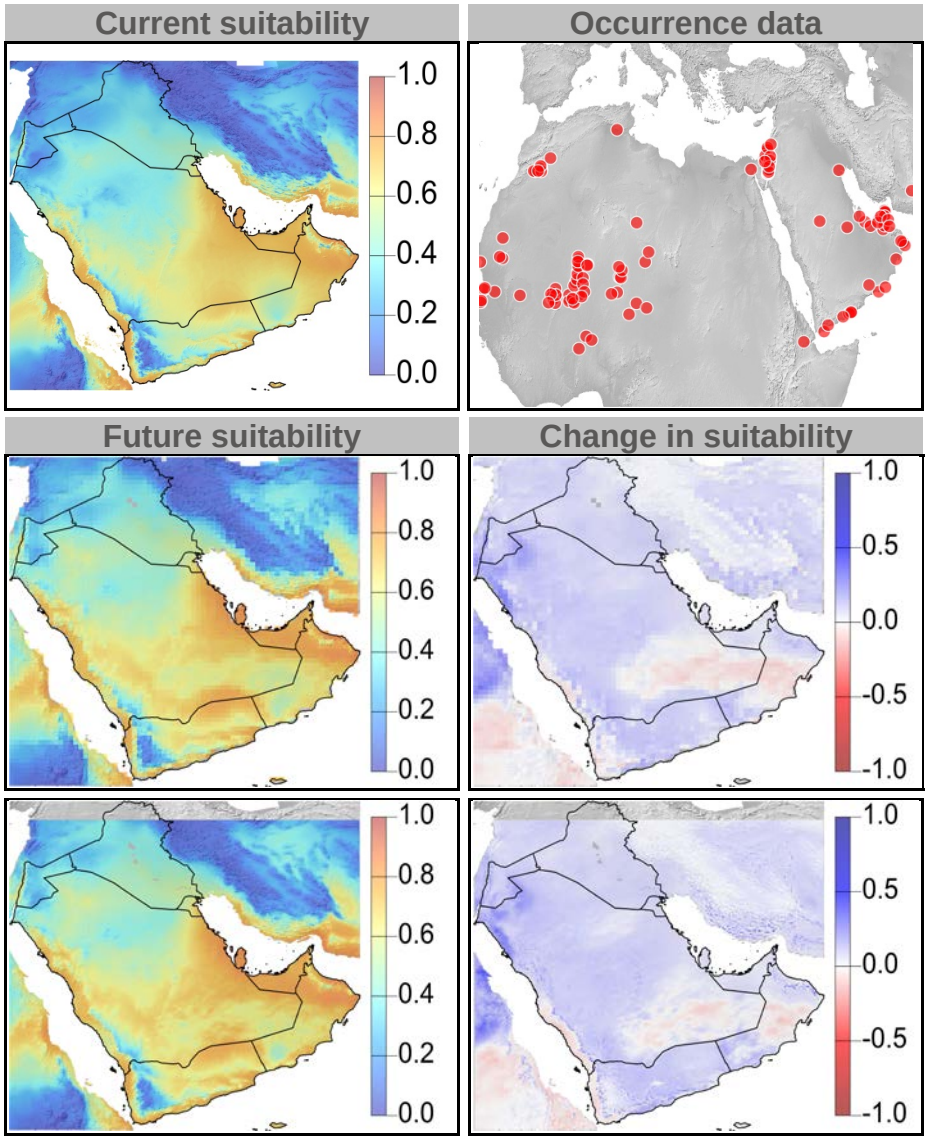

Figure 35: Current and future climate suitability for *Prosopis cineraria*, with associated uncertainty and change in range area based on an ensemble of all future climate scenarios. Range and occurrence data shown for reference.

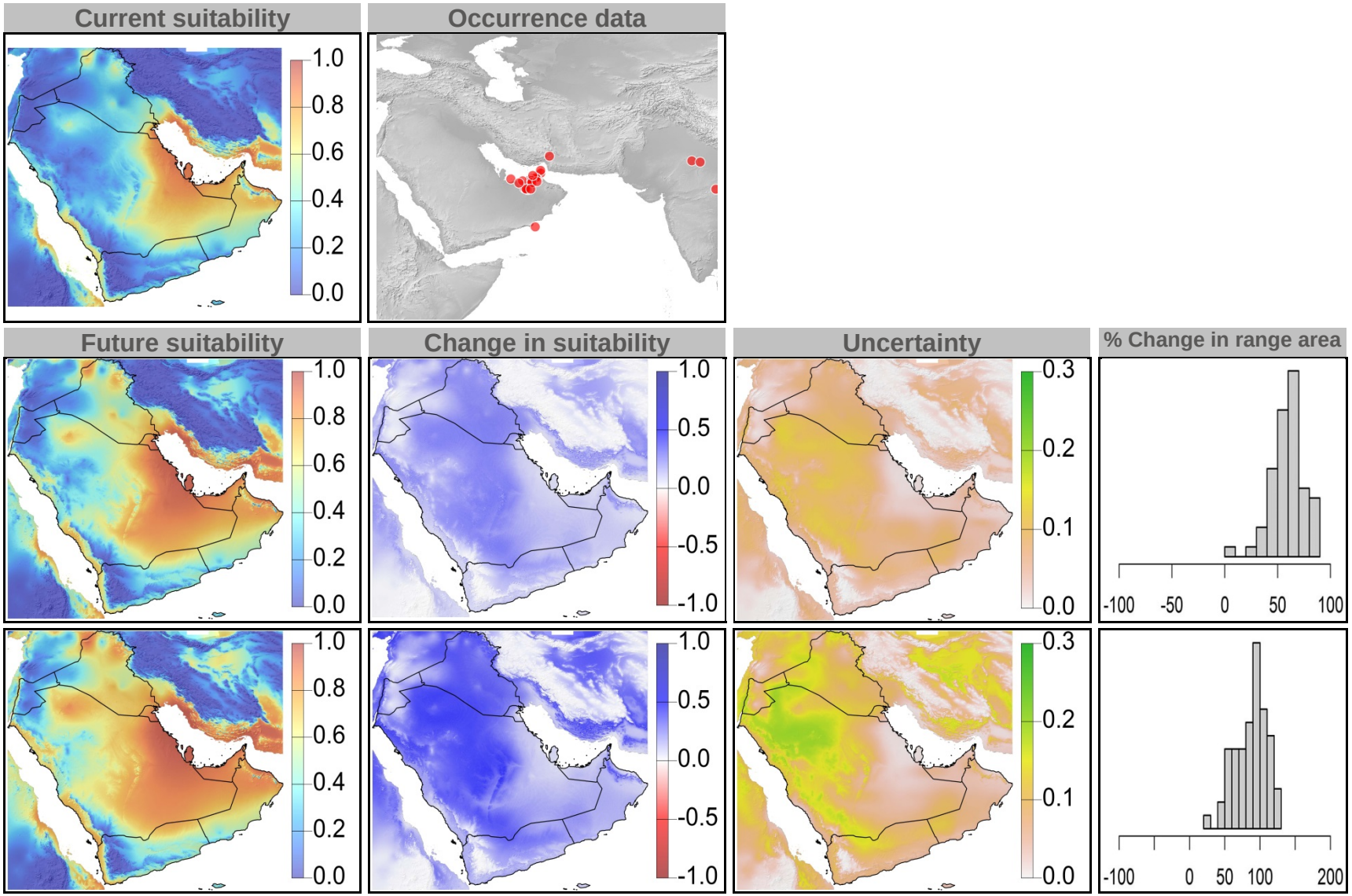

Figure 36: Current and future (2070) climate suitability for *Prosopis cineraria*, based on an ensemble of all future climate scenarios from the regional climate modeling effort at two spatial domains. Range and occurrence data shown for reference.

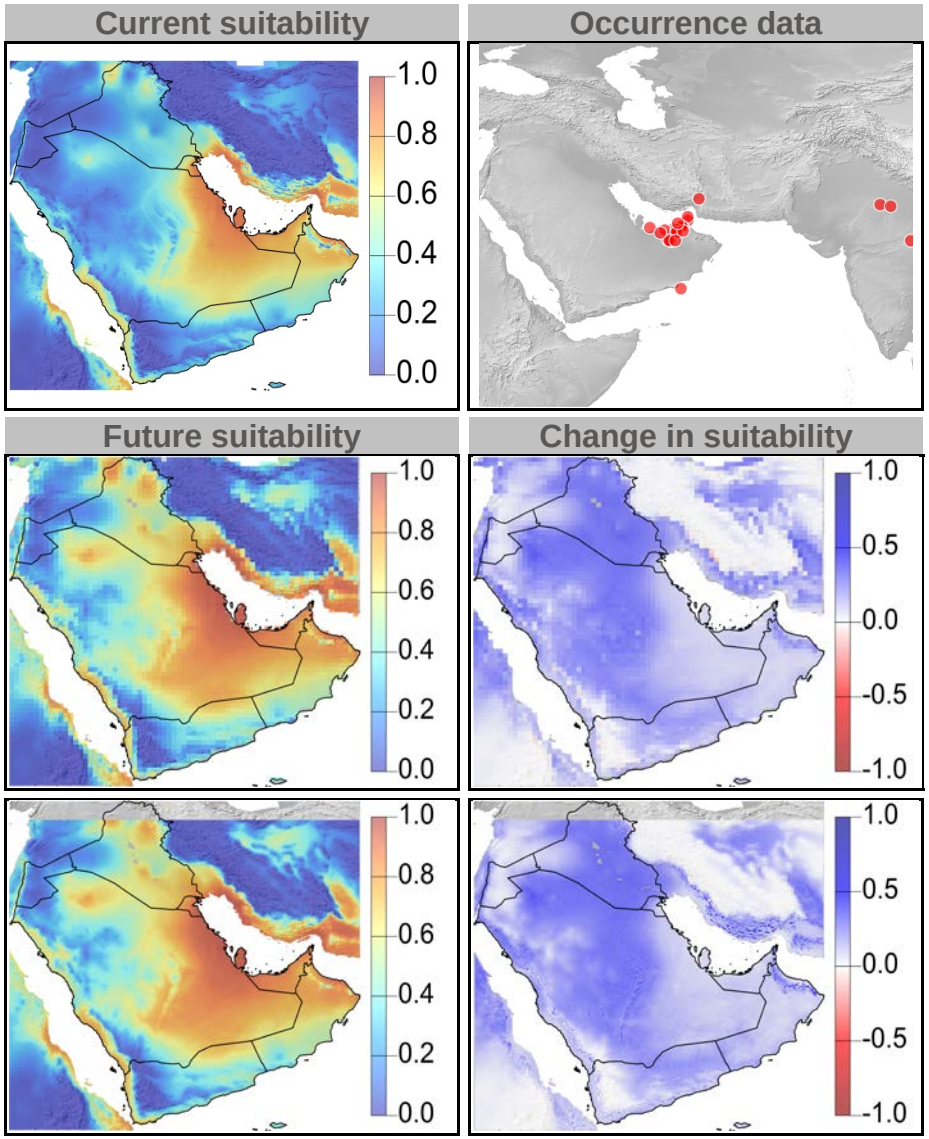

Figure 37: Current and future climate suitability for *Rhazya stricta*, with associated uncertainty and change in range area based on an ensemble of all future climate scenarios. Range and occurrence data shown for reference.

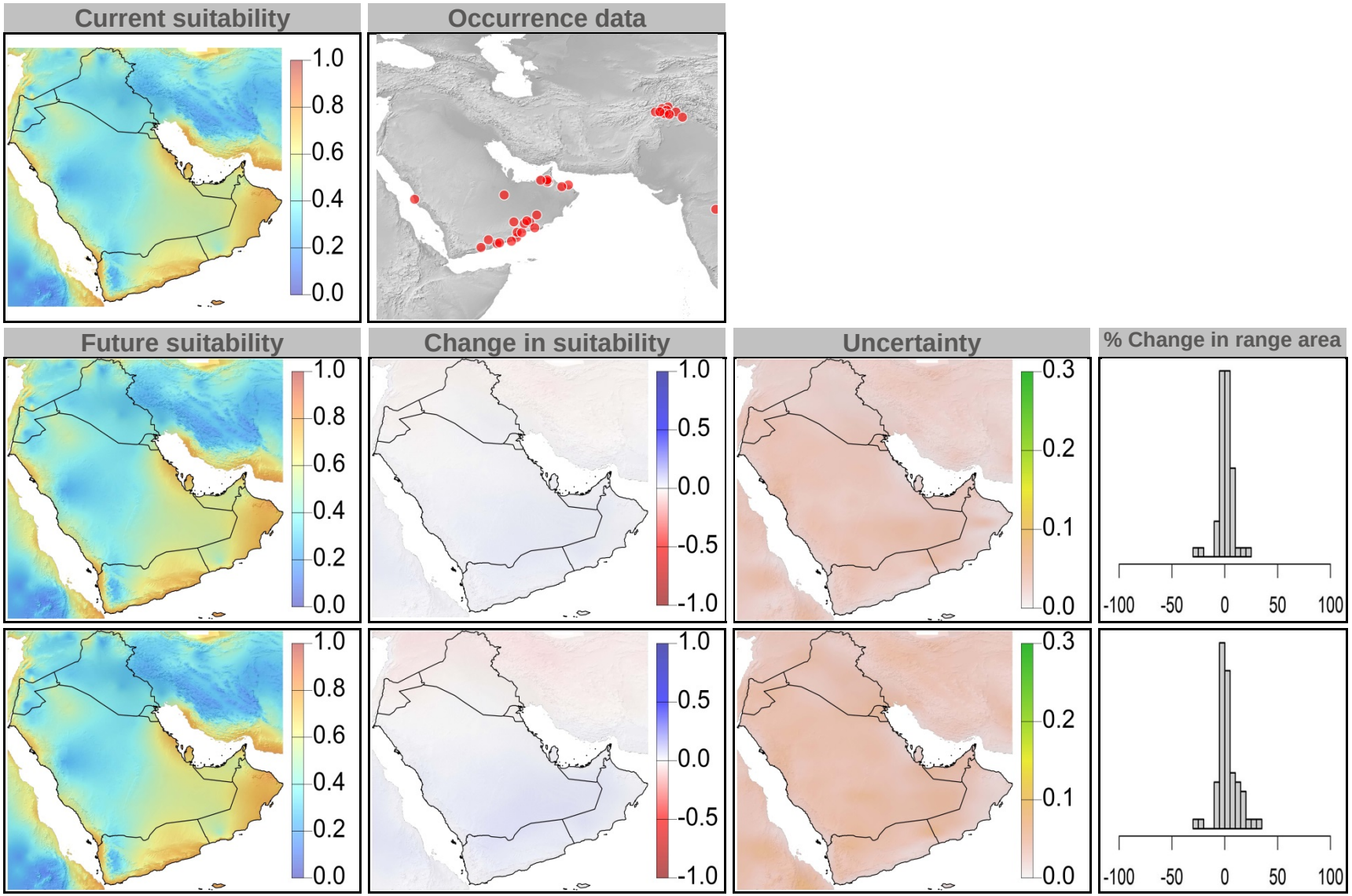

Figure 38: Current and future (2070) climate suitability for *Rhazya stricta*, based on an ensemble of all future climate scenarios from the regional climate modeling effort at two spatial domains. Range and occurrence data shown for reference.

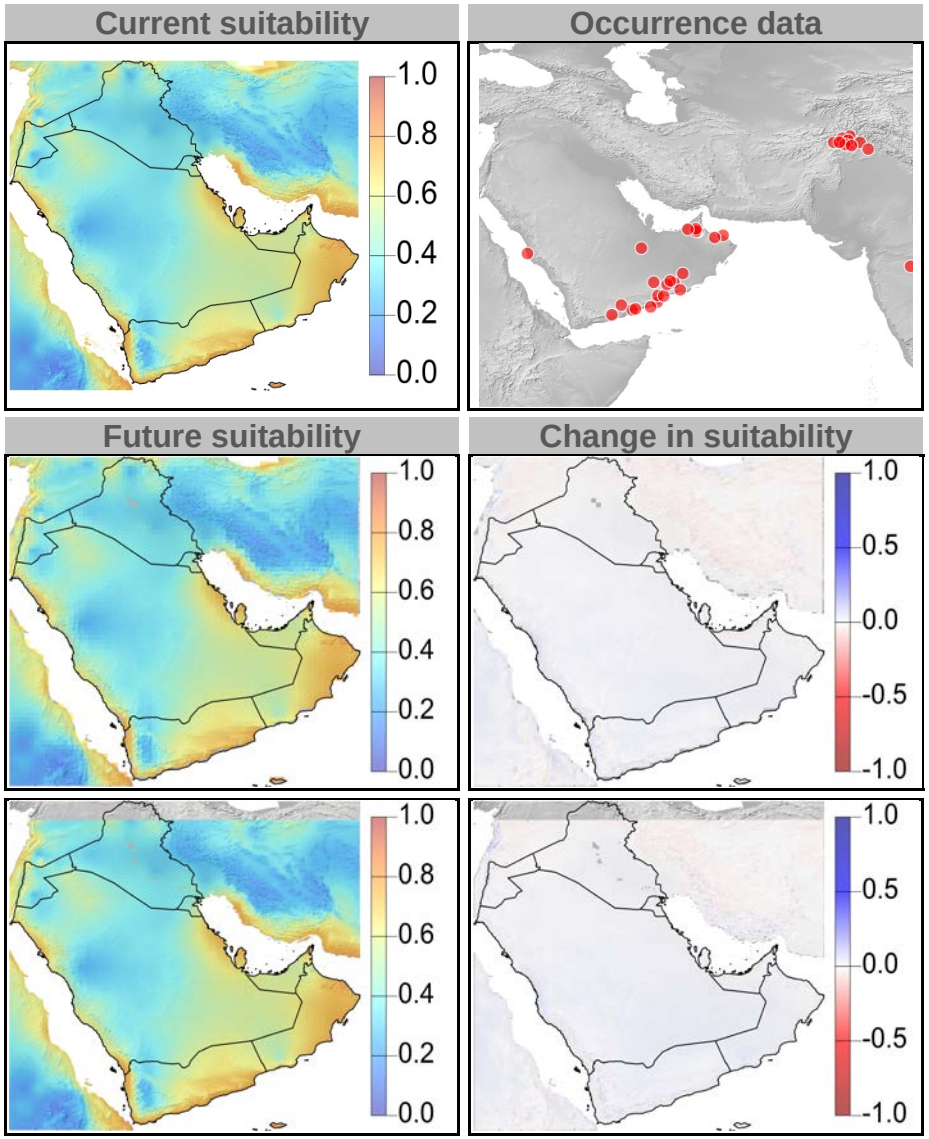

Figure 39: Current and future climate suitability for *Ziziphus spina-christi*, with associated uncertainty and change in range area based on an ensemble of all future climate scenarios. Range and occurrence data shown for reference.

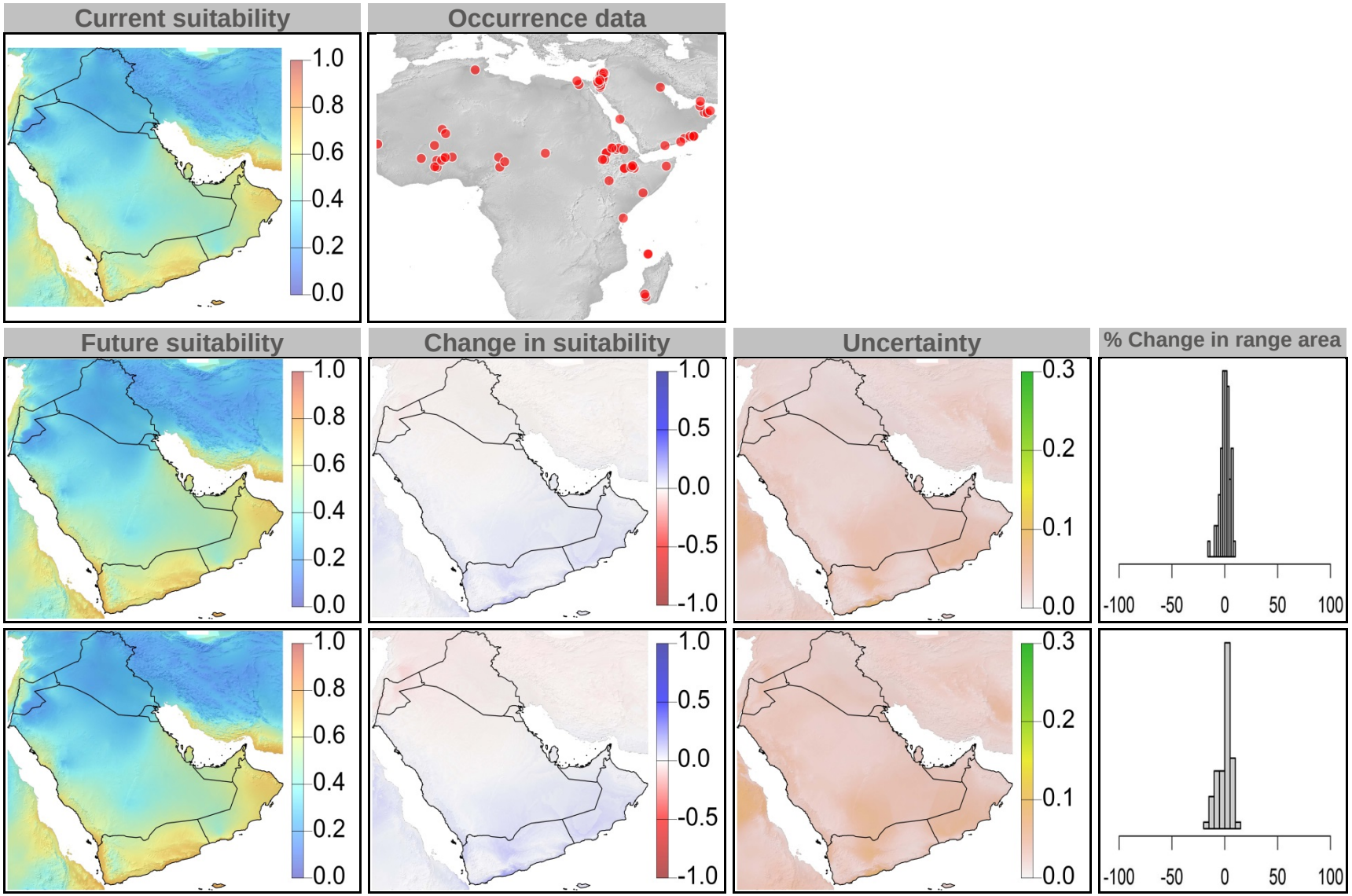

Figure 40: Current and future (2070) climate suitability for *Ziziphus spina-christi*, based on an ensemble of all future climate scenarios from the regional climate modeling effort at two spatial domains. Range and occurrence data shown for reference.

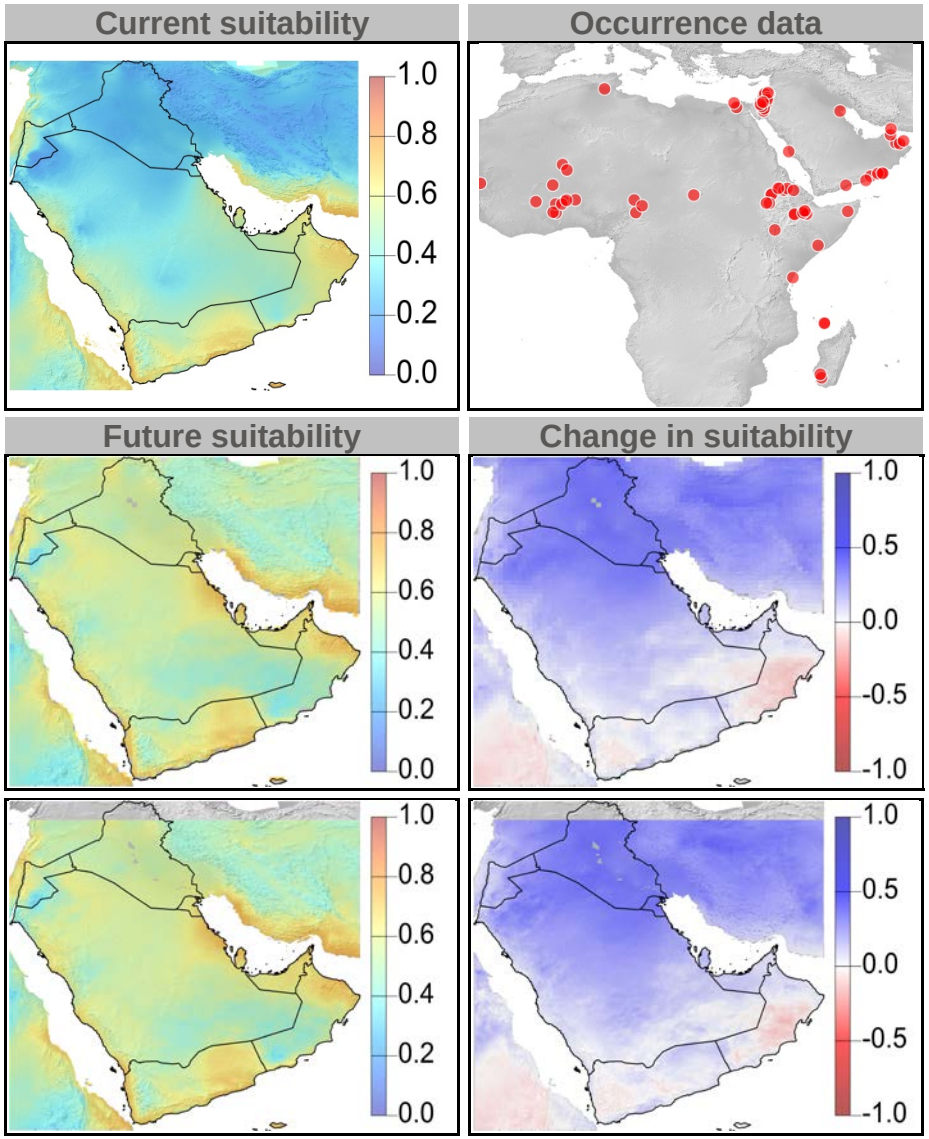

AGEDI
مبادرة أبوظبي العالمية للبيانات البيئية
Abu Dhabi Global Environmental Data Initiative

Annex IX – MaxEnt results combined across all priority reptile species for RCP4.5 and RCP8.5

Climate Change Research Group

University of Maryland
CENTER FOR ENVIRONMENTAL SCIENCE

Figure 1: Current and future climate suitability for *Bunopus tuberculatus*, with associated uncertainty and change in range area based on an ensemble of all future climate scenarios. Range and occurrence data shown for reference.

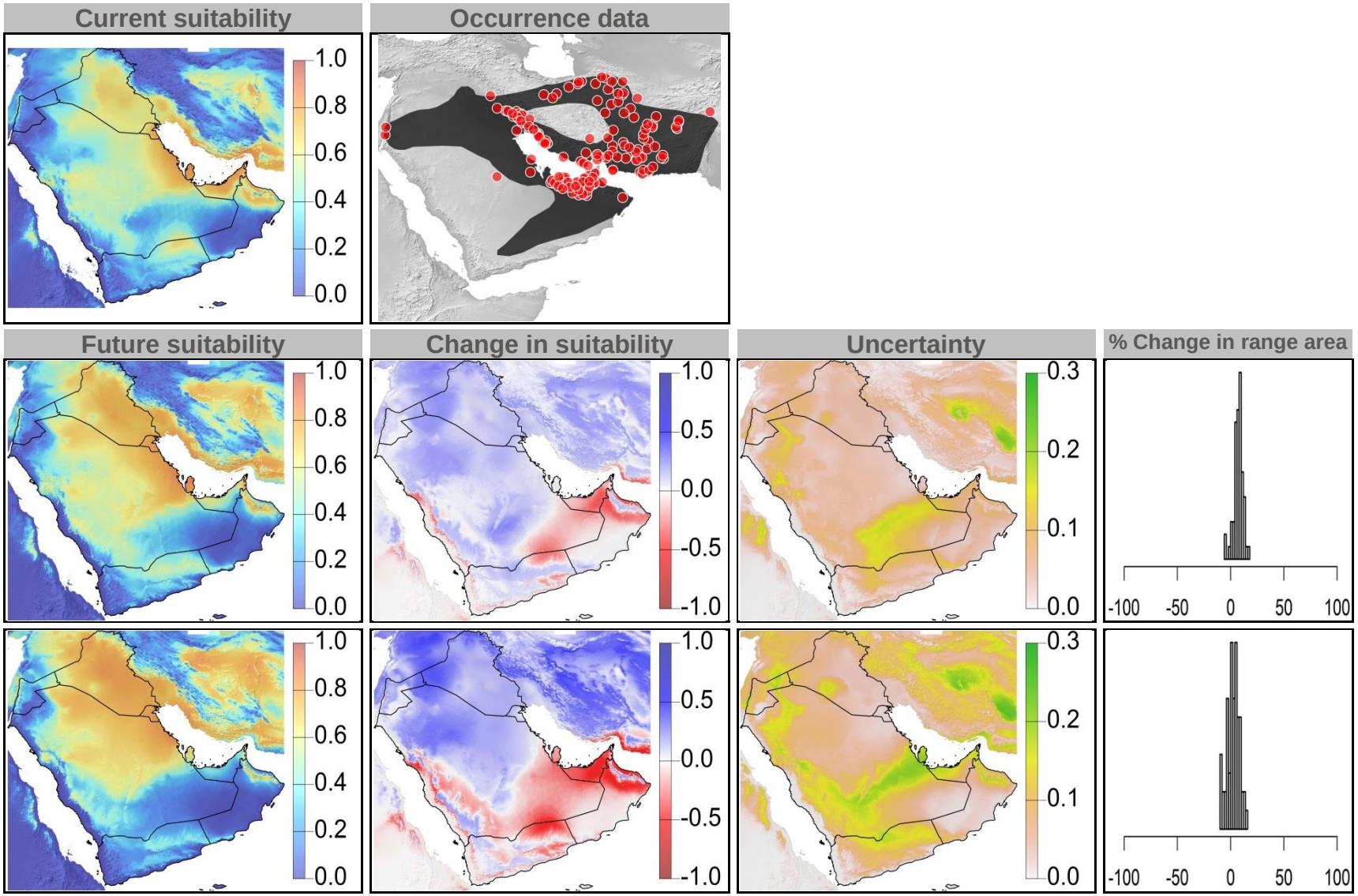

Figure 2: Current and future (2070) climate suitability for *Bunopus tuberculatus*, based on an ensemble of all future climate scenarios from the regional climate modeling effort at two spatial domains. Range and occurrence data shown for reference.

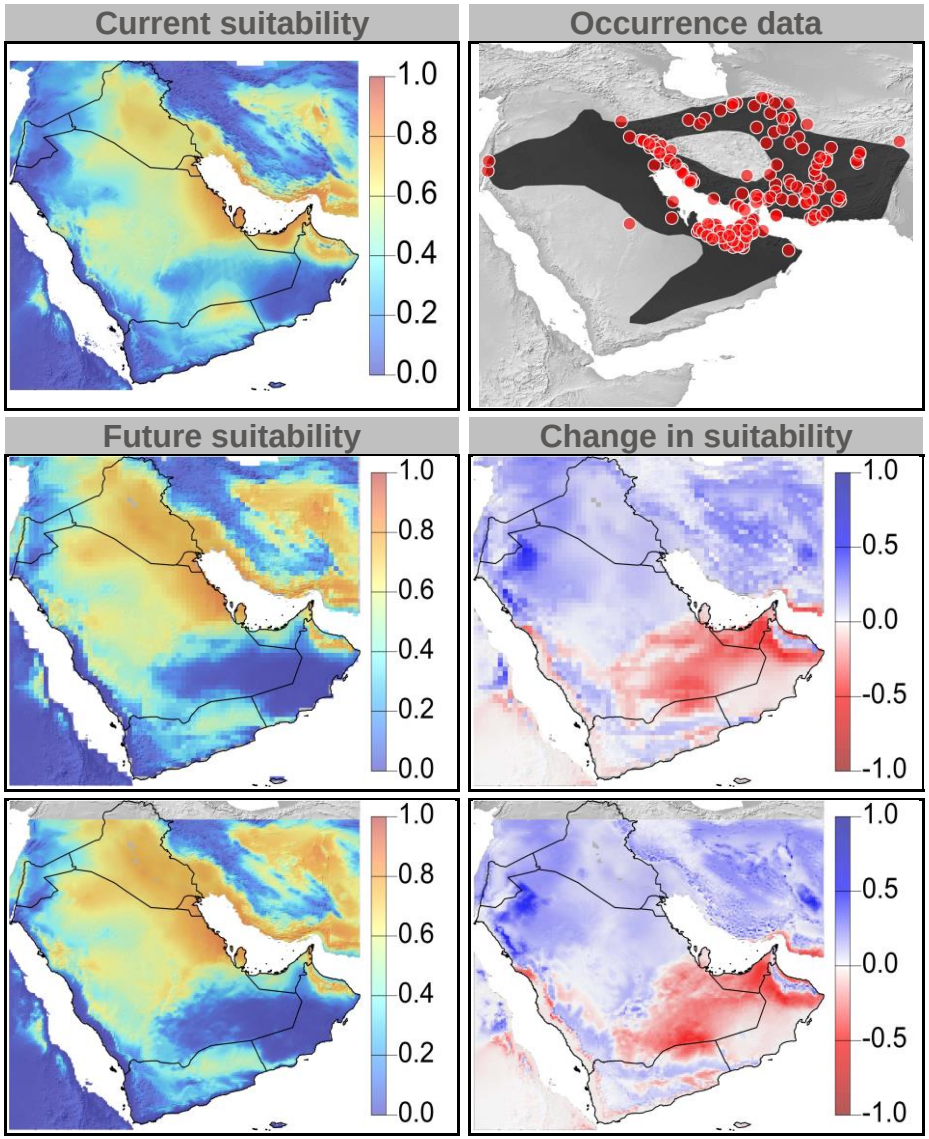

Figure 3: Current and future climate suitability for *Cerastes cerastes*, with associated uncertainty and change in range area based on an ensemble of all future climate scenarios. Range and occurrence data shown for reference.

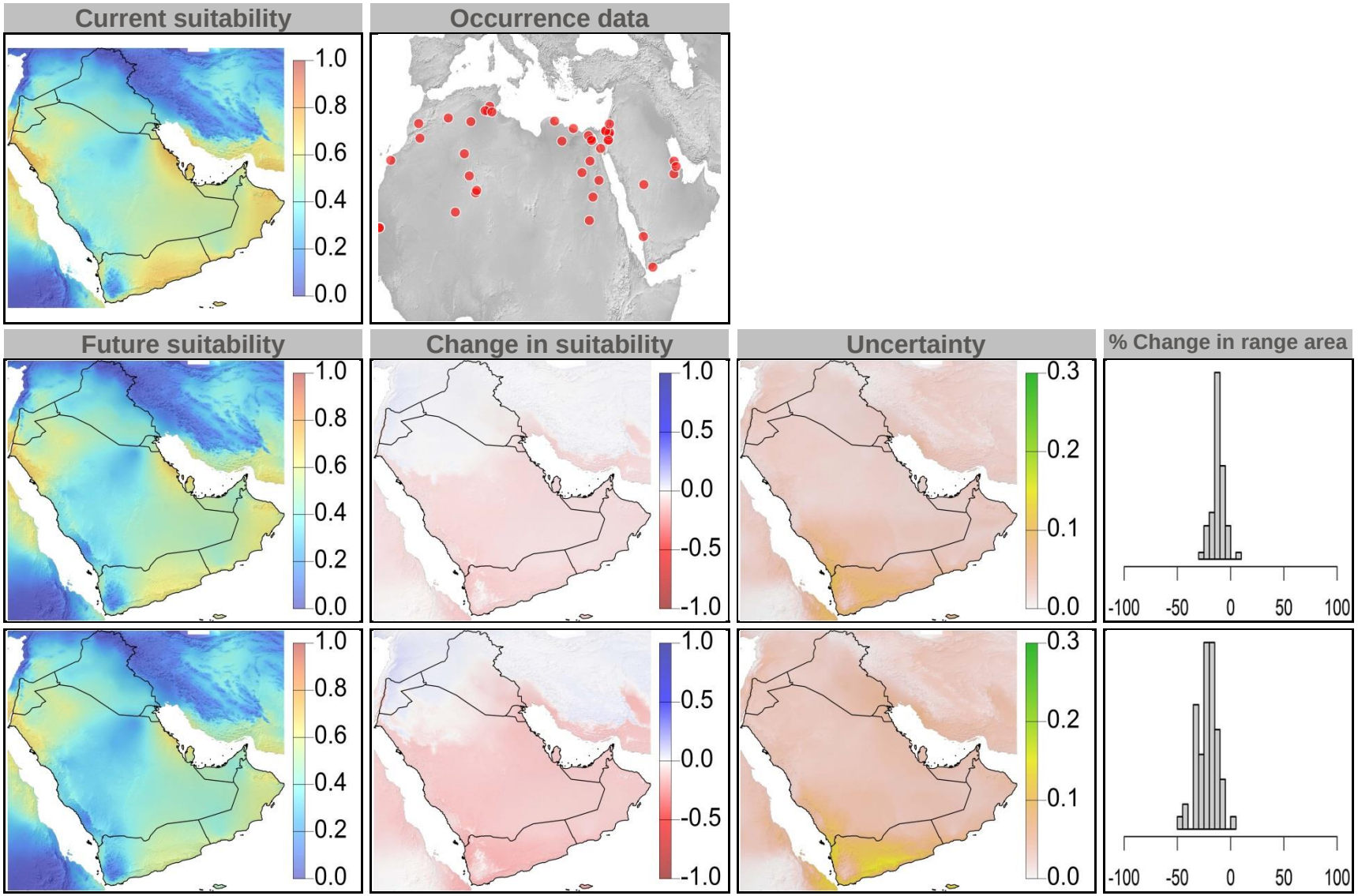

Figure 4: Current and future (2070) climate suitability for *Cerastes cerastes*, based on an ensemble of all future climate scenarios from the regional climate modeling effort at two spatial domains. Range and occurrence data shown for reference.

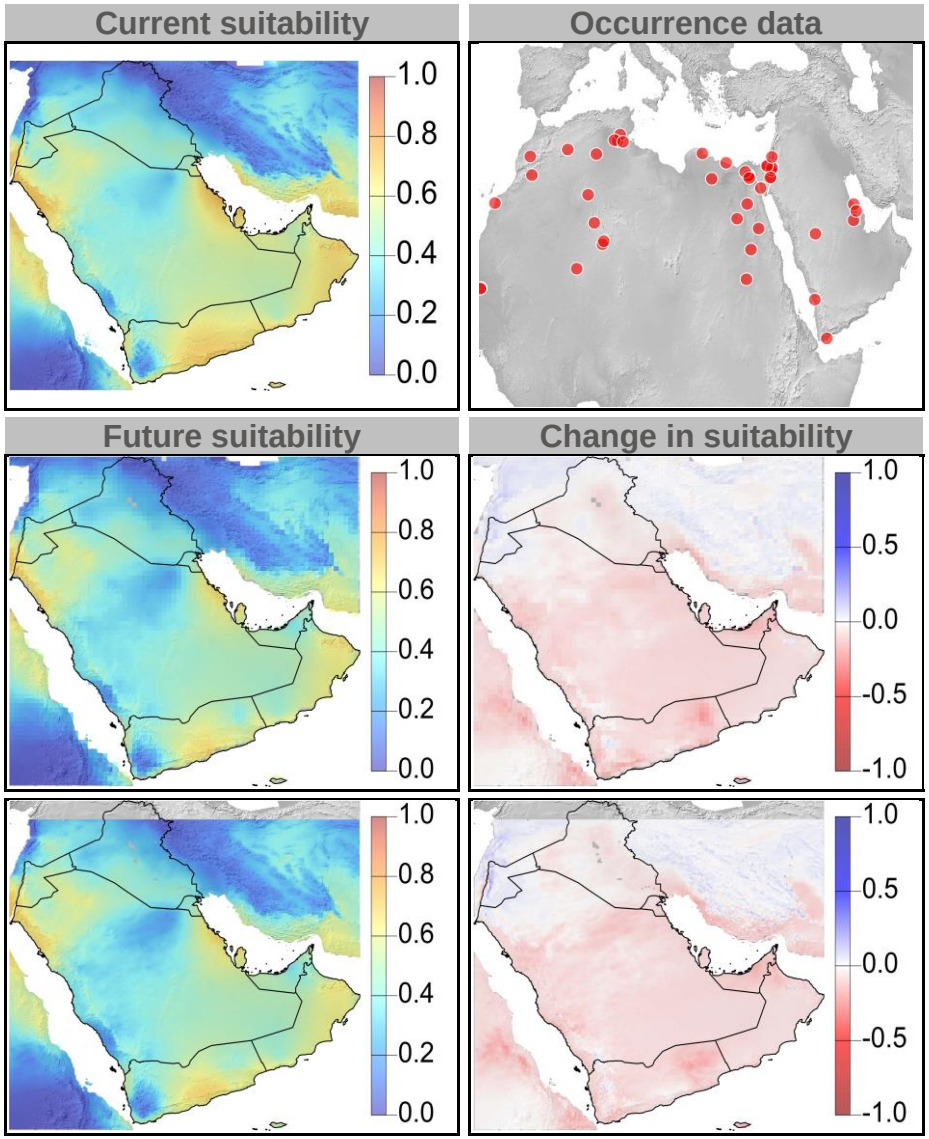

Figure 5: Current and future climate suitability for *Chamaeleo chamaeleon*, with associated uncertainty and change in range area based on an ensemble of all future climate scenarios. Range and occurrence data shown for reference.

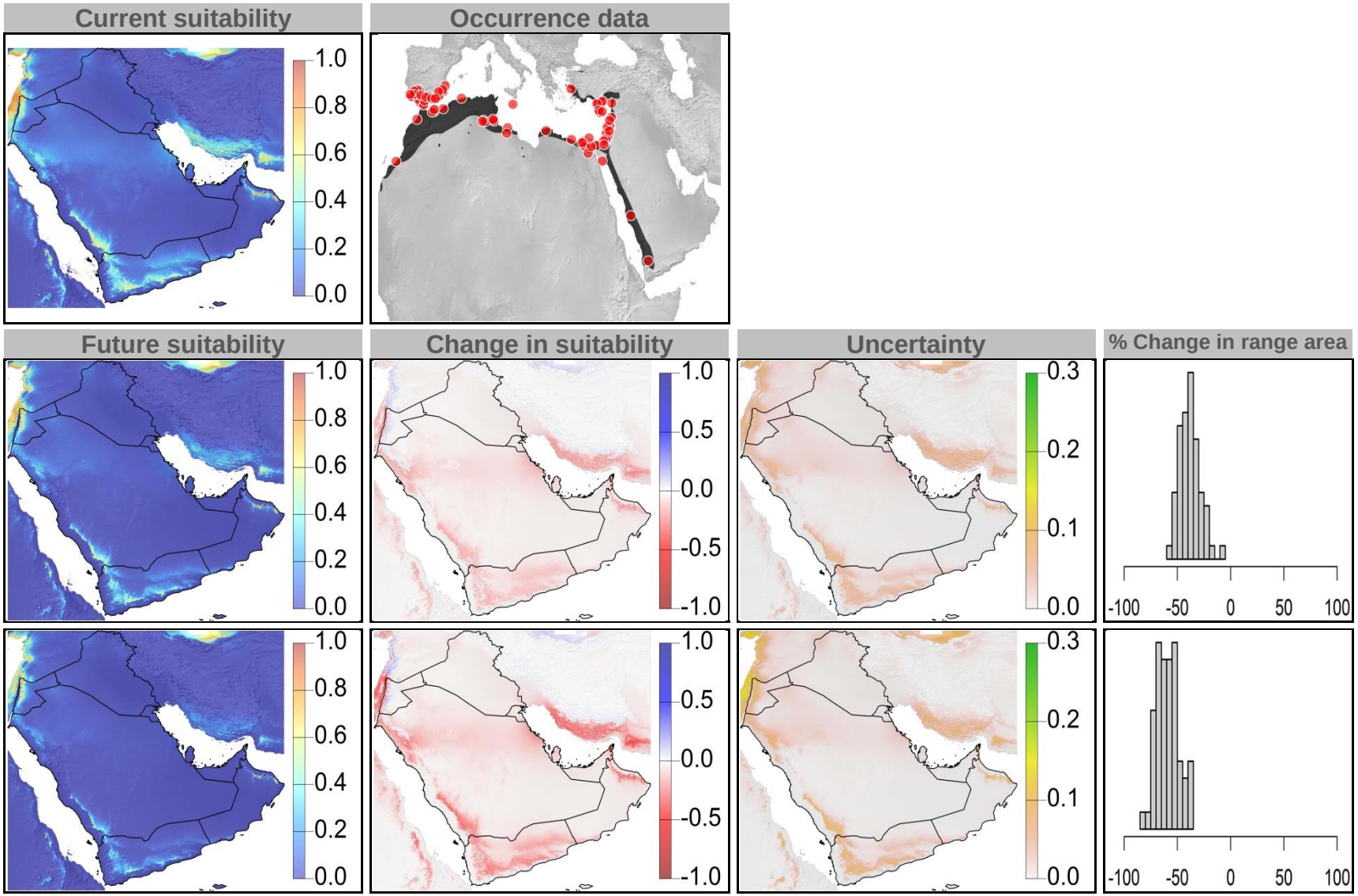

Figure 6: Current and future (2070) climate suitability for *Chamaeleo chamaeleon*, based on an ensemble of all future climate scenarios from the regional climate modeling effort at two spatial domains. Range and occurrence data shown for reference.

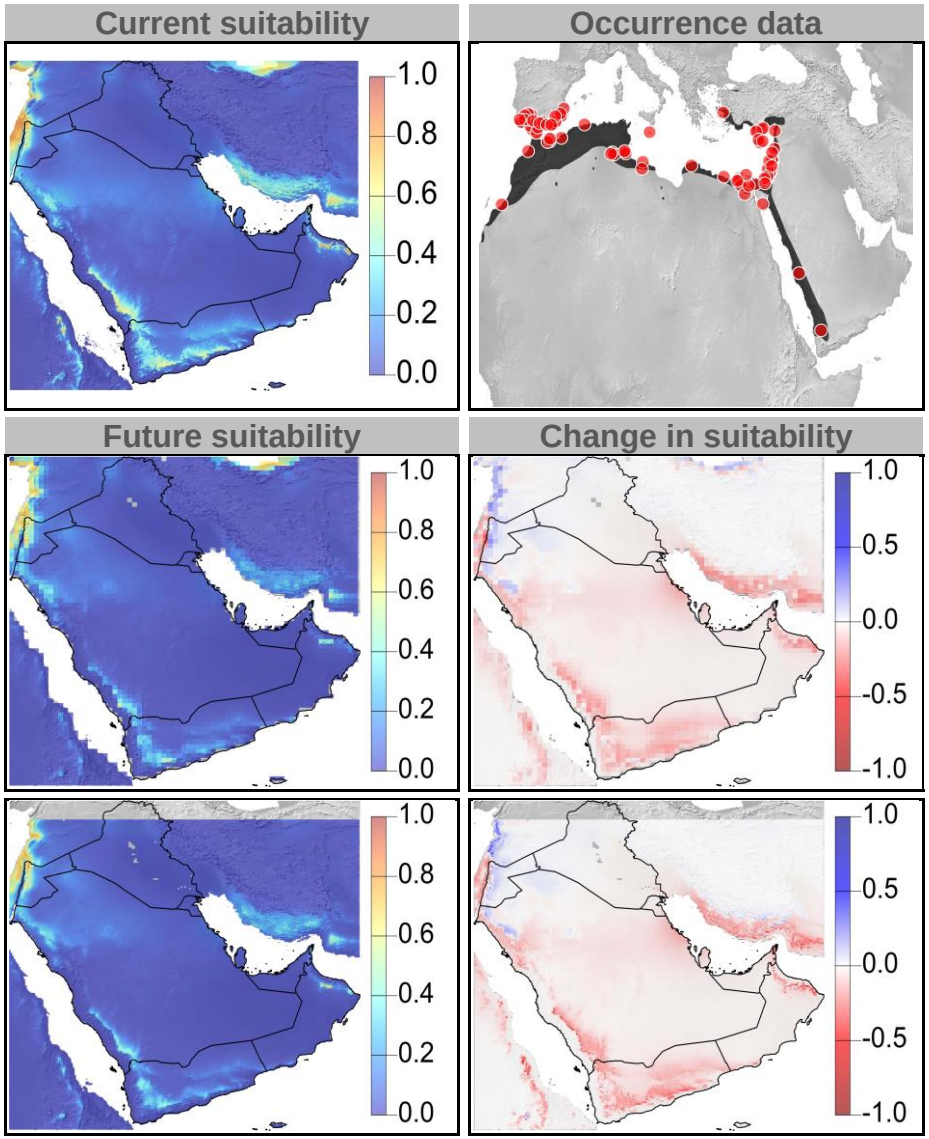

Figure 7: Current and future climate suitability for *Cyrtopodion scabrum*, with associated uncertainty and change in range area based on an ensemble of all future climate scenarios. Range and occurrence data shown for reference.

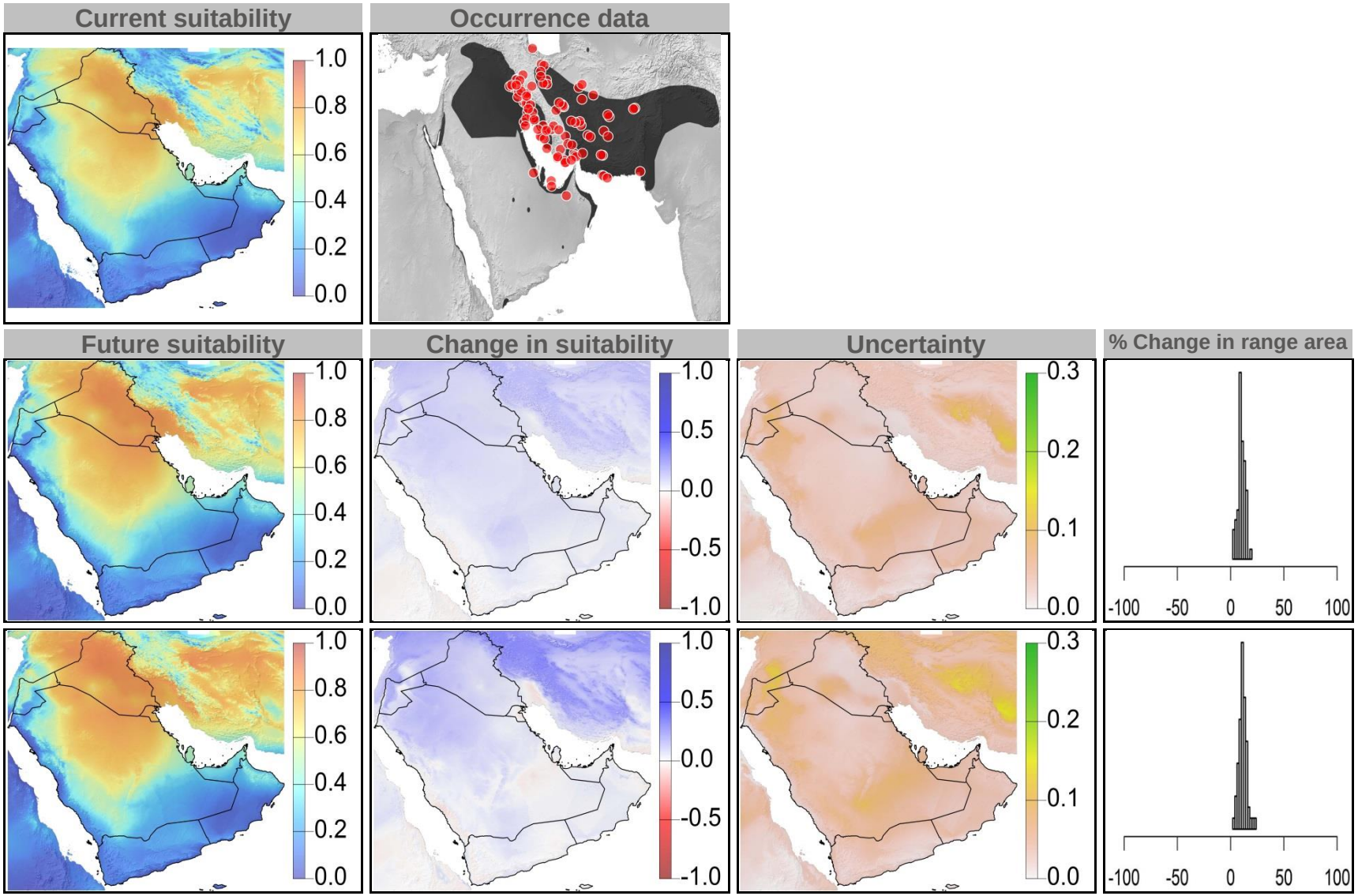

Figure 8: Current and future (2070) climate suitability for *Cyrtopodion scabrum*, based on an ensemble of all future climate scenarios from the regional climate modeling effort at two spatial domains. Range and occurrence data shown for reference.

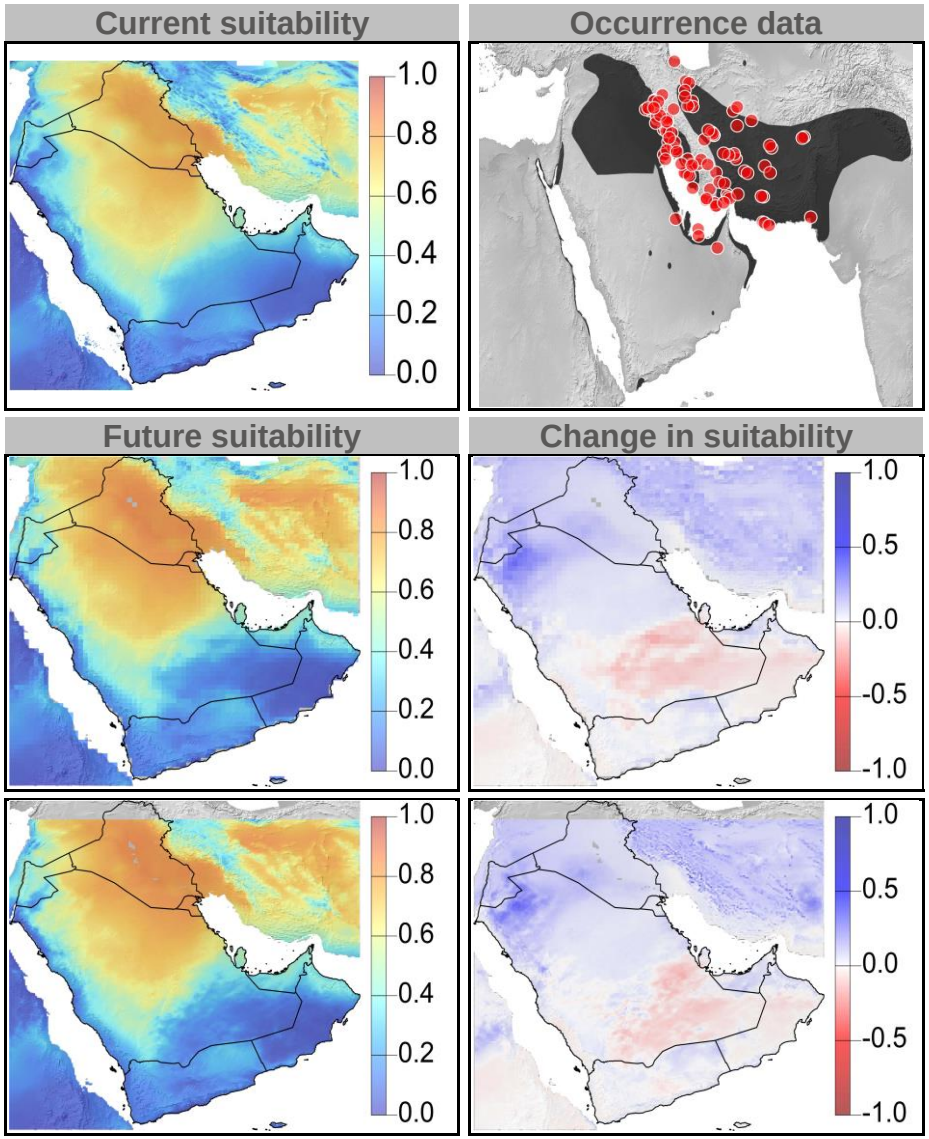

Figure 9: Current and future climate suitability for *Echis carinatus*, with associated uncertainty and change in range area based on an ensemble of all future climate scenarios. Range and occurrence data shown for reference.

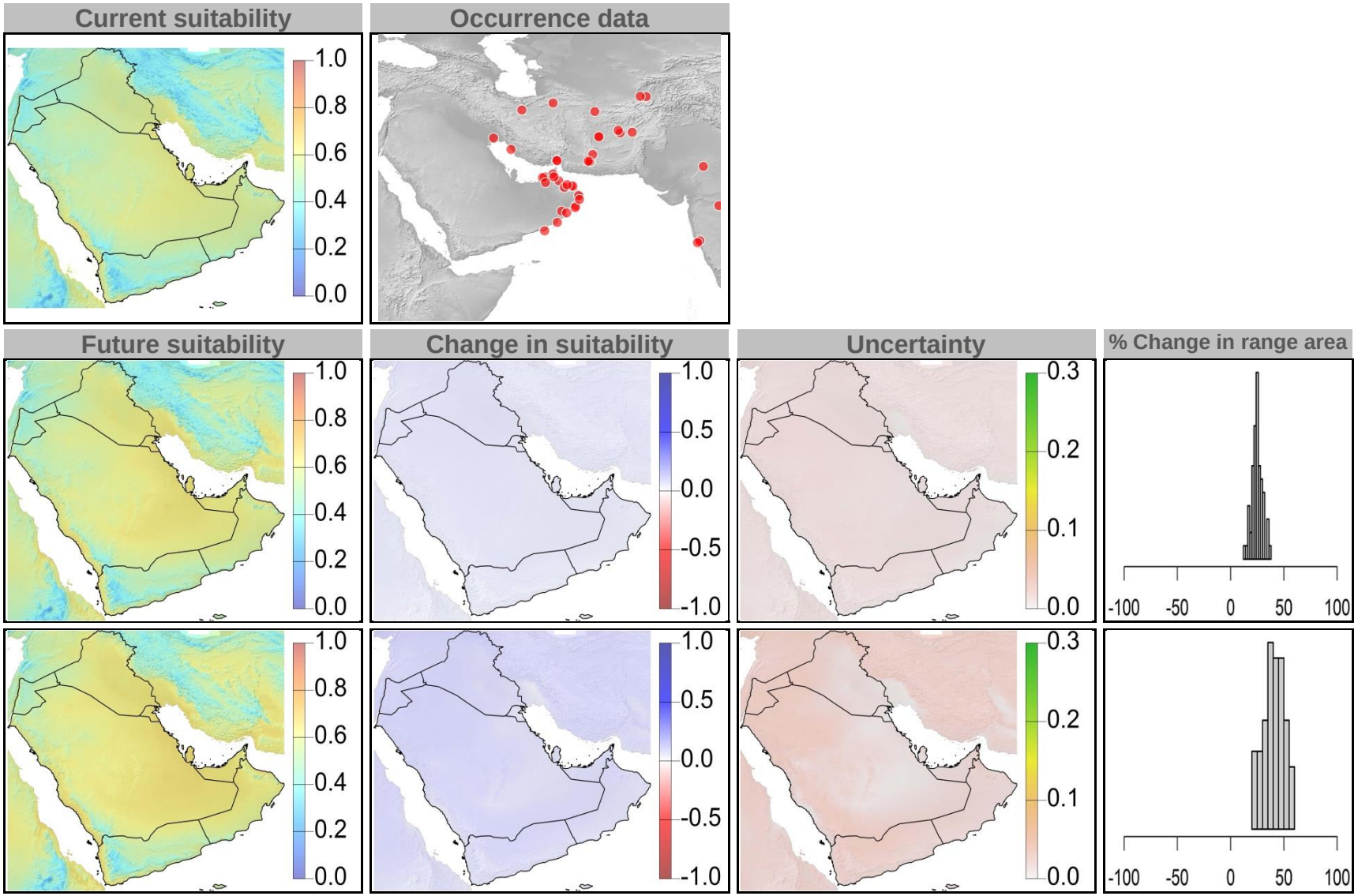

Figure 10: Current and future (2070) climate suitability for *Echis carinatus*, based on an ensemble of all future climate scenarios from the regional climate modeling effort at two spatial domains. Range and occurrence data shown for reference.

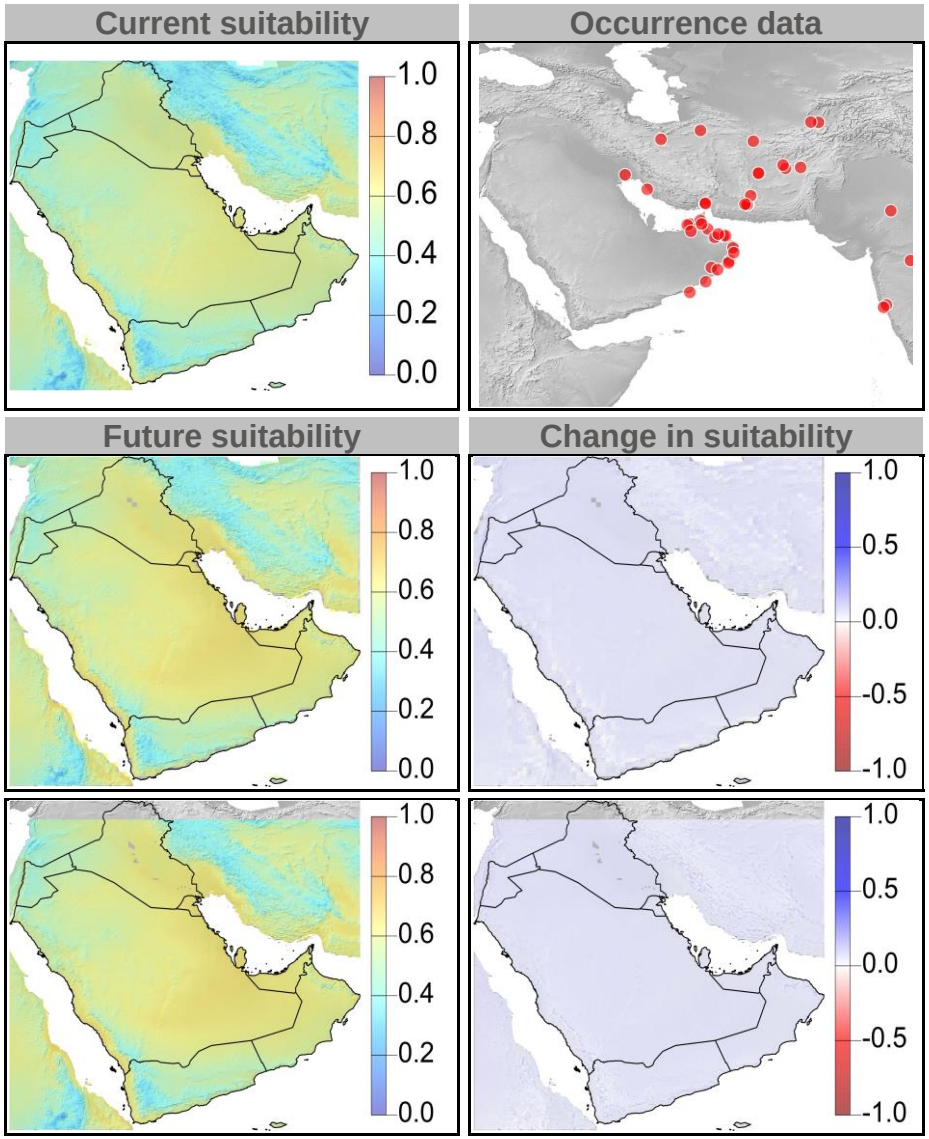

Figure 11: Current and future climate suitability for *Echis coloratus*, with associated uncertainty and change in range area based on an ensemble of all future climate scenarios. Range and occurrence data shown for reference.

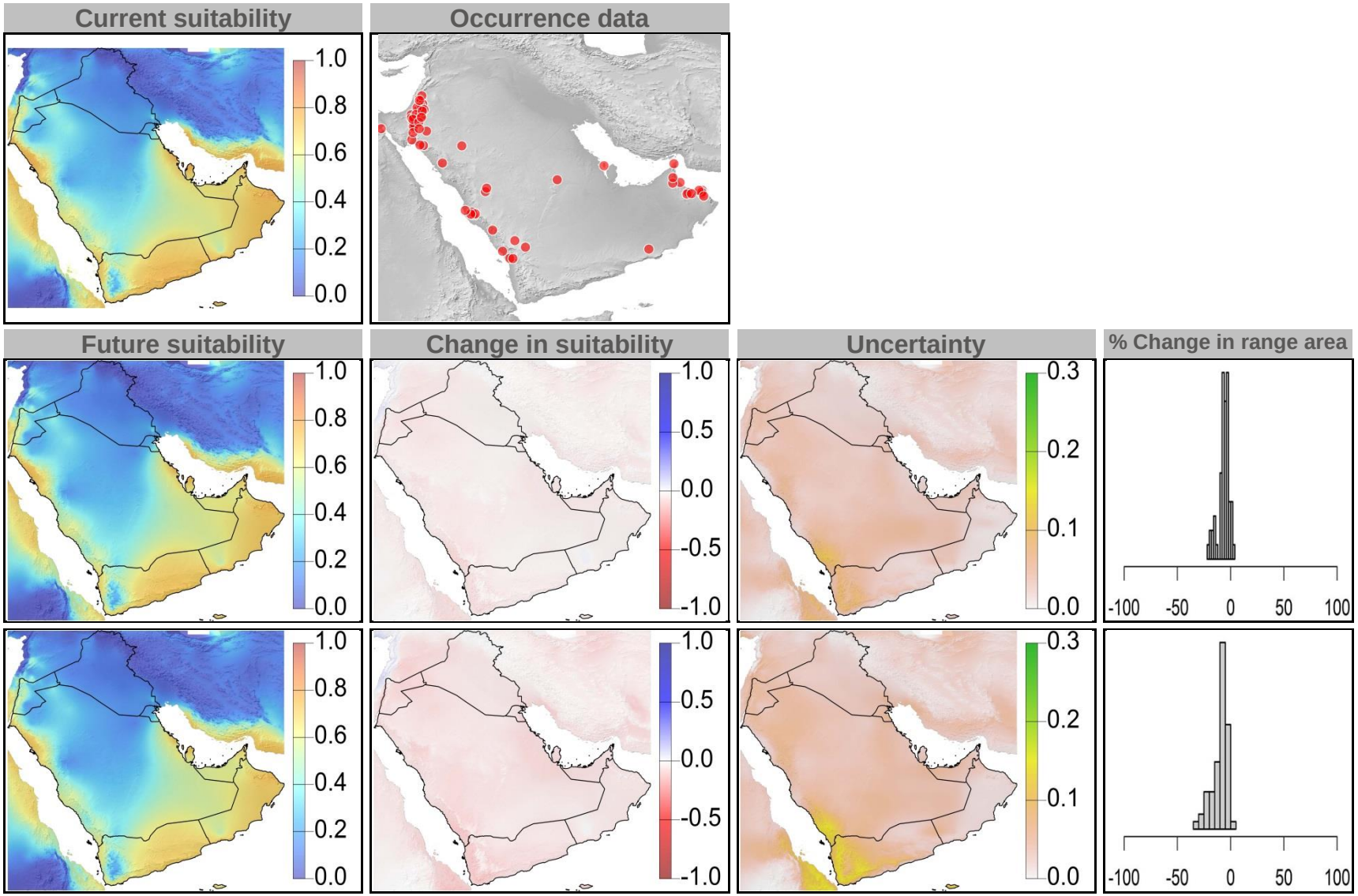

Figure 12: Current and future (2070) climate suitability for *Echis coloratus*, based on an ensemble of all future climate scenarios from the regional climate modeling effort at two spatial domains. Range and occurrence data shown for reference.

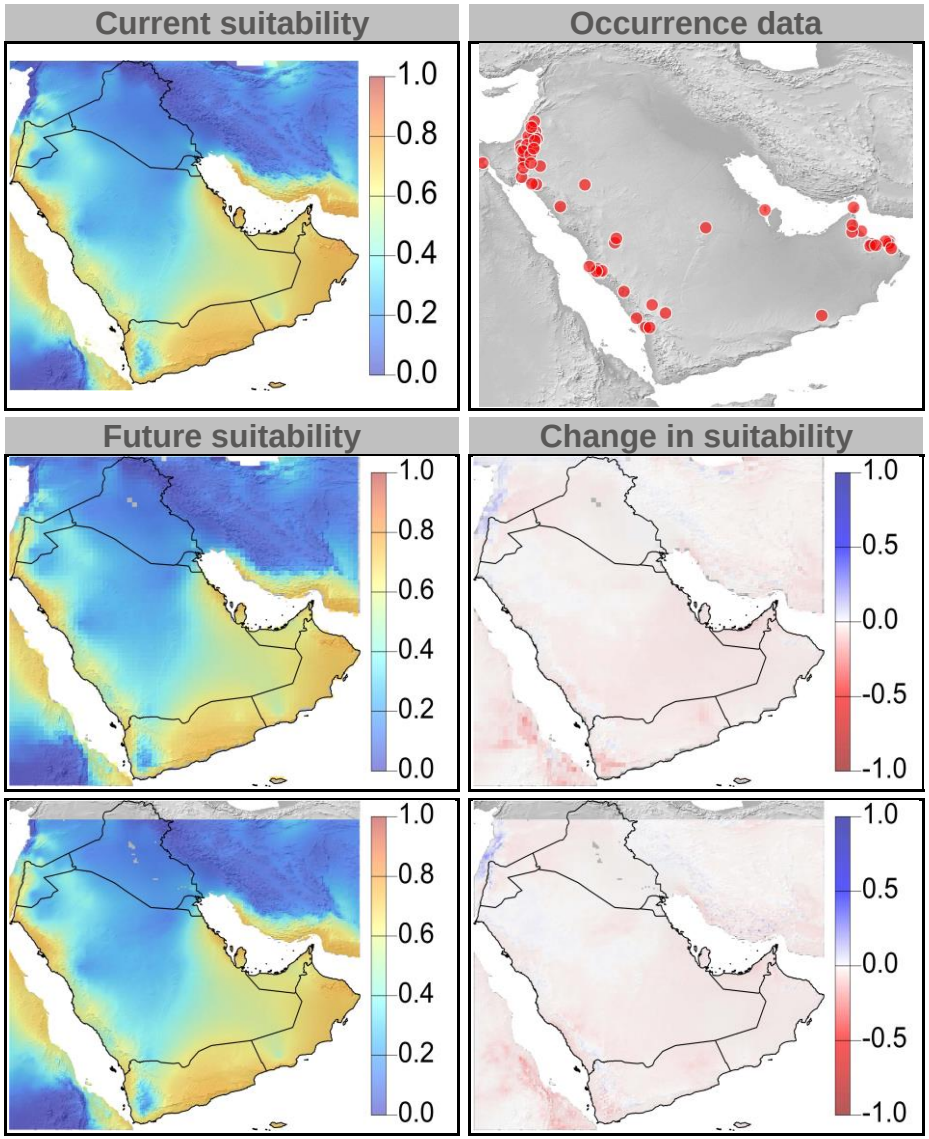

Figure 13: Current and future climate suitability for *Eryx jayakari*, with associated uncertainty and change in range area based on an ensemble of all future climate scenarios. Range and occurrence data shown for reference.

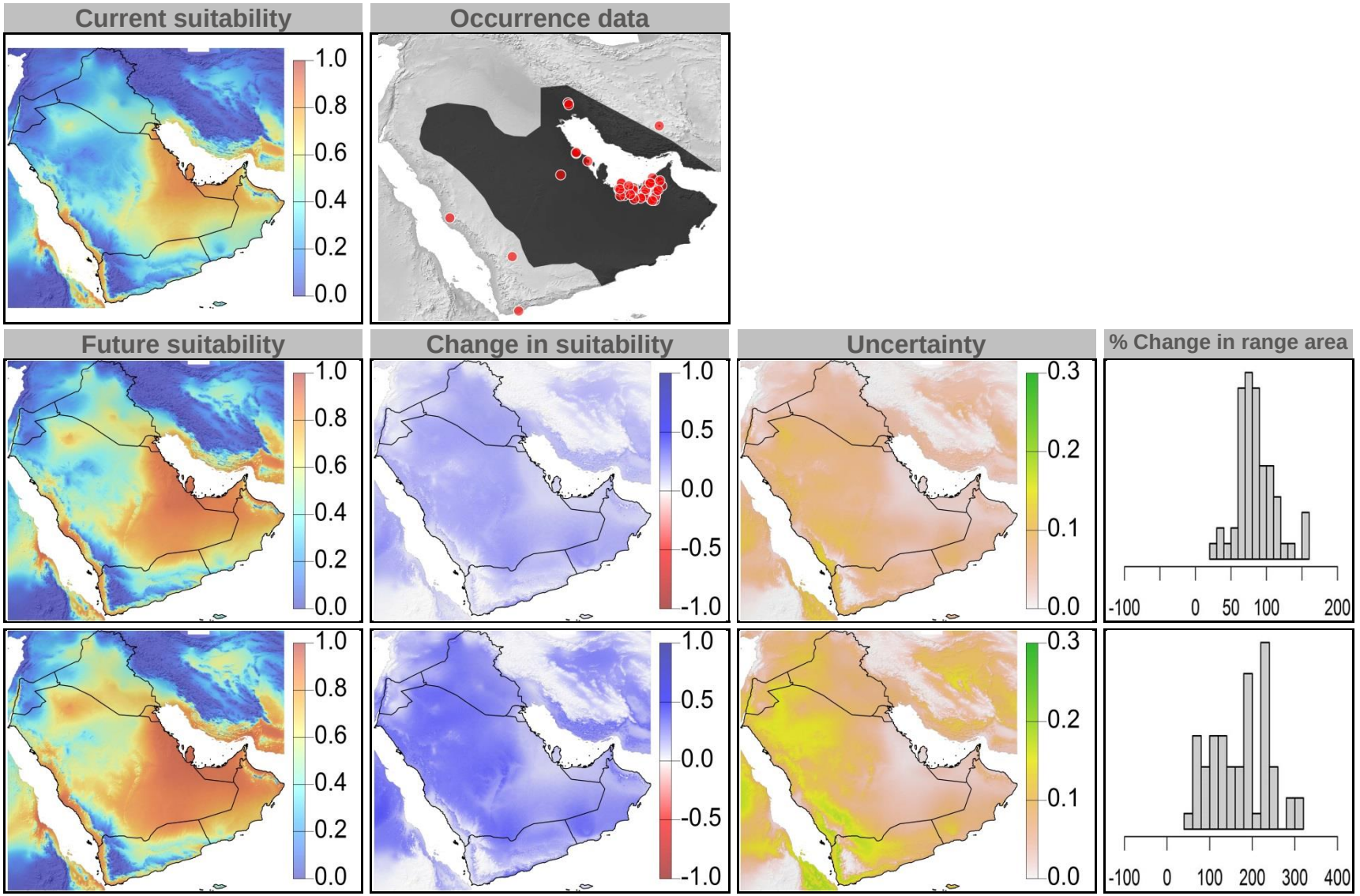

Figure 14: Current and future (2070) climate suitability for *Eryx jayakari*, based on an ensemble of all future climate scenarios from the regional climate modeling effort at two spatial domains. Range and occurrence data shown for reference.

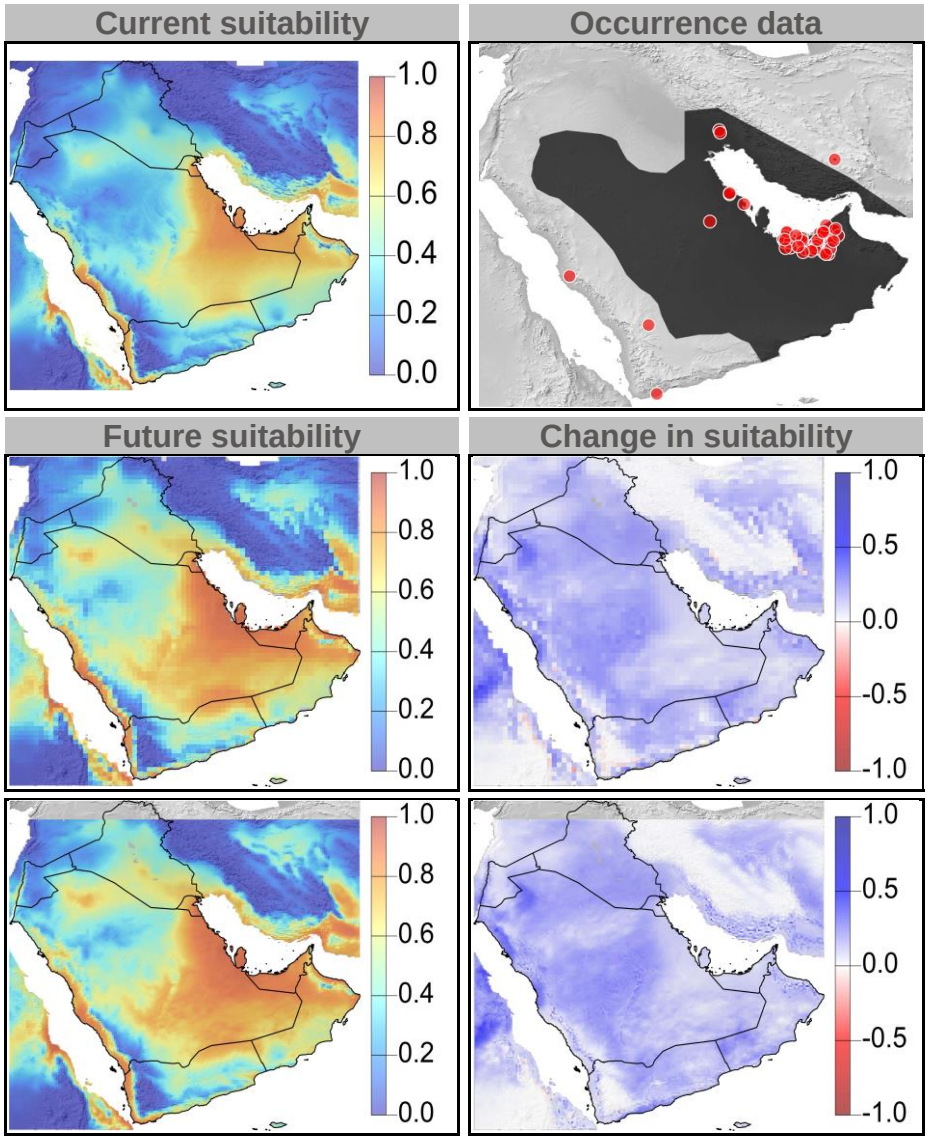

Figure 15: Current and future climate suitability for *Hemidactylus persicus*, with associated uncertainty and change in range area based on an ensemble of all future climate scenarios. Range and occurrence data shown for reference.

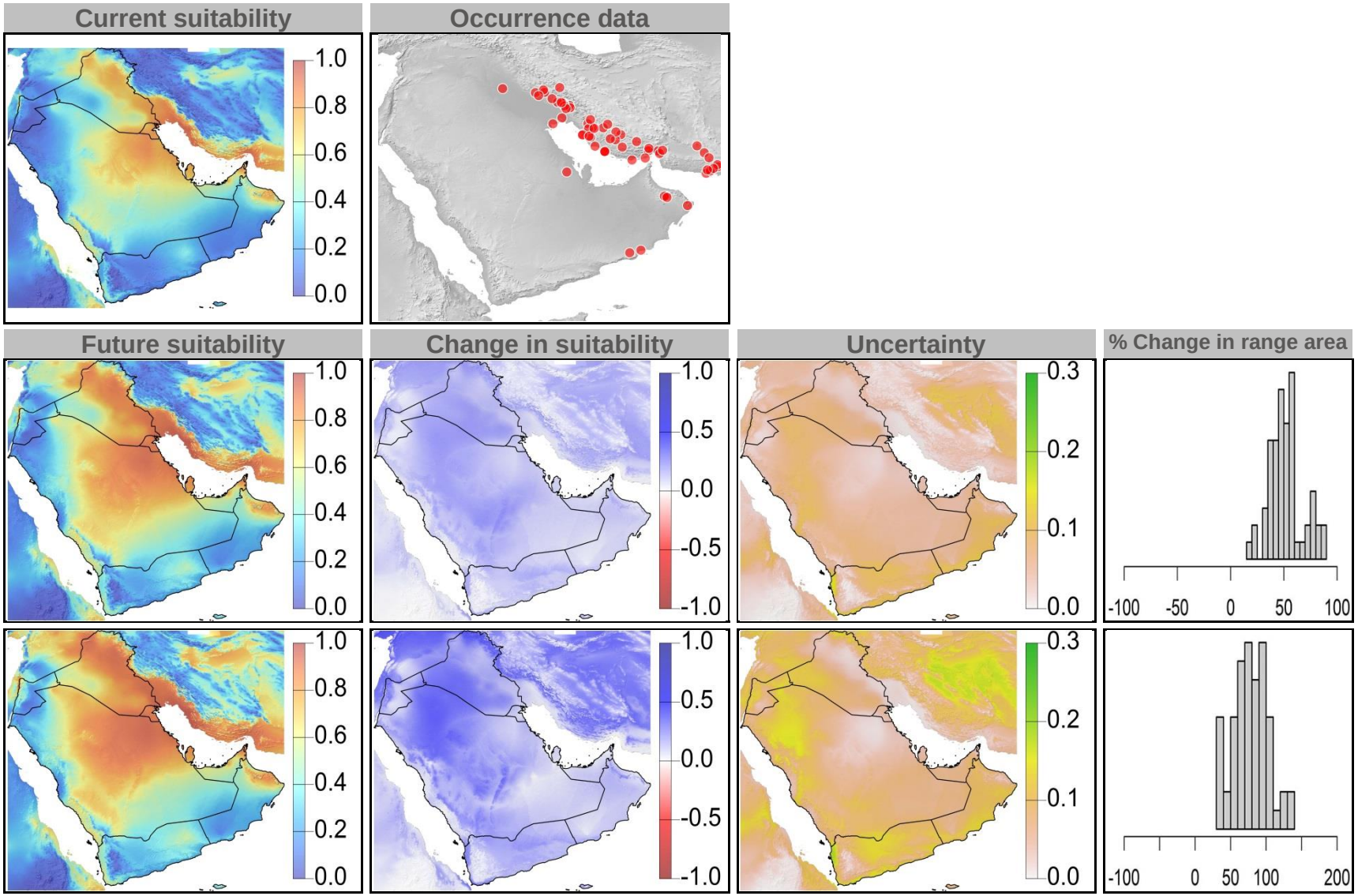

Figure 16: Current and future (2070) climate suitability for *Hemidactylus persicus*, based on an ensemble of all future climate scenarios from the regional climate modeling effort at two spatial domains. Range and occurrence data shown for reference.

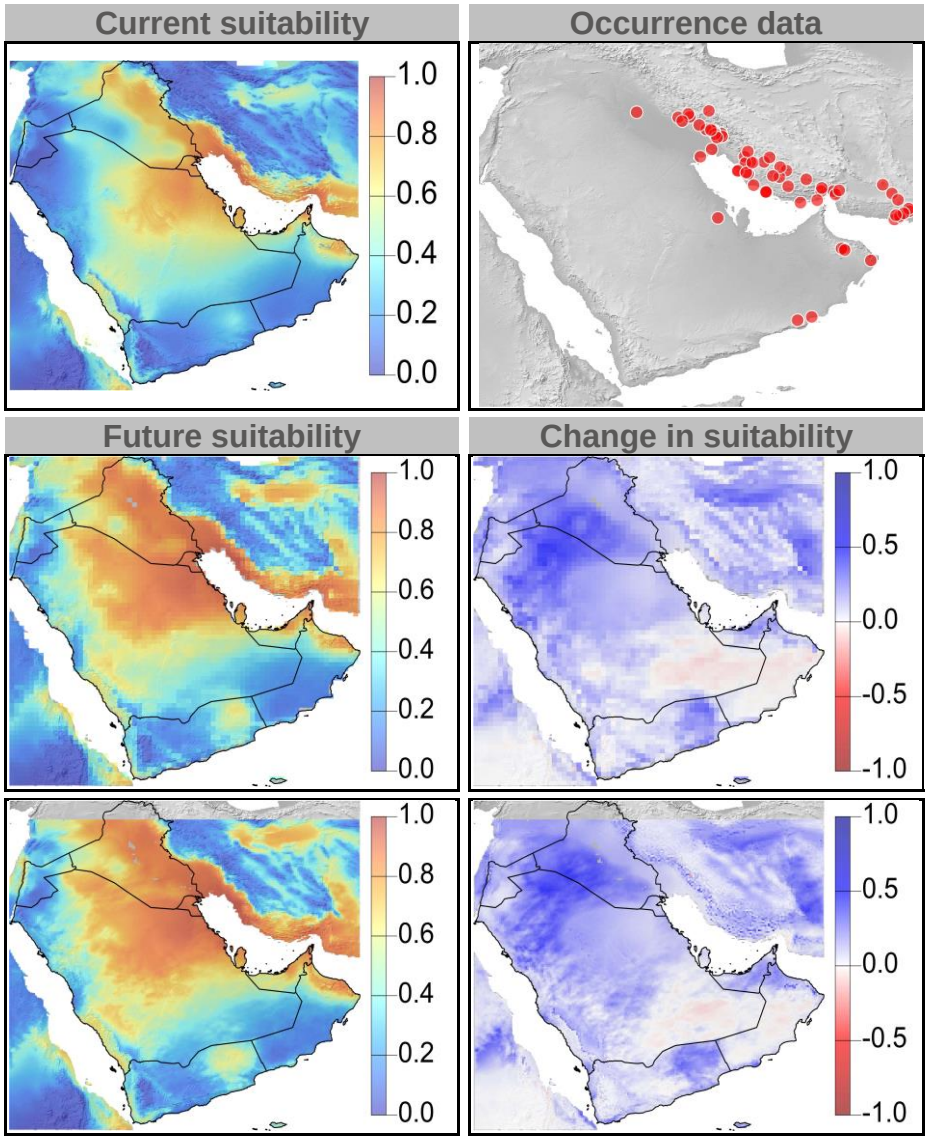

Figure 17: Current and future climate suitability for *Pristurus carteri*, with associated uncertainty and change in range area based on an ensemble of all future climate scenarios. Range and occurrence data shown for reference.

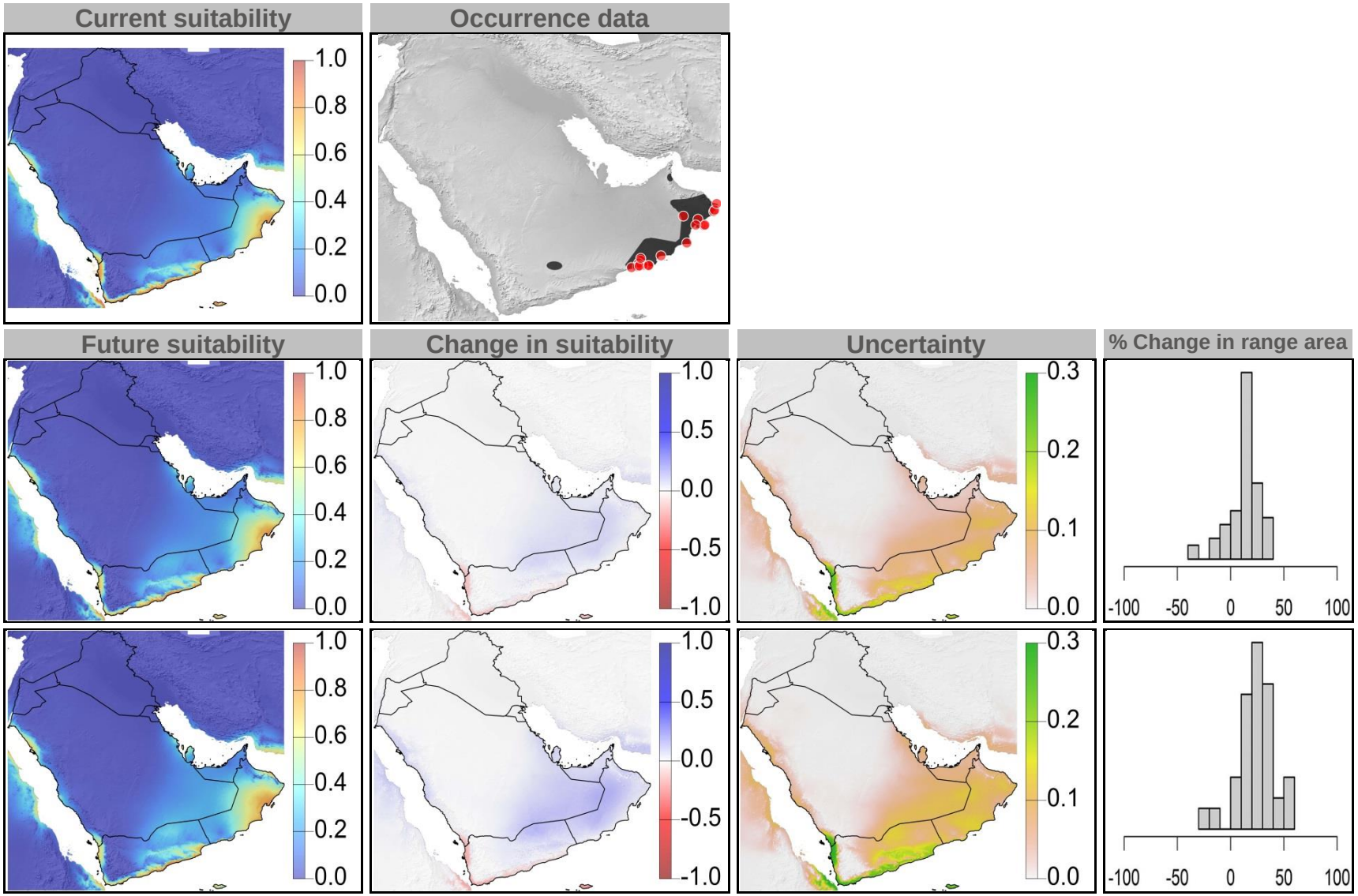

Figure 18: Current and future (2070) climate suitability for *Pristurus carteri*, based on an ensemble of all future climate scenarios from the regional climate modeling effort at two spatial domains. Range and occurrence data shown for reference.

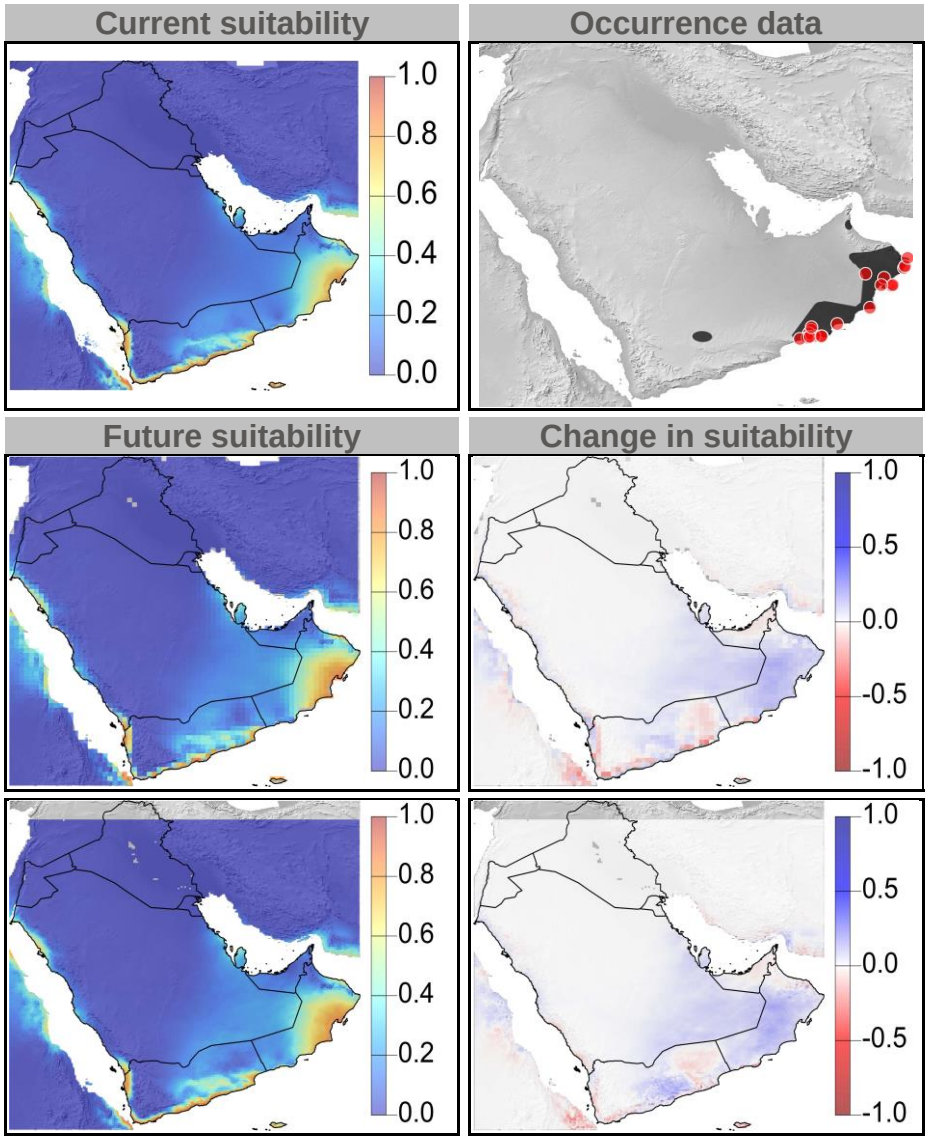

Figure 19: Current and future climate suitability for *Pristurus flavipunctatus*, with associated uncertainty and change in range area based on an ensemble of all future climate scenarios. Range and occurrence data shown for reference.

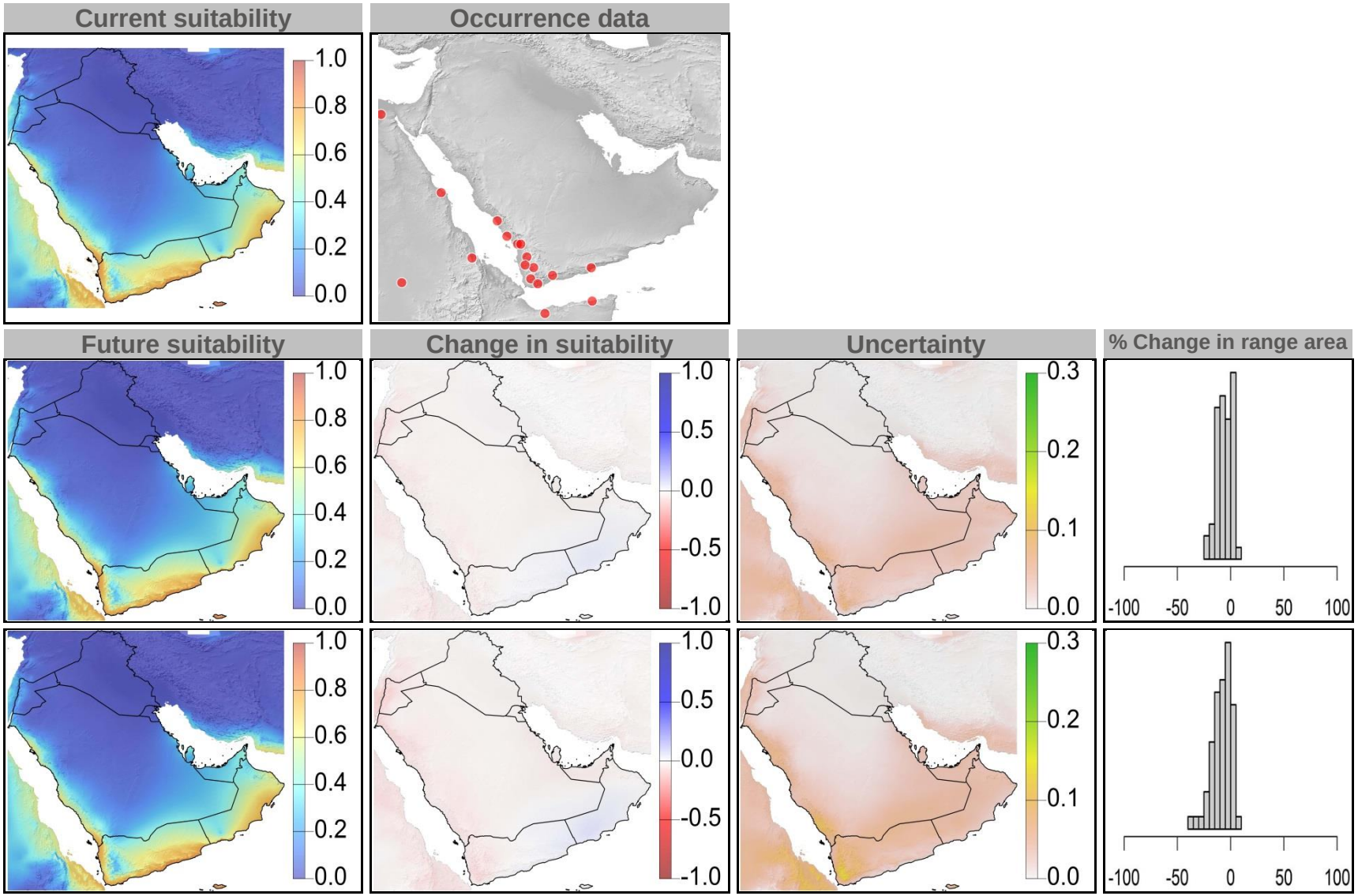

Figure 20: Current and future (2070) climate suitability for *Pristurus flavipunctatus*, based on an ensemble of all future climate scenarios from the regional climate modeling effort at two spatial domains. Range and occurrence data shown for reference.

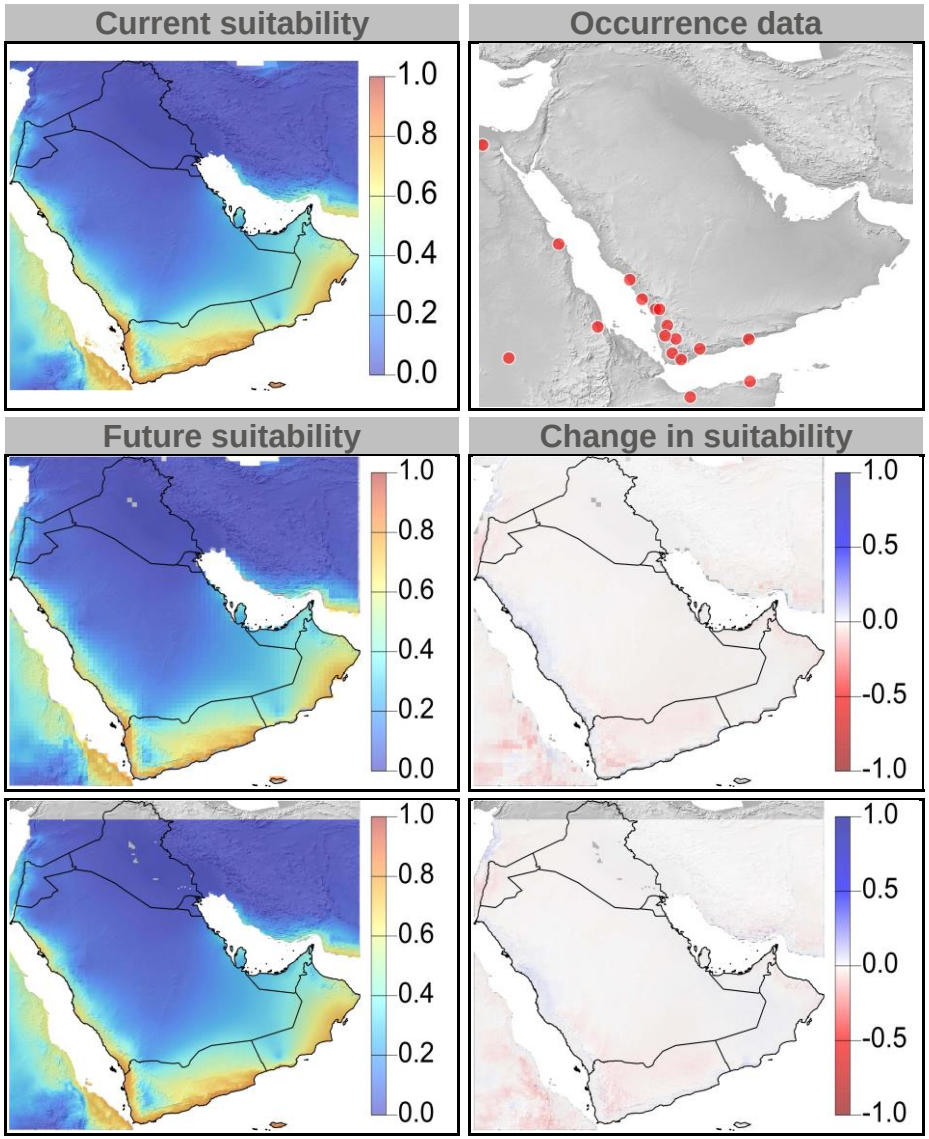

Figure 21: Current and future climate suitability for *Pristurus rupestris*, with associated uncertainty and change in range area based on an ensemble of all future climate scenarios. Range and occurrence data shown for reference.

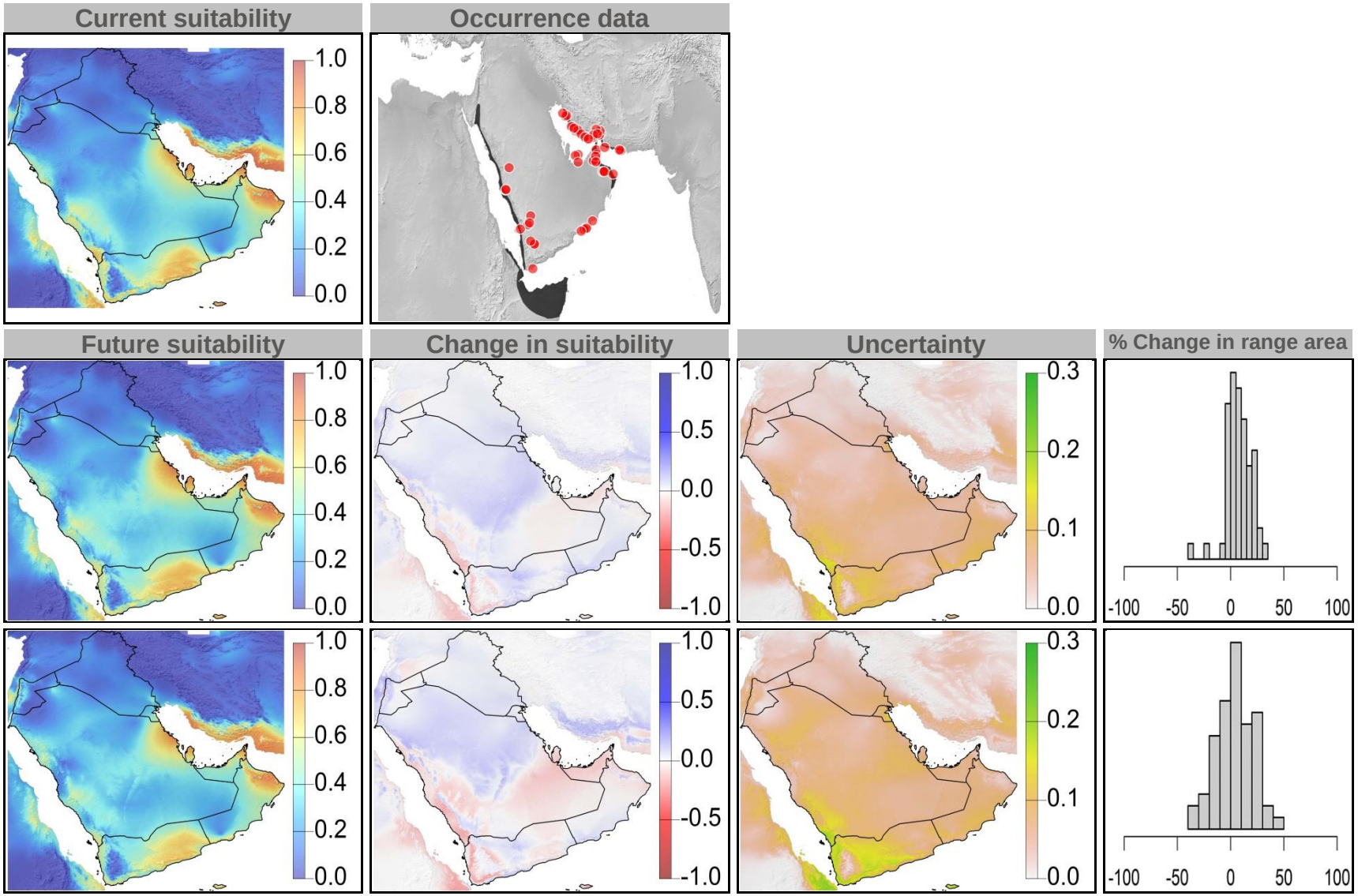

Figure 22: Current and future (2070) climate suitability for *Pristurus rupestris*, based on an ensemble of all future climate scenarios from the regional climate modeling effort at two spatial domains. Range and occurrence data shown for reference.

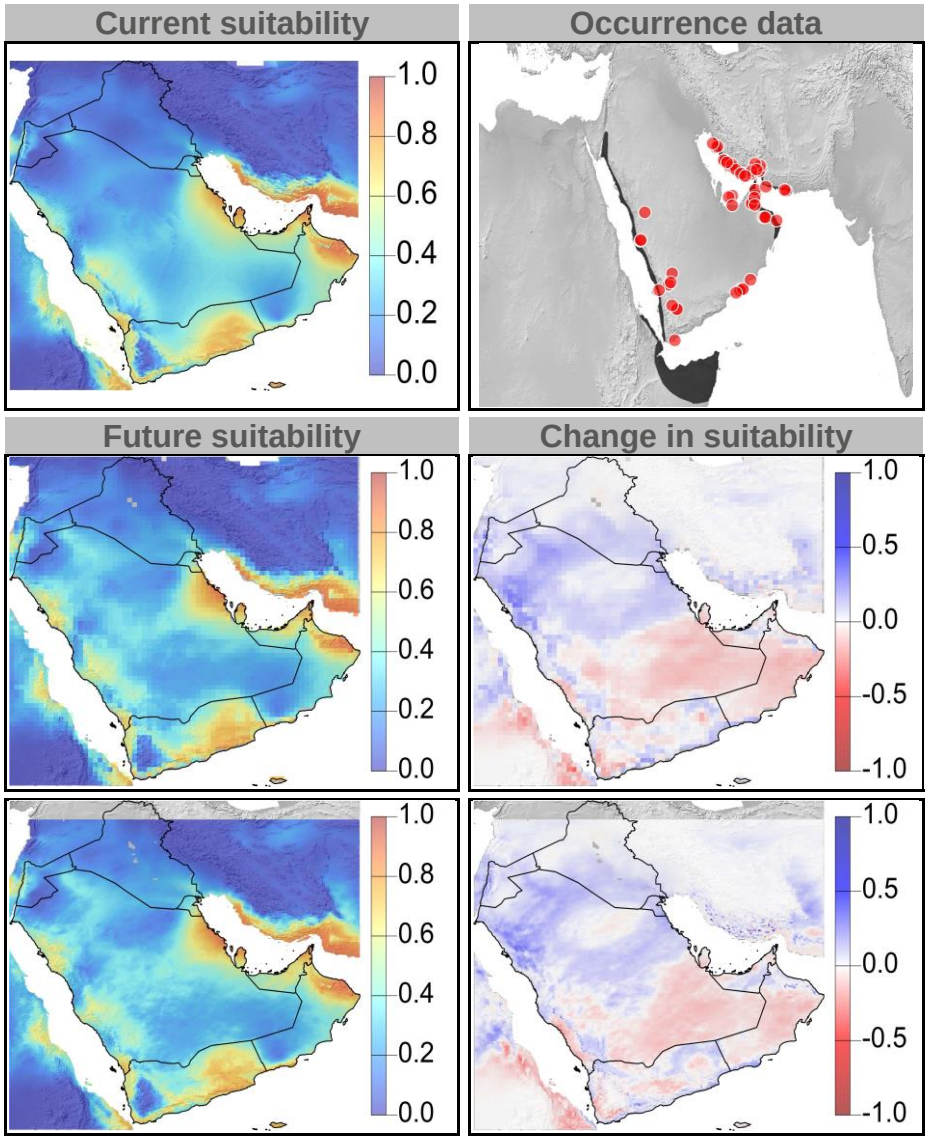

Figure 23: Current and future climate suitability for *Stenodactylus doriae*, with associated uncertainty and change in range area based on an ensemble of all future climate scenarios. Range and occurrence data shown for reference.

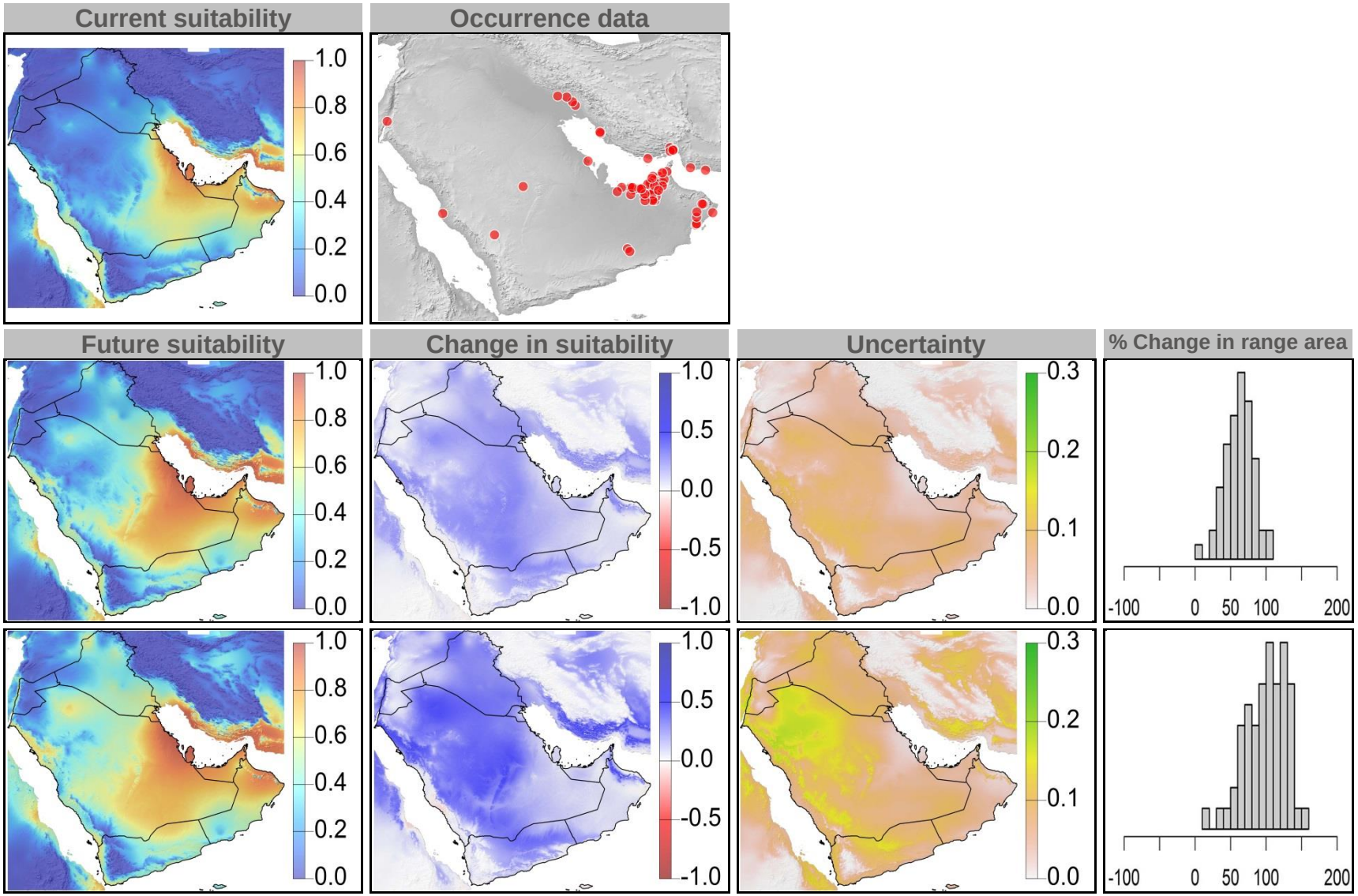

Figure 24: Current and future (2070) climate suitability for *Stenodactylus doriae*, based on an ensemble of all future climate scenarios from the regional climate modeling effort at two spatial domains. Range and occurrence data shown for reference.

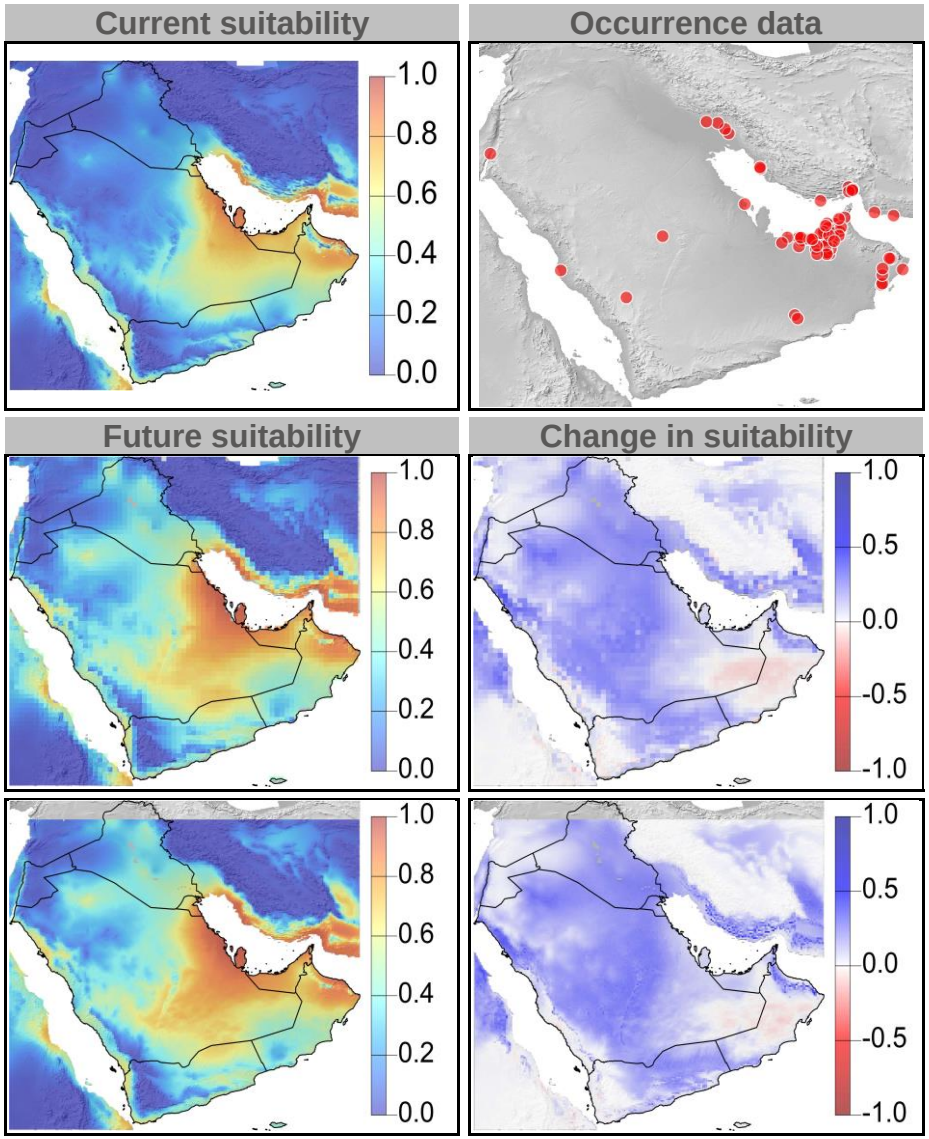

AGEDI
مبادرة أبوظبي العالمية للبيانات البيئية
Abu Dhabi Global Environmental Data Initiative

an initiative of

UNEP

هيئة البيئة - أبوظبي
Environment Agency - ABU DHABI

Abu Dhabi Global Environmental Data Initiative (AGEDI)
P.O Box: 45553
Al Mamoura Building A, Murour Road
Abu Dhabi, United Arab Emirates

Phone: +971 (2) 6934 444
Email : info@AGEDI.ae

AGEDI.org

LNRClimateChange@ead.ae